Investigating the mechanism of non-catalytic tyrosine-phosphorylated receptor triggering

Eleanor Mary Denham

Sir William Dunn School of Pathology



St. Edmund Hall, University of Oxford

A thesis submitted for the degree of Doctor of Philosophy

January 2016

Abstract

Non-catalytic tyrosine-phosphorylated receptors (NTRs) are a large group of leukocyte receptors that bind to surface-associated ligands and include both activating and inhibitory members. They contain, or associate with adaptor molecules which contain, tyrosine residues within conserved cytoplasmic motifs that are phosphorylated and dephosphorylated by extrinsic kinases and phosphatases respectively. The mechanism by which NTR-ligand engagement leads to sustained phosphorylation of receptor tyrosine-based motifs and initiation of downstream signalling (termed "receptor triggering"), is as yet unknown.

Our hypothesis is that the NTRs signal using the kinetic-segregation (KS) model. The model proposes that large inhibitory phosphatases, but not inner leaflet-bound activating kinases, are segregated in a size-dependent manner from engaged receptors upon ligand binding. This favours kinase activity and drives sustained receptor phosphorylation.

To systematically test whether predictions of the KS model hold for all NTRs, we have developed an artificial generic ligand system in which biophysical and biochemical properties of NTR-ligand interactions can be manipulated. These include NTR-ligand dimensions, ligand densities and valency. Our system exploits the interaction between a Strep-Tag II, which is attached to the ectodomain of the NTR, and StrepTactin protein. We first demonstrate that representative NTRs, both activating and inhibitory, can be triggered through ligation of this Strep-Tag II. In agreement with a key KS model prediction, we next show that only ligation by surface-associated ligand leads to triggering, whilst ligation by soluble ligand does not. Additionally, by altering ligand valency and mobility, we provide evidence that receptor clustering can enhance activation. Also in agreement with the KS model, we show that elongation of the artificial ligand dramatically affects activation of a representative NTR. Finally, we provide evidence to suggest that increased receptor clustering may be able to compensate for ligand elongation-mediated defects in NTR signalling.

The flexibility of this system will allow us to analyse other NTRs, test further predictions of the model, and investigate the role of other properties of NTR signalling.

Acknowledgements

I cannot submit this work without thanking my supervisors Professor Anton van der Merwe and Dr Jesse Goyette for the immense amount of support and guidance they have given me. In these last few years I have learned more about science, and how to think about science, than I thought possible, and your continuous encouragement has made my time here truly memorable. I must also thank a number of other people, namely Dr Marion Brown, Dr Omer Dushek, and Professor Neil Barclay, for their help and advice throughout my DPhil, and Professors Oreste Acuto and Simon Davis for their helpful suggestions during my transfer and confirmation processes.

Special thanks also go to my examiners, Professors Mark Howarth and Ben Willcox, for taking the time to read this thesis and discussing my work with me.

More generally, I would like to acknowledge and thank the past and present members of the van der Merwe and Dushek groups for their support, both academic and personal. In particular, to Hong Sheng Lim, for making my time in tissue culture go faster with some interesting discussion topics, to Rachel Paterson, for providing unrelenting optimism (and gossip), to Ben de Wet (and Jesse again!), for the YouTube videos, and to Marcus Bridge, for the commiserative, and celebratory, pints. And of course, my foam sword.

Every DPhil has a time(s!) when nothing works and you have no idea why. I am grateful to Maria and Janet for letting me vent my frustrations to them, and for them in turn sharing their experimental woes with me. I would also like to thank them for their patience during the time I have spent writing this thesis. I have completely neglected you. I promise: I can come out to play now.

I would also like to thank Unilever because I have drunk more PG tips while writing up than a person really ever should. This thesis is basically 75$\%$ tea.

I am very grateful to my nans for their love and kindness throughout my life, and to my grandads, who never got to see this.

A special thank you goes to my brother, Nathan, who essentially inspired me to go into science in the first place. This is all your fault and I'm telling mum!

To my Corwin. I can't express how grateful I am for your support and encouragement. Thank you for believing in me. And thank you for the times you told me everything was going to be OK when I was convinced the world was ending just because I had not met my writing goal for the day. You were right. I made it. I did the thing!

And finally, of course, to my incredible parents. Thank you for your unwavering support. Thank you for always being there when I needed you. Thank you for not making it obvious you thought I was incompetent when I told you "no, that experiment with the DNA didn't work again". And thank you for the help I know is to come. I really will never be able to thank you enough.

In memory of Nanny Ada and Nanny Dot who both

died shortly after submission of this thesis

Contents

1. General introduction **1**

1.1 Non-catalytic tyrosine-phosphorylated receptors 3

1.2 The interaction between NTR and ligand 5

1.3 The variety of NTRs and ligands 8

1.4 NTRs that associate with adaptor proteins containing cytoplasmic tyrosine-based motifs 9

1.4.1 Adaptor proteins 9

1.5 NTRs with intrinsic cytoplasmic tyrosine-based motifs 11

1.6 Regulation of NTR phosphorylation by the opposing activities of Src-family kinases and protein tyrosine phosphatases 13

1.6.1 Signalling induced by prolonged receptor phosphorylation 21

1.7 Regulation of Src family kinases and membrane-associated phosphatases 23

1.7.1 Src family kinases 23

1.7.2 Phosphatases 24

1.8 The mechanism of NTR triggering 25

1.9 Conformational change 29

1.9.1 The "safety" model of TCR triggering 29

1.9.2 Transduction of extracellular binding to the intracellular region . . . 31

1.9.3 Mechanical-induced conformational change 31

1.9.4 Evidence for a mechanical force model 32

1.9.5 How can ligand binding generate a mechanical force? 34

1.10 Clustering/ Aggregation 35

1.10.1 Conformational change-induced oligomerisation model of BCR activation 36

1.10.2 The permissive geometry model 38

1.10.3 Homoclustering 39

1.10.4 Pseudodimerisation model of TCR activation 40

1.10.5 Heterodimerisation model of TCR activation 41

1.10.6 How can ligand binding induce clustering? 42

1.11 Segregation or redistribution 44

1.11.1 Lipid rafts in NTR activation 45
1.11.2 Kinetic-segregation 46
1.11.2.1 The TCR 48
1.11.2.2 CD28 55
1.11.2.3 NK cell receptors 56
1.11.2.4 Dectin-1 57
1.11.2.5 The positive regulatory role of CD45 and the KS model . 57
1.12 Aims and hypothesis 59

2. Materials and methods **61**
2.1 NTR and adaptor construct design and synthesis 61
2.1.1 Receptors 62
2.1.2 Adaptor proteins 63
2.2 Transduction of cell lines with receptor and adaptor constructs 66
2.2.1 Cell lines 66
2.2.2 Lentiviral transduction 66
2.2.2.1 X-tremeGENE™ 9 66
2.2.2.2 Polyethylenimine 67
2.2.3 Cell expression analysis using flow cytometry 67
2.2.4 Cell sorting with magnetic beads or fluorescence-activated cell sorting 68
2.3 Cloning of artificial ligand constructs 68
2.4 Transduction of cell lines with artificial ligand 70
2.4.1 Cell lines 70
2.4.2 CHO 70
2.4.2.1 Nucleofection 70
2.4.3 HEK293T 71
2.4.3.1 PEI 71
2.4.4 Cell expression analysis using flow cytometry 71
2.5 Expression and purification of StrepTactin 72
2.5.1 Using biotin-4-fluorescein to estimate valency of StrepTactin tetramers 74
2.5.2 StrepTactin labelling with atto 647 dye 75
2.6 SNAP tag:Strep-Tag II 75
2.6.1 Cloning of SNAP tag:Strep-Tag II 75
2.6.2 Expression and purification of SNAP tag:Strep-Tag II protein 75
2.6.3 SNAP tag:Strep-Tag II labelling with SNAP-surface® Alexa Fluor® 488 76
2.7 Forming supported lipid bilayers on silica beads 76

2.8 Testing cell lines or phospholipid bilayer-coated beads for StrepTactin binding and available binding sites on StrepTactin-bound cells/beads . . . 77
2.9 Expression and purification of monovalent and tetravalent StrepTactin-Spycatcher . . . 78
2.9.1 Using biotin-4-fluorescein to estimate valency of StrepTactin-SpyCatcher tetramers . . . 80
2.9.2 StrepTactin-SpyCatcher labelling with atto 647 . . . 80
2.10 Stimulation of representative Strep-Tag II-tagged non-catalytic tyrosine-phosphorylated receptors expressed in THP-1 cells by anti-Strep-Tag II antibody immobilised onto 96 well plates . . . 81
2.11 Stimulation of THP-1 NKp30 cells with lipid bilayer-coated beads presenting ST3dSA1 . . . 82
2.12 Stimulating THP-1 NKp30 cells and THP-1 SIRPβ1 cells with CHO ligand cells presenting StrepTactin-SpyCatcher . . . 82
2.12.1 Stimulation of THP-1 cells expressing representative NTRs with plate-immobilised StrepTactin or StrepTactin:atto 647 . . . 83
2.12.1.1 THP-1 NKp30 . . . 83
2.12.1.2 THP-1 FcγRIA, THP-1 SIGLEC-14 and THP-1 SIRPβ1 . . . 84
2.13 Stimulation of example NTRs expressed in THP-1 cells with soluble StrepTactin . . . 84
2.13.1 THP-1 NKp30 . . . 84
2.13.2 THP-1 FcγRIA, THP-1 SIGLEC-14 and THP-1 SIRPβ1 . . . 84
2.14 Flow cytometry analysis of soluble tetravalent StrepTactin binding to NTR-expressing THP-1 cells . . . 85
2.14.1 Direct staining of NTR-expressing THP-1 cells with atto 647-labelled tetravalent StrepTactin . . . 85
2.15 Using flow cytometry to show tetravalent StrepTactin-SpyCatcher binds to NTR-expressing THP-1 cells multivalently . . . 85
2.15.1 Dissociation of atto 647-labelled monovalent or tetravalent StrepTactin-SpyCatcher from THP-1 SIRPβ1 cells . . . 85
2.15.2 Equilibrium binding of atto 647-labelled monovalent or tetravalent StrepTactin-SpyCatcher to THP-1 SIRPβ1 cells . . . 86
2.16 Stimulation of representative NTR-expressing THP-1 cells with immobilised StrepTactin/StrepTactin-SpyCatcher of different valencies . . . 87
2.16.1 Stimulation of THP-1 NKp30 cells with immobilised StrepTactin of different valencies alone or with poly-L-lysine or polyethylenimine . . . 87
2.16.1.1 StrepTactin alone . . . 87
2.16.1.2 Comparison of StrepTactin immobilised alone or with poly-L-lysine or polyethylenimine . . . 87

2.17 Stimulation of THP-1 cells expressing representative NTRs with monovalent or tetravalent StrepTactin-SpyCatcher immobilised on a 96 well plate . 88
2.17.1 Stimulation of THP-1 SIRPβ1 cells 89
2.17.2 Measuring how much StrepTactin-SpyCatcher is immobilised and number of biotin-binding sites 90
2.17.3 Using 6M guanidinium hydrochloride pH 1.5 to denature StrepTactin-SpyCatcher - biotin:atto 680 interaction 91
2.17.3.1 Analysing the effect of guanidinium hydrochloride on biotin:atto 680 fluorescence 91
2.18 Stimulation of THP-1 SIRPβ1 cells with CHO cells expressing artificial ligands of different lengths coupled to monovalent or tetravalent StrepTactin-SpyCatcher 91
2.18.1 Measuring IL-8 release from THP-1 cells expressing NTRs incubated with CHO ligand-expressing cells coupled to StrepTactin-SpyCatcher 91

3. Development of the strategy to artificially stimulate non-catalytic tyrosine -phosphorylated receptors (NTRs) **95**
3.1 Introduction 95
3.1.1 Using physiological ligands 95
3.1.2 Utilising interactions used in biotechnology 96
3.1.3 First generic ligand strategy 98
3.1.4 Second generic ligand strategy 103
3.2 Results 106
3.2.1 Cloning of receptor and adaptor protein constructs 106
3.2.2 Transduction of human cell lines with tagged NTRs and adaptor proteins 112
3.2.2.1 Transduction of Jurkat cells 113
3.2.2.2 Transduction of NKL and NK92 cells 123
3.2.2.3 Transduction of THP-1 cells 124
3.2.3 Cloning of artificial ligand constructs 129
3.2.4 Transfection of mammalian cell lines with artificial ligand constructs 130
3.2.5 Expression and purification of StrepTactin 137
3.2.6 Synthesis of SNAP-Strep-Tag II:488 146
3.2.7 Soluble StrepTactin can bind cells expressing Strep-Tag II-tagged receptors but remaining available binding sites cannot be detected 146
3.2.8 Soluble StrepTactin of different valency can bind cells expressing biotinylated ligands of different lengths with varying numbers of remaining available biotin-binding sites 150

3.2.9 Soluble StrepTactin of different valency can bind biotin presented on supported lipid bilayers with varying numbers of remaining available biotin-binding sites. . . . 160
3.2.10 Second strategy to stimulate NTRs . . . 164
3.2.10.1 Expression and purification of monovalent and tetravalent StrepTactin-SpyCatcher . . . 165
3.2.10.2 Monovalent and tetravalent StrepTactin-SpyCatcher can bind THP-1 SIRPβI cells . . . 174
3.2.10.3 Monovalent and tetravalent StrepTactin-SpyCatcher will conjugate to SpyTagged ligand-expressing cells with accessible biotin-binding site/s . . . 174
3.3 Discussion . . . 176
3.3.1 Receptor cell lines . . . 176
3.3.2 Ligand cell lines . . . 178
3.3.3 StrepTactin and StrepTactin-SpyCatcher . . . 179
3.3.4 Putting the system components together . . . 180

4. A selection of non-catalytic tyrosine-phosphorylated receptors can be stimulated with artificial ligand presented on a surface but not by soluble ligand **183**
4.1 Introduction . . . 183
4.1.1 2B4 . . . 183
4.1.2 FcγRIA . . . 184
4.1.3 LAIR-1 . . . 184
4.1.4 NKp30 . . . 185
4.1.5 SIGLEC-14 . . . 185
4.1.6 SIRPβ1 . . . 186
4.1.7 Comparison between physiological ligand- and artificial ligand-binding site . . . 186
4.1.8 Using the artificial ligand system to test a key prediction of the KS model of NTR activation . . . 189
4.2 Results . . . 192
4.2.1 Representative activating and inhibitory NTRs can be stimulated by ligation of the extracellular Strep-Tag II . . . 192
4.2.2 A representative NTR can be stimulated with StrepTactin presented on phospholipid bilayer-coated beads . . . 197
4.2.3 Stimulation of NTRs with artificial ligand-expressing cells . . . 200
4.2.4 NTRs can be stimulated with plate-immobilised StrepTactin but not soluble protein . . . 204
4.2.5 Tetravalent StrepTactin binds to tagged NTRs multivalently . . . 210

4.3 Discussion . . . 214
4.3.1 Confirming NTRs are stimulated by ligation of the Strep-Tag II . . . 214
4.3.2 Other read-outs of receptor activation and further validation 216
4.3.3 Receptor activation with plate-immobilised versus soluble stimulus 217

5. Ligand valency and ectodomain length affect stimulation of a representative non-catalytic tyrosine-phosphorylated receptor **221**
5.1 Introduction . . . 221
5.1.1 The role of ligand spacing in NTR activation . . . 221
5.1.2 The effect of altering ligand mobility on activation . . . 224
5.1.3 Varying the receptor-ligand complex extracellular dimensions affects NTR signalling . . . 225
5.2 Results . . . 228
5.2.1 NTR activation with plate-immobilised StrepTactin of different valencies . . . 228
5.2.2 Comparing NTR activation using plate-immobilised monovalent and tetravalent StrepTactin-SpyCatcher . . . 234
5.2.3 Investigating the effect of increasing valency of ligands presented on cells on representative NTR activation . . . 243
5.2.4 Elongating monovalent artificial ligand but not tetravalent artificial ligand abolishes representative NTR activation . . . 249
5.3 Discussion . . . 254
5.3.1 Immobilisation of StrepTactin or StrepTactin-SpyCatcher onto wells of a 96 well plate . . . 254
5.3.2 Comparing the activation of SIRPβ1 in response to either plate-immobilised ST1-pD-C or plate-immobilised ST4-pD-C . . . 255
5.3.2.1 The maximum cytokine release . . . 255
5.3.2.2 Potency of the response . . . 258
5.3.3 Immobilised monovalent ligand can stimulate a representative NTR 265
5.3.4 Comparing the activation of SIRPβ1 in response to either monovalent or tetravalent StrepTactin-SpyCatcher presented on a cell surface . . . 266
5.3.5 Investigating the effect of elongating monovalent and tetravalent artificial ligand on NTR activation . . . 273

6. General discussion **279**

List of Figures

1.1 Non-catalytic tyrosine-phosphorylated receptors share a number of features 4
1.2 NTR-ligand complex structures indicate that they have small, comparable dimensions 7
1.3 Proposed mechanisms of NTR triggering 27
1.4 Proposed mechanism for integrin clustering 44

3.1 Strep-Tag II and desthiobiotin occupy the same binding site on StrepTactin 98
3.2 Generic ligand system design 100
3.3 A number of properties of the NTR-ligand interaction can be investigated using the artificial ligand system 102
3.4 Second generic ligand system design 105
3.5 Type I and Type I plasmid design 107
3.6 Representative NTRs and adaptor proteins 109
3.7 NKG2D structure and sequence changes 111
3.8 Jurkat cells transduced with 2B4, LAIR-1 or NKp30 and sorted with magnetic beads express high levels of the NTR 114
3.9 Jurkat cells transduced with either FcγRIA and FcRγ, or SIGLEC-14 and DAP12, or SIRPβI and DAP12, express both receptor and adaptor protein 116
3.10 Jurkat cell lines sorted using magnetic beads express both receptor and adaptor protein 117
3.11 Jurkat cell lines sorted by FACS express both receptor and adaptor protein 118
3.12 Jurkat cells transduced with NKG2D, or NKG2D and DAP10_EmGFP do not express NKG2D with accessible Strep-Tag II 120
3.13 Jurkat cells transduced with NKG2D, NKG2D-1x linker and NKG2D-2x linker express the NTR on the cell surface but with Strep-Tag II inaccessible while NKG2D-loop transduced cells do not express NKG2D 122
3.14 NKL cells transduced with LAIR-1 or NKp30 do not express either receptor 123
3.15 THP-1 cells lentivirally transduced with 2B4, LAIR-1, or NKp30 express the NTR on the cell surface 124
3.16 THP-1 cells expressing 2B4, LAIR-1, or NKp30 were sorted for high receptor expression 125

3.17 THP-1 cells lentivirally transduced with FcγRIA and FcRγ, or SIGLEC-14 and DAP12, or SIRPβI and DAP12, express both NTR and adaptor protein 126
3.18 THP-1 cells expressing FcγRIA, SIGLEC-14, or SIRPβI along with their adaptor protein were sorted using magnetic beads 127
3.19 THP-1 cells expressing FcγRIA, SIGLEC-14, or SIRPβI along with their adaptor protein were sorted using FACS 128
3.20 THP-1 cells co-transduced with NKG2D and DAP10_EmGFP plasmids do not have a double positive population 129
3.21 Partial plasmid maps and cartoon diagrams of the artificial ligands 131
3.22 A small population of CHO cells nucleofected with BirA-ER express the protein 132
3.23 A number of single clones of CHO cells nucleofected with BirA-ER express the HA-tagged protein 133
3.24 CHO BirA-ER cells nucleofected with CD80, CD80-CD2 or CD80-CD4 did not surface express the ligand 135
3.25 HEK293T cells transfected with ligand constructs transiently express the introduced protein 136
3.26 Arrangements of bivalent StrepTactin 138
3.27 Separation of refolded StrepTactin tetramers using anion exchange chromatography 140
3.28 StrepTactin tetramers visualised by SDS-PAGE 142
3.29 Measuring the number of biotin-binding sites on StrepTactin tetramers using biotin-4-fluorescein 144
3.30 Samples of SNAP-Strep-Tag II purification visualised by SDS-PAGE 146
3.31 ST4:647 can bind to THP-1 NKp30 cells 147
3.32 ST3dSA1:647 and anti-Strep-Tag II antibody bind to THP-1 2B4 cells, THP-1 LAIR-1 cells, and THP-1 NKp30 cells 148
3.33 ST3dSA1 can bind THP-1 NKp30 cells but remaining available biotin-binding sites cannot be detected 149
3.34 ST3dSA1:647 can bind to HEK293T cells expressing either CD80, CD80-CD2, or CD80-CD4 ligand 151
3.35 ST3dSA1:647 binds to HEK293T CD80, HEK293T CD80-CD2, and HEK293T CD80-CD4 cells with sites available for biotin to bind 153
3.36 Biotin-binding sites can be detected on HEK293T CD80 cells bound by either ST3dSA1 or the mixture of 1,3 trans-ST2 and 1,4 ST2, but not 1,2 cis-ST2 156
3.37 Biotin-binding sites can be detected on HEK293T CD80-CD2 cells bound by either ST3dSA1 or the mixture of 1,3 trans-ST2 and 1,4 ST2, but not 1,2 cis-ST2 158

3.38 StrepTactin can bind biotin presented on phospholipid bilayer-coated beads with remaining sites available for biotin binding 162
3.39 Both 1,3 trans-ST2 and 1,4 ST2 may bind to presented biotin bivalently . . 163
3.40 Cartoon diagrams of the SpyTagged artificial ligands 165
3.41 Overview of monovalent and tetravalent StrepTactin-SpyCatcher 167
3.42 Separation of StrepTactin-Spycatcher tetramers refolded to synthesise ST1-pD-C 169
3.43 Separation of StrepTactin-Spycatcher tetramers refolded to synthesise ST4-pD-C 170
3.44 Valency of ST1-pD-C and ST4-pD-C as determined using biotin-4-fluorescein171
3.45 Cartoon diagrams of the SpyTagged artificial ligands bound by StrepTactin-SpyCatcher 173
3.46 ST1-pD-C:647 and ST4-pD-C:647 can both bind to THP-1 SIRPβI cells . . 174
3.47 ST1-pD-C and ST4-pD-C can both bind to CHO CD80-Spy cells with the biotin-binding site/s accessible from solution 175

4.1 Structures of example NTRs in complex with their ligand 188
4.2 THP-1 NKp30 cells can be stimulated by plate-immobilised anti-Strep-Tag II antibody 194
4.3 THP-1 LAIR-1 cells can be stimulated by plate-immobilised anti-Strep-Tag II antibody 195
4.4 THP-1 2B4 cells can be stimulated by plate-immobilised anti-Strep-Tag II antibody 196
4.5 StrepTactin presented on phospholipid bilayer-coated beads can stimulate THP-1 NKp30 cells to release IL-8 199
4.6 CHO CD80-Spy cells coupled with ST1-pD-C can stimulate THP-1 SIRPβ1 but not THP-1 NKp30 cells to release IL-8 201
4.7 CHO CD80-CD4-Spy cells presenting ST4-pD-C cannot stimulate THP-1 NKp30 cells to release detectable levels of IL-8 203
4.8 THP-1 NKp30 cells are activated by plate-immobilised but not soluble ST4 205
4.9 THP-1 FcγRIA cells are activated by plate-immobilised but not soluble ST4:647 207
4.10 THP-1 SIGLEC-14 cells are activated by plate-immobilised but not soluble ST4:647 208
4.11 THP-1 SIRPβ1 cells are activated by plate-immobilised but not soluble ST4:647 209
4.12 Dissociation of ST1-pD-C:647 or ST4-pD-C:647 cannot be visualised using flow cytometry 212
4.13 ST4-pD-C:647 binds to THP-1 SIRPβ1 cells multivalently 213

5.1 Plate-immobilised bi-, tri-, and tetra-valent but not monovalent StrepTactin stimulate THP-1 NKp30 cells to secrete IL-8 229
5.2 Pre-coating wells of a 96 well flat bottom plate with poly-L-lysine or PEI abolishes activation of THP-1 NKp30 cells by plate-immobilised StrepTactin 232
5.3 Comparable amounts of ST1-pD-C and ST4-pD-C are immobilised onto 96 well flat bottom plates 236
5.4 Cartoon illustrating the method used to indicate number of biotin-binding sites in StrepTactin-SpyCatcher coated wells 237
5.5 Guanidinium hydrochloride does not affect the fluorescence of biotin:atto 680 238
5.6 Guanidinium hydrochloride denatures the ST-pD-C - biotin:atto 680 interaction 239
5.7 Immobilised ST4-pD-C activates THP-1 SIRPβ1 cells to secrete more IL-8 than immobilised ST1-pD-C 241
5.8 Immobilised ST4-pD-C activates THP-1 SIRPβ1 cells to secrete more IL-8 than immobilised ST1-pD-C when plotted against number of biotin-binding sites and site density 242
5.9 Cartoon illustrating the method used to indicate the number of biotin-binding sites on StrepTactin-SpyCatcher coupled ligand cells 245
5.10 THP-1 SIRPβ1 cells are stimulated by ST1-pD-C and ST4-pD-C presented on ligand cells but not untransfected CHO cells alone 246
5.11 THP-1 SIRPβ1 cells incubated with ST4-pD-C presented on CHO CD80-Spy cells release more IL-8 per biotin-binding site than THP-1 SIRPβ1 cells incubated with CHO CD80-Spy ST1-pD-C cells 248
5.12 Cartoon illustrating the artificial ligand complexes of CD80-Spy or CD80-CD4-Spy and either ST1-pD-C or ST4-pD-C 251
5.13 Elongation of monovalent artificial ligand presented on cells abolishes THP-1 SIRPβ1 cell activation but elongation of tetravalent artificial ligand does not significantly affect receptor activation 253
5.14 At the maximum protein capacity of the wells the number of accessible biotin-binding sites is higher for ST4-pD-C than ST1-pD-C 257
5.15 Increased small-scale proximity of ST4-pD-C - bound receptors compared to ST1-pD-C - bound receptors may affect tension acting on the bonds . . 259
5.16 The close proximity of ST4-pD-C binding sites may increase the likelihood of further receptor - ST-pD-C interactions 261
5.17 Provided there is no bias in binding orientation, the proportion of inaccessible binding sites between plate-immobilised ST1-pD-C and ST4-pD-C are the same 263

5.18 ST1-pD-C and ST4-pD-C bound to CHO CD80-Spy cells will be presented in a specific orientation . . . 269
5.19 Clustering affects multiple properties of the receptor-artificial ligand interaction . . . 272
5.20 Elongation of the receptor - monovalent ligand complex may abolish receptor signalling by reduced engaged receptor clustering and/or reduced segregation of inhibitory phosphatases . . . 276

List of Tables

1.1 The NTR families . . . 20

2.1 StrepTactin and StrepTactin-SpyCatcher abbreviations used . . . 61
2.2 NTRs cloned into either Type I or Type II plasmid . . . 64
2.3 Receptor and adaptor protein primers . . . 65
2.4 Ligand primers . . . 69
2.5 StrepTactin and dead streptavidin amino acid sequences . . . 72
2.6 Strep-Tag II primers . . . 75
2.7 StrepTactin-SpyCatcher, dead streptavidin, and StrepTactin amino acid sequences . . . 79

3.1 Dissociation constants measured or estimated for interactions between Strep-Tag II or biotin, and StrepTactin or streptavidin . . . 97
3.2 Representative non-catalytic tyrosine-phosphorylated receptors cloned into either the Type I or Type II plasmid . . . 108
3.3 Some of the NTRs are normally expressed by a number of the cell lines used for receptor expression . . . 113
3.4 Abbreviations used to refer to StrepTactin/streptavidin tetramer configurations . . . 138
3.5 Predicted isoelectric points of various StrepTactin and streptavidin tetramers created during synthesis of bivalent StrepTactin . . . 141
3.6 Subunit ratio of StrepTactin tetramer peaks are consistent with those expected . . . 141
3.7 Number of biotin-binding sites measured per StrepTactin tetramer . . . 145
3.8 StrepTactin of different valency can bind biotin presented on phospholipid bilayer-coated beads with remaining sites available for biotin binding . . . 163

3.9 Abbreviations used to refer to StrepTactin-SpyCatcher proteins and cell lines 166
3.10 Ratios of ST-pD-C:ST or dSA in ST1-pD-C and ST4-pD-C 171
3.11 Valency of ST1-pD-C and ST4-pD-C determined using biotin-4-fluorescein is in line with that expected 172

5.1 THP-1 SIRPβ1 cells presented to plate-immobilised ST1-pD-C or immobilised ST4-pD-C have significantly different activation responses 243

Abbreviations

°C	degrees celsius
%	percent
1,2 cis-ST2	1,2 cis-bivalent StrepTactin
1,3 trans-ST2	1,3 trans-bivalent StrepTactin
APC	antigen-presenting cell
BCR	B cell receptor
BSA	bovine serum albumin
CAR	chimeric antigen receptor
CD	cluster of differentiation
CHO	chinese hamster ovary
CLEC	C-type lectin domain family
CO_2	carbon dioxide
CTL	cytotoxic T-lymphocyte
CTLA-4	cytotoxic T-lymphocyte-associated protein 4
Da	dalton
DAP10	DNAX-activating protein of 10kDa
DAP12	DNAX-activating protein of 12kDa
DC-SIGN	dendritic cell-specific intercellular adhesion molecule-3 -grabbing non-integrin
DMEM	Dulbecco's modified eagle medium
DNA	deoxyribonucleic acid
DTT	dithiothreitol
EAT-2	Ewing's sarcoma-associated transcript 2
EDTA	ethylenediaminetetraacetic acid
ELISA	enzyme-linked immunosorbent assay
ER	endoplasmic reticulum
F(ab)	fragment antigen-binding
FACS	fluorescence-activated cell sorting
FcR	Fc receptor
FcRL	Fc receptor-like
FcRγ	Fc receptor gamma chain
FCS	foetal calf serum
FKBP	FK506 binding protein
FRB	FKBP rapamycin-binding domain
FRAP	fluorescence recovery after photobleaching
FRET	förster resonance energy transfer
FSC	forward scatter
G	glycine
GFP	green fluorescent protein
GPI	glycosylphosphatidylinositol
GPVI	glycoprotein VI
Grb2	growth factor receptor-bound protein 2
GST	glutathione-S-transferase
HBS	HEPES-buffered saline
HEK293T	human embryonic kidney 293 T
HEPES	4-(2-hydroxyethyl)-1-piperazineethanesulfonic acid
HLA	human leukocyte antigen
I	isoleucine
ICAM-1	intercellular adhesion molecule-1

Ig	immunglobulin
IL-8	interleukin-8
IPTG	isopropyl β-D-1-thiogalactopyranoside
IRES	internal ribosome entry site
ITAM	immunoreceptor tyrosine-based activation motif
ITIM	immunoreceptor tyrosine-based inhibitory motif
ITSM	immunoreceptor tyrosine-based switch motif
KD	equilibrium dissociation constant
KIR	killer cell immunoglobulin-like receptor
KLR	killer cell lectin-like receptor
KS	kinetic-segregation
L	leucine
LAIR-1	leukocyte-associated immunoglobulin-like receptor-1
LAT	linker of activated T cells
LFA-1	lymphocyte function-associated antigen 1
LILR (LIR)	leukocyte immunoglobulin-like receptor
M	methionine
MCMV	mouse cytomegalovirus
MES	2-(N-morpholino)ethanesulfonic acid
MFI	mean/median fluorescence intensity
MHC	major histocompatability complex
mIg	membrane immunoglobulin
MINCLE	macrophage inducible calcium-dependent (C-type) lectin
N	asparagine
NaCl	sodium chloride
Nck	non-catalytic region of tyrosine kinase adaptor protein
NK	natural killer
NKG2D	natural-killer group 2, member D
NTA	nitrilotriacetic acid
NTR	non-catalytic tyrosine-phosphorylated receptor
OSCAR	osteoclast associated, immunoglobulin-like receptor
PAG	phosphoprotein associated with glycosphingolipid-enriched microdomains
PBMC	peripheral blood mononuclear cell
PBS	phosphate-buffered saline
PC	Phosphatidylcholine
PCNA	proliferating cell nuclear antigen
PD-1	Programmed cell death protein 1
PE	phosphoethanolamine
PEI	polyethylenimine
PFA	paraformaldehyde
PI3	phosphoinositide 3
PILR	paired immunoglobulin-like receptor
pMHC	peptide major histocompatability complex
PTP	protein tyrosine phosphatase
RBC	red blood cell
RNA	ribonucleic acid
rpm	revolutions per minute
RPMI	Roswell Park Memorial Institute (medium)
S	serine

SAP	SLAM-associated protein
SBP	streptavidin-binding peptide
SDS-PAGE	sodium dodecyl sulfate polyacrylamide gel electrophoresis
sf.	significant figures
SFK	Src-family kinase
SH2	Src homology 2
SH3	Src homology 3
SHIP-1	Src homology 2 domain-containing inositol-5-phosphatase 1
SHP-1	Src homology domain 2 domain-containing phosphatase-1
SHP-2	Src homology domain 2 domain-containing phosphatase-2
SIGLEC	sialic acid-binding immunoglobulin-type lectin
SIRP	signal regulatory protein
SLAM	signalling lymphocytic activation molecule
SLB	supported lipid bilayer
SLP-76	SH2 domain-containing leukocyte protein of 76 kDa
SOS1	Son Of Sevenless homologue 1
SSC	side scatter
ST	StrepTactin
ST1dSA3	monovalent StrepTactin
ST1-pD-C	monovalent StrepTactin-SpyCatcher
ST1-pD-C:647	monovalent StrepTactin-SpyCatcher:atto 647
ST3dSA1	trivalent StrepTactin
ST3dSA1:647	trivalent StrepTactin: atto 647
ST4	tetravalent StrepTactin
ST4:647	tetravalent StrepTactin: atto 647
ST4-pD-C	tetravalent StrepTactin-SpyCatcher
ST4-pD-C:647	tetravalent StrepTactin-SpyCatcher: atto 647
ST-pD-C	StrepTactin-SpyCatcher
TBS	tris-buffered saline
TCR	T cell receptor
TIM	T-cell immunoglobulin and mucin domain
TMB	3,3',5,5'-tetramethylbenzidine
TREM	triggering receptor expressed on myeloid cells
V	valine
Y	tyrosine
ZAP70	zeta-chain-associated protein kinase 70kDa

1. GENERAL INTRODUCTION

The human body is constantly exposed to microorganisms. These can be potentially harmful and cause disease. To prevent and fight pathogen invasion, the body has a number of defences. These include skin, which acts as a protective barrier, and mucous membranes, which are able to inhibit adherence of, and clear, the microorganisms [Alberts et al., 2008, Murphy, 2011]. Humans also have another highly organised system of cells and tissues, known as the immune system, which surveys the body and removes pathogens. The immune system consists of numerous cell types with specific functions that co-operate to elicit an effective response and remove the threat. In addition to fighting pathogens, a major role of the immune system is to recognise and remove tumourigenic material which can also be very harmful.

The immune system is divided into two main strands: the innate and adaptive immune system which work together to mount the most effective response [Murphy, 2011]. While the innate side provides a generalised and fast response, the adaptive side responds specifically to particular targets or antigens. While slower than the innate system, the adaptive immune system is able to retain immunological memory of the pathogen, allowing a faster specific response to the pathogen if it is encountered again.

The immune response to a pathogen is made up of many stages which each play a vital role in the removal of the threat [Murphy, 2011]. These stages include recognition of the microorganism, an effector response, and resolution of the response. Underlying these processes are interactions that occur at the interface between the surfaces of leukocytes and the surface of the invading pathogens, infected cells, or other leukocytes as appropriate. During a viral infection, for example, dendritic cells recognise and respond to the pathogen, natural killer (NK) cells recognise and respond to infected cells, and the interaction between dendritic and T cells activates the adaptive immune response.

If a viral pathogen is able to break through the initial physical barriers and enter the body it will encounter a number of cell types [Murphy, 2011]. This includes dendritic cells, which are present in many tissues. These innate immune cells express pattern recognition receptors, e.g. toll-like receptors, which are able to recognise pathogen-associated molecular patterns (PAMPs) that are part of the virus. This recognition initiates dendritic cell activation and phagocytosis of the virus. The dendritic cell processes the ingested virus, loads viral peptide onto a major histocompatibility complex (MHC) molecule and presents the peptide-MHC complex on the cell surface. Following this, the dendritic cell migrates to lymphoid organs where it encounters T cells and other cells of the adaptive immune system. If a T cell expressing a T cell receptor (TCR) that specifically binds to the viral peptide-MHC is encountered by the dendritic cell, the TCR and pMHC will bind. The TCR-pMHC interaction, in combination with co-stimulatory signals, activates that T cell to initiate an effector response. This response involves proliferation of the T cell, creating a population of cells that are able to recognise the virus. These T cells can migrate to the site of infection where they help eliminate the virus.

While the adaptive immune response is being initiated, other cells of the innate immune system can respond to, and help control, the viral infection [Murphy, 2011]. For example, NK cells express activating receptors like NKG2D which binds to stress ligands that are themselves up-regulated by infected cells. NK cells also express natural cytotoxicity receptors, e.g NKp30 which binds to viral haemaglutinins. The interaction between NK cell and virus-infected cell activates the leukocyte to secrete the enzymes perforin and granzyme, which create pores in the infected cell membrane and induce cell death. Killing infected cells helps control the spread of infection. This NK cell response is increased by type I interferons which are released by dendritic cells following activation.

In addition to mounting a successful immune response, it is as important for the immune system to remain tolerant to self [Murphy, 2011]. Unwanted immune responses to self antigens are harmful and associated with autoimmune disease. To prevent this, many leukocytes express inhibitory receptors that bind to host targets and regulate the immune response through signal integration. For example, NK cells express inhibitory receptors eg. inhibitory members of the killer-cell immunoglobulin-like receptor (KIR) family, which

bind to MHC class I molecules expressed by healthy cells. Inhibitory KIR-MHC class I binding stimulates inhibitory signalling which suppresses an immune response from the NK cell, and so the healthy cell is not killed. In infected cells however, the surface-presented MHC I molecules may become down-regulated. If the infected cell comes into contact with an NK cell, the stimulus for inhibitory NK cell receptors is no longer present. Therefore any activating signals initiated by NK cell-infected cell contact dominate and the infected cell is killed. This mechanism not only prevents NK cells responding to self, but allows the cells to recognise and kill virus-infected cells.

1.1 Non-catalytic tyrosine-phosphorylated receptors

The receptors involved in these, and many more, immune processes are members of a large class of immune receptors called non-catalytic tyrosine-phosphorylated receptors (NTRs). The TCR, which is responsible for T cell activation in response to antigen presentation by dendritic cells, NKG2D and NKp30 which play a role in NK cell cytotoxicity, and inhibitory KIRs which are involved in NK cell regulation, are just a few examples of NTRs.

These receptors are hugely diverse, rapidly evolving, and classified into families based upon sequence or functional homology. Despite this diversity, the receptors share multiple features that may be important for signalling and so are grouped together under the title of NTRs - so-called based on the properties that they share [Dushek et al., 2012]. These properties are outlined below and illustrated in figure **1.1**.

- NTRs generally have relatively small extracellular domains that bind to surface-associated ligands which also have small extracellular domains
- The receptors have no intrinsic catalytic activity but either contain, or associate with adaptor proteins that contain, cytoplasmic tyrosine-based signalling motifs
- Tyrosine residues within these motifs are phosphorylated by membrane-associated Src-family kinases (SFKs) like Lck and Fyn and dephosphorylated by membrane-associated protein tyrosine phosphatases (PTPs) like CD45 and CD148
- Receptor-ligand engagement induces prolonged phosphorylation of the cytoplas-

mic motifs which, depending on the motif, initiates activating or inhibitory signalling

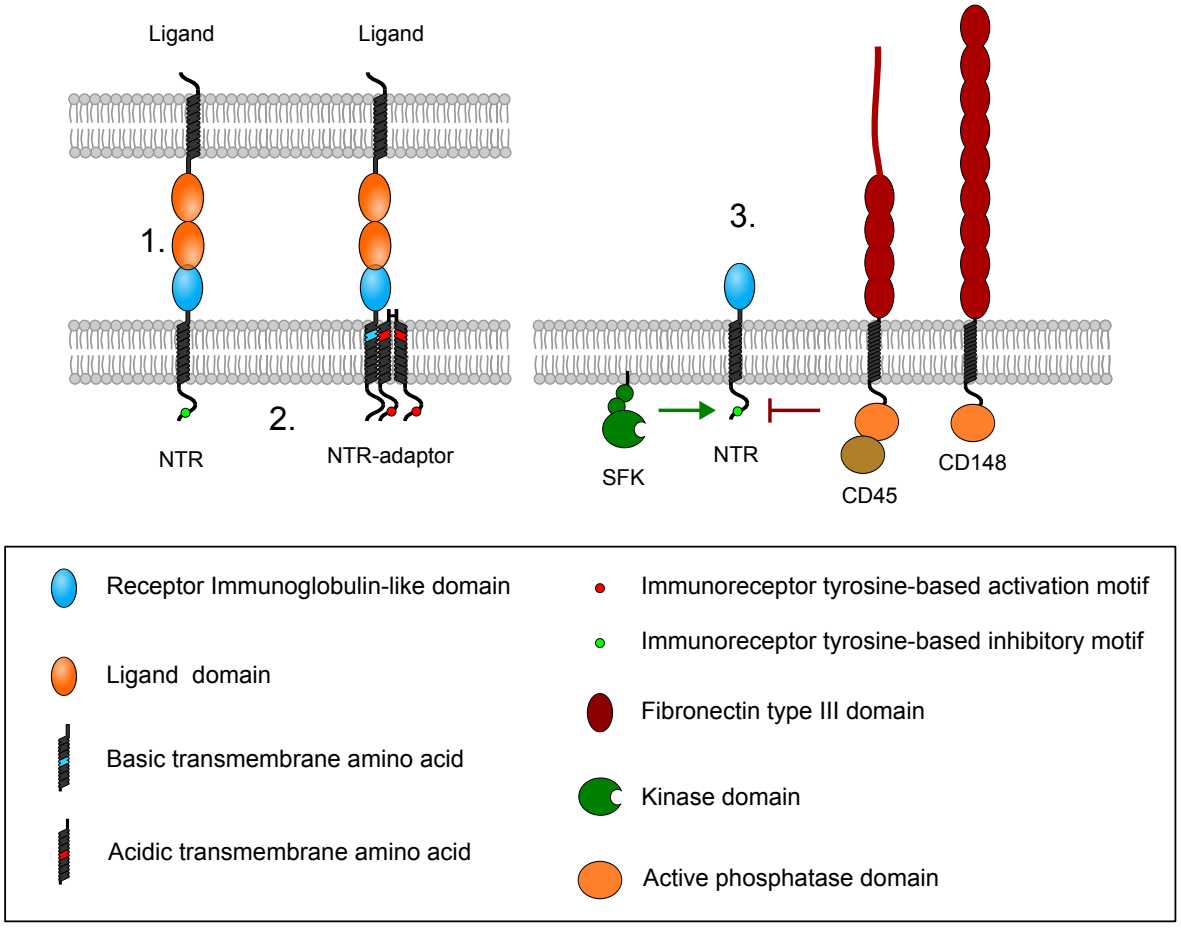


Fig. 1.1: **Non-catalytic tyrosine-phosphorylated receptors share a number of features.** NTRs are either type I or II single pass transmembrane proteins with an ectodomain made up of modular domains (typically immunoglobulin-like domains) and an unstructured cytoplasmic region. **1.** The NTR ectodomain (shown in blue) is relatively small and generally binds to a surface-associated ligand which also has a smaller extracellular domain (shown in orange). **2.** The receptors have no intrinsic catalytic activity but either contain, or associate with adaptor proteins that contain, cytoplasmic tyrosine-based signalling motifs. For example, the immunoreceptor tyrosine-based activation motif (ITAM) or immunoreceptor tyrosine-based inhibition motif (ITIM) which are shown. **3.** Tyrosine residues within the cytoplasmic motifs are phosphorylated by membrane-associated Src-family kinases (SFKs) and dephosphorylated by membrane-associated protein tyrosine phosphatases like CD45 and CD148. Ligand binding induces prolonged tyrosine phosphorylation and initiation of downstream receptor signalling.

NTRs play a major part in almost all the stages and processes that govern an immune response, not just those briefly described above. An understanding of the activation mechanisms of these receptors is therefore hugely important in both our understanding of the immune system and in clinical situations where modulation of the activity of these receptors is required. The mechanism by which binding of an NTR to its ligand induces activation of the receptor and associated signalling is currently unknown.

Here, we discuss the NTR group of receptors and the features that they share. We also discuss the models of NTR activation that have been proposed and consider evidence that supports or opposes the models.

1.2 The interaction between NTR and ligand

The ectodomain of NTRs consists of varying numbers of modular domains, predominantly from the immunoglobulin-like (Ig-like) or C-type lectin domain families. Generally the NTR ectodomain is small and binds to surface-associated ligand proteins to form a complex with small extracellular dimensions. Partial or full structures of a number of NTRs in complex with ligand have been solved. The structures suggest that the complex dimensions, and thus intermembrane distance, are not only small but also quite similar ($\sim$15 nm) (figure **1.2**). This intermembrane distance has been confirmed for the TCR-pMHC receptor-ligand interaction [Choudhuri et al., 2005, James and Vale, 2012].

Although most NTRs have short extracellular regions, there are a few exceptions with large dimensions. The ectodomain of Leukocyte immunoglobulin-like receptor 1 (LIR-1) consists of four Ig-like domains which is longer than many other NTRs which have one or two modular domains. Structural studies however, show that LIR-1 binds to the membrane proximal region of MHC class I [Willcox et al., 2003]. This suggests that upon engagement, despite the large ectodomain of LIR-1, the complex dimensions are comparable to those of other NTR-ligand complexes as shown in figure **1.2**.

CD22 similarly has a large ectodomain with seven Ig-like domains. Expressed in B cells, it has been shown to associate with sialylated glycoproteins on the same cell surface including itself, the BCR and CD45 [Stamenkovic et al., 1991, Sgroi et al., 1993, Peaker and Neuberger, 1993, Razi and Varki, 1998, Han et al., 2005, Gasparrini et al., 2015]. This is in contrast to the majority of NTRs that, where the ligand is known, bind to ligand presented on an opposing surface like a cell membrane.

A small number of NTRs do not bind to cell membrane-presented ligands. LAIR-1, OSCAR and GPVI all bind to collagen, and CLEC9A binds to filamentous actin [Ezumi et al., 2000, Lebbink et al., 2006, Barrow et al., 2011, Zhang et al., 2012]. The much larger size of collagen fibrils and filamentous actin compared to the receptors means that they could

be considered to be a surface. For example, collagen fibrils are $\sim$1 μm in length and $\sim$100 nm in diameter [Chang and Buehler, 2014]. During engagement of LAIR-1, the membrane of the LAIR-1-expressing cell will come into close contact with the insoluble collagen fibril in a similar manner that other NTRs come into close contact with a ligand-expressing cell surface.

Fc receptors also have unusual ligands compared to other NTRs. They bind to immunoglobulins which in turn bind to antigen. This might suggest that the Fc receptor-Ig-antigen complex will be quite large. However structural studies have shown that the Fc receptors are typically in a bent conformation and the Ig binds in an orientation that would position the antigen-binding site close to the membrane [Sondermann et al., 2000, Lu et al., 2015]. This suggests that the receptor-Ig-antigen dimensions could be relatively small (figure **1.2**).

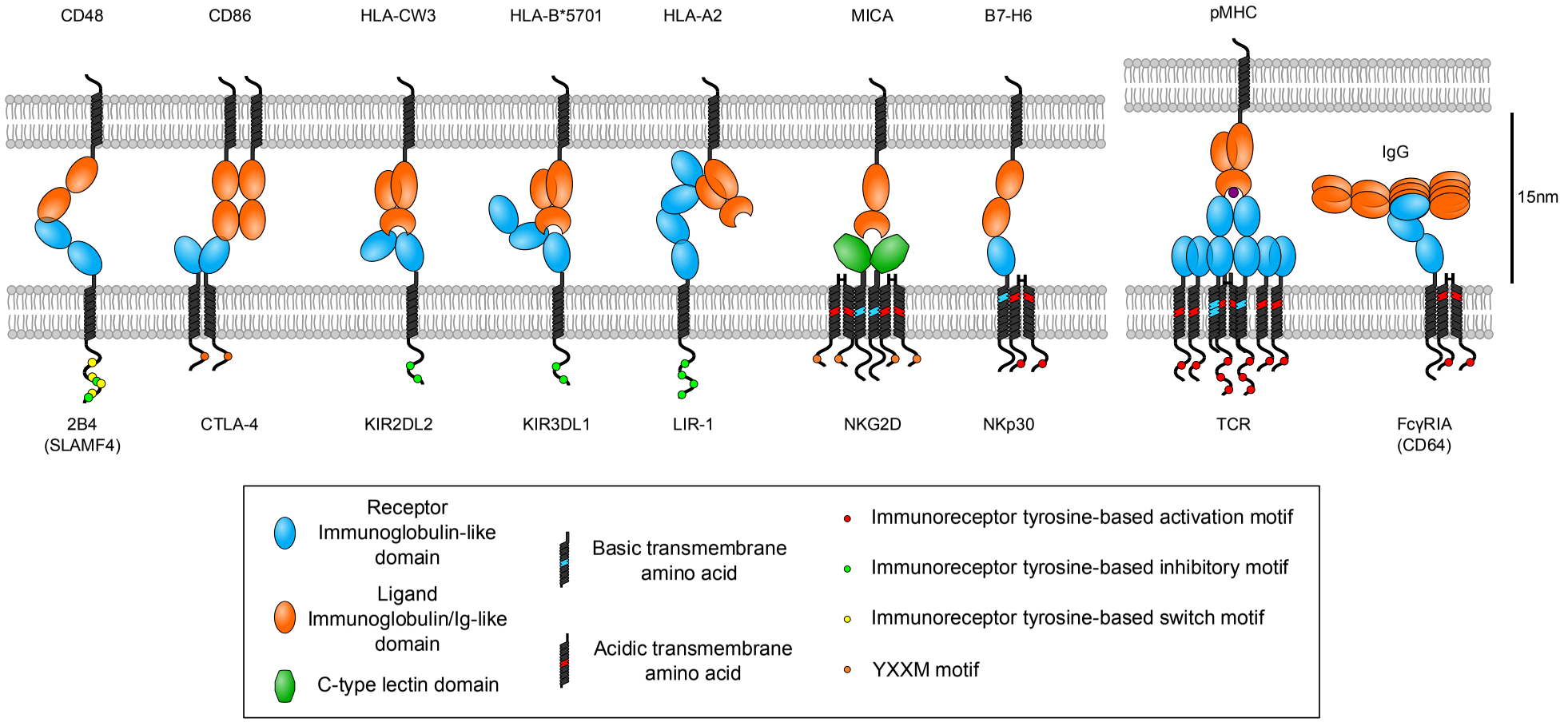


Fig. 1.2: **NTR-ligand complex structures indicate that they have small, comparable dimensions.** Representative diagrams of a number of NTR-ligand complexes based on X-ray crystal structures are illustrated to compare the estimated intermembrane dimensions. FcγRIA is shown in complex with IgG. The receptors are shown associated with the adaptor protein where appropriate. The structures used are as follows: 2B4:CD48 (PDB accession number 2PTT) [Velikovsky et al., 2007], CTLA-4:CD86 (1I85) [Schwartz et al., 2001], KIR2DL2:HLA-CW3 (1EFX) [Boyington et al., 2000], KIR3DL1:HLA-B*5701 (3VH8) [Vivian et al., 2011], LIR-1:HLA-A2 (1P7Q) [Willcox et al., 2003], NKG2D:MICA (1HYR) [Li et al., 2001], NKp30:B7-H6 (3PV6) [Li et al., 2011], TCR:pMHC (3T0E) [Yin et al., 2012], FcγRIA:IgG (4W4O) [Kiyoshi et al., 2015]. This figure is adapted from [Dushek et al., 2012].

1.3 The variety of NTRs and ligands

The ligands of activating NTRs are commonly pathogenic material allowing the immune system to detect, and mount a response to, invading organisms. Pathogens can manipulate this system by evolving and adapting to evade the immune system. In return the host must co-adapt to maintain effective immune responses in an effect described as the "Red Queen hypothesis" [Van Valen, 1974, Akkaya and Barclay, 2013]. The large number and diversity of immune receptors that exist suggest that these proteins are indeed constantly evolving. In addition, the human and mouse immune receptor repertoire are very different [Mestas and Hughes, 2004]. The pathogens that infect humans will differ from those that infect mice which may have led to divergent evolution of the receptors.

A significant proportion of NTRs show very high ectodomain sequence similarity to another NTR but have a different transmembrane and intracellular region. One of the pair of NTRs lacks a cytoplasmic signalling motif and is instead associated with an adaptor protein that contains an activating cytoplasmic motif/s. In contrast, the second NTR of the pair contains intrinsic inhibitory signalling motif/s [Yamada and McVicar, 2008, Akkaya and Barclay, 2013]. Therefore the receptors, termed "paired receptors", usually have opposite roles in the immune system as has been shown for one example pair, Sialic acid-binding immunoglobulin-type lectin-5 (SIGLEC-5) and SIGLEC-14 [Ali et al., 2014].

The existence of these paired receptors is also consistent with the NTRs being a rapidly evolving collection of proteins and may provide a mechanism by which the host can overcome pathogen immune evasion [Barclay and Hatherley, 2008, Akkaya and Barclay, 2013]. It has been suggested that Ly49H, a mouse natural killer (NK) cell activating paired receptor evolved from the inhibitory receptor Ly49I under selection pressure from a pathogen mouse cytomegalovirus (MCMV). MCMV acquired a ligand for Ly49I called m157 such that upon contact between NK cell and MCMV-infected cell, and thus Ly49I-m157 binding, the immune response would be inhibited. It has been proposed that a mutated form of Ly49I, that could still bind to the natural ligand of Ly49I (host major histocompatability complex (MHC) class I) but not the viral protein, was selected for by the host NK cell. In addition, a gene duplication event resulted in another copy of Ly49I that could not bind host MHC class I but still bound viral m157, and also had acquired the

transmembrane and intracellular region of an activating receptor, thereby giving rise to the activating Ly49H receptor. Upon NK cell - virus-infected cell contact, m157 would no longer bind Ly49I and evade the immune system but would instead bind the newly formed Ly49H, initiating an immune response to the infected cell [Arase et al., 2002, Akkaya and Barclay, 2013, Arase and Lanier, 2004].

1.4 NTRs that associate with adaptor proteins containing cytoplasmic tyrosine-based motifs

NTR signalling is mediated by phosphorylation of cytoplasmic tyrosine-based motifs. The three main motifs are the immunoreceptor tyrosine-based activation motif (ITAM) which mediates activating signalling, the immunoreceptor tyrosine-based inhibitory motif (ITIM) which mediates inhibitory signalling, and the immunoreceptor tyrosine-based switch motif (ITSM) which can mediate either activating or inhibitory signalling depending on the context of receptor triggering. The group of NTRs can be divided into two subsets: receptors that have intrinsic signalling motif/s, and receptors that do not. NTRs that lack intrinsic motifs instead associate with an adaptor protein that contains tyrosine-based signalling motif/s. For reference, each NTR is listed in table **1.1** along with features of the receptor including intrinsic signalling motif or adaptor protein and ectodomain structure.

1.4.1 Adaptor proteins

CD3ζ, CD3δ, CD3γ, CD3ϵ

The adaptor CD3ζ contains three intracellular ITAMs, a small extracellular domain, and forms a homodimer in the cell membrane linked by a disulphide bond in the transmembrane region [Rutledge et al., 1992]. CD3δ, CD3γ and CD3ϵ each contain one ITAM and an extracellular region made up of one Ig-like domain. Each ITAM follows the Yxx(L/I)x6-8Yxx(L/I) consensus sequence where x is any amino acid. The TCR antigen receptor complex uses these adaptor proteins. It consists of the TCRα and β chains, associated with a CD3ζ homodimer, CD3$\delta\epsilon$ heterodimer and CD3$\gamma\epsilon$ heterodimer [Call and

Wucherpfennig, 2004]. Together therefore, the TCR complex contains 10 ITAMs. The NK cell cytotoxicity receptors NKp30 and NKp46 can also associate with the CD3ζ adaptor homodimer [Vitale et al., 1998, Pende et al., 1999].

Igα/β

Igα and Igβ each have one Ig-like extracellular domain and contain one ITAM. The two adaptor proteins form a disulphide-linked heterodimer and associate with a membrane-bound immunoglobulin (mIg) to form the B cell receptor (BCR) complex [Siegers et al., 2006].

FcRγ

FcRγ has a very small extracellular domain and contains one ITAM. It exists in the cell membrane as a homodimer mediated by a disulphide bond linking the transmembrane regions of both proteins, or as a heterodimer with the CD3ζ adaptor protein [Orloff et al., 1990]. Numerous NTRs associate with the FcRγ homodimer including activating Fc receptors. One Fc receptor, the FcϵRI complex is more complex in that it consists of the antigen-binding FcϵRα bound to FcϵRβ which associates with the FcRγ homodimer [Howard et al., 1990].

DAP12

DNAX-activating protein of 12kDa (DAP12) contains one ITAM. It forms a homodimer via disulphide bonds between cysteine residues in the small extracellular region [Call and Wucherpfennig, 2007]. A number of activating NTRs associate with DAP12 including activating KIR and SIGLEC receptors, and SIRPβ1 [Wu et al., 2000, Dietrich et al., 2000, Angata et al., 2006].

DAP10

DNAX-activating protein of 10kDa (DAP10) does not contain an ITAM but instead has a YxxM motif. The adaptor protein has a small extracellular domain and forms a homodimer linked by disulphide bonds in the extracellular region of two DAP10 proteins [Call and Wucherpfennig, 2007]. The C-type lectin NK cell receptor NKG2D associates with and signals through the DAP10 homodimer [Wu et al., 1999].

Association between NTR and adaptor protein

Receptors and adaptor proteins generally associate through oppositely charged residues within the transmembrane domain of the proteins. CD3ζ, FcRγ, DAP12, and DAP10 homodimers all contain two acidic transmembrane residues, one from each protein in the dimer, that interact with a basic residue in the transmembrane domain of the partner NTR. Both FcRγ and DAP12 show preferential binding to specific residues. DAP12 will associate with lysine-containing receptors over arginine-containing receptors. Conversely, FcRγ binds arginine-containing receptors over lysine-containing receptors [Feng et al., 2006]. Instead of charged residues, the association between the mIg and Igα/β of the BCR is between polar residues in the transmembrane region of the membrane-bound immunoglobulin [Grupp et al., 1995].

Generally, receptors are specific for particular adaptors and do not pair promiscuously. This is due to the complementary positions of the charged residues in the transmembrane region of receptor and adaptor. DAP10, DAP12, and CD3δ/ϵ have a charged residue in the central area of the transmembrane region. In contrast, CD3ζ and FcRγ both have a charged residue in the more extracellular area of the transmembrane region, which may explain why NKp30 can bind either CD3ζ or FcRγ [Pende et al., 1999, Call and Wucherpfennig, 2007]. Similarly, the TCR alpha chain contains both central and more extracellular transmembrane region charged residues allowing it to associate with multiple sets of homodimers [Call and Wucherpfennig, 2007].

1.5 NTRs with intrinsic cytoplasmic tyrosine-based motifs

A number of NTRs do not associate with an adaptor protein but instead have an intrinsic signalling motif. For example, the activating Fc receptor FcγRIIA is the single Fc receptor that has an intrinsic ITAM. Some NTRs have intrinsic motifs that resemble half of an ITAM (YxxL) and are so called hemITAMs. A number of C-type lectin family NTRs contain a hemITAM and some of which, including CLEC-2, have been shown to form a homodimer [Watson et al., 2009]. It has been suggested that the formation of a homodimer will bring two tyrosine-containing hemITAMs into close proximity effectively reconstituting a full ITAM, allowing the recruitment of similar downstream signalling proteins [Watson et al.,

2009].

Inhibitory NTRs do not associate with an adaptor but instead have intrinsic ITIMs which have a consensus sequence of (S/I/V/L)xYxx(I/V/L) or ITIM-like motifs with a consensus sequence of (E/N)YxE(V/I)(R/K). A number of Killer-cell immunoglobulin-like receptors (KIRs) have intrinsic ITIMs including KIR2DL1 which has two inhibitory motifs. Inhibitory receptors of the SIGLEC family also contain an ITIM but some of them like SIGLEC-9 also contain an ITIM-like motif. The ITIM usually has the dominant activity [Avril et al., 2004].

ITSM-containing receptors like SLAM family receptors can mediate either activating or inhibitory activity depending on the presence of a downstream protein, SAP [Sayos et al., 1998]. Like the ITIM, the ITSM consensus sequence contains a single tyrosine TxYxx(I/V), but has a threonine residue at the -2 position.

The intrinsic motifs are not always functional however as, for example, has been shown for the NTR PD-1. PD-1 contains two types of signalling motif, an ITIM and ITSM, although it has been shown that the ITIM is not required for the inhibitory activity of the receptor [Yokosuka et al., 2012]. Another NTR, NKp44, associates with the adaptor DAP12 but also has an intrinsic ITIM-like sequence. There are conflicting results over the role of this ITIM-like motif. One study used chimeric NKp44 to show that the tyrosine residue of the ITIM-like motif can be phosphorylated but does not recruit downstream signalling proteins. Nor does mutation of the motif affect NK cell activation induced by antibody to the chimeric receptor [Campbell et al., 2004]. In contrast, another study showed that binding of the ligand PCNA to NKp44 induced inhibition of NK cell activity and this was dependent upon the NKp44 ITIM-like motif. This suggests that inhibitory signalling through the ITIM-like motif may be induced by certain interactions [Rosental et al., 2011]. A number of Fc receptor-like receptors (FcRLs) similarly contain more than one type of motif. FcRL3 contains one ITAM and one ITIM but the precise role of these motifs in FcRL3 signalling is unknown.

1.6 Regulation of NTR phosphorylation by the opposing activities of Src-family kinases and protein tyrosine phosphatases

NTR signalling motif phosphorylation is regulated by the opposing activities of Src family kinases (SFKs) and membrane-associated phosphatases like CD45 and CD148. The activities of these two enzymes are held in a dynamic equilibrium in resting cells. The experimental evidence for the regulation of individual NTRs and families by SFKs and evidence for the balance between kinase and phosphatase activity regulating receptor signalling is outlined in table **1.1**.

Name	UniProtKB Accession	Intrinsic motif	Adaptor	Ectodomain	Membrane protein	paired receptors	Src phosphorylation and phosphorylation / dephosphorylation balance evidence
Antigen receptors							
T cell receptor		10 ITAM	CD3ζ, CD3ϵ, CD3δ, CD3γ	2 Ig - TCRα, TCRβ 1 Ig - CD3ζ, CD3ϵ, CD3δ, CD3γ	type I	not paired	[Straus and Weiss, 1992] [Secrist et al., 1993]
B cell receptor		2 ITAM	Igα, Igβ	Membrane immunoglobulin 1 Ig - Igα, Igβ	type I	not paired	[Takata et al., 1994]
C-type lectin family							
CLEC12A	Q5QGZ9	1 ITIM		1 C-type lectin	type II	paired	
CLEC12B	Q2HXU8	1 ITIM		1 C-type lectin	type II		[Hoffmann et al., 2007]
CLEC1A	Q8NC01	1 hemiTAM		1 C-type lectin	type II		
CLEC1B	Q9P126	1 hemiTAM		1 C-type lectin	type II		
CLEC4A	Q9UMR7	1 ITIM		1 C-type lectin	type II		
CLEC2A	Q6UVW9	-	-	1 C-type lectin	type II		
CLEC2B	Q92478	-	-	1 C-type lectin	type II		
CLEC2C (CD69)	Q07108	-	-	1 C-type lectin	type II		
CLEC2D	Q9UHP7	-	-	1 C-type lectin	type II		
Langerin (CLEC4K)	Q9UJ71	-	-	1 C-type lectin	type II		
DC-SIGN (CLEC4L)	Q9NNX6	-	-	1 C-type lectin, 7 short tandem repeats	type II		
DC-SIGN2 (CLEC4M)	Q9H2X3	-	-	1 C-type lectin, 7 short tandem repeats	type II		
BDCA2 (CLEC4C)	Q8WTT0		FcRγ	1 C-type lectin	type II		
CLEC4D	Q8WXI8		FcRγ	1 C-type lectin	type II		[Graham et al., 2012]

MINCLE (CLEC4E)	Q9ULY5		FcRγ	1 C-type lectin	type II		
Dectin-2 (CLEC6A)	Q6EIG7		FcRγ	1 C-type lectin	type II		
Dectin-1 (CLEC7A)	Q96PA5	1 hemiTAM		1 C-type lectin	type II		[Lee et al., 2009]
CLEC8A	P78380	1 hemiTAM		1 C-type lectin	type II		
DNGR-1 (CLEC9A)	Q6UXN8	1 hemiTAM		1 C-type lectin	type II		
CLEC10A	Q8IUN9	-	-	1 C-type lectin	type II		
CLEC13A	Q8IX05	-	-	1 C-type lectin	type I		
CLEC13B (CD205)	O60449	-	-	1 ricin B-type lectin, 1 fibronectin II, 10 C-type lectin	type I		
NKG2C	P26717		DAP12	1 C-type lectin	type II		
NKG2D	P26718		DAP10	1 C-type lectin	type II		[Billadeau et al., 2003]
NKG2E	Q07444		DAP12	1 C-type lectin	type II		
NKG2F	O43908		DAP12	1 C-type lectin	type II		
NKG2A	P26715	2 ITIM		1 C-type lectin	type II		[Kabat et al., 2002]
NKG2B	P26715	2 ITIM		1 C-type lectin	type II		
Killer cell lectin-like receptor subfamily							
KLRB1 (CLEC5B, CD161)	Q12918	1 hemiTAM		1 C-type lectin	type II		
KLRF1 (CLEC5C, NKp80)	Q9NZS2	1 hemiTAM		1 C-type lectin	type II		[Dennehy et al., 2011]
KLRF2 (NKp65)	D3W0D1	1 hemiTAM		1 C-type lectin	type II		
KLRG1 (CLEC15a, MAFA)	Q96E93	1 ITIM		1 C-type lectin	type II		
CD300 family							
CD300a	Q9UGN4	4 ITIM		1 Ig	type I	paired	[Alvarez-Errico et al., 2004]
CD300b	A8K4G0		DAP12	1 Ig	type I		[Hornbeck et al., 2012]
CD300c	Q08708		-	1 Ig	type I		
CD300d	Q6UXZ3		-	1 Ig	type I		
CD300e	Q496F6		DAP12	1 Ig	type I		
CD300f	Q8TDQ1	3 ITIM		1 Ig	type I		
CD300g	Q6UXG3	-	-	1 Ig, mucin	type I		

Fc receptor-like family							
Fc receptor-like protein 1	Q96LA6	2 ITAM		3 Ig	type I	paired	
Fc receptor-like protein 2	Q96LA5	1 ITAM, 2 ITIM		4 Ig	type I		[Xu et al., 2001]
Fc receptor-like protein 3	Q96P31	1 ITAM, 1 ITIM		6 Ig	type I		[Xu et al., 2002] [Won et al., 2006]
Fc receptor-like protein 4	Q96PJ5	2 ITIM		4 Ig	type I		
Fc receptor-like protein 5	Q96RD9	1 ITAM, 2 ITIM		8 Ig	type I		
Fc receptor-like protein 6	Q6DN72	1 ITIM		3 Ig	type I		
Fc receptor-like protein A	Q7L513	-	-	2 Ig	soluble		
Fc receptor-like protein B	Q6BAA4	-	-	2 Ig	soluble		
Classical Fc receptor family							
FcγRI (CD64)	P12314		Fc$R\gamma$	3 Ig	type I	not paired	
FcγRIIa (CD32)	P12318	1 ITAM		2 Ig	type I		
FcγRIIb (CD32)	P31994	1 ITIM		2 Ig	type I		[Suzuki et al., 2000]
FcγRIIc (CD32)	P31995	1 ITAM		2 Ig	type I		
FcγRIII (CD16)	P08637		Fc$R\gamma$	2 Ig	type I		[Pignata et al., 1993]
Immunoglobulin alpha Fc receptor	Q53X38		Fc$R\gamma$	2 Ig	type I		
FcϵRIα	P12319		Fc$R\gamma$	2 Ig	type I		[Eiseman and Bolen, 1992]
Killer cell immunoglobulin-like receptor family							
KIR2DL1	P43626	2 ITIM		2 Ig	type I	paired	[Yu et al., 2008]
KIR2DL2	P43627	2 ITIM		2 Ig	type I		[Burshtyn et al., 1996]
KIR2DL3	P43628	2 ITIM		2 Ig	type I		[Binstadt et al., 1996]
KIR2DL4	Q99706	1 ITIM		2 Ig	type I		[Yusa et al., 2002]
KIR2DL5	Q8N109	2 ITIM		2 Ig	type I		[Marti et al., 1998]
KIR2DS1	Q14954		DAP12	2 Ig	type I		
KIR2DS2	P43631		DAP12	2 Ig	type I		
KIR2DS3	Q14952		DAP12	2 Ig	type I		
KIR2DS4	P43632		DAP12	2 Ig	type I		
KIR2DS5	Q14953		DAP12	2 Ig	type I		
KIR3DL1	P43629	2 ITIM		3 Ig	type I		

KIR3DL2	P43630	2 ITIM		3 Ig	type I		
KIR3DL3	Q8N743	1 ITIM		3 Ig	type I		
KIR3DS1	Q14943		DAP12	3 Ig	type I		
Leukocyte immunoglobulin-like receptor family							
LILRA1	O75019		FcRγ	4 Ig	type I	paired	[Hornbeck et al., 2012]
LILRA2	Q8N149		FcRγ	4 Ig	type I		[Cosman et al., 1997]
LILRA4	P59901		FcRγ	4 Ig	type I		
LILRA5	A6NI73		FcRγ	2 Ig	type I		
LILRA6	Q6PI73		FcRγ	2 Ig	type I		
LILRB1	Q8NHL6	4 ITIM		4 Ig	type I		
LILRB2	Q8N423	3 ITIM		4 Ig	type I		
LILRB3	O75022	3 ITIM		4 Ig	type I		
LILRB4	Q8NHJ6	3 ITIM		2 Ig	type I		
LILRB5	O75023	2 ITIM		4 Ig	type I		
Natural cytotoxicity triggering receptor family							
NKp46	O76036		CD3ζ, FcRγ	2 Ig	type I	not paired	[Augugliaro et al., 2003]
NKp44 (NCR2, CD336)	O95944		DAP12	1 Ig	type I		
NKp30	O14931		CD3ζ, FcRγ	1 Ig	type I		
paired immunoglobulin-like receptor family							
PILR A	Q9UKJ1	2 ITIM		1 Ig	type I	paired	[Fournier et al., 2000] [Mousseau et al., 2000]
PILR B	Q9UKJ0		DAP12	1 Ig	type I		
Sialic acid-binding Ig-like lectin family							
Sialoadhesin (SIGLEC-1)	Q9BZZ2	-	-	17 Ig	type I		
CD22 (SIGLEC-2)	Q9UQA6	4 ITIM		7 Ig	type I	paired	[Bobbitt and Justement, 2000]
CD33 (SIGLEC-3)	P20138	1 ITIM, 1 ITSM		2 Ig	type I		[Pillai et al., 2012]
Myelin-associated glycoprotein (SIGLEC-4)	P20916	Fyn kinase phosphorylation site		5 Ig	type I		

SIGLEC-5	O15389	1 ITIM, 1 ITSM		3 Ig	type I		[Avril et al., 2005]
SIGLEC-6	O43699	1 ITIM, 1 ITSM		3 Ig	type I		
SIGLEC-7	Q9Y286	1 ITIM, 1 ITSM		3 Ig	type I		[Falco et al., 1999] [Ikehara et al., 2004]
SIGLEC-8	Q9NYZ4	1 ITIM, 1 ITSM		3 Ig	type I		
SIGLEC-9	Q9Y336	1 ITIM, 1 ITSM		3 Ig	type I		
SIGLEC-10	Q96LC7	2 ITIM		4 Ig	type I		
SIGLEC-11	Q96RL6	1 ITIM		4 Ig	type I		[Angata et al., 2002]
SIGLEC-12	Q96PQ1	1 ITIM, 1 ITSM		4 Ig	type I		[Yu et al., 2001]
SIGLEC-14	Q08ET2		DAP12	3 Ig	type I		
SIGLEC-15	Q6ZMC9		DAP12	2 Ig	type I		
SIGLEC-16	A6NMB1		DAP12	4 Ig	type I		
Signaling lymphocytic activation molecule family							
SLAMF1	Q13291	2 ITSM		2 Ig	type I	not paired	[Latour et al., 2003]
Ly9 (SLAMF3)	Q9HBG7	6 ITIM, 2 ITSM		4 Ig	type I		[Lee et al., 2004]
2B4 (SLAMF4)	Q9BZW8	2 ITIM, 4 ITSM		2 Ig	type I		[Chen et al., 2004]
SLAMF5	Q9UIB8	2 ITSM		2 Ig	type I		
SLAMF6	Q96DU3	2 ITSM		2 Ig	type I		
SLAMF7 (CRACC)	Q9NQ25	1 ITSM		2 Ig	type I		
CD28 family							
CD28	Q9BYV0	1 ITTM		1 Ig	type I	paired	[Lu et al., 1994]
CTLA-4	P16410	1 ITTM		1 Ig	type I		[Raab et al., 1995]
ICOS	Q9Y6W8	1 ITTM		1 Ig	type I		
PD-1	Q15116	1 ITIM, 1 ITSM		1 Ig	type I		
CD28H	Q96BF3	1 ITTM, 2 non-classical motifs		1 Ig	type I		[Zhu et al., 2013]
BTLA	Q7Z6A9	2 ITIM		1 Ig	type I		
CD200R family							

CD200R1	Q8TD46	non-classical inhibitory motif		2 Ig	type I	paired	[Wright et al., 2000] [Zhang and Phillips, 2006]
CD200R2	Q6Q8B3		DAP12	2 Ig	type I		
Signal-regulatory protein family							
SIRPα	P78324	4 ITIM		3 Ig	type I	paired	[Veillette et al., 1998]
SIRPβ1	O00241		DAP12	3 Ig	type I		
SIRPγ	Q9P1W8	-	-	3 Ig	type I		
SIRPδ	Q9H106	-	-	1 Ig	soluble		
CD5 family							
CD5	P06127	2 ITIM-like		3 SRCR	type I	not paired	[Raab et al., 1994] [Dennehy et al., 2001]
CD6	P30203	non-classical activation motifs		3 SRCR	type I		
Collagen receptors							
LAIR1	Q6GTX8	2 ITIM		1 Ig	type I	not paired	[Meyaard et al., 1997] [Xu et al., 2000]
Glycoprotein VI (GPVI)	Q9HCN6		FcRγ	2 Ig	type I		
OSCAR	Q8IYS5		FcRγ	2 Ig	type I		
T cell immunoglobulin and mucin family							
TIM-1	O46598	2 ITTM		1 Ig, mucin	type I		[de Souza et al., 2008]
TIM-3	Q8TDQ0	non-classical inhibitory motifs	type I	1 Ig, mucin			[Lee et al., 2011]
Nectin-binding family							
CD226 (DNAM-1)	Q15762	1 ITTM		2 Ig	type I		[Zhang et al., 2015b]
TIGIT	Q495A1	1 ITIM		1 Ig	type I		[Liu et al., 2013]
CRTAM	O95727	?		2 Ig	type I		
CD96	P40200	1 ITTM		3 Ig	type I		
Triggering receptor expressed on myeloid cells family							
TREM1	Q9NP99		DAP12	1 Ig	type I		[Bouchon et al., 2000]

TREM2	Q9NZC2		DAP12	1 Ig	type I		
TREML1	Q86YW5	2 ITIM		1 Ig	type I		
TREML2	Q5T2D2	?		1 Ig	type I		
TREML3				1 Ig	type I		
TREML4	Q6UXN2		DAP12	1 Ig	type I		
Miscellaneous							
CD7	P09564	1 ITTM		1 Ig	type I	not paired	
PECAM-1 (CD31)	P16284	2 ITIM		6 Ig	type I		[Jackson et al., 1997]
Junctional adhesion molecule-like (JAML)	Q86YT9	1 ITTM		2 Ig	type I		
CD19	P15391	7 ITTM		2 Ig	type I		[Fujimoto et al., 2000]

Tab. 1.1: **The NTR families.** NTRs are grouped within families with shared structural and/or functional features. Experimental evidence that the receptors are acted on by Src-family kinases, and that a dynamic balance between kinase and phosphatase activity regulates receptor signalling is also listed. This table is adapted and extended from table S1 of [Dushek et al., 2012]. SCRC - scavenger receptor cysteine-rich domain.

The TCR is one example receptor where the the opposing kinase and phosphatase regulation of ITAM phosphorylation has been investigated in more detail. Hui and Vale reconstituted CD3ζ onto liposomes along with varying membrane densities of both Lck and CD45 relative to CD3ζ to analyse the opposing activities of the enzymes on TCR ITAM phosphorylation. With increasing Lck density, CD3ζ phosphorylation increased and with increasing CD45 density, phosphorylation decreased. At equal kinase and phosphatase densities there was strong phosphorylation of CD3ζ but at physiological densities of the two proteins on T cells (Lck: 200 molecules μm^{-2}, CD45: 600 molecules μm^{-2}) little phosphorylation was measured. ITAM phosphorylation was also more sensitive to changes in CD45 density than Lck density. This data illustrated the directly opposing roles of Lck and CD45 in CD3ζ phosphorylation and activation. It also suggested that CD45 may be expressed at higher levels in cells than both receptor and kinase to allow the negative regulatory activity of CD45 to prevent receptor signalling in resting cells [Hui and Vale, 2014].

1.6.1 Signalling induced by prolonged receptor phosphorylation

NTR-ligand engagement induces sustained phosphorylation of the tyrosine-based motifs and this leads to recruitment of downstream signalling proteins which mediate either activating or inhibitory responses. Which proteins are recruited to the phosphorylated cytoplasmic motifs depends on the cell type and motif present.

ITAM-mediated signalling

In T cells and NK cells, the kinases Syk and ZAP70 are recruited to phosphorylated ITAM tyrosines via tandem SH2 domains. These kinases are phosphorylated and activated by SFKs and then phosphorylate further downstream substrates to give cellular activation. This signalling cascade involves LAT and SLP-76 phosphorylation, changes in calcium flux, and changes in gene transcription leading to the production and secretion of cytokines like IL-2 [Wang et al., 2010b, Mócsai et al., 2010]. The very fast timescale of these signalling events for the TCR have been measured using photo-activatable pMHC. LAT phosphorylation occurs at 4 seconds following TCR-pMHC binding with calcium flux occuring 2-3 seconds later [Huse et al., 2007].

In B cells, Syk is recruited to phosphorylated ITAMs and induces cellular activation. Syk recruitment to the phosphorylated ITAMs of the BCR activates downstream signalling proteins to drive cellular responses like changes in gene transcription, and proliferation [Rickert, 2013]. ITAM signalling in other cell types leads to other cellular responses like phagocytosis and antibody-dependent cell-mediated cytotoxicity (ADCC) by Fc receptors, and target cell killing by NK cell receptors [Nimmerjahn and Ravetch, 2008, Pegram et al., 2011].

Signalling by other activating motifs

HemITAMs

Like with phosphorylated ITAMs, Syk family kinases are recruited to the two adjacent phosphorylated hemITAMs of an NTR dimer to mediate downstream signalling [Watson et al., 2009].

YxNM motifs

These are found in several receptors including CD28 and the NKG2D-associated adaptor DAP10. When phosphorylated, they recruit PI3 kinase via the SH2 domain-containing p85 subunit and/or Grb2/Vav1 or Grb2/SOS1 complexes [Lanier, 2009].

ITIM-mediated signalling

Phosphorylated ITIMs and ITIM-like motifs recruit the inhibitory phosphatases SHP-1, SHP-2 and SHIP-1 [Billadeau and Leibson, 2002, Crocker et al., 2007]. These phosphatases can then dephosphorylate and so inhibit the activity of nearby substrates including proteins involved in activating NTR signalling [Billadeau and Leibson, 2002]. By dephosphorylating activating NTR signalling components, inhibitory NTRs can negatively regulate immune responses by signal integration.

ITSM-mediated signalling

The activity downstream of phosphorylated ITSMs depends on the presence of the cytosolic adaptor proteins SAP and EAT-2 [Sayos et al., 1998, Tassi and Colonna, 2005, Le Borgne and Shaw, 2012]. When SAP is absent, the inhibitory phosphatases SHP-1, SHP-2, and SHIP-1 are recruited to the phosphorylated ITSMs leading to inhibitory signalling like that which occurs with phosphorylated ITIMs. When SAP is present however,

it is recruited to phosphorylated ITSMs via its SH2 domain. This blocks inhibitory phosphatase binding to the ITSM and allows recruitment of the Src kinase Fyn and initiation of activating cell responses [Sayos et al., 1998, Le Borgne and Shaw, 2012].

1.7 Regulation of Src family kinases and membrane-associated phosphatases

Adding further complexity to the control of NTR activation and signalling, the activities of Src family kinases and membrane-associated phosphatases are also regulated. These regulatory activities not only affect the kinases and phosphatases but also directly impact NTR activation. Therefore, a thorough understanding of SFK and PTP regulation will improve our understanding of NTR regulation as well.

1.7.1 Src family kinases

The Src family is made up of nine tyrosine kinases which share a conserved domain structure of an SH3 and SH2 domain followed by a C terminal kinase domain. The kinases do not have an extracellular region but are attached to the inner leaflet of the plasma membrane by a myristoylated and sometimes palmitoylated N terminal region [Koegl et al., 1994, Resh, 1999]. Src family kinase activity is regulated by the phosphorylation and dephosphorylation of two conserved tyrosine residues [Roskoski, 2005]. In human Lck, for example, these are positions Y394 and Y505, and Y416 and Y527 in human Src [Smart et al., 1981, Cooper et al., 1986, D'Oro et al., 1996].

The C terminal tyrosine (Y505 in Lck) is phosphorylated by the inhibitory kinase Csk or homologous Chk or Ctk [Nada et al., 1991, Okada et al., 1991, Klages et al., 1994, Bergman et al., 1992]. Phosphorylation promotes intramolecular binding of the SFK SH2 domain to the phosphotyrosine placing the kinase in a closed, inactive conformation [Sicheri et al., 1997, Xu et al., 1997, Xu et al., 1999]. CD45 opposes the negative regulatory activity of Csk by dephosphorylating the C terminal phosphotyrosine [Ostergaard et al., 1989, D'Oro et al., 1996, Hurley et al., 1993, Cahir McFarland et al., 1993]. There is some evidence that Lck can trans-autophosphorylate itself at the inhibitory C

terminal Y505 site [Hui and Vale, 2014].

Conversely, phosphorylation of the Y394 site in the kinase domain by trans- autophosphorylation promotes SFK activity. This is opposed by inhibitory dephosphorylation by CD45 [Ostergaard et al., 1989, Yamaguchi and Hendrickson, 1996, Veillette and Fournel, 1991, D'Oro et al., 1996, Baker et al., 2000, Hui and Vale, 2014]. Thus CD45 has both a positive and negative regulatory role in SFK activity. Similarly, the phosphatase CD148 dephosphorylates both regulatory SFK tyrosines [Stepanek et al., 2011]. This dual role of the phosphatases has made the results of receptor activation studies difficult to interpret, particularly those that manipulate phosphatase activity. It has been suggested that the dual role of CD45/CD148 in regulation of SFKs may act to control the threshold of receptor activation and also that spatial distribution of the phosphatases with respect to SFKs are important for their regulatory activity [McNeill et al., 2007, Hermiston et al., 2009].

1.7.2 Phosphatases

CD45 is one of the most abundant cell surface proteins. It has one active cytoplasmic phosphatase domain and exists as various alternatively spliced isoforms which have different length extracellular regions [Barclay et al., 1997]. The variable regions are followed by a cysteine-rich domain and three type III fibronectin domains meaning that CD45 has a relatively large extracellular domain of approximately 28-50 nm depending on the isoform [McCall et al., 1992, Barclay et al., 1997].

CD148 similarly has a large extracellular region made up of 8-10 fibronectin domains and mucin-like region, and also has a cytoplasmic phosphatase domain. The extracellular region of CD148 is predicted to be $\sim$47-55 nm long [Cordoba et al., 2013].

In contrast to Src family kinases, there is no current evidence that CD45 and CD148 are regulated by interactions with other proteins. No ligand for either protein has been identified other than lectins which bind CD45 glycans [Hermiston et al., 2009]. Artificial dimerisation of a CD45 chimera inhibits phosphatase activity and it has been suggested that dimerisation of CD45 is mediated by a wedge domain in the intracellular region of the protein [Desai et al., 1993, Majeti et al., 1998]. However, structural data of the full

CD45 cytoplasmic region showed that dimerisation of the phosphatase by the wedge domain would be sterically prohibited [Nam et al., 2005]. There is also conflicting evidence concerning whether CD45 dimerises physiologically and so the role of this activity is not clear [Xu and Weiss, 2002, James et al., 2011, Hermiston et al., 2009].

1.8 The mechanism of NTR triggering

The mechanism by which NTR-ligand engagement leads to sustained phosphorylation, a process termed receptor activation or receptor triggering, is currently unknown. The triggering mechanism of a number of individual NTRs, in particular the TCR and BCR, has been investigated and studied in depth but the sequence of events that are both required and sufficient for activation has yet to be conclusively defined. Much less is known about the triggering mechanism of many of the other NTRs.

If, in resting cells, activating kinase and inhibitory phosphatase activity is balanced to prevent receptor activation, engagement of the receptor and ligand must shift this balance in favour of the kinase. This could be by a change in the receptor or a change in the enzymes. For example, ligand binding could induce a conformational change in the receptor (or associated adaptor protein) that increases the accessibility of the receptor-associated signalling motifs for phosphorylation and so result in receptor triggering. Another mechanism to shift the balance in favour of the kinase is to change the proximity of the receptor to the two enzymes. This can be mediated by bringing activating kinases into closer proximity with the NTR, or by segregation of inhibitory phosphatases from the receptor.

It follows that the main proposed models of NTR triggering are based on at least one of these mechanisms and are considered here under the three categories: conformational change, clustering/aggregation, and segregation.

A number of models have been proposed specifically for the TCR. Due to the shared features of the TCR and other NTRs, we consider these models here in the wider view of NTR signalling. Numerous lines of evidence for clustering models of NTR activation or the kinetic-segregation model are discussed in more detail in Chapter 4 and 5 and so are only briefly discussed here. Simplified diagrams of the proposed NTR triggering models

are shown in figure **1.3**. They are referred to again in the individual sections.

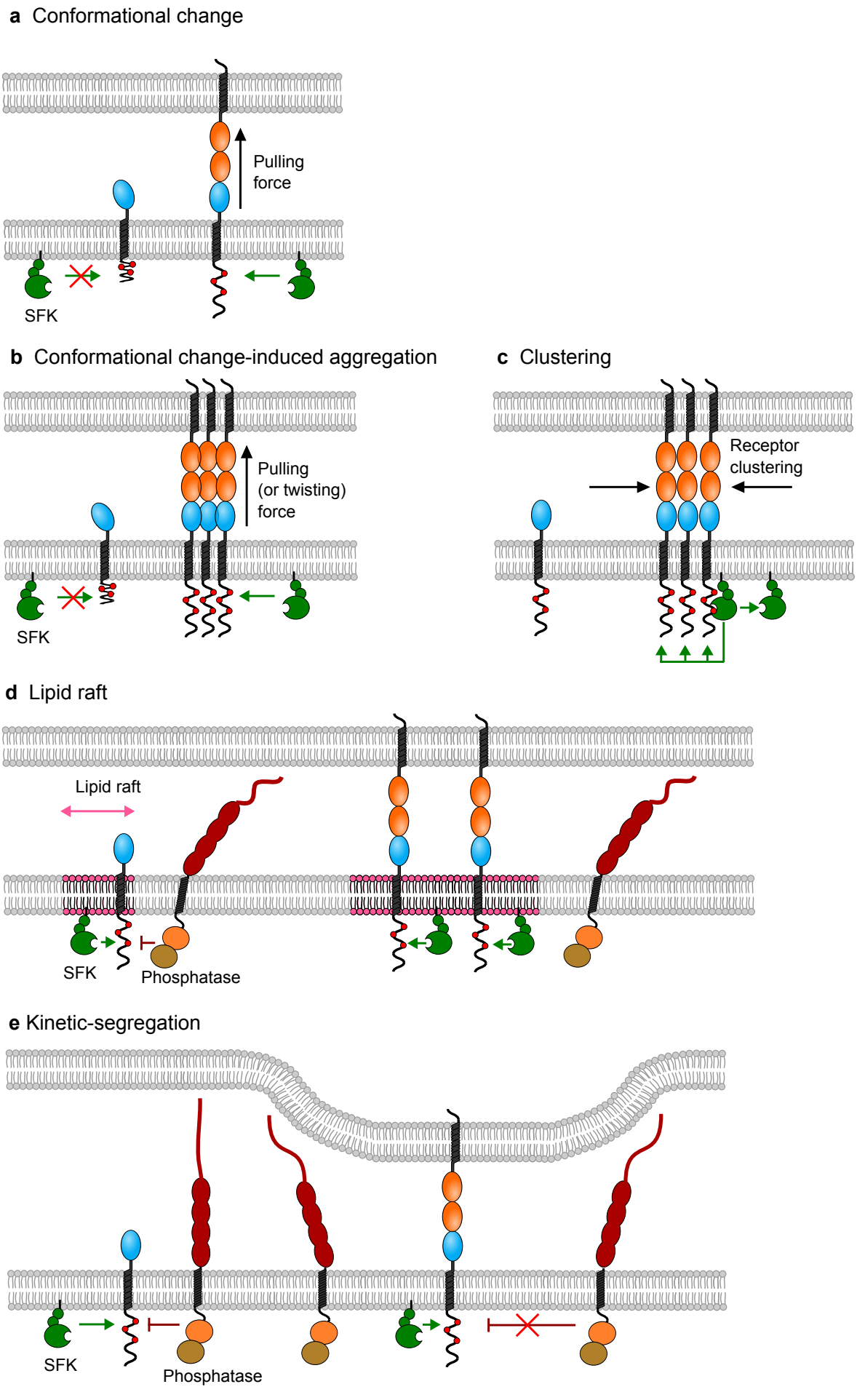


Fig. 1.3: **Proposed mechanisms of NTR triggering.** *Continued on next page.*

Fig. 1.3: **Proposed mechanisms of NTR triggering. Continued.** Simplified diagrams are shown to illustrate proposed models of NTR triggering. A generic NTR and ligand are shown in blue ■ and orange ■ respectively. **a - Conformational change**. In resting cells, the NTR cytoplasmic tyrosine-based signalling motifs are inaccessible to SFK-mediated phosphorylation. Upon ligand binding, a pulling force is generated that acts on the receptor-ligand bond. This force induces a conformational change which increases the accessibility of the intracellular tyrosine residues for phosphorylation by SFKs. **b - Conformational change-induced aggregation**. Upon ligand binding to the NTR, a pulling force acts on the receptor-ligand bond which causes an extracellular conformational change in the receptor. This change increases the propensity of the receptor to aggregate which enhances receptor phosphorylation in a similar manner as that described for clustering models. **c - Clustering/aggregation**. In resting cells, the monomeric NTR is randomly diffusing within the membrane. Ligand binding drives receptor clustering which brings receptors into close proximity with each other. This increases associated SFK activity by trans-autophosphorylation and so also increases NTR signalling motif phosphorylation. **d - Lipid rafts model for TCR activation**. It has been proposed that Lck is associated with lipid rafts whereas phosphatases like CD45 are not. The NTR (in this case the TCR) may be loosely associated with rafts and accessible to phosphatase-mediated dephosphorylation. Upon ligand binding, the lipid rafts aggregate and/or the NTR becomes more closely associated with the rafts. This increases the proximity between active SFKs and NTRs, and segregation from CD45, and increases receptor phosphorylation. Also following ligand binding, phosphatases come into close proximity with rafts to positively regulate SFKs. **e - Kinetic-segregation**. In resting cells, the NTR is both phosphorylated and dephosphorylated by SFKs and phosphatases respectively, with the phosphatase activity dominating. Upon ligand binding, the opposing cell membranes come into close proximity at sites of receptor-ligand complexes which excludes large phosphatases. SFKs are not excluded and so phosphorylation of engaged receptors now dominates over dephosphorylation, leading to sustained NTR phosphorylation.

1.9 Conformational change

Many non-NTR receptors are activated using conformational change-based mechanisms including the epidermal growth factor receptor and the erythropoietin receptor [Burgess et al., 2003, Lu et al., 2006].

Conformational change models that have been proposed for the activation of individual NTRs either involve a mechanism that increases the accessibility of the signalling motifs for tyrosine phosphorylation, or a mechanism that increases the propensity of the receptor to aggregate. Models that use the latter conformational change are discussed under the aggregation heading.

The former models propose that unbound NTRs are held in a conformation whereby the associated signalling motifs are inaccessible to SFK phosphorylation. Upon ligand binding, the NTR conformation changes increasing the accessibility of the signalling motifs, favouring kinase activity and receptor signalling. For this to occur, SFK kinase activity must dominate over phosphatase activity so that sustained motif phosphorylation can proceed.

A conformational change model of NTR activation could plausibly explain the sensitivity of some NTRs. For example, the TCR can be activated by very few pMHC ligands and so ligand-induced conformational change has seemed more plausible to some than other proposed mechanisms that require clustering of multiple receptors.

1.9.1 The "safety" model of TCR triggering

One ligand-specific conformational change model that has been proposed for TCR triggering is the "safety" model [Aivazian and Stern, 2000, Xu et al., 2008, Kuhns and Davis, 2008]. The model postulates that prior to ligand engagement the cytoplasmic regions of the CD3ζ and CD3ϵ chains are associated with the plasma membrane such that the ITAMs are inaccessible for tyrosine phosphorylation. pMHC binding to the TCR induces dissociation of the cytoplasmic regions from the membrane thereby allowing SFKs to phosphorylate the signalling motifs. In agreement with this model, association of both CD3ζ and CD3ϵ to the plasma membrane or acidic phospholipids has been shown to

be dependent on basic residue rich sequences, and binding of the CD3ζ chain to acidic phospholipids inhibits Src-mediated phosphorylation of the ζ chain [Aivazian and Stern, 2000, Sigalov et al., 2006, Xu et al., 2008, Deford-Watts et al., 2009, Zhang et al., 2011]. In addition, TCR engagement by pMHC leads to dissociation of the CD3ζ chain from the membrane [Zhang et al., 2011]. A number of studies have provided evidence that is inconsistent with this mechanism however. Firstly, pervanadate treatment of TCR-expressing cells in the absence of ligand engagement leads to tyrosine phosphorylation which suggests that the ITAMs are accessible to SFK in resting cells [O'Shea et al., 1992, Secrist et al., 1993, Imbert et al., 1994, Fernandes et al., 2010, Zhang et al., 2011]. In addition, mutation of the basic rich region of CD3ζ which should decrease chain association with the membrane and increase ITAM accessibility to SFKs reduced CD3ζ phosphorylation [Zhang et al., 2011, DeFord-Watts et al., 2011]. Mutation of the basic rich region of a CD3ϵ chimeric protein also did not lead to increased phosphorylation which is inconsistent with the safety model [Fernandes et al., 2010]. In addition, dissociation of the CD3ζ chain from the plasma membrane was dependent on phosphorylation of the ITAMs suggesting it occurs after initial triggering [Zhang et al., 2011]. More recently, calcium-induced dissociation of the TCR cytoplasmic chains from the membrane has been suggested to enhance signalling rather than initiate it [Shi et al., 2013]. Therefore, while there is evidence that TCR-pMHC ligand engagement does cause dissociation of TCR cytoplasmic regions from the membrane, this does not appear to be the mechanism responsible for receptor triggering. Others have suggested alternative explanations for these conflicting results and so this model remains controversial [Gagnon et al., 2010].

Membrane association of cytoplasmic regions has been reported for the FcRγ adaptor protein but not any other receptors or adaptors suggesting a similar process is unlikely to occur across the NTR group [Sigalov et al., 2006, Lee and Tolar, 2013]. In fact, for the BCR it has been proposed that upon receptor activation one cytoplasmic chain of the BCR complex increases rather than decreases membrane proximity [Lee and Tolar, 2013]. This conformational change of the Igα chain cytoplasmic region requires phosphorylation of the Igα ITAM by SFKs, thus indicating that the conformational change is secondary to BCR phosphorylation and activation [Lee and Tolar, 2013]. It has been

recently proposed that the mIgG cytoplasmic region of the BCR, which contains an activating YxNM motif, interacts with the plasma membrane via basic residues in the receptor chain and that upon BCR engagement and phosphorylation, the short chain dissociates from the plasma membrane, contributing to enhanced BCR signalling rather than signal initiation [Chen et al., 2015].

Another TCR conformational change upon engagement by pMHC or antibody has been described. This is shown to involve a proline-rich region in the cytoplasmic region of CD3ϵ which is exposed upon ligand binding to the TCR and then recruits the adaptor protein Nck. The conformational change was shown to be independent of tyrosine phosphorylation so is not secondary to receptor activation [Gil et al., 2002, Gil et al., 2005]. However, later studies have shown that the proline-rich region is important for regulation of TCR expression levels and T cell development rather than activation [Mingueneau et al., 2008, Wang et al., 2010a].

1.9.2 Transduction of extracellular binding to the intracellular region

A major challenge facing conformational change models however is that it is not clear how the extracellular binding event is transduced across the membrane to induce intracellular changes and initiation of signalling processes. In addition to this, a conformational change upon ligand binding is unlikely to be shared by all NTRs. For this to be a common mechanism, the binding of each individual ligand to the appropriate receptor would need to induce the same or comparable conformational change that results in increased accessibility of the signalling motif. Many NTRs can be activated by antibody to the receptor as well as physiological ligand, and so antibody binding to the receptor would need to similarly induce the same stimulatory conformational change if it was a requirement for triggering. It is unclear how this could occur.

1.9.3 Mechanical-induced conformational change

One model that may be able to provide a mechanism for inducing comparable conformational changes in multiple/all NTRs, and also transduction of extracellular changes to the cytoplasmic regions, is a mechanically-induced change that is not specific to

the receptor-ligand pair (illustrated in figure **1.3a**) [Choudhuri et al., 2005, Ma et al., 2012,Chen and Zhu, 2013]. Such a force-induced mechanism has been proposed for the TCR in the form of the receptor deformation model [Ma et al., 2008a, Ma et al., 2008b]. This model postulates that following TCR-pMHC interaction, the binding pair is pulled away from each other by a detaching force generated, for example, by the T cell actin cytoskeleton as it acts to move the T cell away from the antigen-presenting cell (APC). A pulling force acting on the TCR may induce a conformational change or deformation of the receptor cytoplasmic region which increases accessibility of the signalling motifs and favours tyrosine phosphorylation. Pushing or twisting of the TCR due to ligand engagement has also been proposed to activate the TCR but is arguably less plausible [Ma et al., 2008a, Minguet and Schamel, 2008].

Structural analyses of CD3$\epsilon\gamma$, which is associated with the TCR$\alpha\beta$ dimer, show the heterodimer to be rigid and that a conserved stalk is required for CD3ϵ/CD3γ association. It has been suggested that this interaction and rigidity may provide a means for extracellular tension acting on the engaged TCR$\alpha\beta$ dimer to be transduced across the membrane via the CD3 heterodimer to induce activation [Sun et al., 2001]. Another mechanism for transduction of extracellular binding events to cytoplasmic signalling has been recently proposed. Lee et al. report that cytoplasmic membrane proximal regions of the TCR$\zeta\zeta$ homodimer are spread apart in resting cells and come together upon TCR activation, perhaps due to a mechanical influence. This movement of the cytoplasmic regions of the homodimer is proposed to form an 'on' TCR conformation that favours kinase activity and signalling [Lee et al., 2015].

While the role of mechanical forces in activation of many NTRs has yet to be investigated, the binding event between any NTR and surface-associated ligand could conceivably generate a similar pulling force on the receptor and so mechanical force could play a role in the activation of this diverse group of receptors.

1.9.4 Evidence for a mechanical force model

In support of a mechanical force model, T cell calcium flux is induced by application of a force to the TCR using anti-CD3 antibody- or pMHC- coated beads [Kim et al., 2009]. Kim

et al. observed that a force parallel to the membrane was required for this to occur and proposed that the TCR acts as a mechanosensor. Another study similarly found that a shearing force acting on a cell-presented anti-CD3 antibody bound to cell-presented TCR induced a calcium response [Li et al., 2010]. In contrast to the conformational change model suggested by these studies it has been proposed that the shearing force may have acted to increase collisions between TCR complexes and Lck and thereby trigger the receptor [Ma et al., 2012]. However, T cell activation was also induced when a force was applied to pull the T cell away from the antibody-presenting cell [Li et al., 2010]. Two membrane-associated antibodies were used in these experiments with different length ectodomains. The elongated antibody was only able to induce a T cell calcium response in the presence of the applied force [Li et al., 2010]. This could be due to different levels of force required or as has been suggested, the applied force induced segregation of large surface molecules like the phosphatase CD45 from the bound elongated TCR and thereby initiated receptor activation [Chen and Zhu, 2013].

More recent studies using a red blood cell (RBC) presenting pMHC as an APC, or RBC with pMHC-coated bead, and micropipette to apply a pulling force to the TCR-pMHC interaction have also observed T cell calcium release in response to the applied force [Pryshchep et al., 2014, Liu et al., 2014]. Increasing the pMHC-presenting RBC membrane stiffness, and so increasing the applied force, increased the calcium response in line with mechanical force affecting TCR activation [Pryshchep et al., 2014]. Liu et al. took the studies further to propose that TCR and agonist pMHC bind with a catch bond and that an optimal force applied to the TCR-pMHC bond triggers TCR activation by increasing the catch bond lifetime and that force provides a means for the TCR to discriminate between ligands [Liu et al., 2014].

The force generated upon a soluble ligand binding to a receptor is likely to be smaller than that upon binding of a surface-presented ligand. In line with the idea that mechanical force increases receptor activation, multiple studies have shown surface-immobilised ligand induces greater TCR responses than soluble ligand does, or that soluble monomeric ligand does not induce activation at all [Geppert and Lipsky, 1987, Cebecauer et al., 2005a, Cebecauer et al., 2005b, Angelov et al., 2006]. This has also been shown for other NTRs (see Chapter 4 introduction). There are a number of other factors which will

vary between soluble and surface-presented ligand binding to a receptor however which may affect signalling. For example the local concentration of ligand will differ and also a close contact between the receptor surface and a ligand surface will induce spatial redistribution of large receptor cell surface molecules. This will not occur with soluble ligand unless the density of receptor-ligand complexes is very high and the ligand is multivalent.

A mechanical model is further supported by studies presenting T cells to ligand on surfaces that can be created with different elastic modulus values. Two studies show that T cell activation responses to surface-presented antibody varies with rigidity of the surface suggesting that the force induced by the surface upon receptor engagement can affect the receptor response [Judokusumo et al., 2012, O'Connor et al., 2012]. Activation of the BCR is also affected by the rigidity of a ligand-presenting surface. Antigen immobilised on stiffer gel surfaces induced greater B cell activation responses than antigen immobilised on softer surfaces [Wan et al., 2013, Zeng et al., 2015]. It is possible that this sensitivity to surface rigidity applies to other NTRs.

Studies with a number of NTRs have observed that receptor activation is decreased if either the receptor or ligand ectodomain is elongated (see Chapter 5 introduction for detailed discussion). While manipulation of the NTR-ligand complex in this manner could affect several properties of receptor activation, these results are also consistent with the importance of a mechanical force acting on the engaged receptor in the activation mechanism. The force generated by a ligand binding to the receptor and the impact this has on intracellular signalling may be reduced by elongation of either receptor or ligand.

1.9.5 How can ligand binding generate a mechanical force?

Various techniques are being used to measure the forces generated upon receptor-ligand interaction. For example, using atomic force microscopy, rupture forces of interactions between T cells and APCs have been measured [Puech et al., 2011]. The forces generated by T cells contacting arrays of nanopillars presenting anti-CD3 antibody or pMHC have also been measured [Bashour et al., 2014]. In addition, using a biomembrane force

probe, the interaction between anti-CD3 coated beads and a T cell was observed to generate a force with both a pushing and pulling phase which is consistent with the proposed mechanical force models [Husson et al., 2011]. With improvements, these techniques may help elucidate the magnitude of forces created by physiological receptor-ligand binding events and whether they are sufficient for activation [Ma et al., 2012].

A number of physiological sources of force have been suggested that could result in receptor activation. The relatively small size of NTR-ligand complexes compared to other cell surface molecules means that upon engagement of the receptor, the two opposing surfaces will come into close proximity which will place pressure on the larger surface molecules [Allard et al., 2012]. If these large proteins are not flexible, the bending of the extracellular region will likely place pressure on the two opposing membranes and in doing so place tension on the receptor-ligand bond. This could generate the pulling force that has been proposed to result in receptor activation. T cell migration away from the APC and cytoskeleton movements have also been suggested to place tension on receptor-ligand complexes [Ma et al., 2008a, Chen and Zhu, 2013]. In support of this, cytoskeleton disrupting agents have been observed to decrease the mechanical force acting on TCRs bound by pMHC at the cell-cell interface and also lead to a reduced T cell calcium response [Valitutti et al., 1995a, Lim et al., 2011].

As with ligand-specific conformational change models of NTR activation, a major challenge to a mechanical force-induced conformational change model is that enzymatic inhibition of phosphatases in the absence of ligand engagement can initiate tyrosine phosphorylation and signalling. In addition to this, soluble antibody complexes that cross-link or aggregate the receptor have been shown to initiate receptor, including TCR, activation (discussed in more detail in the next section). It is possible that binding of large soluble complexes to NTRs can generate a mechanical force sufficient to initiate signalling but more investigations are required to confirm this.

1.10 Clustering/ Aggregation

Another group of models propose that receptor clustering upon ligand binding is sufficient for receptor activation. There are many studies that indeed show NTR cross-linking with

antibodies and multivalent protein can initiate signalling. Because of this evidence, for some of the NTRs, a clustering mechanism for receptor triggering is generally accepted but little in-depth work has been conducted to develop a detailed model. A small number of NTRs have been studied in more detail including the TCR and BCR.

There are two main types of aggregation model. One proposes that ligand binding to the receptor induces a conformational change, like those discussed in the previous section, and that this conformational change increases the propensity of the receptor to aggregate (figure **1.3b**). The second does not involve a conformational change but postulates that ligand binding induces clustering of the receptor and this initiates signalling (figure **1.3c**).

Conformation-induced aggregation models have been proposed for both the TCR and BCR. For example, Kuhns et al. propose that upon ligand binding the TCR alpha chain undergoes a conformational change that mediates dimerisation of the receptor. They report that the TCR dimerises and that mutating the Cα domain of the TCR both reduces receptor dimerisation and leads to a decreased T cell calcium response upon ligand binding [Kuhns et al., 2010].

1.10.1 Conformational change-induced oligomerisation model of BCR activation

The BCR can be activated by binding multivalent antigens or antibody, but not soluble F(ab) fragments, suggesting that aggregation or clustering of the receptor is required for activation [Woodruff et al., 1967, Puffer et al., 2007, Minguet et al., 2010]. Monovalent antigen can induce B cell responses however, when it is presented on a surface like a supported lipid bilayer [Tolar et al., 2009]. In addition to this, it has been observed using single molecule imaging that upon BCR binding to surface-presented monovalent and multivalent antigen, BCR microclusters form which is also consistent with a clustering mechanism [Tolar et al., 2009]. There are however a small number of studies which report that soluble monomeric antigen can activate the BCR which argues against clustering being required for activation [Kim et al., 2006, Avalos et al., 2014].

Tolar et al. report that the engaged BCRs within microclusters become immobilised

and suggest they are oligomeric. They show that this immobilisation/oligomerisation is dependent on the Cμ4 extracellular domain and N terminal region of the BCR transmembrane domain because antigen binding to BCR fusion proteins that lack this Cμ4 domain was unable to induce B cell activation nor oligomerisation. Resulting from these studies, Tolar et al. propose that a force-mediated conformational change in the BCR upon ligand binding exposes the oligomerisation-promoting Cμ4 domain which is inaccessible in resting B cells [Tolar et al., 2009, Tolar and Pierce, 2010]. In support of this, they found that deleting part of the BCR extracellular region to expose the Cμ4 domain in resting cells led to the BCR aggregating spontaneously [Tolar et al., 2009]. While there is no structural evidence that a conformational change in the soluble BCR occurs upon ligand binding it has been suggested that in cells, like with the TCR, a pulling force is generated by BCR-antigen binding that can induce the ectodomain conformational change in the receptor to expose the Cμ4 domain and promote oligomerisation [Tolar and Pierce, 2010].

Using FRET, it was observed that upon antigen binding a conformational change in the BCR cytoplasmic regions occurs. The cytoplasmic domains come into close proximity and then move apart in a motion suggested to be the ITAM-containing cytoplasmic regions opening up to increase tyrosine phosphorylation [Tolar et al., 2005].

Linking these mechanisms together to form a conformational change-induced oligomerisation mechanism, Tolar et al. propose that in resting cells the ITAMs are inaccessible for kinase binding. Upon antigen binding, a pulling force acts on the BCR which exposes the Cμ4 domain and induces BCR oligomerisation. This oligomerisation is followed by changes in the local lipid environment and conformational changes to the cytoplasmic regions [Tolar et al., 2005, Tolar and Pierce, 2010]. These conformational changes could leave the BCR in a signalling active form that increases Lyn- or Syk- mediated phosphorylation of the BCR ITAMs and thereby initiates signalling [Tolar et al., 2008]. It has been suggested however that the cytoplasmic conformational changes may be secondary to activation and so play a role in regulation of signalling rather than initiation [Tolar et al., 2005, Lee and Tolar, 2013].

In conflict with this model are reports that the BCR is already oligomeric in resting B cells. It has been suggested that this oligomeric structure is inhibitory and that antigen

binding causes dissociation of the oligomers and formation of clustered BCR monomers which initiates signalling [Schamel and Reth, 2000, Yang and Reth, 2010]. The presence of oligomers in resting cells was not observed by Tolar et al. however so the exact events involved in BCR activation are not clear [Tolar et al., 2005].

1.10.2 The permissive geometry model

The permissive geometry model of TCR activation does not propose conformational change-induced aggregation but instead postulates that binding of the TCR to a pMHC dimer causes the two adjacent engaged TCRs to rotate within the membrane relative to each other. This rotation alters the conformation of the TCR cytoplasmic domains to favour tyrosine phosphorylation [Minguet et al., 2007, Minguet and Schamel, 2008]. The model predicts that pMHCs that bind the TCR in an altered geometry would not be able to activate the TCR because they would not induce the required conformational change. In line with this prediction, Adams et al. observed that while pMHCs that bind the TCR with the same geometry activated the receptor, a pMHC that binds with a different geometry could not [Adams et al., 2011]. The model also predicts that binding of a pMHC monomer to the TCR would be unable to induce the required conformational change and so would not activate the TCR. This proposal is in conflict with studies that report the TCR can be activated by surface-associated monomeric pMHC [Sykulev et al., 1996, Ma et al., 2008b, Huang et al., 2013]. In addition, there is conflicting evidence as to whether pMHCs exist as dimers and therefore whether such a conformational change would occur physiologically [Cherry et al., 1998, Krishna et al., 1992, Yin et al., 2012].

A second type of aggregation mechanism does not involve a conformational change but postulates that receptor clustering or dimerisation itself is sufficient for activation. We will discuss aggregation models proposed for the TCR but note that similar reports exist for other NTRs. Studies that specifically look at evidence for the role of clustering in activation of a number of other individual NTRs are discussed further in Chapter 4 introduction.

1.10.3 Homoclustering

Like with the BCR there is extensive evidence that cross-linking the TCR with antibodies and multivalent protein can initiate signalling but that binding of soluble monovalent pMHC or F(ab) fragments cannot [Kaye and Janeway Jr., 1984, Abastado et al., 1995, Boniface et al., 1998, Cochran et al., 2000, Doucey et al., 2001, Cebecauer et al., 2005a, Cebecauer et al., 2005b, Stone and Stern, 2006, Xie et al., 2012, Perica et al., 2014]. These studies which compare soluble monovalent to multivalent antigen-induced activation are the main evidence for a clustering mechanism. There are a number of studies that investigate cross-linking of the TCR and BCR in more detail and are discussed in Chapter 5 introduction.

In conflict with a clustering model of TCR activation is a report that soluble monovalent pMHC could activate the TCR [Delon et al., 1998]. However, it was later suggested that this result was due to the peptide of the soluble pMHC being transferred to T cell-expressed endogenous MHC molecules such that TCRs on opposing membranes bound to, and were activated by, the surface-presented pMHC [Ge et al., 2002]. Indeed, other studies that found soluble pMHC monomers could activate the TCR found this was dependent on expression of endogenous MHC by the T cells [Ge et al., 2002, Schott et al., 2002]. Further to this, the majority of studies do not reproduce the finding that soluble pMHC can activate the TCR. This includes a study that showed cross-linking monomeric pMHC to the TCR did not induce a T cell calcium response unless the pMHC-bound TCRs were aggregated using multivalent protein (or also bound to a supported lipid bilayer) [Xie et al., 2012].

Receptor dimerisation or clustering is proposed to lead to activation by favouring activating kinase activity and thereby shifting the balance between kinase and phosphatase activity. This NTR activation mechanism (illustrated in figure **1.3c**) is supported by a recent mathematical model consisting of an NTR-like protein, SFK and tyrosine phosphatase to reflect the physiological signalling components. The model postulated that bringing receptors and receptor-associated kinases into close proximity would increase the rate of SFK trans-autophosphorylation thereby increasing SFK activity and receptor phosphorylation. SFK trans-autophosphorylation and activation will be increased in SFKs that

are bound to clustered receptors because the local concentration of SFKs will be much higher. Increased proximity of receptors will also increase signalling motif phosphorylation by allowing activated SFKs associated with one NTR to trans-phosphorylate an adjacent receptor [Cooper and Qian, 2008]. Indeed, Cooper and Qian show using the model that provided there is a SFK-receptor association that is phosphorylation-dependent and that a receptor-bound SFK can phosphorylate an adjacent receptor or another receptor-bound SFK, clustering of NTRs can lead to SFK and receptor activation. In agreement with this, in a reconstituted system Hui and Vale show that co-clustering CD3ζ with Lck can induce tyrosine phosphorylation [Hui and Vale, 2014].

The homoclustering model of TCR activation has been challenged by observations that agonist pMHCs are presented to the T cell at low density and therefore the levels of clustering required to induce activation may not be reached physiologically. In addition, a number of studies have provided evidence that the T cell can be activated by very few surface-presented pMHCs which suggests that aggregation is not required for activation [Valitutti et al., 1995b, Sykulev et al., 1996, Irvine et al., 2002, Purbhoo et al., 2004, Ma et al., 2008b, Huang et al., 2013]. Such an argument could apply to aggregation models of other NTRs as well.

Two models have been proposed to explain how pMHC at low density can aggregate TCRs. These are termed the pseudodimerisation and heterodimerisation models.

1.10.4 Pseudodimerisation model of TCR activation

The pseudodimerisation model proposes that the TCR is activated by pseudodimers of one agonist pMHC and one endogenous (self) pMHC. Both agonist and endogenous pMHC each bind one TCR while the agonist pMHC also interacts with a co-receptor (CD4 or CD8) that is associated with the endogenous pMHC-bound TCR effectively dimerising the TCRs. The TCR-endogenous pMHC will unbind but the interaction between co-receptor and agonist pMHC keeps the two TCRs in close proximity and in doing so activates both receptors [Irvine et al., 2002, Krogsgaard et al., 2005]. As one agonist pMHC can activate two TCRs, and endogenous pMHCs are present on APCs at higher density, it is conceivable that low numbers of agonist pMHC could activate a T cell using

this mechanism.

There is however conflicting evidence over whether endogenous pMHCs enhance TCR triggering, particularly between CD4+ T cell studies and CD8+ T cell studies. In support of the model, endogenous pMHCs have been shown to cluster at the CD4+ T cell-APC interface [Irvine et al., 2002, Wülfing et al., 2002, Krogsgaard et al., 2005]. In addition, removing endogenous pMHC recognition from CD4+ cells was shown to dramatically reduce agonist pMHC-induced TCR activation [Stefanová et al., 2002]. Krogsgaard et al. took these studies further by creating soluble dimers consisting of one agonist pMHC and one endogenous pMHC and found that some combinations of dimers activated T cells whereas monomeric pMHC or an endogenous-only pMHC dimer did not. In addition, mutation of the agonist pMHC CD4-binding domain reduced T cell activation [Krogsgaard et al., 2005].

In contrast, the contribution of endogenous pMHC to CD8+ TCR activation varies between pMHC molecules with some endogenous pMHCs having no effect on signalling [Spörri and Reis e Sousa, 2002, Yachi et al., 2005, Juang et al., 2010]. It has been suggested that the contrast between the role of endogenous pMHC in CD4+ and CD8+ T cell activation may be due to the different affinities between CD4 and MHC class II versus CD8 and MHC class I [Hoerter et al., 2013]. The evidence suggests endogenous pMHC molecules may play a role in TCR activation in some cases.

1.10.5 Heterodimerisation model of TCR activation

The heterodimerisation model of TCR activation also emphasises the importance of the CD4 and CD8 co-receptors. Agonist pMHC is bound by both TCR and the co-receptor. By binding to the same pMHC as the TCR, the co-receptor, which is associated with Lck, brings the kinase into close proximity with the receptor, thereby favouring kinase activity and phosphorylation of the TCR [Delon et al., 1998]. This model was reported following the observation that monomeric pMHC could trigger TCR activation in CD8+ T cells but not CD8- T cells, nor when the interaction between CD8 and MHC or Lck was blocked [Delon et al., 1998]. In conflict with the heterodimerisation model however, are studies that showed TCR triggering could be induced by pMHC in the absence of

co-receptors, and also that the TCR could be activated by antibodies which do not bind to the co-receptor [Kaye and Janeway Jr., 1984, Locksley et al., 1993, Schilham et al., 1993]. In addition, many studies have observed that soluble monomeric pMHC could not activate the TCR which would occur if heterodimerisation of the TCR and co-receptor alone was sufficient for activation [Abastado et al., 1995, Boniface et al., 1998, Stone and Stern, 2006, Xie et al., 2012]. Therefore, it does not appear that a heterodimerisation mechanism is sufficient for TCR triggering.

A further argument against clustering models of activation comes from reports that the TCR (and also the BCR) is clustered, or present in both monomeric and multimeric forms, in resting cells [Fernandez-Miguel et al., 1999, Schamel et al., 2005, Kumar et al., 2011, Schamel and Alarcón, 2013, Crites et al., 2014]. The TCR is also reported to be present in "protein islands" in resting cells [Lillemeier et al., 2010]. It has been proposed that these small TCR nanoclusters aggregate into larger clusters upon ligand binding or aggregate with separate membrane domains containing downstream signalling molecules during activation [Lillemeier et al., 2010, Crites et al., 2014]. In contrast, a number of studies report the TCR to be predominantly in a monomeric form in the absence of ligand engagement [Reich et al., 1997, James et al., 2007]. Further study may be required in order to reconcile the conflicting findings.

1.10.6 How can ligand binding induce clustering?

Altogether, there is clear evidence that cross-linking the TCR or other NTRs can induce receptor activation and a plausible mechanism by which dimerisation or clustering can initiate intracellular signalling by increasing kinase activity has been proposed. In addition, upon ligand engagement, the TCR for example has been observed to aggregate into microclusters at the cell-surface interface using imaging techniques [Bunnell et al., 2002, Yokosuka et al., 2005, Campi et al., 2005, Varma et al., 2006]. These microclusters are signalling-active and can form in the presence of SFK inhibitors suggesting they are not secondary to TCR triggering [Yokosuka et al., 2005, Campi et al., 2005, Varma et al., 2006]. Formation of the clusters is dependent on the actin cytoskeleton, however. Inhibition of actin polymerisation abrogates microcluster formation and TCR activation

suggesting that the cytoskeleton plays an important role in receptor activation [Campi et al., 2005, Varma et al., 2006].

The main challenge to aggregation models is how clustering can be induced physiologically in the first place. The majority of NTR ligands are monomeric and therefore it is not initially obvious how monomeric ligand binding can drive increased receptor proximity. We note however, that there a small number of NTRs that are dimeric or bind dimeric ligands. For example NKG2D, which is a member of the C-type lectin family of NTRs, is present as a homodimer in the membrane but binds to one monomeric ligand [Li et al., 2001]. The dimeric form of NKG2D in resting cells suggests this dimerisation does not activate the receptor and there is no structural evidence to suggest that binding of the ligand induces further multimerisation [Li et al., 2001]. Therefore the dimeric form may not be functionally important for the triggering mechanism. The receptor CD28 is also a homodimer that binds monovalently to ligand (either CD80 or CD86). CD80 is a dimer so may cross-link two CD28 proteins but CD86 is not and both ligands can activate the receptor suggesting that the dimeric form of CD80 is not required for CD28 activation [Ikemizu et al., 2000, Zhang et al., 2003].

FcαRI is one NTR that is directly cross-linked upon ligand binding. Co-crystallisation of FcαRI with the Fc region of IgA1 shows that 2 receptors bind to one IgA which may be important for triggering [Herr et al., 2003]. This property is not shared throughout the NTR group however so if ligand binding does induce receptor dimerisation/clustering in all NTRs, another mechanism must be responsible.

One possible mechanism may involve the glycocalyx and other large surface molecules. Recently, it was shown that the cell glycocalyx can drive areas of integrin clustering at a cell-surface interface [Paszek et al., 2014]. Paszek et al. observed that large glycopolymers (80nm) representing the glycocalyx were excluded from regions of integrin (20nm) contact at the cell-surface interface whereas short glycopolymers with comparable lengths to the integrins (3nm or 30nm) were not. The authors also observed increased integrin clustering in cells expressing the large glycopolymers and postulate the difference in size serves to create regions of the cell membrane where the likelihood of integrin binding to ligand is increased in a "kinetic trap" mechanism (illustrated in figure **1.4**). Localised, increased rates of integrin-ligand binding will lead to integrin cluster-

ing in these areas. Regions of clustered engaged integrins as opposed to numerous spread-out single engagements amongst the much larger glycocalyx is also more energetically favourable as this minimises deformation of the cell membrane. It is proposed that other cell surface receptors may similarly be clustered upon ligand binding by the glycocalyx kinetic trap mechanism. This includes the NTRs and so a similar mechanism may occur upon ligand binding to physiologically drive receptor clustering and initiate signalling.

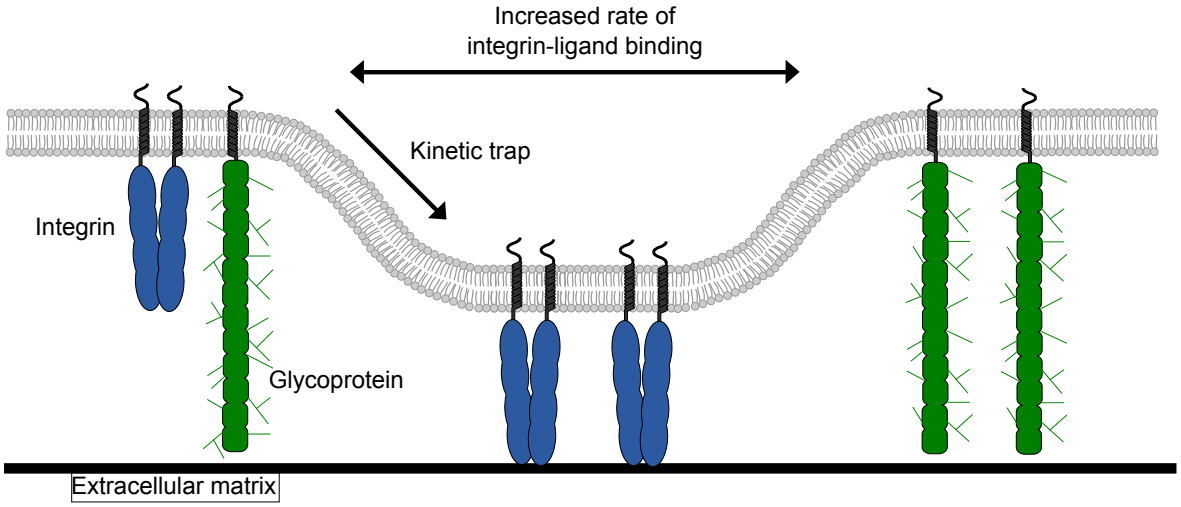


Fig. 1.4: **Proposed mechanism for integrin clustering.** At sites of integrin-ligand binding an intermembrane distance forms that is smaller than glycoproteins and other glycocalyx components expressed by the cell. The rate of integrin-ligand bond formation will increase at these sites of close cell-surface contact and decrease outside them thereby inducing clusters of engaged integrins to form. The regions of increased binding kinetics are referred to as "kinetic traps" [Paszek et al., 2014].

1.11 Segregation or redistribution

There are two types of proposed NTR triggering mechanisms that are based on the redistribution of a number of cell surface components upon ligand binding. In both cases, signalling is initiated because the redistribution serves to favour activating kinase activity over inhibitory phosphatase activity. The lipid raft model proposes, in a similar manner to aggregation models, that ligand binding induces increased proximity between receptors and kinases, whereas the kinetic-segregation model proposes that ligand binding induces segregation of inhibitory phosphatases from engaged receptors.

1.11.1 Lipid rafts in NTR activation

The cell membrane is proposed to contain microdomains termed lipid rafts (or membrane rafts) that are enriched in sphingolipids, cholesterol and lipid-modified proteins like GPI-anchored proteins [Simons and Ikonen, 1997, Brown and London, 2000]. The lipid raft hypothesis postulates that a number of membrane proteins either associate with, or are excluded from, lipid raft structures and also that raft-associated membrane proteins exhibit reduced diffusion within the membrane which may contribute to regulation of protein-protein interactions. Lipid rafts have been implicated in a number of immune cell processes including immunoreceptor signalling [Simons and Ikonen, 1997].

There are a number of similar models of TCR activation that place emphasis on the role of lipid rafts in the spatial segregation and redistribution of TCR triggering components, the TCR, Lck and CD45. The proposed spatial redistribution shifts the balance between kinase and phosphatase activity leading to receptor activation. An illustration of proposed lipid raft receptor activation models is shown in figure **1.3d**. In one such model both the TCR and kinase Lck are raft-associated whereas CD45 is not. The lipid rafts are sufficiently small that in resting cells CD45 is able to regulate both TCR and Lck activity. Upon antigen binding, lipid rafts aggregate into larger structures, both bringing multiple TCR and Lck proteins into close proximity, and increasing the distance between these raft-associated proteins and the excluded CD45. This favours kinase activity and leads to TCR activation [Janes et al., 2000].

An alternative model developed from that described above postulates that in resting cells the TCR only weakly interacts with lipid rafts and that raft-associated Lck activity is inhibited by the PAG/Cbp-Csk complex. Upon antigen binding, TCR-raft association increases which favours kinase activity. In addition, CD45 is redistributed to the lipid rafts increasing dephosphorylation of Lck at position Y505, thereby also favouring Lck activity and leading to TCR activation [Kabouridis, 2006]. CD45 is also inhibitory however so, if this model is accurate, there must be a mechanism for how its inhibitory activity is regulated upon recruitment to the rafts.

Lipid rafts have also been implicated in BCR and FcγRIIB activation models [Tolar et al., 2008, Liu et al., 2010]. As part of the conformational change-induced aggregation model

for BCR activation Tolar et al. propose that upon clustering of the BCR, SFK-containing lipid rafts are aggregated around the BCR. This increases the proximity between activating SFKs and the BCR and so may initiate signalling in the same manner proposed by receptor clustering models by favouring kinase activity [Tolar et al., 2008]. This has also been proposed by others [Gupta and DeFranco, 2007]. Additionally, they postulate that due to the presence of saturated lipids in lipid rafts, the cell membrane will be thicker in these areas which may place strain on raft-associated BCRs and induce the conformational change they observe [Tolar et al., 2008].

There has been a lot of work investigating the role of lipid rafts in NTR activation initiation and signalling (reviews include [Simons and Toomre, 2000, Horejsí, 2005, Harder and Sangani, 2009, Filipp et al., 2012]) but these studies and even the existence of lipid raft structures remain a controversial topic [Munro, 2003, Horejsí, 2005]. This mostly stems from arguments against early work that used detergent solubility experiments to determine the presence of lipid rafts. The addition of detergent to cells could both destroy lipid structures or create structural artefacts that may be identified as raft-like regions of the cell membrane. As well as this, a number of studies have failed to provide evidence consistent with lipid raft models [Pizzo et al., 2002, Glebov and Nichols, 2004, Hashimoto-Tane et al., 2010]. For example, one study did not visualise TCR microclusters associated with a lipid raft probe upon antigen binding [Hashimoto-Tane et al., 2010].

Due to the small scale of proposed lipid rafts it has been suggested that the field would benefit from super-resolution imaging studies. Such techniques would be required to fully visualise the small raft-like regions and elucidate some of the questions and controversy surrounding rafts and their role in immunoreceptor activation [Dushek and van der Merwe, 2011, Owen et al., 2012, Kuokkanen et al., 2015]. This includes techniques like stimulated emission depletion (STED) microscopy which is able to track single diffusing lipids in nanoscale regions of the cell membrane [Eggeling et al., 2009].

1.11.2 Kinetic-segregation

In contrast to lipid raft-based models, the kinetic-segregation (KS) model proposes that segregation of inhibitory phosphatases like CD45 and CD148 from engaged recep-

tors, rather than increased proximity with activating kinases, is a driver in signal initiation.

As discussed above and shown in figure **1.2** the extracellular dimensions of NTRs and their ligands are generally relatively small and so upon engagement the two opposing membranes or surfaces will come into close contact. These dimensions are smaller than those of other protein-protein complexes present like ICAM - LFA-1 ($\sim$40 nm) and also much smaller than the cell glycocalyx [Barclay et al., 1997]. Springer noted that these size differences mean that for the TCR and pMHC, or for other small binding partners like CD2 and CD48 to interact, the larger proteins and cellular components would either have to be excluded from regions of receptor-ligand interaction, or change conformation to permit such close cell-cell contact and prevent exclusion. It was also postulated that such a mechanism may affect immune signalling [Springer, 1990]. Following structural analysis of the CD2-CD48 interaction that provided evidence for the small complex dimensions, this mechanism was extended and the kinetic-segregation model of TCR activation was proposed [van der Merwe et al., 1995, Davis and van der Merwe, 1996, van der Merwe et al., 2000]. A similar model based on the same mechanism was also proposed around the same time [Shaw and Dustin, 1997]. While the KS model was initially postulated to explain TCR triggering, it has since also been proposed for the activation of other NTRs as well [Köhler et al., 2010, Brzostek et al., 2010, Dushek et al., 2012, Lim et al., 2015].

The KS model (figure **1.3e**) proposes that in a resting immune cell, the receptor cytoplasmic signalling motifs (for example an ITAM) are continuously phosphorylated by Src family kinases like Lck and dephosphorylated by protein tyrosine phosphatases, for example CD45 and CD148. Under resting conditions, the phosphatase activity dominates, and results in a net zero phosphorylation of tyrosine residues in the receptor. When an immune cell comes into contact with a ligand-expressing cell, regions of close contact form at sites of receptor-ligand interaction. The intermembrane distance at these sites is small, reflecting the small complex dimensions. Whereas the kinase has no extracellular region and can diffuse within the membrane and interact with engaged receptors, the phosphatase, which has a large extracellular region, is physically excluded and cannot. This shifts the balance between kinase and phosphatase activity acting on the engaged

receptors in favour of the kinase thereby permitting sustained receptor tyrosine phosphorylation and initiation of downstream signalling [Davis and van der Merwe, 1996, van der Merwe et al., 2000, Davis and van der Merwe, 2006].

Most of the work conducted that provides evidence consistent with the model has been done with the TCR although there is also evidence with other NTRs. We will, for the most part, consider the evidence with different NTRs separately.

1.11.2.1 The TCR

A dynamic balance between kinase and phosphatase activity and the KS model

Like aggregation models, the KS model places emphasis on there being a dynamic balance between activating kinase and inhibitory phosphatase activity and that altering this balance alone is sufficient for activation. As discussed previously, there is clear evidence that inhibiting phosphatase activity in T cells by pervanadate treatment leads to tyrosine phosphorylation and other cellular activation responses [Secrist et al., 1993, Imbert et al., 1994, O'Shea et al., 1992]. There is also evidence that pervanadate treatment of other NTR-expressing cells similarly induces tyrosine phosphorylation. For example, pervanadate treatment of NK cells leads to DAP10 phosphorylation which is the adaptor protein of NKG2D, and phosphorylation of Ly49 receptors [Mason et al., 1997, Wu et al., 1999, Billadeau et al., 2003]. These observations are consistent with both aggregation models and the KS model. The work by Hui and Vale investigating the dynamic balance between kinase and phosphatase activity on CD3ζ phosphorylation in a reconstituted system clearly showed that CD3ζ phosphorylation was more sensitive to changes in CD45 levels than Lck levels. This suggests that changes to CD45 activity may be the crucial factor in receptor activation rather than changes in kinase activity [Hui and Vale, 2014]. This is more consistent with the KS model than aggregation models that propose increases in kinase activity on the receptor are important for activation.

It has been reported that a significant proportion of Lck in resting T cells is active and that this level does not change upon activation [Nika et al., 2010]. These results do not indicate whether the same Lck molecules remain active throughout receptor activation or if this is a dynamic population of Lck molecules constantly being activated and inactivated.

However, it does suggest that kinase-mediated receptor phosphorylation is inhibited in resting cells perhaps by dominant phosphatase activity. By segregating inhibitory phosphatases, but not kinases, from ligand-bound receptors, this dominant inhibitory activity is decreased and kinase activity dominates. The results of Nika et al. have recently been disputed by another study that reports the level of active Lck in resting cells to be much lower [Ballek et al., 2015]. While it conflicts with these results it does not provide evidence against the KS model.

How can ligand binding induce segregation?

Fundamental to the KS model is how receptor-ligand interactions can drive segregation of larger surface molecules. By generating a model and applying it to images of proteins at immune synapses Burroughs et al. provided evidence that protein segregation patterns at immune cell interfaces can be explained by size-based differences between the proteins alone. They show this for the segregation of ICAM-1 from CD2-CD58 interactions at the interface between T cell and lipid bilayer, and ICAM-1 from KIR2DL1 - HLA-Cw6 interactions at an NK cell-target cell interface [Burroughs et al., 2011]. Alakoskela et al. used nanoscale fluorescent particles (quantum dots) to observe segregation following engagement of KIR2DL1 and HLA-Cw6 at the NK cell immune synapse [Alakoskela et al., 2011]. Membrane-bound nanoparticles with comparable dimensions to the KIR2DL1 - HLA-Cw6 complex co-localised with the engaged receptors at the immune synapse. Whereas particles with dimensions larger than those of the receptor-ligand complex were segregated from sites of engagement. It is proposed that the size difference will cause a membrane curvature defect and that segregation of large molecules is favourable to minimise this membrane bending [Alakoskela et al., 2011]. This process may also act to cluster receptors in areas of close membrane contact using a mechanism like that proposed for integrin receptors (discussed in section 1.10.6) [Paszek et al., 2014]. Alakoskela et al. analysed segregation over the immune synapse which is a larger scale than the proposed scale of segregation in the KS model and so does not seek evidence that this segregation was associated with changes in receptor activation. The study does however provide evidence to suggest that size differences can lead to protein redistribution.

The small-scale protein segregation proposed by the KS mechanism has been sug-

gested to be plausible using mathematical modelling [Allard et al., 2012]. The nanometre-scale model takes into account the membrane bending and compression of large surface molecules like inhibitory phosphatases that will occur at sites of close cell-cell contact. It predicts that even a single receptor-ligand bond could induce segregation of large surface molecules from the site of engagement. A recent structure of CD45 extracellular domains D1-D4 indicates that the extracellular region is rigid, further supporting the idea that CD45 will be excluded from sites of close cell-cell contact rather than changing conformation in order to allow the ectodomain to fit within the close-contact areas [Chang et al., 2016].

These studies provide evidence that NTR-ligand binding could drive exclusion of inhibitory phosphatases from sites of engaged receptors. Further to this, imaging NTRs and inhibitory phosphatases at cell-cell or cell-surface interfaces has shown that the large surface molecules are indeed segregated from engaged receptors. At the interface between T cell and supported lipid bilayer presenting ICAM-1 and pMHC, CD45 is segregated from sites of TCR-signalling microclusters [Johnson et al., 2000, Varma et al., 2006]. CD45 is similarly segregated from the TCR at the interface between T cell and glass coverslips presenting immobilised antibody, and from sites of tyrosine phosphorylation at the T cell-APC interface [Bunnell et al., 2002, Leupin et al., 2000, Chang et al., 2016]. Likewise, CD45 is excluded from BCR- and phosphotyrosine- positive microclusters that form upon interaction between B cells, and ICAM-1 and antigen presented on a supported lipid bilayer [Depoil et al., 2008].

The ectodomain of inhibitory phosphatases mediates segregation

One of the predictions the KS model makes about NTR activation is that truncation of the ectodomain of inhibitory phosphatases will reduce segregation of the protein from receptor-ligand complexes. This increased proximity between receptor and phosphatase will decrease the receptor phosphorylation and activation upon ligand binding. Consistent with this prediction, CD45-deficient T cells or T cell hybridoma lines expressing truncated versions of CD45 showed dramatically reduced levels of activation in response to APC or immobilised antibody compared to cells expressing wild-type CD45 [He et al., 2002, Irles et al., 2003, Cordoba et al., 2013]. In contrast, T cells expressing chimeric CD45 with the ectodomain of CD43, which is a comparable length to that of CD45, were

activated upon ligand presentation [Irles et al., 2003, Cordoba et al., 2013]. In addition to this, wildtype-length CD45 was observed to be excluded from TCR microclusters whereas truncated CD45 was not [Irles et al., 2003]. These results indicate that the size of the ectodomain is important for both segregation and the inhibitory function of CD45.

In a reconstituted system where HEK293T cells expressing the TCR, Lck, CD45, Csk and proteins to mediate adhesion are presented to APCs, CD45 was excluded from TCR-pMHC interactions at the cell-cell interface [James and Vale, 2012]. Similar results were observed using an articifial receptor-ligand interaction that spanned the same intermembrane distance as the TCR and pMHC. In contrast to other studies, even truncated CD45 was also partially excluded from engaged TCRs but CD45 lacking an ectodomain was not excluded. Forcing the truncated CD45 into the close cell-cell interface and into close proximity with the TCR abolished receptor triggering consistent with phosphatase segregation being required for signalling. James and Vale propose that additional forces may have induced exclusion of the truncated CD45 from the TCR-pMHC complexes [James and Vale, 2012]. It has been suggested that high levels of TCR clustering at the cell-cell interface may have driven lateral segregation of CD45 by a "crowding out" mechanism [Cordoba et al., 2013].

The role of ectodomain size in protein exclusion from cell-cell contacts has also been shown using chimeric forms of Lck. Lck with a transmembrane domain and the extracellular region of CD45, that was transduced into T cells, was excluded from contacts between the T cell and anti-CD3 antibody-coated coverslips and co-localised with CD45. Chimeric Lck with no ectodomain did not co-localise with CD45 at cell-surface contacts suggesting the large ectodomain of chimeric Lck was responsible for the exclusion. Lck exclusion was also associated with reduced T cell activation indicating that for TCR triggering to occur phosphatase segregation and the presence of Lck at sites of receptor engagement are required [Chang et al., 2016].

Like CD45, T cells expressing truncated forms of CD148 showed dramatically reduced signalling responses to pMHC or antibody [Cordoba et al., 2013]. CD148 is also excluded from CD3 and TCR microclusters at the immunological synapse whereas truncated CD148 is not [Lin and Weiss, 2003, Cordoba et al., 2013]. Targeting the truncated

CD148 into sites of TCR engagement within the immunological synapse inhibited TCR activation providing evidence that CD148 exclusion from TCR-pMHC complexes is mediated by the large extracellular domain and that this exclusion is required for activation [Lin and Weiss, 2003, Cordoba et al., 2013].

As well as decreasing the inhibitory dephosphorylation of receptor tyrosine-based motifs, CD45 segregation from engaged receptors may increase receptor phosphorylation and activation by increasing phosphorylation and clustering of Lck. Rossy et al. show using super-resolution microscopy that the conformational state of Lck controls the distribution of Lck in the cell membrane. The open active conformation, which CD45 can negatively regulate, induces Lck clustering whereas the inactive conformation does not. The authors suggest this clustering will increase interactions between Lck and the TCR. Segregation of CD45 from engaged TCRs upon TCR-pMHC binding may increase the fraction of active Lck within these regions of engaged TCR and close membrane contact leading to increased Lck clustering and receptor tyrosine phosphorylation [Rossy et al., 2013].

In agreement with these studies that CD45/CD148 segregation from the receptor is required for activation, it has been shown for multiple NTRs that ligand or antibody cannot activate the receptor unless immobilised on a surface (or cross-linked) (examples include [Geppert and Lipsky, 1987, Goodridge et al., 2011, Xie et al., 2012]). This is discussed further for a number of receptors in Chapter 4 introduction. Binding of soluble monovalent ligands to the receptor is unlikely to induce exclusion of phosphatases because the soluble ligand will not put strain on the phosphatase ectodomain like a ligand-presenting surface would upon close contact. This may explain why soluble monovalent ligand cannot activate NTRs.

Further cross-linking of soluble ligand-bound or antibody-bound receptors by either a secondary antibody or multivalent protein can also induce NTR activation (examples include [Pende et al., 1999, Saverino et al., 2002, Hayashi et al., 2004, Merlo et al., 2005]). This is also discussed further for a number of NTRs in Chapter 4 introduction. This suggests that large-scale clustering of receptors is required for activation to be induced by soluble ligand. In agreement with this, in a reconstituted system of the CD3ζ chain, Lck and CD45 cytoplasmic regions expressed on a liposome membrane, homoclustering of

the CD3ζ chain induced tyrosine phosphorylation [Hui and Vale, 2014]. This might suggest that CD45 exclusion is not required for activation. Alternatively, this clustering may have induced lateral segregation of CD45 from regions of clustered CD3ζ. Similar lateral exclusion of CD45/CD148 may occur when receptors are clustered by soluble ligand and further multivalent protein, favouring kinase activity and initiating signalling. Hui and Vale observed that heteroclustering of CD3ζ and Lck in the reconstituted system also induced tyrosine phosphorylation, to greater levels than that induced by CD3ζ homoclustering [Hui and Vale, 2014]. Perhaps in this case, in combination with the possible lateral segregation of CD45 from CD3ζ,, Lck is now held in close contact to CD3ζ allowing the kinase activity to dominate further and lead to higher levels of phosphorylation.

Ligand-independent TCR activation

Further suggesting that the dynamic balance between kinase and phosphatase activity is fundamental to TCR triggering, Chang et al. show ligand-independent TCR activation associated with exclusion of the inhibitory phosphatase CD45 from the TCR [Chang et al., 2016]. T cells were allowed to make contacts with supported lipid bilayers by use of the CD2-CD48 interaction. CD45 was excluded from these contacts whereas the TCR, Lck and truncated CD45 were not. T cells expressing wildtype length CD45 were activated upon contact with the supported lipid bilayer in the absence of ligand. TCRs within the contacts were freely diffusing and segregated from CD45 as long as they remained within the contact region. This segregation may have induced receptor activation. Calcium signalling in T cells expressing truncated CD45 in contact with the lipid bilayer was much lower. Truncated CD45 is not segregated from any TCR so will be able to dephosphorylate the receptor. This suggests that phosphatase segregation from TCRs in the absence of TCR ligand is sufficient to activate TCR signalling [Chang et al., 2016].

One challenge to the KS model is that such a mechanism could conceivably lead to ligand-independent receptor activation in vivo and consequent unwanted immune responses. Immune cells will often be in close contact with other cells and surfaces physiologically and this close contact may induce segregation of large surface molecules. If all that is required for activation is segregation of phosphatases from the receptor then a question is why are immune cells not non-specifically activated by contact with other

cells? Indeed, Chang et al. show that ligand-independent TCR activation can occur due to exclusion of CD45 from TCRs present at cell-surface interfaces [Chang et al., 2016]. Why does this not happen physiologically? Using mathematical modelling it has been postulated that in a physiological setting, unbound TCRs present in membrane regions from which CD45 is excluded will remain within these regions for very short timescales in the order of milliseconds. It was suggested that these short timescales are not sufficient for full TCR activation to occur and that keeping receptors within these regions by ligand binding is required [Burroughs et al., 2006]. Chang et al. propose a similar mechanism [Chang et al., 2016]. They also note that APCs will present many molecules that were not incorporated into the lipid bilayers they used in their studies. The presence of these other molecules, like the glycocalyx, may act to make the regions of close cell-cell contact smaller or more short-lived than those observed experimentally. Therefore physiologically, TCRs are not segregated from phosphatases for long enough for activation to occur unless they are bound by ligand [Chang et al., 2016].

Altering the intermembrane distance at sites of receptor engagement affects activation

Another prediction of the KS model is that increasing the intermembrane distance at sites of receptor-ligand engagement, by elongating the ectodomain of the receptor and/or ligand, will reduce phosphatase exclusion and ligand-induced activation. Elongation of the ligand for receptors including the TCR, CD28 and NK cell receptors has been shown to either abolish or dramatically reduce receptor activation [Choudhuri et al., 2005, Choudhuri et al., 2009, Lim et al., 2015, Köhler et al., 2010, Brzostek et al., 2010]. Where tested, this was associated with reduced segregation of phosphatases [Choudhuri et al., 2009, Lim et al., 2015]. In Chapter 5 we conduct similar experiments and so this work is discussed in Chapter 5 introduction.

Altering the distance between the membrane and ligand epitope position for receptor binding will also alter the intermembrane distance. Bluemel et al. used bi-specific antibodies targeted at CD3 and an antigen expressed on CHO cells to induce T cell-mediated lysis. There was a correlation between antigen epitope distance from the membrane and potency, with antibodies that targeted the most membrane proximal epitopes eliciting the most potent response. Antibodies that bound antigens with smaller ectodomains were

similarly more potent [Bluemel et al., 2010]. A negative correlation between epitope distance from the membrane and T cell-mediated lysis was also observed with a chimeric TCR against CD22. A chimeric TCR that bound truncated CD22, or CD20 which has a shorter ectodomain than CD22, gave an increased response upon binding [James et al., 2008].

T cells expressing a recombinant immunoreceptor were also sensitive to the position of the epitope it binds. T cells expressing an immunoreceptor that bound a membrane proximal antigen epitope showed increased activation responses to antigen binding compared to T cells expressing an immunoreceptor that bound a membrane distal epitope. Similarly, truncation of the antigen and so moving the epitope to a more membrane proximal position was associated with increased T cell activation. When the antigen was immobilised onto a surface, and the two epitopes were present at equal distances from the surface, the response of the two recombinant immunoreceptors to antigen binding did not differ [Hombach et al., 2007]. These results are consistent with the KS model. The increased intermembrane distance when the receptor (or chimeric TCR or recombinant immunoreceptor) bound a more membrane distal epitope could potentially result in decreased exclusion of phosphatases and this may account for the decreased receptor response to antigen.

Further to this, the epitope distance from the membrane was shown to be important for T cell responses to an ImmTAC (Immune mobilising monoclonal T cell receptor against cancer) [Adams, 2013]. The ImmTAC consisted of the single chain fragment (scFv) of the UCHT-1 anti-CD3 antibody and soluble monoclonal TCR. An ImmTAC with the UCHT-1 scFv fused to the N terminal end of the TCR compared to the C terminus induced a more potent response. This orientation of binding with the scFv fused to the TCR N terminus would likely give a smaller intermembrane distance at contact points which may contribute to the increased potency in line with the KS model.

1.11.2.2 CD28

CD28 co-localises with the TCR in signalling active microclusters at the cell-cell interface. CD45, which is segregated from these microclusters, will therefore also be segregated

from CD28 and indeed has been shown to be segregated from sites of CD28 engagement [Yokosuka et al., 2008, Lim et al., 2015]. Similarly, both CTLA-4 and PD-1 co-localise with TCR signalling microclusters and so will be segregated from CD45 [Yokosuka et al., 2010, Yokosuka et al., 2012]. We note that while this segregation may be functionally significant, it was not shown whether this segregation of CTLA-4 or PD-1 from CD45 was required for receptor activation so does not provide evidence for the KS model.

Like with the TCR, epitope position has been shown to be important for responses to anti-CD28 antibody-mediated stimulation. Conventional anti-CD28 antibodies bind to relatively membrane distal epitopes and cannot activate T cells in the absence of TCR engagement [Hünig and Dennehy, 2005]. In contrast, so called super-agonist anti-CD28 antibodies bind a more membrane proximal epitope of CD28 and can activate the T cell in the absence of TCR engagement [Lühder et al., 2003, Hünig and Dennehy, 2005, Evans et al., 2005]. Binding of anti-CD28 antibodies to membrane proximal epitopes will result in a smaller intermembrane distance and so the differences in antibody potency observed may be due to differences in phosphatase segregation from CD28.

1.11.2.3 NK cell receptors

McCann et al. showed using fluorescence microscopy that CD45 is excluded from the inhibitory NK cell synapse [McCann et al., 2003]. It was not investigated whether this was important for NK cell activation. CD45 was not excluded from the activating NK cell synapse however. The intermembrane distance across the activating synapse varied with some areas of increased distance. It was suggested that these wider areas might accommodate CD45 whereas the close contact areas with intermembrane distances measured as $\sim$10-30nm are likely to contain engaged NK receptors. They suggest that CD45 segregation at smaller scales than those visualised in these studies may occur at the NK cell activating synapse.

1.11.2.4 Dectin-1

The C-type lectin receptor Dectin-1 is activated by particulate forms of β-glucan but is only activated by monomeric β-glucan when it is immobilised [Goodridge et al., 2011]. Upon contact between Dectin-1- expressing macrophages and β-glucan in particulate form or immobilised onto plates, CD45 and CD148 are segregated from Dectin-1 and sites of tyrosine phosphorylation at the interface. CD45 was co-localised with Dectin-1 when it was bound by soluble β-glucan suggesting the opposing surface was important for segregation. Forcing co-localisation of CD45 with Dectin-1 at the interface reduced the ligand-induced activation of macrophages. This evidence is consistent with CD45 segregation being required for Dectin-1 activation, in line with the KS model.

1.11.2.5 The positive regulatory role of CD45 and the KS model

A challenge to the KS mechanism is that CD45 has both positive and negative regulatory roles in SFK activity (discussed in section 1.7) [Alexander, 2000, Hermiston et al., 2009, Chakraborty and Weiss, 2014]. If CD45 is segregated from receptor-ligand complexes it will also be segregated from Lck proteins within these cell areas. Inhibitory Csk, which opposes the positive regulatory activity of CD45, will not be excluded from the activated Lck and so will be able to inactivate it. This may decrease Lck activity at sites of close membrane contact and so also decrease receptor phosphorylation. If the KS mechanism is sufficient for NTR triggering it must account for this.

Johnson et al. provided evidence that upon antigen engagement by the TCR, CD45 is segregated from the cell-surface interface and then was recruited to an area of the cell membrane adjacent to engaged TCRs. They proposed that this CD45 position may allow CD45-mediated positive regulation of nearby SFKs and therefore favour both kinase activity and receptor activation [Johnson et al., 2000].

In addition to this, a number of studies have demonstrated that Lck phosphorylated at both the activating and inhibitory tyrosine exhibits some activity [D'Oro et al., 1996, Nika et al., 2010, Hui and Vale, 2014]. This suggests that phosphorylation of the activatory Y394 site of Lck can overcome inhibitory phosphorylation at Y505. Hui and Vale further

propose that the order of Lck phosphorylation is important. If Y505 is phosphorylated first, Lck is inactive. Whereas, if Y394 is phosphorylated first, Lck remains active even if it is subsequently phosphorylated at inhibitory Y505 [Hui and Vale, 2014]. Perhaps at sites of CD45 exclusion from engaged receptors, trans-autophosphorylation of Lck at Y394 (without opposition from CD45) induces Lck activity and this activity is not completely abolished by unopposed inhibitory Csk Y505 phosphorylation.

1.12 Aims and hypothesis

The precise mechanism by which NTRs are activated has yet to be defined. There is a lot of evidence that is consistent with each of the 3 general proposed mechanisms of NTR triggering. Some of this evidence is consistent with more than one model which has made it hard to identify the exact events required to take a receptor-ligand binding event to initiation of signalling, whether activating or inhibitory. It is possible that multiple mechanisms co-operate and are required for receptor activation. It is also possible that some of the mechanisms discussed in Chapter 1 play a role in enhancing activation rather than initiation which is important to elicit the most effective immune response.

Our hypothesis is that all NTRs trigger using the same mechanism: the KS mechanism. This is because there is evidence with multiple NTRs in support of the KS model and also the properties that they share are consistent with the requirements of triggering by this mechanism. The aim of this thesis is to test our hypothesis using a representative selection of NTRs.

Testing this hypothesis requires analysis of many individual receptor-ligand interactions. Previous experiments to test predictions of the KS model have focused on one or a small number of receptors and involved receptor or ligand manipulation. A similar approach in our investigations would potentially require manipulation of many NTR-ligand complexes.

We aim to instead develop an artificial ligand system whereby a single ligand can bind to any NTR, and where biophysical and biochemical properties of the receptor-ligand interaction can be easily manipulated. We further aim to use this system to test predictions the KS model makes about NTR activation and investigate other properties of receptor activation. By using a single ligand that can bind any NTR, manipulation of the single ligand will alter the NTR-artificial ligand interaction of any receptor. This allows us to conduct a high-throughput, systematic investigation of the group of receptors. In addition, the ligand for some of the NTRs has yet to be identified and so we can use the artificial ligand to investigate activation of these receptors.

This wider aim can be broken down into a number of objectives and questions that will

be covered by this thesis:

- Develop an artificial ligand system that is easily manipulatable and can bind to members of the NTR group with physiological affinity, valency and dimensions (Chapter 3)
- Confirm that the artificial ligand can activate representative NTRs including receptors from multiple families, and with diverse features. For example, activating and inhibitory receptors, and receptors with variable ectodomains (Chapter 4)
- Test the KS model prediction that for NTR activation to occur, the ligand must be presented on a surface (Chapter 4)
- Use the artificial ligand to investigate the role of ligand valency in NTR activation (Chapter 5)
- Test the KS model prediction that elongation of the receptor-ligand complex will reduce NTR activation (Chapter 5)
- Combine the changes to ligand dimensions and valency to investigate the requirements for NTR activation (Chapter 5)

This systematic investigation of NTR triggering will elucidate the requirements for receptor activation and the mechanisms involved. This will improve our understanding of the processes that regulate immune signalling. The artificial ligand system will be a useful tool that can be used to investigate further questions about the properties of NTR triggering, and could also be applied to examine other receptor-ligand interactions.

2. MATERIALS AND METHODS

All flow cytometry data collection was conducted using either a FACScan™ Cytek 8 flow cytometer or FACS Calibur™flow cytometer. All data was analysed using FlowJo software and gated for single cells or beads (unless otherwise stated) using FSC and SSC readings before fluorescence intensity was analysed. Unless otherwise stated, the flow cytometry wash buffer used throughout is phosphate-buffered saline (PBS), 1% bovine serum albumin (BSA), 0.05% sodium azide.
Protein immobilisation and stimulation data was analysed using GraphPad Prism.

We use a number of abbreviations to refer to proteins we use throughout this work. Table **2.1** lists these abbreviations and full name of the protein.

2.1 NTR and adaptor construct design and synthesis

Two inserts were designed for cloning either individual type I or type II transmembrane NTRs. These were synthesised and cloned into the pHR-SIN-BX-IRES-EmGFP plasmid (a gift from Professor Oreste Acuto) using the GENEWIZ® gene synthesis service.

Abbreviation	Full protein name
ST	StrepTactin
ST1dSA3	monovalent StrepTactin
1,2 cis-ST2	1,2 cis-bivalent StrepTactin
1,3 trans-ST2, 1,4 ST2	mixture of 1,3 trans-bivalent and 1,4 bivalent StrepTactin
ST3dSA1	trivalent StrepTactin
ST4	tetravalent StrepTactin
ST-pD-C	StrepTactin-SpyCatcher
ST1-pD-C	monovalent StrepTactin-SpyCatcher
ST4-pD-C	tetravalent StrepTactin-SpyCatcher

Tab. 2.1: **StrepTactin and StrepTactin-SpyCatcher abbreviations used.** Listed are the abbreviations we use to refer to various forms of StrepTactin and StrepTactin-SpyCatcher protein throughout the text.

These two plasmids are hereafter referred to as the Type I and Type II plasmids.

The inserted region of Type I plasmid begins with the Igκ mammalian signal peptide, a Strep-Tag II tag with SA linker (SA-WSHPQFEK) and a $(GS)_3$ linker. These are followed by a short multiple cloning site (referred to as MCS I) comprising the XhoI, **BamHI**, *SpeI* and BsiWI restriction enzyme recognition sites (ctcgag**GGATCC***actagt*CGTACG), a FLAG tag (DYKDDDDK) and a second short multiple cloning site (referred to as MCS II). MCS II comprises the NdeI, Bsu36I and *MluI* recognition sites, and ends with a **STOP** codon (catatgCCTGAGG*acgcgt***ga**).

The inserted region of Type II plasmid comprises the MCS II sequence minus STOP codon, followed by a start methionine and FLAG tag, the MCS I sequence, a $(GS)_2$ linker and the Strep-Tag II sequence ending with a STOP codon.

2.1.1 Receptors

All receptors used are human and were amplified without the native signal sequence and STOP codon. Table **2.2** outlines the NTRs that have been cloned into the appropriate plasmid, along with the template DNA from which the sequence was amplified, and the primers used for amplification. Primer sequences are displayed in table **2.3**. Each amplified receptor was inserted directly into the plasmid using the restriction enzyme sites highlighted in bold in each primer pair (table **2.3**). Exceptions to this were SIGLEC-14 and NKG2D. SIGLEC-14 was first amplified using nested primers # 9a and 9b, then amplified from this PCR product using primers # 10a and 10b. NKG2D was first subcloned into pCR2.1®TOPO® TA vector using the TOPO® TA Cloning® Kit (Thermo Fisher Cat. # 451641) as per manufacturer's instructions before being transferred to the Type II plasmid.

Template cDNA generated from either PBMC RNA or macrophage RNA was synthesised using Thermo Fisher's SuperScript® III First-Strand Synthesis System (Cat. # 18080-051) as per manufacturer's instructions. All sequences were verified using the Source BioScience Sanger sequencing service. Hereafter these individual plasmids are referred to by the vector and the receptor insert, for example Type I LAIR-1, or Type II NKG2D.

NKG2D-1x linker and NKG2D-2x linker

Primers # 12a and 12b encoding a 15 amino acid linker flanked by two BsiWI sites were annealed to each other and inserted either once or twice into Type II NKG2D using the plasmid BsiWI restriction recognition site yielding the NKG2D-1x linker or NKG2D-2x linker plasmids respectively. Amino acid sequence of the linker is GSSGGSGGS-GSSGGS.

NKG2D-loop

Two amino acid changes at positions 186 and 187 were introduced into the sequence of NKG2D in the pCR2.1®-TOPO®subcloning vector by QuikChange®PCR mutagenesis (Agilent Technologies) using primers # 13a and 13b. This introduced an NheI restriction recognition site and altered the amino acid sequence from ...EMQKGDCA... to ...EMQASDCA... . Primers # 14a and 14b encoding Strep-Tag II flanked by NheI restriction recognition sites were annealed to each other and inserted into this mutated pCR2.1®-TOPO®NKG2D. The NKG2D with Strep-Tag II sequence was then amplified from this plasmid using primers # 5a and 15 and inserted into the Type II vector using BamHI and NotI, replacing the Strep-Tag II sequence already present.

2.1.2 Adaptor proteins

Primers # 16a and 16b encoding a c-Myc tag were annealed together to form an adaptor and inserted into the pHR-SIN-BX-IRES-EmGFP plasmid using the NotI site. Upon insertion of the adaptor, the 5' NotI site was retained while the 3' site was destroyed thereby permitting insertion of human DAP10, DAP12 or FcRγ using this single NotI site. Primer sequences are shown in table **2.3**.

DAP10, DAP12 and FcRγ were all amplified with native signal sequence but without the STOP codon. DAP10 was amplified from cDNA synthesised from human PBMC RNA first using nested primers # 17a and 17b and then primers # 18a and 18b. Digested PCR product was then inserted into pHR-SIN-BX-IRES-EmGFP c-Myc using the BamHI and NotI restriction sites. DAP12 and FcRγ were also amplified from PMBC cDNA and inserted into the pHR-SIN-BX-IRES-EmGFP-c-Myc plasmid using the BamHI and NotI

Receptor	Target plasmid	Source of DNA	Primers used
2B4	Type I	Plasmid provided by Dr Marion H Brown	1a, 1b
CD5	Type I	Plasmid provided by Dr Marion H Brown	2a, 2b
FcγRIA	Type I	cDNA synthesised from activated human macrophage RNA provided by Dr Sally Cowley	3a, 3b
LAIR-1	Type I	Plasmid provided by Dr Jesse Goyette	4a, 4b
NKG2D	Type II	cDNA synthesised from human PBMC RNA	5a, 5b
NKp30	Type I	cDNA clone Source Bioscience IMAGE ID:5934651	6a, 6b
NKp44	Type I	cDNA clone Genscript Clone ID:OHu32157 NCBI Reference Sequence: NM_004828.3	7a, 7b
PD-1	Type I	Plasmid provided by Rachel Paterson	8a, 8b
SIGLEC-14	Type I	cDNA synthesised from activated human macrophage RNA provided by Dr Sally Cowley	9a, 9b then 10a, 10b
SIRPβ1	Type I	Plasmid provided by Dr Debbie Hatherley	11a, 11b

Tab. 2.2: **NTRs cloned into either Type I or Type II plasmid.** Each receptor cloned into the appropriate lentivector is listed along with which plasmid it was cloned into, the source of the DNA amplified and the primers used to amplify the sequence. Primer sequences are outlined in table **2.3**

sites. DAP12 was amplified using nested primers # 19a and 19b and then re-amplified from this PCR product with primers # 20a and 20b. FcRγ was amplified using nested primers # 21a and 21b and then # 22a and 22b.

To synthesise adaptor protein constructs that make use of the pHR-SIN-BX-IRES-EmGFP vector IRES-EmGFP sequence, DAP10, DAP12 and FcRγ were amplified individually from the above plasmids using primers # 18a, 20a or 22a respectively along with primer # 23 and inserted into pHR-SIN-BX-IRES-EmGFP using the BamHI and XhoI sites thus retaining the c-Myc tag and IRES-EmGFP sequence. All sequences were confirmed using Sanger sequencing.

Primer #	**Sequence**
1a	ttatta**CTCGAG**tgccagggatcagctgacc
1b	ttatta**CGTACG**ggaataaacatcaaagttctccagc
2a	ttatta**CTCGAG**cggctcagctggtatgacc
2b	ttatta**CGTACG**cagcctctgagccccatg
3a	ttatta**GGATCC**caagtggacaccacaaaggc
3b	ttatta**CGTACG**cgtggccccctgggg
4a	ttatta**GGATCC**caggaggaagatctgcccag
4b	ttatta**CGTACG**gtgtctggcaacggctgc
5a	ttatta**GGATCC**atggggtggattcgtggtcgg
5b	ttatta**CGTACG**cacagtcctttgcatgcagatgtacg
6a	ttatta**CTCGAG**ctctgggtgtcccagcc
6b	ttatta**CGTACG**gcctcctgggactggg
7a	ttatta**GGATCC**caatccaaggctcaggtacttc
7b	ttatta**CGTACG**caaagtgtgttcatcatcatcatcg
8a	ttatta**GGATCC**ccaggatggttcttagactcc
8b	ttatta**CGTACG**gaggggccaagagcagtg
9a	gcatttccttccctgacagc
9b	agttctgtcttgagcgggag
10a	ttatta**CTCGAG**gagaagccagtgtacgagc
10b	ttatta**CGTACG**gccaggcctctcagcc
11a	ttatta**GGATCC**gaggacgagctacaggtg
11b	ttatta**CGTACG**ggccttctgtttccagcag
12a	gtacggggtccagcggcggctccggcggaagcggcagcagcggaggaagcc
12b	gtacggcttcctccgctgctgccgcttccgccggagccgccgctggacccc
13a	caataattgaaatgcag**GCTAGC**gactgtgcactctatgc
13b	gcatagagtgcacagtc**GCTAGC**ctgcatttcaattattg
14a	ctagcagcgcctggagccacccccagttcgagaagg
14b	ctagccttctcgaactgggggtggctccaggcgctg
15	ttatta**GCGGCCGC**ttacacagtcctttgcatgcagatg
16a	ggccgccagcggtggtgaacaaaaacttatttctgaagaagatctgtgata
16b	ggcctatcacagatcttcttcagaaataagtttttgttcaccaccgctggc
17a	ctggacttctctggaccaca
17b	aagtcaaaggtccaagctgc
18a	ttatta**GGATCC**atgatccatctgggtcacatcc
18b	ttatta**GCGGCCGC**gcccctgcctggcatgttg
19a	cccttacactgtggtgtcca
19b	ttgctgactgtcatgattcg
20a	ttatta**GGATCC**atgggggacttgaaccctg
20b	ttatta**GCGGCCGC**tttgtaatacggcctctgtgtg
21a	cagaacggccgatctcca
21b	agctggtgttaatggcatgc
22a	ttatta**GGATCC**atgattccagcagtggtcttgc
22b	ttatta**GCGGCCGC**ctgtggtggtttctcatgcttc
23	ttatta**CTCGAG***TCA*cagatcttcttcagaaataagtttttg

Tab. 2.3: **Receptor and adaptor protein primers.** *Continued on the next page.*

Tab. 2.3: **Receptor and adaptor protein primers.** *Continued.* For each primer, where appropriate, complete restriction recognition sites are in **bold**. Amplified PCR products of receptors were inserted into either the Type I or Type II vector using these restriction sites. Adaptor proteins were also inserted into the appropriate plasmid using the highlighted restriction sites. STOP codons are highlighted in *italics*. Primer # 8a was provided by Rachel Paterson.

2.2 Transduction of cell lines with receptor and adaptor constructs

2.2.1 Cell lines

For one week prior to transfection for lentivirus production HEK293T cells were maintained in complete RPMI 1640 media (RPMI 1640, 10% FCS, 100 U mL^{-1} penicillin/streptomycin) at 37°C 5% CO_2. THP-1 cells and Jurkat cells were maintained in complete RPMI 1640 media at 37°C 5% CO_2. NKL and NK92 cells were maintained in complete RPMI 1640 media supplemented with 100 U mL^{-1} recombinant IL-2 at 37°C 5% CO_2.

2.2.2 Lentiviral transduction

Unless otherwise stated, lentiviral transductions were conducted using virus made in HEK293T cells transfected with the X-tremeGENE™ 9 transfection reagent.

2.2.2.1 X-tremeGENE™ 9

X-tremeGENE™ 9 DNA transfection reagent (29 μL) (Sigma-Aldrich Cat. # XTG9-RO) was added slowly to 0.5mL RPMI 1640 10mM HEPES media prewarmed to 37°C , mixed, and incubated at room temperature for 20 minutes. Packaging DNA pRSV.REV and pGAG (3 μg of each) was mixed with 1.17 μg pVSV-G packaging DNA before 2.5 μg of the appropriate lentiviral vector or positive control was added. Where co-transduction was attempted 1.25 μg of each lentiviral vector was mixed with the packaging DNA. The premixed DNA was then added to the RPMI 1640 transfection reagent mixture and incubated at room temperature for 30 minutes. Media was removed from a T25 flask containing HEK293T cells at 50% confluency and replaced with the RPMI 1640 transfection

reagent-DNA mix. After 1 minute incubation, 9.5mL of RPMI 1640 10% FCS, 100U mL^{-1} penicillin/streptomycin, 10mM HEPES, was added to the flask and incubated overnight at 37°C in a 5% CO_2 containing incubator. After 24 hours, the media was transferred to a sterile tube and replaced with 10mL of fresh RPMI 1640 10% FCS, 100U mL^{-1} penicillin/streptomycin, 10mM HEPES, and incubated for a further 24 hours at 37°C in a 5% CO_2 containing incubator before this media was also collected. The 24 and 48 hour media was centrifuged at 524xg for 6 minutes at 4°C before 10 μL 5 $mgmL^{-1}$ polybrene was added and the solution filtered through a 0.22μm syringe filter. Virus-containing media (3mL) was then added to ∼3 x 10^6 Jurkat cells, THP-1 cells, or NKL cells in one well of a 6 well flat bottom plate. The plate was centrifuged at 2095xg for 2 hours at 32°C , incubated at 32°C 8% CO_2 for 6 hours, followed by culturing at 37°C 5% CO_2 for 72 hours. For transduced NKL cells, the media was supplemented with 100 U mL^{-1} recombinant human IL-2 following the 6 hour incubation at 32°C .

2.2.2.2 Polyethylenimine

Packing DNA pRSV and pGAG (2.5 μg of each) was mixed with 0.97 μg pVSV-G and 2.1μg appropriate lentiviral vector in 400 μL RPMI 1640 media. Polyethylenimine (PEI) (16 μg) was mixed with 400 μL RPMI 1640 media in a separate tube before the two solutions were mixed together and incubated at room temperature for 20 minutes. This mixture was added dropwise to HEK293T cells at 50% confluency in a T25 flask and incubated at 37°C 5% CO_2 for 4 hours. The media was then replaced with complete RPMI 1640 media and returned to the incubator for 24 hours. Virus-containing media was collected 24 hour and 48 hours later, treated and added to 3 x 10^6 Jurkat cells as described above.

2.2.3 Cell expression analysis using flow cytometry

Receptor expression was analysed using intracellular staining with anti-FLAG antibody (Sigma-Aldrich, clone M2) and anti-mouse IgG1:Alexa Fluor® 488 antibody (Thermo Fisher Cat. # A-21121) or extracellular staining with anti-Strep-Tag II antibody (iba Cat. # 2-1507-001) and anti-mouse IgG1:Alexa Fluor® 647 antibody (Thermo Fisher Cat. #

A-21240). Specific NKG2D surface expression was analysed using anti-NKG2D antibody (Abcam, clone 1D11) or mouse IgG1 isotype control (AbD Serotec Cat. # MCA928) and anti-mouse IgG1:Alexa Fluor® 647.

Expression of adaptors with IRES-EmGFP was analysed for GFP.

For each flow cytometry analysis of transfected/nucleofected/transduced cells, either cells of the same line that were not transfected (/nucleofected/transduced) or were mock transfected (/nucleofected/transduced) were treated and analysed the same as test samples to act as negative controls.

For intracellular staining, cells were pretreated with 4% paraformaldehyde (PFA) in phosphate buffered saline (PBS) for 15 minutes at room temperature and subsequent washes (before and after antibody incubation) were conducted using saponin wash buffer (PBS, 1% bovine serum albumin (BSA), 0.1% saponin, 0.05% sodium azide). All samples stained for an extracellular target were washed (before and after antibody incubation) with flow cytometry wash buffer (PBS, 1% BSA, 0.05% sodium azide). All antibodies were incubated with cells at 10μg mL^{-1} for 30 minutes at room temperature unless otherwise stated. Prior to flow cytometry analysis, cells were resuspended in 1% PFA in PBS.

2.2.4 Cell sorting with magnetic beads or fluorescence-activated cell sorting

Jurkat cells or THP-1 cells expressing NTRs were sorted using anti-Strep-Tag II antibody immobilised on anti-mouse IgG magnetic beads (ThermoFisher Cat # 112-01D) as per manufacturer's instructions. Alternatively cells were sorted for high expression levels by fluorescence-activated cell sorting (FACS) using a Beckman Coulter MoFlo® Astrios™.

2.3 Cloning of artificial ligand constructs

A sequence containing the Igκ mammalian signal sequence, followed by a HA tag and Avitag was amplified from a plasmid provided by Dr Jesse Goyette using primers # 24a and 24b (sequences in table **2.4**) and then inserted into pcDNA3.1(+) vector (a gift from

Professor Shona Murphy) using the KpnI and BamHI restriction recognition sites. The intracellular, transmembrane and short extracellular stalk regions of mouse CD80 were amplified from a plasmid provided by Dr Hong Sheng Lim using primers # 25a and 25b and inserted into pcDNA3.1(+)-Igκ-HA-Avitag (this entire construct hereafter is referred to as pcDNA3.1(+)CD80 for simplicity). To synthesise constructs with extracellular domains elongated by the 2 immunoglobulin domains of human CD2 or 4 immunoglobulin domains of human CD4 the DNA sequences for insertion were amplified from constructs provided by Dr Jesse Goyette using primers # 26a and 26b or # 27a and 27b respectively. These amplified sequences were then inserted into pcDNA3.1(+)CD80 using the BamHI restriction recognition site. These plasmids are hereafter referred to as pcDNA3.1(+)CD80-CD2 and pcDNA3.1(+)CD80-CD4 respectively. To synthesise a ligand with extracellular region elongated by the immunoglobulin domains of both human CD4 and CD2, the CD4 immunoglobulin domains were amplified from a construct provided by Dr Jesse Goyette using primers # 27a and 28 and inserted in pcDNA3.1(+)CD80 using the BamHI site. The insertion of this sequence leaves the 5' BamHI site intact but the 3' BamHI site is destroyed. The immunoglobulin domains of CD2 were then amplified as above using primers # 26a and 26b and inserted into the remaining BamHI site of this plasmid to create the construct hereafter referred to as pcDNA3.1(+)CD80-CD4-CD2. Sequences were verified using Sanger sequencing.

Primer #	**Sequence**
24a	ttatta**GGTACC**atggagacagacacactcctg
24b	ttatta**GGATCC**ctcgtgccactcgatctt
25a	ttatta**GGATCC**cacgtgtcagaggacttcac
25b	ttatta**GCGGCCGC**ctaaaggaagacggtctgttc
26a	ttatta**GGATCC**gagattacgaatgccttggaaacc
26b	attatt**GGATCC**tttctctggacagctgacagg
27a	ttactc**GGATCC**aaagtggtactgggcaaaaaagg
27b	ttaatc**GGATCC**tgtgggcagaaccttgatgtttg
28	ttatta**AGATCT**tgtgggcagaaccttgatgtttgattccagca

Tab. 2.4: **Ligand primers.** For each primer, complete restriction recognition sites are in **bold**. Primers # 26a to 27b were provided by Dr Jesse Goyette.

2.4 Transduction of cell lines with artificial ligand

2.4.1 Cell lines

Unless otherwise stated, HEK293T cells and CHO cells were maintained in complete DMEM media (DMEM 10% FCS 100U mL^{-1} penicillin/streptomycin) unless otherwise stated at 37°C in a 10% CO_2 containing incubator.
Transfected cells lines are referred to by the cell line and construct expressed. For example: HEK293T CD80, or CHO CD80-CD4.

2.4.2 CHO

2.4.2.1 Nucleofection

BirA nucleofection

To allow biotinylation of introduced ligand proteins, CHO cells were nucleofected with a plasmid encoding the BirA biotin-protein ligase with endoplasmic reticulum retention signal sequence (BirA-ER) (pDISPLAY-BirA-ER). CHO cells were nucleofected using the Lonza Amaxa Cell line Nucleofector™kit V according to manufacturer's instructions. Briefly 1 x 10^6 cells were mixed with Nucleofector™ solution and 3 μg pDisplay-BirA-ER, transferred to a kit cuvette and nucleofected with the Amaxa apparatus using programme U-024. Cells were then transferred to one well of a 24 well flat bottom plate containing complete DMEM media and cultured for 48 hours at 37°C , 10% CO_2. After 48 hours the media was replaced with complete DMEM media supplemented with 400μg mL^{-1} Geneticin®. Cells were analysed 2-3 weeks later by flow cytometry. Following analysis, transfected cells were serially diluted to 1 cell per 100μL complete DMEM media supplemented with 400μg mL^{-1} Geneticin®and 100μL added to each well of a 96 well plate. After 3 weeks, individual clones of CHO BirA-ER cells were analysed by flow cytometry (section 2.4.4).

Ligand nucleofection

CHO BirA-ER cells (1 x 10^6) were nucleofected as described above for pDisplay-BirA-

ER with 3 μg appropriate ligand construct or positive control (truncated CD148). After 48 hours the media was replaced with complete DMEM media supplemented with 400 μg mL^{-1} Geneticin® , 300 μg mL^{-1} Hygromycin B and 20 μM biotin. Cells were then analysed by flow cytometry. Cells nucleofected with pMAX-GFP positive control provided with the Lonza Amaxa Cell line Nucleofector™kit V (Lonza Cat. # VACA-1003) were treated as per manufacturer's instructions.

2.4.3 HEK293T

2.4.3.1 PEI

pDisplay-BirA-ER (4 μg) pre-mixed with 4 μg appropriate ligand plasmid were added to 400 μl DMEM media. As a negative control 4 μg of pDisplay-BirA-ER alone was mixed with DMEM media. PEI (16 μg) was mixed with 400 μl DMEM in a separate tube before the two solutions were mixed together and incubated at room temperature for 20 minutes. This was added dropwise to ∼4 x 10^6 HEK293T cells in a T25 flask and incubated at 37°C 10% CO_2 for 4 hours. The media was then replaced with complete DMEM media supplemented with 20 μM biotin. After 24 hours, surface expression was analysed using flow cytometry (section 2.4.4).

2.4.4 Cell expression analysis using flow cytometry

Expression of the BirA biotin ligase was analysed by intracellular anti-HA tag:Alexa Fluor® 647 antibody (Cell Signalling Technology® , clone 6E2) staining. Surface expression of the ligands or truncated CD148 positive control was analysed by extracellular anti-HA tag:Alexa Fluor® 647 antibody staining. Expression of the pmaxGFP positive control was analysed for GFP.

For each flow cytometry analysis of transfected/nucleofected cells, either cells of the same line that were not transfected (/nucleofected) or were mock transfected (/nucleofected) were treated and analysed the same as test samples to act as negative controls.

For intracellular staining, cells were pretreated with 4% PFA for 15 minutes at room temperature and subsequent washes (before and after antibody incubation) were conducted using saponin wash buffer (PBS, 1% BSA, 0.1% saponin, 0.05% sodium azide). All samples stained for an extracellular target were washed (before and after antibody incubation) with flow cytometry wash buffer. All antibodies and fluorescent proteins were incubated with cells at 10μg mL^{-1} for 30 minutes at room temperature unless otherwise stated. Prior to flow cytometry analysis, cells were resuspended in 1% PFA in PBS.

2.5 Expression and purification of StrepTactin

StrepTactin tetramers of different valencies were expressed and purified using a modified version of the protocol described in [Howarth and Ting, 2008] which involves the expression of two separate subunits before refolding of the monomers into tetrameric protein. These subunits are a StrepTactin monomer and a mutated streptavidin monomer which is unable to bind biotin and termed 'dead' streptavidin. The loss of biotin-binding by dead streptavidin has previously been reported [Howarth et al., 2006]. The amino acid sequences of these subunits are outlined in table 2.5. The dead streptavidin subunit has a polyaspartate sequence inserted to allow separation of StrepTactin of different valencies by ion exchange chromatography.

StrepTactin	MAEAGITGTWYNQLGSTFIVTAGADGALTGTYVTAR GNAESRYVLTGRYDSAPATDGSGTALGWTVAWKNNY RNAHSATTWSGQYVGGAEARINTQWLLTSGTTEANA WKSTLVGHDTFTKVKPSAAS
dead streptavidin	MAEAGITGTWYAQLGDTFIVTAGADGALTGTYEAAVG **DDDGDDDGDDDG**AESRYVLTGRYDSAPATDGSGTALGW TVAWKNNYRNAHSATTWSGQYVGGAEARINTQWLL TSGTTEANAWKSTLVGHDTFTKVKPSAAS

Tab. 2.5: **StrepTactin and dead streptavidin amino acid sequences** *E. coli* cells were transformed with a plasmid encoding either the StrepTactin or dead streptavidin monomer to allow synthesis of StrepTactin tetramers of different valency. The dead streptavidin monomer has a polyaspartate sequence inserted (shown in **bold**) in order to permit separation of the tetramers by valency and arrangement using ion exchange chromatography.

Escherichia coli BL21 (DE3) cells were transformed with a plasmid encoding either Strep-

Tactin monomer (pET21a-StrepTactin) or dead streptavidin monomer (pET21a-polyD-dead streptavidin). Both plasmids were gifts from Professor Mark Howarth. Transformed *E. coli* cells were grown in LB supplemented with 100μg mL^{-1} ampicillin in a shaking incubator at 37°C , 180rpm until OD_{600nm} reached 0.9. Protein expression was then induced with addition of 1mM isopropyl-β-d-thiogalactopyranoside (IPTG) and incubation at 37°C for a further 4 hours.

Inclusion bodies were purified in wash buffer (50 mM Tris, 100 mM NaCl, 10 mM EDTA, 0.5$\%$ Triton X-100 pH 7.4) by sonicating in rounds of 3 x 30 seconds, alternated with centrifugation at 30996 x g for 10 minutes at 4°C . These steps were repeated until the inclusion body pellet turned white and chalky in consistency. A final wash of inclusion bodies with resuspension buffer (50 mM Tris, 100 mM NaCl, 10 mM EDTA pH 7.4) at 30996 x g, 10 minutes at 4°C was followed by dissolving of the inclusion bodies in 6M guanidinium hydrochloride pH 1.5. StrepTactin and dead streptavidin subunits were mixed at a 1:1 molar ratio as determined by OD_{280} values of the unfolded proteins in guanidinium hydrochloride. Mixed subunits were then refolded at 4°C in PBS by rapid dilution. Refolded proteins were collected by ammonium sulphate precipitation and resuspension of the pellet in 20mM Tris pH 8.0. The refolded protein was dialysed thrice in 20mM Tris pH 8.0, filtered through a 0.22 μm syringe filter and loaded onto a Mono Q HR 5/5 column (GE Healthcare Life Sciences). StrepTactin tetramers of different valencies were separately eluted using ion exchange chromatography by gradually increasing the concentration of 1M NaCl in 20mM Tris pH 8.0. Fractions (0.75mL) were collected, pooled into the various valencies and redialysed twice in PBS before being sterile filtered through a 0.22μm filter and stored at -80°C.

To confirm the correct purification of tetramers, 1 μg samples of each protein peak were either boiled in 5x SDS loading buffer (0.25M Tris-Cl pH 6.8, 10$\%$ SDS, 0.5M DTT, 50$\%$ glycerol, 0.25$\%$ bromophenol blue) and loaded onto a 16$\%$ SDS PAGE gel, or loaded unboiled in 5x SDS loading buffer onto a 10$\%$ SDS-PAGE gel and electrophoresis run at 4°C. Protein gels were stained using InstantBlue™ protein stain (Sigma-Aldrich Cat. # ISB1L). Gel images were analysed and band densities measured using ImageJ software.

2.5.1 Using biotin-4-fluorescein to estimate valency of StrepTactin tetramers

StrepTactin tetramer valency was estimated using a biotin-4-fluorescein fluorescence quenching protocol modified from [Kada et al., 1999]. Briefly, 0.9 μM of each StrepTactin tetramer (or the same volume of PBS only as negative control) was mixed with titrating concentrations of biotin-4-fluorescein (Sigma-Aldrich Cat. # B9431), covering a range of below to above saturation and incubated for 15 minutes at room temperature. Fluorescence was measured with excitation 485nm and emission at 520nm, and data analysed using GraphPad Prism software to estimate the number of binding sites per StrepTactin.

Mean fluorescence values of PBS-only control wells were substracted from all test values. These were then plotted against concentration of biotin-4-fluorescein added to the well. Values for wells containing biotin-4-fluorescein diluted in PBS only were fit with a linear regression line. Monovalent StrepTactin (ST1dSA3), 1,2 cis-bivalent StrepTactin (1,2 cis-ST2), the mixture of 1,3 and 1,4 bivalent StrepTactin (1,3 trans-ST2, 1,4 ST2), and trivalent StrepTactin (ST3dSA1) values were individually fit with a segmental linear regression line by GraphPad prism software using equations **2.1** to **2.4**:

$$Y1 = \text{intercept1} + \text{slope1} \cdot X \tag{2.1}$$

$$Y \text{ at } X0 = \text{slope1} \cdot X0 + \text{intercept1} \tag{2.2}$$

$$Y2 = Y \text{ at } X0 + \text{slope2} \cdot (X - X0) \tag{2.3}$$

$$Y = IF(X<X0, Y1, Y2) \tag{2.4}$$

where X is the concentration of biotin-4-fluorescein (μM), Y is fluorescence (arbitrary units (AU)), X0 is the concentration of biotin-4-fluorescein at which the line segments intersect (μM), slope1 is the gradient of the first line segment, slope2 is the gradient of the second line segment and intercept1 is the Y value at which the first line segment intersects the Y axis.

Intercept1 was constrained to 0 and slope2 constrained to that calculated for the PBS

negative control. The protein valency was determined by dividing the X0 value in μM by the StrepTactin concentration (μM).

2.5.2 StrepTactin labelling with atto 647 dye

Both trivalent (ST3dSA1) and tetravalent (ST4) StrepTactin were fluorescently labelled with the amine reactive atto 647N-NHS ester (ATTO-TEC Cat. # AD 647N) as per manufacturer's instructions. Excess dye was removed by 2 rounds of dialysis in PBS. The degree of labelling was determined using the absorbance readings of the protein at 280nm and 644nm and molar extinction coefficient for atto 647N provided by the manufacturer. Proteins are referred to as ST3dSA1:647 and ST4:647.

2.6 SNAP tag:Strep-Tag II

2.6.1 Cloning of SNAP tag:Strep-Tag II

The Strep-Tag II sequence was cloned into the pSNAP-tag® (T7)-2 vector (NEB Cat. # N9181S) by annealing primers # 29a and 29b (table **2.6**) together and inserting the sequence between the plasmid's BamHI and XhoI restriction recognition sites. The Strep-Tag II sequence was codon optimised for *E. coli* expression. This plasmid is hereafter referred to as pSNAP-Strep-Tag II. The sequence was verified using Sanger sequencing.

Primer #	**Sequence**
29a	gatccagcgcgtggagccatccgcagtttgaaaaac
29b	tcgagtttttcaaactgcggatggctccacgcgctg

Tab. 2.6: **Strep-Tag II primers.** Primer # 29a and 29b were annealed to each other and inserted into pSNAP-tag® (T7)-2 using the BamHI and XhoI recognition sites.

2.6.2 Expression and purification of SNAP tag:Strep-Tag II protein

E. coli BL21 (DE3) cells were transformed with pSNAP-Strep-Tag II and grown in LB supplemented with 100μg mL^{-1} ampicillin in a shaking incubator at 37°C , 180 rpm until OD_{600nm} reached 0.5. IPTG was added to 0.4mM before the *E. coli* cells were returned

to the incubator at 37°C for 4 hours (unless otherwise indicated). Bacterial pellets were lysed in wash buffer (50 mM Tris, 100 mM NaCl, 10 mM EDTA, 0.5% Triton pH 7.4) by sonicating 6 x 30 seconds. Insoluble material was pelleted at 30996 x g for 10 minutes at 4°C . The supernatant containing SNAP-tag:Strep-Tag II protein was collected and purified using a gravity column packed with 2mL StrepTactin resin (Qiagen Cat. # 30002) as per manufacturer's instructions. Samples of fractions collected (10 μL) throughout the purification steps of one expression and purification cycle were boiled for 5 minutes at 99°C in 5 x SDS loading buffer (0.25M Tris-Cl pH 6.8, 10% SDS, 0.5M DTT, 50% glycerol, 0.25% bromophenol blue) and visualised on a 16% SDS-PAGE gel using InstantBlue™ protein stain.

2.6.3 SNAP tag:Strep-Tag II labelling with SNAP-surface® Alexa Fluor® 488

Eluted SNAP-tag:Strep-Tag II was labelled with SNAP-surface® Alexa Fluor® 488 as per manufacturer's instructions, incubating the protein and substrate in the dark at 37°C for 30 minutes. Unreacted substrate was removed by 2 rounds of dialysis in PBS. The degree of protein labelling, as calculated using manufacturer's instructions, was 1:0.4(SNAP-tag:Strep-Tag II : Alexa Fluor®488). Labelling was repeated a number of times with the protocol altered as per manufacturer's suggestions ie. less protein was added to the reaction mix and a longer incubation time was used but degree of labelling was not improved with these changes. This reagent is hereafter referred to as SNAP:Strep-Tag II:488.

2.7 Forming supported lipid bilayers on silica beads

Liposomes were prepared by sonication and a modified protocol of that described by [Smith and Morrissey, 2004] using 1,2-dioleoyl-sn-glycero-3-phosphoethanolamine-N-(cap biotinyl)(cap biotinyl PE) and 1,2-dioleoyl-sn-glycero-3-phosphocholine (PC) (Avanti Polar Lipids, Inc. Cat. # 870273C and 850375C respectively). Briefly, molar ratios of biotinyl cap PE : PC ranging from 1:99 to 0.03:99.97 made by 2-fold serial dilutions (total 2 μmole lipid) and a 2 μmole PC alone sample were dried down in glass tubes under argon. To remove residual chloroform, the tubes were placed under high vacuum for

one hour. The lipids were then resuspended for 1 hour at room temperature in HEPES-buffered saline (HBS) to give a final concentration of 1mM and then sonicated using a bath sonicator for 3x 10 minute sonications. Liposomes were then mixed with 5 μm silica beads as previously described [Dustin et al., 2007] to create a set of supported bilayers with varying amounts of biotin presented on the surface.

2.8 Testing cell lines or phospholipid bilayer-coated beads for StrepTactin binding and available binding sites on StrepTactin-bound cells/beads

To determine if StrepTactin can bind to Strep-Tag II-tagged receptor-expressing cells or biotinylated ligand-expressing cells, ST3dSA1:647 or ST4:647 made in section **2.5.2** were added to cells at 10μg mL^{-1} unless otherwise stated, and incubated at 4°C for 1 hour. Cells were then washed thrice in flow cytometry wash buffer and analysed for StrepTactin binding by flow cytometry.

To confirm the presence of free binding sites for biotin on StrepTactin-bound receptor-expressing cells or StrepTactin-bound ligand cells, 10μg mL^{-1} (unless otherwise stated) biotinylated mouse IgG1 (AbD Serotec Cat. # MCA928B) was incubated with the StrepTactin-bound cells for 15 minutes at 4°C . The cells were then washed thrice with flow cytometry wash buffer and then incubated with 10μg mL^{-1} anti-mouse IgG1:Alexa Fluor®647 or anti-mouse IgG1:Alexa Fluor®488 at 4°C for 15 minutes. Alternatively, StrepTactin-bound ligand cells were incubated with 10μg mL^{-1} (unless otherwise stated) SNAP:Strep-Tag II:488 made in section **2.6.3** at 4°C for 15 minutes. All cells were washed thrice with flow cytometry wash buffer before being fixed in PBS, 1$\%$ PFA and analysed for fluorescence protein binding using flow cytometry.

StrepTactin of different valencies were incubated individually with cells at 10μg mL^{-1} and analysed for free biotin-binding sites using biotinylated mouse IgG1 as for ligand-expressing cells. StrepTactin binding to phospholipid bilayer-coated beads and available binding sites was tested as above for ligand-expressing cells. Cells or beads were washed 3 times in flow cytometry wash buffer before and after protein incubations. Expression analyses were conducted using FlowJo software. Median fluorescence intensity was measured using the software to compare number of binding sites between cells or

phospholipid bilayered-coated beads bound by StrepTactin of different valencies.

2.9 Expression and purification of monovalent and tetravalent StrepTactin-Spycatcher

Monovalent StrepTactin-SpyCatcher (referred to as ST1-pD-C) and tetravalent StrepTactin-SpyCatcher (referred to as ST4-pD-C) were expressed and purified using a modified version of the protocol described in [Howarth and Ting, 2008]. Monovalent and tetravalent StrepTactin-SpyCatcher are abbreviated as such to refer to the number of Strep-Tag II or biotin-binding sites per tetramer. ST**1**-pD-C has a single binding site and ST**4**-pD-C has four binding sites. The 'pD' and 'C' refer to the single polyaspartate sequence and SpyCatcher per tetramer. ST-pD-C is used to generically refer to StrepTactin-SpyCatcher. Synthesising StrepTactin-SpyCatcher tetramers involves the expression of two separate subunits before refolding of the monomers into tetrameric protein. For monovalent StrepTactin-SpyCatcher these subunits are a StrepTactin-SpyCatcher fusion monomer and dead streptavidin monomer which are refolded in a 1:3 molar ratio. For tetravalent StrepTactin-SpyCatcher, a StrepTactin-SpyCatcher monomer and StrepTactin monomer are refolded in a 1:3 molar ratio. The amino acid sequences of these subunits are outlined in table 2.7. The StrepTactin-SpyCatcher subunit has a polyaspartate sequence inserted between the StrepTactin and SpyCatcher to allow separation of tetramers of different configurations by ion exchange chromatography. Refolding the monomers in this manner means that both monovalent and tetravalent StrepTactin-SpyCatcher have a single SpyCatcher and polyaspartate sequence per tetramer.

To make monovalent StrepTactin-SpyCatcher (referred to as ST1-pD-C), *E. coli* BL21-CodonPlus (DE3)-RIPL cells (Agilent Technologies Cat. # 230280) were transformed with pET-21a-StrepTactin-polyD-SpyCatcher or pET-21a-dead streptavidin (both plasmids modified by Dr Jesse Goyette from plasmids provided by Professor Mark Howarth). Transformed *E. coli* cells were grown in LB supplemented with 100μg mL^{-1} ampicillin, 25μg mL^{-1} chloramphenicol in a shaking incubator at 37°C , 180rpm until OD_{600nm}

StrepTactin-SpyCatcher	MAEAGITGTWYNQLGSTFIVTAGADGALTGTYVTAR GNAESRYVLTGRYDSAPATDGSGTALGWTVAWKNNY RNAHSATTWSGQYVGGAEARINTQWLLTSGTTEAN AWKSTLVGHDTFTKVKPSAAS**DDDGDDDGDDDD** SATHIKFSKRDEDGKELAGATMELRDSSGKTISTW ISDGQVKDFYLYPGKYTFVETAAPDGYEVATAITF TVNEQGQVTVNGKATKGDAHI
dead streptavidin	MAEAGITGTWYAQLGDTFIVTAGADGALTGTYEAAVG NAESRYVLTGRYDSAPATDGSGTALGWTVAWKNNYRN AHSATTWSGQYVGGAEARINTQWLLTSGTTEANAWKS TLVGHDTFTKVKPSAAS
StrepTactin	MAEAGITGTWYNQLGSTFIVTAGADGALTGTYVTAR GNAESRYVLTGRYDSAPATDGSGTALGWTVAWKNN YRNAHSATTWSGQYVGGAEARINTQWLLTSGTTEAN AWKSTLVGHDTFTKVKPSAAS

Tab. 2.7: **StrepTactin-SpyCatcher, dead streptavidin, and StrepTactin amino acid sequences.** StrepTactin-SpyCatcher monomers and dead streptavidin monomers were mixed in a 1:3 molar ratio before refolding to synthesise monovalent StrepTactin-SpyCatcher. StrepTactin-SpyCatcher monomers and StrepTactin monomers were mixed in a 1:3 molar ratio before refolding to synthesise tetravalent StrepTactin-SpyCatcher. The StrepTactin-SpyCatcher monomer has a polyaspartate sequence (shown in **bold**) between StrepTactin and SpyCatcher sequences such that the desired monovalent or tetravalent StrepTactin-SpyCatcher has a single polyaspartate sequence and can be purified by ion exchange chromatography.

reached 0.9. Protein expression was induced with 1mM IPTG and incubation at 37°C 180rpm, for a further 4 hours. Bacterial pellets were resuspended in 1 x BugBuster® (Novagen Cat. # 70921) 20μg mL^{-1} lysozyme, 20μg mL^{-1} DNase I, 2mM $MgSO_4$ and protease inhibitor cocktail (Sigma-Aldrich Cat. # P8340) as per manufacturer's instructions and incubated at room temperature for 15 minutes. The solution was then centrifuged at 30996xg for 15 minutes at 4°C. The inclusion body pellet was then resuspended in tris-buffered saline (TBS) and centrifuged again at 30996 x g for 15 minutes at 4°C. Inclusion bodies were then dissolved in 6M guanidinium hydrochloride pH 1.5. StrepTactin-SpyCatcher and dead streptavidin subunits were then mixed in a 1:3 molar ratio as determined by OD_{280nm} values of the dissolved proteins.

To make tetravalent StrepTactin-SpyCatcher (referred to as ST4-pD-C), pET-21a-StrepTactin-polyD-SpyCatcher and pET-21a-StrepTactin were expressed, extracted and dissolved as above. These subunits were also mixed in a 1:3 molar ratio of StrepTactin-SpyCatcher:StrepTactin.

Mixed subunits were then separately refolded at 4°C in PBS by rapid dilution. Refolded

ST1-pD-C or ST4-pD-C were collected by ammonium sulphate precipitation and resuspension of the pellet in 20mM Tris pH 8.0. The refolded proteins were then dialysed thrice in 20mM Tris pH 8.0, filtered through a 0.22 μm syringe filter and loaded onto a Mono Q HR 5/5 column. ST1-pD-C or ST4-pD-C were separated from other subunit compositions with a linear gradient of 0 to 0.5 M NaCl in 20mM Tris pH 8.0. Fractions (2mL) containing either ST1-pD-C or ST4-pD-C were collected, pooled, concentrated, and exchanged into 20mM MES, 140mM NaCl pH 6.0 using a centrifugal filter unit (Merck Millipore Cat. # UFC901024) before being sterile filtered through a 0.22 μm filter and stored at -80°C.

To confirm the correct purification of ST1-pD-C 1 μg samples of each protein peak were boiled at 99°C for 5 minutes in 5x SDS loading buffer (0.25M Tris-Cl pH 6.8, 10% SDS, 0.5M DTT, 50% glycerol, 0.25% bromophenol blue), loaded onto a 4-12% Bis-Tris protein gel (Thermo Fisher Cat. # NP0322) and analysed by SDS-PAGE using InstantBlue™protein stain. Correct purification of ST4-pD-C was confirmed in the same way. Gel images were analysed and band densities measured using ImageJ software.

2.9.1 Using biotin-4-fluorescein to estimate valency of StrepTactin-SpyCatcher tetramers

StrepTactin-SpyCatcher tetramer valency was estimated as per section **2.5.1** using 50 nM of either ST1-pD-C or ST4-pD-C per well. The data was analysed as per section **2.5.1** and StrepTactin-SpyCatcher estimated using the calculated X0 value.

2.9.2 StrepTactin-SpyCatcher labelling with atto 647

Both ST1-pD-C and ST4-pD-C were fluorescently labelled as per section **2.5.2**. Proteins are referred to as ST1-pD-C:647 and ST4-pD-C:647.

2.10 Stimulation of representative Strep-Tag II-tagged non-catalytic tyrosine-phosphorylated receptors expressed in THP-1 cells by anti-Strep-Tag II antibody immobilised onto 96 well plates

All 96 well plates used in this section (unless stated otherwise) are from Thermo Scientific Cat # 456537. All IL-8 ELISAs were conducted using a kit from eBioscience Cat # 88-8086-88.

Anti-Strep-Tag II antibody (ranging from 40 μg mL^{-1} to 1.25 μg mL^{-1}) in PBS (or PBS alone) was added to wells of a 96 well flat bottom plate and incubated overnight at 4°C. These plates were washed thrice with 200 μL PBS before PBS, 1$\%$ BSA was added and incubated at room temperature for a further hour to block the plate. The plate was then washed again three times with PBS. Untransduced THP-1 cells or THP-1 NKp30 cells (1 x 10^5) in complete RPMI 1640 media were then added to the appropriate wells and incubated at 37°C 5$\%$ CO_2 for 20 hours. Supernatants were then collected and IL-8 protein concentrations determined by ELISA.

THP-1 cells were previously stimulated by Dr Jesse Goyette with various concentrations of anti-FcγRIA antibody (R$\&$D Systems Cat. # mab1257) immobilised on 96 well plates to determine the concentration that gives optimal activation to inhibit with LAIR-1 or 2B4 activity. For the stimulation of these inhibitory NTRs, titrating concentrations of anti-Strep-Tag II antibody (final concentration ranging from 10μg mL^{-1} to 0.156μg mL^{-1}) (or no anti-Strep-Tag II antibody) were pre-mixed with 2.5μg mL^{-1} anti-FcγRIA antibody (final concentration) in PBS. Antibody mixtures were added to wells of a 96 well plate and incubated overnight at 4°C. The plate was then washed and blocked with PBS, 1$\%$ BSA as for THP-1 NKp30 stimulation before 1 x 10^5 untransduced THP-1 cells, THP-1 2B4 cells, or THP-1 LAIR-1 cells were added in complete RPMI 1640 media and incubated as with THP-1 NKp30 stimulation. After 20 hours, supernatants were collected and IL-8 protein concentrations determined by ELISA.

2.11 Stimulation of THP-1 NKp30 cells with lipid bilayer-coated beads presenting ST3dSA1

Lipid bilayer-coated beads made according to the protocol outlined in section **2.7** were incubated with 0.18 μM ST3dSA1 for 30 minutes at room temperature and then washed thrice with PBS, 1% BSA. The beads were resuspended in serum-free DMEM 100U mL^{-1} penicillin/streptomycin and either 1 x 10^5, 2 x 10^5 or 4 x 10^5 beads were added to appropriate wells of a 96 well flat bottom plate in 50 μL volume. Untransduced THP-1 cells or THP-1 NKp30 cells were washed thrice with PBS, resuspended in serum-free DMEM 100U mL^{-1} penicillin/streptomycin and 1 x 10^5 cells in 50 μL volume added to appropriate wells. The beads and cells were mixed by gentle shaking for 1-2 minutes before being incubated at 37°C 10% CO_2 for 20 hours. Cell supernatants were then analysed for IL-8 protein secretion by ELISA. For stimulation with beads presenting trans-ST2, the protocol above was replicated, but incubating the beads with 0.18 μM trans-ST2 instead of ST3dSA1.

2.12 Stimulating THP-1 NKp30 cells and THP-1 SIRPβ1 cells with CHO ligand cells presenting StrepTactin-SpyCatcher

As a positive control wells of a 96 well flat bottom plate were incubated with 20μg mL^{-1} anti-Strep-Tag II antibody at 4°C overnight. The wells were washed thrice with 200 μL PBS before PBS, 1% BSA was added and incubated at room temperature for a further hour to block the wells. The plate was then washed again three times with PBS. Untransduced THP-1 cells, THP-1 NKp30 cells or THP-1 SIRPβ1 cells (1 x 10^5) pre-washed three times with sterile PBS and resuspended in complete DMEM media, 2μg mL^{-1} avidin (Sigma-Aldrich Cat # A9275), were added to the wells in 100 μL volume and incubated for 20 hours at 37°C 10% CO_2 before the supernatant was collected and analysed for IL-8 by ELISA.

For stimulation with ligand cells a 96 well flat bottom plate was blocked for 1 hour at room temperature with PBS, 1% BSA and washed twice with sterile PBS and once with 2-(N-morpholino)ethanesulfonic acid (MES)-BSA buffer (20mM MES, 140mM NaCl, 1%

BSA, pH 6.0). CHO CD80-Spy cells were washed twice with PBS 1% BSA and resuspended in MES-BSA buffer. Titrating concentrations of ST1-pD-C ranging from 10 μM to 0.31 μM (or 0 μM) in MES-BSA buffer were added to the cells and left to conjugate at room temperature for 10 minutes. The conjugated cells were then washed three times with PBS, 1% BSA, resuspended in complete DMEM media, 2μg mL^{-1} avidin, and 1 x 10^5 cells added to appropriate wells of the pre-blocked and washed flat bottom plate in 50 μL volume. Untransduced THP-1 cells, THP-1 NKp30 cells or THP-1 SIRPβ1 cells were washed thrice with sterile PBS, resuspended in complete DMEM media, 2μg mL^{-1} avidin, and 1 x 10^5 cells were added to the appropriate wells in 50 μL media. Plates were shaken gently for 1-2 minutes and incubated at 37°C 10% CO_2 for 20 hours. The supernatants were then collected and analysed for IL-8 by ELISA.

In a separate experiment, untransduced THP-1 cells or THP-1 NKp30 cells were incubated with 2 x 10^5 CHO CD80-CD4-Spy cells coupled with varying concentrations of ST4-pD-C (rather than CHO CD80-Spy cells coupled with ST1-pD-C) using the same protocol as described above.

2.12.1 Stimulation of THP-1 cells expressing representative NTRs with plate-immobilised StrepTactin or StrepTactin:atto 647

2.12.1.1 THP-1 NKp30

Tetravalent StrepTactin (ranging from 1.49 μM to 0.001 μM) in sterile PBS was added to wells of a 96 well flat bottom plate and incubated overnight at 4°C . The plate was then washed thrice with 200 μL PBS before PBS, 1% BSA was added and incubated at room temperature for a further hour to block the plate. The plate was then washed again three times with PBS. Untransduced THP-1 cells or THP-1 NKp30 cells were washed three times in sterile PBS and resuspended in serum-free DMEM 100U mL^{-1} penicillin/streptomycin. Cells (1 x 10^5) were then added to appropriate wells and incubated at 37°C 10% CO_2 for 20 hours before supernatants were collected and analysed for IL-8 by ELISA.

2.12.1.2 THP-1 FcγRIA, THP-1 SIGLEC-14 and THP-1 SIRPβ1

THP-1 FcγRIA cells, THP-1 SIGLEC-14 cells or THP-1 SIRPβ1 cells (or negative control untransduced THP-1 cells) were treated as described for THP-1 NKp30 cells in section **2.12.1.1**. ST4:647 (ranging from varying from 0.74 μM to 0.001 μM) was added to the 96 well plate however instead of non-fluorescent ST4.

2.13 Stimulation of example NTRs expressed in THP-1 cells with soluble StrepTactin

2.13.1 THP-1 NKp30

Wells of a 96 well flat bottom plate were blocked for 1 hour at room temperature with sterile PBS, 1% BSA and then washed three times with sterile PBS. Varying concentrations of ST4 were then added to the blocked wells followed by 1 x 10^5 untransduced THP-1 cells or THP-1 NKp30 cells that were pre-washed three times with sterile PBS and re-suspended in serum-free DMEM, 100U mL^{-1} penicillin/streptomycin. ST4 was added to the wells in the same supplemented media at final concentrations that match those used in section **2.12.1.1**. The plate was incubated and supernatants analysed as for THP-1 NKp30 plates in section **2.12.1.1**.

2.13.2 THP-1 FcγRIA, THP-1 SIGLEC-14 and THP-1 SIRPβ1

THP-1 FcγRIA cells, THP-1 SIGLEC-14 cells or THP-1 SIRPβ1 cells (or negative control untransduced THP-1 cells) were treated as described for THP-1 NKp30 cells in section **2.13.1**. ST4:647 was added to the cells however instead of non-fluorescent ST4. The protein was added at final concentrations that match those added to the wells for presentation to THP-1 cells expressing FcγRIA, SIGLEC-14 or SIRPβ1 in section **2.12.1.2**.

2.14 Flow cytometry analysis of soluble tetravalent StrepTactin binding to NTR-expressing THP-1 cells

2.14.1 Direct staining of NTR-expressing THP-1 cells with atto 647-labelled tetravalent StrepTactin

THP-1 FcγRIA cells, THP-1 SIGLEC-14 cells or THP-1 SIRPβ1 cells (1 x 10^5 cells) were washed three times with PBS wash buffer and incubated in complete DMEM media, 2μg mL^{-1} avidin, for 15 minutes at 4°C . The media was then replaced with fresh media containing varying concentrations of ST4:647 to match those added to THP-1 cells for stimulation analysis in section **2.12.1**. The concentrations ranged from 0.74 μM to 0.001 μM. A sample of the cells were also not incubated with ST4:647 as a negative control. The cells were incubated with the protein for 30 minutes at room temperature before being washed three times with PBS wash buffer, resuspended in PBS 1% PFA and analysed by flow cytometry. As further negative controls, untransduced THP-1 cells were incubated with 0.74 μM ST4:647 or no protein, and treated as above before analysis. The measured events were analysed using FlowJo software and median fluorescence intensities (MFIs) calculated to reflect binding of ST4:647. Negative control MFIs of cells not incubated with ST4:647 were subtracted from the appropriate values which were then plotted against concentration of ST4:647 added to the cells.

2.15 Using flow cytometry to show tetravalent StrepTactin-SpyCatcher binds to NTR-expressing THP-1 cells multivalently

2.15.1 Dissociation of atto 647-labelled monovalent or tetravalent StrepTactin-SpyCatcher from THP-1 SIRPβ1 cells

THP-1 SIRPβ1 cells (1 x 10^6 cells) were washed three times with flow cytometry wash buffer. Cells were then incubated with 1.55 μM ST1-pD-C:647 or ST4-pD-C:647 (made in section 2.9.2) for 30 minutes at 4°C . Room temperature PBS, 1% BSA was then added to the cells, diluting the sample more than 30 fold. The cells were then immedi-

ately analysed using flow cytometry. Median fluorescence intensity (MFI) of the bound StrepTactin-SpyCatcher:647 was plotted against time. To measure background fluorescence levels, duplicate samples of THP-1 SIRPβ1 cells incubated with ST1-pD-C:647 or ST4-pD-C:647 were diluted more than 30 fold with room temperature PBS, 1$\%$ BSA, 2 μM d-biotin (final biotin concentration) before being immediately analysed by flow cytometry. The free d-biotin will block the StrepTactin-SpyCatcher and prevent it binding to Strep-Tag II-tagged NTRs. Again, the MFIs measured for the cells were plotted against time.

2.15.2 Equilibrium binding of atto 647-labelled monovalent or tetravalent StrepTactin-SpyCatcher to THP-1 SIRPβ1 cells

THP-1 SIRPβ1 cells (1 x 10^6) were washed thrice with flow cytometry wash buffer. Cells were then resuspended in varying concentrations of either ST1-pD-C:647 or ST4-pD-C:647 in flow cytometry wash buffer for 15 minutes at room temperature and then analysed by flow cytometry. The concentrations of ST-pD-C:647 used ranged from 6 μM to 0.03 μM. To determine background fluorescence, duplicate samples of washed THP-1 SIRPβ1 cells were incubated with the same set of ST1-pD-C:647 or ST4-pD-C:647 concentrations but in PBS, 1$\%$ BSA, 4 μM d-biotin, 0.05$\%$ sodium azide. MFI of cells incubated with ST-pD-C:647 and d-biotin were subtracted from the corresponding MFIs of cells incubated with ST-pD-C:647 alone. These were then plotted against concentration of ST-pD-C:647 added to the cells using GraphPad Prism software. GraphPad Prism was also used to fit a saturation binding equation - one site, specific binding, to both ST1-pD-C:647 and ST4-pD-C:647 binding to THP-1 SIRPβ1 cells. Equation **2.5** was used:

$$Y = \frac{Bmax \cdot X}{Kd + X} \tag{2.5}$$

where Y is the MFI of bound protein (AU), Bmax is the maximum specific protein binding also in units of MFI (AU), X is the concentration of ST-pD-C:647 added (M), and Kd is

the equilibrium binding constant (M).

2.16 Stimulation of representative NTR-expressing THP-1 cells with immobilised StrepTactin/StrepTactin-SpyCatcher of different valencies

All 96 well plates used in this section (unless stated otherwise) are from Thermo Scientific Cat. # 456537. All IL-8 ELISAs were conducted using a kit from eBioscience Cat. # 88-8086-88.

2.16.1 Stimulation of THP-1 NKp30 cells with immobilised StrepTactin of different valencies alone or with poly-L-lysine or polyethylenimine

2.16.1.1 StrepTactin alone

Wells of a 96 well flat bottom plate were incubated with varying concentrations of either ST1dSA3, 1,2 cis-ST2, the mixture of 1,3 trans-ST2 and 1,4 ST2, ST3dSA1 or ST4 overnight at 4°C . Concentrations ranged from 1.49 μM to 0.01 μM (or PBS alone) in sterile PBS. Wells were then washed thrice with PBS, blocked with PBS, 1% BSA for 1 hour at room temperature, and washed three times again with PBS. Untransduced THP-1 cells or THP-1 NKp30 cells were washed thrice with sterile PBS, resuspended in serum-free DMEM, 100U mL^{-1} penicillin/streptomycin, and 1 x 10^5 cells added to appropriate wells. The plate was then incubated for 20 hours at 37°C 10% CO_2 before supernatants were collected and analysed for IL-8 by ELISA.

2.16.1.2 Comparison of StrepTactin immobilised alone or with poly-L-lysine or polyethylenimine

Wells of a 96 well flat bottom plate were incubated with PBS or PBS 0.01% poly-L-lysine, or 0.01% PEI for 1 hour at room temperature. Wells were washed thrice with sterile PBS, blocked with PBS 1% BSA, and then incubated with varying concentrations of ST1dSA3 or ST3dSA1 as described above. Duplicates of the plates were made, one for stimulation

analysis, and one for measuring how much StrepTactin had been immobilised.

Stimulation of THP-1 NKp30 cells

Untransduced THP-1 cells or THP-1 NKp30 cells were washed thrice with sterile PBS, resuspended in serum-free DMEM 100U mL^{-1} penicillin/streptomycin and 1 x 10^5 cells added to appropriate wells prepared above. Plates were incubated for 20 hours at 37°C 10% CO_2 and then supernatants collected for analysis of IL-8 secretion.

Measuring how much StrepTactin protein had been immobilised

A duplicate plate to that prepared above was incubated with 10μg mL^{-1} biotinylated mouse IgG1 (AbD Serotec Cat. # MCA928B) in PBS, 1% BSA for 1 hour at room temperature. The wells were then washed thrice with PBS and incubated with anti-mouse Ig antibody:HRP (Dako Cat. # P0447) as per manufacturer's instructions, incubating the wells for 1 hour at room temperature. Wells were then washed 5 times with PBS and incubated with TMB substrate (eBioscience Cat. # 00-4201) as per manufacturer's instructions and reaction was stopped with 1M H_3PO_4. Absorbance at 450nm was measured using a Spectramax® M2 microplate reader (Molecular Devices).

2.17 Stimulation of THP-1 cells expressing representative NTRs with monovalent or tetravalent StrepTactin-SpyCatcher immobilised on a 96 well plate

All 96 well plates used in this section (unless stated otherwise) are from Thermo Scientific Cat # 456537. All IL-8 ELISAs were conducted using a kit from eBioscience Cat # 88-8086-88.

ST1-pD-C or ST4-pD-C (ranging from 100 μM to 0.01 μM), or PBS alone, were incubated with wells of a 96 well flat bottom plate overnight at 4°C. Wells were then washed thrice with sterile PBS, blocked for 1 hour with PBS, 5% BSA at room temperature and washed again three times with PBS. Duplicate plates were made, one for stimulation analysis and one for analysing how much ST-pD-C had been immobilised.

2.17.1 Stimulation of THP-1 SIRPβ1 cells

Untransduced THP-1 cells or THP-1 SIRPβ1 were washed thrice with sterile PBS, re-suspended in complete DMEM media, 2 μg mL^{-1} avidin, and 1 x 10^5 cells added to appropriate wells prepared as above. Avidin was added to block any biotin present within the complete DMEM media. Wells were then incubated for 20 hours at 37°C 10% CO_2 before the supernatants were collected and analysed for IL-8 by ELISA. IL-8 values measured in wells not incubated with ST1-pD-C or ST4-pD-C were subtracted from wells that were. These values were plotted against concentration of ST-pD-C incubated with the well, intensity of biotin:atto 680 fluorescence measured using duplicates of the wells, or measures of binding sites calculated using these fluorescence values. GraphPad Prism software was used to fit a dose response - stimulation curve to both ST1-pD-C and ST4-pD-C data using log[ST-pD-C]. The data was fit with both a three parameter (equation **2.6**) and four parameter (equation **2.7** - Hill equation) curve:

$$\text{Y} = \text{Bottom} + \frac{\text{Top - Bottom}}{1+10^{\text{LogEC50-X}}} \tag{2.6}$$

$$\text{Y} = \text{Bottom} + \frac{\text{Top - Bottom}}{1+10^{(\text{LogEC50-X})\cdot\text{HillSlope}}} \tag{2.7}$$

where Y is the normalised IL-8 concentration (AU), Top and Bottom are the Y values at the maximum and minimum plateaus respectively (in the same arbitrary units as Y), X is either the concentration of ST-pD-C added to the plate (μM), the fluorescence of bound biotin:atto 680 (relative fluorescence units), number of biotin-binding sites (absolute values) or density of biotin-binding sites (μm^{-2}) and EC_{50} is the X value that gives a response half-way between Top and Bottom (in the same units as X).

The equation that best fit the data is declared on the figures.

To allow collation of data from experiments conducted on different days, IL-8 concentrations determined within one experiment were normalised to the calculated maximum

(Top) of THP-1 SIRPβ1 cells incubated with immobilised ST1-pD-C.

2.17.2 Measuring how much StrepTactin-SpyCatcher is immobilised and number of biotin-binding sites

Duplicates of the wells prepared above were incubated with 10μg mL^{-1} anti-streptavidin antibody (Abcam, clone S10D4) for 30 minutes at room temperature and then washed thrice with PBS wash buffer (PBS, 1$\%$ BSA). Wells were then incubated with anti-mouse IgG (H+L):Dylight® 800 (Thermo Scientific Cat. # SA5-10176) as per manufacturer's instructions and 10 μM biotin:atto 680 (ATTO-TEC Cat. # AD 680-71) for 30 minutes at room temperature. Wells were then washed thrice with PBS wash buffer and scanned using the LI-COR Odyssey Sa scanner using the 800nm channel to measure anti-streptavidin signal. Unless otherwise stated, 6M guanidinium hydrochloride pH 1.5 was added to the wells, the plates shaken for 10 minutes at room temperature and rescanned using the LI-COR scanner using the 700nm channel to measure biotin:atto 680 signal. Raw intensity values in both channels in wells not incubated with ST-pD-C were subtracted from values measured in corresponding wells that were. These values were then plotted against concentration of ST-pD-C added to the well and also used to compare IL-8 release measured from cells incubated with these plates.

To calculate absolute number of biotin-binding sites present in the wells, a standard curve of biotin:atto 680 was created. Varying concentrations of biotin:atto 680 in 6M guanidinium hydrochloride pH 1.5 ranging from 2 μM to picomolar were added to wells of a 96 well flat bottom plate and scanned using the LI-COR system with the 700nm channel at the same intensity used as wells incubated with ST-pD-C. The raw exported values were used to convert raw intensity values of ST-pD-C incubated wells to number of binding sites using equation **2.8**.

$$\#\text{ of binding sites} = [\text{biotin:atto 680}]\ (\text{M}) \cdot \text{volume (L)} \cdot \text{Avogadro's constant} \qquad (2.8)$$

2.17.3 Using 6M guanidinium hydrochloride pH 1.5 to denature StrepTactin-SpyCatcher - biotin:atto 680 interaction

2.17.3.1 Analysing the effect of guanidinium hydrochloride on biotin:atto 680 fluorescence

Concentrations of biotin:atto 680 ranging from 100nM to 0.20nM in either 6M guanidinium hydrochloride pH 1.5 or Milli-Q® H_2O were added to a 96 well flat bottom plate and incubated for 15 minutes. Wells were then scanned using the LI-COR Odyssey Sa system using the 700nm channel. Integrated intensity values in wells with 6M guanidinium hydrochloride pH 1.5 or H_2O alone were subtracted from the corresponding values in wells with biotin:atto 680. These values were then plotted against concentration of biotin:atto 680 added to the well.

2.18 Stimulation of THP-1 SIRPβ1 cells with CHO cells expressing artificial ligands of different lengths coupled to monovalent or tetravalent StrepTactin-SpyCatcher

2.18.1 Measuring IL-8 release from THP-1 cells expressing NTRs incubated with CHO ligand-expressing cells coupled to StrepTactin-SpyCatcher

Positive controls for the experiment were set up as described in section **2.12** by incubating wells of a 96 well flat bottom plate with 0.15 μM ST4-pD-C at 4°C overnight before the plate was washed, blocked and untransduced THP-1 cells or THP-1 SIRPβ1 cells added.

Preparing ligand cells and stimulation of THP-1 cells

Wells were prepared in a similar manner to those described in section **2.12**. Wells of a 96 well filter plate (Merck Millipore Cat. # MSHVN4550) were blocked with sterile PBS, 1% BSA by centrifuging PBS, 1% BSA through the filter at 300 x g for 2 minutes, room temperature, and then leaving fresh PBS, 1% BSA in the wells at 4°C overnight. The

wells were then washed by centrifuging through MES-BSA buffer and the spin-through discarded. Mock transduced CHO cells, CHO CD80-Spy cells or CHO CD80-CD4-Spy cells were washed twice with PBS, 1% BSA, resuspended in MES-BSA buffer and 2 x 10^5 cells added to each appropriate well of the pre-blocked and washed filter plate. The CHO cells within the plate were washed for a final time with MES-BSA buffer before titrating concentrations of ST1-pD-C or ST4-pD-C in MES-BSA buffer were added to the cells. Concentrations of ST1-pD-C and ST4-pD-C used range from 7 μM to 0.3 nM. The plates were gently shaken for 2 minutes before being incubated at room temperature for a further 8 minutes. The coupled cells were then washed in the filter plates three times with PBS, 1% BSA and resuspended in complete DMEM media, 2μg mL^{-1} avidin.
Untransduced THP-1 cells or THP-1 SIRPβ1 cells were washed thrice with sterile PBS, resuspended in complete DMEM media, 2μg mL^{-1} avidin, and 1 x 10^5 cells were added to the appropriate wells in a total volume of 100 μL. Filter plates were shaken gently for 1-2 minutes and incubated at 37°C 10% CO_2 for 20 hours. The supernatants were then centrifuged through the filters into a 96 well flat bottom plate (Thermo Scientific Cat. # 442404) and analysed for IL-8 by ELISA. IL-8 values measured in wells where THP-1 cells were incubated with uncoupled CHO cells were subtracted from the corresponding IL-8 values of THP-1 cells incubated with coupled CHO cells.

Measuring number of biotin-binding sites on ligand cells

CHO CD80-Spy cells and CHO CD80-CD4-Spy cells were washed and coupled with either ST1-pD-C or ST4-pD-C as described above. For the first repeat 2 x 10^5 CHO cells were coupled to ST-pD-C in filter plates. Following coupling and washing of the cells thrice with PBS, 1% BSA, 10 μM biotin:atto 680 was added to each well and incubated for 20 minutes at room temperature. The cells were then washed again with PBS, 1% BSA three times. 6M guanidinium hydrochloride pH 1.5 (50 μL) was added to each well and the plate shaken at room temperature for 10 minutes before the samples were centrifuged through the filter into a fresh 96 well flat bottom plate. The flat bottom plate was then scanned using LI-COR Odyssey Sa scanner using the 700nm channel.
For the second and third repeat 4 x 10^5 CHO cells per well were washed, coupled with ST-pD-C, and biotin:atto 680 added in 96 well conical bottom plates (Sarstedt Cat. # 82.1583.001) (instead of filter plates). For wash steps the plate was centrifuged at 525

x g for 5 minutes, room temperature and supernatant discarded. Following incubation of 6M guanidinium hydrochloride pH 1.5 with the coupled cells, the samples were transferred to a 96 well flat bottom plate before scanning for the biotin:atto 680 signal. 0.5 μM biotin:atto 680 was added to each well of cells during the third repeat instead of 10 μM used in the first and second.

Titrating concentrations of biotin:atto 680 ranging from 2 μM to picomolar in 6M guanidinium hydrochloride pH 1.5 were also added to a 96 well flat bottom plate to create a standard curve. Standard curve plates were scanned in the same manner as the ligand cell test plates.

3. DEVELOPMENT OF THE STRATEGY TO ARTIFICIALLY STIMULATE NON-CATALYTIC TYROSINE-PHOSPHORYLATED RECEPTORS (NTRS)

3.1 Introduction

3.1.1 Using physiological ligands

Upon NTR-ligand binding, prolonged phosphorylation of either intrinsic or associated tyrosine-based motifs is induced which initiates downstream immune signalling of the receptor. The mechanism by which receptor-ligand binding leads to triggering of NTR signalling has yet to be defined. Here we hypothesise that NTRs signal using the kinetic-segregation mechanism and this is a common feature of this group of receptors. To test this, it is possible to study the activation of each NTR with its ligand/s (where the ligand is known) in isolation and then collate this data to look for trends and commonalities between the receptors. This would require many ligand-expressing cell lines. In addition, to investigate specific properties of receptor activation, each receptor-ligand interaction would need to be manipulated. For some of the NTRs a ligand has yet to be identified so we would not be able to investigate these receptors. Together, these reasons led us to pursue an alternative method to permit a systematic, high throughput investigation of the NTRs as a collective group. For this, we aimed to develop a single artificial, generic ligand which can engage any NTR.

It is possible to utilise one well-characterised NTR-ligand interaction. The artificial ligand would be identical to the characterised ligand and each NTR would have its native extracellular region replaced with the extracellular region of the characterised NTR. Each NTR-ligand interaction would therefore be identical in the extracellular portions but each receptor would have its native transmembrane and cytoplasmic regions.

An artificial ligand system that involves as little manipulation of the receptor as possible is more desirable however, in order to keep the receptor environment relatively physiological and maintain native folding of the receptor. We therefore aimed to make use of an established peptide-protein interaction. The small peptide would be fused to the extracellular region of each NTR thus allowing all tagged receptors to be ligated by a single ligand fused to the protein binding partner. Ideally the protein binding partner will engage the peptide monovalently, and the peptide and binding partner pair will bind with a relatively physiological affinity to replicate native NTR-ligand interactions.

3.1.2 Utilising interactions used in biotechnology

A number of peptide tags are unsuitable for the system. For example, the interaction between Glutathione-S-transferase (GST) and glutathione is commonly used for affinity protein purification but GST is a relatively large protein ($\sim$25 kDa) and has also been shown to exist as a homodimer [Ji et al., 1992, Armstrong, 1997]. Much smaller peptide tags have been developed, for example FLAG^{TM} tag, HA-tag, c-Myc tag, but purification uses antibodies to the tag rather than small, protein binding partners [Hopp et al., 1988, Field et al., 1988, Evan et al., 1985]. The S-tag - S-protein interaction could be utilised but has a very high affinity [Connelly et al., 1990].

The interaction between biotin (vitamin H) and streptavidin is commonly used in biotechnology. The vitamin and tetrameric streptavidin bind with a dissociation constant of $\sim$ 4 x 10 $^{-14}$ M (first reported in [Green, 1990]). Biotin will also bind to an analagous protein, avidin, with a similar dissociation constant ($\sim$ 0.6 x 10^{-15} M) [Green, 1990]. While this affinity is too high to replicate physiological receptor-ligand interactions there are variants of the biotin-streptavidin interaction which are more useful, specifically Strep-Tag II-StrepTactin. StrepTactin is identical to streptavidin apart from 3 amino acid mutations (E44V, S45T, V47R) and is able to bind both biotin and a short peptide tag named Strep-Tag II [Voss and Skerra, 1997a]. The affinity between Strep-Tag II and StrepTactin at $K_D \sim$ 1 x 10^{-6} M is much lower than that for biotin-streptavidin and is also the most physiological affinity of the various interaction combinations (shown in table **3.1**).

Other small peptide tags that bind streptavidin, for example Streptavidin-Binding Peptide

Pairing	Dissociation constant K_D	Reference/s
Strep-Tag II - StrepTactin	$\sim$ 1 x 10^{-6} M	[Voss and Skerra, 1997a] [Schmidt et al., 2013]
biotin - StrepTactin	< 1 x 10^{-13} M (estimated)	[Knabel et al., 2002]
Strep-Tag II - streptavidin	13 x 10^{-6} - 72 x 10^{-6} M	[Voss and Skerra, 1997a] [Schmidt et al., 1996]
biotin - streptavidin	$\sim$ 4 x 10^{-14} M	[Green, 1990]

Tab. 3.1: **Dissociation constants measured or estimated for interactions between Strep-Tag II or biotin, and StrepTactin or streptavidin.**

(SBP)-tag and nano-tag, do so with a higher affinity than Strep-Tag II does, and the interaction of these tags with StrepTactin has yet to be characterised [Keefe et al., 2001, Wilson et al., 2001, Lamla and Erdmann, 2004]. We therefore sought to use the pairing between Strep-Tag II and StrepTactin as the artificial receptor-ligand interaction.

Like streptavidin, StrepTactin exists as a tetramer with four binding sites for Strep-Tag II, whereas we only require one. A fusion protein of a streptavidin mutant that is monomeric has been created for cell surface expression but the biotin-binding property was not detected [Gotoh and Matsumoto, 2007]. This is likely because the binding site of biotin lies at the interface of streptavidin subunits [Sano and Cantor, 1995, Weber et al., 1989, Chilkoti et al., 1995]. The binding site of Strep-Tag II on StrepTactin/streptavidin overlaps that of biotin (shown in figure **3.1**) and so it is likely that creating a monomeric StrepTactin would similarly affect the Strep-Tag II-binding affinity [Schmidt et al., 1996].

More recently, monomeric streptavidin that retains its biotin-binding property was created. The affinity of monomeric streptavidin for biotin was significantly reduced however from a K_D value in the femtomolar range to nanomolar [Lim et al., 2013, Qureshi et al., 2001]. It is possible that introducing the same mutations into StrepTactin would similarly decrease its affinity for Strep-Tag II.

Avidin mutants that are monomeric have also been made. Like for streptavidin, introduction of the mutations necessary to express avidin as a monomer reduced the affinity for biotin from a K_D value in the femtomolar range to above nanomolar [Laitinen et al., 2003]. Other monomeric avidin mutants were also created but these were shown to

reform tetramers upon addition of biotin [Laitinen et al., 2001].

Using a method developed by Howarth et al., it is possible to express streptavidin as a tetramer but with different valencies. This uses a mutated streptavidin subunit that has negligible biotin-binding activity, termed 'dead streptavidin'. The approximate dissociation constant of dead streptavidin binding to biotin is $\sim$ 1.2 x 10^{-3} M [Howarth et al., 2006]. Individual subunits of streptavidin are refolded with dead streptavidin subunits at different ratios to create tetramers of different valencies [Howarth et al., 2006]. We postulate that similarly refolding StrepTactin subunits with dead streptavidin could yield StrepTactin tetramers of different valency.

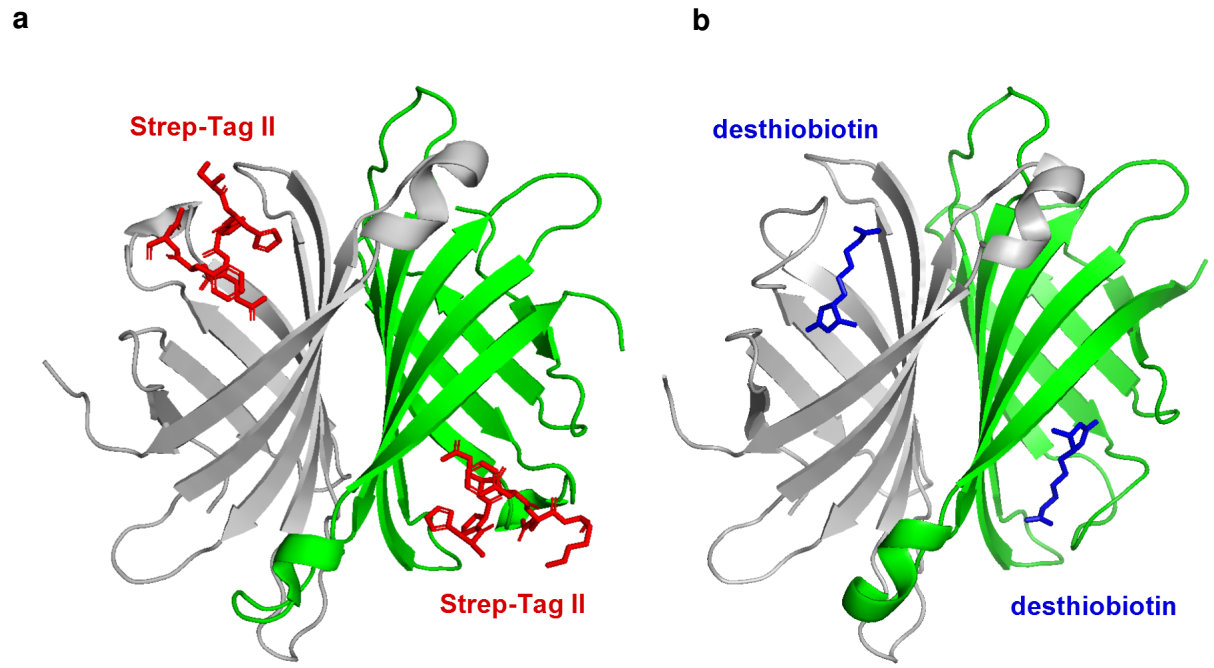


Fig. 3.1: **Strep-Tag II and desthiobiotin occupy the same binding site on Strep-Tactin.** The structure of StrepTactin bound by either Strep-Tag II ■ (**a**) or desthiobiotin ■ (**b**) shows the peptide and biotin derivative share the same binding site. The structure of desthiobiotin in complex with dimeric StrepTactin only was obtained (PDB accession # 4DNE) [Panwar et al., 2012]. StrepTactin in complex with Strep-Tag II is also shown as a dimer for comparison purposes (PDB accession # 1KL3) [Korndörfer and Skerra, 2002]. Both figures were created using PyMOL.

3.1.3 First generic ligand strategy

We will construct NTR plasmids such that they have an N-terminal Strep-Tag II (or C-terminal if the receptor is a type II transmembrane protein). An example tagged NTR is shown in cartoon form in figure **3.2**a. The Strep-Tag II will then be ligated by the generic

ligand made of StrepTactin bound to a cell surface-expressed protein.

The biotin-binding activity of StrepTactin will be utilised to allow it to bind to a cell surface-expressed ligand protein. It has previously been shown that proteins containing a biotin ligase target sequence termed Avitag can be biotinylated in vivo and then expressed on the surface of mammalian cells. For this, cells are co-transfected with a plasmid encoding the BirA biotin ligase with an endoplasmic reticulum retention signal sequence and a second plasmid encoding the Avitagged target protein [Howarth et al., 2008]. We will use this method to create cell lines expressing a generic protein with N-terminal Avitag for biotinylation. This generic protein will make up the surface-expressed component of the artificial ligand. Ideally the ligand protein will be a single-pass transmembrane protein that is easily expressed by mammalian cells, does not form homodimers or interact with other proteins expressed on the cell surface, and finally has no signalling activity itself.

Trans-bivalent StrepTactin will be expressed, purified and then added to the biotinylated ligand-expressing cell lines such that one of the binding sites binds to the biotinylated transmembrane protein leaving the other free for Strep-Tag II-tagged receptor binding (figure **3.2b**). Trans-bivalent StrepTactin bound to the biotinylated transmembrane protein constitutes the generic ligand. We predict that bivalent StrepTactin with binding sites in a trans orientation will allow ligation of both biotinylated ligand and tagged receptor simultaneously. A method for purifying trans-bivalent streptavidin has already been developed which we will use to generate trans-bivalent StrepTactin [Fairhead et al., 2014a].

Figure **3.2c** depicts the entire receptor-artificial ligand complex. By adding trans-bivalent StrepTactin to biotinylated ligand-expressing cells in excess and at 4°C to slow kinetics, we postulate that a significant portion of bivalent StrepTactin will bind monovalently to the biotinylated protein allowing interaction between receptor and ligand. With a dissociation constant around a million fold lower than for Strep-Tag II-StrepTactin, the interaction between biotin and StrepTactin will be much more stable (values in table **3.1**).

This system can be manipulated to investigate a number of questions about receptor triggering. The number of ligands per cell will be controlled by pre-mixing trans-bivalent

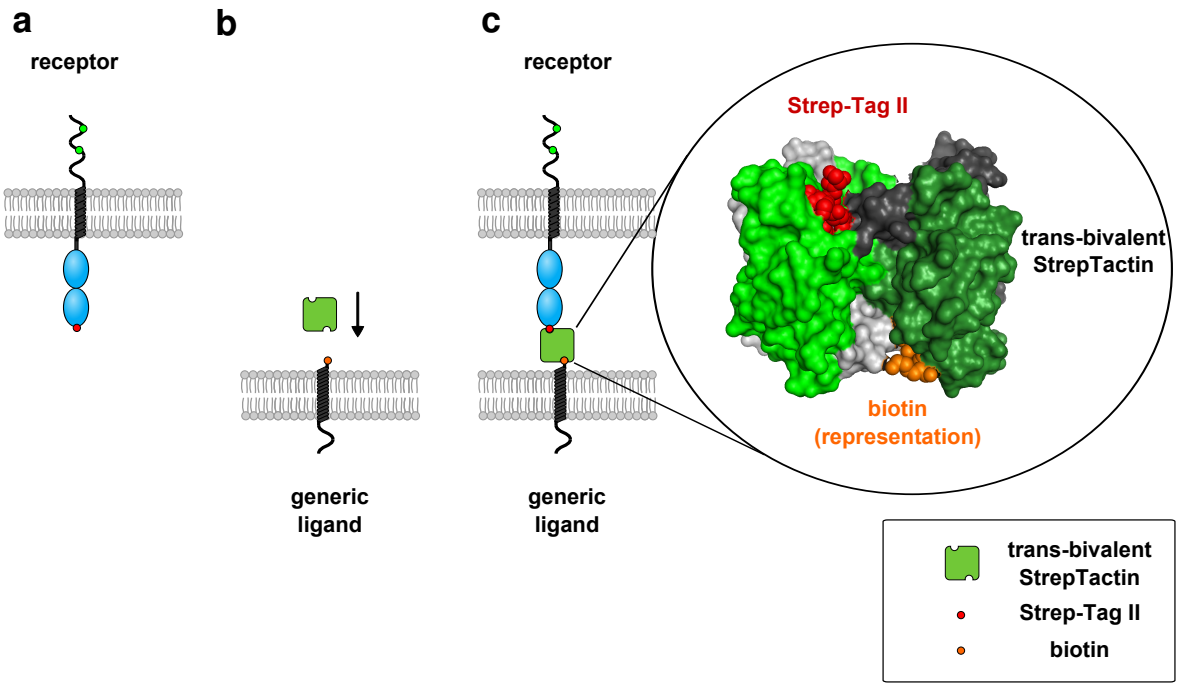


Fig. 3.2: **Generic ligand system design.** Each NTR is constructed with a Strep-Tag II at the extracellular terminus and expressed in cell lines (**a**). Trans-bivalent StrepTactin is incubated with cells expressing a biotinylated transmembrane protein (biotin) to form the generic ligand complex (**b**). Trans-bivalent StrepTactin will bind to the biotinylated protein with one binding site leaving the other available for ligation of the tagged NTR (**c**). The structure of StrepTactin with a single Strep-Tag II bound is also shown. Biotin is displayed on this structure in a representative form only to illustrate the complex. This figure is modified from a figure created by Dr Jesse Goyette. The structure was visualised using PyMOL (PDB accession # 1KL3) [Korndörfer and Skerra, 2002].

StrepTactin with monovalent StrepTactin at different ratios before adding the mixture to ligand-expressing cells. Monovalent StrepTactin will bind to biotinylated ligand but will not be able to ligate a tagged NTR so at lower ratios of trans-bivalent to monovalent StrepTactin fewer ligands per cell will be available for receptor interaction. This method is illustrated in figure **3.3a**. Alternatively, ligand-expressing cells could be saturated with trans-bivalent StrepTactin and then different concentrations of biotin added to block varying numbers of the ligand.

The effect of altering the dimensions of receptor-ligand interactions will also be investigated. The extracellular region of the generic ligand will be elongated by insertion of inert domains to create a set of ligands of different size that can be used to ligate any tagged NTR (figure **3.3b**).

The stoichiometry of receptor-ligand interactions can also be altered using StrepTactin of different valencies. The response of receptor-expressing cells when engaged by trivalent or tetravalent StrepTactin will be compared to the response when receptors are bound by bivalent StrepTactin. Thus the effect of bringing receptors into close proximity on their activation will be analysed (figure **3.3c**).

Finally, the affinity of StrepTactin for Strep-Tag II (and so the affinity of the receptor for the ligand) can be altered by creating StrepTactin mutants. By doing this, the activation of NTRs in response to ligands of different affinity can be compared (figure **3.3d**). Streptavidin mutants with various affinities for biotin and Strep-Tag II have already been developed and so would be of use to us here [Reznik et al., 1998, Chu et al., 1998, Meyer et al., 2001, Aslan et al., 2005, Magalhães et al., 2011].

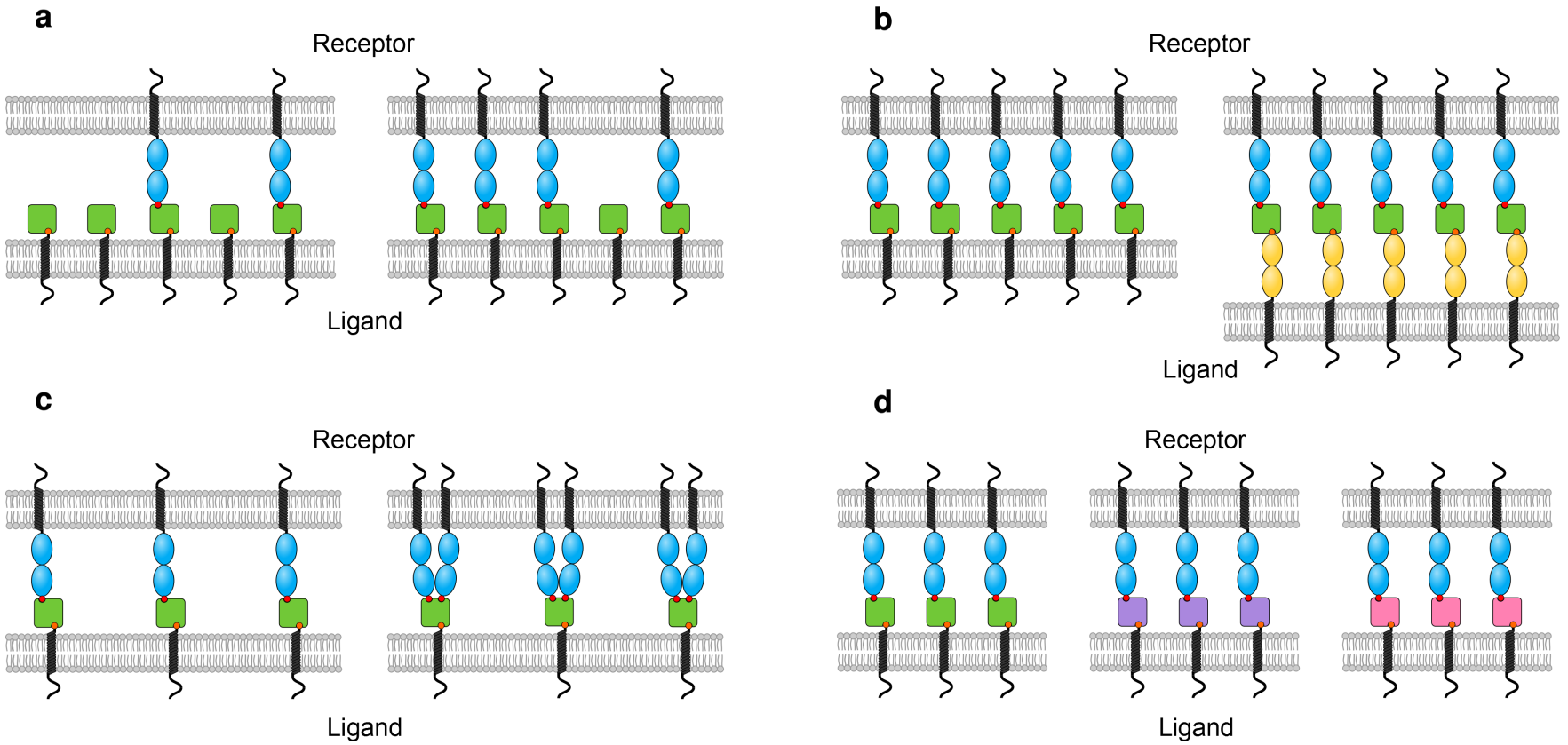


Fig. 3.3: **A number of properties of the NTR-ligand interaction can be investigated using the artificial ligand system.** By incubating ligand cells with different ratios of monovalent StrepTactin and trans-bivalent StrepTactin (the tetramers are shown in green) the number of ligands per cell can be varied (**a**). The extracellular region of the generic ligand can be elongated. Receptor responses to cells expressing this elongated ligand can be compared to responses by NTRs ligated with the shorter ligand (**b**). Ligand cells can be incubated with trivalent or tetravalent StrepTactin to analyse the effect of small-scale receptor clustering on signalling (**c**). Mutated forms of StrepTactin/streptavidin with different affinities for Strep-Tag II can be used to form the generic ligand complex and presented to NTRs (**d**). StrepTactin of different affinities are shown as different colours.

3.1.4 Second generic ligand strategy

The second strategy that will be used for some of the presented work does not involve the interaction between StrepTactin and biotinylated protein. Instead, the interaction between the peptide SpyTag and its binding partner SpyCatcher will be used. The two components are derived from the fibronectin-binding protein (FbaB) of *Streptococcus pyogenes*. The immunoglobulin-like collagen adhesin domain from this protein has been shown to be stabilised by an intramolecular covalent bond formed between two regions of the domain [Oke et al., 2010, Hagan et al., 2010]. When the two regions are expressed separately as a peptide (SpyTag) and binding partner (SpyCatcher), they will couple to form a spontaneous, irreversible, isopeptide bond [Zakeri et al., 2012, Li et al., 2014].

The surface-expressed generic ligand protein of the second strategy will have an N-terminal SpyTag instead of Avitag (figure **3.4**). StrepTactin will be expressed and purified but as a fusion protein of monovalent StrepTactin and a single SpyCatcher at the C-terminus of the StrepTactin subunit. This fusion protein will consist of 3 "dead" streptavidin subunits and a single StrepTactin subunit fused to the SpyCatcher. SpyCatcher fusion proteins have previously been successfully created [Zhang et al., 2013, Sun et al., 2014, Nguyen et al., 2014]. Monovalent StrepTactin-SpyCatcher will be covalently conjugated to the SpyTagged generic protein expressed on the ligand cell surface leaving the single binding site available for ligation of the NTR. The components of the system are outlined in figure **3.4**.

This system is as flexible as the first and so can be used to ask the same questions. By adding different concentrations of StrepTactin-SpyCatcher to the ligand cells, the number of ligands per cell will be controlled. The role of receptor-ligand dimensions in signalling will also be explored by again creating a set of generic ligands with different length extracellular regions. By refolding a single StrepTactin-SpyCatcher subunit with three StrepTactin (no SpyCatcher) subunits instead of "dead" streptavidin, tetravalent StrepTactin-SpyCatcher will be synthesised and used to investigate the effect of increasing ligand valency on receptor activation. Note that tetravalent StrepTactin-SpyCatcher will have four Strep-Tag II-binding sites but only one SpyCatcher. Finally, mutated forms

of StrepTactin-SpyCatcher that have different affinities for Strep-Tag II can be created and used to explore the role of affinity in receptor signalling.

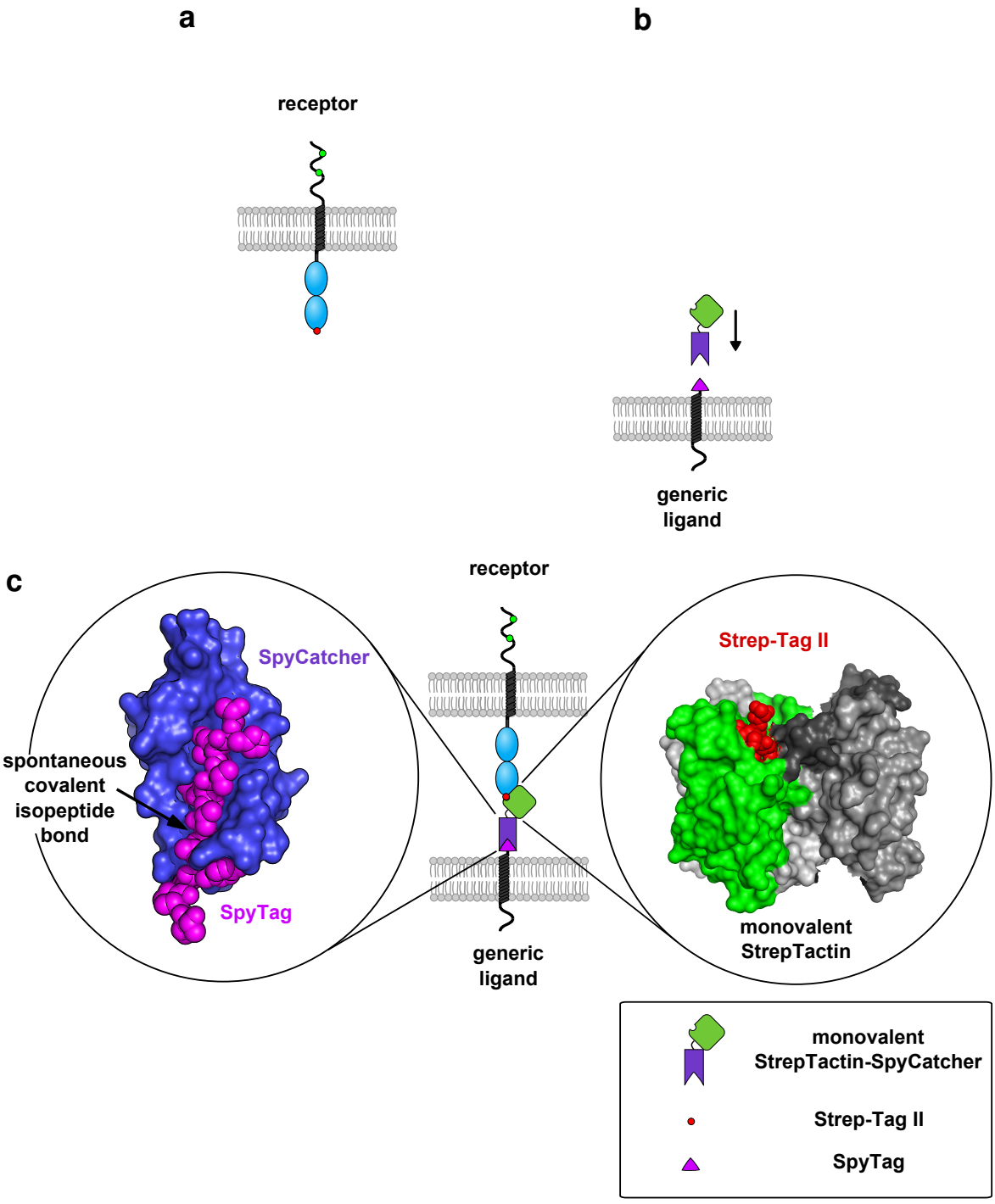


Fig. 3.4: **Second generic ligand system design.** Just as with the first system each NTR is constructed with a Strep-Tag II at the extracellular terminus and expressed in cell lines (**a**). Monovalent StrepTactin-SpyCatcher (StrepTactin , SpyCatcher) is incubated with cells expressing a SpyTagged transmembrane protein allowing a covalent bond to form between SpyTag and SpyCatcher. This complex forms the generic ligand (**b**). The single binding site of monovalent StrepTactin-SpyCatcher is available for ligation of the tagged NTR (**c**). The structure of StrepTactin with a single Strep-Tag II bound is shown. The structure of the SpyTag-SpyCatcher complex is also shown. This figure is modified from a figure created by Dr Jesse Goyette. Structures were visualised using PyMOL (PDB accession # 4MLI and # 1KL3 [Li et al., 2014, Korndörfer and Skerra, 2002]).

3.2 Results

3.2.1 Cloning of receptor and adaptor protein constructs

In order to clone both type I and II transmembrane protein NTRs two sequences were designed and synthesised using the GENEWIZ gene synthesis service and inserted into the pHR-SIN-BX-EmGFP plasmid, replacing the EmGFP sequence. Illustrations of these plasmids, referred to as Type I and Type II plasmid, are shown in figure 3.5. Cloning of NTRs into multiple cloning site I (MCS I) of these plasmids means that when expressed, the NTR will have a Strep-Tag II tag at the extracellular terminus (to enable binding to artificial ligand) and FLAG tag at the intracellular terminus (to enable immunoprecipitation and detection of the receptor). Each plasmid also has a second multiple cloning site (MCS II) to permit insertion of further sequences, for example fluorescent proteins, into the intracellular region of the receptor.

Table **3.2** summarises the cloned NTRs. Cartoon diagrams of the receptors and adaptor proteins that have been cloned are shown in figure **3.6**. NKG2D is shown as a dimer in accordance with the crystal structure of NKG2D in complex with its ligand MHC class I polypeptide-related sequence A (MICA) [Li et al., 2001] . DAP10, DAP12, and FcRγ are also shown as dimers in accordance with evidence that they exist as dimers in the membrane [Garrity et al., 2005, Lanier et al., 1998, Perez-Montfort et al., 1983]. For simplicity, the plasmids containing representative NTRs that have been cloned are hereafter referred to by the plasmid and receptor name, for example, Type I LAIR-1 or Type II NKG2D or just the receptor name, for example, LAIR-1 or NKG2D.

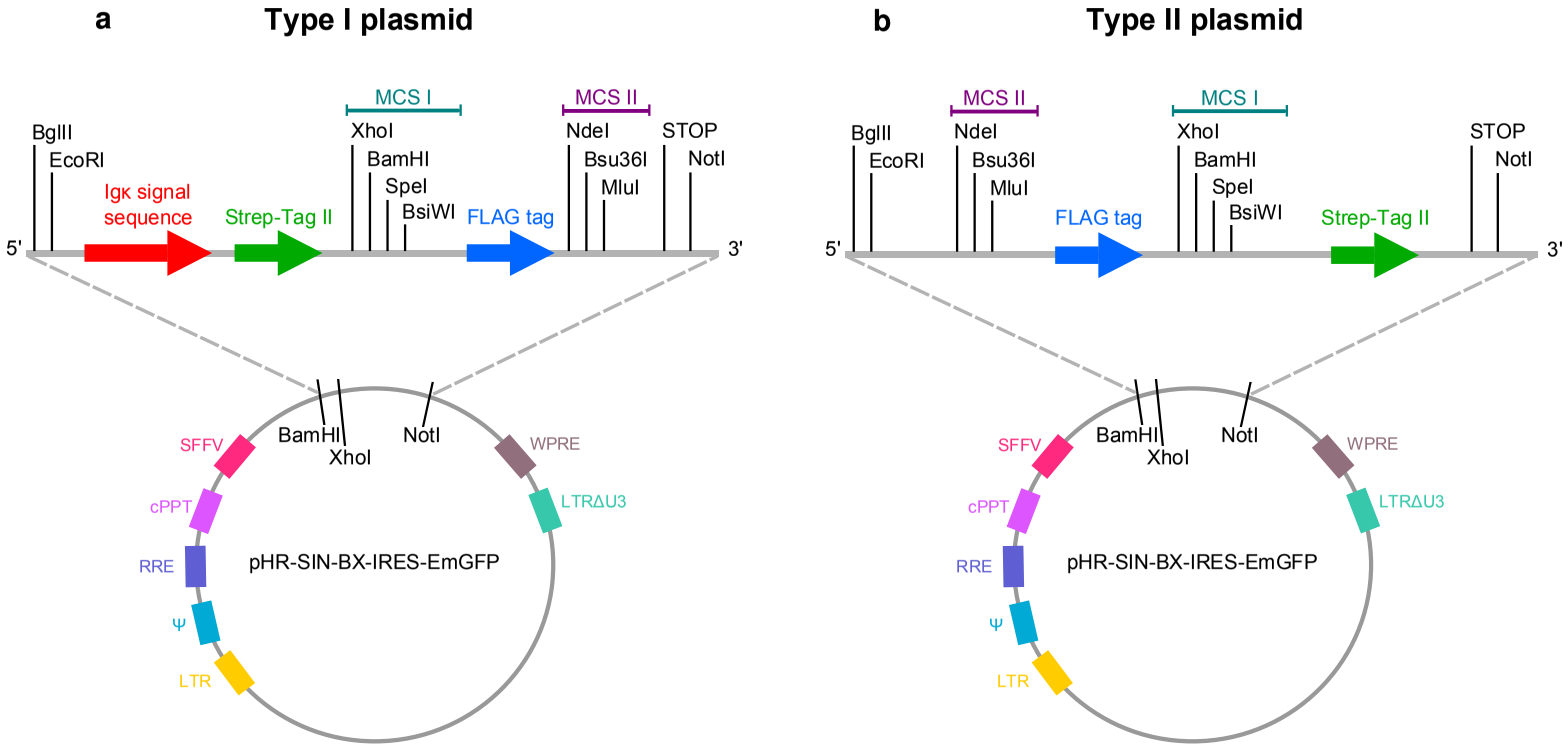


Fig. 3.5: **Type I and Type I plasmid design.** DNA sequences for expressing NTRs in mammalian cells with extracellular Strep-Tag II and intracellular FLAG tag were inserted between the BamHI and NotI sites of pHR-SIN-BX-IRES-EmGFP plasmid to create the Type I plasmid (a) for type I transmembrane protein NTRs and the Type II plasmid (b) for type II transmembrane protein NTRs. Type I NTRs will use the Igκ mammalian signal sequence. The FLAG tag in the Type II plasmid is immediately preceded by a methionine to ensure the FLAG tag is translated. NTRs can be cloned into Multiple Cloning Site I (MCS I) while extra sequences can be cloned into Multiple Cloning Site II (MCS II). LTR - long terminal repeat, ψ packaging signal, RRE - Rev response element, cPPT - HIV central polypurine tract, SFFV - Spleen focus forming virus promoter, WPRE - Woodchuck hepatitis virus post-transcriptional regulatory element, LTRδU3 - Long terminal repeat, transcriptional activator of HIV

NTR cloned	Type I/II	Adaptor	Activating/Inhibitory
2B4	I	-	Both
CD5	I	-	Inhibitory
FcγRIA	I	Fc$R\gamma$	Activating
LAIR-1	I	-	Inhibitory
NKG2D	II	DAP10	Activating
NKp30	I	CD3ζ Fc$R\gamma$	Activating
NKp44	I	Fc$R\gamma$	Activating
PD-1	I	-	Inhibitory
SIGLEC-14	I	DAP12	Activating
SIRPβI	I	DAP12	Activating

Tab. 3.2: **Representative non-catalytic tyrosine-phosphorylated receptors cloned into either the Type I or Type II plasmid.** Both activating and inhibitory NTRs were cloned. Receptors that do not use an adaptor protein for signalling, and also those that use either Fc$R\gamma$, DAP10 or DAP12 adaptor proteins were also cloned.

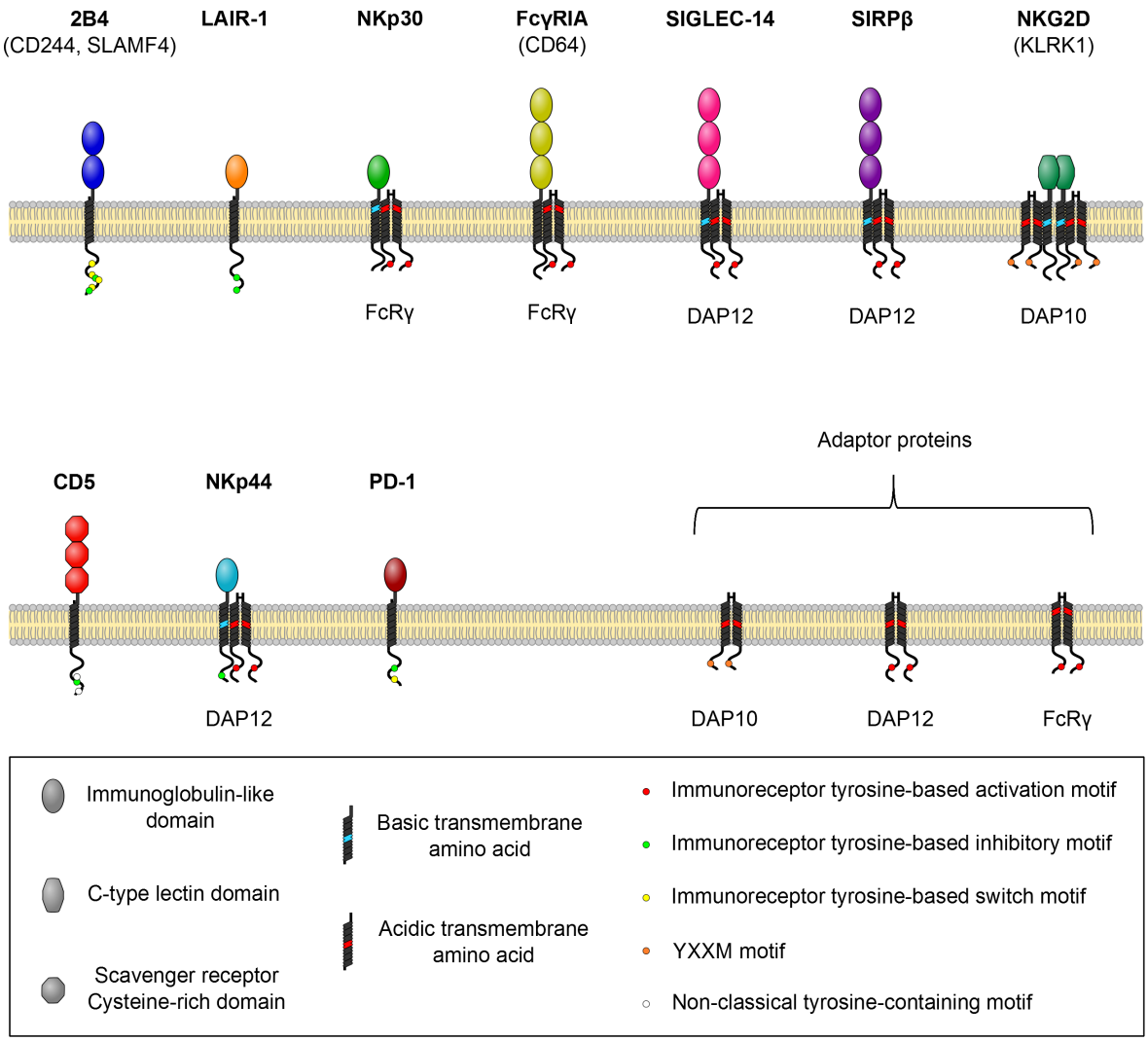


Fig. 3.6: **Representative NTRs and adaptor proteins.** Representative NTRs that have been cloned into the corresponding plasmid (either Type I or Type II) are labelled and shown in cartoon form in a cell membrane. Where appropriate, the receptor is drawn in complex with the adaptor protein it uses for signalling. This interaction is mediated by basic transmembrane residues in the receptor (shown in blue ▬) and acidic transmembrane residues in the adaptor (shown in red ▬). The three adaptor proteins DAP10, DAP12 and FcRγ are also shown alone in dimer form. The tyrosine-based signalling motifs used by each receptor are also highlighted. NKG2D is shown in dimer form. This figure is modified from a version created by Dr Jesse Goyette.

Following transduction of Type II NKG2D into Jurkat cells and THP-1 cells (presented and discussed in sections 3.2.2.1 and 3.2.2.3) we found that the Strep-Tag II was inaccessible to antibody binding and therefore would likely not engage artificial ligand. This was supported by the NKG2D X-ray crystal structure (PBD accession 1HYR) where the C terminus appears to lie in a position likely very close to the cell membrane (figure **3.7a**) [Li et al., 2001]. To improve accessibility of the tag, we designed alternative NKG2D constructs: one with a 15 amino acid linker between the NKG2D C terminus and Strep-Tag II (Type II NKG2D-1x linker or NKG2D-1x linker), one with 2 copies of the 15 amino acid linker between the NKG2D C terminus and Strep-Tag II (Type II NKG2D-2x linker or NKG2D-2x linker), and one where the Strep-Tag II sequence was instead inserted into the β5'-β5 stirrup loop of the NKG2D C-type lectin domain (Type II NKG2D-loop or NKG2D-loop). The position of insertion, highlighted in figure **3.7**, was predicted to be exposed by analysis of the NKG2D structure, and also positioned away from the surface of NKG2D homodimer interactions [Li et al., 2001].

Many NTRs do not contain cytoplasmic tyrosine-based motifs for signalling but instead associate with adaptor proteins which contain the motifs. We therefore inserted human DAP10, DAP12 or FcRγ into pHR-SIN-BX-IRES-EmGFP with an intracellular c-Myc tag, and the IRES-EmGFP sequence retained. The IRES-EmGFP sequence enables easy analysis of tagged-adaptor protein expression in mammalian cells. These plasmids are hereafter referred to as pHR DAP10_EmGFP (or DAP10_EmGFP), pHR DAP12_EmGFP (or DAP12_EmGFP) and pHR FcRγ_EmGFP (or FcRγ_EmGFP). Cartoon diagrams of the adaptor proteins are shown in figure **3.6**.

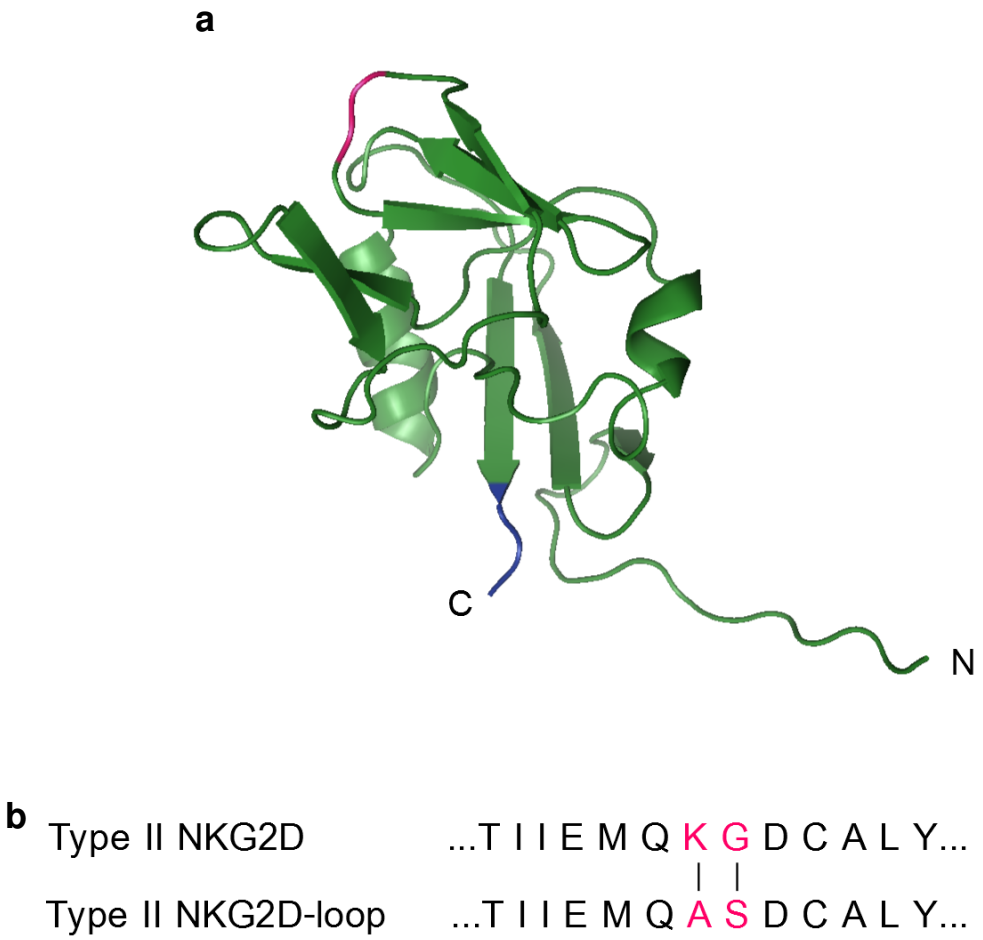


Fig. 3.7: **NKG2D structure and sequence changes.** (**a**) The structure of the C-type lectin domain of human NKG2D with C terminal amino acids highlighted in blue ▬. For Type II NKG2D, the Strep-Tag II sequence was inserted at the C terminus. The C terminus is also the site where one or two 15 amino acid linkers were inserted to create Type II NKG2D-1x linker and NKG2D-2x linker respectively. To create Type II NKG2D-loop, amino acids # 186 and 187 (highlighted in pink ▬) were altered. A small section of the amino acid sequence of NKG2D is shown in **b** with altered amino acids highlighted in pink ▬. Position 186 was altered from basic polar lysine to hydrophobic neutral alanine, and position 187 was altered from non-polar neutral glycine to polar neutral serine. **a** is based on the published X-ray crystal structure (PDB accession 1HYR) [Li et al., 2001]. Structure was visualised using PyMOL.

3.2.2 Transduction of human cell lines with tagged NTRs and adaptor proteins

Four human cell lines were investigated as lines in which to express NTRs and their adaptor protein, if appropriate. These are the CD4+ T cell line Jurkat, the NK cell lines NKL and NK92, and the monocytic line THP-1. The receptors 2B4, FcγRIA, LAIR-1, NKG2D, NKp30, SIGLEC-14 and SIRPβI were those chosen to transduce into the 4 cell lines. Table **3.2.2** indicates the cell lines relevant to this work that these receptors are, or are not, expressed in.

Receptor	**Cell lines the receptor is expressed by**	**Cell lines the receptor is not expressed by**	**References**
2B4	CD4+ T cells (low levels) NK cells monocytes		[Romero et al., 2004]
FcγRIA	THP-1 cells	Jurkat cells	[Fleit and Kobasiuk, 1991] [Zhang et al., 2015a]
LAIR-1	Jurkat cells THP-1 cells	NKL cells NK92 cells	[Meyaard et al., 1997] [Kang et al., 2015]
NKG2D	NKL		[Wu et al., 2011] [Jimenez-Perez et al., 2012]
NKp30	NKL		[Pende et al., 1999]
SIGLEC-14	monocytes	CD4+ T cells THP-1 cells	[Yamanaka et al., 2009] [Ali et al., 2014]
SIRPβ1	monocytes	T cells	[Dietrich et al., 2000] [Piccio et al., 2005]

Tab. 3.3: **Some of the NTRs are normally expressed by a number of the cell lines used for receptor expression.** The representative NTRs are listed along with the cell lines used in this work they have been shown to be expressed by and also cell lines they are not expressed by. In some cases, where cell line data does not exist, the primary cell types that do or do not express the receptors are listed.

3.2.2.1 Transduction of Jurkat cells

Jurkat transduction with 2B4, LAIR-1 and NKp30

Jurkat cells were investigated as a cell line in which to express Strep-Tag II-tagged NTRs. Lentiviral particles of 2B4, LAIR-1 or NKp30 constructs, collected 24 hours after transfection of packaging cells, were transduced into Jurkat cells. This lentiviral transduction yielded cell populations with high levels of receptor surface expression (figure **3.8a-c**). Transductions and flow cytometry analysis of protein expression was conducted by Dr Jesse Goyette. Re-analysis of receptor surface expression following cell sorting with magnetic beads showed a much higher proportion of cells expressing the individual receptors (figure **3.8d-f**). In addition to FcRγ, NKp30 associates with CD3ζ as a signalling adaptor [Pende et al., 1999]. NKp30 transduced into Jurkat cells will therefore associate with endogenous CD3ζ present in these cells.

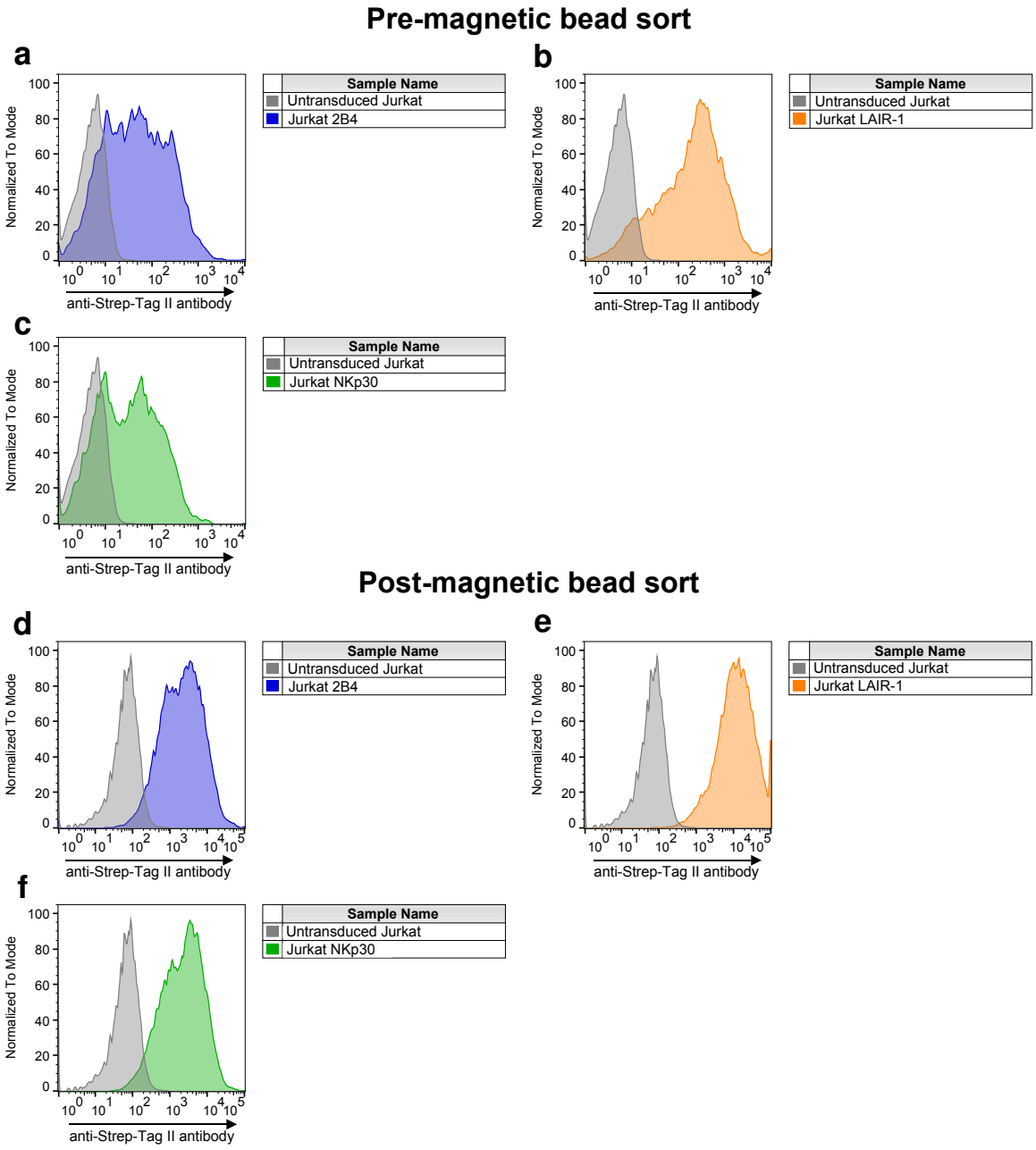


Fig. 3.8: **Jurkat cells transduced with 2B4, LAIR-1 or NKp30 and sorted with magnetic beads express high levels of the NTR.** Strep-Tag II-tagged receptor surface expression of Jurkat cells transduced with 2B4 (**a**), LAIR-1 (**b**) or NKp30 (**c**) was analysed by flow cytometry using anti-Strep-Tag II antibody staining. Transductions and flow cytometry was conducted by Dr Jesse Goyette. The cell lines were then sorted by magnetic beads coated with anti-Strep-Tag II antibody and re-analysed by flow cytometry for surface expression (**d**-**f**).

Jurkat transduction with FcγRIA, SIRPβI and SIGLEC-14

Jurkat cells transduced with lentivirus of either FcγRIA and FcRγ_EmGFP, or SIGLEC-14 and DAP12_EmGFP, or SIRPβI and DAP12_EmGFP were analysed for expression of the NTR and adaptor. Adaptor protein expression was inferred from expression of EmGFP which is encoded with an IRES sequence on the same plasmid as the adaptors. A significant population of cells in all three cell lines were positive for both proteins (figure **3.9**). The proportion of double positive cells within the populations increased after sorting them for high receptor expression using anti-Strep-Tag II antibody-coated magnetic beads (figure **3.10**). The proportions of cells positive for both NTR and adaptor protein then increased further following FACS sorting (figure **3.11**). There is also a good correlation between receptor and adaptor protein expression in these sorted cell lines (figure **3.11**).

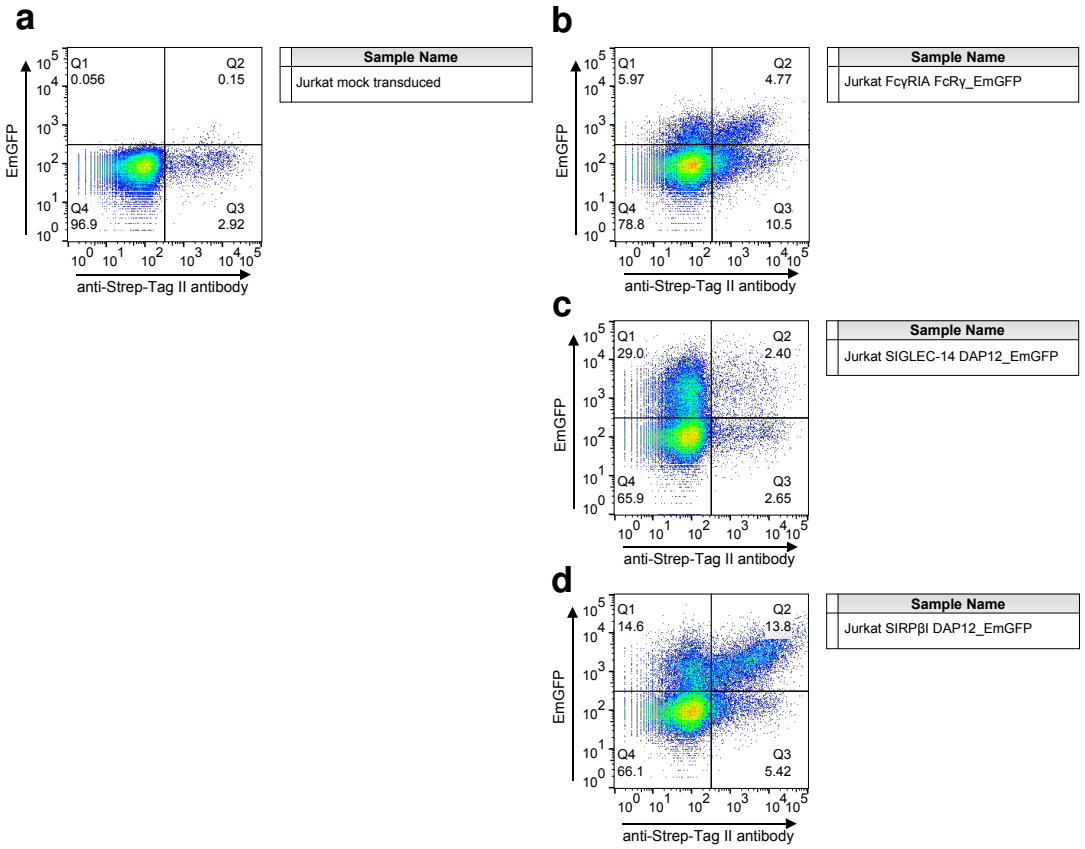


Fig. 3.9: **Jurkat cells transduced with either FcγRIA and FcRγ, or SIGLEC-14 and DAP12, or SIRPβI and DAP12, express both receptor and adaptor protein.** Jurkat cells that were mock transduced (**a**), or transduced with either FcγRIA and FcRγ_EmGFP (**b**), or SIGLEC-14 and DAP12_EmGFP (**c**), or SIRPβI and DAP12_EmGFP (**d**), were analysed for receptor surface expression (x-axis) using anti-Strep-Tag II antibody by flow cytometry. The cells were also analysed for adaptor protein expression (y-axis) making use of the EmGFP signal encoded on the same plasmid as each adaptor protein.

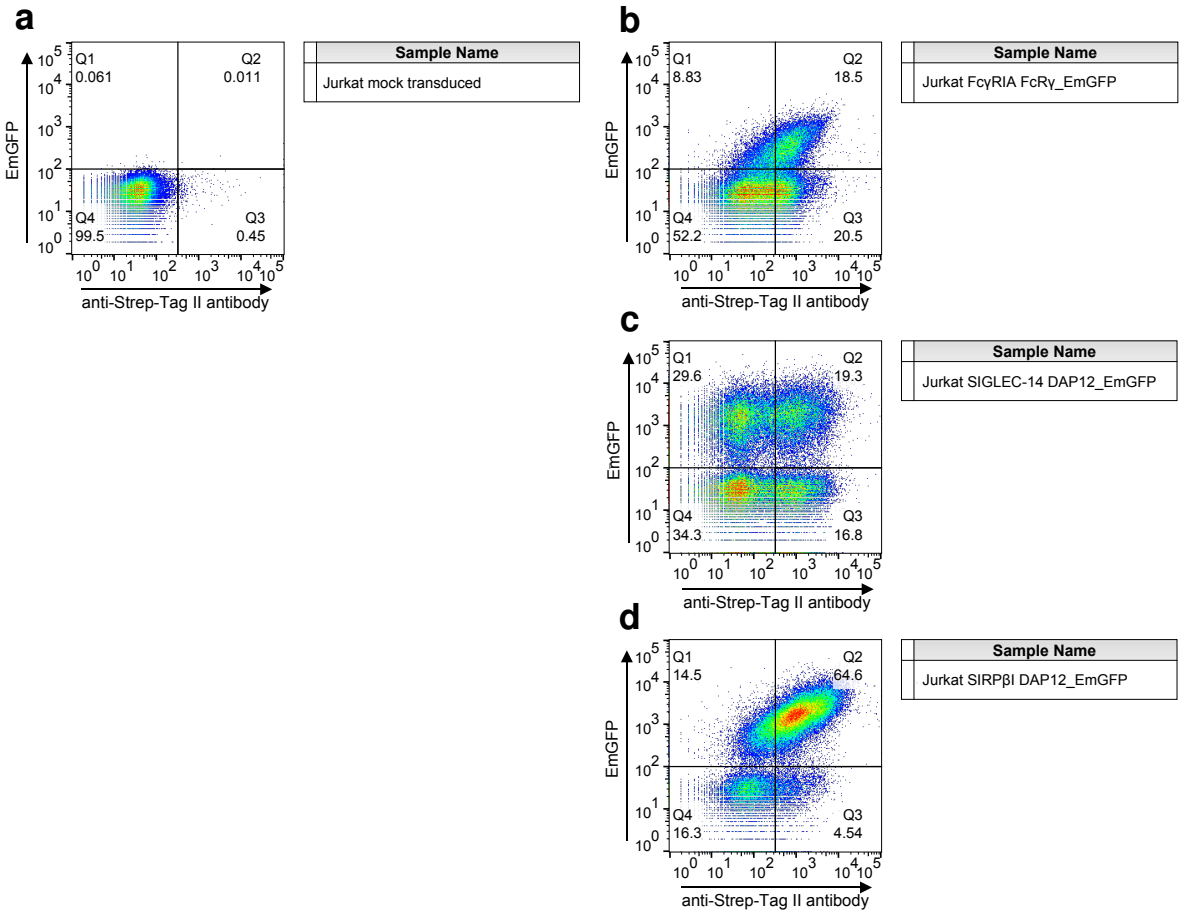


Fig. 3.10: **Jurkat cell lines sorted using magnetic beads express both receptor and adaptor protein.** Jurkat cells (**a**) were analysed by flow cytometry for non-specific antibody binding (x-axis) and background fluoresence in the channel used for adaptor protein signal (y-axis). Jurkat FcγRIA FcRγ_EmGFP cells (**b**), Jurkat SIGLEC-14 DAP12_EmGFP cells (**c**) and Jurkat SIRPβI DAP12_EmGFP cells (**d**) from figure **3.9** were sorted using anti-Strep-Tag II antibody-coated magnetic beads and then re-analysed by flow cytometry for receptor surface expression (x-axis) using anti-Strep-Tag II antibody. The cells were also analysed for adaptor protein expression (y-axis) making use of the EmGFP signal encoded on the same plasmid as each adaptor protein.

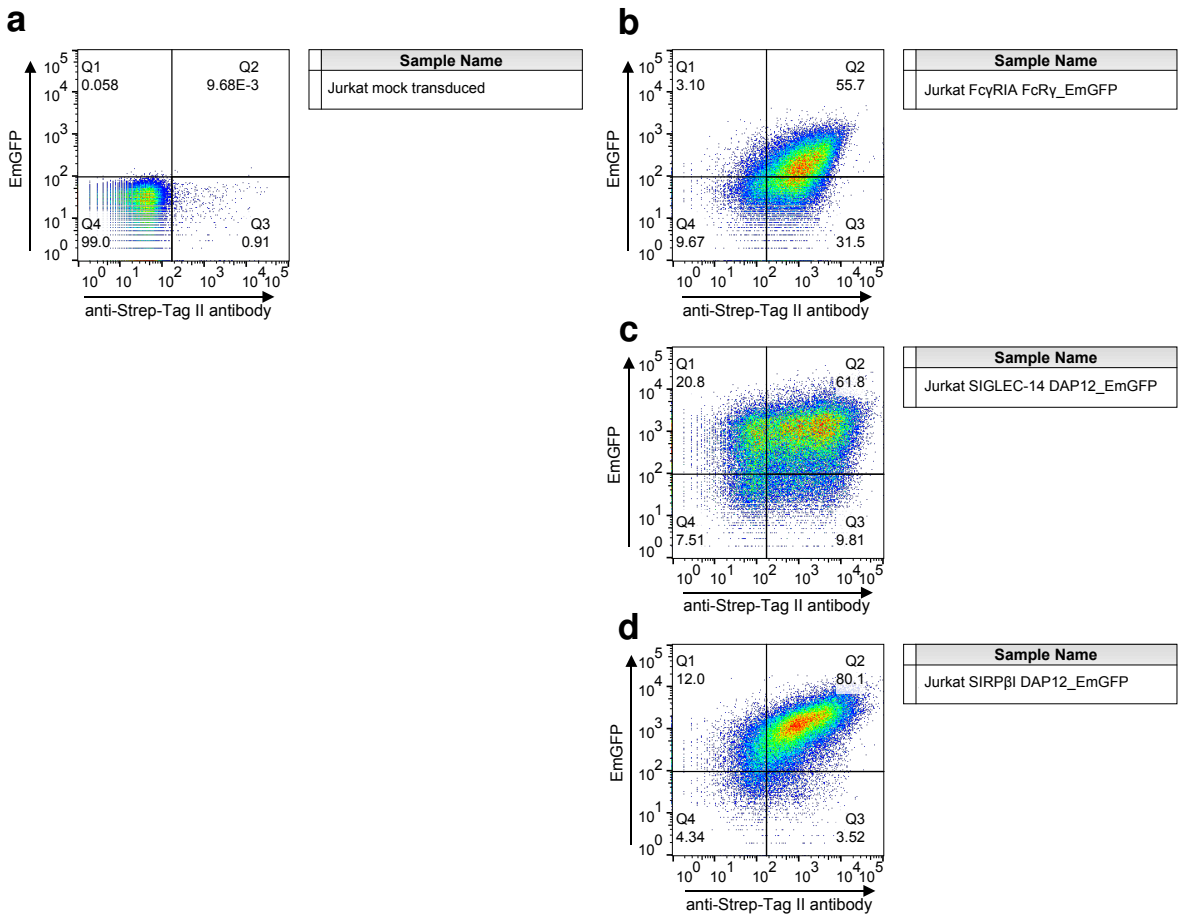


Fig. 3.11: **Jurkat cell lines sorted by FACS express both receptor and adaptor protein.** Jurkat cells (**a**) were analysed by flow cytometry for non-specific antibody binding (x-axis) and background fluoresence in the channel used for adaptor protein signal (y-axis). Jurkat FcγRIA FcRγ_EmGFP cells (**b**), Jurkat SIGLEC-14 DAP12_EmGFP cells (**c**) and Jurkat SIRPβI DAP12_EmGFP cells (**d**) shown in figure **3.10** were sorted using FACS and then re-analysed by flow cytometry for receptor surface expression (x-axis) using anti-Strep-Tag II antibody. The cells were also analysed for adaptor protein expression (y-axis) making use of the EmGFP signal encoded on the same plasmid as each adaptor protein.

Jurkat transduction with NKG2D and DAP10

Lentiviral particles of NKG2D or NKG2D and DAP10_EmGFP collected 24 hours after transfection of HEK293T packaging cells were added to Jurkat cells. Flow cytometry analysis using anti-Strep-Tag II antibody showed these two Jurkat cell lines were negative (figure **3.12ai-ii**). To determine whether the transduced Jurkat cells were positive for NKG2D surface expression the cells were analysed by flow cytometry using anti-NKG2D antibody. While as expected, untransduced Jurkat cells were negative for NKG2D surface expression, both the NKG2D- and NKG2D plus DAP10_EmGFP -transduced cells contained a positive population (figure **3.12bi-iii**). Using the crystal structure of NKG2D, the C terminus of NKG2D which is where the Strep-Tag II is inserted, is predicted to be positioned close to the membrane which may make it inaccessible for anti-Strep-Tag II antibody binding [Li et al., 2001].

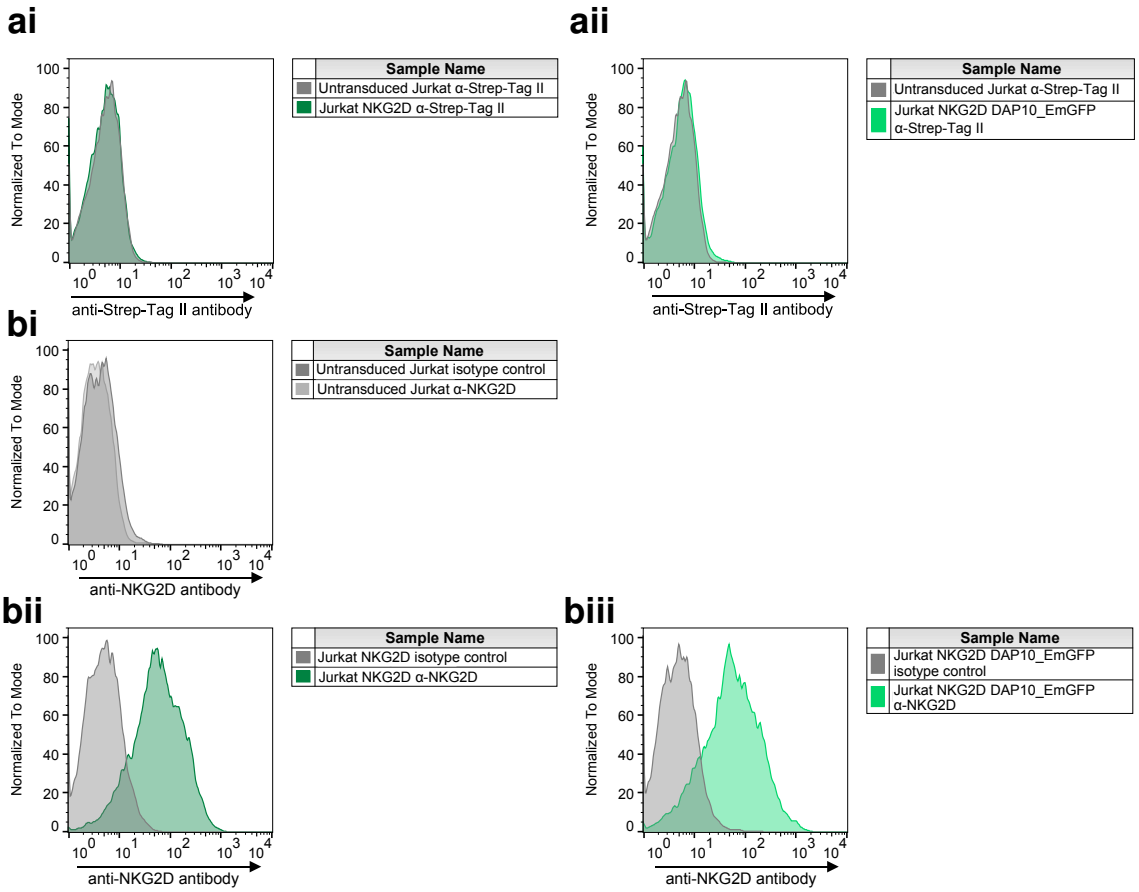


Fig. 3.12: **Jurkat cells transduced with NKG2D, or NKG2D and DAP10_EmGFP do not express NKG2D with accessible Strep-Tag II.** Jurkat cells transduced with NKG2D ■ (**ai**) or NKG2D and DAP10_EmGFP ■ (**aii**) were analysed for surface expression of NKG2D by anti-Strep-Tag II antibody. Jurkat cells (**bi**), Jurkat NKG2D cells (**bii**) and Jurkat NKG2D DAP10_EmGFP cells (**biii**) were also analysed using anti-NKG2D antibody. Cells in bi-iii were also incubated with an IgG negative isotype control. Anti-Strep-Tag II and anti-NKG2D staining was conducted on different days.

Three alternative NKG2D lentiviral vectors were synthesised to improve accessibility of the Strep-Tag II (described in section 3.2.1) : NKG2D-1x linker, NKG2D-2x linker and NKG2D-loop. Jurkat cells lentivirally co-transduced with one of these vectors and DAP10_EmGFP or transduced with NKG2D alone in the case of NKG2D-1x linker were analysed by flow cytometry for both the accessibility of Strep-Tag II and surface expression of NKG2D (figure **3.13**). The method of transduction was additionally altered slightly to improve efficiency. Specifically, packaging cells were transfected using PEI reagent instead of X-tremeGENE^{TM} 9. Cells previously transduced with NKG2D or NKG2D plus DAP10_EmGFP from figure **3.12** were included as positive controls, again showing the inaccessibility of Strep-Tag II but a population of cells positive for NKG2D surface expression (figure **3.13a-d**). The population of positive cells are smaller than those seen in figure **3.12** though. NKG2D-1x linker, NKG2D-1x linker plus DAP10_EmGFP, and NKG2D-2x linker plus DAP10_EmGFP transduced cells showed a similar lack of Strep-Tag II accessibility but a small population of cells positive for NKG2D surface expression (3.13e-j). NKG2D-loop plus DAP10_EmGFP transduced cells were negative for both anti-Strep-Tag II and anti-NKG2D staining (3.13k-l). This suggests insertion of the Strep-Tag II into a loop of the C-type lectin domain disrupted the correct folding of the domain and thereby abolished anti-NKG2D binding.

We were therefore unable to create NKG2D-expressing Jurkat cell lines that have an accessible Strep-Tag II. Transduction of Jurkats with NKG2D was consequently moved to lower priority to allow investigation of alternative receptors.

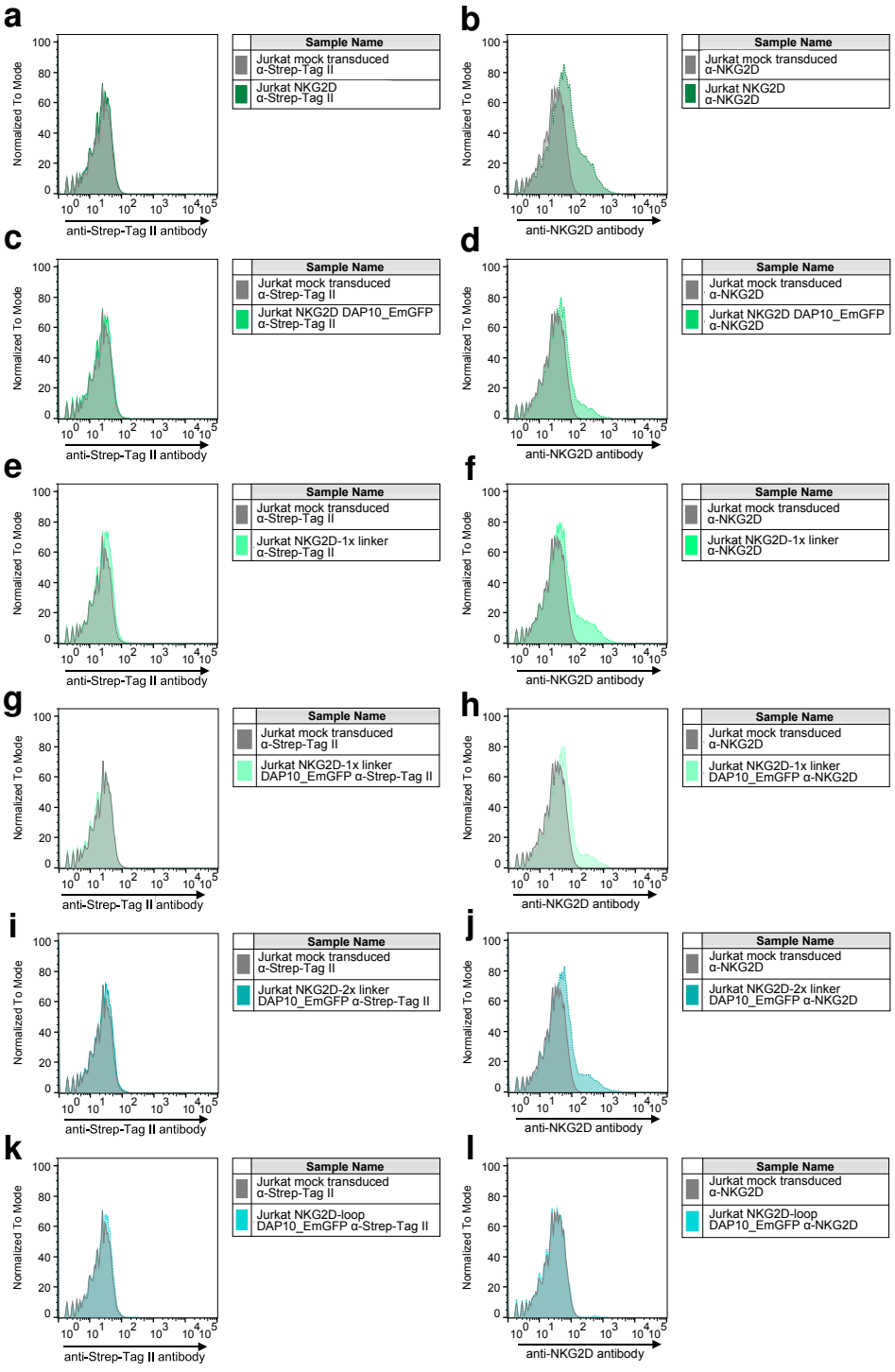


Fig. 3.13: **Jurkat cells transduced with NKG2D, NKG2D-1x linker and NKG2D-2x linker express the NTR on the cell surface but with Strep-Tag II inaccessible while NKG2D-loop transduced cells do not express NKG2D.** Jurkat cells transduced with NKG2D ■ or NKG2D and DAP10_EmGFP ■ analysed in figure **3.12** were re-analysed for Strep-Tag II accessibility (**a** and **c** respectively) and NKG2D surface expression (**b** and **d**) for comparison purposes. *Continued on the next page.*

Fig. 3.13: **Jurkat cells transduced with NKG2D, NKG2D-1x linker and NKG2D-2x linker express the NTR on the cell surface but with Strep-Tag II inaccessible while NKG2D-loop transduced cells do not express NKG2D.** *Continued.* Jurkat cells transduced with NKG2D-1x linker, NKG2D-1x linker and DAP10_EmGFP, NKG2D-2x linker and DAP10_EmGFP or NKG2D-loop and DAP10_EmGFP were also analysed for Strep-Tag II accessibility using anti-Strep-Tag II antibody (**e, g, i, k** respectively) and NKG2D surface expression using anti-NKG2D antibody (**f, h, j, l** respectively).

3.2.2.2 Transduction of NKL and NK92 cells

The human NK cell line NKL was also investigated as a receptor-expressing cell line. NKL cells were lentivirally transduced with NKp30 or LAIR-1 using virus known to be competent by successful transduction of THP-1 cells (figure **3.15**). Flow cytometry analysis indicated however that transduction of NKL cells using these viruses was unsuccessful (figure **3.14**). We also attempted to lentivirally transduce NKL cells with other NTRs and also co-transduce cells with NKp30 and the adaptor protein FcRγ. Flow cytometry analysis showed however that the NKL cells did not express the receptors or adaptor protein. Nucleofection of NKL cells with a number of the receptors was unsuccessful. We also investigated another human NK cell line, NK92 as receptor-expressing cells but nucleofection of NK92 cells was unsuccessful. This data has been omitted for brevity. Creating NTR-expressing NK cell lines was therefore changed to a lower priority so work with other cell lines could be pursued.

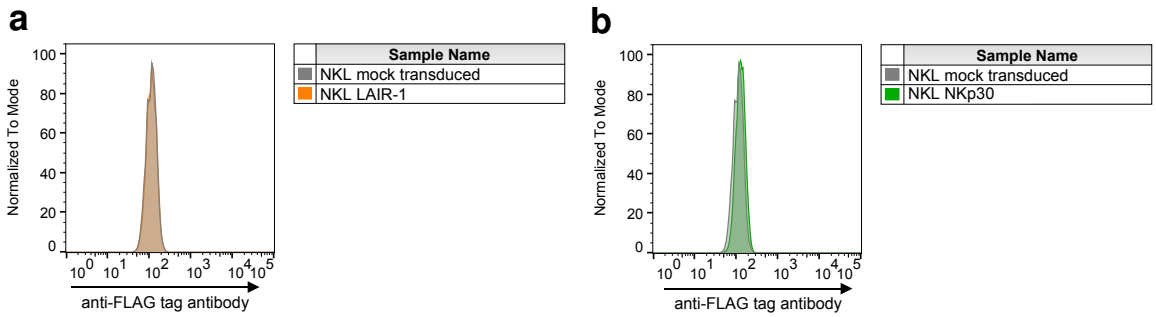


Fig. 3.14: **NKL cells transduced with LAIR-1 or NKp30 do not express either receptor.** NKL cells transduced with virus of LAIR-1 (**a**) or NKp30 (**b**) were analysed for receptor expression by flow cytometry using anti-FLAG tag antibody intracellular staining.

3.2.2.3 Transduction of THP-1 cells

THP-1 transduction with 2B4, LAIR-1 and NKp30

THP-1 cells were transduced with the receptors 2B4, LAIR-1 or NKp30 using lentivirus collected 48 hours after transfection of HEK293T packaging cells. THP-1 cells contain endogenous FcRγ so introduced NKp30 will be able to associate with the adaptor protein already expressed for signalling transduction [Scholl and Geha, 1993]. Receptor surface expression of the three cell lines was analysed using anti-Strep-Tag II antibody staining (figure **3.15**). All three THP-1 cell lines each had a large population of cells that expressed the introduced Strep-Tag II-tagged forms of 2B4, LAIR-1 or NKp30. The staining of cells with anti-Strep-Tag II antibody also showed that the Strep-Tag II was accessible. The proportion of cells within the population that expressed the Strep-Tag II-tagged NTR increased upon sorting of the lines with anti-Strep-Tag II antibody-coated magnetic beads (figure **3.16**).

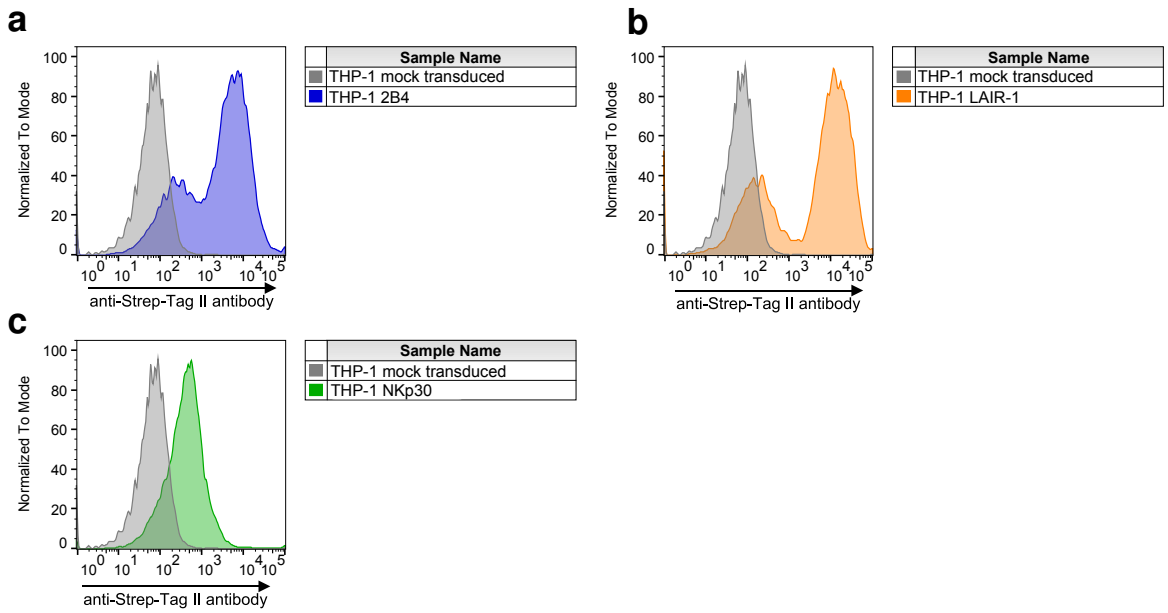


Fig. 3.15: **THP-1 cells lentivirally transduced with 2B4, LAIR-1, or NKp30 express the NTR on the cell surface.** THP-1 cells lentivirally transduced with 2B4 (**a**), LAIR-1 (**b**), or NKp30 (**c**) were analysed for receptor surface expression using anti-Strep-Tag II antibody.

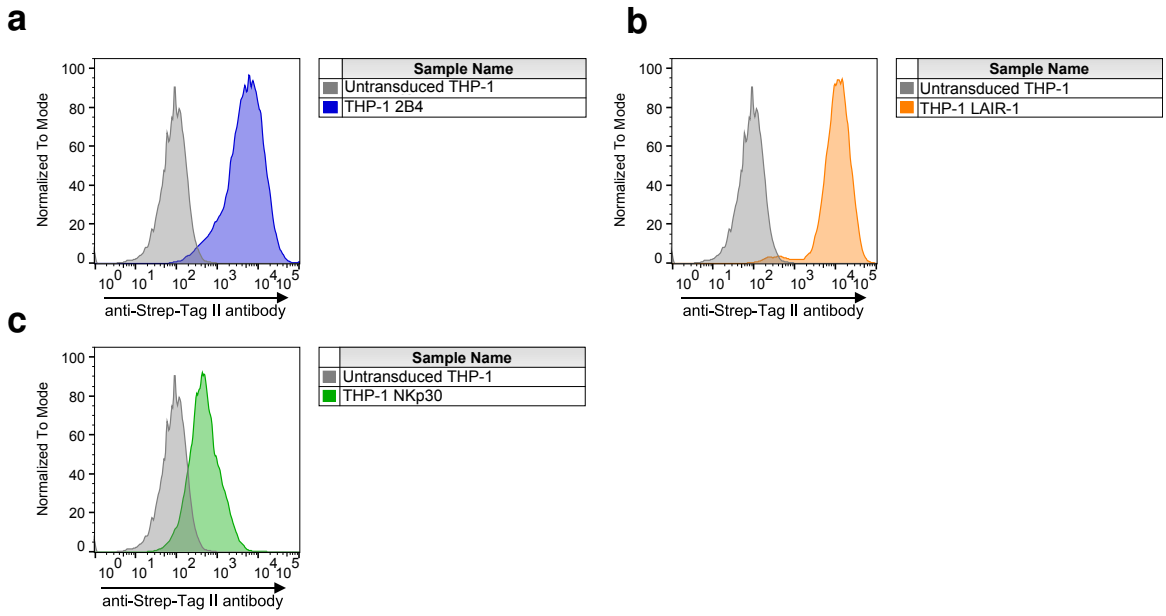


Fig. 3.16: **THP-1 cells expressing 2B4, LAIR-1, or NKp30 were sorted for high receptor expression.** Transduced THP-1 cells from figure **3.15** were sorted for NTR expression using magnetic beads coated with anti-Strep-Tag II antibody. Surface expression of 2B4 (**a**), LAIR-1 (**b**), or NKp30 (**c**) was then re-analysed using anti-Strep-Tag II antibody staining and flow cytometry.

THP-1 transduction with FcRγRIA, SIGLEC-14, SIRPβI, or NKG2D, along with the appropriate adaptor protein

THP-1 cells co-transduced with lentivirus of FcγRIA and FcRγ_EmGFP, or SIGLEC-14 and DAP12_EmGFP, or SIRPβI and DAP12_EmGFP, were analysed for expression of the receptor and adaptor protein using flow cytometry. Adaptor protein expression was inferred from expression of EmGFP which is encoded with an IRES sequence on the same plasmid as the adaptors. A significant proportion of cells in each transduced cell line stained double positive for receptor and adaptor (figure **3.17**). The proportion of double positive cells increased in all three lines after sorting with anti-Strep-Tag II antibody-coated magnetic beads (figure **3.18**) and again after FACS sorting (figure **3.19**).

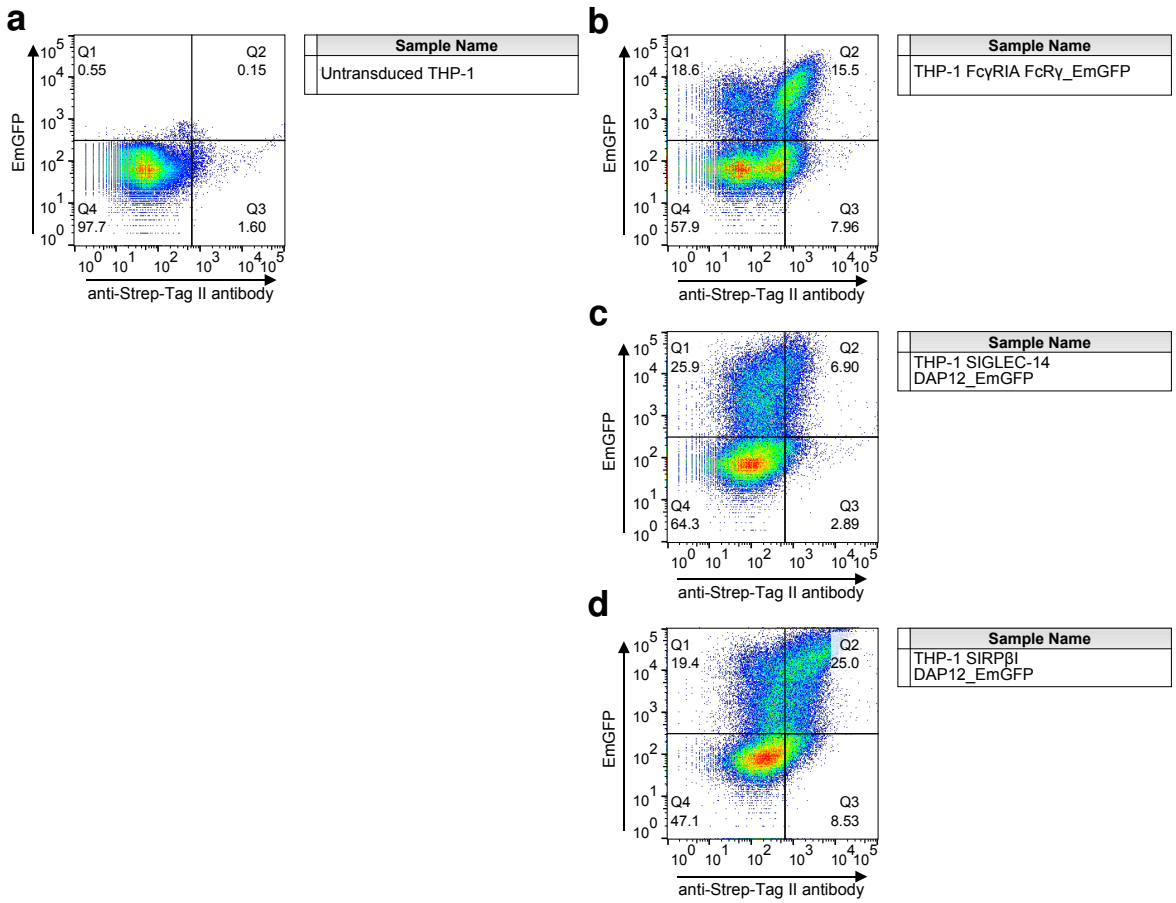


Fig. 3.17: **THP-1 cells lentivirally transduced with FcγRIA and FcRγ, or SIGLEC-14 and DAP12, or SIRPβI and DAP12, express both NTR and adaptor protein.** Untransduced THP-1 cells (**a**) were analysed for non-specific antibody binding (x-axis) and background fluorescence in the channel used to infer adaptor protein signal (y-axis). THP-1 cells lentivirally transduced with FcγRIA and FcRγ_EmGFP (**b**), or SIGLEC-14 and DAP12_EmGFP (**c**), or SIRPβI and DAP12_EmGFP (**d**) were analysed for receptor expression (x-axis) and adaptor protein expression (y-axis). The antibody target of the receptors was Strep-Tag II (extracellular). Adaptor protein expression was inferred using EmGFP expression.

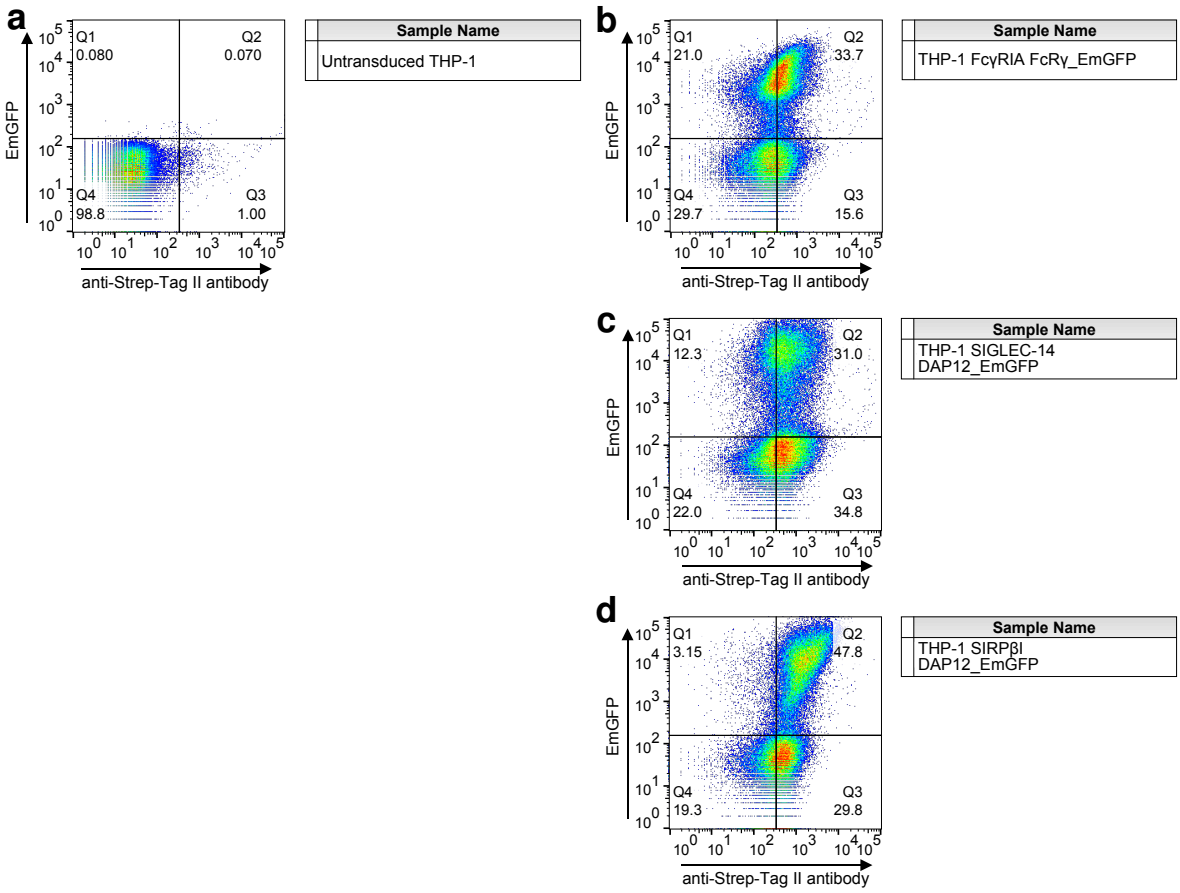


Fig. 3.18: **THP-1 cells expressing FcγRIA, SIGLEC-14, or SIRPβI along with their adaptor protein were sorted using magnetic beads.** THP-1 cells (**a**) were analysed for non-specific antibody binding (x-axis) and background fluorescence in the channel used to infer adaptor protein signal (y-axis). THP-1 cells transduced with FcγRIA and FcRγ_EmGFP (**b**), or SIGLEC-14 and DAP12_EmGFP (**c**), or SIRPβ and DAP12_EmGFP (**d**) shown in figure **3.17** were sorted using magnetic beads coated with anti-Strep-Tag II antibody. The lines were then re-analysed by flow cytometry for receptor surface expression (x-axis) using anti-Strep-Tag II antibody and adaptor expression (y-axis) using the IRES-EmGFP on the adaptor plasmids.

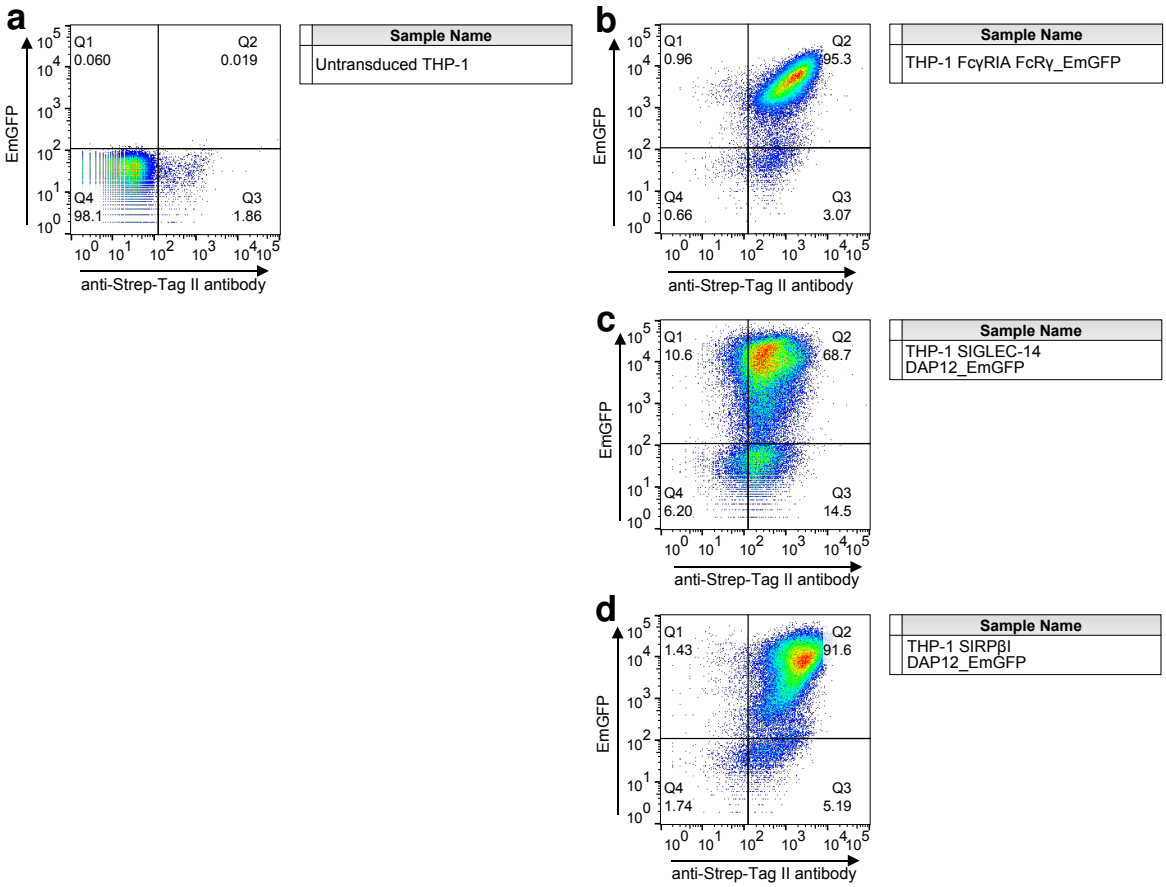


Fig. 3.19: **THP-1 cells expressing FcγRIA, SIGLEC-14, or SIRPβI along with their adaptor protein were sorted using FACS.** THP-1 cells (**a**) were analysed for non-specific antibody binding (x-axis) and background fluorescence in the channel used to infer adaptor protein signal (y-axis). THP-1 cells expressing FcγRIA and FcRγ_EmGFP (**b**), or SIGLEC-14 and DAP12_EmGFP (**c**), or SIRPβ and DAP12_EmGFP (**d**) shown in figure **3.18** were sorted using FACS. The lines were then re-analysed by flow cytometry for receptor surface expression (x-axis) using anti-Strep-Tag II antibody and adaptor expression (y-axis) using the IRES-EmGFP on the adaptor plasmids. FACS was conducted with Nigel Rust.

In an effort to create THP-1 NKG2D cell lines, THP-1 cells were co-transduced with lentivectors encoding NKG2D and DAP10_EmGFP using virus collected 48 hours after HEK293T packaging cell transfection. The cells were then analysed for NKG2D and DAP10 expression using flow cytometry (figure **3.20**). While a small population of cells expressed DAP10_EmGFP , the cells did not express NKG2D as shown by anti-NKG2D antibody staining.

Lentiviral transduction of THP-1 cells with the NKG2D variants, for example, NKG2D-1x linker, along with DAP10_EmGFP was also attempted but was not successful. These data suggest NKG2D is not surface expressed at all in the transduced THP-1 cells. In contrast, other receptors have been successfully transduced into THP-1 cells such as 2B4, and NKG2D has been transduced into Jurkat cells (with inaccessible Strep-Tag II) (section 3.2.2.1). Based on these results, it is possible that THP-1 cells cannot correctly fold and transport NKG2D to the cell surface, or NKG2D at the cell surface may not be stable and so the transduced cell lines do not stain for NKG2D expression. The data has been omitted for brevity.

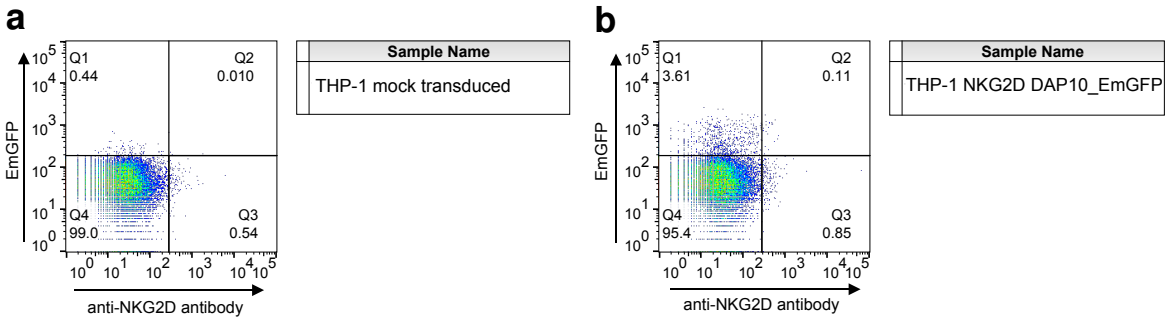


Fig. 3.20: **THP-1 cells co-transduced with NKG2D and DAP10_EmGFP plasmids do not have a double positive population.** THP-1 cells mock transduced (**a**) or co-transduced with NKG2D and DAP10_EmGFP (**b**) were analysed for double positive expression profiles using anti-NKG2D antibody (x-axis) and the DAP10_EmGFP signal (y-axis).

3.2.3 Cloning of artificial ligand constructs

The artificial ligand component of our system uses the intracellular, transmembrane and short extracellular hinge-like region of mouse CD80 as a base (figure **3.21**). Mouse CD80 has previously been used to create chimeric ligand proteins that are expressed in CHO cells [Lim et al., 2015]. In addition, removal of the immunoglobulin-like domain

of mouse CD80 will ensure that the protein will most likely not bind any protein that is surface expressed on the human receptor-expressing cell lines.

The shortest length artificial ligand we designed consists just of this truncated mouse CD80, along with an N terminal HA tag and Avitag, and is referred to as 'CD80 ligand' for simplicity. The extracellular Avitag is the target for enzymatic biotinylation of the ligand which will enable it to be bound by StrepTactin protein. Elongated versions of the ligand were created by insertion of immunoglobulin-like domain spacers between the mouse CD80 hinge-like region and Avitag sequence. The spacers consist of the immunoglobulin-like domains from human CD2 and/or CD4 which have previously been used to elongate NTR ligands [Choudhuri et al., 2005, Choudhuri et al., 2009, Köhler et al., 2010, Brzostek et al., 2010, Lim et al., 2015]. The extracellular region of CD80 ligand when bound to StrepTactin will largely be the same as the dimensions of the StrepTactin tetramer, which is $\sim$5nm as predicted from the X-ray crystal structure of streptavidin [Hendrickson et al., 1989]. Insertion of the two antiparallel β-barrel immunoglobulin-like domains of CD2 is predicted to increase the extracellular dimensions by $\sim$7nm using the crystal structure of the CD2 extracellular region [Bodian et al., 1994]. Insertion of the four immunoglobulin-like domains of CD4 is predicted to increase the extracellular dimensions by $\sim$12nm [Harrison, 1993, Wu et al., 1997]. The ligand-binding regions of CD2 and CD4 lay at the most membrane-distal end of the proteins where StrepTactin binds to the Avitag and so we do not predict any binding by CD2 or CD4 within the artificial ligands to their native binding partners [Wang et al., 2001, Davis and van der Merwe, 1996]. Partial plasmid maps of the artificial ligands along with cartoon diagrams of the proteins are shown in figure **3.21**.

3.2.4 Transfection of mammalian cell lines with artificial ligand constructs

Chinese hamster ovary (CHO) cells were used to create artificial ligand-expressing cell lines. As hamster cells, they are unlikely to express proteins that will interact with the human receptor-expressing cells and so will not interfere with our experiments. CHO cells were first nucleofected with a plasmid encoding the BirA biotin-protein ligase with endoplasmic reticulum retention signal sequence (pDISPLAY-BirA-ER). Expression of

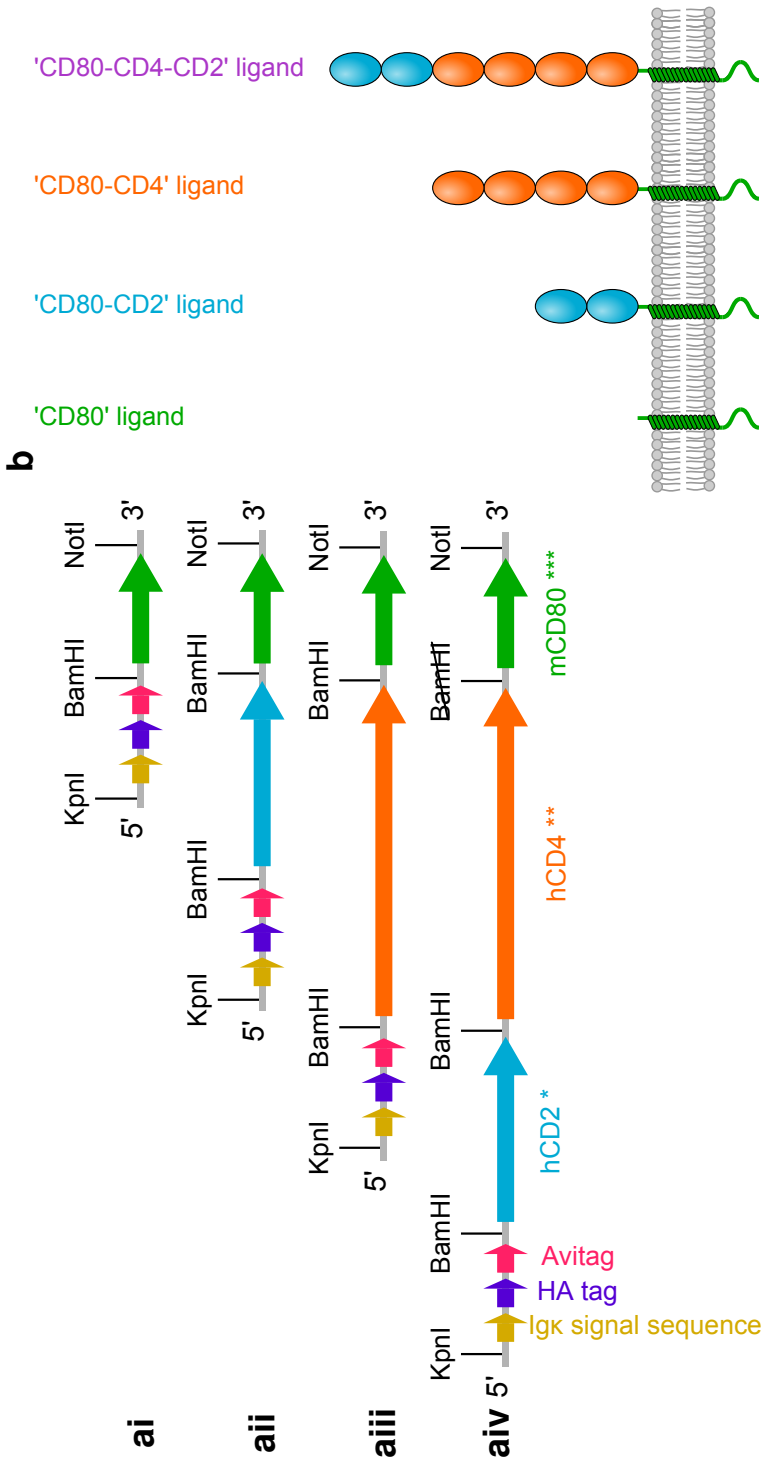


Fig. 3.21: **Partial plasmid maps and cartoon diagrams of the artificial ligands.** All of the ligand constructs synthesised have the Igκ mammalian signal sequence followed by HA tag and Avitag sequences. This segment was inserted into pcDNA3.1(+) using the restriction enzymes KpnI and BamHI. The shortest ligand (termed CD80 for simplicity) (**ai**) consists of the extracellular hinge-like, transmembrane and intracellular region of mouse CD80 (mCD80***) inserted into the plasmid using the BamHI and NotI restriction sites. CD80-CD2 (**aii**) and CD80-CD4 (**aiii**) ligands have identical sequences to CD80 with the addition of the immunoglobulin-like domains of human CD2 (CD2 *) or human CD4 (CD4 **) respectively, inserted using the restriction site BamHI. For synthesis of CD80-CD4-CD2 (**aiv**) ligand, the immunoglobulin domains of human CD4 flanked by BamHI and BglII sites were first inserted into the CD80 ligand using its BamHI site. This permits insertion of CD4, destroying the C terminal BamHI site while the N terminal site remains. Human CD2 immunoglobulin-like domains were then inserted using BamHI. Cartoon diagrams of these proteins in a cell membrane are also shown (**b**).

the biotin-protein ligase will allow biotinylation of the Avitag of introduced ligand proteins. The BirA-ER construct was a gift from Professor Mark Howarth. Transfection of the BirA-ER construct into mammalian cells for biotinylation of proteins in the endoplasmic reticulum before trafficking to the cell surface has been described and previously used [Parrott and Barry, 2001, Howarth et al., 2008, Howarth and Ting, 2008].

Nucleofected cells were selected for geneticin resistance and then analysed using flow cytometry for intracellular expression of the BirA protein, which has a HA tag. A small population of nucleofected cells were positive for HA-tagged BirA protein expression (figure **3.22**). These nucleofected CHO cells were diluted and cultured to yield single clones of cells which were expanded and then individually analysed for BirA protein expression (figure **3.23**). A number of colonies expressed the biotin-protein ligase including clone # 8 (figure **3.23g**) (hereafter termed CHO BirA-ER) which was selected for progression of ligand cell line production.

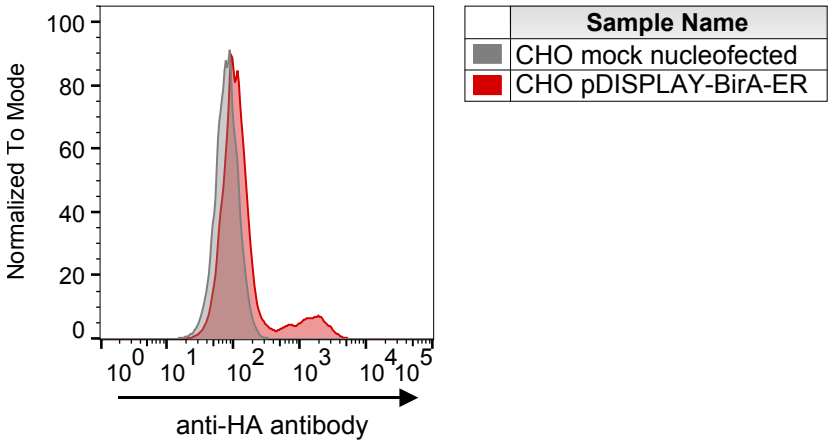


Fig. 3.22: **A small population of CHO cells nucleofected with BirA-ER express the protein.** CHO cells nucleofected with pDISPLAY-BirA-ER were analysed for protein expression by flow cytometry using intracellular anti-HA tag staining.

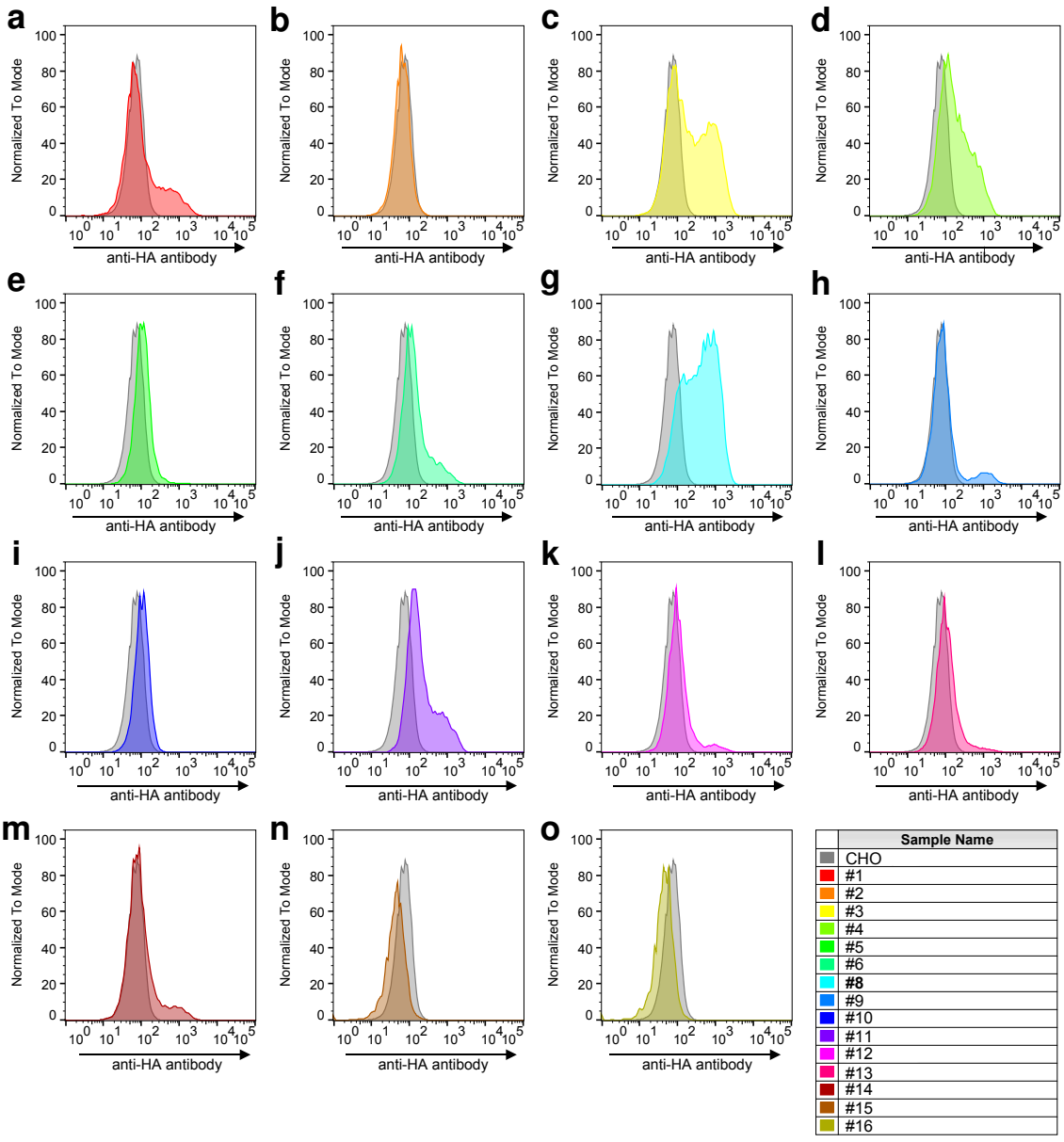


Fig. 3.23: **A number of single clones of CHO cells nucleofected with BirA-ER express the HA-tagged protein.** CHO cells nucleofected with pDISPLAY-BirA-ER were diluted and cultured to create single clones. A selection of these clones (**a-o**) were analysed by flow cytometry for expression of the BirA protein using anti-HA tag intracellular staining. Clone #8 in g was chosen.

CHO BirA-ER cells were nucleofected with the CD80 ligand, CD80-CD2 ligand, or CD80-CD4 ligand construct, or a positive control previously nucleofected into CHO cells. This positive control is a pcDNA3.1(+) vector encoding mouse CD148 with truncated ectodomain. Following selection for antibiotic resistance, the nucleofected cells were analysed for ligand expression by flow cytometry using anti-HA antibody. All ligand constructs and the positive control have an extracellular HA tag. The nucleofected CHO cells did not express any of the ligand constructs or positive control (figure **3.24a-d**).

To determine whether the CHO cells were nucleofection competent, CHO BirA-ER cells were nucleofected with a GFP positive control plasmid provided with the Lonza Nucleofector kit V. This was conducted on a different day to the data in (figure **3.24a-d**). Nucleofected cell analysis showed a large population of cells highly expressing the GFP plasmid indicating the CHO BirA-ER cells were nucleofection competent (figure **3.24e**).

We attempted a number of alternative methods to create ligand-expressing CHO cells but these were also unsuccessful. For example, shortly after nucleofection, cells were sorted using magnetic beads to enrich for the ligand-expressing cells. The sorted cells did not express the ligands however. Transfection of CHO cells with ligand constructs using the X-treme-GENE 9 transfection reagent was also not successful. To determine if the previous nucleofection of CHO cells with the BirA-ER plasmid had interfered with the CHO cells such they could not be nucleofected with the ligand plasmids, CHO cells (without BirA-ER) were nucleofected with the ligand constructs and analysed for ligand protein expression. The cell lines did not express the ligands however. These results are not shown.

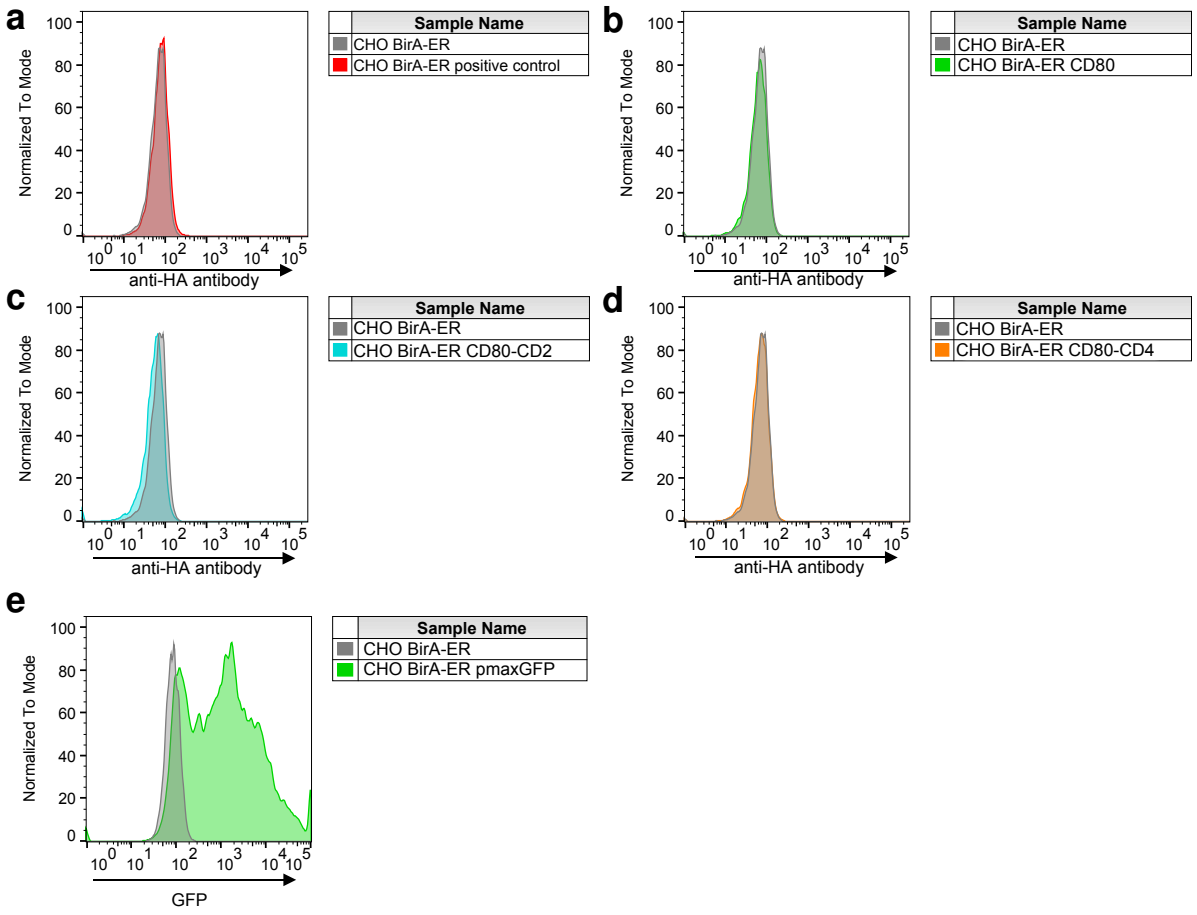


Fig. 3.24: **CHO BirA-ER cells nucleofected with CD80, CD80-CD2 or CD80-CD4 did not surface express the ligand.** CHO BirA-ER cells were nucleofected with either a positive control (**a**), CD80 (**b**), CD80-CD2 (**c**), or CD80-CD4 (**d**). Following antibiotic selection, protein expression was analysed by flow cytometry using anti-HA tag extracellular staining. (**e**) CHO BirA-ER cells were nucleofected with a pmaxGFP positive control vector. GFP expression was then analysed using flow cytometry. The experiment in e was conducted on a different day to a-d.

To test if the ligand plasmids can be transfected into a cell line and surface expressed, CD80, CD80-CD2, or CD80-CD4 were individually co-transfected into HEK293T cells with pDISPLAY-BirA-ER. Analysis of ligand surface expression using flow cytometry showed all three transfected cell lines contained a population of cells that expressed the introduced ligand protein (figure **3.25**). This indicates that the plasmids are able to be transfected into, and proteins expressed by, HEK293T cells but not CHO cells.

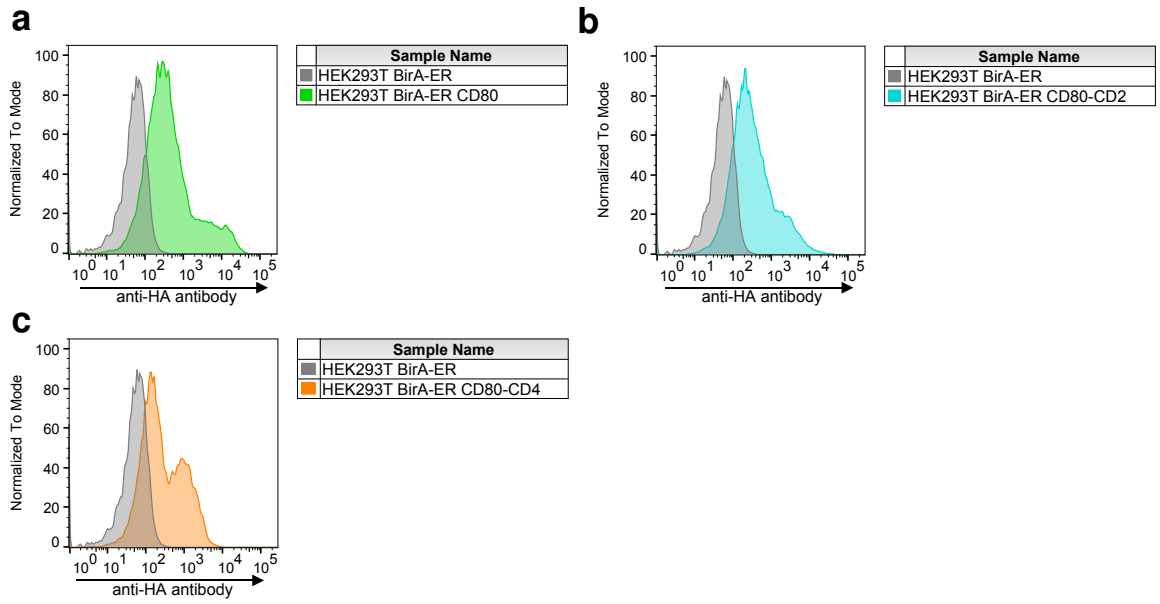


Fig. 3.25: **HEK293T cells transfected with ligand constructs transiently express the introduced protein.** HEK293T cells co-transfected with BirA-ER and either CD80 (**a**), CD80-CD2 (**b**), or CD80-CD4 (**c**) were analysed for protein expression using flow cytometry and extracellular anti-HA tag staining.

HEK293T cells are a human cell line and therefore their use as the cell line for artificial ligand expression is not ideal; they may endogenously express native ligands for various NTRs and thereby interfere with our studies. However, to allow validation and investigation with the artificial ligand system we used HEK293T cells transiently expressing the ligand proteins as the ligand-expressing cell lines. Transfection of CHO cells with the CD80-based artificial ligand plasmids outlined here was not pursued further.

Further investigation of CHO cells as the cell line for these ligands could involve protein expression analysis of cells 2-3 days following nucleofection/transfection and prior to antibiotic selection. There may be a mutation in the hygromycin resistance gene of the pcDNA3.1(+) vector used as a backbone for the ligand constructs. This would interfere with the creation of stable ligand-expressing cell lines. An alternative vector or different transmembrane domains of the ligands themselves could also be investigated to improve

surface expression.

3.2.5 Expression and purification of StrepTactin

Bivalent StrepTactin tetramers were synthesised as described in section 2.5 using a protocol modified from [Howarth and Ting, 2008]. StrepTactin subunit and a mutated streptavidin subunit unable to bind biotin (referred to as "dead" streptavidin and previously described in [Howarth et al., 2006]) were expressed individually in *E. coli* before being mixed in a 1:1 molar ratio and refolded.

Mixing of these subunits will yield a number of various tetramer valencies including tetravalent, trivalent, bivalent, and monovalent StrepTactin where, for example, trivalent StrepTactin is a tetramer consisting of three StrepTactin subunits and a single dead streptavidin subunit thereby giving the tetramer three possible Strep-Tag II- (or biotin-) binding sites. For monovalent, trivalent and tetravalent StrepTactin there is a single arrangement of subunits that will yield each valency. Conversely, there are three possible subunit arrangements that will yield bivalent StrepTactin, each giving a different orientation of the two Strep-Tag II/biotin-binding sites relative to each other. These different forms are illustrated in figure **3.26** and listed in table **3.4** along with the abbreviations we use to refer to them with.

The Strep-Tag II-binding sites of both 1,3 trans-bivalent StrepTactin and 1,4 bivalent StrepTactin are located such that they face away from each other whereas the binding sites of 1,2 cis-bivalent StrepTactin are facing in the same direction. This arrangement of 1,2 cis-bivalent StrepTactin binding sites may affect the ability of the tetramer to simultaneously bind a Strep-Tag II and biotin which is a requirement of our system. We therefore sought to purify only the 1,3 and 1,4 bivalent StrepTactin proteins which we predicted would be able to bind both biotinylated protein and Strep-Tag II-tagged receptor.

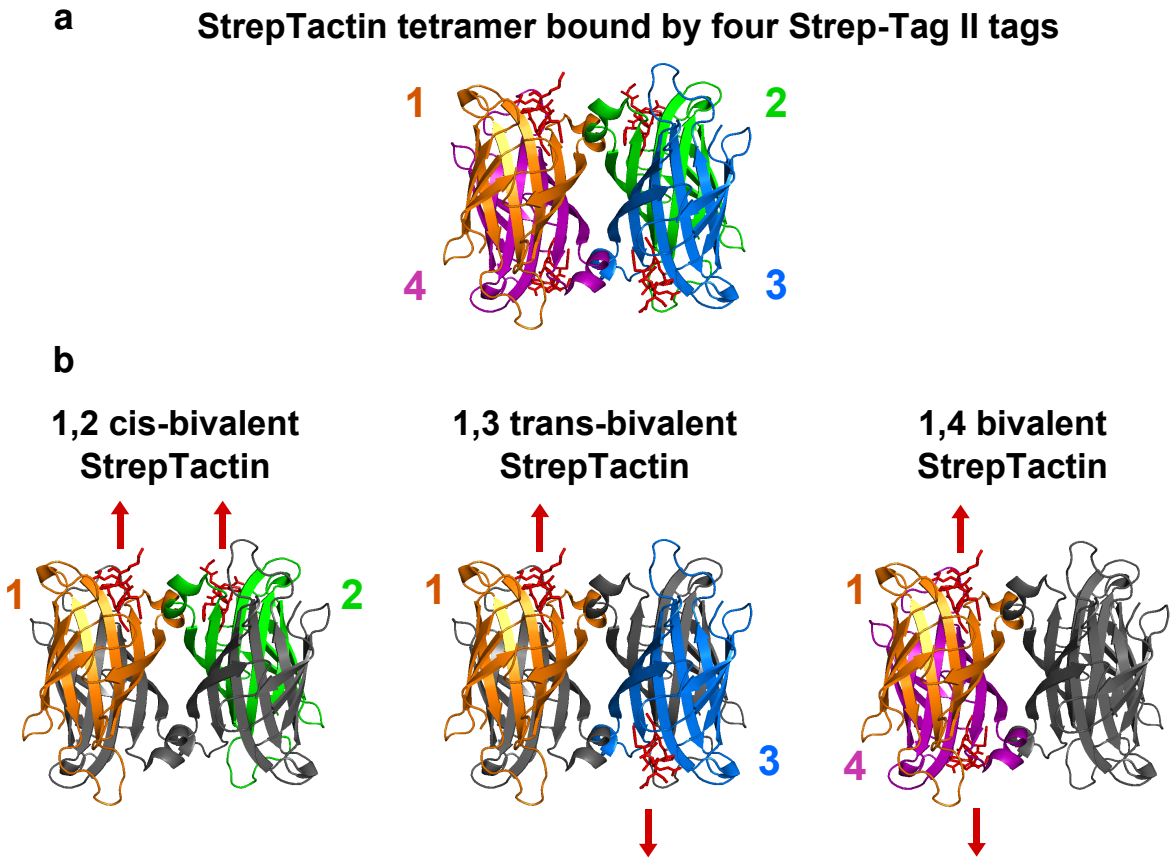


Fig. 3.26: **Arrangements of bivalent StrepTactin.** The structure of tetrameric StrepTactin in complex with four Strep-Tag II tags is shown in **a** (PDB accession # 1KL3) [Korndörfer and Skerra, 2002]. Each monomer is labelled from one to four and shown in a different colour. The bound Strep-Tag II tags are shown in red ▬. Bivalent StrepTactin can form in three different arrangements: 1,2 bivalent, 1,3 bivalent and 1,4 bivalent StrepTactin. Illustrations of these tetramers are shown in **b**. For each bivalent tetramer, the appropriate two subunits that would correspond to dead streptavidin and so would not have a Strep-Tag II binding site are coloured in gray ▬. The remaining StrepTactin subunits are again shown bound to a Strep-Tag II. For 1,2 bivalent StrepTactin (left), the binding sites face in the same direction (shown by the red arrows) and so 1,2 bivalent StrepTactin is defined as cis-bivalent StrepTactin. The two binding sites of 1,3 bivalent StrepTactin (middle) face in different directions (red arrows) and so this tetramer is defined as 1,3 trans-bivalent StrepTactin. The Strep-Tag II/biotin- binding sites of 1,4 bivalent StrepTactin also do not point in the same direction (red arrows). The structures of both 1,2 cis-bivalent and 1,3 trans-bivalent streptavidin have been solved using x-ray crystallography [Fairhead et al., 2014a]. All figures were created using PyMOL.

Abbreviation	Protein
ST4	tetravalent StrepTactin
ST3dSA1	trivalent StrepTactin
1,2 cis-ST2	1,2 cis-bivalent StrepTactin
1,3 trans-ST2	1,3 trans-bivalent
1,4 ST2	1,4 bivalent StrepTactin
ST1dSA3	monovalent StrepTactin
dSA4	dead streptavidin

Tab. 3.4: **Abbreviations used to refer to StrepTactin/streptavidin tetramer configurations.**

In order to do this we used a protocol previously used by [Fairhead et al., 2014a] to separate and purify streptavidin of different valencies. For this, the dead streptavidin subunit contains a polyaspartate sequence and so tetramers of different valency and arrangement can be resolved using a MonoQ column (anion exchange). As the polyaspartate sequence is inserted into the dead streptavidin subunit only it should not interfere with binding of Strep-Tag II or biotin to the StrepTactin subunits of the tetramer.

A representative chromatogram of StrepTactin tetramer separation (figure **3.27a**) is comparable to chromatograms of streptavidin tetramers prepared in a similar manner [Fairhead et al., 2014a]. Based on this comparison, and taking into consideration the predicted isoelectric points of the various tetramer arrangements which are listed in table **3.5**, we made an initial prediction of which tetramer each peak of the chromatogram represented. Each peak in figure **3.27a** is labelled according to these predictions. We believe that the 1,3 and 1,4 bivalent StrepTactin tetramers were collected in the same peak in agreement with the separation of streptavidin in [Fairhead et al., 2014a]. The peak we believe to contain the desired 1,3 bivalent and 1,4 bivalent tetramers (annotated as 1,3 trans-ST2, 1,4 ST2) is highlighted in figure **3.27a** in red.

To determine whether the peaks contained the tetramers we expected, boiled samples of the tetravalent StrepTactin (ST4), 1,2 cis-ST2, the mixture of 1,3 trans-ST2 and 1,4 ST2, monovalent StrepTactin (ST1dSA3) and dead streptavidin tetramer (dSA4) peaks were visualised on an SDS-PAGE gel (figure **3.27b**). The gel band density was then measured using ImageJ and converted into a ratio of StrepTactin:dead streptavidin subunit for each peak (table **3.6**). For each peak analysed the protein ratio was consistent with the tetramer configuration expected.

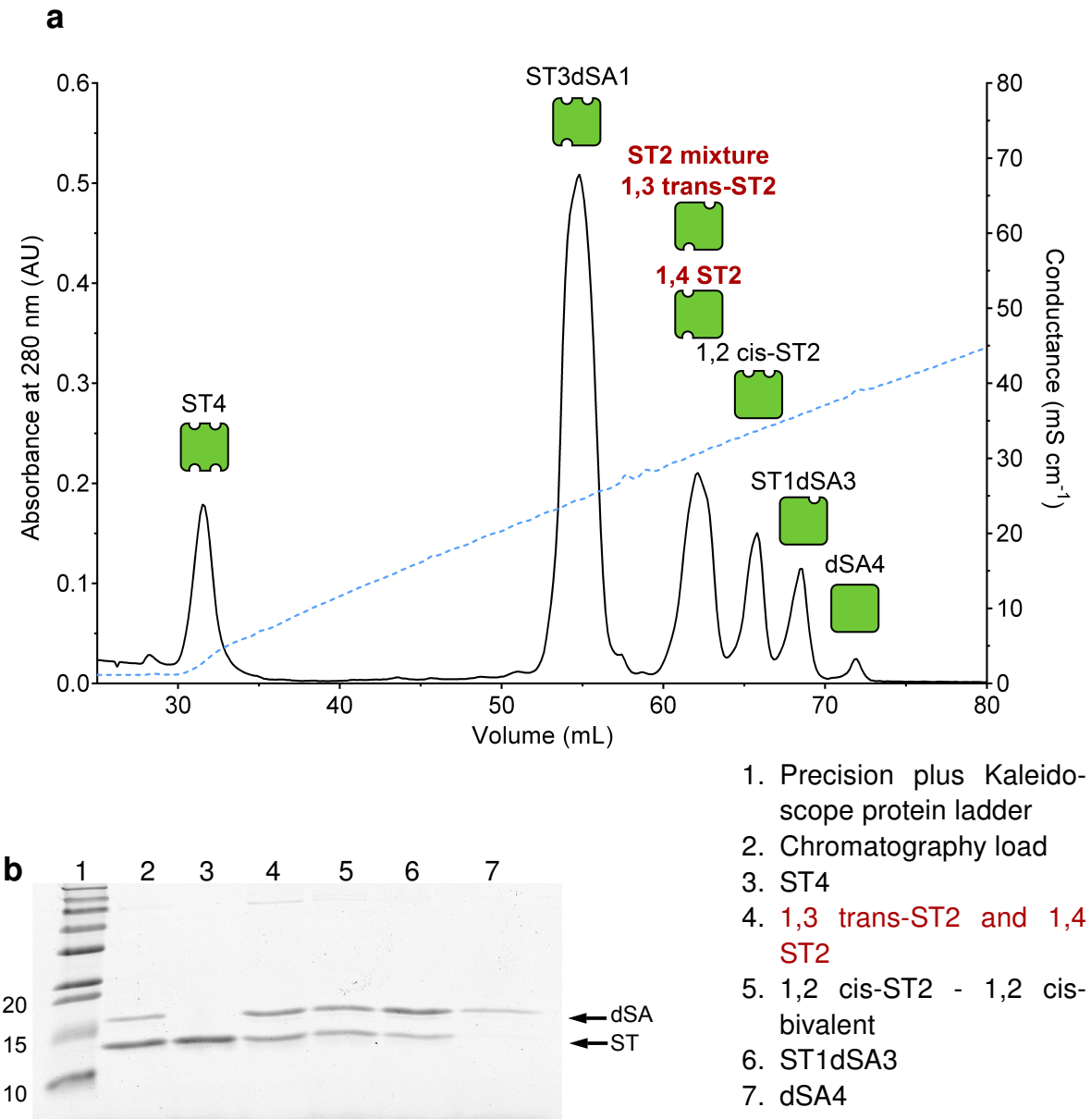


Fig. 3.27: **Separation of refolded StrepTactin tetramers using anion exchange chromatography.** Refolded tetramers of StrepTactin were loaded onto a MonoQ column and separated using anion exchange chromatography. Absorbance of the eluted fractions are shown in black and conductance is shown by the blue dashed line (**a**). The expected tetramer configuration of each peak is labelled on the figure along with cartoon diagrams of the tetramers. Peak samples and a protein sample prior to chromatography were boiled and visualised by SDS-PAGE and coomassie staining (**b**). StrepTactin (ST) and dead streptavidin (dSA) subunits are labelled. The desired ST2 mixture is highlighted in red.

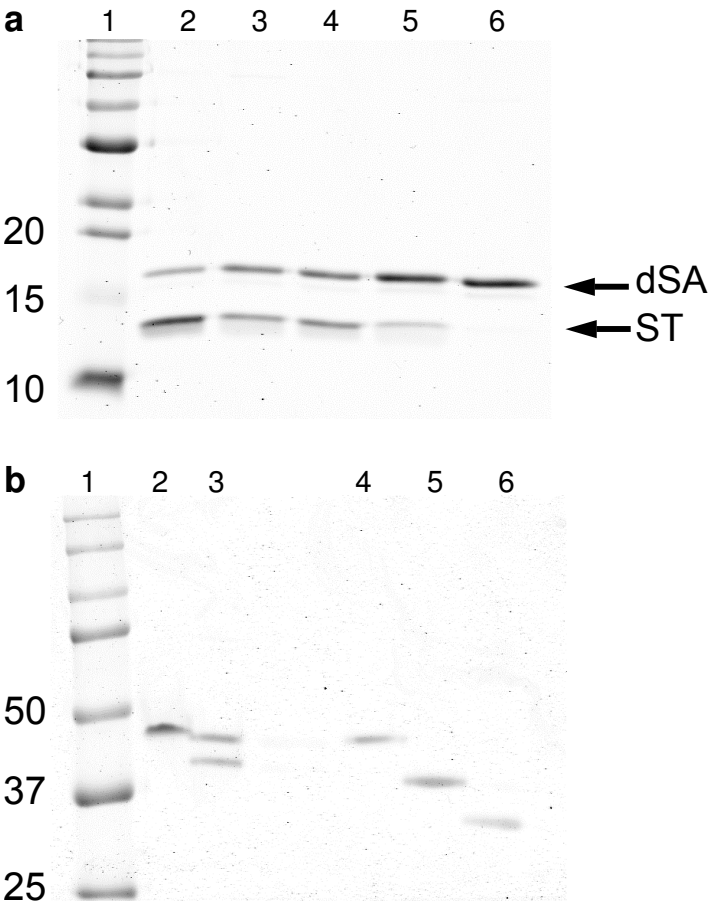
Tetramer	Predicted isoelectric point
ST4	8.91
ST3dSA1	5.53
1,2 cis-ST2	4.73
1,3 trans-ST2, 1,4 ST2	4.73
ST1dSA3	4.40
dSA4	4.20

Tab. 3.5: **Predicted isoelectric points of various StrepTactin and streptavidin tetramers created during synthesis of bivalent StrepTactin.** The predicted isoelectric points of the tetramers listed were used to infer which tetramer arrangements the peaks shown in figure 3.27a represent.

	StrepTactin:dead streptavidin ratio
ST4	1 : 0.0
1,3 trans-ST2 and 1,4 ST2	1 : 1.0
1,2 cis-ST2	1 : 1.1
ST1dSA3	1 : 2.3
dSA4	0.1 : 1

Tab. 3.6: **Subunit ratio of StrepTactin tetramer peaks are consistent with those expected.** Density of gel bands shown in figure **3.27** were calculated using ImageJ and converted to a ratio of StrepTactin and dead streptavidin subunits to confirm the identity of the eluted protein peaks.

Boiled samples along with unboiled samples of the protein peaks from a separate expression and purification cycle again show each peak has the expected subunit ratio (figure **3.28a**) and also expected mobility (figure **3.28b**) in accordance with streptavidin tetramer mobility seen in [Fairhead et al., 2014a]. Tetramers with more dead streptavidin subunits have a higher negative charge due to the polyaspartate loop and so have faster mobility. There are also two bands present in figure **3.28b** in the lane loaded with the mixture of 1,3 trans-ST2 and 1,4 ST2. These two bands are likely to correspond to the two species of tetramer present in this sample.



1. Precision plus Kaleidoscope protein ladder
2. ST3dSA1
3. 1,3 trans-ST2 and 1,4 ST2
4. 1,2 cis-ST2
5. ST1dSA3
6. dSA4

1. Precision plus Kaleidoscope protein ladder
2. ST3dSA1
3. 1,3 trans-ST2 and 1,4 ST2
4. 1,2 cis-ST2
5. ST1dSA3
6. dSA4

Fig. 3.28: **StrepTactin tetramers visualised by SDS-PAGE.** Boiled (**a**) or unboiled (**b**) samples of protein peaks were visualised using SDS-PAGE and coomassie staining to analyse subunit ratios or tetramer mobility respectively. The desired mixture of 1,3 trans-ST2 and 1,4 ST2 is highlighted in red.

Further to this, protein valency was estimated using a protocol modified from [Kada et al., 1999]. This protocol makes use of the self-quenching activity of biotin-4-fluorescein when bound to streptavidin or avidin (and in our case StrepTactin).

Titrating concentrations of biotin-4-fluorescein were mixed with StrepTactin and the fluorescence of the solutions measured. Because of the extremely high affinity of StrepTactin for biotin, below saturating concentrations, all biotin-4-fluorescein added is bound to the tetramer and will self-quench if the proteins are close enough to each other. At biotin-4-fluorescein concentrations above saturation, some the fluorescent biotin remains in solution and so shows no further self-quenching activity. At this point the fluorescence profile alters to match the gradient seen in the absence of StrepTactin (figure **3.29**). The concentration of biotin-4-fluorescein that saturates each tetramer is calculated from the fluorescent protein concentration at which the profile changes (figure **3.29**). This is then used to calculate the number of biotin-binding sites per tetramer. The number of binding sites measured for each tetramer, outlined in table **3.7**, are similar to those expected although the number of binding sites estimated for the sample containing 1,3 trans-ST2 and 1,4 ST2 is lower than for 1,2 cis-ST2. This may reflect the difference in binding site orientation between the two tetramers.

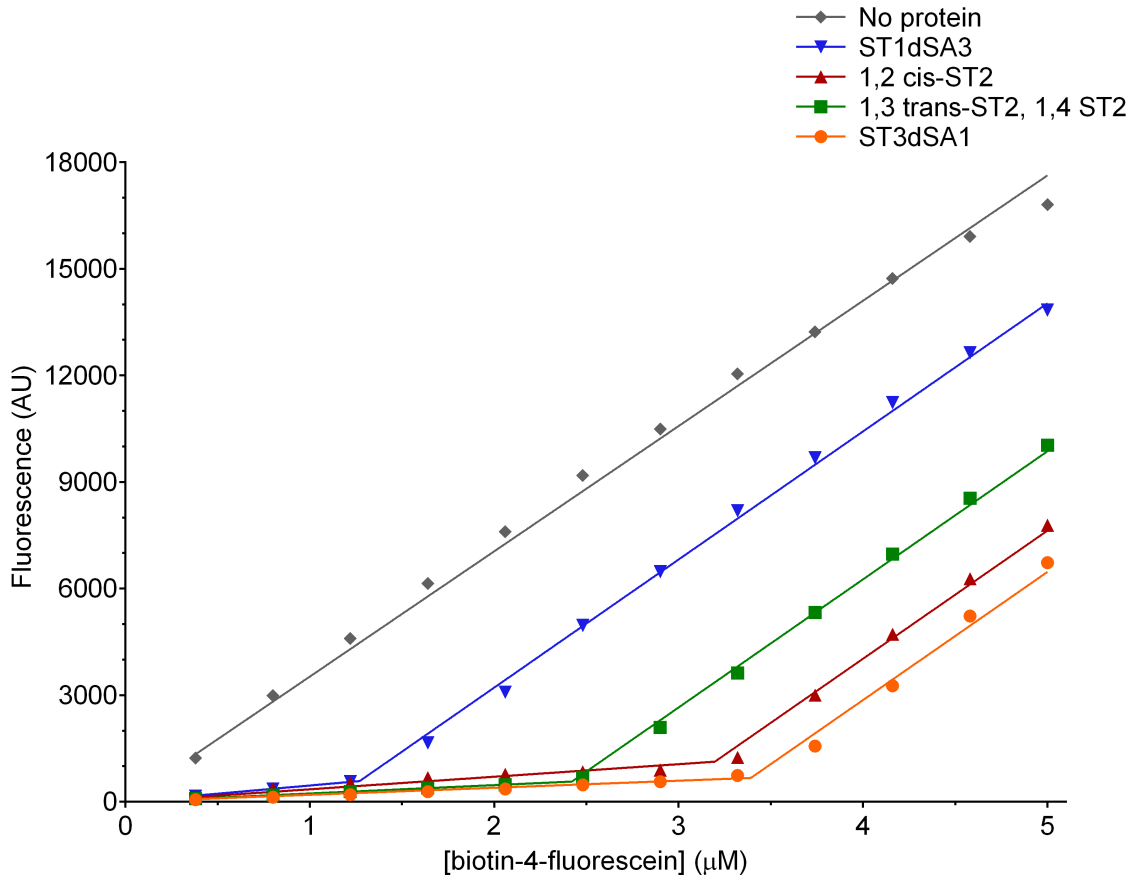


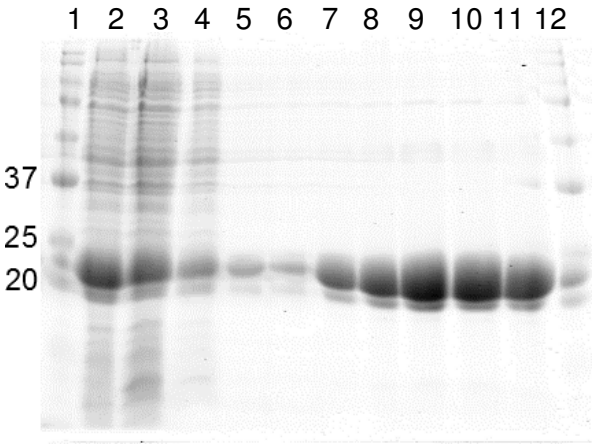
Fig. 3.29: **Measuring the number of biotin-binding sites on StrepTactin tetramers using biotin-4-fluorescein.** ST1dSA3, 1,2 cis-ST2, the mixture of 1,3 trans-ST2 and 1,4 ST2, or ST3dSA1, (0.9 μM) or PBS was mixed with titrating concentrations of biotin-4-fluorescein. Fluorescence of the mixtures was then measured. Mean fluorescence values of PBS-only control wells were subtracted from all test values. These are plotted here against concentration of biotin-4-fluorescein added to the well. Each StrepTactin dataset was fit with a segmental linear regression and used to calculate the number of biotin-binding sites for each tetramer.

Tetramer	# binding sites per StrepTactin
ST3dSA1	3.7
1,3 trans-ST2 and 1,4 ST2	2.7
1,2 cis-ST2	3.5
ST1dSA3	1.4

Tab. 3.7: **Number of biotin-binding sites measured per StrepTactin tetramer.** The number of biotin-binding sites per StrepTactin tetramer was calculated using the fluorescence profiles shown in figure **3.29**.

3.2.6 Synthesis of SNAP-Strep-Tag II:488

Soluble Strep-Tag II fused to a SNAP tag (SNAP-Strep-Tag II) was synthesised and purified using a StrepTactin resin column as described in section 2.6.3. Samples of protein taken at various points throughout the expression and purification of SNAP-Strep-Tag II were visualised using SDS-PAGE to confirm the successful purification of the protein (figure **3.30**). The eluted fractions of SNAP-Strep-Tag II were reasonably pure with the predominant band migrating at the predicted size of ∼21 kDa. The purified protein was then labelled with Alexa Fluor®488 (SNAP-Strep-Tag II:488) to be used in flow cytometry experiments.



1. Precision plus Kaleidoscope protein ladder
2. Cleared lysate
3. Flow-through
4. Wash # 1
5. Wash # 2
6. Eluted fraction # 1
7. Eluted fraction # 2
8. Eluted fraction # 3
9. Eluted fraction # 4
10. Eluted fraction # 5
11. Eluted fraction # 6
12. Precision plus Kaleidoscope protein ladder

Fig. 3.30: **Samples of SNAP-Strep-Tag II purification visualised by SDS-PAGE.** Boiled samples of protein taken at various points throughout the expression and purification of SNAP-Strep-Tag II were visualised using SDS-PAGE. SNAP-Strep-Tag II was purified using a StrepTactin resin column.

3.2.7 Soluble StrepTactin can bind cells expressing Strep-Tag II-tagged receptors but remaining available binding sites cannot be detected

Both ST4 and ST3dSA1 were labelled with Atto 647 dye (termed ST4:647 and ST3dSA1:647 respectively) for analysis of these tetramers binding to cells expressing tagged NTRs. Firstly, we determined an optimal concentration of StrepTactin to incubate with the NTR-expressing cell lines for flow cytometry analysis. THP-1 NKp30 cells were used as an example cell line. Figure **3.31** shows 0.19 μM ST4:647 appears to saturate the cells and

so this concentration was used for future incubation of cells with StrepTactin.

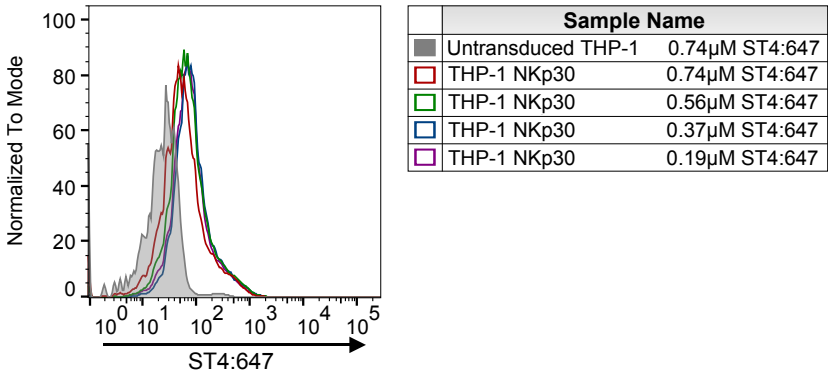


Fig. 3.31: **ST4:647 can bind to THP-1 NKp30 cells.** ST4:647 was incubated with THP-1 NKp30 cells at concentrations varying from 0.19 µM to 0.74 µM. The cells were then analysed for ST4:647 binding using flow cytometry.

ST3dSA1:647 was then incubated with three different NTR-expressing THP-1 cell lines to confirm the protein is able to specifically bind to the Strep-Tag II (figure **3.32**). Indeed ST3dSA1:647 (and also anti-Strep-Tag II antibody) is able to bind to the Strep-Tag II-tagged receptors expressed on cells indicating that the Strep-Tag II is accessible and can be ligated by StrepTactin protein.

To confirm the presence of available biotin-binding sites on THP-1 NKp30 cells bound by StrepTactin, we incubated cells with non fluorescent ST3dSA1 followed by biotinylated mouse IgG1 and fluorescent secondary antibody (figure **3.33a**). Incubation of cells with the various proteins was conducted at 4°C in order to slow kinetics, and ST3dSA1 was added at a saturating concentration in order to minimise the likelihood of StrepTactin cross-linking receptors, which would reduce the number of sites free for biotin binding. While ST3dSA1:647 could bind THP-1 NKp30 cells as shown using flow cytometry (figure **3.33b**) binding of biotinylated mouse IgG1 was not detected (figure **3.33c**).

These data suggest that while StrepTactin can indeed bind the receptor, it does so with all three sites, or that StrepTactin binds to the tagged receptor such that the binding of biotinylated IgG1 or a further antibody is sterically hindered.

Alternatively, there is evidence that mouse IgG1 can bind to human Fc receptors (discussed in [Bruhns, 2012]). THP-1 cells are known to express Fc receptors and therefore it is possible any specific binding of biotinylated mouse IgG1 to StrepTactin was masked by non-specific binding of the IgG1 to Fc receptors [Fleit and Kobasiuk, 1991]. This

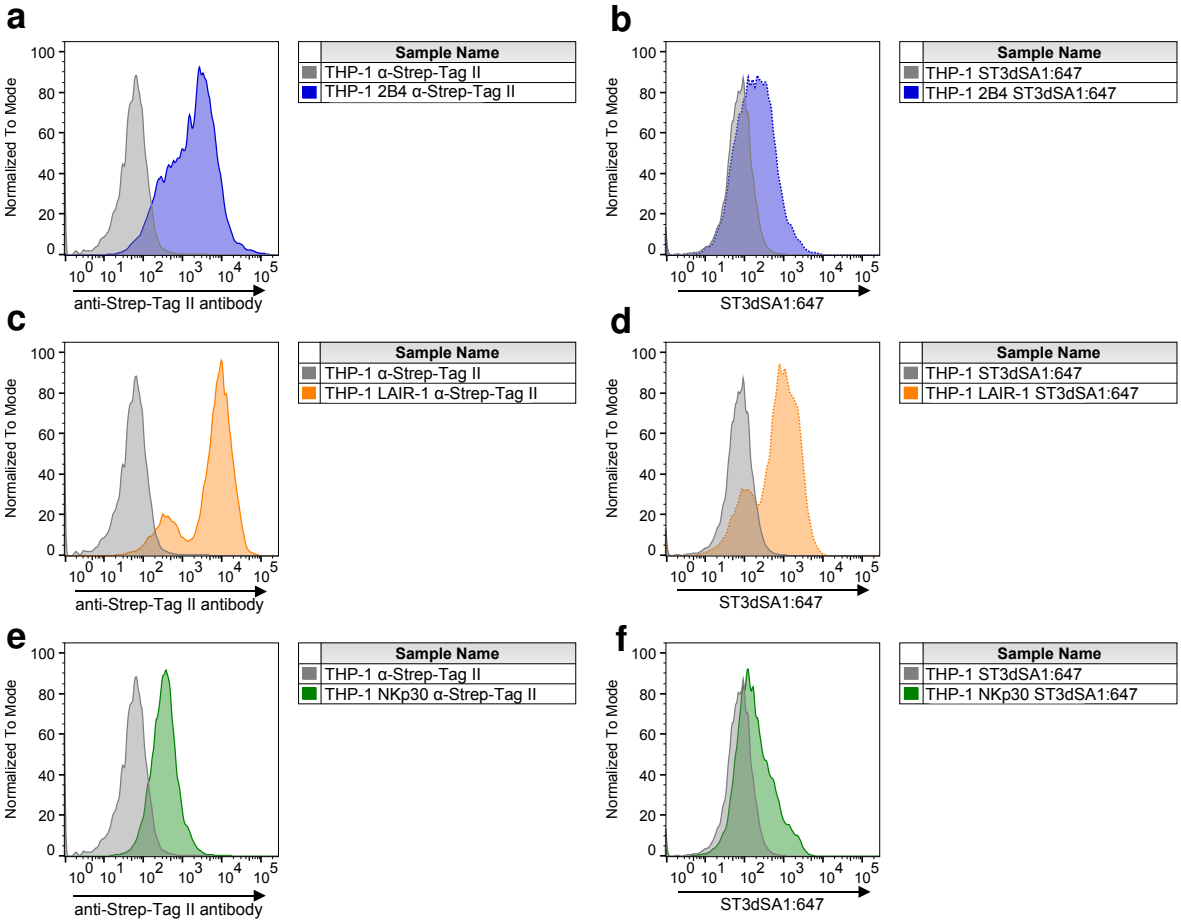


Fig. 3.32: **ST3dSA1:647 and anti-Strep-Tag II antibody bind to THP-1 2B4 cells, THP-1 LAIR-1 cells, and THP-1 NKp30 cells.** THP-1 2B4 cells were stained using anti-Strep-Tag II antibody (**a**) or incubated with ST3dSA1:647 (**b**), and then analysed for protein binding using flow cytometry. THP-1 LAIR-1 cells (**c-d**), or THP-1 NKp30 cells (**e-f**) were also stained using anti-Strep-Tag II antibody or incubated with ST3dSA1:647 respectively and then analysed.

could explain the difference in fluorescence intensity between negative control samples incubated with biotinylated mouse IgG1 and those not (figure **3.33d**).

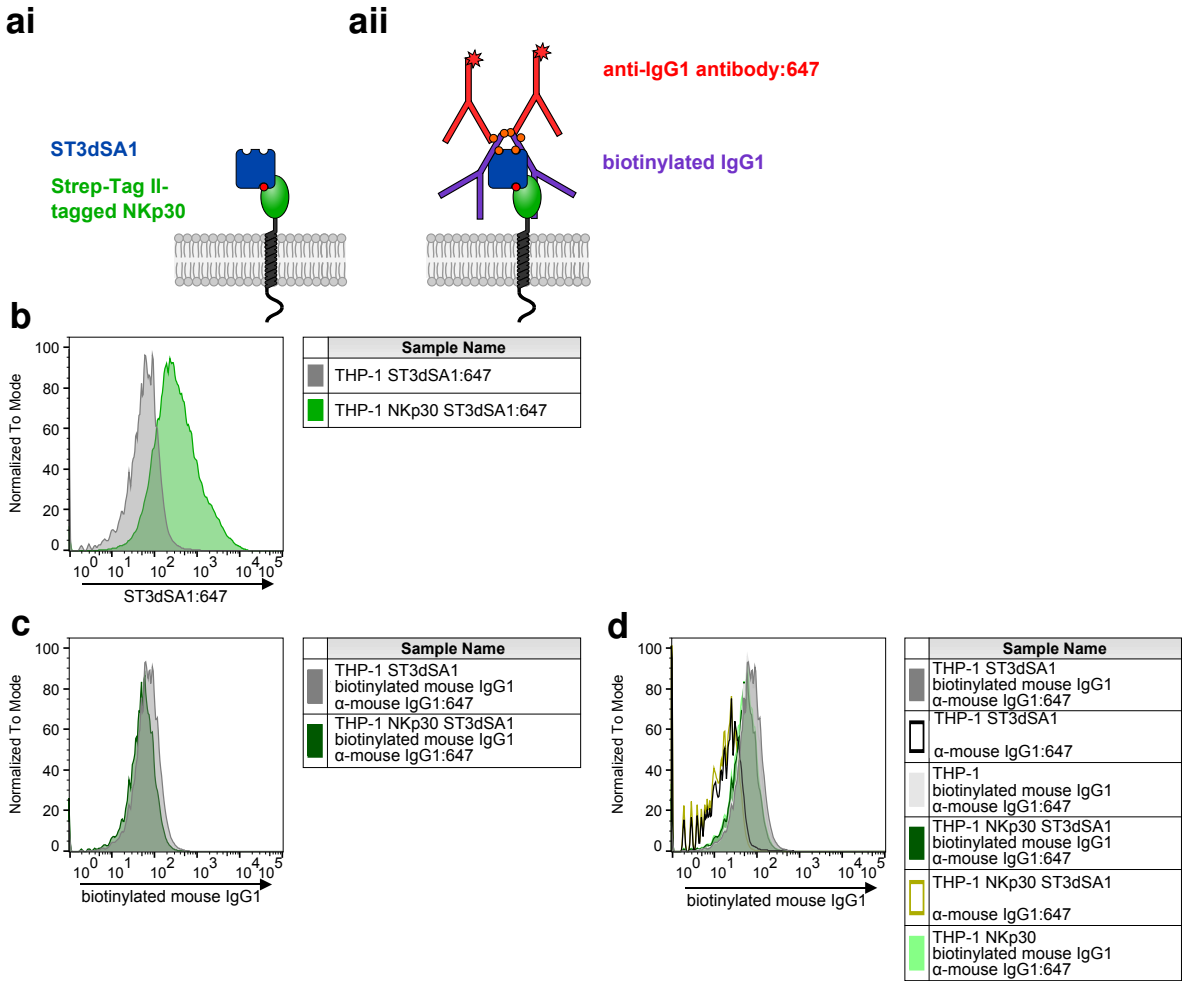


Fig. 3.33: **ST3dSA1 can bind THP-1 NKp30 cells but remaining available biotin-binding sites cannot be detected.** Cartoons depicting the set-ups used to produce the data in **b** and **c-d** are shown in **ai** and **aii** respectively. In **b**, THP-1 NKp30 cells were incubated with fluorescent ST3dSA1:647 and then analysed by flow cytometry. In **c**, THP-1 NKp30 cells were incubated with ST3dSA1 followed by biotinylated mouse IgG1 and anti-mouse IgG1:alexa 647. Negative controls were also included where cells were not incubated with ST3dSA1 or not incubated with biotinylated mouse IgG1 (**d**). Untransduced THP-1 cells were also incubated with the proteins as a further negative control.

3.2.8 Soluble StrepTactin of different valency can bind cells expressing biotinylated ligands of different lengths with varying numbers of remaining available biotin-binding sites

For the analysis of both StrepTactin binding to ligand cells, and the available biotin-binding sites on StrepTactin-bound cells, transiently transfected HEK293T cells were used.

As shown in figure **3.34** ST3dSA1:647 could bind to the biotinylated ligand in HEK293T CD80, HEK293T CD80-CD2, or HEK293T CD80-CD4 ligand cells. This indicates that StrepTactin can bind the biotinylated ligand. The ligand cells had not been sorted for ligand expression prior to this flow cytometry analysis so contained populations of positive and negative cells. The cell lines were therefore also stained for ligand expression using anti-HA tag antibody for comparative purposes (figure **3.34**).

To determine whether StrepTactin bound to the biotinylated ligand had free binding sites that could engage Strep-Tag II-tagged receptor, either fluorescent soluble Strep-Tag II (SNAP-Strep-Tag II:488) (figure **3.35a**) or biotinylated mouse IgG1 (figure **3.35b**) were incubated with StrepTactin-bound ligand cells. Soluble Strep-Tag II and biotinylated mouse IgG1 should bind to any free binding sites on StrepTactin bound to the ligand cells. The cells were then analysed for protein binding using flow cytometry.

Available Strep-Tag II-binding sites on ST3dSA1:647-bound ligand cells were not detected with SNAP-Strep-Tag II:488 (figure **3.35c-g**). In contrast, incubating ST3dSA1:647-bound HEK293T CD80, HEK293T CD80-CD2, or HEK293T CD80-CD4 with biotinylated mouse IgG1 followed by a fluorescent secondary antibody did indicate the presence of available biotin-binding sites on StrepTactin-bound ligand cells (figure **3.35h-k**).

The signals of ST3dSA1:647 and biotinylated IgG1 mouse (with fluorescent secondary antibody) binding are also well correlated for the population of cells that express ligand in all three cell lines (figure **3.35i, j, k**). The signal for biotinylated mouse IgG1 binding on HEK293T CD80-CD4 cells was lower than that for HEK293T CD80 and HEK293T CD80-CD2 cells (figure **3.35k** versus **i** and **j**) which corresponds in part with a consistently lower fluorescence signal seen with ST3dSA1:647 binding to HEK293T CD80-CD4 cells

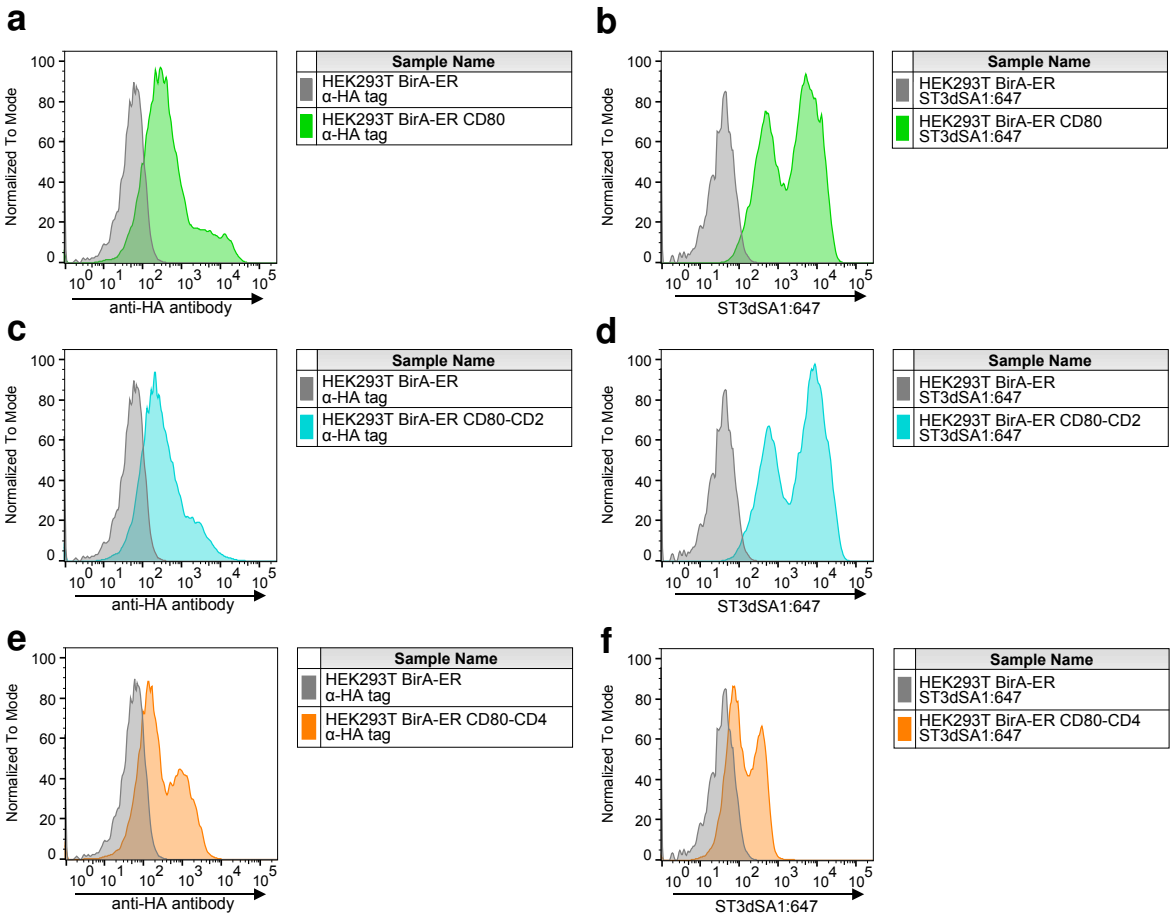


Fig. 3.34: **ST3dSA1:647 can bind to HEK293T cells expressing either CD80, CD80-CD2, or CD80-CD4 ligand.** HEK293T cells transiently co-transfected with BirA-ER and either CD80 ■, CD80-CD2 ■, or CD80-CD4 ■ were either stained with anti-HA tag antibody:alexa 647 (**a, c, e**) or incubated with ST3dSA1:647 (**b, d, f**). Cells were then analysed for antibody or protein binding using flow cytometry. Cells transfected with just BirA-ER were also analysed as a negative control.

compared to the other lines (seen in figure **3.34f**).

Increasing the concentration of SNAP-Strep-Tag II:488 incubated with the StrepTactin-bound cells did not improve the signal (data not shown). The degree of labelling of this protein was quite poor (calculated at $\sim$0.4 moles of dye to 1 mole of SNAP-Strep-Tag II) and despite a number of attempts, it was not improved. It is therefore possible that the fluorescence of this reagent is not detectable in our experiments. Alternatively, it is possible that the interaction between StrepTactin and soluble Strep-Tag II is too short-lived to be useful as a reagent in our flow cytometry studies.

As a result of this, detection of binding sites on StrepTactin-bound cells was only continued with biotinylated mouse IgG1.

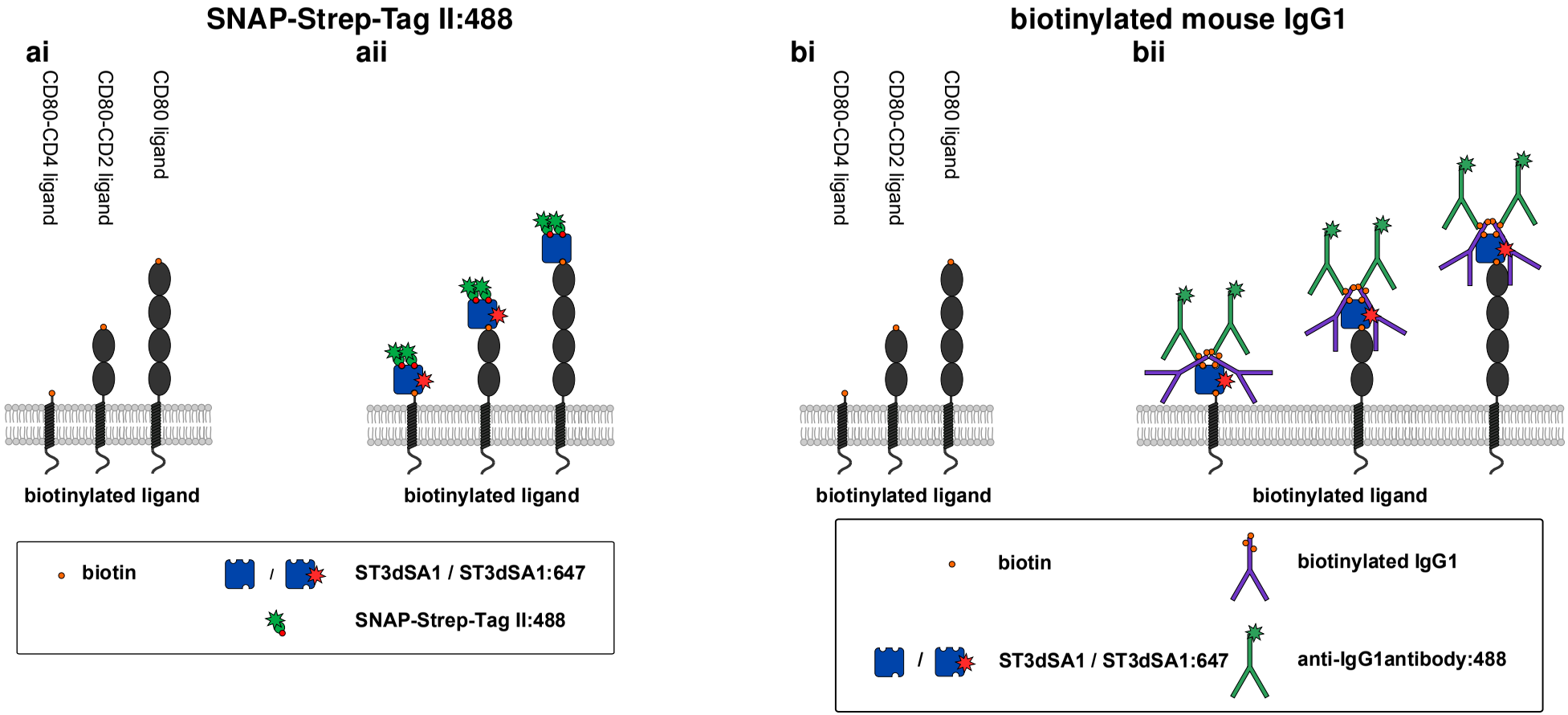


Fig. 3.35: **ST3dSA1:647 binds to HEK293T CD80, HEK293T CD80-CD2, and HEK293T CD80-CD4 cells with sites available for biotin to bind.** Cartoons depicting the set-ups used to produce the data in **c-g** and **h-k** are shown in **ai-aii** and **bi-bii** respectively. HEK293T cells expressing either CD80, CD80-CD2, or CD80-CD4 ligand (shown in **ai** and **bi**) were incubated with ST3dSA1 or ST3dSA1:647, and then either SNAP-Strep-Tag II:488 (**aii**), or biotinylated IgG1 and anti-IgG1 antibody:488 (**bii**), was used to determine whether free biotin-binding sites are present on the StrepTactin-bound ligand. *Continued on the next page.*

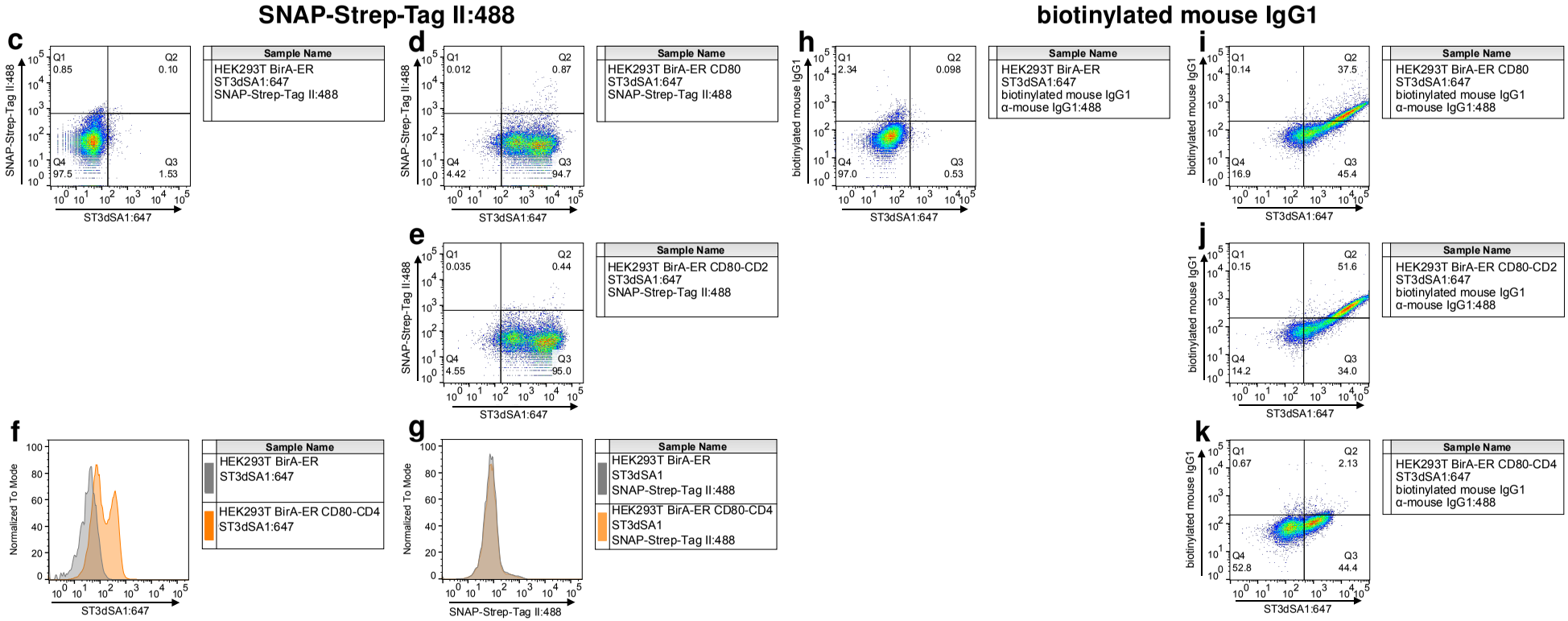


Fig. 3.35: **ST3dSA1:647 binds to HEK293T CD80, HEK293T CD80-CD2, and HEK293T CD80-CD4 cells with sites available for biotin to bind.***Continued.* Mock transfected HEK293T cells (BirA-ER alone) were incubated with ST3dSA1:647 (x-axis) and SNAP-Strep-Tag II:488 (y-axis) to analyse background protein binding (**c**). HEK293T CD80 cells (**d**) or HEK293T CD80-CD2 cells (**e**) were incubated with ST3dSA1:647 (x-axis) and then SNAP-Strep-Tag II:488 (y-axis), before being analysed by flow cytometry. HEK293T CD80-CD4 cells were incubated with ST3dSA1:647 (**f**) or ST3dSA1 and then SNAP-Strep-Tag II:488 (**g**) and then analysed for protein binding. Mock transfected HEK293T cells (BirA-ER alone) were also incubated with ST3dSA1:647 (x-axis) and biotinylated mouse IgG1 and fluorescent secondary antibody (y-axis) to analyse background protein binding (**h**). HEK293T CD80 cells (**i**), HEK293T CD80-CD2 cells (**j**), or HEK293T CD80-CD4 cells (**k**) were incubated with ST3dSA1:647 (x-axis) and biotinylated mouse IgG1 and fluorescent secondary antibody (y-axis) and then protein binding was analysed using flow cytometry. Figures **f-g** were conducted on a different day to the rest of the figure.

The availability of biotin-binding sites on ligand-expressing cells bound by StrepTactin of different valencies was also analysed. Again, biotinylated mouse IgG1 followed by fluorescent secondary antibody were incubated with StrepTactin-bound cells before being analysed for protein binding using flow cytometry (figure **3.36a**). HEK293T CD80 cells were not sorted for ligand expression prior to these experiments and so there is a population of cells that express the biotinylated ligand, and a population of cells that does not. HEK293T CD80 cells were therefore also stained with anti-HA tag antibody for comparison purposes (figure **3.36b**). Biotin-binding sites could not be detected on HEK293T CD80 cells bound by 1,2 cis-ST2 (figure **3.36c**). Conversely, sites were detected on HEK293T CD80 cells incubated with either ST3dSA1 or the mixture of 1,3 trans-ST2 and 1,4 ST2 (figure **3.36d-e**). The same results were seen with HEK293T CD80-CD2 cells: biotin-binding sites were detected on cells bound by ST3dSA1 or the sample containing 1,3 trans-ST2 and 1,4 ST2, but not 1,2 cis-ST2 (figure **3.37**).

The negative controls shown in figures **3.36** and **3.37** (panels cii, dii and eii) whereby transfected cell lines were not incubated with StrepTactin or not incubated with biotinylated mouse IgG1 overlay both each other and the mock transfected cell negative control indicating that there is no non-specific binding of the immunoglobulins or StrepTactin to the ligand-expressing cells.

The results presented in figures **3.36** and **3.37** indicate the mixture of 1,3 trans-bivalent and 1,4 bivalent StrepTactin does bind to ligand-expressing cells with available binding sites which is required for the artificial ligand to engage Strep-Tag II-tagged receptors. This suggests that biotinylated ligand bound by the bivalent StrepTactin mixture can be used as an artificial ligand for Strep-Tag II-tagged NTRs.

These results also confirm that 1,2 cis-ST2 is not a suitable reagent for our experiments. The data suggest that 1,2 cis-ST2 binds to the cell using both of its biotin-binding sites and therefore no free sites remain. Alternatively, as the two biotin-binding sites of 1,2 cis-ST2 are relatively close to each other and face the same direction the tetramer may not be able to bind two biotinylated proteins simultaneously.

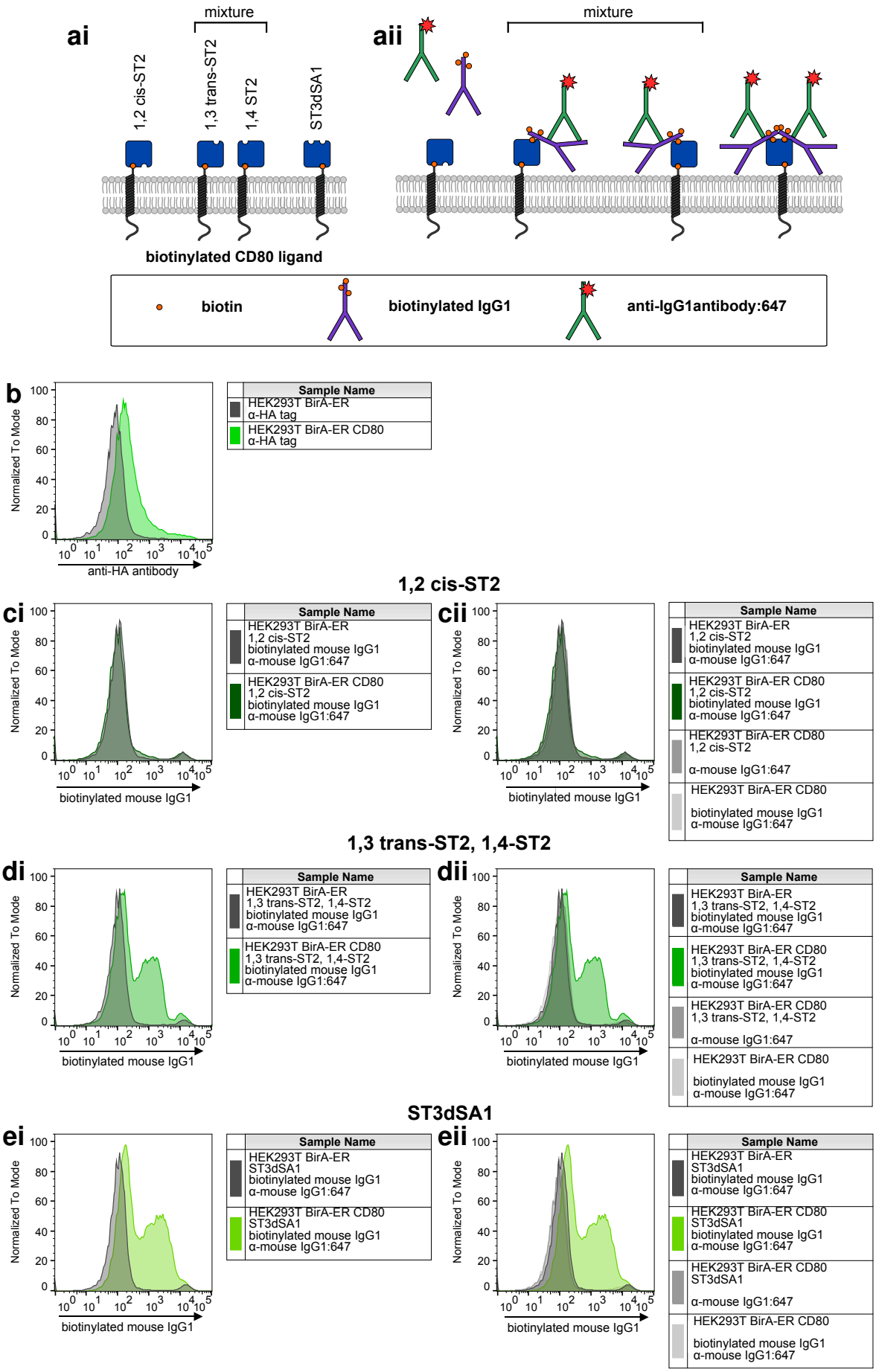


Fig. 3.36: **Biotin-binding sites can be detected on HEK293T CD80 cells bound by either ST3dSA1 or the mixture of 1,3 trans-ST2 and 1,4 ST2, but not 1,2 cis-ST2.** *Continued on the next page.*

Fig. 3.36: **Biotin-binding sites can be detected on HEK293T CD80 cells bound by either ST3dSA1 or the mixture of 1,3 trans-ST2 and 1,4 ST2, but not 1,2 cis-ST2.** *Continued.* A cartoon illustrating the set-up used to produce the data in **c-e** is shown in **a**. HEK293T CD80 cells were incubated with either 1,2 cis-ST2, or the mixture of 1,3 trans-ST2 and 1,4 ST2, or ST3dSA1 (**ai**) before the cells were incubated with biotinylated IgG1 and then anti-IgG1 antibody to determine whether free biotin-binding sites were present on the StrepTactin-bound ligands (**aii**). For comparative purposes, transiently transfected HEK293T CD80 cells were incubated with anti-HA tag antibody and then analysed for antibody binding using flow cytometry (**b**). HEK293T CD80 cells were incubated with either 1,2 cis-ST2 (**ci, cii**), or the mixture of 1,3 trans-ST2 and 1,4 ST2 (**di, dii**), or ST3dSA1 (**ei, eii**) followed by biotinylated mouse IgG1 and then fluorescent secondary antibody. Cells were then analysed by flow cytometry. As negative controls, mock transfected HEK293T cells were also incubated with these proteins (shown in dark grey). Further to this, HEK293T CD80 cells were incubated with either 1,2 cis-ST2, or the mixture of 1,3 trans-ST2 and 1,4 ST2, or ST3dSA1, followed by the fluorescent secondary antibody only (**cii**, **dii**, and **eii** respectively in mid grey), or cells were incubated with only biotinylated mouse IgG1 and fluorescent secondary antibody (shown in **cii**, **dii**, and **eii** in light grey).

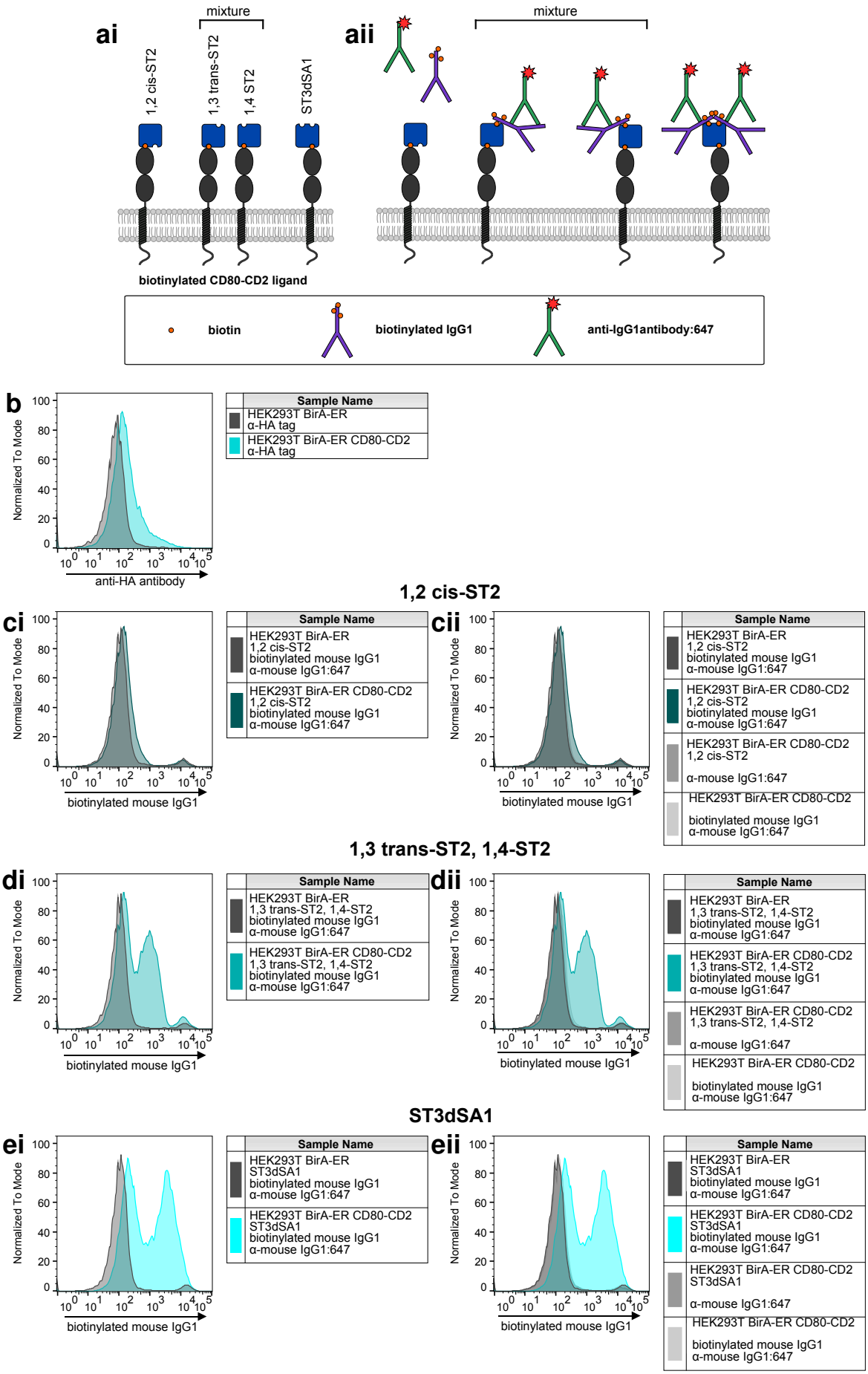


Fig. 3.37: **Biotin-binding sites can be detected on HEK293T CD80-CD2 cells bound by either ST3dSA1 or the mixture of 1,3 trans-ST2 and 1,4 ST2, but not 1,2 cis-ST2.** *Continued on the next page.*

Fig. 3.37: **Biotin-binding sites can be detected on HEK293T CD80-CD2 cells bound by either ST3dSA1 or the mixture of 1,3 trans-ST2 and 1,4 ST2, but not 1,2 cis-ST2.** *Continued.* A cartoon illustrating the set-up used to produce the data in **c-e** is shown in **a**. HEK293T CD80-CD2 cells were incubated with either 1,2 cis-ST2, or the mixture of 1,3 trans-ST2 and 1,4 ST2, or ST3dSA1 (**ai**) before the cells were incubated with biotinylated IgG1 and then anti-IgG1 antibody to determine whether free biotin-binding sites were present on the StrepTactin-bound ligands (**aii**). For comparative purposes, transiently transfected HEK293T CD80-CD2 cells were incubated with anti-HA tag antibody and then analysed for antibody binding using flow cytometry (**b**). HEK293T CD80-CD2 cells were incubated with 1,2 cis-ST2 (**ci, cii**), or the mixture of 1,3 trans-ST2 and 1,4 ST2 (**di, dii**), or ST3dSA1 (**ei, eii**) followed by biotinylated mouse IgG1 and then fluorescent secondary antibody. Cells were analysed by flow cytometry. As negative controls, mock transfected HEK293T cells were also incubated with these proteins (shown in dark grey). Further to this, HEK293T CD80-CD2 cells were incubated with either 1,2 cis-ST2, or the mixture of 1,3 trans-ST2 and 1,4 ST2, or ST3dSA1, followed by the fluorescent secondary antibody only (**cii**, **dii**, and **eii** respectively in mid grey), or cells were incubated with only biotinylated mouse IgG1 and fluorescent secondary antibody (shown in **cii**, **dii**, and **eii** in light grey).

3.2.9 Soluble StrepTactin of different valency can bind biotin presented on supported lipid bilayers with varying numbers of remaining available biotin-binding sites.

Phospholipid bilayer-coated beads were synthesised with varying proportions of biotinyl cap phosphoethanolamine (PE) mixed with phosphatidylcholine to simulate ligand- expressing cells. A selection of these beads were incubated with ST3dSA1:647 to confirm that StrepTactin is able to bind the biotin presented on them (figure **3.38b**).

Just as conducted for ligand-expressing HEK293T cells, biotinylated mouse IgG1 and then fluorescent secondary antibody were incubated with lipid bilayer-coated beads pre-incubated with either the mixture of 1,3 trans-ST2 and 1,4 ST2, or ST3dSA1, or ST4, to crudely compare the number of remaining available biotin-binding sites (figure **3.38a**). Beads coated in varying proportions of biotinyl cap PE were analysed in this way although only a representative set of data is shown in figure **3.38**. Beads coated with either 1,3 trans-ST2 and 1,4 ST2, or ST3dSA1, or ST4 were all shown to have available biotin-binding sites (figure **3.38c-e**). Negative controls, where beads were not incubated with StrepTactin, or where beads were not incubated with biotinylated mouse IgG1, were also analysed (panels cii, dii, eii). The histograms of these data overlap both each other and the histograms of beads that did not present biotin (negative control beads) that were incubated with StrepTactin and immunoglobulins (figures **3.38cii, dii, eii**). This indicates that neither StrepTactin nor immunoglobulins non-specifically bind to the phospholipid bilayer-coated beads.

The median fluorescence intensites (MFI) of the beads incubated with StrepTactin of different valency and then biotinylated mouse IgG1 and fluorescent secondary antibody (shown in figure **3.38ci, di** and **ei**) were measured to crudely compare the available binding sites between StrepTactin-bound beads. These values are shown in table **3.8**. As expected, ST4-bound beads had the highest number of available biotin-binding sites, followed by ST3dSA1 and then the mixture of 1,3 trans-ST2 and 1,4 ST2. The MFI of the 1,3 bivalent and 1,4 bivalent StrepTactin-bound beads was much lower than expected though in comparison to ST3dSA1 and ST4. It is possible that, in line with what we suggest for 1,2 cis-ST2 binding to ligand-expressing cells, a significant proportion of the 1,3

trans-bivalent and 1,4 bivalent StrepTactin proteins are binding to the biotin presented on the bilayer-coated beads bivalently and so fewer binding sites are available for biotinylated IgG1 binding. This effect is illustrated in figure **3.39**. Incubation of the proteins with the beads was conducted at 4°C to slow kinetics and the proteins were also added at saturating concentrations in order to minimise the possibility of multivalent binding. It appears the protein still bound bivalently to the beads however.

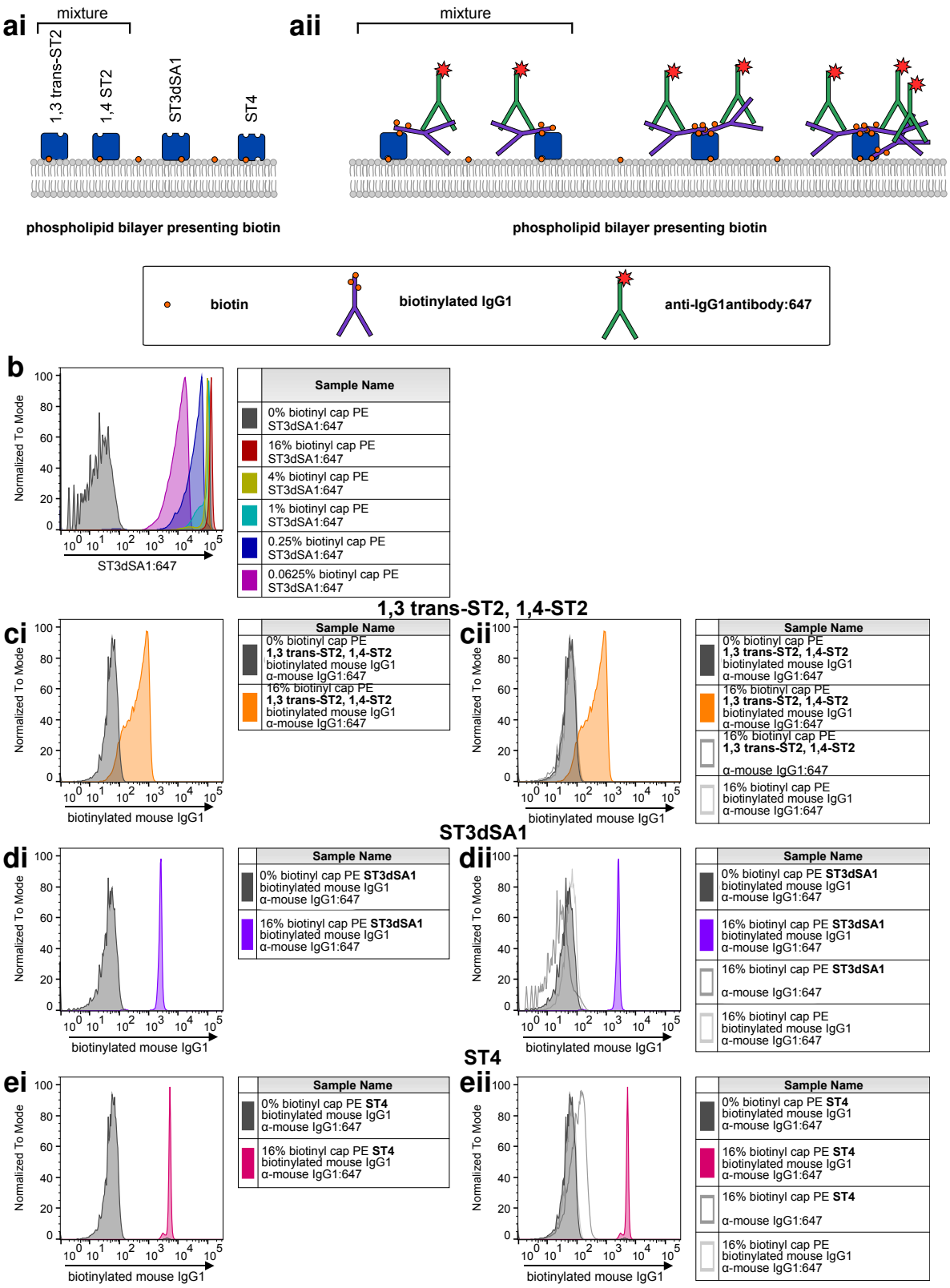


Fig. 3.38: **StrepTactin can bind biotin presented on phospholipid bilayer-coated beads with remaining sites available for biotin binding.** A cartoon illustrating the set-up used to produce the data in **c-e** is shown in **a**. Silica beads were coated with a phospholipid bilayer containing varying concentrations of biotinyl cap PE to simulate ligand cells. A selection of these beads were incubated with either the mixture of 1,3 trans-ST2 and 1,4 ST2, or ST3dSA1, or ST4 (**ai**) before the beads were incubated with biotinylated IgG1 and then anti-IgG1 antibody to determine whether free biotin-binding sites were present on the StrepTactin bound to the presented biotin (**aii**). *Continued on the next page.*

Fig. 3.38: **StrepTactin can bind biotin presented on phospholipid bilayer-coated beads with remaining sites available for biotin binding.** *Continued.* To first show that StrepTactin can bind to the biotin presented on the bilayer, the beads with varying proportions of biotinyl cap PE were incubated with ST3dSA1:647 and analysed for protein binding by flow cytometry (**b**). In **c-e** beads coated with a bilayer with 16% biotinyl cap PE were incubated with the mixture of 1,3 trans-ST2 and 1,4-ST2 (**ci, cii**), or ST3dSA1 (**di, dii**), or ST4 (**ei, eii**), followed by biotinylated mouse IgG1 and then fluorescent secondary antibody. The beads were then analysed by flow cytometry. As a negative control, beads not presenting biotin were treated as above (shown in dark grey). As further negative controls, 16% cap biotinyl PE bilayer-coated beads were incubated with either the mixture of 1,3 trans-ST2 and 1,4 ST2, or ST3dSA1, or ST4, and fluorescent secondary antibody only (**cii**, **dii**, and **eii** respectively in mid grey), or beads were incubated with only biotinylated mouse IgG1 and fluorescent secondary antibody (shown in **cii**, **dii**, and **eii** in light grey).

StrepTactin	Median fluorescence intensity
1,3 trans-bivalent and 1,4 bivalent StrepTactin	402
ST3dSA1	2442
ST4	5089

Tab. 3.8: **StrepTactin of different valency can bind biotin presented on phospholipid bilayer-coated beads with remaining sites available for biotin binding.** Median fluorescence intensities (MFI) of histograms in figure **3.38** were extracted using FlowJo software. The MFIs of negative control beads that were incubated with ST4, or ST3dSA1, or both 1,3 trans-ST2 and 1,4 ST2, and then biotinylated mouse IgG1 and secondary antibody were subtracted first from the corresponding 16% biotinyl cap PE bead values.

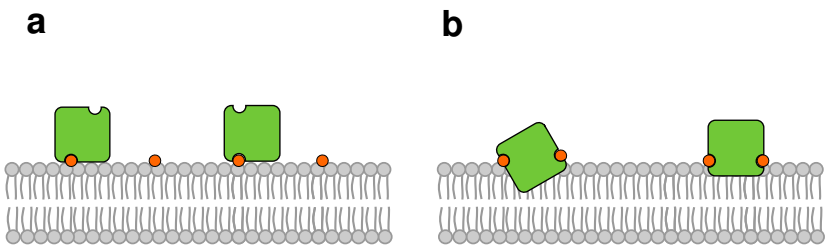


Fig. 3.39: **Both 1,3 trans-ST2 and 1,4 ST2 may bind to presented biotin bivalently.** Under the conditions of our experiments we expected 1,3 trans-ST2 and 1,4 ST2 to bind to presented biotin with one biotin-binding site leaving the other accessible for ligation of Strep-Tag II tagged NTRs or biotinylated protein. This is shown in **a** as 1,3 trans-ST2 and 1,4 ST2 bound to biotin presented on a lipid bilayer. We predict from our results however that a significant proportion of the bivalent StrepTactin is binding to the presented biotin bivalently such that there are no free sites for ligation of the receptor (**b**). Bivalent StrepTactin is shown in green and biotin in orange.

Although this analysis would need to be repeated to confirm the results seen here, bivalent binding of the desired 1,3 trans-bivalent and 1,4 bivalent StrepTactin proteins presents a challenge for our artificial ligand strategy. For receptor-artificial ligand interactions to occur, at least a significant proportion of the bivalent StrepTactin added to

the cells is required to bind monovalently to one biotinylated ligand, leaving the other binding site free for binding to the Strep-Tag II-tagged receptor.

3.2.10 Second strategy to stimulate NTRs

The results presented in sections 3.2.8 and 3.2.9 indicate that bivalent StrepTactin binds bivalently to biotinylated ligand. However, the system we present requires StrepTactin to bind monovalently in order to allow engagement of the Strep-Tag II-tagged receptor. For this reason a new system was developed. This system makes use of the irreversible covalent interaction between a peptide tag SpyTag and its protein partner SpyCatcher [Zakeri et al., 2012]. Using this system did not require the receptor constructs or cell lines to be remade as it still uses StrepTactin to ligate the Strep-Tag II of the NTR. However, the artificial ligands are different: in the new approach, the N terminal Avitag peptide motif (for biotinylation) is replaced with a SpyTag peptide (sequence AHIVMVDAYKPTK). The ligand construct therefore had to be remade. Elongated versions of the ligand were also constructed by insertion of the 2 immunoglobulin-like domains of human CD2 or the 4 immunoglobulin-like domains of human CD4. The inserted immunoglobulin-like domains were also point mutated with previously characterised mutations in order to prevent unwanted interactions between the ligands and binding partners of human CD2 and CD4 ie. CD58 and MHC class II [Piatier-Tonneau et al., 1991, van der Merwe et al., 1995]. The new ligand constructs termed CD80-Spy, CD80-CD2-Spy, and CD80-CD4-Spy were created by Dr Jesse Goyette and Rachel Paterson and are shown in cartoon form in figure **3.40**.

In this second strategy, soluble StrepTactin is still bound to the ligand for presentation to the receptor, but instead of binding via a biotin:StrepTactin interaction, one of the four subunits in the StrepTactin tetramer is expressed fused to the SpyTag binding partner SpyCatcher. This conjugates to the SpyTagged ligand, leaving any biotin/Strep-Tag II-binding sites of the tetramer free. This removes the problems we saw using biotinylated ligand whereby bivalent StrepTactin tetramers were most likely binding to more than one ligand and therefore unable to ligate the tagged receptor. We produced StrepTactin-SpyCatcher tetramers which have either one (monovalent) or four (tetravalent) binding

sites for Strep-Tag II. Each tetramer also has a single SpyCatcher for coupling to a single SpyTagged ligand. The abbreviations we use to refer to the various StrepTactin-SpyCatcher proteins and cell lines throughout this work are listed in table **3.9**.

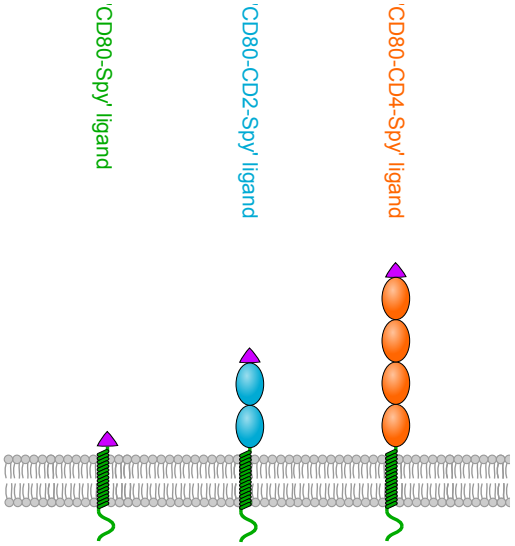


Fig. 3.40: **Cartoon diagrams of the SpyTagged artificial ligands.** CD80-Spy ligand is made up of the cytoplasmic, transmembrane and extracellular hinge-like regions of mouse CD80 with an N terminal SpyTag. The immunoglobulin-like domains of human CD2 or CD4 were inserted between the SpyTag and mouse CD80 protein to create the elongated CD80-CD2-Spy and CD80-CD4-Spy ligands. Mutations were introduced into CD2 (K43E) and CD4 (R54D) to prevent binding to the natural ligands. These constructs were created by Dr Jesse Goyette and Rachel Paterson.

3.2.10.1 Expression and purification of monovalent and tetravalent StrepTactin-SpyCatcher

Monovalent (ST1-pD-C) and tetravalent (ST4-pD-C) StrepTactin-Spycatcher were synthesised as described in section 2.5. We made StrepTactin-SpyCatcher tetramers of the desired valency by mixing monomers of StrepTactin fused to SpyCatcher (StrepTactin-SpyCatcher monomer) with monomers of dead streptavidin (for monovalent StrepTactin-SpyCatcher) or mixing monomers of StrepTactin-SpyCatcher with monomers of StrepTactin (for tetravalent StrepTactin-SpyCatcher) at a 1:3 molar ratio before refolding. During separation of StrepTactin tetramers by ion exchange chromatography we noticed that the tetramer with a single polyaspartate sequence was resolved the best (figure **3.27**). We therefore sought to purify StrepTactin-SpyCatcher tetramers with a single polyaspartate sequence. To do this, the polyaspartate sequence was inserted into the

Abbreviation	Protein/cell line
ST-pD-C	StrepTactin-SpyCatcher (no valency specified) ST - StrepTactin pD - polyaspartate sequence (one per tetramer) C - SpyCatcher
ST**1**-pD-C	**mono**valent StrepTactin-SpyCatcher
ST**4**-pD-C	**tetra**valent StrepTactin-SpyCatcher
CHO CD80-Spy : ST1-pD-C	CHO CD80-Spy cells with ST1-pD-C covalently bound to the CD80 ligand
CHO CD80-CD4-Spy : ST4-pD-C	CHO CD80-CD4-Spy cells with ST4-pD-C covalently bound to the CD80-CD4 ligand

Tab. 3.9: **Abbreviations used to refer to StrepTactin-SpyCatcher proteins and cell lines.** The "ST1" or "ST4" part of ST1-pD-C and ST4-pD-C identify the number of Strep-Tag II/biotin-binding sites per tetramer, and the "pD" and "C" identify that each tetramer has a single polyaspartate sequence and SpyCatcher respectively.

StrepTactin-SpyCatcher monomer. As both monovalent and tetravalent StrepTactin-SpyCatcher tetramers contain one subunit of StrepTactin-SpyCatcher monomer, both tetramers will contain a single polyaspartate sequence. The two tetramers are illustrated in figure **3.41a-b**.

The polyaspartate sequence was inserted between the StrepTactin and SpyCatcher sequences of the StrepTactin-SpyCatcher monomer. As the polyaspartate sequence is inserted at the C terminus of the StrepTactin and away from the Strep-Tag II binding site (shown in figure **3.41c**), we do not predict it will interfere with the interaction between StrepTactin-SpyCatcher and Strep-Tag II.

Both StrepTactin-SpyCatcher and dead streptavidin subunit constructs were created by Dr Jesse Goyette using templates provided by Professor Mark Howarth.

Chromatograms of ST1-pD-C or ST4-pD-C purification are shown in figures **3.42a** and **3.43a**. Based upon the separation of StrepTactin tetramers we predicted that the peaks highlighted in figures **3.42a** and **3.43a** correspond to monovalent and tetravalent StrepTactin-SpyCatcher respectively. To test this, samples of all peaks in both figures were boiled and analysed by SDS-PAGE (figures **3.42b** and **3.43b**). The density of the appropriate gel bands was measured using ImageJ and then used to calculate the ratio of StrepTactin-SpyCatcher subunit to either StrepTactin or dead streptavidin subunit for each peak and compared to the ratio predicted for each tetramer. The protein ratios for monovalent and tetravalent StrepTactin-SpyCatcher were not entirely consistent with that

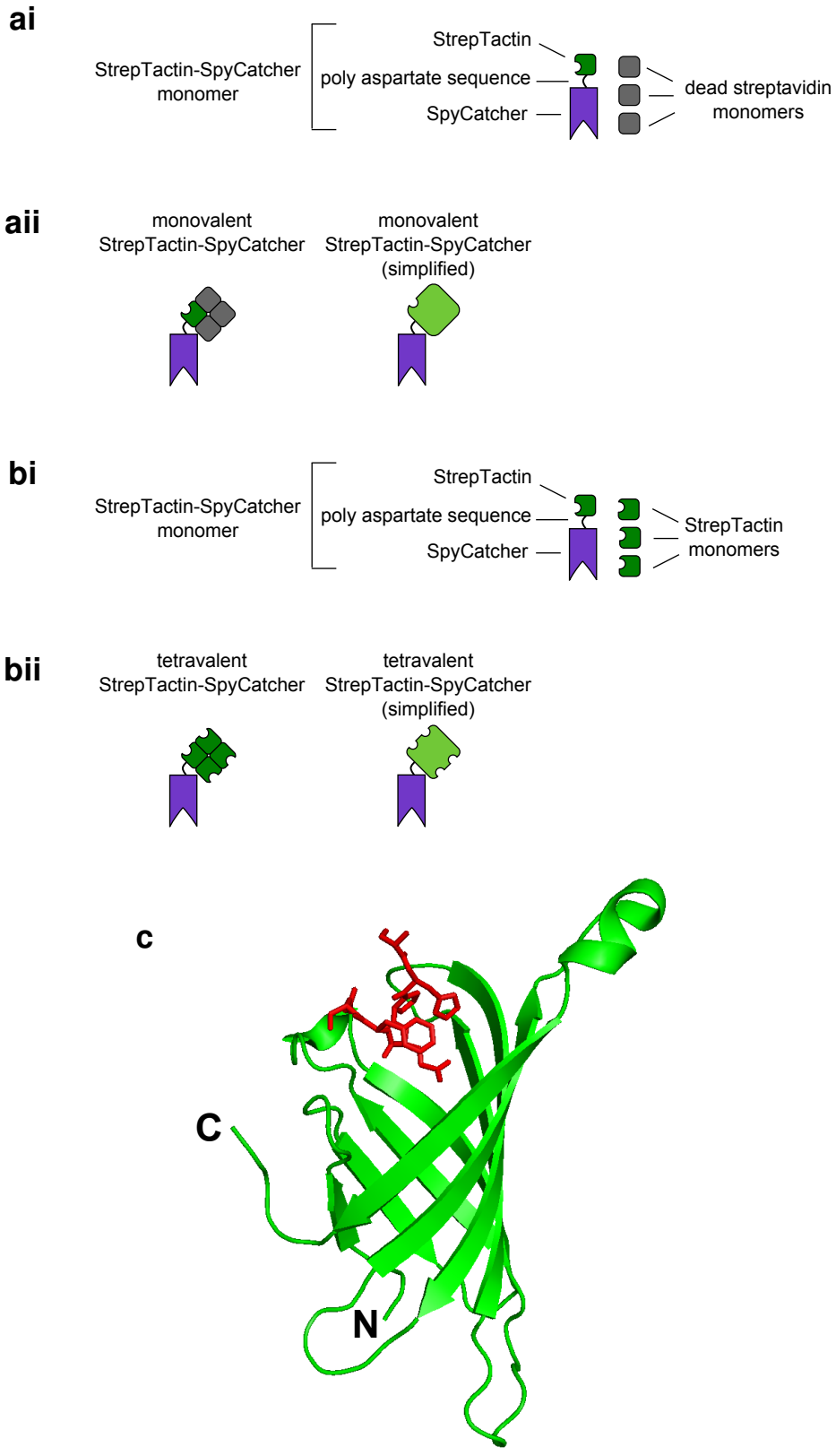


Fig. 3.41: **Overview of monovalent and tetravalent StrepTactin-SpyCatcher.** Monovalent StrepTactin-SpyCatcher is synthesised from StrepTactin-SpyCatcher monomers and dead streptavidin monomers mixed in a 1:3 ratio. These monomers are shown in (**ai**). The StrepTactin-SpyCatcher monomer consists of a StrepTactin sequence, followed by a polyaspartate sequence and then SpyCatcher sequence. Refolding this mix of monomers will produce tetramers of monovalent StrepTactin-SpyCatcher (among others). *Continued on the next page.*

Fig. 3.41: **Overview of monovalent and tetravalent StrepTactin-SpyCatcher.** *Continued.* A cartoon of the monovalent StrepTactin-SpyCatcher tetramer is shown in (**aii**, left) along with a simplified cartoon of the tetramer fusion protein which we use throughout the thesis (**aii**, right). Tetravalent StrepTactin-SpyCatcher is synthesised from StrepTactin-SpyCatcher monomers and StrepTactin monomers mixed in a 1:3 ratio. These monomers are shown in (**bi**). Refolding this mix of monomers will produce tetramers of tetravalent StrepTactin-SpyCatcher (among others). A cartoon of the tetravalent StrepTactin-SpyCatcher tetramer is shown in (**bii**, left) along with a simplified cartoon of the tetramer fusion protein which we use throughout the thesis (**bii**, right). The structure of one subunit of a StrepTactin tetramer (in green) bound to Strep-Tag II (in red) is shown in **c** (PDB accession # 1KL3 [Korndörfer and Skerra, 2002]). The N and C termini of StrepTactin are also labelled. The polyaspartate sequence and SpyCatcher of the StrepTactin-SpyCatcher subunit are positioned after the C terminus of StrepTactin. We predict the insertion of these sequences will not affect StrepTactin-Strep-Tag II binding. The structure was visualised using PyMOL.

expected (table **3.10**). Proteins with different sequences bind coomassie dye to differing extents which may explain these results.

Like with the StrepTactin tetramers in section 3.2.5, we measured the valency of the proteins predicted to be ST1-pD-C and ST4-pD-C using biotin-4-fluorescein binding (figure **3.44**). The number of biotin-binding sites measured using this technique (shown in table **3.11**) are consistent with what we expect and so we believe the purified proteins are indeed monovalent and tetravalent StrepTactin-SpyCatcher.

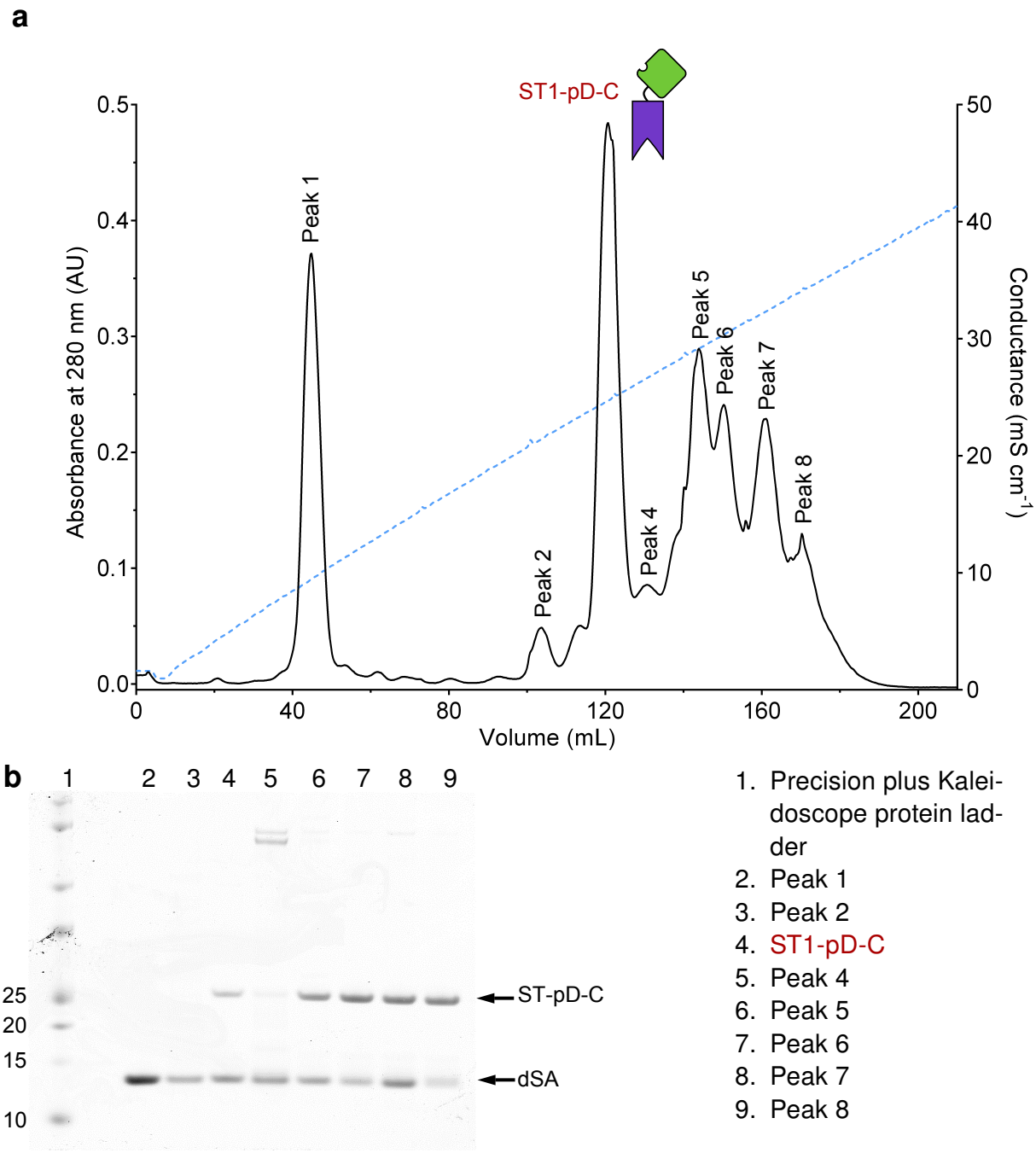


Fig. 3.42: **Separation of StrepTactin-Spycatcher tetramers refolded to synthesise ST1-pD-C.** Representative chromatogram of StrepTactin-Spycatcher tetramers separated using ion exchange chromatography. Absorbance of the eluted fractions are shown in black and conductance is shown by the blue dashed line (**a**). Each peak is numbered with the exception of the expected ST1-pD-C tetramer which is labelled with a representative cartoon diagram of the protein. Samples of the peaks (1 µg) were boiled and visualised using SDS-PAGE electrophoresis and coomassie staining to support identification of the desired peak (**b**). The desired ST1-pD-C is highlighted in red. dSA - dead streptavidin.

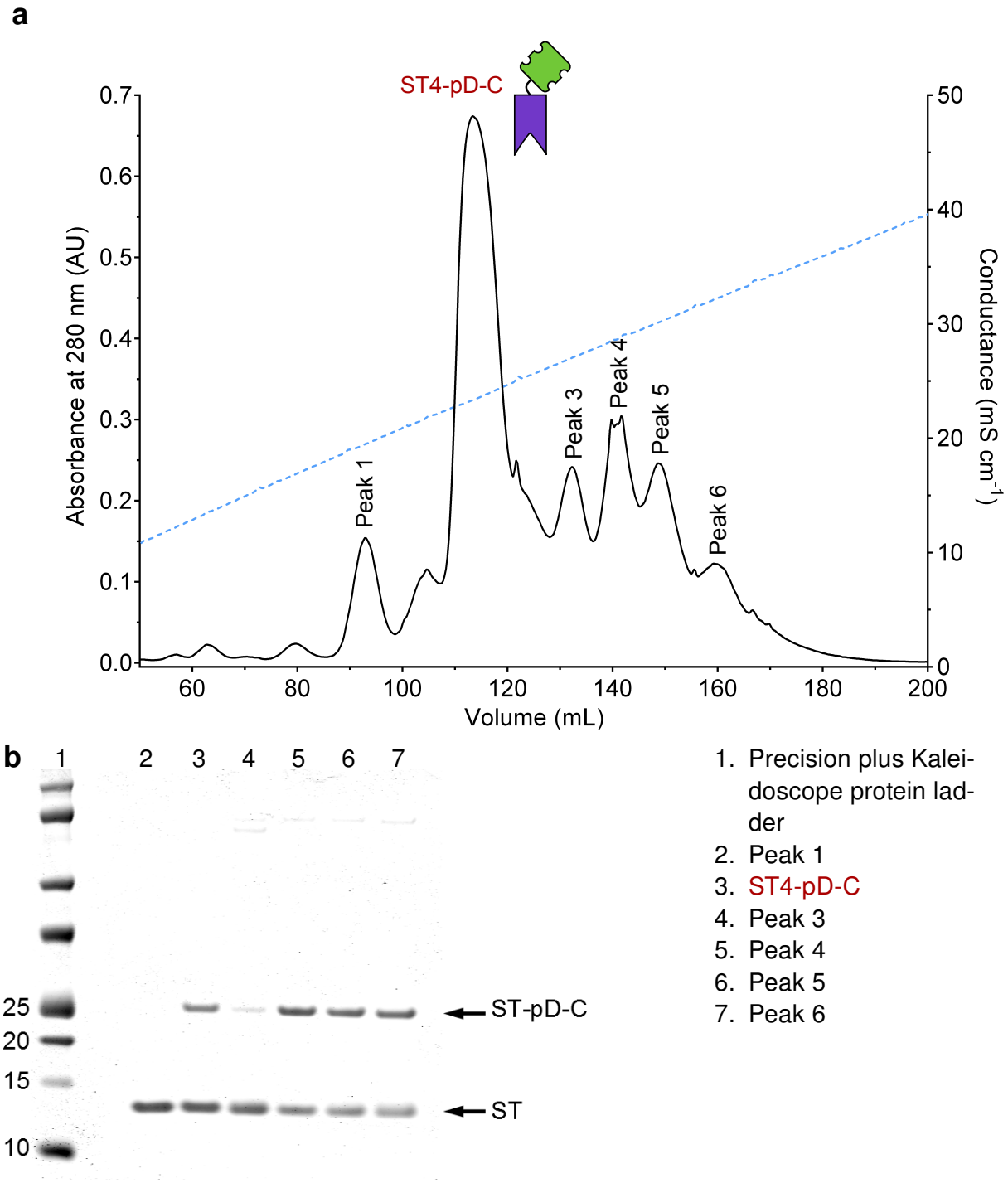


Fig. 3.43: **Separation of StrepTactin-Spycatcher tetramers refolded to synthesise ST4-pD-C.** Representative chromatogram of StrepTactin-Spycatcher tetramers separated using ion exchange chromatography. Absorbance of the eluted fractions are shown in black and conductance is shown by the blue dashed line (**a**). Each peak is numbered with the exception of the expected ST4-pD-C tetramer which is labelled with a representative cartoon diagram of the protein. Samples of the peaks (1 µg) were boiled and visualised using SDS-PAGE electrophoresis and coomassie staining to support identification of the desired peak (**b**). The desired ST4-pD-C is highlighted in red.

StrepTactin tetramer	StrepTactin-Spycatcher:StrepTactin/Dead streptavidin ratio
ST1-pD-C	1:2.3
ST4-pD-C	1:1.7

Tab. 3.10: **Ratios of ST-pD-C:ST or dSA in ST1-pD-C and ST4-pD-C.** The gel band densities of ST1-pD-C and ST4-pD-C subunits from figures **3.42b** and **3.43b** were exported using ImageJ and converted into a ratio of ST-pD-C:ST or dSA subunits.

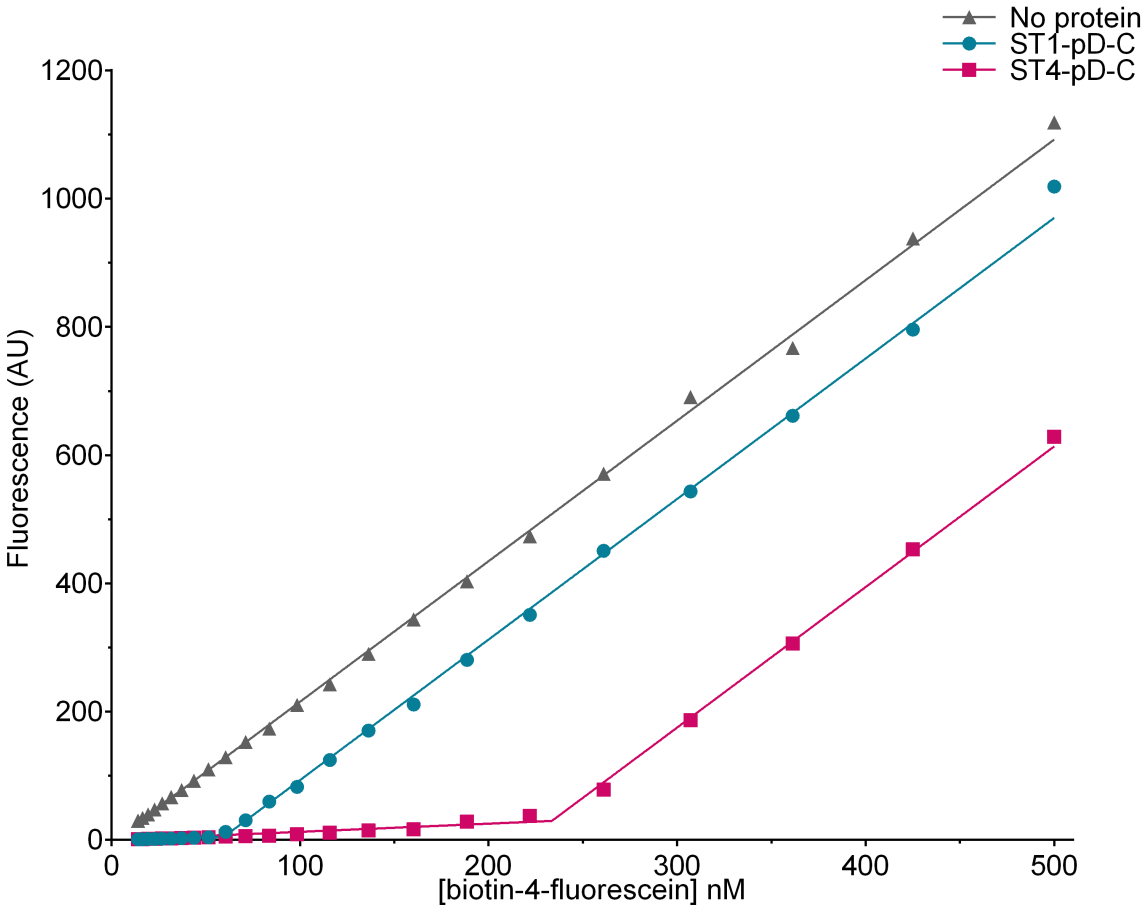


Fig. 3.44: **Valency of ST1-pD-C and ST4-pD-C as determined using biotin-4-fluorescein.** The valency of ST1-pD-C and ST4-pD-C was calculated using biotin-4-fluorescein as previously described with StrepTactin tetramers. ST1-pD-C or ST4-pD-C, (50nM) or PBS 1% BSA was mixed with varying concentrations of biotin-4-fluorescein. Fluorescence of the mixtures was then measured. Mean fluorescence values of PBS-only control wells were subtracted from all test values. These are plotted here against concentration of biotin-4-fluorescein added to the well. Both ST1-pD-C and ST4-pD-C dataset was fit with a segmental linear regression and used to calculate the number of biotin-binding sites for each tetramer.

StrepTactin tetramer	Number of binding sites per tetramer
ST1-pD-C	1.2
ST4-pD-C	4.7

Tab. 3.11: **Valency of ST1-pD-C and ST4-pD-C determined using biotin-4-fluorescein is in line with that expected.** Figure **3.44** was used to calculate the number of biotin-binding sites per tetramer of StrepTactin-Spycatcher.

Either monovalent or tetravalent StrepTactin-SpyCatcher will be conjugated to one of the SpyTagged transmembrane proteins to create different length ligands of varying valency. StrepTactin-SpyCatcher tetramers bound to the SpyTagged proteins are shown in cartoon form in figure **3.45**.

Binding StrepTactin-SpyCatcher to the ligand proteins will give the whole complex a different length to that of the StrepTactin-bound ligand shown in section 3.2.3. The length of StrepTactin-SpyCatcher coupled to CD80-Spy ligand is predicted to be $\sim$11 nm compared to $\sim$5 nm of StrepTactin coupled to CD80 ligand. Dimensions were calculated using the structures of streptavidin and the immunoglobulin-like collagen adhesin domain of the *Streptococcus pyogenes* protein FbaB from which the SpyTag and SpyCatcher partners were created [Hendrickson et al., 1989, Oke et al., 2010]. Insertion of the immunoglobulin-like domains are CD2 and CD4 will increase the length of this by $\sim$7nm and $\sim$12 nm respectively [Bodian et al., 1994, Harrison, 1993, Wu et al., 1997].

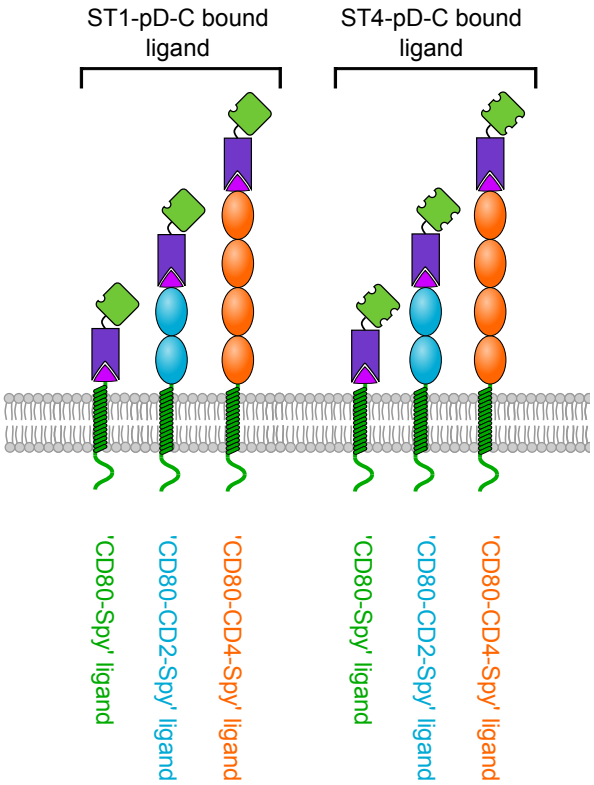


Fig. 3.45: **Cartoon diagrams of the SpyTagged artificial ligands bound by StrepTactin-SpyCatcher.** Monovalent (ST1-pD-C) or tetravalent (ST4-pD-C) StrepTactin-SpyCatcher is incubated with the ligand-expressing cells, allowing a covalent bond to form between the SpyTag and SpyCatcher. Conjugating ST1-pD-C or ST4-pD-C to the SpyTagged proteins will give artificial ligands with either one (monovalent) or four (tetravalent) binding sites for Strep-Tag II-tagged receptor.

3.2.10.2 Monovalent and tetravalent StrepTactin-SpyCatcher can bind THP-1 SIRPβI cells

To confirm that both monovalent and tetravalent StrepTactin-SpyCatcher can bind to Strep-Tag II-tagged receptors, THP-1 SIRPβI cells were incubated with fluorescently labelled ST1-pD-C (ST1-pD-C:647) or fluorescently labelled ST4-pD-C (ST4-pD-C:647) and then immediately analysed for protein binding by flow cytometry. As a negative control, cells were incubated with either ST1-pD-C:647 or ST4-pD-C:647 and an excess amount of free biotin. This will block all of the binding sites of StrepTactin-SpyCatcher and so the protein will not specifically bind to the receptor-expressing cells. Figure **3.46** shows that both ST1-pD-C:647 and ST4-pD-C:647 bind to THP-1 SIRPβI cells.

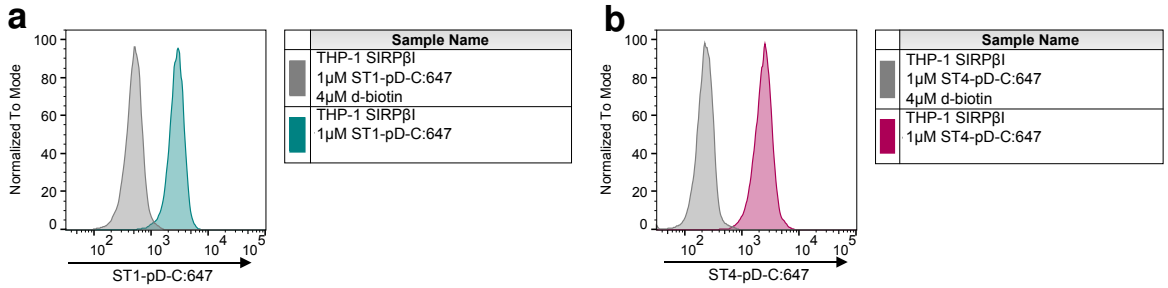


Fig. 3.46: **ST1-pD-C:647 and ST4-pD-C:647 can both bind to THP-1 SIRPβI cells.** THP-1 SIRPβI cells were incubated with 1 μM ST1-pD-C:647 alone or with 4 μM d-biotin (**a**). THP-1 SIRPβI cells were also incubated with 1 μM ST4-pD-C:647 alone or with 4 μM biotin (**b**). Cells were then analysed for protein binding using flow cytometry.

3.2.10.3 Monovalent and tetravalent StrepTactin-SpyCatcher will conjugate to SpyTagged ligand-expressing cells with accessible biotin-binding site/s

CHO cell lines stably expressing either CD80-Spy or CD80-CD4-Spy were created by Dr Jesse Goyette. The optimal conditions for coupling ST-pD-C to ligand-expressing CHO cells were also determined by Dr Jesse Goyette.

To confirm that ST1-pD-C and ST4-pD-C will not only conjugate to ligand-expressing CHO cells but will also do so with biotin-binding site/s accessible from solution, ST1-pD-C or ST4-pD-C were conjugated to CHO CD80-Spy cells. Then a soluble fluorescently labelled biotin (biotin:atto 680) was used as described in the materials and methods

(section 2.18.1) to determine the number of free biotin-binding sites (figure **3.47a**). ST1-pD-C and ST4-pD-C conjugated to CHO CD80-Spy cells were both shown to have accessible biotin-binding sites as indicated by the fluorescence signal of ST-pD-C - bound biotin:atto 680 (figure **3.47b**). As expected, ST4-pD-C coupled to cells has many more biotin-binding sites than ST1-pD-C coupled to the same cells. These results confirm that this second strategy is a more promising approach for our investigations.

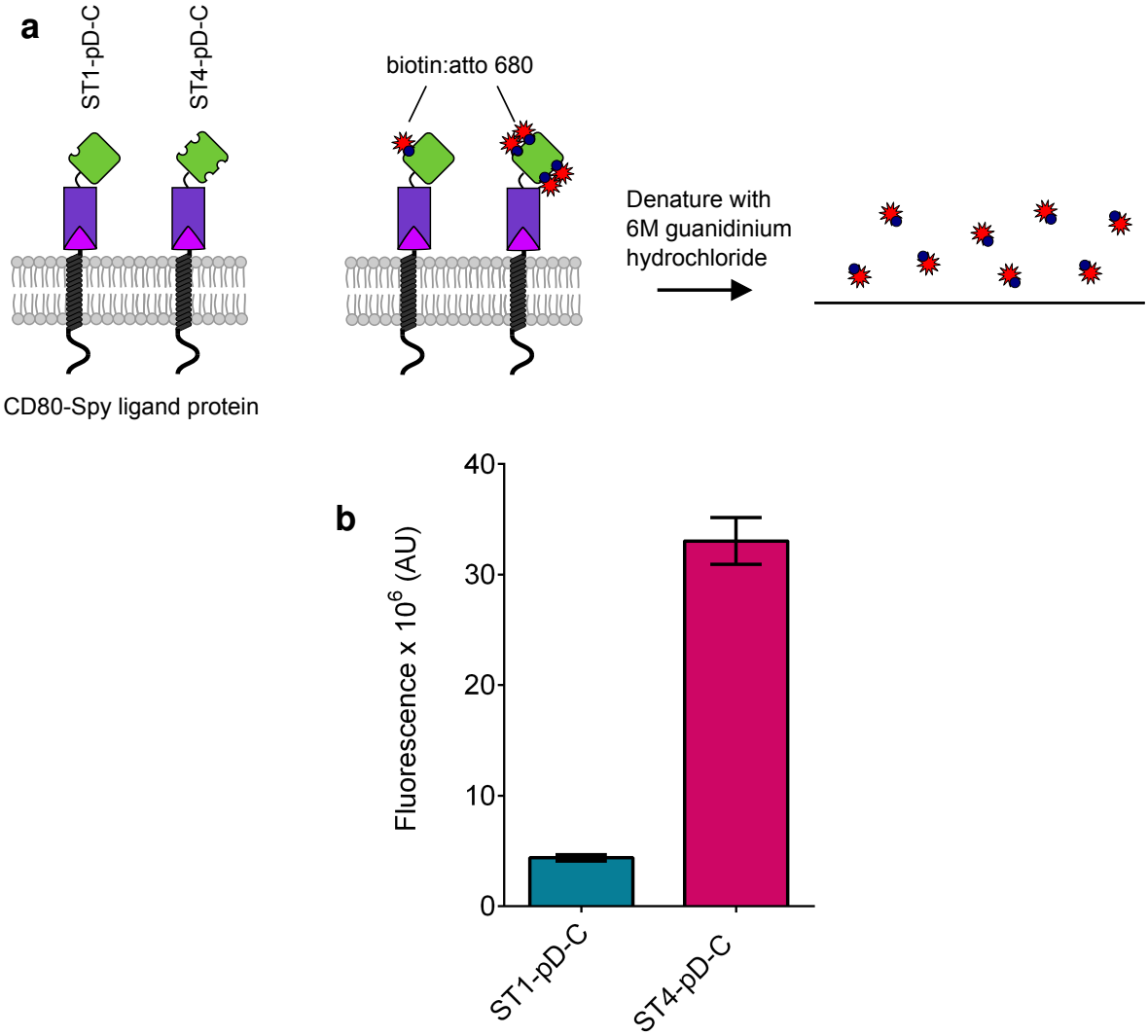


Fig. 3.47: **ST1-pD-C and ST4-pD-C can both bind to CHO CD80-Spy cells with the biotin-binding site/s accessible from solution.** A cartoon illustrating the set-up used to produce the data in **b** is shown in **a**. CHO CD80-Spy cells were incubated with either 0.5 μM ST1-pD-C or 0.53 μM ST4-pD-C. The conjugated cells were then incubated with biotin:atto 680, washed and then the ST-pD-C:biotin interaction disrupted by addition of guanidinium hydrochloride. The fluorescence of the biotin:atto 680 was then measured. CHO-CD80-Spy cells were also mock conjugated with 0 μM ST1-pD-C or ST4-pD-C as a negative control. Fluorescence values exported for these mock conjugated cells were subtracted from the values for cells that were conjugated. These values were then plotted in a bar graph format in **b**. Fluorescence values shown are mean±range.

3.3 Discussion

The work presented in this Chapter consisted of the development and validation of two artificial ligand systems. This required the development of receptor-expressing cell lines and cell lines presenting a transmembrane artificial ligand protein that can bind monovalently to the representative receptors.

3.3.1 Receptor cell lines

A group of ten representative NTRs have been cloned into a lentiviral vector. Stable cell lines of six of these receptors have been created using both THP-1 cells and Jurkat cells. When expressed in a cell line, these receptors have an N-terminal Strep-Tag II for ligation by the artificial ligand. The group of ten NTRs includes receptors representing different families within the larger NTR group. While we are yet to have synthesised plasmids of at least one NTR from each family to truly cover the variety of receptors within this group, we have both NTRs that have activating or inhibitory activity, as well as a receptor that can exhibit both depending on the context of activation. We also have NTRs which contain intrinsic signalling motifs and also those which associate with an adaptor protein to mediate immune signalling. In addition, we have chosen NTRs with a variety of functions within the immune system and that differ in the cells in which they are expressed. With continuation of the investigation, the selection of NTRs will be extended. Some specific receptors we would like to investigate include CD22 (SIGLEC-2), the TCR, and NK cell receptors.

The extracellular region of full length human CD22 is made up of seven immunoglobulin-like domains and is one of the largest NTRs [Wilson et al., 1991, Stamenkovic et al., 1991]. CD22 has also been shown to bind to itself in cis as well as binding to glycoproteins both in cis and on the surface of other cells [Han et al., 2005, Powell et al., 1993, Engel et al., 1993]. These properties of CD22 make it a good candidate for more focused study using the proposed system.

Likewise, the TCR is an interesting example NTR. It forms a complex that contains 10 ITAMs which is the highest number of motifs of any NTR [Dushek et al., 2012]. It also

shows a very sensitive response to pMHC [Valitutti et al., 1995b, Sykulev et al., 1996, Irvine et al., 2002, Purbhoo et al., 2004, Ma et al., 2008b, Huang et al., 2013]. We could test whether this sensitivity is retained when the TCR is used within our artificial ligand system. The activation of the TCR using our system could also be compared to the artificial ligand-mediated activation of other NTRs that have fewer motifs to investigate how this affects receptor activation. Combining our results with the current literature could potentially lead to further understanding of the activity of this receptor, both alone, and in the context of the NTR group.

NKG2D is one of the NTRs chosen to be investigated using the proposed system. It is expressed in NK cells, is a type II transmembrane protein and its extracellular domain is made of a single C-type lectin domain whereas many other NTRs have extracellular regions made up of immunoglobulin-like domains [Wu et al., 2011, Jimenez-Perez et al., 2012, Li et al., 2001]. We did create a lentivector encoding NKG2D and were able to transduce it into Jurkat cells but found that the Strep-Tag II was inaccessible.

To counter the inaccessibility of the Strep-Tag II on NKG2D we transduced Jurkat cells (and also THP-1 cells) with lentivectors of NKG2D where the tag was moved to make it more accessible. The plasmids with a linker between the receptor and tag were expressed in Jurkat cells but again the Strep-Tag II was not accessible. It is possible that even with addition of the linker the Strep-Tag II is buried within the structure. Alternatively, perhaps the Strep-Tag II is not translated. The plasmid does have a start methionine before the Strep-Tag II but it is possible that the translation is not being initiated upstream of the tag.

NKG2D-loop was not transduced successfully into Jurkat cells. It is possible that the amino acid mutations made to permit insertion of the Strep-Tag II into a loop of the receptor caused it to be misfolded and therefore not trafficked to the cell surface, or unable to bind anti-NKG2D antibody. More conservative mutations in the loop could be investigated to improve the probability of NKG2D retaining the correct folding. Other positions for insertion could also be investigated.

Other NK cell C-type lectin receptors were considered as a representative receptor rather than NKG2D. However, analysis of the structures of the extracellular region of these re-

ceptors (where structures exist and in some cases the structure of the murine analogue) indicated that as for NKG2D, the C terminus is likely to be inaccessible from solution (PDB accession # 2BPD [Brown et al., 2007], PDB accession # 2C6U [Watson et al., 2007], PDB accession # 4IOP [Li et al., 2013], PDB accession # 3FF7 [Li et al., 2009]). Therefore, if we wish to study the triggering mechanism of C-type lectin NTRs we may need to use the physiological ligand instead of the proposed artificial one.

We would also like to extend the work by transducing receptors into other cell lines. For example, NKp30 and NKG2D are NK cell receptors so transducing them into an NK cell line would be more suitable. Transduction of NKL and NK92 cells with a number of the NTRs in this work was not successful. To improve transduction efficiency an alternative method of transduction could be utilised. For example, retroviral transduction has previously been used to introduce proteins into NKL cells for surface expression [Miah and Campbell, 2010].

3.3.2 Ligand cell lines

Plasmids encoding artificial ligands of different length were created but not nucleofected successfully into CHO BirA-ER cells. By nucleofecting a positive control plasmid into the CHO BirA-ER cells we confirmed that the cells were competent. This positive control plasmid for CHO nucleofection is smaller than the ligand plasmids which may explain why the nucleofection efficiency was much higher. An alternative reason for the poor nucleofection efficiency may lie with the ligand construct plasmid: pcDNA3.1(+). Selection of the positive cell population relies on expression of a hygromycin resistance gene encoded by the pcDNA3.1(+) vector. While unlikely, perhaps there is a mutation within the hygromycin resistance gene of the sample of this vector we used to create the ligand plasmids such that the selection system is disrupted.

HEK293T cells were successfully transfected with the CD80, CD80-CD2 or CD80-CD4 plasmids to create cell lines transiently expressing the ligands thereby confirming that the chimeric artificial ligands could be expressed on the surface of cells. HEK293T cells are not the desired line for ligand cell expression because they are a human cell line so could therefore express NTR ligands which would interfere with our investigation. We

did however, use them as ligand cell lines to confirm the ligation of StrepTactin to the biotinylated ligand protein.

3.3.3 StrepTactin and StrepTactin-SpyCatcher

We have also expressed and purified both StrepTactin of different valency and monovalent or tetravalent StrepTactin-SpyCatcher fusion proteins. Analysis of the purified proteins using SDS-PAGE and biotin-4-fluorescein binding provided evidence that the proteins were the expected tetramers.

SDS-PAGE and the biotin-4-fluorescein experiments do not distinguish between the different forms of bivalent StrepTactin however and so it is possible that we have mislabelled the 1,2, 1,3 and 1,4 bivalent forms. To distinguish between the various bivalent species we could make use of large biotinylated ligands. To characterise the interaction between the two biotin-binding sites of cis- and trans-bivalent streptavidin, Fairhead et al. used both mono-biotinylated DNA (439bp long) and a mono-biotinylated affibody [Fairhead et al., 2014a]. They found that when in excess, the pre-defined trans-bivalent streptavidin bound two biotinylated affibodies whereas the cis-bivalent form bound one. Only at higher concentrations of affibody would cis-bivalent streptavidin bind two affibodies. Similar results were seen with biotinylated DNA binding where trans-bivalent streptavidin bound two biotinylated DNA molecules whereas cis-bivalent streptavidin bound to either one or two DNA molecules. We could test the binding of mono-biotinylated ligands to the bivalent StrepTactin species we have synthesised here to infer which protein is likely to be the 1,2 cis-bivalent tetramer and which is the 1,3 trans-bivalent tetramer. Our results may differ slightly from those of Fairhead et al. as we believe the purified 1,3 trans-bivalent StrepTactin also contains the 1,4 bivalent species.

To more definitively confirm the identity of the bivalent StrepTactin tetramers we have synthesised, other structural analyses could be used, for example native mass spectrometry and x-ray crystallography. Indeed, Fairhead et al. was able to confirm the 1,2 cis-bivalent streptavidin and 1,3 trans-bivalent streptavidin proteins using x-ray crystallography [Fairhead et al., 2014a].

A number of steps could also be taken to further confirm the identity of monovalent and

tetravalent StrepTactin-SpyCatcher.

As the single biotin- (and Strep-Tag II-) binding competent monomer used to synthesise monovalent StrepTactin-SpyCatcher contains the SpyCatcher protein, the range of tetramers created during synthesis will not only differ in the number of biotin-binding sites but also the number of SpyCatcher proteins. Varying the number of SpyCatcher proteins per tetramer will vary the size of the complex. It should therefore be possible to further validate the monovalent StrepTactin-SpyCatcher using native SDS-PAGE. Native SDS-PAGE allows the tetramers to remain intact and would indicate if the complex migrates at the correct size. Similarly, synthesising tetravalent StrepTactin-SpyCatcher yields a number of species which vary in the number of SpyCatcher proteins per tetramer and so vary in size. Native SDS-PAGE could be used again to confirm that the protein is the correct species and migrates at the expected size. With increasing StrepTactin-SpyCatcher monomers per tetramer, not only will the size of the protein increase but the charge will as well because each StrepTactin-SpyCatcher monomer contains a polyaspartate sequence. This difference in charge may affect the mobility of the proteins in native SDS-PAGE and so affect the analysis of the gels.

Additionally, the identity of monovalent and tetravalent StrepTactin-SpyCatcher could be confirmed using native mass spectrometry. This technique would determine the protein present and validate that the correct monovalent and tetravalent StrepTactin-SpyCatcher species have been purified. If further purification of the proteins was required, gel filtration chromatography could be used to separate out the tetramers based on size. The desired monovalent or tetravalent StrepTactin-SpyCatcher species will differ in size from all the other tetramers present and so can be purified in this way.

3.3.4 Putting the system components together

Fluorescent ST3dSA1 and ST4 were used to confirm that StrepTactin can bind to both tagged NTRs and biotinylated ligand proteins expressed in cell lines, as well as biotin presented on supported lipid bilayers. Unexpectedly, available biotin-binding sites were not detected on receptor-expressing cells bound by StrepTactin. This is possibly due to non-specific binding of the probe used (biotinylated mouse IgG1) to the receptor-expressing

cells thereby masking the specific signal.

Available biotin-binding sites were detected on both ligand-expressing cells and supported bilayers bound by ST3dSA1 and ST4. However, available sites were not detected on ligand cells bound by 1,2 cis-ST2 and the availability of biotin-binding sites on supported bilayers bound by the mixture of 1,3 trans-ST2 and 1,4 ST2 was much lower than predicted. We suspect that bivalent StrepTactin is binding to the ligand cell (or simulated ligand cell) with both binding sites leaving none available for ligation of the tagged receptor or probe. This presents a challenge to the fundamental requirements of the system: a significant proportion of StrepTactin-bound ligand must bind the tagged NTR as well. So while we have developed the necessary components for the system, they do not behave desirably.

This led us to develop an alternative system that makes use of the SpyTag and SpyCatcher covalent interaction as opposed to that of biotin and StrepTactin. The StrepTactin-SpyCatcher plasmids and new ligand-expressing CHO cell lines required for this system were developed by Dr Jesse Goyette outside of the work of this thesis.

We confirmed that StrepTactin-SpyCatcher can bind to both receptor-expressing cells and ligand-expressing cell lines, and that StrepTactin-SpyCatcher conjugated to the generic ligand protein on these cells has accessible biotin-binding site/s.

In summary, most of the components of the original artificial ligand system have been developed and analysed but shown to not be entirely suitable for our investigations here. The new approach, which is largely based on the first, has also been developed and analysed. We further confirmed that the various components of the second artificial ligand strategy behave and interact as expected thereby presenting a more promising approach to systematically investigate NTR triggering.

4. A SELECTION OF NON-CATALYTIC TYROSINE-PHOSPHORYLATED RECEPTORS CAN BE STIMULATED WITH ARTIFICIAL LIGAND PRESENTED ON A SURFACE BUT NOT BY SOLUBLE LIGAND

4.1 Introduction

In chapter 3 we outlined the development of two artificial ligand strategies to investigate NTR activation. Here we aimed to validate that representative NTRs created with N-terminal Strep-Tag II can be activated by ligation of this tag with plate-immobilised and cell-associated artificial ligands. We use six representative NTRs to look at this: LAIR-1, 2B4, NKp30, FcγRIA, SIRPβ1 and SIGLEC-14. Each of the receptors have been studied individually in terms of their ligands, role within the immune system and signalling mechanisms. The mechanism of activation is less well studied. Here we will briefly discuss the representative six NTRs and consider evidence for the mechanism of activation of these receptors.

4.1.1 2B4

The NTR 2B4 is a member of the SLAM family of receptors and binds to the ligand CD48 which is expressed in lymphoid and myeloid cells [Yokoyama et al., 1991, Brown et al., 1998]. Like other SLAM receptors, 2B4 plays a role in regulation of NK cell and T cell activity (discussed in detail in [Cannons et al., 2011]). It has intrinsic cytoplasmic ITIMs and ITSMs and as a result can mediate either activating or inhibitory signalling upon triggering. Which type of activity is initiated is hypothesised to depend on the association of SAP with the phosphorylated ITSMs. If SAP is present, 2B4 triggering initiates activating triggering and in the absence or low levels of SAP, 2B4 acts as an

inhibitory receptor [Chlewicki et al., 2008]. The process behind this variable signalling is discussed more in section 1.6.1.

4.1.2 FcγRIA

The Fc receptor family contains both activating and inhibitory members and plays a regulatory role in responses to pathogens [Nimmerjahn and Ravetch, 2008]. FcγRIA is expressed on monocytes and macrophages, and also has inducible expression in polymorphonuclear cells [Schiff et al., 1997, Swisher and Feldman, 2015]. It binds to monomeric IgG with high affinity and like a number of other activating Fc receptors it signals through the ITAM-containing FcRγ chain [Bruhns et al., 2009, Duchemin et al., 1994, Ernst et al., 1993]. FcγRIA activation initiates a number of signalling responses including antibody-dependent cell-mediated cytotoxicity (ADCC) and phagocytosis [Van Vugt et al., 1998, Indik et al., 1994].

4.1.3 LAIR-1

LAIR-1 is expressed by many leucocytes including CD4+ and CD8+ T cells, NK cells, B cells, monocytes, dendritic cells and basophils [Meyaard et al., 1997, Omiya et al., 2009, Bonaccorsi et al., 2010, Florian et al., 2006]. LAIR-1 does not bind to a cell surface-associated ligand but instead binds to glycine-proline-hydroxyproline (GPO) repeats of collagen [Meyaard et al., 1997, Lebbink et al., 2006, Brondijk et al., 2010, Tang et al., 2009, Jiang and Barclay, 2009]. The affinity of LAIR-1 for collagen binding is similar to the interactions of the other NTR-ligand interactions with a measured K_D = 26μM [Jiang and Barclay, 2009].

LAIR-1 has two intrinsic ITIMs and so upon receptor triggering recruits inhibitory phosphatases for example SHP-1, to the phosphorylated ITIMs to mediate inhibitory activity. ITIM-mediated signalling is discussed more in section 1.6.1. As expected from its expression in many cell lines, LAIR-1 activity inhibits a large number of immune activities including CD4+ and CD8+ T cell activation responses, NK cell cytotoxicity, and monocyte cytokine secretion [Meyaard et al., 1999, Maasho et al., 2005, Saverino et al., 2002, Meyaard et al., 1997, Lebbink et al., 2006, Son and Diamond, 2014].

Due to the widespread role of LAIR-1 understanding the molecular mechanism of how this receptor is activated will impact our understanding of the regulation of a number of immune cell activities.

4.1.4 NKp30

NKp30 is a member of the natural killer cell cytotoxicity (NCR) family and binds both pathogen and cellular ligands, some of which are inhibitory [Arnon et al., 2005, Hecht et al., 2009, Pogge von Strandmann et al., 2007, Brandt et al., 2009, Li et al., 2011]. Tumour cell-associated heparan sulphates and the B7-H6 tumour antigen are among ligands which activate NKp30 upon binding [Hecht et al., 2009, Brandt et al., 2009]. NKp30 signals through the CD3ζ or FcRγ adaptor proteins to initiate the NK cell-mediated cytotoxicity response to tumour or pathogen [Pende et al., 1999]. Other members of the NCR family similarly associate with activating motif-containing adaptor proteins and initiate NK cell-mediated cytotoxicity [Pessino et al., 1998, Sivori et al., 1999, Campbell et al., 2004].

4.1.5 SIGLEC-14

The SIGLEC receptor family are sialic-acid - binding receptors. Most SIGLECs have intrinsic ITIMs or ITIM-like motifs and so have inhibitory signalling roles. Three human SIGLECs are not inhibitory: SIGLEC-14, -15, and -16 [Macauley et al., 2014].

SIGLEC-14 is expressed in monocytes and binds to sialic acid presented by the bacteria nontypeable *Haemophilus influenzae* (NTHi) and group B Streptococcus (GBS) [Angata et al., 2006, Angata et al., 2013, Ali et al., 2014, Yamanaka et al., 2009]. SIGLEC-14 associates with the ITAM-containing adaptor protein DAP12 and through DAP12 phosphorylation upon SIGLEC-14 - ligand binding elicits activating signalling, for example cytokine secretion [Angata et al., 2006, Angata et al., 2013, Yamanaka et al., 2009, Ali et al., 2014].

The N-terminal two extracellular Ig-like domains of SIGLEC-14 are nearly identical to those of the inhibitory receptor, SIGLEC-5 [Angata et al., 2006]. SIGLEC-5 and SIGLEC-

14 are paired receptors, opposing the activity of the other receptor [Ali et al., 2014, Angata et al., 2006, Crocker et al., 2007].

The activation mechanism of the relatively recently discovered SIGLEC-14 has not been studied in detail. Our artificial ligand strategy will allow further investigation.

4.1.6 SIRPβ1

SIRPβ1 is expressed in a number of leucocytes including monocytes, dendritic cells and neutrophils [Dietrich et al., 2000, Liu et al., 2005]. The ligand for SIRPβ1 has yet to be determined but the receptor has a number of activating functions, for example in PMN cell transepithelial migration, phagocytosis of target cells by mouse macrophages and serotonin release by rat basophils [Liu et al., 2005, Hayashi et al., 2004, Tomasello et al., 2000].

SIRPβ1, which has been shown to form a disulphide-linked homodimer, associates with the ITAM-containing adaptor protein DAP12 which likely mediates the signalling of SIRPβ1 activation [Tomasello et al., 2000, Hayashi et al., 2004, Dietrich et al., 2000, Liu et al., 2005]. Another SIRP receptor, SIRPα is a paired receptor of SIRPβ1 and has a negative regulatory role in macrophages [Yamao et al., 2002, Okazawa et al., 2005].

4.1.7 Comparison between physiological ligand- and artificial ligand-binding site

Our strategy to investigate NTR activation uses an artificial ligand which binds to a tag located at the extracellular terminus of the receptor. The extracellular terminus is not necessarily the region of the receptor that interacts with physiological ligand. This distance between natural and artificial ligand-binding site position, and also the difference in ligand size, may mean the artificial ligand-receptor dimensions do not match the natural dimensions. The KS model of NTR activation in particular places emphasis on the role of receptor-ligand complex dimensions in receptor activation and so a contrast between natural and artificial receptor-ligand dimensions may affect signalling. We therefore looked at the structures of the representative NTRs in complex with their ligand, where struc-

tures are available, to compare the ligand-binding site and predicted Strep-Tag II location. These structures are shown in figure **4.1**.

Only the structure of Ig-like domain 1 of mouse 2B4 in complex with the Ig-like domain 1 of mouse CD48 has been determined (figure **4.1a**). The full 2B4-CD48 complex has been modelled however and predicted to span 11.5 nm [Velikovsky et al., 2007]. As shown in figure **4.1a** the CD48-binding site of 2B4 lies very close to the N terminus (position of Strep-Tag II). The predicted dimensions of the artificial ligands CD80 with StrepTactin and CD80-Spy coupled with ST-pD-C are $\sim$ 5 nm and $\sim$ 11 nm respectively. While binding of CD80 with StrepTactin to tagged 2B4 is likely to give similar intermembrane dimensions to those of 2B4 and CD48, binding of CD80-Spy with ST-pD-C might give a slightly larger intermembrane distance.

The binding site for IgG1 on human FcγRIA lies within Ig-like domain 2 [Kiyoshi et al., 2015]. Based on the structure in figure **4.1b** the binding site of physiological and artificial ligand will not differ significantly in distance from the membrane. The structure of unbound FcγRIA shows that there is a conformational change in the receptor upon ligand binding (PDB accession # 3RJD28) [Lu et al., 2011, Kiyoshi et al., 2015]. The position of the N-terminus however does not alter significantly relative to the rest of the structure. The intermembrane distance between the receptor cell with IgG-bound FcγRIA and the antigen-presenting surface has not been determined and will depend on the position of the antibody epitope. We note however, that because of the orientation of IgG1 binding to FcγRIA, the antigen-binding region of the immunoglobulin will lie within $\sim$10 nm of the receptor cell surface.

A structure of LAIR-1 in complex with the ligand collagen has not been determined. LAIR-1 residues that are predicted to be involved in collagen binding have been identified using mutagenesis studies and modelling [Brondijk et al., 2010]. The predicted collagen-binding site (figure **4.1c**) and position of Strep-Tag II (N-terminus) are in close proximity. However, we predict the distance between the LAIR-1-expressing cell surface and the collagen 'surface' will at most be the distance covered by the single Ig-like domain of LAIR-1. The dimensions of Strep-Tag II-tagged LAIR-1 bound to artificial ligand will be longer than this. This will need to taken into consideration when analysing experimental data.

NKp30 has been crystallised in complex with the ligand B7-H6. The ligand-binding site is in close proximity to the N terminus of NKp30 as shown in figure **4.1d**. We predict that NKp30-artificial dimensions will be comparable or slightly longer than the dimensions of the NKp30 - B7-H6 complex ($\sim$10 nm) [Li et al., 2011].

No structure of SIGLEC-14 has been determined. It is predicted that the sialic acid-binding site is positioned in the N terminal Ig-like domain [Angata et al., 2006]. As the dimensions of the NTR-ligand complex is unknown however we cannot compare it to predicted dimensions of the NTR-artificial ligand complex.

The ligand of SIRPβ1 has yet to be identified and therefore we cannot compare the physiological SIRPβ1-ligand interaction with the SIRPβ1-artificial ligand. There is also not a crystal structure of the receptor.

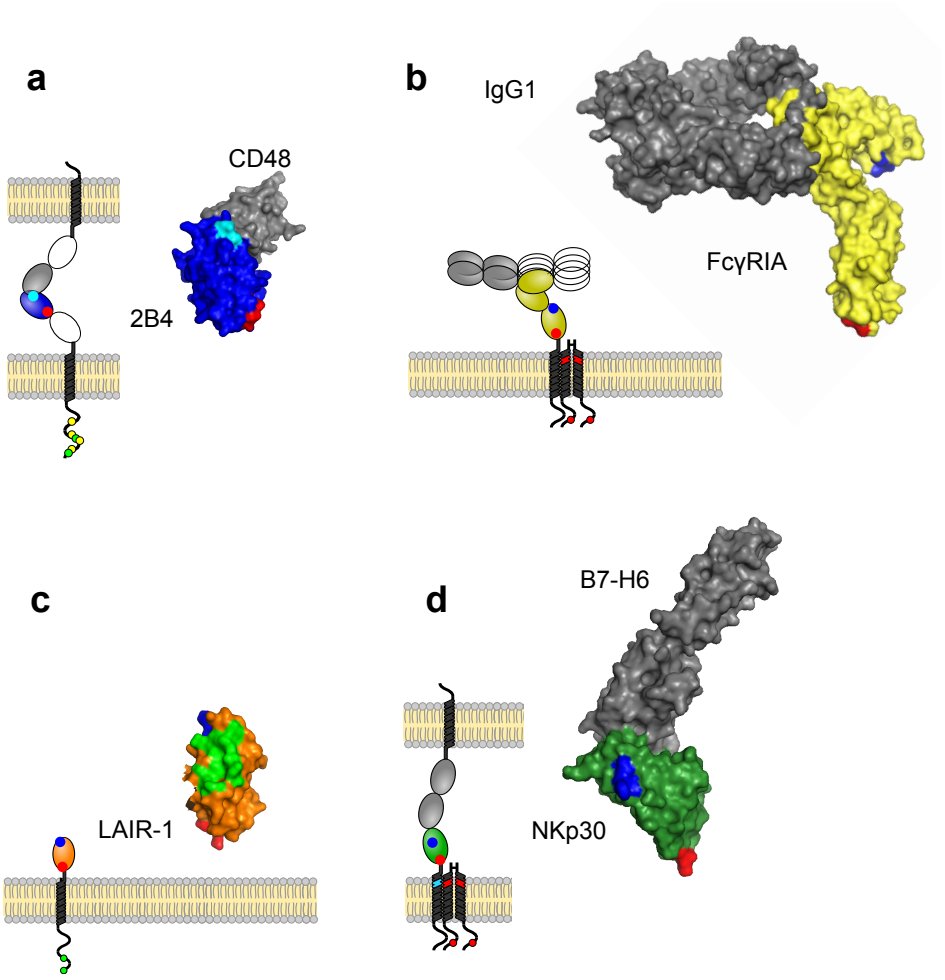


Fig. 4.1: **Structures of example NTRs in complex with their ligand.** *Continued on the next page.*

Fig. 4.1: **Structures of example NTRs in complex with their ligand.** *Continued.* (**a**) Cartoon of human 2B4 in complex with CD48 alongside the crystal structure of mouse 2B4 Ig-like domain 1 (in blue) in complex with mouse CD48 Ig-like domain 1 (in grey) (PDB accession # 2PTT) [Velikovsky et al., 2007]. (**b**) Cartoon of FcγRIA bound to IgG1 and structure of FcγRIA extracellular region (in yellow) in complex with the CH2 and CH3 domains of human IgG1 (in grey) (PDB accession # 4W4O) [Kiyoshi et al., 2015]. (**c**) Cartoon and structure of the Ig-like domain of human LAIR-1 (PDB accession # 3KGR) [Brondijk et al., 2010]. The residues predicted to be involved in collagen binding of LAIR-1 are shown in green . (**d**) Cartoon of NKp30 in complex with B7-H6 alongside the structure of NKp30 (in green) in complex with B7-H6 (in grey) (PDB accession # 3PV6) [Li et al., 2011]. The receptor and ligand domains that are not present in the crystal structures are shown as hollow ovals in the predicted position. The N- and C-terminal 3 residues of each receptor are coloured in blue (or cyan for 2B4) and red respectively on both the structure and cartoon to illustrate where the termini are. Figures of the structures were created using PyMOL.

4.1.8 Using the artificial ligand system to test a key prediction of the KS model of NTR activation

Our hypothesis is that NTRs trigger using the KS mechanism. We can investigate this by using the artificial ligand system to test predictions that the KS model makes about NTR activation. One key prediction is that for activation to occur, the ligand must be presented on a surface. This would provide a means for segregation of inhibitory phosphatases like CD45 and CD148 from the receptor-ligand complex, which is a key component of the KS model. According to the model, soluble monovalent ligand would not induce this segregation of membrane-bound inhibitory phosphatases and so receptor triggering would not occur.

In studies of the NTRs, receptor activation is usually initiated by surface-presented ligand or antibody. For example, the activity of NK cell receptors NKp30 and 2B4 is commonly investigated using anti-receptor antibody bound to Fc receptor-expressing target cells [Tangye et al., 2000a, Tangye et al., 2000b, Parolini et al., 2000, Sivori et al., 2000, Chlewicki et al., 2008, Spaggiari et al., 2001]. The requirement for the ligand to be presented on a surface has not been examined in detail.

As discussed in section 4.1.3, as collagen forms fibres and basement membranes, LAIR-1 - collagen binding could be considered as the receptor binding to a solid surface-presented ligand.

There is evidence consistent with the hypothesis that LAIR-1 activation requires ligation by a surface-presented ligand in an NK cell-mediated cytotoxicity assay. LAIR-1 - mediated inhibition of NK cell-mediated cytotoxicity was observed when LAIR-1 - expressing NK cells bound by anti-LAIR-1 antibody were presented to Fc receptor-expressing target cells. In contrast, LAIR-1 inhibitory activity was not seen when the same anti-LAIR-1 antibody-bound NK cells were presented to target cells that did not express Fc receptors. In the absence of Fc receptors which bind to the anti-LAIR-1 antibody, LAIR-1 receptor is not held within the cell-cell contact [Meyaard et al., 1997, Meyaard et al., 1999]. It is possible that LAIR-1 needs to be confined between two surfaces for it to be triggered which is consistent with the KS model. Alternatively, as suggested by the authors, the further cross-linking provided by Fc receptor binding may be required for LAIR-1 activation [Meyaard et al., 1997, Meyaard et al., 1999]. A third possibility is that soluble antibody does activate LAIR-1 but for the inhibitory signalling to be integrated with the NK cell activation, which will be triggered by interactions at the cell-cell interface, activated LAIR-1 must be in close proximity to the activating receptor. More detailed study of LAIR-1 activation, using our artificial ligand system may help elucidate this.

While NTRs bind to surface-presented ligands there is evidence that receptor-cross-linking by soluble antibodies and multivalent protein is sufficient for activation. For example, cross-linking of LAIR-1 with primary and secondary antibody activates LAIR-1 to inhibit T cell activation and TCR-mediated cytotoxicity of CD8+ cells [Saverino et al., 2002, Maasho et al., 2005]. SIRPβ1 is also commonly stimulated in studies by anti-SIRPβ1 antibody and a secondary antibody [Dietrich et al., 2000, Hayashi et al., 2004, Tomasello et al., 2000]. Engagement of NKp30 by soluble antibody and then secondary antibody or F(ab')2 fragments is similarly sufficient for receptor activation responses including NK cell-mediated cytotoxicity [Spaggiari et al., 2001, Chen et al., 2007]. These results favour clustering models of NTR activation (discussed further in section 1.10).

These results are inconsistent with the KS model as it predicts soluble ligand would not be able to segregate inhibitory phosphatases from the receptor. It has been argued however, that upon binding of primary and secondary antibodies, the complexes formed by this high level of cross-linking are large enough to laterally exclude phosphatases from

the receptor-ligand complex by a crowding effect [Cordoba et al., 2013]. In support of this, a number of studies have shown that the further cross-linking induced by a secondary antibody is required for activation by soluble antibody.

For example, addition of soluble anti-LAIR-1 antibody alone to CD4+ T cells did not inhibit the cytotoxic activity of the cells whereas further cross-linking with a secondary antibody did [Saverino et al., 2002]. The same was seen for IgG production in activated B cells incubated with anti-LAIR-1 antibody alone or anti-LAIR-1 antibody and a secondary antibody [Merlo et al., 2005].

The further cross-linking mediated by secondary antibody was shown to be a requirement for an NK cell calcium response to soluble anti-NKp30 antibody. Calcium flux was not observed in response to soluble antibody unless it was further cross-linked by secondary antibody [Pende et al., 1999].

FcγRIA cross-linking with IgG or antibody F(ab')2 fragments and also further cross-linking by secondary antibody are required to induce downstream signalling of the receptor including calcium signalling and PI3 kinase activation [Melendez et al., 1998, Rankin et al., 1993]. Other activating Fc receptors show the same requirement for both IgG and secondary antibody binding for activation [Liao et al., 1992, Rankin et al., 1993]. However, one soluble monoclonal antibody (m197) can activate FcγRIA without the requirement for a secondary antibody. This antibody binds trivalently to FcγRIA and so it has been suggested that the minimum level of cross-linking required for activation is three receptors [Akerley et al., 1991, Liao et al., 1992].

There is conflicting evidence concerning activation of SIRPβ1 with soluble antibody. One study found that cross-linking of SIRPβ1 with soluble antibody alone was not sufficient to induce phagocytosis in macrophage cells. Addition of a secondary antibody was required [Hayashi et al., 2004]. In contrast however, a number of studies have found that the addition of soluble anti-SIRPβ1 antibody alone is sufficient to activate macrophages to release nitric oxide, and to positively regulate transepithelial migration of neutrophils [Adams et al., 1998, Liu et al., 2005]. It is currently unclear therefore whether cross-linking of SIRPβ1 with the developed artificial ligand will be sufficient for receptor activation.

As well as confirming Strep-Tag II-tagged NTRs can be activated by artificial ligand, we further aimed in this Chapter to test whether NTR activation requires engagement of a surface-presented ligand. This will test a key KS model prediction. To do this, we directly compared the activation of NTRs in response to plate-immobilised artificial ligand to activation in response to soluble artificial ligand.

Clustering models of NTR activation propose that receptor cross-linking, independent of the ligand being surface-immobilised, is sufficient for receptor activation. To test this, we added soluble tetravalent artificial ligand to Strep-Tag II-tagged receptor-expressing cells and investigated whether this could activate the receptors. Upon binding of soluble tetravalent StrepTactin or StrepTactin-SpyCatcher to receptor-expressing cells the maximum number of receptors that can be engaged per protein is four. While binding of multivalent soluble ligand will likely cause cross-linking of the receptor, we predict this level of cross-linking will not be sufficient to induce lateral segregation of inhibitory phosphatases. Therefore, if receptor activation is triggered by this soluble tetravalent ligand, it will likely be a result of receptor clustering rather than phosphatase segregation. These results will help elucidate what conditions of receptor engagement are sufficient for NTR activation.

4.2 Results

4.2.1 Representative activating and inhibitory NTRs can be stimulated by ligation of the extracellular Strep-Tag II

To determine if NTRs can be stimulated by ligation of the Strep-Tag II, transduced Jurkat and THP-1 cell lines expressing representative tagged NTRs were presented to varying concentrations of anti-Strep-Tag II antibody or multivalent StrepTactin immobilised onto 96 well flat bottom plates. Secretion of the cytokine IL-8 was measured as a read-out of cell activation. IL-8 secretion has previously been used as an indicator of both Jurkat and THP-1 cell activation (for example [Kuno et al., 1993, Bartelt et al., 2009, Liu et al., 1997, Baqui et al., 1999]). Experiments with the Jurkat cell lines were less successful than those with THP-1 cell lines. Therefore, to allow detailed analysis of Strep-Tag II-

tagged NTR stimulation, experiments were continued using THP-1 cell lines only. The results with Jurkat cell lines have been omitted for brevity.

THP-1 cells expressing the activating Strep-Tag II-tagged NTR NKp30 were presented to varying concentrations of plate-immobilised anti-Strep-Tag II antibody. As shown in figure **4.2**, Strep-Tag II-tagged NKp30 can be stimulated by ligation of the tag by immobilised antibody.

As an example of an inhibitory NTR, LAIR-1 was also activated by ligation of the tag by plate-immobilised anti-Strep-Tag II antibody (figure **4.3**). In order to detect the inhibitory activity of LAIR-1, a single concentration of anti-FcγRIA antibody was co-immobilised onto the 96 well flat bottom plate with varying concentrations of anti-Strep-Tag II antibody. The concentration of anti-FcγRIA antibody was chosen following a pilot experiment conducted by Dr Jesse Goyette that indicated this concentration gave a strong, but not saturated, stimulation of THP-1 cells. The activating signal of endogenous FcγRIA is inhibited by Strep-Tag II-tagged LAIR-1 activity, visualised as a decrease in IL-8 release by THP-1 cells (figure **4.3**).

Some NTRs exhibit either activating or inhibitory activity depending on the context of their stimulation. For example, the SLAM family receptor 2B4 associates with the SLAM-Associated Protein (SAP) [Tangye et al., 1999]. In the presence of SAP 2B4 exhibits activating activity, while in the absence of functional SAP 2B4 has inhibitory activity [Tangye et al., 1999, Parolini et al., 2000]. Our results indicate that in THP-1 cells, 2B4 acts as an inhibitory receptor and Strep-Tag II-tagged 2B4 is stimulated by plate-immobilised anti-Strep-Tag II antibody (figure **4.4**). Identical to LAIR-1, THP-1 2B4 cells were incubated in wells co-immobilised with a single concentration of anti-FcγRIA antibody and various concentrations of anti-Strep-Tag II antibody in order to visualise the 2B4-mediated inhibition of IL-8 secretion.

The activation of these receptors with plate-immobilised anti-Strep-Tag II antibody was specific to ligation of the tag. Untransduced THP-1 cells treated in the same way either did not release detectable levels of IL-8 (for the NKp30 experiment) or released the same level of IL-8 across the test wells (for LAIR-1 and 2B4 experiments). This indicates that any cell response measured was specific to the tagged NTR and not due to non-specific

activation of THP-1 cell Fc receptors by the antibody.

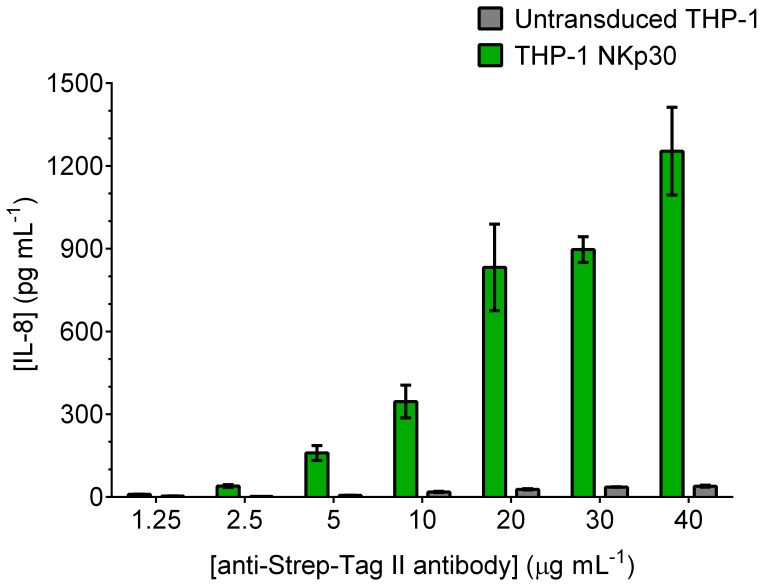


Fig. 4.2: **THP-1 NKp30 cells can be stimulated by plate-immobilised anti-Strep-Tag II antibody.** Varying concentrations of anti-Strep-Tag II antibody were immobilised onto 96 well flat bottom plates. Untransduced THP-1 or THP-1 NKp30 cells were added to these plates and incubated at 37°C , 5% CO_2 for 20 hours before the supernatants were analysed for IL-8 protein levels. IL-8 values in supernatants from unstimulated cells have been subtracted from all values shown. Bars shown are from 1 experiment (n=2) with values given as mean±range of duplicate wells.

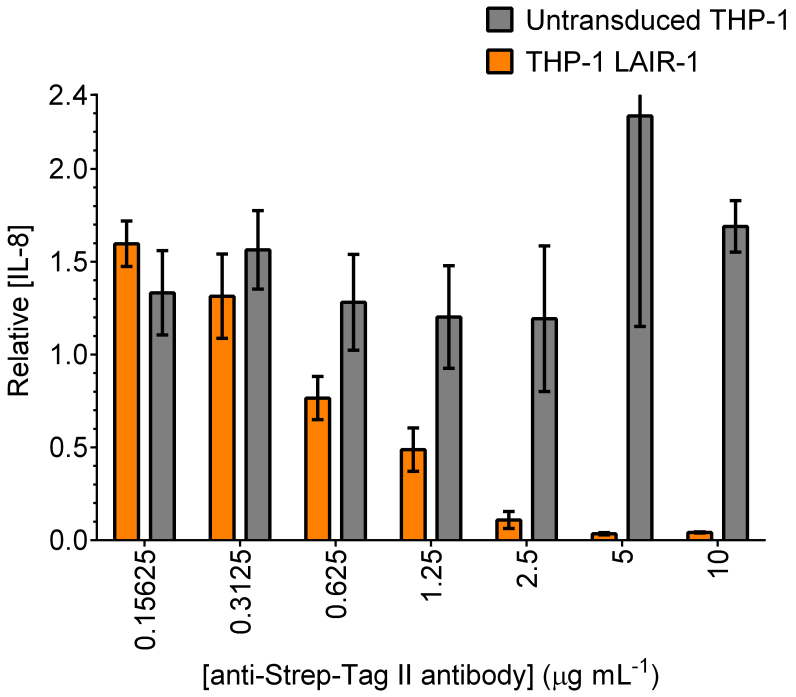


Fig. 4.3: **THP-1 LAIR-1 cells can be stimulated by plate-immobilised anti-Strep-Tag II antibody.** Anti-FcγRIA antibody (2.5μg mL^{-1}) was co-immobilised with varying concentrations of anti-Strep-Tag II antibody onto 96 well flat bottom plates. Untransduced THP-1 or THP-1 LAIR-1 cells were incubated in these wells at 37°C , 5% CO_2 for 20 hours before the supernatants were analysed for IL-8. IL-8 values in supernatants from unstimulated cells have been subtracted from all values shown which are normalised to the mean IL-8 concentration from the supernatants of cells presented to anti-FcγRIA antibody alone. Bars shown are from 1 experiment (n=2) with values given as mean$\pm$range of duplicate wells.

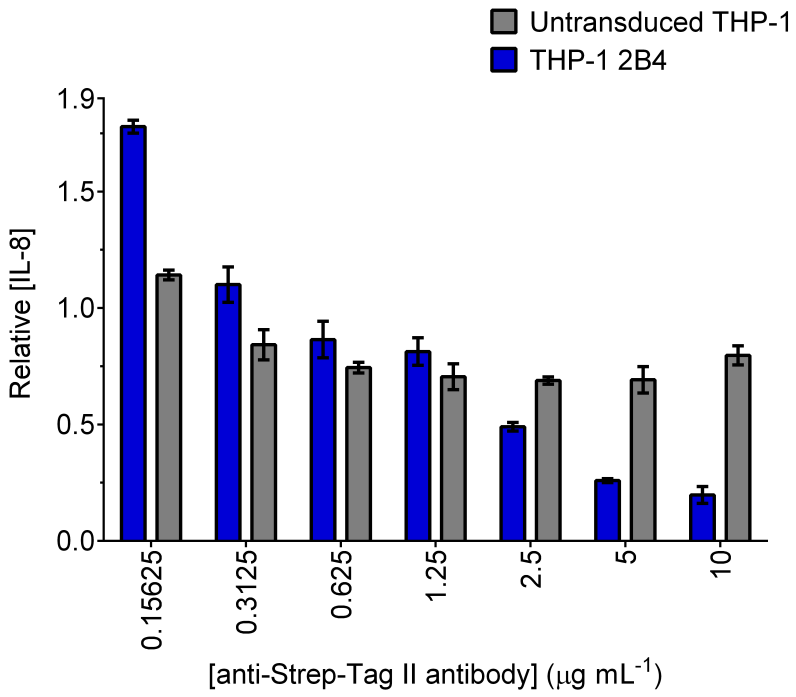


Fig. 4.4: **THP-1 2B4 cells can be stimulated by plate-immobilised anti-Strep-Tag II antibody.** Anti-FcγRIA antibody (2.5μg mL^{-1}) was co-immobilised with varying concentrations of anti-Strep-Tag II antibody onto 96 well flat bottom plates. Untransduced THP-1 or THP-1 2B4 cells were incubated in these wells at 37°C, 5% CO_2 for 20 hours before the supernatants were analysed for IL-8. IL-8 values in supernatants from unstimulated cells were subtracted from all values shown which were then normalised to the mean IL-8 concentration measured in the supernatant of cells that were presented to anti-FcγRIA antibody alone. Bars shown are from 1 experiment (n=2) with values given as mean$\pm$range of duplicate wells.

4.2.2 A representative NTR can be stimulated with StrepTactin presented on phospholipid bilayer-coated beads

To confirm tagged NTRs can be stimulated through ligation of the tag in a different setting we used phospholipid bilayer-coated silica beads to simulate ligand cells. A set of phosphatidylcholine-coated beads with varying proportions of a biotinyl cap lipid were created. StrepTactin binds to the biotin presented by the beads leaving a number of remaining binding site/s for ligation of the tagged NTR. The number of remaining sites depends on the valency of StrepTactin used. Incubating StrepTactin with a set of beads coated with varying proportions of biotinyl cap lipid will yield a set of beads with varying numbers of artificial ligand presented per bead. The ligands should also be mobile within the phospholipid bilayer.

A number of cell culture mediums such as RPMI 1640 media, as well as foetal calf serum which is a supplement of cell culture medium, contain biotin [Moore et al., 1967]. This free biotin would block the StrepTactin presented by lipid bilayer-coated beads and prevent binding between StrepTactin and Strep-Tag II-tagged receptor. Therefore this experiment, and further experiments using StrepTactin as a ligand were carried out in serum-free DMEM media unless otherwise stated because DMEM media does not contain biotin [Barford, 1995]. Biotin would not block the binding of Strep-Tag II to anti-Strep-Tag II antibody and so serum-free DMEM was not required for previous experiments using antibody as stimulus.

THP-1 NKp30 cells were stimulated to secrete IL-8 following incubation with ST3dSA1-bound lipid bilayer-coated beads (figure **4.5a**). Incubating THP-1 NKp30 cells with the ST3dSA1-bound beads at a 1:4 ratio led to a higher level of IL-8 release than either a 1:2 or 1:1 ratio (figure **4.5a**). Untransduced THP-1 cells incubated with the beads did not release detectable levels of IL-8 confirming the response we saw is specific to the receptor-ST3dSA1 interaction.

With all three ratios of receptor cell to bead, the level of IL-8 released increased with more artificial ligand presented per bead to a peak and then decreased again. This decrease does not appear to be a result of fewer StrepTactin tetramers bound per bead. This

is shown by a sample of the IL-8 release data plotted against the median fluorescence intensity (MFI) of fluorescent ST3dSA1 bound to the various beads (figure **4.5b**). Upon incubation of THP-1 NKp30 cells with beads bound by the highest amounts of ST3dSA1, as indicated by higher MFI values, the level of IL-8 release decreases. This should be confirmed by repeating the experiment.

The results shown here confirm that THP-1 NKp30 cells can be stimulated with ST3dSA1 presented on phospholipid bilayer-coated beads. The desired presentation of artificial ligand for our system however is bivalent StrepTactin as opposed to trivalent. This is to ensure a 1:1 interaction between receptor and ligand. Incubating THP-1 NKp30 cells with beads presenting 1,3 trans-ST2 and 1,4 ST2 did not produce detectable levels of IL-8 however (data not shown). This is in line with flow cytometry data (figure **3.38**) crudely comparing the number of available biotin-binding sites on beads bound by StrepTactin of different valencies. Bilayer-coated beads presenting 1,3 trans-ST2 and 1,4 ST2 had much fewer available binding sites in comparison to beads bound by ST3dSA1 or ST4. It is likely that tagged NKp30 could not interact with the bivalent StrepTactin presented on the beads and so the cells were not stimulated to release IL-8. Presentation of beads bound by 1,2 cis-ST2 was not attempted.

These data, among other results (see section 3.2.8), led us to alter the artificial ligand in order to optimise the interaction between receptor and ligand. This system has previously been described in section 3.1.4.

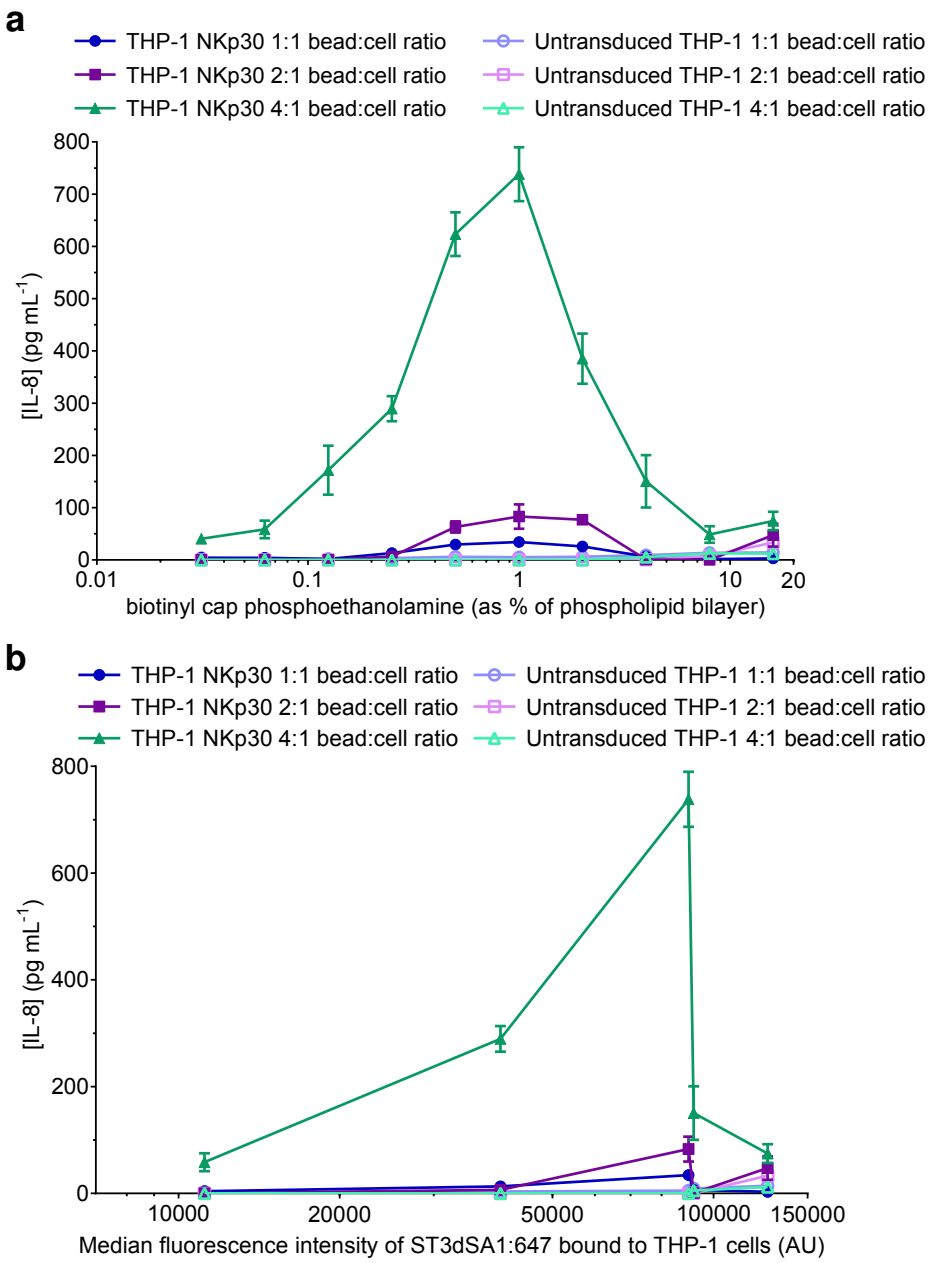


Fig. 4.5: **StrepTactin presented on phospholipid bilayer-coated beads can stimulate THP-1 NKp30 cells to release IL-8.** Silica beads were coated in a phosphatidylcholine phospholipid bilayer containing different proportions of biotinyl cap phosphoethanolamine. (**a**) ST3dSA1 was incubated with these beads to bind to the biotinyl cap and then the beads were presented to THP-1 NKp30 cells or untransduced THP-1 cells and incubated for 20 hours. Cell activation was measured by IL-8 release. Beads were presented to THP-1 cells at either a 1:1 ■, 2:1 ■, or 4:1 ■ ratio. (**b**) A sample of the phospholipid bilayer-coated beads were incubated with fluorescent ST3dSA1:647 instead of ST3dSA1 and analysed by flow cytometry to measure the median fluorescence intensity (MFI). IL-8 release data from (a) was then plotted against the MFI values. IL-8 secretion levels measured for either untransduced THP-1 or THP-1 NKp30 cells incubated with lipid bilayer-coated beads containing 0% biotinyl cap PE were subtracted from all values shown which are plotted against % of biotinyl cap PE in the bilayers or MFI. Data are from 1 experiment (n=2) with values shown mean±range of duplicate wells.

4.2.3 Stimulation of NTRs with artificial ligand-expressing cells

As described in section 3.2.8 we were unable to create CHO cell lines expressing the artificial ligand proteins for StrepTactin to bind. We did however create HEK293T cell lines transiently expressing the ligand proteins. Even though HEK293T cells are not the desired ligand cell line we used these transiently expressing cells to determine whether a representative tagged NTR could be activated by artificial ligand cells. IL-8 release could not be detected from THP-1 NKp30 cells incubated with ST3dSA1 bound to either HEK293T CD80 cells, HEK293T CD80-CD2 cells, or HEK293T CD80-CD4 cells (data not shown). Different ratios of ligand cell:receptor cell were used in an effort to optimise the experiment but even when added at a 4:1 ratio, the ligand cells did not elicit a response from the THP-1 NKp30 cells above background levels. In the same experiment THP-1 NKp30 cells did release IL-8 in response to plate-immobilised anti-Strep-Tag II, comparable to that seen in figure **4.2**, indicating that the reason for the ligand cells not stimulating THP-1 NKp30 cells was not a lack of sensitivity of the receptor cells. It is possible that ST3dSA1 bound multivalently to the ligand-expressing cells leading to fewer binding sites for Strep-Tag II-tagged receptor binding and the receptors cells were not activated to give a response above background. The StrepTactin presented on ligand cells may also not be able to engage NKp30 receptor. We also encountered problems stimulating Strep-Tag II-tagged NKp30 with cells expressing the artificial ligand of the second strategy (StrepTactin-SpyCatcher) (see next section).

Following the development of the second artificial ligand strategy, we re-investigated if artificial ligand presented on mammalian cells could stimulate tagged NTR-expressing cell lines. CHO CD80-Spy cells were covalently coupled with different concentrations of monovalent StrepTactin-SpyCatcher (ST1-pD-C) and then presented to THP-1 cells expressing either tagged NKp30 or tagged SIRPβ1. THP-1 SIRPβ1 cells were stimulated by the CHO CD80-Spy cells with ST1-pD-C covalently bound to the CD80 ligand protein (CHO CD80-Spy : ST1-pD-C cells) (figure **4.6a**) with a clear trend in levels of IL-8 secreted and concentration of ST1-pD-C used for conjugation to the CHO CD80-Spy cells. Untransduced THP-1 cells were not stimulated to release IL-8 under the same conditions indicating that the activation seen with THP-1 SIRPβ1 was specific to the

receptor-artificial ligand interaction.

In contrast, THP-1 NKp30 cells did not release detectable levels of IL-8 in response to incubation with CHO CD80-Spy : ST1-pD-C cells (figure **4.6a**). THP-1 NKp30 cells did release IL-8 following incubation with plate-immobilised anti-Strep-Tag II antibody (4.6b). This result, and the activation of THP-1 SIRPβ1 cells with the CHO CD80-Spy : ST1-pD-C cells provides evidence that both the THP-1 NKp30 cells and CHO CD80-Spy : ST1-pD-C cells are functional.

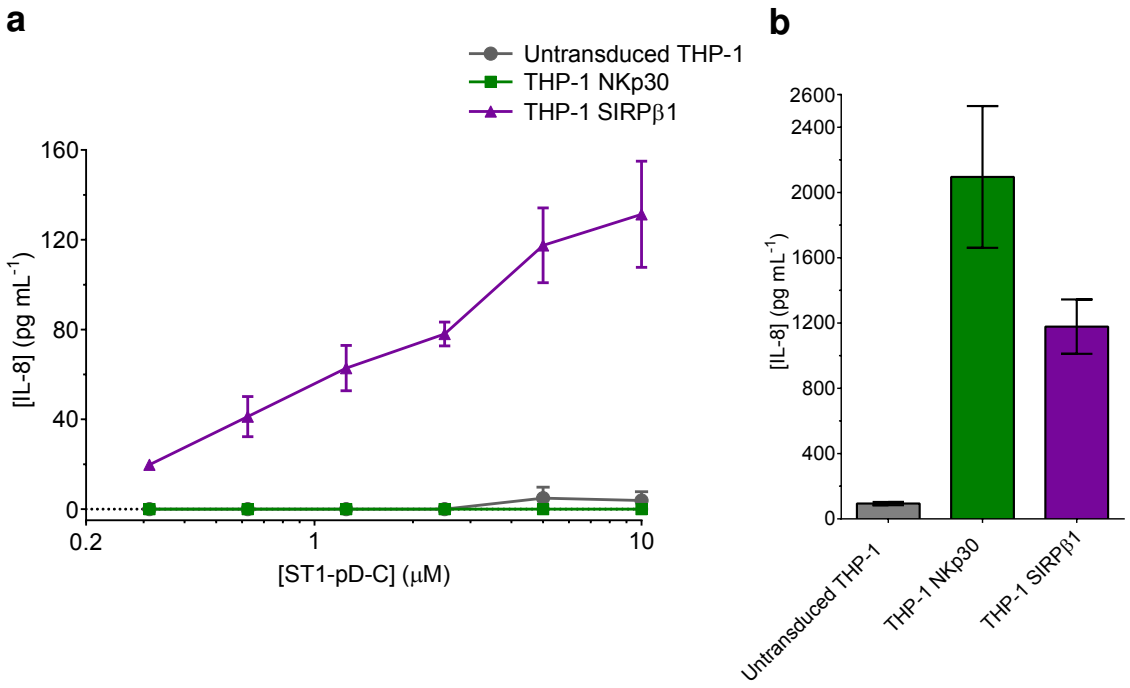


Fig. 4.6: **CHO CD80-Spy : ST1-pD-C cells can stimulate THP-1 SIRPβ1 but not THP-1 NKp30 cells to release IL-8.** CHO CD80-Spy cells were coupled with different concentrations of ST1-pD-C. These cells were then presented at a 1:1 ratio to untransduced THP-1 cells, THP-1 NKp30 cells, or THP-1 SIRPβ1 cells and incubated for 20 hours (**a**). Cell stimulation was measured by IL-8 release. As a positive control untransduced THP-1 cells, THP-1 NKp30 cells, or THP-1 SIRPβ1 cells were instead incubated for 20 hours with 96 well flat bottom plates pre-coated using 20μg mL^{-1} anti-Strep-Tag II antibody (**b**). Cell stimulation was measured by IL-8 release. Negative control IL-8 values measured in the supernatants from THP-1 cells incubated with mock conjugated ligand cells have been subtracted from all values shown which are plotted in a against concentration of ST1-pD-C added to the ligand cells. Data are from one experiment (n=2) with values shown as mean$\pm$range of duplicate wells.

NKp30 has a smaller extracellular region than SIRPβ1 with one immunoglobulin-like domain compared to three [Pende et al., 1999, Kharitonenkov et al., 1997]. Therefore it is possible that NKp30 is less able to form contacts with the short CD80-Spy ligand, and so THP-1 NKp30 cells are not stimulated to release IL-8. It is also possible that THP-

1 NKp30 cells may require more receptor-ligand interactions, or receptor cross-linking, for stimulation to occur. The structure of NKp30 in complex with one of its ligands B7-H6 revealed a 1:1 stoichiometry, and NKp30 has previously been immunoprecipitated as a monomer from the NK cell surface [Pende et al., 1999, Li et al., 2011]. In contrast, the structure of NKp30 extracellular domain alone shows the Ig-like domain to exist as a dimer and soluble forms of the extracellular domain of NKp30 were found to form oligomers so it may be possible that cross-linking of the receptor plays a role in activation [Joyce et al., 2011, Herrmann et al., 2014]. In an effort to stimulate Strep-Tag II-tagged NKp30 with artificial ligand-expressing cells, ST4-pD-C (to cross-link the receptor) was conjugated onto CHO cells stably expressing the longer ligand CD80-CD4-Spy (to potentially improve contacts between receptor and artificial ligand) and presented to THP-1 NKp30 cells. The ratio of ligand cells:receptor cells was also increased to a 2:1 ratio with the aim of increasing the number of receptor-ligand contacts. THP-1 NKp30 cells did not release detectable levels of IL-8 in response to these conditions however (figure **4.7a**). In contrast, THP-1 NKp30 cells were again shown to release IL-8 in response to plate-immobilised anti-Strep-Tag II antibody (figure **4.7b**).

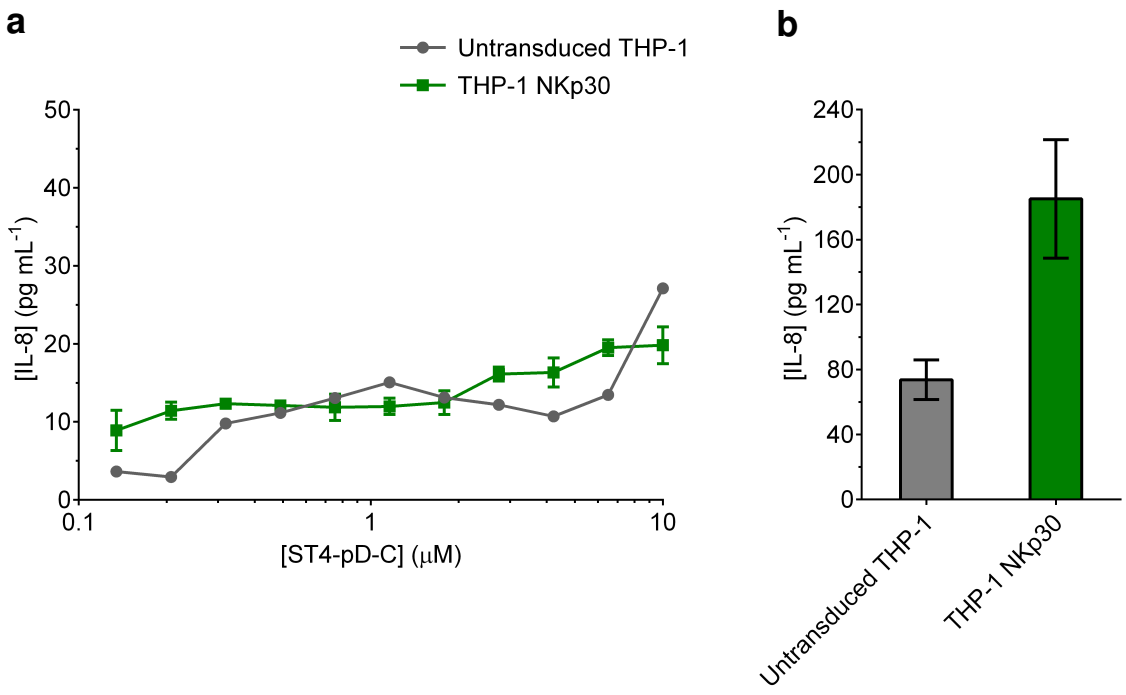


Fig. 4.7: **CHO CD80-CD4-Spy cells presenting ST4-pD-C cannot stimulate THP-1 NKp30 cells to release detectable levels of IL-8.** CHO CD80-CD4-Spy cells were coupled with different concentrations of ST4-pD-C. These cells were then presented at a 2:1 ratio to untransduced THP-1 cells or THP-1 NKp30 cells and incubated for 20 hours (**a**). Cell stimulation was measured by IL-8 release. As a positive control untransduced THP-1 cells or THP-1 NKp30 cells were instead incubated with 96 well flat bottom plates pre-coated using 20μg mL^{-1} anti-Strep-Tag II antibody (**b**). Cell stimulation was measured by IL-8 release. For (a) negative control IL-8 values measured in the supernatants of THP-1 cells incubated with mock conjugated ligand cells have been subtracted from all values shown which are plotted against concentration of ST4-pD-C added to the ligand cells. For (b), IL-8 values in the supernatants of cells incubated in blank wells was first subtracted from the plotted data. Data are from one experiment (n=2 for THP-1 NKp30 cells in (a) and (b), and untransduced THP-1 cells in (b), n=1 for untransduced THP-1 cells in (a) with values shown as mean$\pm$range of duplicate wells or individual values.

4.2.4 NTRs can be stimulated with plate-immobilised StrepTactin but not soluble protein

One of the predictions of the KS model of NTR triggering is that surface-immobilised monovalent ligand can activate the NTR whereas soluble monovalent ligand cannot. We used our system to test this prediction by comparing the activation of representative NTRs in response to surface-presented artificial ligand and activation in response to soluble artificial ligand.

Initially, we attempted to stimulate Strep-Tag II-tagged NTR-expressing cells with plate-immobilised ST1dSA3. However, as discussed in more detail in section 5.2.1, we discovered that ST1dSA3 could not be efficiently immobilised onto 96 well flat bottom plates whereas other StrepTactin tetramers such as ST4 could be efficiently adsorbed onto the plates. We therefore used ST4 to determine whether Strep-Tag II-tagged NTR-expressing cell lines could be activated by plate-immobilised or soluble StrepTactin. These experiments were conducted in serum-free DMEM because it does not contain biotin which would otherwise block the StrepTactin - Strep-Tag II interaction.

THP-1 NKp30 cells were stimulated to release IL-8 by plate-immobilised ST4 (figure **4.8a**). The levels were significantly higher than IL-8 levels released by untransduced THP-1 cells incubated with plate-immobilised ST4. When ST4 was presented to THP-1 NKp30 cells in solution however, IL-8 release could not be detected (figure **4.8b**). We also saw that THP-1 NKp30 cells released IL-8 when incubated with plate-immobilised anti-Strep-Tag II antibody but not soluble antibody (data not shown). This is consistent with the hypothesis that for NTR activation to occur, the ligand must be presented on a surface.

Whilst the values of IL-8 released by cells incubated with plate-immobilised StrepTactin or soluble StrepTactin cannot be directly compared, the values are plotted using the same axis for ease of visualisation.

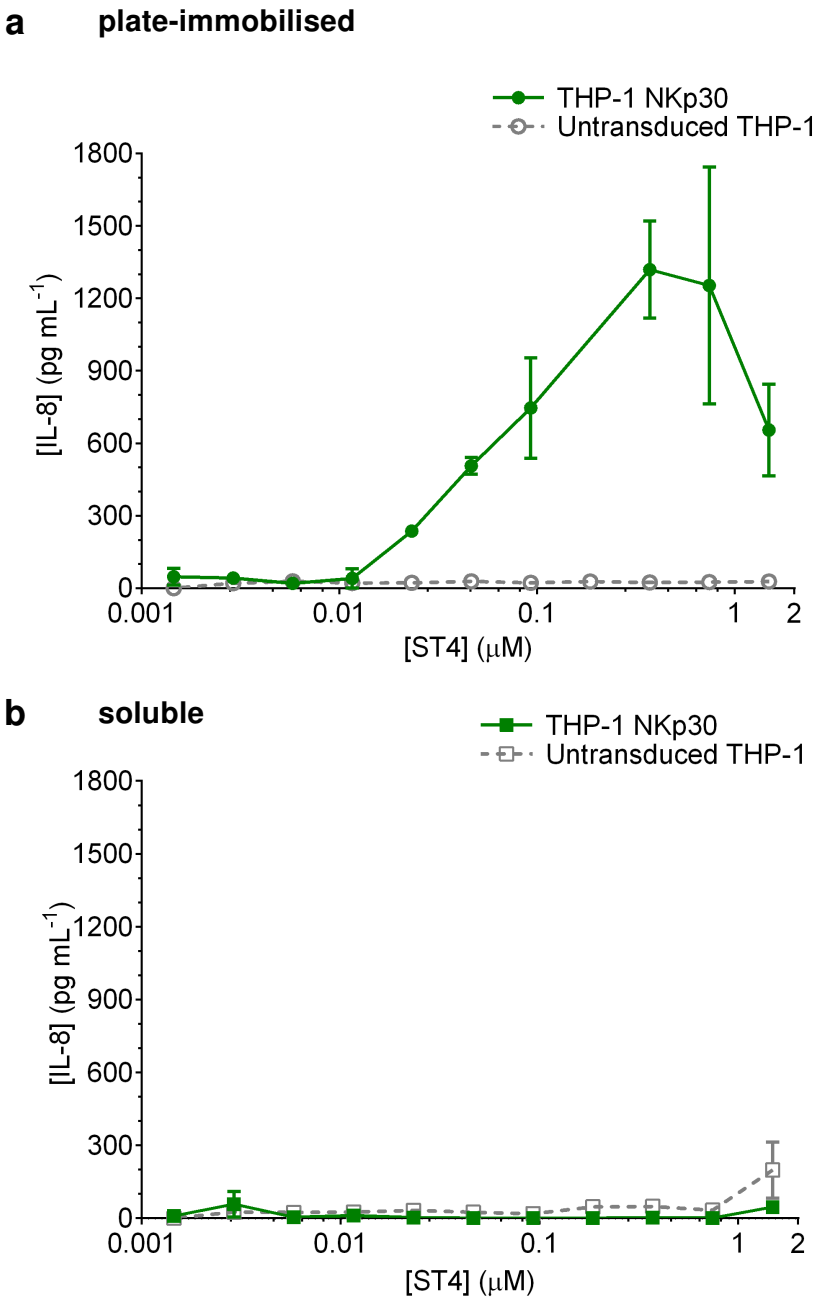


Fig. 4.8: **THP-1 NKp30 cells are activated by plate-immobilised but not soluble ST4.** Untransduced THP-1 cells or THP-1 NKp30 cells were incubated with varying concentrations of plate-immobilised ST4 (**a**) or soluble ST4 (**b**) in serum-free DMEM media. Serum-free DMEM does not contain biotin which would otherwise block interactions between StrepTactin and the Strep-Tag II-tagged NTR. After 20 hours, cell supernatants were analysed for IL-8. Supernatant IL-8 levels measured for cells incubated in blank wells have been subtracted from all values shown which are plotted against concentration of ST4 added to the wells. Data are from one experiment with values (n=2) given as mean±range of duplicate wells.

THP-1 FcγRIA cells were also incubated with either plate-immobilised or soluble ST4. In this case, the ST4 used was fluorescently labelled (ST4:647). Using fluorescent ST4:647 allowed us to show not only that THP-1 FcγRIA cells were activated by plate-immobilised ST4:647 but not soluble ST4:647 (figure **4.9a-b**), but also that soluble ST4:647 bound specifically to the Strep-Tag II-tagged NTR (figure **4.9ci**). Binding of soluble ST4:647 to THP-1 FcγRIA cells was determined by incubating the Strep-Tag II-tagged NTR-expressing cells with the same concentrations of soluble ST4:647 used in figure **4.9b** and then analysing the cells for StrepTactin binding using flow cytometry. Plotting the median fluorescence intensities from figure **4.9ci** of THP-1 FcγRIA cells incubated with various concentrations of soluble ST4:647 (figure **4.9cii**) shows that the cells are saturated with protein at the higher concentrations. Therefore, soluble ST4:647 is able to specifically bind to tagged FcγRIA expressed in THP-1 cells but is unable to stimulate the cells. ST4:647 did not bind to untransduced THP-1 cells (figure **4.9ci**) nor stimulate the cells, either in immobilised or soluble form (figure **4.9a-b**), thus indicating that the cell response was specific to ST4 binding to the Strep-Tag II-tagged receptor.

In agreement with what was seen for THP-1 NKp30 cells (figure **4.8**) and THP-1 FcγRIA cells (figure **4.9**), THP-1 SIGLEC-14 cells and THP-1 SIRPβ1 cells (figures **4.10** and **4.11** respectively) were only stimulated by plate-immobilised ligand and not soluble ligand. The flow cytometry data also showed that soluble ST4:647 was binding to the cells (figures **4.10ci** and **4.11ci**) but not causing activation even when it was added to cells at saturating concentrations (figures **4.10cii** and **4.11cii**).

Together, these data are consistent with the hypothesis that for the artificial ligand to activate NTRs, it needs to be presented on a surface.

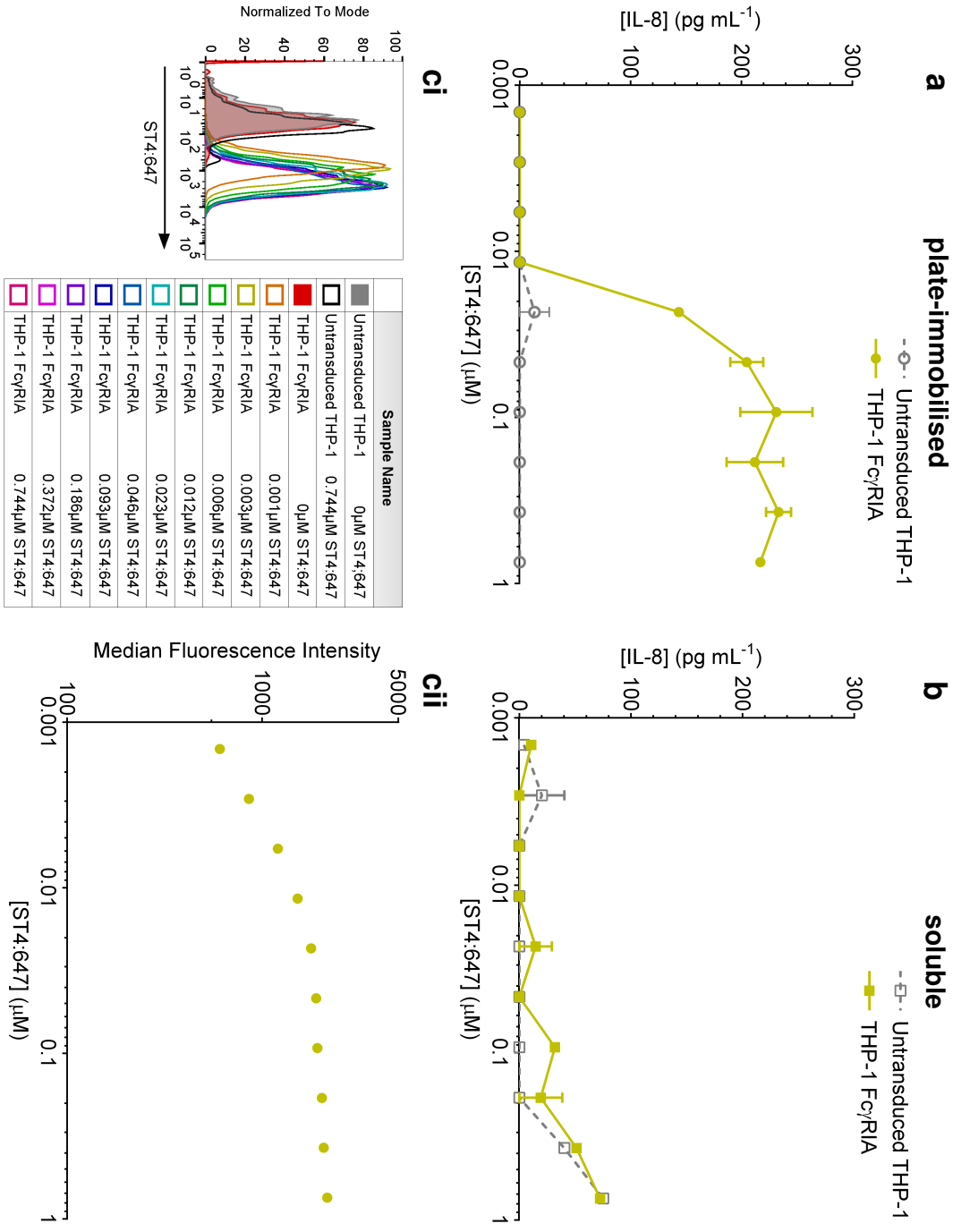


Fig. 4.9: **THP-1 FcγRIA cells are activated by plate-immobilised but not soluble ST4:647.** Untransduced THP-1 cells or THP-1 FcγRIA cells were incubated with varying concentrations of plate-immobilised ST4:647 (**a**) or soluble ST4:647 (**b**) for 20 hours and then the cell supernatants were analysed for IL-8. Untransduced THP-1 cells or THP-1 FcγRIA cells were incubated with the identical concentrations of soluble ST4:647 used in (b) and then analysed by flow cytometry (**ci**). Median fluorescence intensities from (ci) are plotted in (**cii**). The concentration of soluble ST4:647 added to the cells in (ci) is indicated on the figure key. For (a) and (b), supernatant IL-8 levels measured for cells incubated in blank wells were subtracted from the data, which was plotted against concentration of ST4:647 added to the wells. For (cii), MFIs of cells not incubated with ST4:647 were first subtracted from the values shown. Data are from one experiment with individual values or mean±range shown.

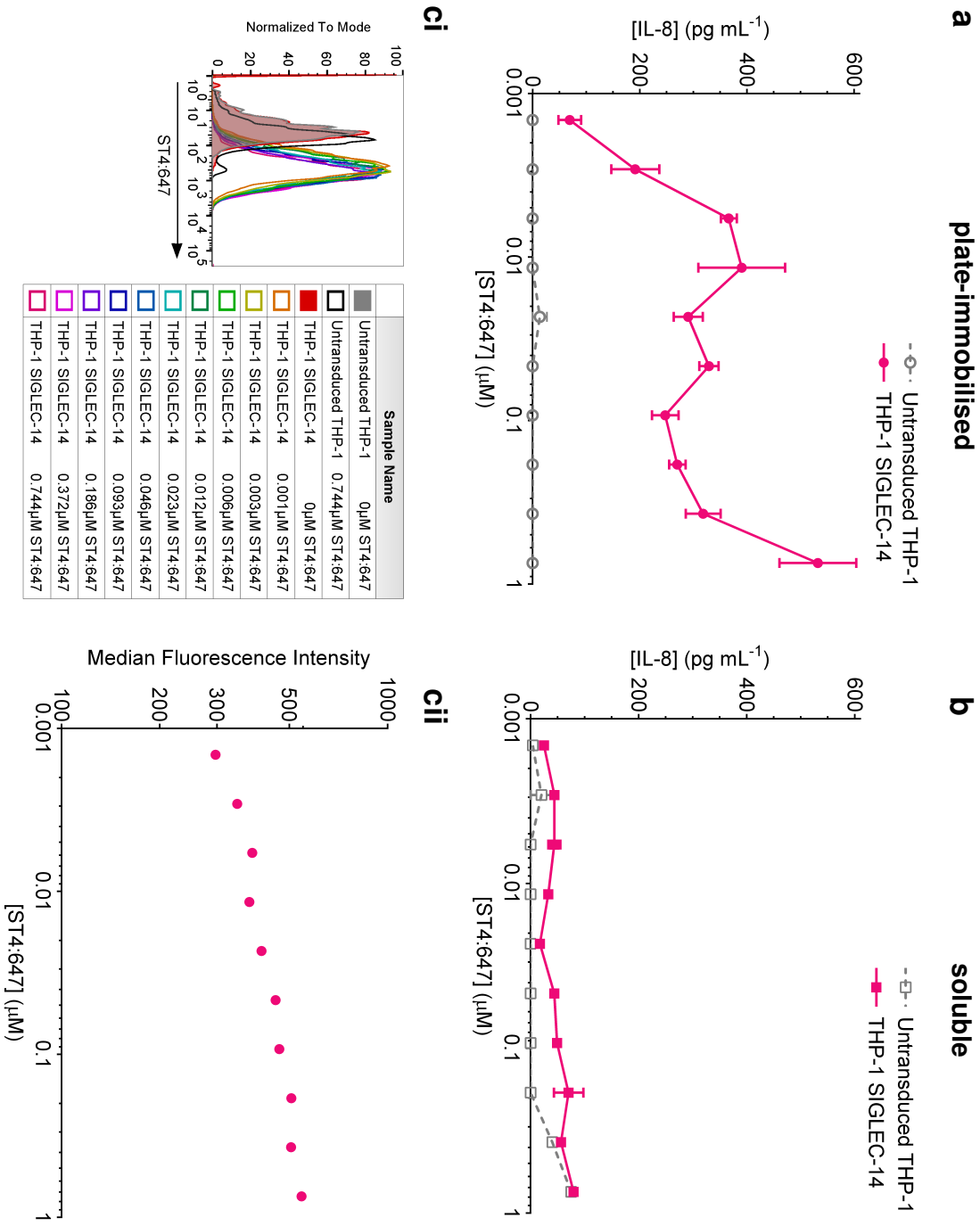


Fig. 4.10: **THP-1 SIGLEC-14 cells are activated by plate-immobilised but not soluble ST4:647.** Untransduced THP-1 cells or THP-1 SIGLEC-14 cells were incubated with varying concentrations of plate-immobilised ST4:647 (**a**) or soluble ST4:647 (**b**) for 20 hours and then the cell supernatants were analysed for IL-8. Untransduced THP-1 cells or THP-1 SIGLEC-14 cells were incubated with the identical concentrations of ST4:647 used in (b) and then analysed by flow cytometry (**ci**). Median fluorescence intensities from (ci) are plotted in (**cii**). The concentration of soluble ST4:647 added to the cells in (ci) is indicated on the figure key. For (a) and (b), supernatant IL-8 levels measured for cells incubated in blank wells were subtracted from the data, which was plotted against concentration of ST4:647 added to the wells. For (cii), MFIs of cells not incubated with ST4:647 were first subtracted from the presented results. Data are from one experiment with individual values or mean±range shown.

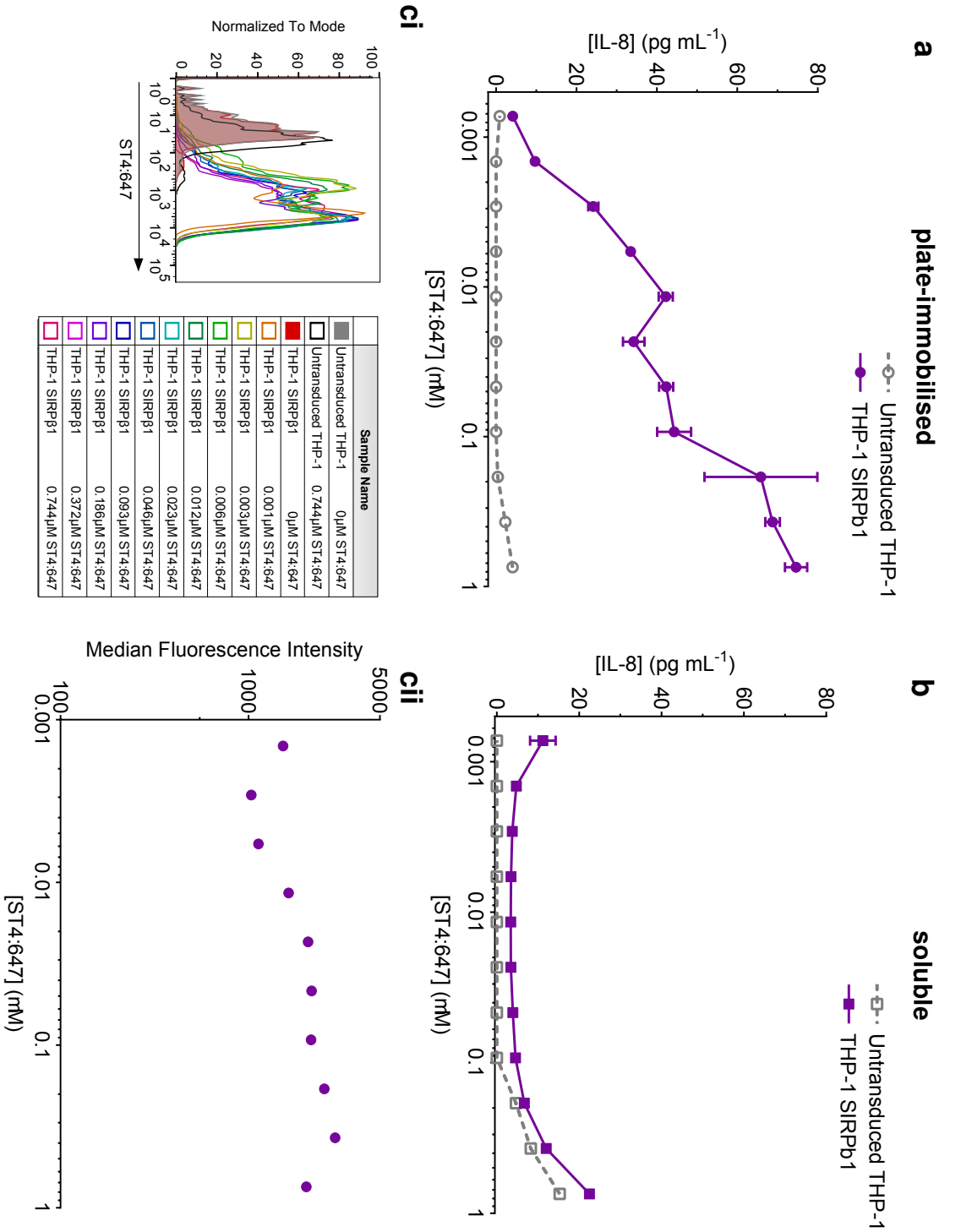


Fig. 4.11: **THP-1 SIRPβ1 cells are activated by plate-immobilised but not soluble ST4:647.** Untransduced THP-1 cells or THP-1 SIRPβ1 cells were incubated with varying concentrations of plate-immobilised ST4:647 (**a**) or soluble ST4:647 (**b**) for 20 hours and then the cell supernatants were analysed for IL-8. Untransduced THP-1 cells or THP-1 SIRPβ1 cells were incubated with the identical concentrations of ST4:647 used in (b) and then analysed by flow cytometry (**ci**). Median fluorescence intensities from (ci) are plotted in (**cii**). The concentration of soluble ST4:647 added to the cells in (ci) is indicated on the figure key. For (a) and (b), supernatant IL-8 levels measured for cells incubated in blank wells were subtracted from the data, which was plotted against concentration of ST4:647 added to the wells. For (cii), MFIs of cells not incubated with ST4:647 were first subtracted from the presented results. Data are from one experiment with individual values or mean±range shown.

4.2.5 Tetravalent StrepTactin binds to tagged NTRs multivalently

Clustering models of activation propose that cross-linking of the receptor following ligand binding is sufficient to activate the receptor. This does not rely on the ligand being surface-immobilised. We showed in figures **4.8**, **4.9**, **4.10** and **4.11** that soluble ST4:647 did not stimulate the NTRs even though it bound the receptors specifically. We did not however show evidence that tetravalent StrepTactin:647 was binding to the receptors multivalently and thereby cross-linking the receptors. If soluble ST4:647 does bind to tagged receptors multivalently, these results together provide evidence that receptor cross-linking at this scale is insufficient for receptor activation to occur. We therefore analysed the binding of ST4:647 to the cells in more detail to determine whether ST4:647 was binding to the Strep-Tag II-tagged NTRs multivalently.

For these experiments the StrepTactin-SpyCatcher fusion protein was used, not StrepTactin. We do not believe the presence of the SpyCatcher will affect our experiments and so consider the results in conjunction with the stimulation experiments in figures **4.8**, **4.9**, **4.10** and **4.11** that use StrepTactin without a SpyCatcher. StrepTactin-SpyCatcher that is binding multivalently to receptor-expressing cells will have a different dissociation profile than StrepTactin-SpyCatcher that is binding monovalently. To visualise if ST4-pD-C binds multivalently to THP-1 SIRPβ1 cells, $\sim$1.55μM fluorescent ST4-pD-C:647 was incubated with the cells. The volume in which the cells were suspended was then rapidly increased over 30 fold and the dissociation of ST4-pD-C:647 from THP-1 SIRPβ1 cells was immediately measured using flow cytometry (figure **4.12a**). As a comparison, THP-1 SIRPβ1 cells were incubated with fluorescent ST1-pD-C:647 which will bind to the cells monovalently. Samples of THP-1 SIRPβ1 cells bound by ST1-pD-C:647 or ST4-pD-C:647 were alternatively diluted over 30 fold with excess d-biotin to minimise rebinding of Streptactin-SpyCatcher to tagged SIRPβ1 (figure **4.12b**). The data shown in figure **4.12** are one example of this experiment. To confirm the profiles, the experiment was repeated but we found the traces were not reproducible. It is likely that dissociation of both ST1-pD-C:647 and ST4-pD-C:647 is faster than can be visualised using this set up and that any change in fluoresence intensity seen is a result of the measurement technique used.

As an alternative method, increasing concentrations of ST1-pD-C:647 or ST4-pD-C:647 were incubated with THP-1 SIRPβ1 cells and allowed to reach equilibrium binding before being analysed by flow cytometry. To determine the background signal, samples of THP-1 SIRPβ1 cells were alternatively incubated with the same concentrations of fluorescent ST1-pD-C:647 or ST4-pD-C:647 in the presence of excess free d-biotin. The free d-biotin will saturate the ST-pD-C:647 such that it cannot bind to the THP-1 SIRPβ1 cells. The background levels were subtracted from the corresponding fluorescence intensities of cells incubated with ST-pD-C:647 alone which were then normalised for the different degree of labelling between ST1-pD-C:647 and ST4-pD-C:647 and then plotted in figure **4.13**. With increasing concentration added to the cells, binding of ST1-pD-C:647 increases, but does not reach saturating levels. ST4-pD-C:647 binding however increases and then saturates. The K_D and maximum binding (Bmax) values calculated from the curve fit for ST1-pD-C:647 are 11 x 10^{-6}M (2sf) and 7900 (arbitrary units to 2sf) respectively and for ST4-pD-C:647 are 1.00 x 10^{-6}M (to 3sf) and 1900 (arbitrary units to 2sf) respectively. This is consistent with ST4-pD-C:647 binding to SIRPβ1 multivalently. We note that the K_D for ST4-pD-C:647 is consistent with the K_D given for the interaction of tetravalent StrepTactin and Strep-Tag II [Voss and Skerra, 1997b, Schmidt et al., 2013].

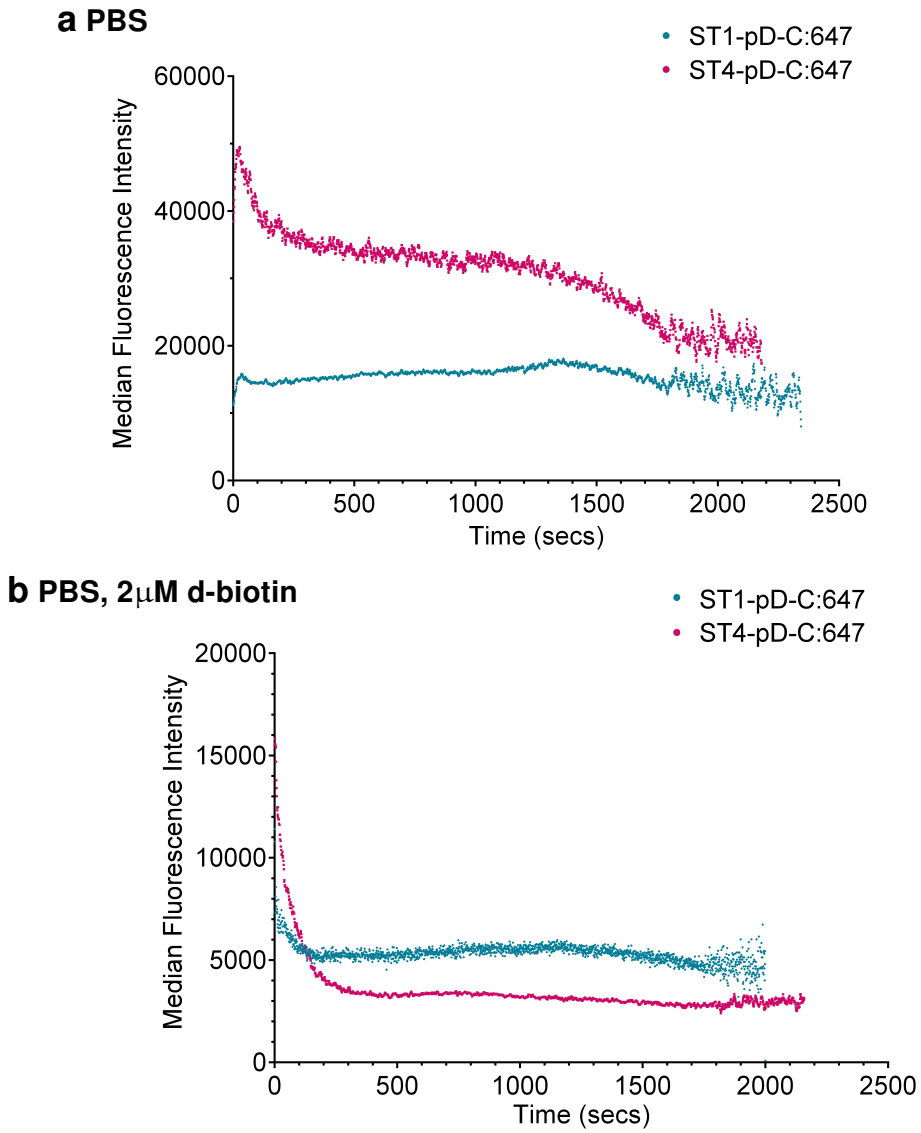


Fig. 4.12: **Dissociation of ST1-pD-C:647 or ST4-pD-C:647 cannot be visualised using flow cytometry.** THP-1 SIRPβ1 cells were incubated with ∼1.55μM ST1-pD-C:647 or ST4-pD-C:647. Cells were then diluted over 30 fold with either PBS (**a**) or PBS, 2μM d-biotin (**b**) and immediately analysed by flow cytometry for ST-pD-C:647 binding for ∼30 minutes.

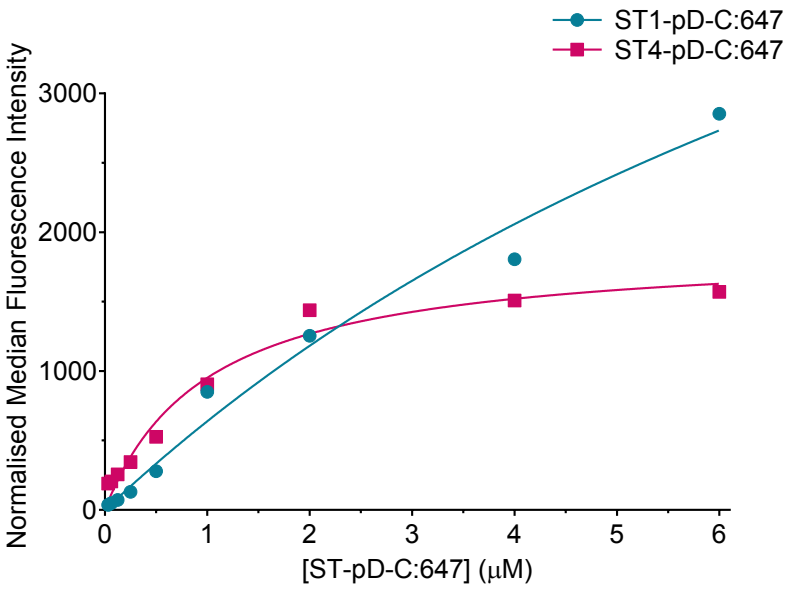


Fig. 4.13: **ST4-pD-C:647 binds to THP-1 SIRPβ1 cells multivalently.** THP-1 SIRPβ1 cells were incubated with varying concentrations of ST1-pD-C:647 or ST4-pD-C:647 and then analysed by flow cytometry. Fluorescence intensity values of THP-1 SIRPβ1 cells incubated with identical concentrations of ST1-pD-C:647 or ST4-pD-C:647, and also 4μM d-biotin were subtracted from the corresponding values of cells incubated with ST-pD-C:647 alone. These median fluorescence intensity values were then normalised for differences in degree of labelling between ST1-pD-C:647 and ST4-pD-C:647 before being plotted. Data is from one experiment and was fit with a saturation binding curve, one site - specific binding, using GraphPad Prism software. ST1-pD-C:647 R^2 = 0.98, ST4-pD-C:647 R^2 = 0.97.

4.3 Discussion

4.3.1 Confirming NTRs are stimulated by ligation of the Strep-Tag II

This chapter shows that 6 representative Strep-Tag II-tagged NTRs expressed in THP-1 cells can be activated by ligation of the Strep-Tag II. This ligation is either by immobilised anti-Strep-Tag II antibody binding or binding to StrepTactin or StrepTactin-SpyCatcher presented either on a plate, lipid bilayer-coated bead, or artificial ligand cell.

To visualise the inhibitory signalling of LAIR-1 and 2B4, transduced THP-1 cells were incubated with plate-immobilised anti-FcγRIA antibody to activate the cells, in combination with anti-Strep-Tag II antibody. While inhibition of IL-8 release was clearly seen with increasing anti-Strep-Tag II antibody concentration, there was a higher level of IL-8 released by untransduced or transduced THP-1 cells incubated with plate-immobilised anti-FcγRIA antibody and the lowest concentration of anti-Strep-Tag II antibody compared to cells incubated with anti-FcγRIA antibody alone (figures **4.3** and **4.4**). This may be a result of non-specific interactions between the anti-Strep-Tag II antibody and Fc receptors expressed on the THP-1 cell surface. Mouse immunoglobulins are known to bind to human Fc receptors present on THP-1 cells [Bruhns, 2012]. The interaction between antibody and Fc receptor could activate the Fc receptors and lead to the observed increase in IL-8 seen. As well as this, the binding of anti-Strep-Tag II antibody to Fc receptors may improve contact between the cell and plate, compared to contacts between cells and plates coated with anti-FcγRIA antibody only, thereby aiding anti-FcγRIA antibody-mediated activation. Isotype control antibodies could be used within the experiment to keep a constant concentration of immunoglobulin per well and keep the binding of IgG1 bound to Fc receptors the same. Alternatively, the Fc receptors could be blocked by the addition of human serum and so prevent Fc receptor-antibody binding.

THP-1 NKp30 cells could similarly be activated to release IL-8 upon incubation with plate-immobilised anti-Strep-Tag II antibody (figure **4.2**) and also released IL-8 in response to phospholipid bilayer-coated beads presenting ST3dSA1 (figure **4.5**). The level of IL-8 released by the cells increased with increasing amount of ST3dSA1 presented per bead to a peak and then unexpectedly decreased again. While this result needs to be confirmed

there are a number of mechanisms that could explain this. Firstly, it is possible that upon incubation of THP-1 NKp30 cells with beads presenting higher levels of ST3dSA1, NKp30 expression is down-regulated and therefore not available for ST3dSA1 binding. A number of NTRs are down-regulated upon ligand or antibody engagement including 2B4, NKp46 and the TCR [Valitutti et al., 1995b, Sivori et al., 2000, Sandusky et al., 2006]. The level of TCR down-regulation has been shown to correlate with the peptide concentration that antigen-presenting cells are pulsed with [Valitutti et al., 1995b]. Alternatively, there may be a higher level of cell death induced by activation. Cell death following activation of T cells for example has been shown (reviewed in [Green et al., 2003, Zhang et al., 2004]. To determine if either of these are the case, flow cytometry can be used to measure levels of receptor expression and cell death during the experiment. This optimum density of ligand may also be a characteristic of NKp30 stimulation. The peak in IL-8 release is not seen with plate-immobilised stimulus but it is possible that THP-1 NKp30 cells are presented with a much higher number and density of ligand in the coated bead experiments compared to experiments with plate-immobilised ligand.

THP-1 NKp30 cells could not be activated with phospholipid bilayer-coated beads bound by 1,3 trans-ST2 and 1,4 ST2 however. We hypothesise this is due to bivalent StrepTactin binding to the beads bivalently leaving very few available binding sites for Strep-Tag II, and so NKp30 is not activated. This is in agreement with previous flow cytometry data shown in section 3.2.9.

THP-1 NKp30 cells were also not activated by ST3dSA1 bound to HEK293T CD80 cells, HEK293T CD80-CD2 cells, or HEK293T CD80-CD4 cells. Previous flow cytometry data confirms that all three ligand-expressing cell lines can bind ST3dSA1 and leave binding sites available for soluble biotinylated IgG1, which suggests it should be possible for the ST3dSA1-bound ligand cells to form contacts with tagged NKp30. HEK293T cells are a human cell line and known to express a number of ligands for inhibitory NTRs which in turn are known to be expressed by THP-1 cells. One example is the NTR SIRPα and ligand CD47 which is expressed on HEK293T cells [Toledano et al., 2013]. The SIRPα-CD47 interaction has previously been shown to inhibit THP-1 cell phagocytosis so it is possible that any THP-1 cell response due to NKp30 activation is masked by the inhibitory activity of SIRPα and other inhibitory NTRs [Tsai and Discher, 2008, Tsai et al.,

2010].

THP-1 NKp30 cells were also not stimulated to release IL-8 by ligand cell lines created for the second artificial ligand strategy. Neither CHO CD80-Spy : ST1-pD-C cells nor CHO CD80-CD4-Spy : ST4-pD-C cells elicited a response from the receptor-expressing cells (figure **4.6** and **4.7**). Both cell lines were shown to be functional however. One possibility is that the Strep-Tag II-tagged NKp30 on THP-1 cells is unable to engage the artificial ligand when presented on ligand cells. Flow cytometry and imaging experiments could be used to determine this and allow further investigation of NKp30 triggering.

THP-1 SIRPβ1 cells were activated to release IL-8 upon incubation with CHO CD80-Spy : ST1-pD-C cells (figure **4.6**). This shows that StrepTactin-SpyCatcher coupled ligand cells are capable of forming conjugates with Strep-Tag II-tagged NTR-expressing THP-1 cells and that the NTR is activated upon this interaction.

These results show that representative NTRs can be stimulated by ligation of an introduced tag with artificial ligand and confirms the strategies developed in chapter 3 behave as expected and can be used to investigate NTR signalling. This also provides evidence against a ligand binding-induced conformational change in the receptor being required for activation. It is unlikely that ligation of the tag in the case of each receptor initiates the required conformational change for that receptor, leading to activation. Work previously described that uses antibodies to activate receptors rather than physiological ligand supports this (discussed in detail in section 4.1). An activation mechanism involving a generic, mechanically-induced, conformational change in the NTR upon ligand binding is consistent with these results however.

4.3.2 Other read-outs of receptor activation and further validation

To support and further confirm that Strep-Tag II-tagged NTRs can be activated by ligation of the tag, additional read-outs of receptor activation could be used for example phosphorylation of the NTR or associated adaptor protein. Signalling motif phosphorylation is a proximal signalling event and also allows investigation of inhibitory receptor signalling. Measuring inhibitory NTR activation with cytokine secretion as the signalling output is not straight-forward as it requires the cells to be stimulated in order to see the inhibitory

receptor signalling. Preliminary work to use signalling motif phosphorylation as a read-out of NTR activation is already under way. We have co-immunoprecipitated a number of the Strep-Tag II-tagged NTRs discussed here, along with the appropriate adaptor protein, from cell lines. Further to this, we have treated THP-1 LAIR-1 cells with the phosphatase inhibitor pervanadate and then immunoprecipitated the NTR and confirmed it was phosphorylated by western blotting and probing for phosphotyrosine. These methods are being further developed and optimised to be used to immunoprecipitate Strep-Tag II-tagged NTRs (with adaptor protein if appropriate) from cell lines following receptor stimulation with artificial ligand.

Another THP-1 cell activation read-out we are exploring is the up-regulation of ICAM-1 expression which has previously been shown in THP-1 cells in response to various stimuli [Al-Numani et al., 2003, Thornton and McDaniel, 2005, Xie and Gu, 2008, Wang et al., 2012]. Preliminary data from Dr Jesse Goyette shows THP-1 SIRPβ1 cells that have been differentiated by vitamin D3 treatment up-regulate ICAM-1 expression in response to stimulation with artificial-ligand expressing cells. This data indicates that ICAM-1 up-regulation could be a useful alternative read-out of NTR activation which has the advantage of providing single cell data rather than population data.

We would also like to validate the system using a selection of NTRs and their physiological ligand. By comparing activation of an NTR by ligation with either StrepTactin or physiological ligand we would also be able to determine any factors specific to the physiological ligand that play a role in receptor activation. For example, the affinity between receptor and ligand, or different dimensions of the receptor-ligand complex.

4.3.3 Receptor activation with plate-immobilised versus soluble stimulus

A key prediction the KS model makes about NTR activation is that ligand generally needs to be presented on a surface to optimally stimulate the receptor. This prediction was tested by presenting either plate-immobilised or soluble StrepTactin to representative Strep-Tag II-tagged NTRs and comparing the cell responses. Consistent with the prediction, all four activating NTRs tested, NKp30, FcγRIA, SIGLEC-14 and SIRPβ1, were only activated following incubation with StrepTactin that was presented on a surface and did

not respond to soluble StrepTactin (figures **4.8**, **4.9**, **4.10** and **4.11**). While this supports the KS model, it is also consistent with a mechanism whereby upon receptor cell-ligand cell interaction, a mechanically induced change in the receptor leads to activation.

Binding of soluble StrepTactin to the transduced cells was confirmed using flow cytometry. In fact, these data indicated that at the higher concentrations of soluble StrepTactin incubated with the cells, the receptors were saturated. The form of StrepTactin used was ST4 and, by using equilibrium binding analysis, it was shown that soluble tetravalent StrepTactin-SpyCatcher not only binds to tagged NTRs on the surface of transduced THP-1 cells but binds to the receptor multivalently. This was shown with THP-1 SIRPβ1 cells (figure **4.13**). While StrepTactin was used for stimulation analysis and StrepTactin-SpyCatcher was used for equilibrium binding we predict that soluble StrepTactin binds to receptor-expressing cells multivalently too.

Together these data indicate that even at saturating concentrations, and when bound multivalently to the receptors, soluble StrepTactin is unable to activate NTRs. This suggests that receptor aggregation alone is not sufficient for NTR triggering. It is also in conflict with data showing that representative NTRs are activated by antibody-induced receptor cross-linking (discussed in section 4.1). Further work should elucidate the reason for this. Firstly, it could be further confirmed that ST4-pD-C binds to transduced THP-1 cells multivalently and that receptors are clustered upon ST4-pD-C binding using FRET. This technique has been used previously to look at clustering of the BCR in B cells for example [Tolar et al., 2005]. Measurement of homo-FRET using fluorescence anisotropy imaging could also be investigated to show receptor clustering. The use of this technique in imaging protein dynamics is discussed in [Ghosh et al., 2012].

If these experiments confirm the clustering of SIRPβ1 upon soluble ST4-pD-C binding, the level of clustering in comparison to receptor cross-linking could be investigated. Perhaps the aggregation of NTRs in our experiments is on too small a scale to give stimulation. Antibody-induced receptor cross-linking, where this has been shown to activate the receptor, generally involves a primary antibody to initially cross-link the receptors and also a secondary antibody to cross-link them further still. It is therefore likely that in these experiments the receptor is more clustered in comparison to when transduced THP-1 cells are incubated with soluble ST4-pD-C. In line with this, it has been shown for

SIRPβ1, and activating Fc receptors that induced receptor dimerisation by soluble IgG alone is insufficient for receptor activation [Kurlander and Gartrell, 1983, Hayashi et al., 2004]. To investigate this further, larger soluble StrepTactin-SpyCatcher complexes could be incubated with receptor-expressing cells to form larger NTR clusters and the cell responses compared to those of cells incubated with soluble StrepTactin-SpyCatcher of a lower valency. Anti-streptavidin antibody that cross-reacts with StrepTactin could be incubated with StrepTactin-bound cells to further cluster the receptors. Alternatively, larger StrepTactin complexes with an increased number of Strep-Tag II binding sites could be used. This is based on streptavidin eicosamers previously created and used to activate the TCR [Fairhead et al., 2014b].

5. LIGAND VALENCY AND ECTODOMAIN LENGTH AFFECT STIMULATION OF A REPRESENTATIVE NON-CATALYTIC TYROSINE-PHOSPHORYLATED RECEPTOR

5.1 Introduction

As discussed in chapter 1, it has been proposed that receptor dimerisation or clustering induced by ligand binding initiates signalling. There is an abundance of evidence with numerous NTRs that higher order cross-linking of the receptor can initiate activation. While we show in Chapter 4 that soluble multivalent artificial ligand binding to representative NTRs was insufficient for activation, other factors may be important, for example the scale of clustering. The role of clustering in signalling may also differ between receptors. A number of studies have been conducted with the TCR, BCR and an NK cell receptor looking in a more detailed manner at the role of ligand clustering and spacing in receptor activation.

5.1.1 The role of ligand spacing in NTR activation

Small-scale patterning of ligand onto solid surfaces and nanometre-scale diffusion barriers positioned on supported lipid bilayers have been used to investigate receptor signalling, immune synapse formation and protein migration at the interface between a receptor-expressing cell and ligand-presenting surface (example studies include [Doh and Irvine, 2006, Culley et al., 2009, DeMond et al., 2008, Mossman et al., 2005, Shen et al., 2009]). Numerous studies have similarly used nanometre-scale arrays of immobilised ligand to investigate the role of ligand spacing on receptor activation at smaller scales.

Arrays of immobilised antibody to the TCR or CD16 were presented to T cells or NK

cells respectively. The antibodies were immobilised onto surface-bound anchors with different length spaces between the anchors. With increasing distance between the antibody-presenting anchors from 25 nm to 104 nm the response of both T and NK cells, measured by phosphotyrosine blotting, decreased. While this is consistent with receptor clustering increasing signalling it is also possible that the absolute number of receptor engagements by the nanometre-scale antibody arrays also varied. Closely spaced immobilised antibodies may be more likely to engage higher numbers of receptors over time, perhaps due to increased rebinding of the receptor by nearby antibody. This may lead to an increased signalling output [Delcassian et al., 2013].

Similarly, increasing the distance between immobilised antigen in a nanometre-scale array decreased activation responses of an antigen-specific chimeric antigen receptor (CAR) presented on T cells. Here, the antigen amount per array was kept constant and only the density of antigen was altered. However, at the highest densities of antigen, CAR activation was reduced. It was suggested that at these high antigen densities the diffusion of proteins like Lck may be hindered leading to reduced interaction between Lck and the CAR, and reduced activation [Fishler et al., 2012].

In addition to immobilised ligand, soluble ligand dimers and multimers have been used to investigate the effect of altering ligand spacing on receptor activation. This work used spatial separation of single ligands rather than small clusters of ligand as used in Delcassian et al. Multiple studies used soluble pMHC dimers with varying length linkers between the proteins to show a negative correlation between linker length and both CD4+ and CD8+ CTL cell responses [Cochran et al., 2001, Cebecauer et al., 2005b, Cebecauer et al., 2005a]. A dimer of pMHCs directly coupled via disulphide bonds induced the largest response. These studies disagree however on the level of binding of the various pMHC dimers to T cells. Cochran et al. found no difference in T cell binding between pMHC dimers separated by different length linkers whereas in other studies binding inversely correlated with linker length. The difference in binding could affect T cell responses but it was argued that the reduction in binding was not sufficient to explain the reduction in activation. These studies also disagree on the linker length at which pMHC dimers are unable to induce TCR activation. These variances, and also the variances in dimer binding measured in each study, may be a result of differences in

the rigidity of the linkers used [Cochran et al., 2001, Cebecauer et al., 2005b, Cebecauer et al., 2005a].

This work was extended to include pMHC tetramers and octamers with similar results. Not only did pMHC multimers with longer linkers induce the lowest TCR aggregation but also the weakest cytotoxic T lymphocyte (CTL) response. The binding of multimers coupled by long linkers to CTLs was again lower than more directly coupled complexes and there was also decreased CTL-target cell conjugate formation which was proposed to be a result of reduced TCR signalling [Angelov et al., 2006].

Similarly, soluble trivalent DNP complexes with different length linkers between were added to a FcϵRI-expressing mast cell line bound by anti-DNP IgE. Like for the TCR, an inverse correlation was seen between linker length and cell responses including FcϵRI phosphorylation, calcium mobilisation and mast cell degranulation although significant changes in other signalling components like PLCγI phosphorylation was not visualised [Sil et al., 2007].

Soluble bivalent NIP haptens with varying length peptide linkers were used to investigate the role of ligand spacing in BCR activation. No difference in BCR calcium responses to the various linked haptens was observed even at longer linker lengths comparable to those used in the TCR studies (longest length linker predicted to be 8 nm if extended). It is possible that if the linker took on a structured rather than extended form however the linker length range would be much smaller and so may be insufficient to significantly affect BCR signalling. Alternatively, the BCR may not be sensitive to changes in ligand spacing. Soluble monovalent hapten was unable to induce BCR activation, indicating that cross-linking of the receptor is required for activation [Minguet et al., 2010].

These studies together provide detailed evidence that induced close proximity of some NTRs by ligand binding results in increased receptor responses although the specific mechanism is unclear.

5.1.2 The effect of altering ligand mobility on activation

Altering the mobility of receptor-ligand complexes can affect the level of receptor clustering and signalling. For example, B cell-expressed BCRs bound by monovalent F(ab) fragments were presented to either immobilised streptavidin or streptavidin on a supported lipid bilayer (SLB). As expected, BCR microclusters on the B cells presented to mobile streptavidin were more mobile. Enhanced phosphotyrosine signals were also visualised in BCR microclusters presented to mobile ligand suggesting this mobility plays a role in BCR signalling [Ketchum et al., 2014].

FcϵRI signalling can also be influenced by ligand mobility. FcϵRI-expressing rat basophilic leukaemia cells were presented to either mono- or multi- valent hapten, either immobilised or presented on a supported lipid bilayer. Multivalent hapten induced degranulation both when immobilised and presented on a lipid bilayer. Monovalent hapten however, could only induce degranulation when presented on a bilayer and mobile. Immobilised monovalent hapten did not activate the cells suggesting that FcϵRI needs to be clustered for activation to occur. Alternatively, the arrangement of immobilised monovalent hapten, which would result in single receptor-ligand interactions spread over a large area, may alter the tension acting on the receptor-ligand bonds and thereby also affect receptor activation [Carroll-Portillo et al., 2010].

The mobility of proteins presented on SLBs can be varied by the lipids that make up the bilayer. Hsu et al. created a set of bilayers made of varying proportions of two lipids and showed that NTA presented on each of the bilayers exhibited different mobilities. Anti-CD3 was bound to the SLB-NTA and presented to T cells for TCR engagement. ZAP70 microclusters located at the interface between T cell and the SLB were more mobile with higher mobility bilayers. Increased central accumulation of CD3ζ at the cell-bilayer interface, increased phosphotyrosine signalling in the interface, and increased calcium flux were also measured in response to more mobile anti-CD3. Hsu et al. suggest that high ligand mobility, and the observed higher central accumulation of CD3ζ at the interface, allows generation of new TCR microclusters and recruitment of downstream signalling molecules to maintain elevated calcium levels [Hsu et al., 2012]. This is unlikely to contribute to the differences in phosphotyrosine signalling observed however,

which occurred earlier than CD3ζ accumulation. The phosphotyrosine signal was also spread throughout the T cell-SLB interface rather than accumulated at the centre with CD3ζ. The effect of ligand mobility on early TCR signalling may therefore occur on a smaller scale than the whole interface.

5.1.3 Varying the receptor-ligand complex extracellular dimensions affects NTR signalling

In addition to ligand spacing and mobility, the role of ligand ectodomain length in receptor signalling has been investigated for a number of NTRs. The KS model which we hypothesise is involved in NTR activation predicts that elongating the extracellular domain of the receptor and/or ligand will decrease receptor signalling. Elongation of the receptor-ligand complex dimensions increases the intermembrane distance at sites of receptor engagement thereby reducing the segregation of large surface molecules like the phosphatases CD45 and CD148 from the bound receptor. The phosphatases will then be able to target bound NTRs and inhibit signalling. A number of studies with a range of NTRs have tested this prediction and provided evidence that supports the KS model.

Binding of a T cell-expressed TCR by a specific single-chain trimer (SCT) expressed on CHO cells can induce TCR signalling. Elongating the extracellular domain of the SCT by the insertion of 2-4 immunoglobulin-like domains from CD2, CD22, or CD4 reduced ligand binding-induced TCR triggering [Choudhuri et al., 2005, Choudhuri et al., 2009]. In fact, there was an inverse correlation between ectodomain length and both early and late readouts of TCR triggering. Ligand elongation also increased the CHO cell-T cell intermembrane distance in line with predictions and resulted in reduced segregation of CD45 from the TCR at the cell-cell interface [Choudhuri et al., 2009]. The same trend was also seen with artificial TCR-pMHC complexes that span similar intermembrane dimensions [Choudhuri et al., 2005]. These results were not associated with changes in binding of elongated SCT to the TCR or co-receptor.

Immobilising pMHC onto a surface via linkers of different length has also been used to vary the distance between the T cell surface and pMHC-presenting surface [Ma et al.,

2014]. Increasing this cell-surface distance by immobilising pMHC on longer linkers decreased TCR activation. pMHCs immobilised by the longest linkers (extended lengths of 190.9 and 381.8 nm) could still activate the TCR however. This is inconsistent with the KS model as these large cell-surface distances would not give physical exclusion of CD45 from engaged TCR-pMHCs. However, the linkers used are flexible and so will not always be fully extended. The average distances between the surface and the pMHC immobilised by the longest linkers (as given by the Flory radius) were predicted to be 14 and 21.3 nm. These smaller intersurface distances at sites of receptor-ligand engagement could mediate exclusion of large surface proteins like CD45. Therefore these results do not provide evidence against a model of TCR triggering that involves inhibitory phosphatase segregation [Ma et al., 2014].

Elongation of the extracellular domain of ligand CD80 by insertion of immunoglobulin-like domains decreased CD28 receptor-mediated co-stimulation of TCR signalling [Lim et al., 2015]. Using a trans co-stimulation assay, this was shown not to be a result of the mismatched dimensions between TCR-pMHC and CD28-CD80 that may result in reduced signal integration and/or reduced engagement of the receptor and ligand pairs. CD45 segregation from CD80 protein at the cell-cell interface was also reduced with elongation of the ligand. CD80 elongation had a much smaller effect on co-stimulation by a CD28 mutant that is not phosphorylated in the YxNM signalling motif indicating that decreased co-stimulation was a result of changes to YxNM motif-mediated signalling [Lim et al., 2015].

The extracellular domain of inhibitory receptors CTLA-4 and PD-1 have similarly been elongated with immunoglobulin-like domains from CD22 or CD4 to investigate the effect on receptor signalling [Yokosuka et al., 2010, Yokosuka et al., 2012]. Elongated CTLA-4 and PD-1 receptors exhibited reduced co-localisation with TCR microclusters compared to wild-type length receptors. The inhibitory effect of either CTLA-4 or PD-1 signalling on TCR-induced IL-2 secretion was also reduced by elongation of the receptor ectodomain. Studies with PD-1 showed decreased ligand binding-induced phosphorylation of the elongated receptor compared to wild-type indicating that increasing the ectodomain length of PD-1 interferes with activation of the receptor [Yokosuka et al., 2012]. In addition, SHP-1 or SHP-2 inhibitory phosphatase was fused to both wild-type

and elongated PD-1 to investigate PD-1-mediated suppression of TCR signalling independent of PD-1 phosphorylation. Suppression of TCR signalling by elongated PD-1-SHP-1 was lower than that of wildtype length fusion proteins. This suggests that signal integration is also affected by elongation of the receptor, perhaps due to spatial segregation of engaged TCRs and elongated PD-1 [Yokosuka et al., 2012]. Similar mechanisms may be responsible for the reduced inhibition of TCR signalling by elongated CTLA-4 [Yokosuka et al., 2010].

An inverse correlation between dimensions of a number of NK cell receptor-ligand complexes and associated signalling has also been shown [Brzostek et al., 2010, Köhler et al., 2010]. Ligands of both activating and inhibitory NK cell NTRs were lengthened by insertion of immunoglobulin-like domains into the ectodomain. Elongated ligands induced lower levels of receptor activation compared to wildtype length ligands. Kohler et al. also show that activating and inhibitory ligand co-localisation at the immune synapse is reduced when one of the ligands is elongated. This segregation was suggested to be due to the mismatched dimensions of wildtype and elongated receptor-ligand complexes which may also contribute to reduced signal integration [Köhler et al., 2010].

Both anti-CD30 and ROR1-specific chimeric antigen receptors (CARs) elongated with the CH2CH3 region of either IgG1 or IgG4 exhibited reduced activation responses to ligand binding compared to shorter versions [Hombach et al., 2000,Hudecek et al., 2013]. The reduced signalling of the anti-CD30 CAR was not due to a reduction in conjugate formation between the CAR-expressing cell and target cell [Hombach et al., 2000].

All of these studies provide evidence consistent with the KS model. In each case elongation of the receptor-ligand complex resulted in reduced signalling and where analysed, was associated with reduced CD45 segregation from the receptor-ligand complex which is key to the model.

Both ligand spacing and ectodomain length are therefore important in activation of a number of NTRs. The artificial ligand system we have developed can be easily manipulated and used to investigate both of these properties further and in other NTRs. To analyse ligand spacing and valency on receptor signalling we use StrepTactin or StrepTactin-SpyCatcher of different valencies to activate representative NTRs. We also

look at the difference in responses to mono- or multi- valent ligands that are either immobilised or presented on cell membranes to further investigate the role of receptor clustering in activation. In addition to this, we use CHO cell lines expressing either a 'short' or 'long' version of the artificial ligand protein to investigate the effect of ligand elongation on signalling. Finally, we combine varying the two ligand properties, valency and ectodomain length, to compare receptor behaviour in response to these combinations. For example, if the activation of a receptor bound by monovalent ligand is altered by ligand elongation, does elongation of tetravalent ligand result in the same changes to receptor signalling?

5.2 Results

5.2.1 NTR activation with plate-immobilised StrepTactin of different valencies

To initially investigate the effect of altering ligand valency on NTR activation we used plate-immobilised StrepTactin of different valencies and THP-1 NKp30 cells as a representative NTR-expressing cell line. Varying concentrations of mono-, bi-, tri- and tetravalent StrepTactin were individually immobilised onto wells of a 96 well flat bottom plate. THP-1 NKp30 cells, or untransduced THP-1 cells as a negative control, were incubated in these wells for 20 hours. The cell supernatants were then analysed for IL-8 levels as an indication of cell activation.

For all StrepTactin proteins apart from monovalent StrepTactin (ST1dSA3), the amount of IL-8 released by THP-1 NKp30 cells increased with increasing concentration of StrepTactin used to coat the wells (figure **5.1**). Untransduced THP-1 cells did not secrete detectable levels of IL-8 in response to any of the plate-immobilised StrepTactin proteins indicating that the response of THP-1 NKp30 cells is specific to the Strep-Tag II-tagged receptor - StrepTactin interaction. There is also a clear trend in the THP-1 NKp30 cell response to StrepTactin of different valencies. Plate-immobilised tetravalent (ST4) and trivalent (ST3dSA1) StrepTactin elicited the highest level of IL-8 secretion from THP-1 NKp30 cells while both 1,2 cis-ST2 and the mixture of 1,3 trans-ST2 and 1,4 ST2 stimulated the release of much lower levels of IL-8. For every StrepTactin protein immobilised,

ST4 will potentially present more receptor-binding sites than ST3dSA1 which in turn will potentially present more receptor-binding sites than bivalent StrepTactin. Therefore the difference in IL-8 secretion seen in figure **5.1**, where IL-8 levels are plotted against concentration of StrepTactin, is likely due, at least in part, to the different numbers of receptor-binding sites presented by the various StrepTactin proteins.

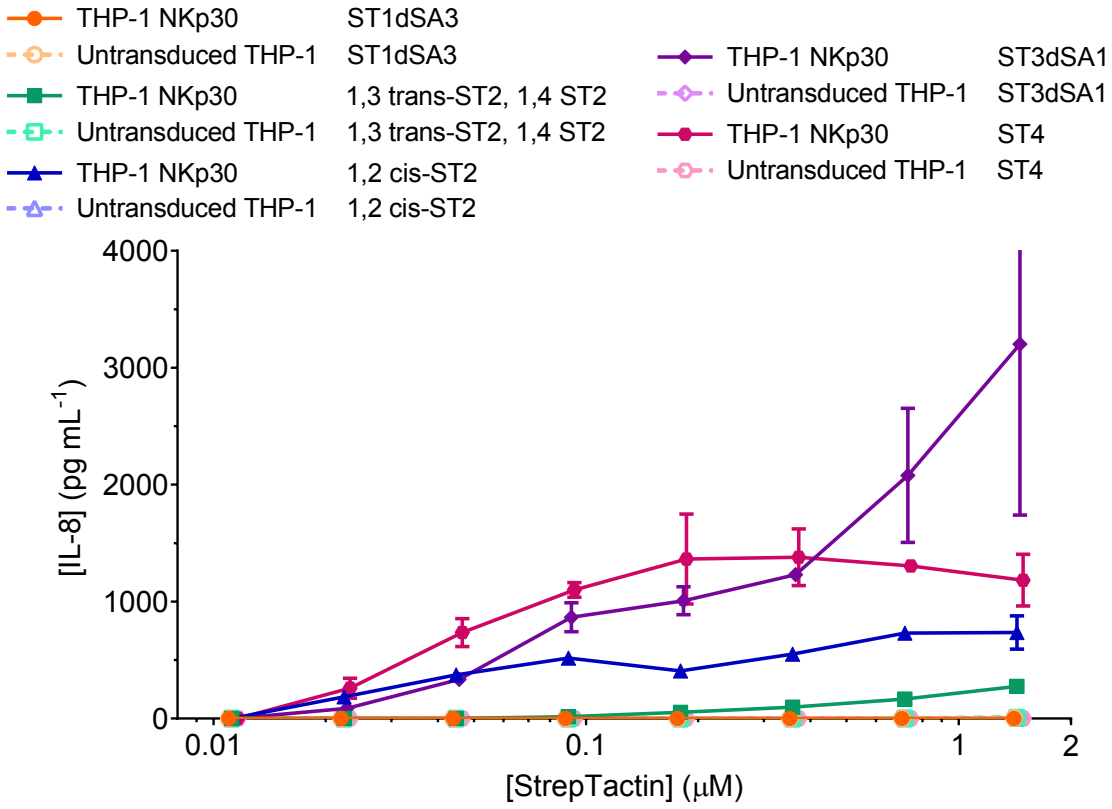


Fig. 5.1: **Plate-immobilised bi-, tri-, and tetra-valent but not monovalent StrepTactin stimulate THP-1 NKp30 cells to secrete IL-8.** THP-1 NKp30 cells were incubated with increasing concentrations of plate-immobilised monovalent StrepTactin (ST1dSA3), or the mixture of 1,3 trans-ST2 and 1,4 ST2, or 1,2 cis-bivalent (1,2 cis-ST2), trivalent (ST3dSA1), or tetravalent (ST4) StrepTactin for 20 hours. The cell supernatants were then analysed for IL-8 levels by ELISA. As negative controls, untransduced THP-1 cells (shown in paler colours) were incubated in identical StrepTactin-coated wells for 20 hours and analysed for IL-8 secretion. IL-8 values measured in wells not coated with StrepTactin protein were first subtracted from the values shown which are plotted against concentration of StrepTactin added to the wells. Data shown are from 1 experiment (n=2) with values shown as mean±range of duplicate wells.

IL-8 secretion by THP-1 NKp30 cells incubated with plate-immobilised ST1dSA3 was not detected (figure **5.1**). This may be due to a low efficiency of ST1dSA3 immobilisation onto wells, a low accessibility of the binding sites for receptor engagement, or because monovalent engagement does not activate the NTR. Cis-bivalent StrepTactin and the mixture of 1,3 trans-ST2 and 1,4 ST2 elicited significantly different levels of IL-8 secretion from THP-1 NKp30 cells. One reason for this could again be different immobilisation efficiencies between the two proteins. If for example, 1,2 cis-ST2 is more efficiently immobilised onto wells than 1,3 trans-ST2 and 1,4 ST2 there will potentially be more receptor-binding sites available in wells coated using 1 μM 1,2 cis-ST2 than in wells coated using 1 μM 1,3 trans-ST2 and 1,4 ST2. As the data in figure **5.1** uses the concentration of StrepTactin used to coat the wells, cell activation in response to plate-immobilised 1,2 cis-ST2 would appear larger.

One way in which the StrepTactin proteins differ that could alter the immobilisation efficiency is the overall charge. To permit separation of the various configurations using ion exchange chromatography the dead streptavidin subunit has a polyaspartate loop. ST4 does not contain a polyaspartate loop whereas ST1dSA3, having 3 dead streptavidin subunits per protein, will contain 3 polyaspartate loops. Thus ST1dSA3 has an overall more negative charge. While each protein will bind to the 96 well plate using electrostatic interactions, this greater net negative charge may inhibit the immobilisation of ST1dSA3. Alternatively, it may bias the orientation of ST1dSA3 binding such that the binding site is oriented towards the plate making it inaccessible. Similarly, the orientation of the two polyaspartate loops of 1,2 cis-ST2 may lead to a higher immobilisation efficiency than 1,3 trans-ST2 and 1,4-ST2, or bias the orientation in which 1,2 cis-ST2 is immobilised leaving the binding sites more accessible for receptor engagement.

To determine if the more negative charge of ST1dSA3 interferes with the immobilisation of the protein we pre-coated the wells of a 96 well flat bottom plate with either positively charged poly-L-lysine or positively charged PEI (or PBS as a control). Either ST1dSA3 or ST3dSA1 were then immobilised onto these wells. (ST1dSA3 was not added to PEI-coated wells). As well as presenting these protein-coated wells to THP-1 NKp30 cells and measuring IL-8 secretion, we used duplicate wells to determine if the StrepTactin was immobilised and also whether the Strep-Tag II/biotin-binding sites on the immobilised

StrepTactin were accessible from solution. For this, biotinylated mouse IgG1, followed by anti-mouse HRP and then HRP substrate was incubated with the StrepTactin-coated wells (figure **5.2a**).

ST1dSA3 was not immobilised onto the blank wells with accessible binding sites (figure **5.2a**) which explains the lack of detectable activation of THP-1 NKp30 cells incubated in these wells (figure **5.2bi**). ST1dSA3 was immobilised onto plates pre-coated with poly-L-lysine however, which is consistent with the negative charge of ST1dSA3 interfering with immobilisation onto blank wells. Despite the immobilisation of ST1dSA3 onto poly-L-lysine - coated wells with accessible binding sites, THP-1 NKp30 cells incubated in these wells did not release detectable levels of IL-8 (figure **5.2bi**). This suggests that either poly-L-lysine interferes with the receptor-ligand interaction or that immobilised ST1dSA3 does not activate NKp30.

As expected, ST3dSA1 was immobilised onto the wells with the highest number of accessible biotin-binding sites (figure **5.2a**). Pre-coating the wells with poly-L-lysine or PEI appeared to inhibit ST3dSA1 immobilisation. ST3dSA1 has a less negative charge than ST1dSA3 and so perhaps pre-coating the wells with positive poly-L-lysine or PEI interferes with the immobilisation. THP-1 NKp30 cells but not untransduced THP-1 cells were activated by incubation with plate-immobilised ST3dSA1 only (figure **5.2bii**) in accordance with previous results (figure **5.1**). Surprisingly, pre-coating the wells with either poly-L-lysine or PEI abolished this activation (figure **5.2bii**) despite detectable levels of accessible biotin-binding sites. This suggests the presence of poly-L-lysine or PEI interferes with receptor engagement and activation.

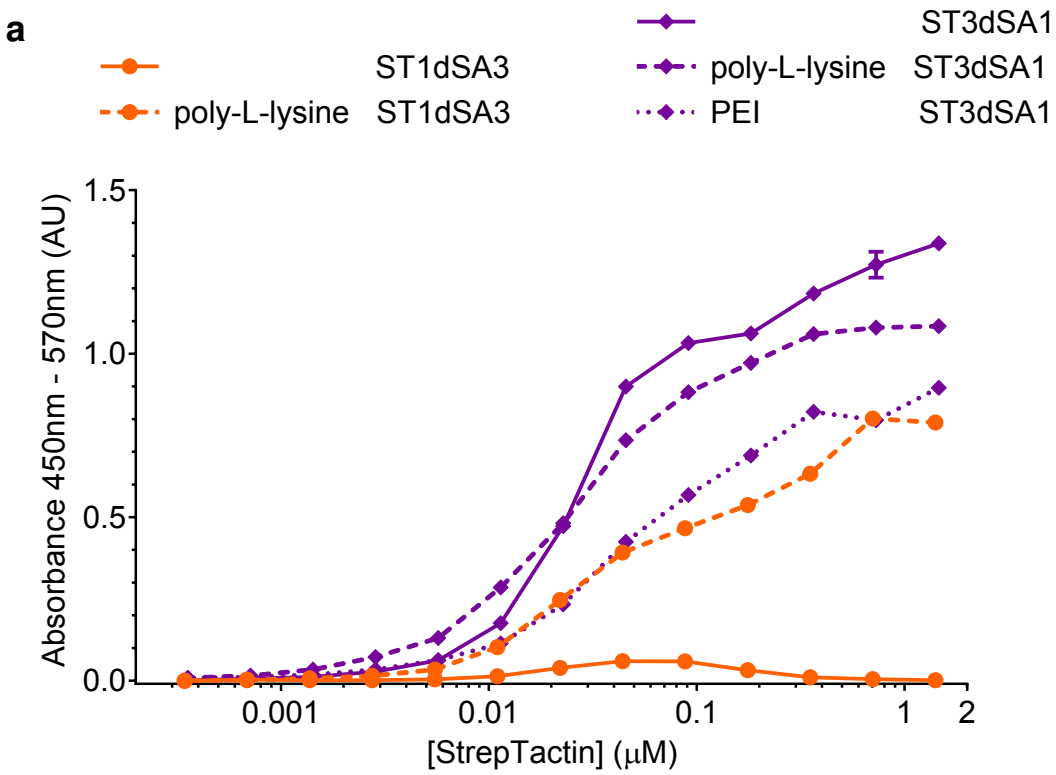


Fig. 5.2: **Pre-coating wells of a 96 well flat bottom plate with poly-L-lysine or PEI abolishes activation of THP-1 NKp30 cells by plate-immobilised StrepTactin.** Wells of a 96 well flat bottom plate were incubated with PBS (solid line), poly-L-lysine (dashed line), or PEI (dotted line). Following washing of the wells, different concentrations of ST1dSA3 or ST3dSA1 were added to the wells. Biotinylated mouse IgG1, then anti-mouse HRP and then HRP substrate were incubated in the wells to indicate StrepTactin immobilisation and number of accessible biotin-binding sites (**a**). Absorbance resulting from biotinylated mouse IgG1 binding (y-axis) is plotted against the concentration of StrepTactin used to coat the wells (x-axis). Absorbance values of wells incubated with no protein, poly-L-lysine alone, or PEI alone were first subtracted from the corresponding values shown. *Continued on the next page.*

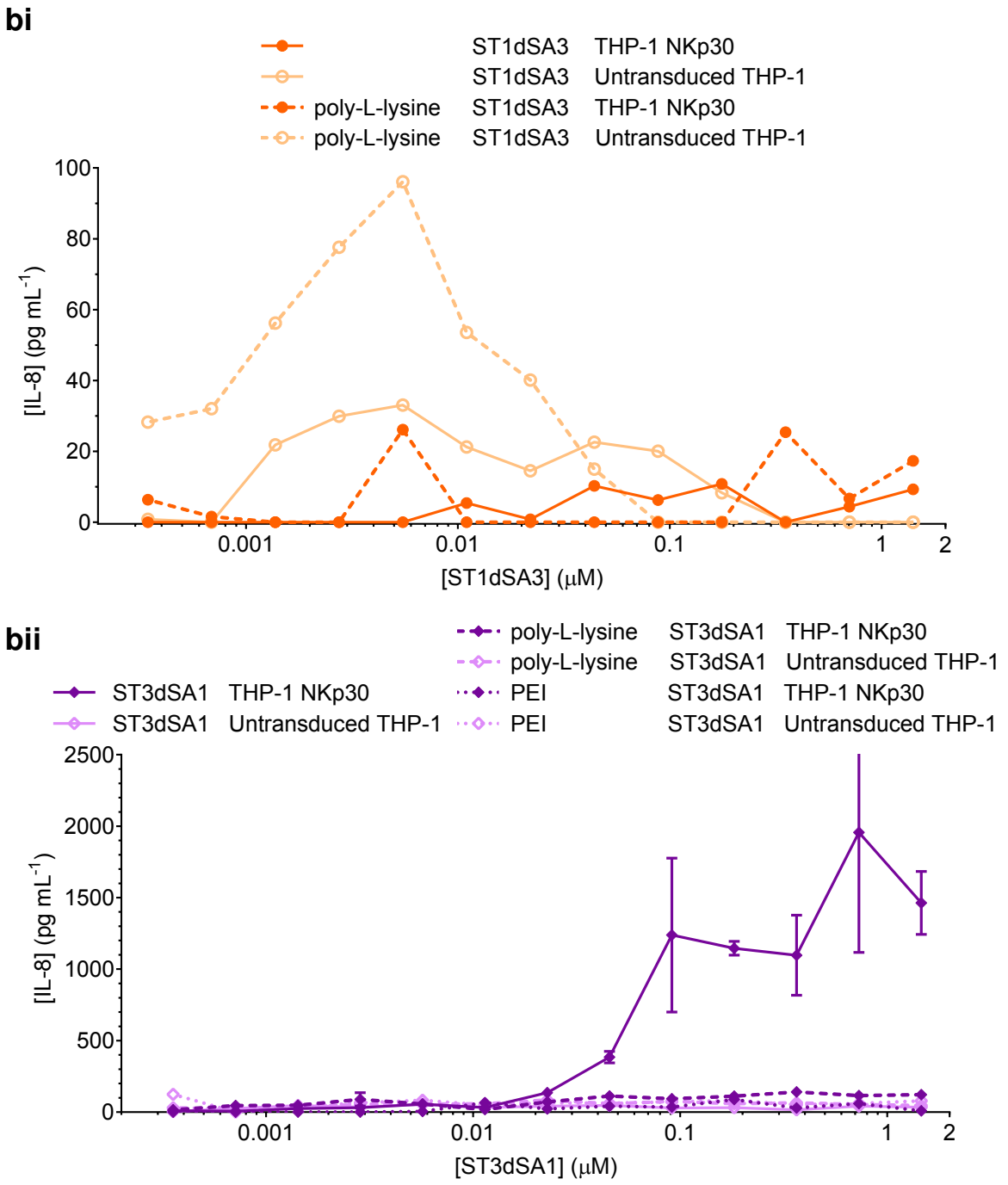


Fig. 5.2: **Pre-coating wells of a 96 well flat bottom plate with poly-L-lysine or PEI abolishes activation of THP-1 NKp30 cells by plate-immobilised StrepTactin.** *Continued.* Untransduced THP-1 cells or THP-1 NKp30 cells were incubated with duplicates of the ST1dSA3-coated wells (**bi**) or ST3dSA1-coated wells (**bii**) for 20 hours. The cell supernatants were then analysed for IL-8 by ELISA. IL-8 secretion (y-axis) is plotted against the concentration of StrepTactin used to coat the wells (x-axis). Note the difference in y-axis scale between bi and bii. IL-8 levels released by untransduced THP-1 cells are shown in paler colours. IL-8 concentrations measured in wells incubated with either PBS, poly-L-lysine or PEI alone were subtracted from the corresponding values shown which are plotted against concentration of StrepTactin added to the wells. Data are from one experiment, n=1 for all ST1dSA3 data and n=2 for all ST3dSA1 data. Values for ST3dSA1 are given as mean±range of duplicate wells.

We also attempted to immobilise comparable levels of ST1dSA3 and ST4 onto wells of a 96 well flat bottom plate by pre-coating the wells with a polyclonal anti-streptavidin antibody that we predicted would also bind to both monovalent and tetravalent StrepTactin. While both ST1dSA3 and ST4 were immobilised onto anti-streptavidin antibody-coated plates, Strep-Tag II-tagged NTR-expressing THP-1 cells added to the wells were activated by the anti-streptavidin antibody. This data has been omitted for brevity.

5.2.2 Comparing NTR activation using plate-immobilised monovalent and tetravalent StrepTactin-SpyCatcher

The adsorption efficiencies of monovalent and tetravalent StrepTactin-SpyCatcher (annotated as ST1-pD-C and ST4-pD-C respectively) onto 96 well flat bottom plates were also analysed. Like StrepTactin, purification of both ST1-pD-C and ST4-pD-C makes use of a polyaspartate loop which in the case of ST1-pD-C and ST4-pD-C is present on the StrepTactin-SpyCatcher subunit (described in section 3.2.10.1). Both ST1-pD-C and ST4-pD-C contain one StrepTactin-SpyCatcher subunit and so each only have one polyaspartate loop per protein. We therefore predicted that the two proteins would have similar immobilisation efficiencies when used to coat 96 well flat bottom plates and so sought to use these proteins to investigate the effect of increasing ligand valency on receptor activation.

To determine whether the adsorption efficiencies of ST1-pD-C and ST4-pD-C onto plastic plates were similar, varying concentrations of ST1-pD-C or ST4-pD-C were incubated in wells of a 96 well flat bottom plate. After washing and blocking of the wells, anti-streptavidin antibody and then a HRP-conjugated secondary antibody were incubated in the wells to measure how much StrepTactin-SpyCatcher had been immobilised per well. At each concentration of StrepTactin-SpyCatcher added to the wells, comparable amounts of ST1-pD-C and ST4-pD-C were immobilised (figure **5.3a**). This indicates that the two proteins have similar immobilisation efficiencies.

The activation of NTR-expressing cells will vary with the number of receptor-ligand interactions. This is likely to differ between cells incubated with a single concentration of ST1-pD-C or ST4-pD-C. The cell activation response therefore needs to be normalised

for the number of receptor-ligand interactions as opposed to concentration of ST-pD-C. To do this, we used biotin fused to a single atto 680 dye (biotin:atto 680) to indicate the number of accessible biotin-binding sites present in wells coated with StrepTactin-SpyCatcher. Duplicates of the ST1-pD-C - or ST4-pD-C - coated wells used in figure **5.3a** were incubated with saturating concentrations of biotin:atto 680, washed and then the atto 680 signal was measured and analysed (figure **5.3b**). The number of accessible biotin-binding sites on immobilised ST1-pD-C, as indicated by biotin:atto 680 fluorescence, increases with higher concentrations of ST1-pD-C used to coat the well. This is in line with the increase in immobilised ST1-pD-C seen in figure **5.3a**. In contrast, the number of accessible biotin-binding sites on immobilised ST4-pD-C increases a small amount and then saturates at a relatively low ST4-pD-C concentration. This fluorescence is consistently much lower than the fluorescence of biotin:atto 680 bound to immobilised ST1-pD-C (figure **5.3b**). As we had seen comparable amounts of ST1-pD-C and ST4-pD-C immobilised onto duplicates of these wells (figure **5.3a**), and there should be four times as many biotin-binding sites on ST4-pD-C than on ST1-pD-C, we would predict many more accessible biotin-binding sites in wells with immobilised ST4-pD-C.

After subsequent reads of the fluorescence of these wells, and so with increased photobleaching of the biotin:atto 680 signal, the fluorescence intensity of wells with immobilised ST4-pD-C increased. We therefore hypothesised that biotin:atto 680 binding to ST4-pD-C brings the atto 680 dyes into close proximity and leads to auto-quenching of the atto 680 fluorescence. This would explain the apparent low level of biotin:atto 680 binding to ST4-pD-C. Auto-quenching of biotin:atto 680 fluorescence was also seen in the laboratory when the reagent was used to indicate the number of biotin-binding sites on artificial ligand-expressing cells presenting ST4-pD-C (data not shown).

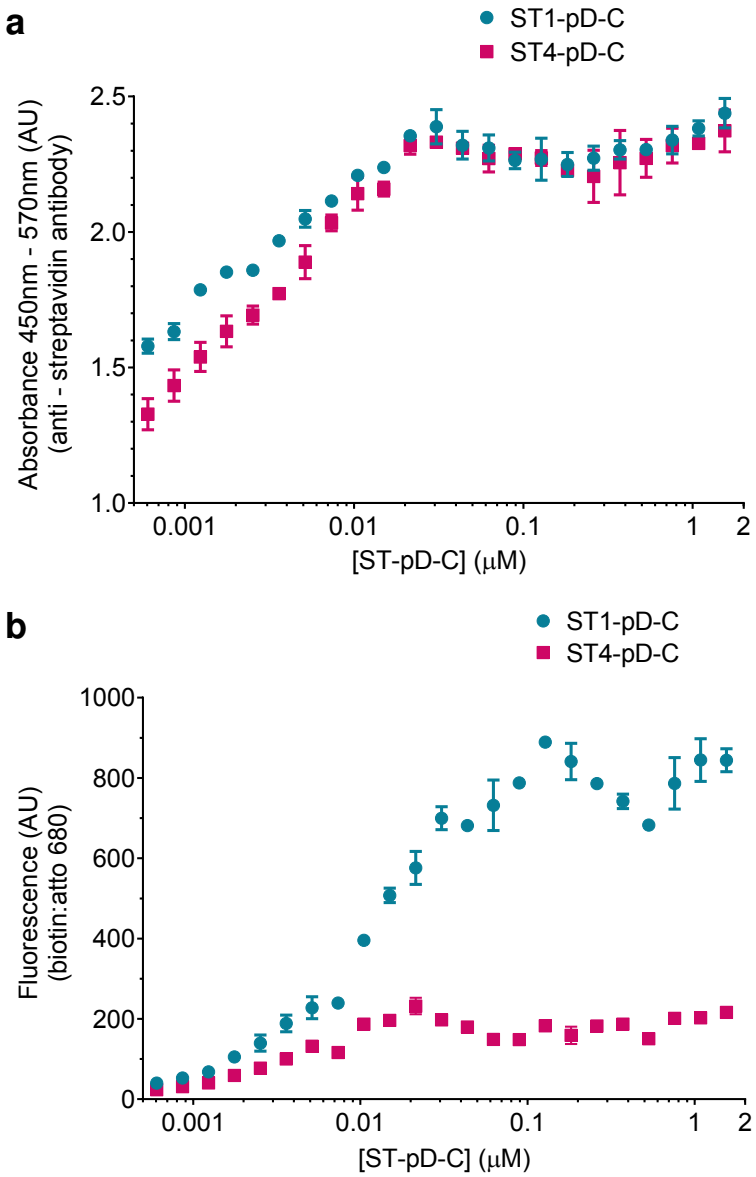


Fig. 5.3: **Comparable amounts of ST1-pD-C and ST4-pD-C are immobilised onto 96 well flat bottom plates.** Varying concentrations of either ST1-pD-C or ST4-pD-C were immobilised on to 96 well flat bottom plates. Anti-streptavidin antibody, followed by anti-mouse HRP and then HRP substrate were incubated in the wells to analyse ST-pD-C immobilisation (**a**). Biotin:atto 680 was incubated with a duplicate set of wells to measure the number of accessible biotin-binding sites (**b**). Fluorescence and absorbance values measured in wells not incubated with ST-pD-C were first subtracted from all corresponding values shown. Data are from 1 experiment (n=2) with values shown as mean±range of duplicate wells.

To counter this auto-quenching of atto 680 fluorescence, after incubation of biotin:atto 680 in StrepTactin-SpyCatcher-coated wells and subsequent washes, the denaturing agent guanidinium hydrochloride was added. We predicted that this would denature the interaction between StrepTactin-SpyCatcher and biotin:atto 680. Immobilised biotin:atto 680 would then be released into solution such that the fluorophores are no longer held in close proximity to each other. A cartoon illustrating this is shown in figure **5.4**.

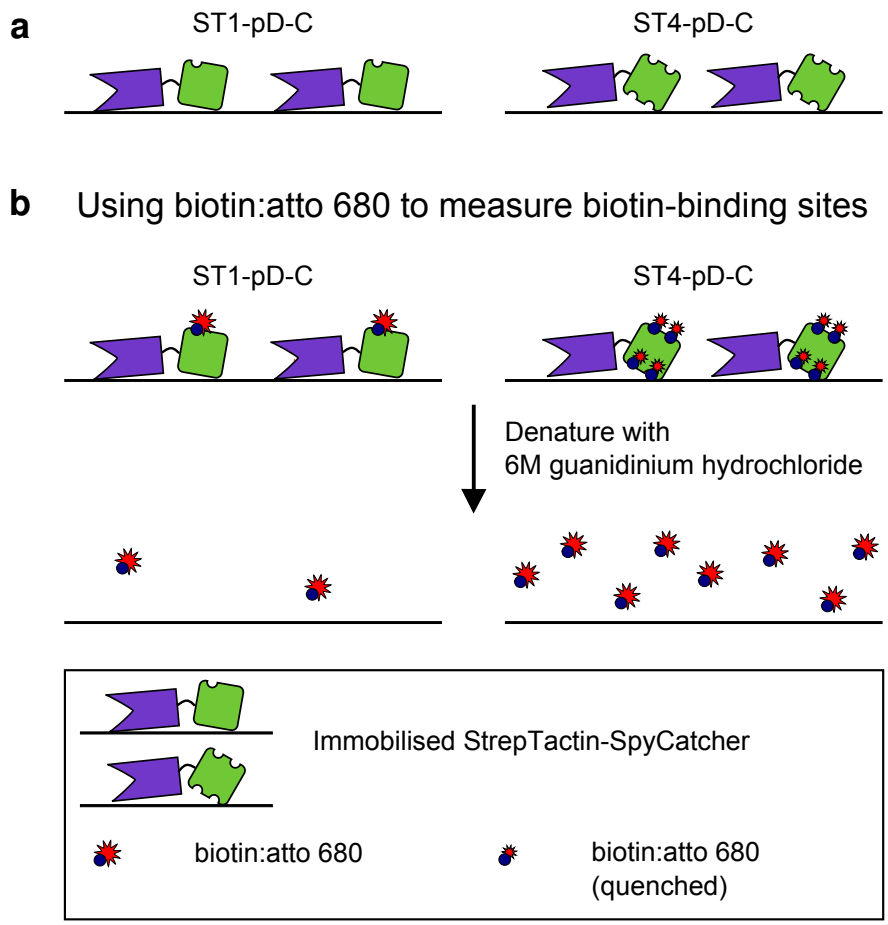


Fig. 5.4: **Cartoon illustrating the method used to indicate number of biotin-binding sites in StrepTactin-SpyCatcher coated wells.** A set of wells are coated in either ST1-pD-C or ST4-pD-C (**a**). Biotin:atto 680 is added to the wells to measure the number of accessible biotin-binding sites (**b**). The fluorophores of multiple biotin:atto 680 complexes are held in close proximity to each other when bound to a single immobilised ST4-pD-C. This leads to auto-quenching of the fluorescence. Upon addition of 6M guanidinium hydrochloride pH 1.5, we predicted that biotin:atto 680 would be released from the interaction with StrepTactin-SpyCatcher into solution. Atto 680 dyes would no longer be held in close proximity to each other and so the fluorescence would no longer be quenched.

It is possible that adding guanidine to biotin:atto 680 will affect the dye fluorescence, independent of denaturing the StrepTactin-SpyCatcher : biotin:atto 680 interaction. To test this, varying concentrations of biotin:atto 680 were diluted in either water or guani-

dinium hydrochloride and added to wells of a 96 well flat bottom plate. The wells were then scanned and fluorescence measured. The fluorescence of biotin:atto 680 diluted in guanidinium hydrochloride was comparable to the fluorescence of the reagent dissolved in water at all concentrations (figure **5.5**). Therefore guanidinium hydrochloride does not affect the fluorescence of biotin:atto 680.

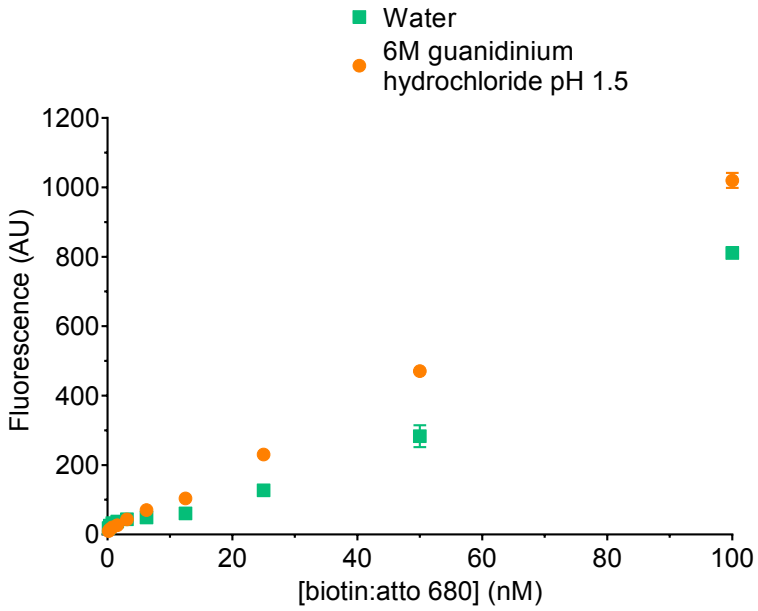


Fig. 5.5: **Guanidinium hydrochloride does not affect the fluorescence of biotin:atto 680.** Varying concentrations of biotin:atto 680 were diluted in either water or 6M guanidinium hydrochloride pH 1.5 and added to wells of a 96 well flat bottom plate. The fluorescence of biotin:atto 680 in these wells was then measured. Fluorescence values of wells containing 6M guanidinium hydrochloride pH 1.5 or H_2O alone have been subtracted from the corresponding values shown. Data are from 1 experiment (n=2) with values shown as mean±range of duplicate wells.

We then sought to confirm that guanidinium hydrochloride denatures the ST-pD-C : biotin:atto 680 interaction. Biotin:atto 680 was incubated in wells coated with either ST1-pD-C or ST4-pD-C as before. The wells were then washed and guanidinium hydrochloride was added before the wells were scanned for atto 680 fluorescence. As shown previously in figure **5.3b**, biotin:atto 680 fluorescence increased with increasing concentration of ST1-pD-C used to coat the wells (figure **5.6**). In addition, biotin:atto 680 fluorescence increased with increasing concentration of ST4-pD-C. The fluorescence levels of ST4-pD-C - coated wells were significantly higher than seen previously and also higher than corresponding ST1-pD-C - coated wells. This suggests that addition of guanidinium hydrochloride does denature the StrepTactin-SpyCatcher - biotin:atto 680

interaction and so removes the atto 680 dye auto-quenching. To determine whether guanidinium hydrochloride had denatured all of the interactions, the wells were washed repeatedly to remove biotin:atto 680 in solution and then re-scanned for atto 680 fluorescence using the same laser intensity. The biotin:atto 680 signal decreased to minimal levels following washing of the plate indicating that all of the immobilised biotin:atto 680 had been released into solution following the addition of guanidinium hydrochloride (figure **5.6**). These results indicate that biotin:atto 680 and guanidinium hydrochloride can be used to qualitatively measure the number of biotin-binding sites on plate-immobilised StrepTactin-SpyCatcher.

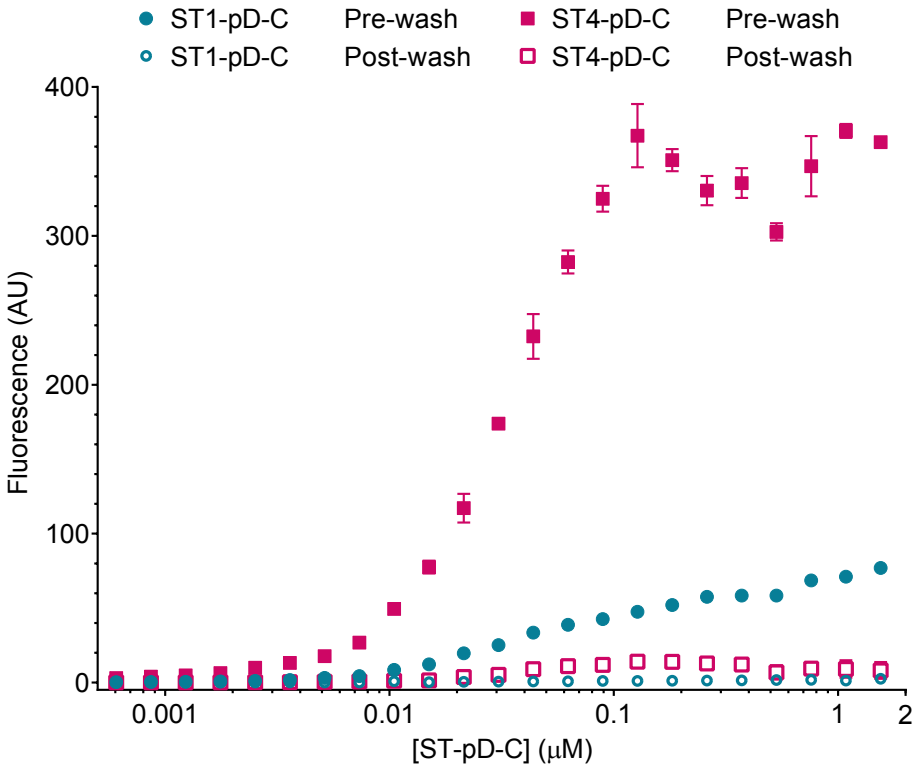


Fig. 5.6: **Guanidinium hydrochloride denatures the ST-pD-C - biotin:atto 680 interaction.** Varying concentrations of ST1-pD-C or ST4-pD-C were immobilised onto wells of a 96 well flat bottom plate. The wells were then incubated with biotin:atto 680 to measure the number of accessible biotin-binding sites. To disrupt the StrepTactin-SpyCatcher - biotin:atto 680 interaction, the wells were incubated with 6M guanidinium hydrochloride pH1.5 and scanned to measure atto 680 fluorescence (pre-wash - solid shapes). The wells were then washed repeatedly and re-scanned for atto 680 fluorescence at the same laser intensity (post wash - empty shapes). Fluorescence values of blank wells have been subtracted from all data shown. Data are from 1 experiment (n=2) with values shown as mean±range of duplicate wells.

To investigate NTR activation in response to plate-immobilised ST1-pD-C or ST4-pD-C, THP-1 cells expressing Strep-Tag II-tagged SIRPβ1 as a respresentative NTR were

used. Varying concentrations of either ST1-pD-C or ST4-pD-C were immobilised onto wells of a 96 well flat bottom plate in duplicate. THP-1 SIRPβ1 cells were incubated in one set of these wells for 20 hours and then analysed for IL-8 secretion. The cells were added in DMEM media supplemented with foetal calf serum and avidin. Avidin was added to block any free biotin present in the serum which would otherwise bind to the StrepTactin-SpyCatcher. As a negative control, untransduced THP-1 cells were incubated in wells pre-coated with the highest concentration of ST1-pD-C or ST4-pD-C and analysed for IL-8 secretion. The second set of the protein-coated wells were used to measure the number of accessible biotin-binding sites using biotin:atto 680 and guanidinium hydrochloride as in figure **5.6**.

The IL-8 secretion measurements taken from one representative experiment are shown in figure **5.7**. Untransduced THP-1 cells incubated with the highest concentrations of either plate-immobilised ST1-pD-C or ST4-pD-C were not stimulated to secrete IL-8 (figure **5.7a**). In contrast, THP-1 SIRPβ1 cells were stimulated to secrete IL-8 in response to both plate-immobilised ST1-pD-C and ST4-pD-C. ST4-pD-C stimulated the cells at lower concentrations than ST1-pD-C (figure **5.7a**). This was expected because ST4-pD-C presents more potential binding sites per protein than ST1-pD-C and so we would also expect more receptor-ligand interactions between SIRPβ1 and ST4-pD-C. To determine if the difference in stimulation seen is a result of the varying numbers of engaged receptors or the distribution of the engaged receptors, the IL-8 secretion data was plotted against the number of potential receptor-binding sites on immobilised ST1-pD-C or ST4-pD-C. As shown in figure **5.7b**, at the same number of potential receptor-binding sites, as indicated by biotin:atto 680 fluorescence, immobilised ST4-pD-C triggers a more potent response from THP-1 SIRPβ1 cells than ST1-pD-C. The maximal response to ST4-pD-C is much higher than the maximal response to ST1-pD-C (figure **5.7b**).

Using a biotin:atto 680 standard curve we were able to convert the biotin:atto 680 fluorescence data from this and subsequent experiments into the number of accessible biotin-binding sites in each well and also the density of binding sites. Levels of IL-8 secretion by THP-1 SIRPβ1 cells from three independent experiments, plotted against either the number of biotin-binding sites (figure **5.8a**) or the density of binding sites (figure **5.8b**) are presented. The absolute levels of IL-8 released by THP-1 SIRPβ1 cells

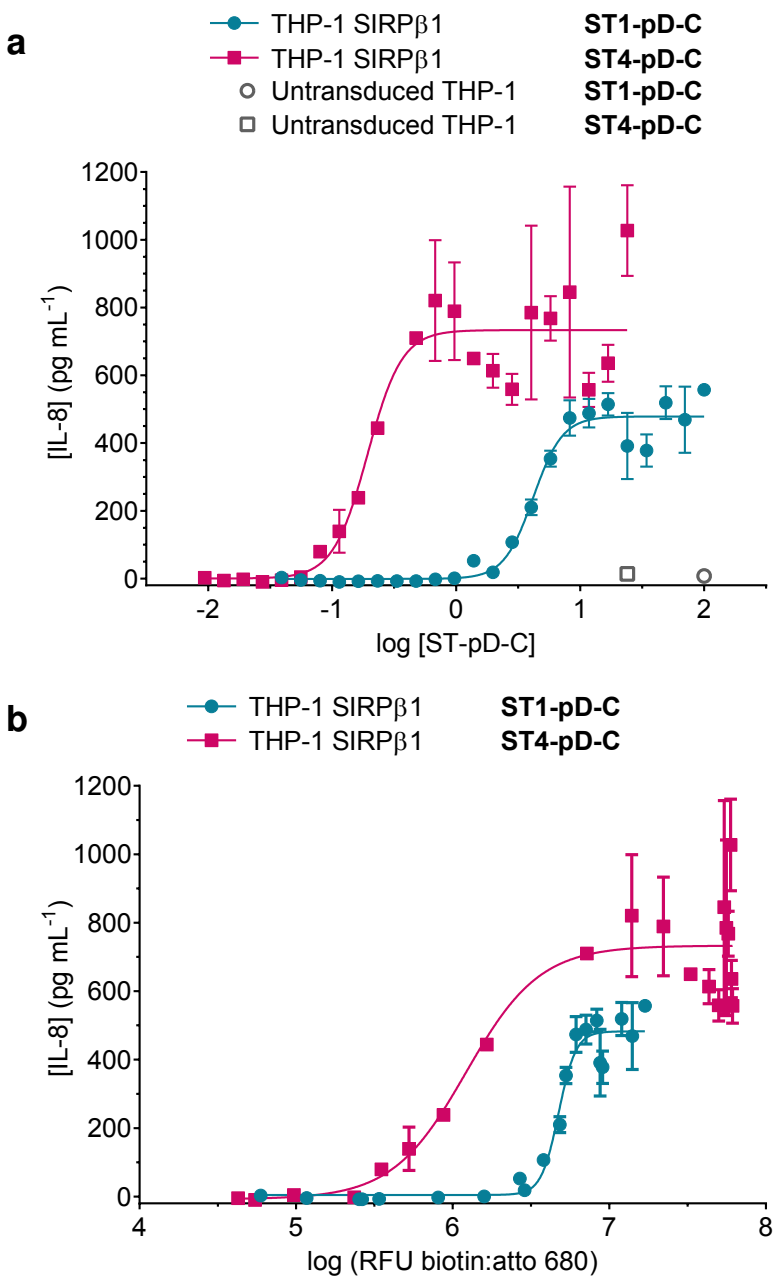


Fig. 5.7: **Immobilised ST4-pD-C activates THP-1 SIRPβ1 cells to secrete more IL-8 than immobilised ST1-pD-C.** Wells of a 96 well flat bottom plate were coated with varying concentrations of either ST1-pD-C or ST4-pD-C. THP-1 SIRPβ1 cells were incubated in the protein-coated wells for 20 hours before the cell supernatants were analysed for IL-8 by ELISA. Untransduced THP-1 cells were incubated in wells coated with the highest concentration of either ST1-pD-C or ST4-pD-C (shown in grey). Duplicate ST1-pD-C - or ST4-pD-C - coated wells were used to measure the number of accessible biotin-binding sites using biotin:atto 680 and guanidinium hydrochloride. IL-8 secretion data was plotted against concentration of ST-pD-C used to coat the wells (**a**) or the biotin:atto 680 fluorescence (**b**). IL-8 concentrations measured in the supernatants of cells incubated in blank wells have been subtracted from all values shown. Data are from one experiment (n=2) with data shown as mean±range of duplicate wells. Biotin:atto 680 fluorescence values in b (x-axis) are the mean values calculated from duplicate wells (n=2). RFU - relative fluorescence units. Both data sets in (a) and (b) are fit using a four parameter stimulation dose-response curve using GraphPad prism software.

varied between each experiment, and so the IL-8 concentrations were normalised to the maximum of the immobilised ST1-pD-C dose response curve within each experiment. This allows analysis of the collated data.

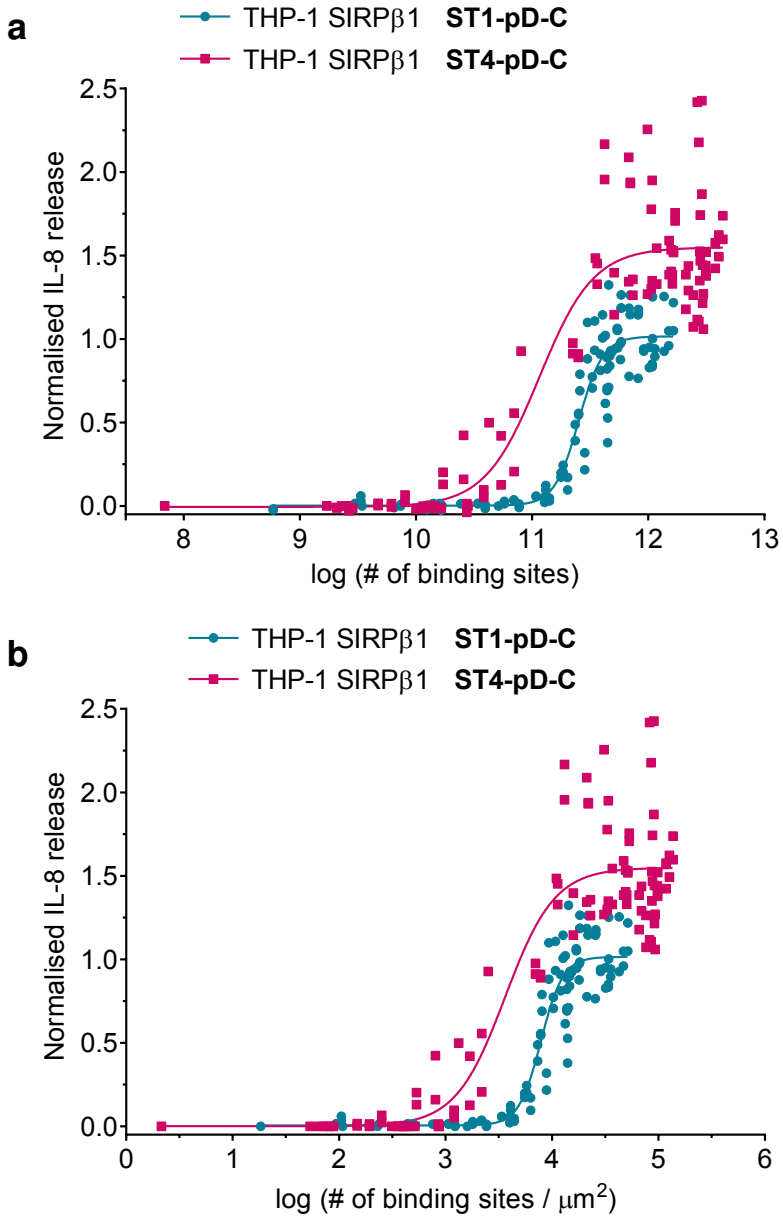


Fig. 5.8: **Immobilised ST4-pD-C activates THP-1 SIRPβ1 cells to secrete more IL-8 than immobilised ST1-pD-C when plotted against number of biotin-binding sites and site density.** IL-8 secretion data from figure **5.7** and 2 other independent experiments were plotted against the total number of biotin-binding sites per well (**a**) or density of biotin-binding sites (**b**). The number and density of binding sites were calculated using biotin:atto 680 fluorescence measurements. Binding site number and density values shown are mean values calculated from duplicate wells. IL-8 concentrations from individual experiments have been normalised to the maximum of the ST1-pD-C dose response curve within that experiment which was allocated a value of 1. Individual IL-8 secretion data points from 3 independent experiments are plotted. Both data sets are fit using a four parameter stimulation dose-response curve using GraphPad prism software.

	ST1-pD-C	ST4-pD-C	p value
Log(EC_{50})	11.4 (11.37-11.43)	11.1 (10.92-11.20)	0.0001
Maximum	1.0 (0.96-1.07)	1.5 (1.47-1.63)	<0.0001

Tab. 5.1: **THP-1 SIRPβ1 cells presented to plate-immobilised ST1-pD-C or immobilised ST4-pD-C have significantly different activation responses.** Log(EC_{50}) values of the number of binding sites and the maximum response best fit values were extracted from the collated data in figure **5.8a**. These values are presented with the 95$\%$ confidence interval range for each value shown in brackets. An F test analysis shows that both Log(EC_{50}) and maximum response values are significantly different between cells presented to immobilised ST1-pD-C and cells presented to ST4-pD-C (p values for these tests are shown). The best fit values are given to 1 decimal place, and confidence intervals to 2dp. Values were calculated and the F test conducted using GraphPad prism software.

It is clear from figure **5.8a** that THP-1 SIRPβ1 cells consistently secrete more IL-8 per binding site in response to plate-immobilised ST4-pD-C than in response to plate- immobilised ST1-pD-C. Stimulation dose-response curves were fit to the ST1-pD-C and ST4-pD-C data. A four parameter curve (used in figure **5.8**) fits both datasets better than a three parameter stimulation dose-response curve. The log(EC_{50}) values of THP-1 SIRPβ1 cells incubated with plate-immobilised ST1-pD-C or immobilised ST4-pD-C were calculated using the dose-response fits (shown in table 5.1). These values were calculated to be significantly different using an F test and GraphPad prism software. The maximum IL-8 secretion response of receptor-expressing cells incubated with plate-immobilised ST1-pD-C or ST4-pD-C were also calculated and found to be significantly different (table 5.1). The difference in log(EC_{50}) between THP-1 SIRPβ1 cells activated with plate-immobilised ST1-pD-C and cells activated with immobilised ST4-pD-C suggests that ligand valency does affect receptor activation. More specifically, the higher potency of ST4-pD-C is consistent with the hypothesis that receptor clustering induced by tetravalent ligand binding enhances receptor activation.

5.2.3 Investigating the effect of increasing valency of ligands presented on cells on representative NTR activation

To further investigate the effect of increasing ligand valency on receptor activation either ST1-pD-C or ST4-pD-C were presented on a cell surface. Receptors engaged by artificial ligand presented on a cell surface will be able to diffuse within the cell membrane as

opposed to when they bind to immobilised protein. This lateral diffusion combined with size-dependent segregation of large surface molecules upon small receptor-monovalent ligand binding would be expected to lead to receptor clustering as discussed in section 1.10.6. If engaged receptors do cluster at the cell-cell interface and clustering does enhance receptor signalling we would expect to see the difference in potency of plate-immobilised ST1-pD-C and ST4-pD-C to be either reduced and abolished. Upon clustering, ST1-pD-C - bound receptors will be held in close proximity to each other in the same way multiple receptors bound to the same ST4-pD-C protein are, and so activation will be enhanced.

Varying concentrations of ST1-pD-C or ST4-pD-C were incubated with CHO CD80-Spy ligand cells allowing the StrepTactin-SpyCatcher to form a covalent bond with the Spy-tagged ligand protein. Duplicate sets of CHO CD80-Spy ST-pD-C ligand cells were used. One set was incubated with THP-1 SIRPβ1 cells for 20 hours. IL-8 release by the THP-1 SIRPβ1 cells was then measured. The second set of ligand cells were incubated with biotin:atto 680 and then guanidinium hydrochloride to measure the number of accessible biotin-binding sites on the ligand cells. This is shown in cartoon form in figure **5.9**.

THP-1 SIRPβ1 cells incubated with CHO CD80-Spy cells presenting ST1-pD-C or ST4-pD-C were stimulated to secrete IL-8 (figure **5.10**). As a negative control, untransfected CHO cells were incubated with ST1-pD-C or ST4-pD-C, washed, and then presented to THP-1 SIRPβ1 cells. The IL-8 levels released by THP-1 SIRPβ1 cells in response to these untransfected CHO cells were below detectable levels for most of the data points (figure **5.10**). This is representative of 2 independent experiments. IL-8 levels below the detection limit of the ELISA were allocated a value of 0.

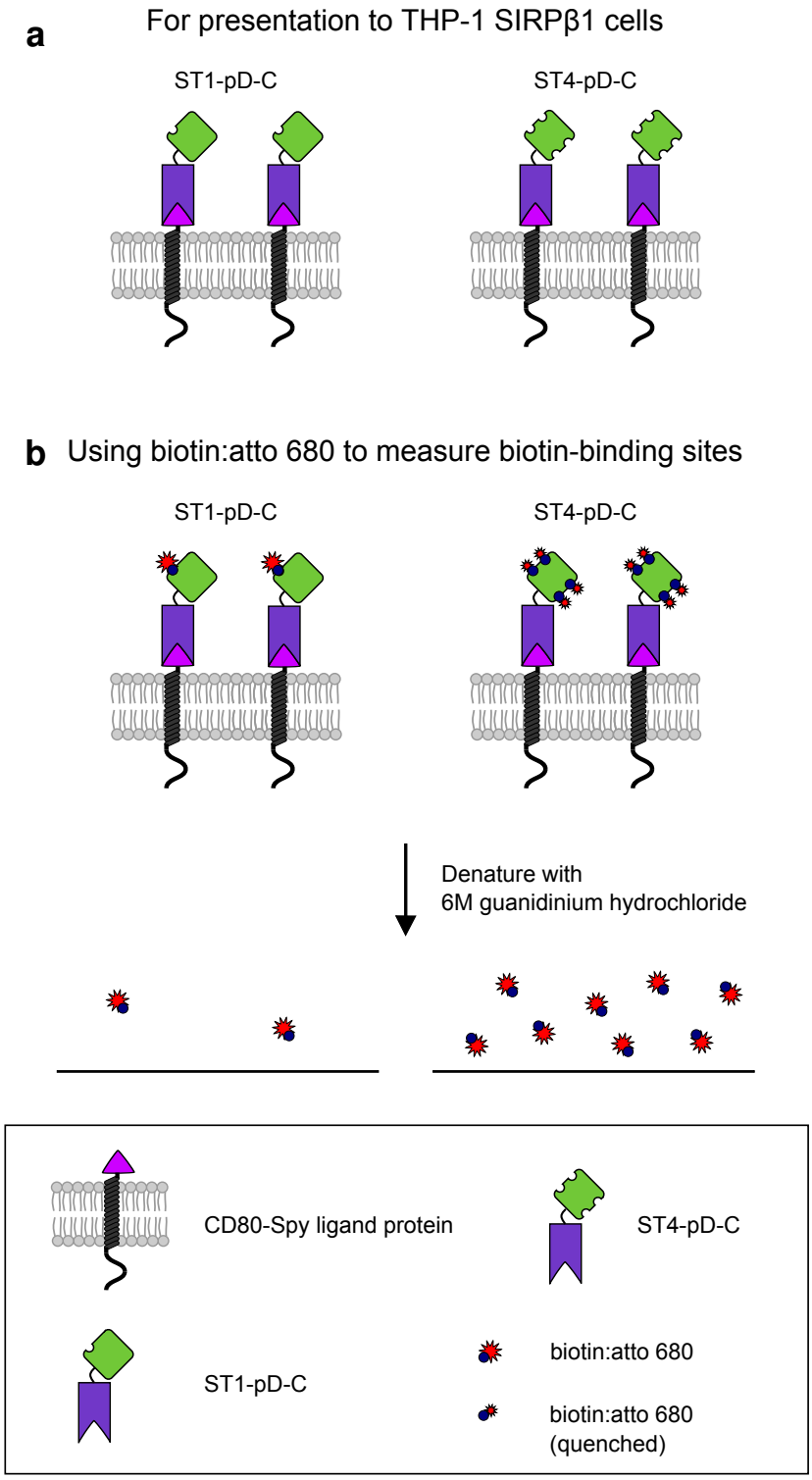


Fig. 5.9: **Cartoon illustrating the method used to indicate the number of biotin-binding sites on StrepTactin-SpyCatcher coupled ligand cells.** CHO CD80-Spy cells presenting either ST1-pD-C or ST4-pD-C are presented to THP-1 SIRPβ1 cells to measure cell activation (**a**). Biotin:atto 680 is added to a duplicate set of ligand-expressing cells to measure the number of accessible biotin-binding sites (**b**). Upon addition of 6M guanidinium hydrochloride pH 1.5, the biotin:atto 680 is released from the interaction with StrepTactin-SpyCatcher into solution. Atto 680 fluorescence is then measured.

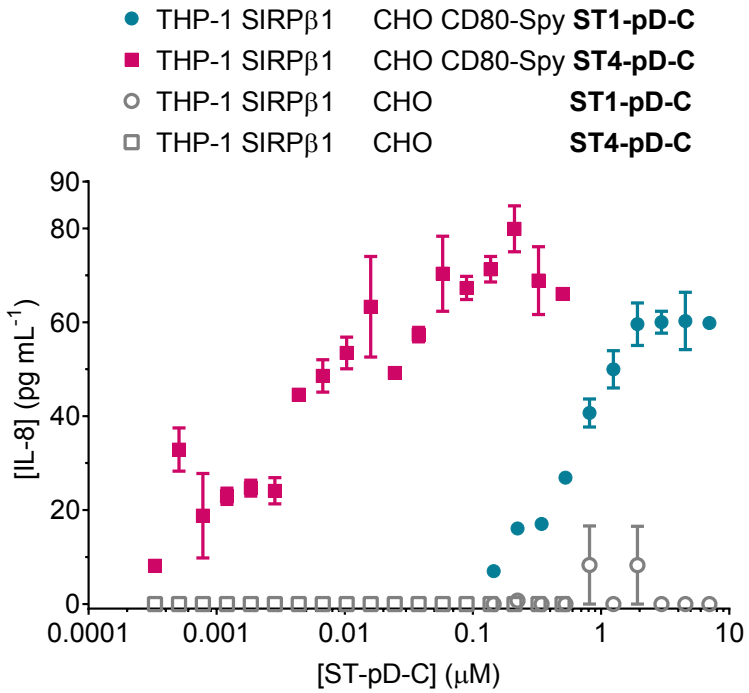


Fig. 5.10: **THP-1 SIRPβ1 cells are stimulated by ST1-pD-C and ST4-pD-C presented on ligand cells but not untransfected CHO cells alone.** CHO CD80-Spy cells were incubated with varying concentrations of ST1-pD-C or ST4-pD-C, to allow covalent binding between CD80-Spy ligand and StrepTactin-SpyCatcher. This concentration is plotted on the x-axis. As negative controls, untransfected CHO cells (CHO) were incubated with the identical range of ST1-pD-C or ST4-pD-C concentrations (shown in grey). These ligand-expressing cells or mock ligand cells were then incubated with THP-1 SIRPβ1 cells. After 20 hours, the cell supernatants were analysed for IL-8 secretion by ELISA. IL-8 concentrations that were below the detectable range of the ELISA were given a value of 0. IL-8 concentrations measured in the supernatants of cells incubated with mock conjugated cells have been subtracted from all values shown. Data shown are representative of 2 independent experiments with values for CHO CD80-Spy cells given as the mean±range (n=2) and values for untransfected CHO cells given as individual values (n=1).

The data from figure **5.10** and a second independent experiment are plotted in figures **5.11a** and **b** respectively against the number of biotin-binding sites measured using biotin:atto 680. This is the total number of biotin-binding sites present over all of the ligand-expressing cells presented to THP-1 SIRPβ1 cells per well. The exact protocol for measuring biotin-binding sites using biotin:atto 680 was found to be less straightforward than that used for plate-immobilised StrepTactin-SpyCatcher. The background levels of biotin:atto 680 measured in the experiment shown in figure **5.11a** were very high leading to a small specific signal. Between the experiments shown in figures **5.11a** and **b**, the protocol was optimised and so the number of binding sites has only been calculated for the ligand cells shown in **5.11b**. The number of binding sites calculated in the second repeat were assigned to the corresponding ligand cells used in 5.11a. This allowed us to visualise IL-8 secretion per biotin-binding site for both repeats. A biotin:atto 680 standard curve was again used to convert fluorescence into the number of biotin-binding sites.

The data does not form a clear dose-response profile as seen with the plate-immobilised data and therefore we were unable to fit a stimulation dose-response curve. For this reason, the IL-8 levels secreted by THP-1 SIRPβ1 cells in each experiment could not be normalised to allow visualisation of the data from both experiments on the same axes. However, in each repeat, there is a clear trend of increasing IL-8 secretion with biotin-binding sites present on both ST1-pD-C - and ST4-pD-C - presenting CHO CD80-Spy cells. As for the plate-immobilised ligand data, the potency of the response to ST1-pD-C - or ST4-pD-C - presenting ligand cells is different although the apparent magnitude of this difference varies between the experiments shown in figures **5.11a** and **b**. This may be because the number of biotin-binding sites in the first repeat were assigned rather than measured. In figure **5.11b**, where the binding sites have been measured, the difference in ST1-pD-C and ST4-pD-C potency is visually much smaller than that seen for the plate-immobilised data.

In order to confirm that the profiles seen in figure **5.11** are reproducible this experiment needs to be repeated with measurement of the biotin-binding sites present on ligand-expressing cells. In addition to this, we would aim to achieve a larger range of binding site numbers on the ligand cells to allow us to visualise the full THP-1 SIRPβ1 cell re-

sponse.

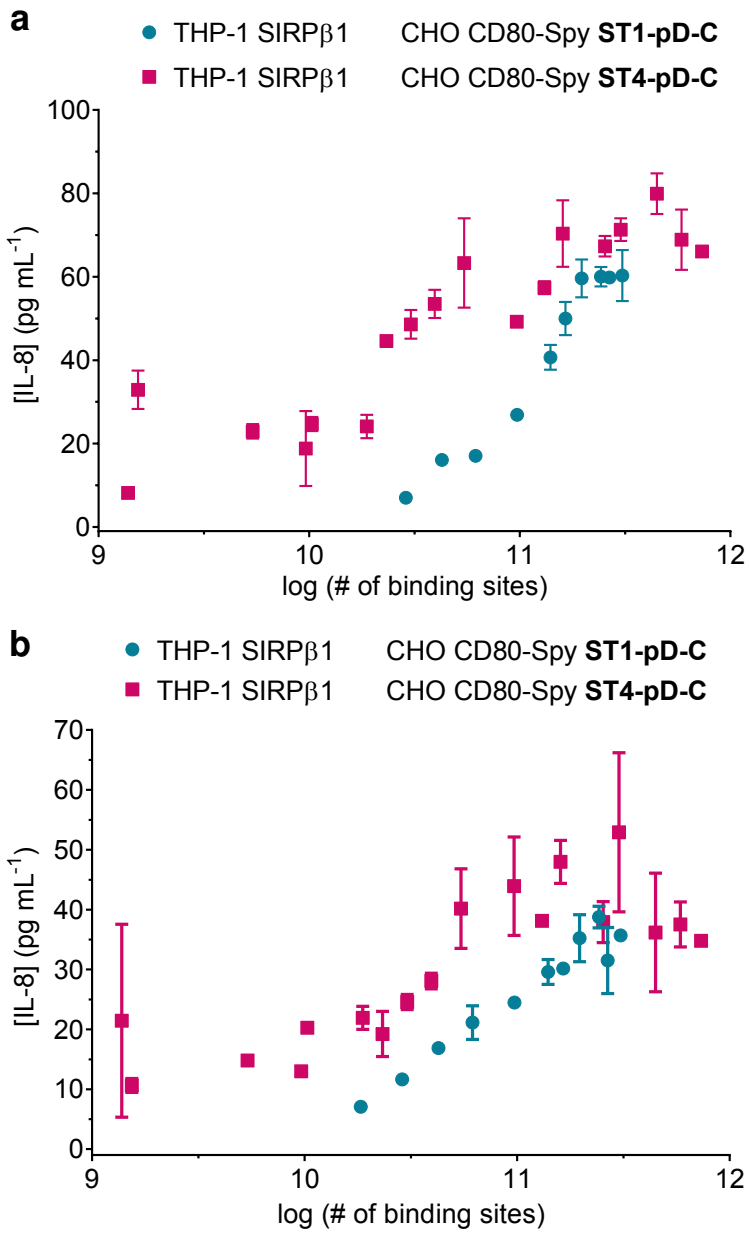


Fig. 5.11: **THP-1 SIRPβ1 cells incubated with ST4-pD-C presented on CHO CD80-Spy cells release more IL-8 per biotin-binding site than THP-1 SIRPβ1 cells incubated with CHO CD80-Spy ST1-pD-C cells.** CHO CD80-Spy cells were incubated with varying concentrations of either ST1-pD-C ▬ or ST4-pD-C ▬ to allow covalent binding of the ST-pD-C to the CD80-Spy protein. One set of these ligand-expressing cells were incubated with THP-1 SIRPβ1 cells for 20 hours before the cell supernatants were analysed for IL-8 secretion by ELISA. A duplicate set of ligand cells were used to measure the number of biotin-binding sites with biotin:atto 680 and guanidinium hydrochloride. IL-8 secretion data (with negative control values subtracted) are plotted against the total number of biotin-binding sites over all the ligand-expressing cells ($\sim$ 2 x 10^5 cells) incubated with THP-1 SIRPβ1 cells per well. Two independent experiments are shown in (**a**) and (**b**). The numbers of biotin-binding sites calculated in b were assigned to the corresponding data points in a. The number of binding sites are the mean value of duplicate wells. IL-8 secretion values (n=2) are shown as mean$\pm$range of duplicate wells.

5.2.4 Elongating monovalent artificial ligand but not tetravalent artificial ligand abolishes representative NTR activation

As discussed previously, one of the key predictions the kinetic-segregation model makes about NTR activation is that elongation of the extracellular dimensions of the receptor-ligand complex will decrease or abolish receptor signalling. By lengthening the receptor-ligand complex, the distance between the receptor cell and ligand cell at sites of NTR engagement increases. Depending on the magnitude of the increase in intermembrane distance, this will potentially decrease exclusion of large surface proteins like inhibitory phosphatases from an engaged receptor. In turn, this will alter the kinase:phosphatase activity balance in favour of phosphatase activity and so lead to reduced or abolished receptor signalling.

As shown in chapter 3, a stable CHO cell line expressing an elongated version of the CD80-Spy ligand used above has been created by Dr Jesse Goyette. This elongated ligand is termed CD80-CD4-Spy due to the insertion of the 4 immunoglobulin-like domains of human CD4 into the extracellular region. CHO CD80-Spy and CHO CD80-CD4-Spy cells were used to investigate the effect of elongating the NTR-artificial ligand complex on receptor signalling. Again, SIRPβ1 was used as a representative NTR.

In the same experiments shown in figure **5.11**, in addition to CHO CD80-Spy cells, CHO CD80-CD4-Spy cells were incubated with varying concentrations of ST1-pD-C. Thus creating a set of cells expressing different numbers of monovalent artificial ligand with a relatively short extracellular length (CHO CD80-Spy : ST1-pD-C), and a set of cells expressing different numbers of a monovalent artificial ligand with a longer extracellular length (CHO CD80-CD4-Spy : ST1-pD-C cells). A cartoon of these cell lines is shown in figure **5.12a**. A sample of these ligand-expressing cells were presented to THP-1 SIRPβ1 cells to measure the receptor activation. The remaining ligand-expressing cells were used to measure the number of accessible biotin-binding sites using biotin:atto 680 and guanindinium hydrochloride.

In addition to investigating the effect of elongating monovalent ligand on receptor activation we also investigated the effect of elongating tetravalent ligand to see if the changes in

dimension affect both receptor-ligand complexes in the same way. For this, CHO CD80-Spy cells or CHO CD80-CD4-Spy cells were incubated with varying concentrations of ST4-pD-C and then treated the same as monovalent ligand-expressing cells. Cartoons of the CHO cells lines bound by ST4-pD-C are shown in figure **5.12b**.

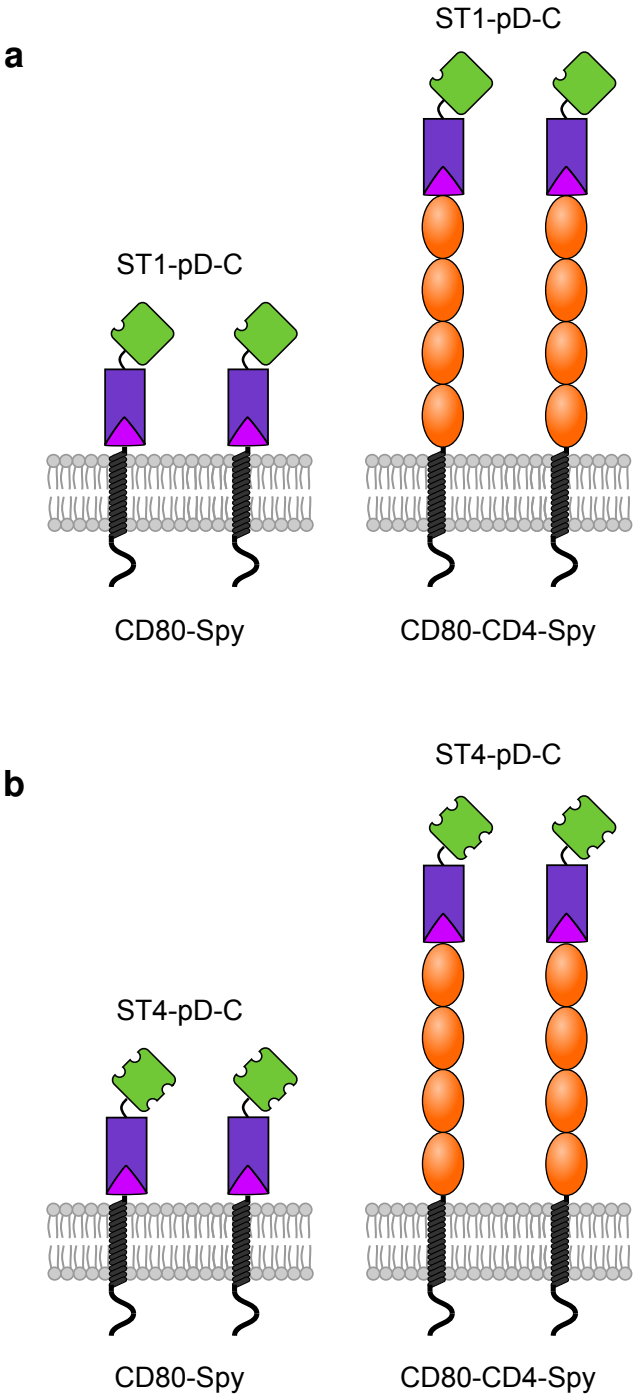


Fig. 5.12: **Cartoon illustrating the artificial ligand complexes of CD80-Spy or CD80-CD4-Spy and either ST1-pD-C or ST4-pD-C.** CHO CD80-Spy cells or CHO CD80-CD4-Spy cells are incubated with ST1-pD-C to give two cell lines expressing either monovalent artificial ligand with a relatively short extracellar length or monovalent artificial ligand with a longer extracellular length respectively (**a**). CHO CD80-Spy cells or CHO CD80-CD4-Spy cells are incubated with ST4-pD-C. This yields two further cell lines presenting tetravalent artificial ligand with either a relatively short or long extracellular length (**b**).

Data from 2 independent experiments are shown in figure **5.13** (ai and bi, aii and bii). The experiment in figures **5.13ai** and **bi** is the same experiment shown in figure **5.11a** and the experiment in figures **5.13aii** and **bii** is the same as the experiment in figure **5.11b** but with the added data. The levels of IL-8 secretion are plotted against the total number of biotin-binding sites present over all ligand-expressing cells per well. As described previously, the number of biotin-binding sites in the first experiment (figure **5.13ai** and **bi**) were not measured so instead were assigned the corresponding numbers of biotin-binding sites measured in the repeat experiment (figure **5.13aii** and **bii**).

ST1-pD-C presented by CHO CD80-Spy cells activated THP-1 SIRPβ1 cells to secrete IL-8 significantly above background levels (figure **5.13ai, aii**). We were unable to create CHO CD80-CD4-Spy : ST1-pD-C cells with the full range of binding sites present on CHO CD80-Spy : ST1-pD-C cells. The same concentrations of ST1-pD-C were incubated with both CHO CD80-Spy and CHO CD80-CD4-Spy cell lines and also both cell lines expressed either CD80-Spy or CD80-CD4-Spy ligand with matched expression levels as detected by flow cytometry using antibody to the extracellular HA tag of the ligands (data not shown). This suggests that the process of ST1-pD-C conjugating to CD80-CD4-Spy ligand is less efficient. Over the range of biotin-binding site numbers that were measured however, it is clear that ST1-pD-C presented by CHO CD80-CD4-Spy cells was unable to stimulate THP-1 SIRPβ1 cells to secrete IL-8 (figure **5.13ai, aii**). This includes ligand surface densities at which there was THP-1 SIRPβI stimulation in response to CHO CD80-Spy : ST1-pD-C cells (figure **5.13ai, aii**). These results suggest that elongation of the receptor-monovalent artificial ligand interaction abolishes receptor activation.

Elongation of tetravalent ligand did not have this effect (figure **5.13bi, bii**). THP-1 SIRPβ1 cells were activated by both CHO CD80-Spy : ST4-pD-C cells and CHO CD80-CD4-Spy : ST4-pD-C cells. The data do not form a complete dose-response curve so cannot be quantitatively analysed. Qualitatively however, there is no significant difference in IL-8 secretion by THP-1 SIRPβ1 cells in response to the two tetravalent ligand cell lines. The data in figure **5.13bi** does appear to show that CHO CD80-CD4-Spy : ST4-pD-C cells elicit a slightly less potent activation response but this will need to be reproduced. A repeat of this experiment using ligand cells with a wider range of biotin-binding site numbers, and where the number of binding sites per ligand cell are measured within that

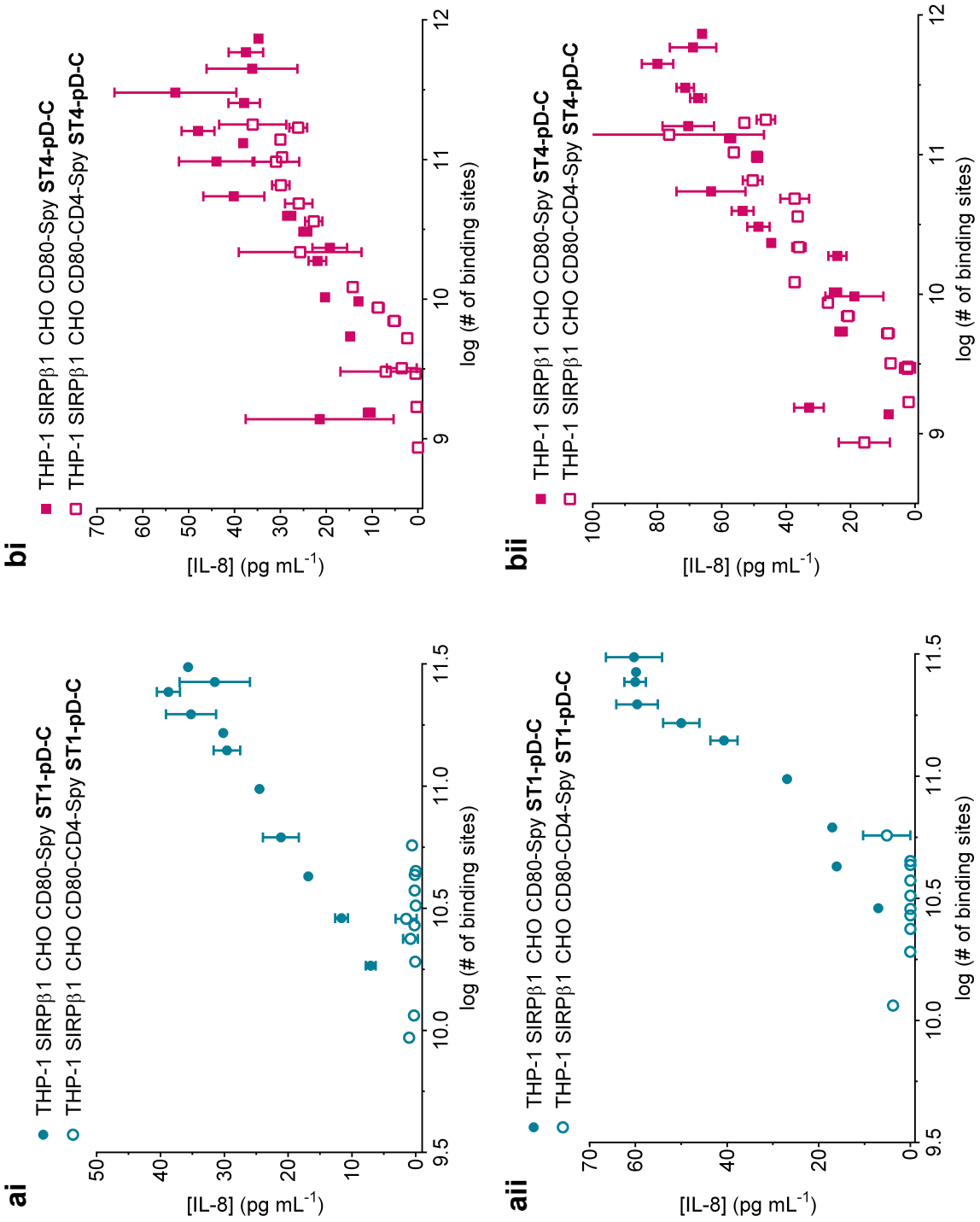


Fig. 5.13: **Elongation of monovalent artificial ligand presented on cells abolishes THP-1 SIRPβ1 cell activation but elongation of tetravalent artificial ligand does not significantly affect receptor activation.** *Continued on the next page.*

Fig. 5.13: **Elongation of monovalent artificial ligand presented on cells abolishes THP-1 SIRPβ1 cell activation but elongation of tetravalent artificial ligand does not significantly affect receptor activation.** *Continued.* (**a**) CHO CD80-Spy cells (filled circle) or CHO CD80-CD4-Spy cells (empty circle) were incubated with varying concentrations of ST1-pD-C ▬. These artificial ligand-presenting cells were incubated with THP-1 SIRPβ1 cells for 20 hours before the cell supernatants were analysed for IL-8 secretion. The IL-8 secretion data (with negative control values subtracted) from 2 independent experiments (**ai** and **aii**) are plotted against the total number of biotin-binding sites present on the ligand-expressing cells per well ($\sim$ 2 x 10^5 cells). The number of binding sites in aii were measured within that experiment and assigned to the corresponding data in ai. (**b**) CHO CD80-Spy cells (filled square) or CHO CD80-CD4-Spy cells (empty square) were incubated with varying concentrations of ST4-pD-C ▬ and then treated as monovalent ligand-presenting cells were. The data from 2 independent experiments are shown in **bi** and **bii** with IL-8 secretion plotted against the number of biotin-binding sites. These numbers were measured for the experiment in bii and assigned to the data in bi. The number of biotin-binding sites are the mean values of duplicate wells. IL-8 secretion values (n=2) are given as the mean$\pm$range of duplicate wells.

experiment, will allow more detailed analysis and show whether the profiles observed here are reproducible.

5.3 Discussion

5.3.1 Immobilisation of StrepTactin or StrepTactin-SpyCatcher onto wells of a 96 well plate

We initially attempted to use StrepTactin protein to investigate the effect of changing ligand valency on NTR activation. Mono-, bi-, tri-, and tetra-valent StrepTactin were immobilised onto wells of a 96 well plate and presented to NTR-expressing cells. Despite using a number of strategies for StrepTactin immobilisation, we were unable to find a method that both allowed immobilisation of ST1dSA3 with accessible biotin-binding sites and also did not interfere with receptor signalling. We believe the poor apparent immobilisation of ST1dSA3, as measured using biotinylated mouse IgG1, is due to the higher number of polyaspartate loops and so more negative charge compared to the other StrepTactin proteins.

Unlike the StrepTactin proteins, ST1-pD-C and ST4-pD-C both have only one polyaspartate loop and are adsorbed onto 96 well plates at comparable levels. We also developed a method to measure the number of accessible biotin-binding sites on immo-

bilised StrepTactin-SpyCatcher using biotin:atto 680 binding. The cytokine release of NTR-expressing cells in response to stimulus can therefore be normalised for the number of possible NTR ligand-binding sites.

5.3.2 Comparing the activation of SIRPβ1 in response to either plate-immobilised ST1-pD-C or plate-immobilised ST4-pD-C

The data from three independent experiments were collated and fit with a stimulation dose-response curve. Two parameters of the immobilised ST1-pD-C and ST4-pD-C dose-response curves differ significantly: the maximum cytokine release and the log(EC_{50}).

5.3.2.1 The maximum cytokine release

The maximal response of THP-1 SIRPβ1 cells incubated with immobilised ST1-pD-C is consistently lower than that of cells incubated with immobilised ST4-pD-C. We believe this is due to a difference in the maximum amount of ST1-pD-C or ST4-pD-C that can be immobilised per well.

The density of ST1-pD-C biotin-binding sites at which the maximal response of THP-1 SIRPβ1 cells is reached is approximately 10^4 binding sites per μm^2 (figure **5.8**). As each ST1-pD-C has one biotin-binding site the density of protein is also $\sim 10^4$ per μm^2. A cartoon illustrating this protein density on the well surface is shown in figure **5.14a**. For simplicity, ST1-pD-C is shown without the SpyCatcher and we approximate the 2D area of the well taken up by a single immobilised monovalent StrepTactin to be a square of 5 nm dimensions. It is possible that each immobilised ST1-pD-C will take up a larger area than the assumed 25 nm^2 because of the SpyCatcher binding to the plate but for ease of presentation we show ST1-pD-C without the SpyCatcher. Figure **5.14a** shows a 1600 nm^2 square section of well with immobilised ST1-pD-C. If individual ST1-pD-C proteins were packed into this area, an absolute maximum of $\sim$64 ST1-pD-C proteins could be immobilised. The maximal response density of 10^4 ST1-pD-C per μm^2 would equate to $\sim$16 ST1-pD-C per 1600 nm^2. Due to this high density, and also because the protein will not bind as closely or in the pattern shown in figure **5.14a**, we predict that in fact the

ST1-pD-C dose-response curve saturates at this density because the well is saturated with protein.

In agreement with this, in figure **5.7** the data points at the highest concentrations of ST1-pD-C added to the well are spread along the x-axis when plotted against ST1-pD-C concentration (figure **5.7a**) but cluster along the x-axis when plotted against biotin:atto 680 fluorescence (figure **5.7b**). This suggests that concentrations of ST1-pD-C higher than the plate saturation concentration are added to some wells which is reflected in the number of biotin-binding sites measured.

To achieve the same density of biotin-binding sites on immobilised ST4-pD-C, approximately a quarter of the number of ST4-pD-C proteins need to be immobilised (figure **5.14b**). If we assume the plate capacity for ST4-pD-C binding is identical to the plate ST1-pD-C capacity, the maximum number of biotin-binding sites on immobilised ST4-pD-C is much higher (figure **5.14c**). This higher capacity for binding sites is consistent with the THP-1 SIRPβ1 cell response to immobilised ST4-pD-C saturating at a higher number of sites. Theoretically, the maximum number of biotin-binding sites on immobilised ST4-pD-C is $\sim$4 x 10^4 binding sites (4x that of the ST1-pD-C maximum). The dose-response curve of THP-1 SIRPβ1 response to plate-immobilised ST4-pD-C indeed saturates around $\sim$4 x 10^4 binding sites. Perhaps therefore, like for ST1-pD-C, the ST4-pD-C dose response curve reaches a maximum due to saturation of the well rather than saturation of the cell response.

To ensure a maximum signalling response is seen for both ST1-pD-C and ST4-pD-C data, THP-1 SIRPβ1 cells with a lower SIRPβ1 expression could be used. Fewer ligands would be required for the maximal response of these receptor-expressing cells. Alternatively, there is evidence with one NTR, the TCR, that increasing the affinity of the receptor-ligand interaction increases the potency of the response (for example [Sykulev et al., 1994,Andersen et al., 2001]). Along the same lines, by immobilising either a monovalent or tetravalent version of a StrepTactin mutant with higher affinity for Strep-Tag II, the THP-1 SIRPβ1 cell response to these stimuli might similarly increase in potency such that the maximal response is reached before the wells are saturated with protein.

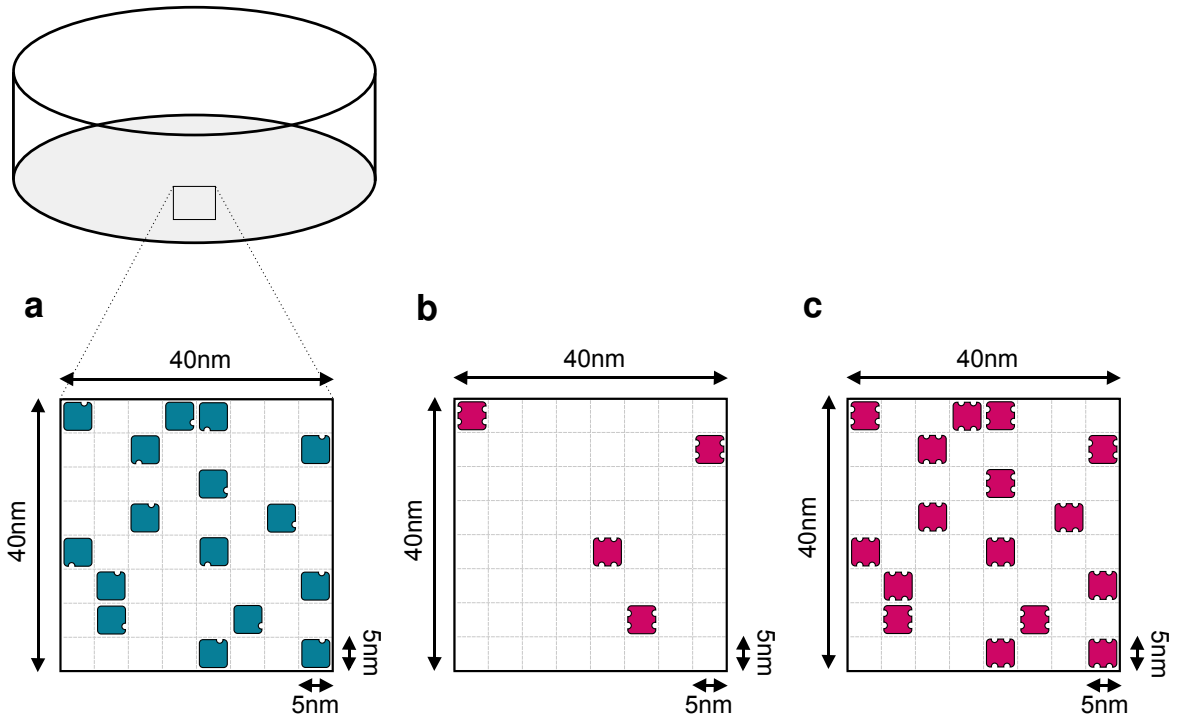


Fig. 5.14: **At the maximum protein capacity of the wells the number of accessible biotin-binding sites is higher for ST4-pD-C than ST1-pD-C.** Three cartoons show a small area (dimensions 40 nm x 40 nm) of a well coated with either ST1-pD-C or ST4-pD-C, each with 2D dimensions given as 5 nm x 5 nm. If ST-pD-C proteins were packed tightly into this selection of a well, the absolute maximum number of immobilised proteins is 64. This distribution is shown by the grids in grey dashed lines, with each square representing one ST-pD-C. The distributions of ST-pD-C are illustrations only to allow visualisation of our hypothesis. (**a**) The number of ST1-pD-C proteins predicted to be bound over this area of a well at the maximum response of THP-1 SIRPβ1 cells incubated with plate-immobilised ST1-pD-C. (**b**) The predicted number of immobilised ST4-pD-C proteins that would give the same number of biotin-binding sites seen in (a). (**c**) The number of ST4-pD-C proteins bound and accessible biotin-binding sites over the selected area of a well at the predicted maximum capacity of the plate.

5.3.2.2 Potency of the response

The log(EC_{50}) values of the THP-1 SIRPβ1 dose-response curves in response to plate-immobilised ST1-pD-C or ST4-pD-C are significantly different. Below we discuss a number of possible reasons for this.

Clustering of the receptors

The difference in log(EC_{50}) may be due to the different distributions of binding sites between immobilised ST1-pD-C and ST4-pD-C. At the same number of binding sites per well, the sites of immobilised ST4-pD-C will be more clustered at a small scale than those of immobilised ST1-pD-C. ST4-pD-C - bound receptors will thus tend to be held in closer proximity to each other than receptors engaged by ST1-pD-C. This higher level of receptor clustering could favour src kinase activity through enhancing trans autophosphorylation and lead to increased ITAM phosphorylation. This mechanism, which is described in more detail in chapter 1 and section 5.1, may give a more potent receptor response to immobilised ST4-pD-C than ST1-pD-C.

The increased small-scale proximity of ST4-pD-C - bound receptors may also give greater adhesion between THP-1 SIRPβ1 cells and the protein-coated wells compared to the adhesion between THP-1 SIRPβ1 cells and ST1-pD-C - coated wells. Binding of THP-1 SIRPβ1 cells to plate-immobilised StrepTactin-SpyCatcher will involve deformation of the cell membrane due to the presence of much larger proteins on the cell surface. A cartoon depicting this is shown in figure **5.15**. This will place tension on the receptor - StrepTactin-SpyCatcher bonds. Per engaged receptor, the THP-1 SIRPβ1 cell membrane will deform over a larger surface area upon interaction with immobilised ST1-pD-C (figure **5.15a**) compared to immobilised ST4-pD-C (figure **5.15b**). This could lead to a larger tension acting on ST1-pD-C - SIRPβ1 bonds. In addition to this, ST4-pD-C has a higher avidity so the tension acting on multiple receptor - one ST4-pD-C interactions will be spread over the potentially four individual bonds whereas the tension acting on ST1-pD-C bound to one receptor will be placed on the single bond. Overall, these factors may lead to a relatively more stable interaction between SIRPβ1 and immobilised ST4-pD-C proteins, and result in increased receptor activation.

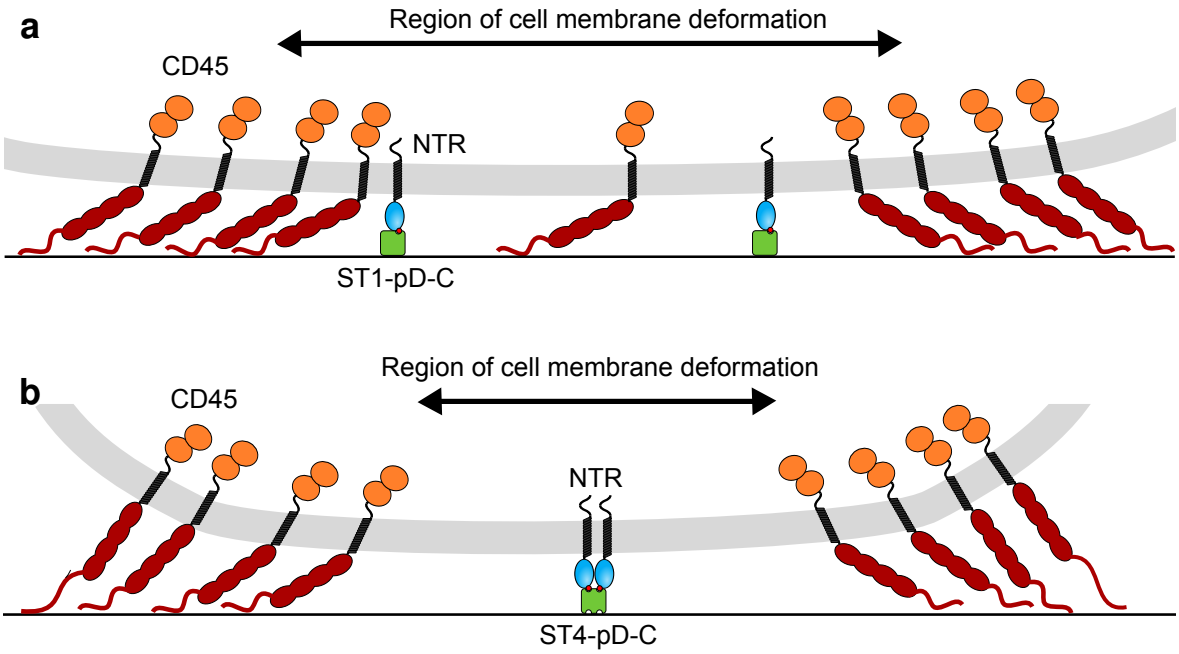


Fig. 5.15: **Increased small-scale proximity of ST4-pD-C - bound receptors compared to ST1-pD-C - bound receptors may affect tension acting on the bonds.** The interaction between an NTR (SIRPβ1 in our experiments) expressed on a cell surface and either plate-immobilised ST1-pD-C (**a**) or ST4-pD-C (**b**) is shown. A cartoon of a generic NTR is shown. The cell surface also expresses large surface molecules like CD45 which is also shown. The receptor-artificial ligand interaction is much smaller than the length of the large surface molecules and therefore to permit receptor-expressing cell - ST-pD-C interaction, the cell membrane must be deformed. For the same number of engaged receptors, the membrane of a cell interacting with immobilised ST1-pD-C (a) will be deformed over a larger surface area than a cell interacting with ST4-pD-C (b). This may lead to a larger tension acting on the ST1-pD-C - receptor interactions.

Likelihood of further receptor-artificial ligand interactions

The close proximity of ST4-pD-C binding sites may increase the likelihood of further receptor-artificial ligand interactions. When an individual receptor unbinds from immobilised ST4-pD-C it will be in closer proximity to additional binding sites (shown in cartoon form in figure **5.16ai**) than a ST1-pD-C - bound receptor will be (figure **5.16aii**). This may increase the probability of a second interaction and increase the potency of immobilised ST4-pD-C relative to immobilised ST1-pD-C.

To test whether there is enhanced rebinding the off-rate of receptors engaged by plate-immobilised ST4-pD-C or ST1-pD-C could be measured. 2D kinetics of the TCR - pMHC interaction have previously been measured using single molecule FRET microscopy and a similar method could be used here [Huppa et al., 2010]. A receptor bound to one ST1-pD-C and a receptor bound to ST4-pD-C that does not rebind to the same ST4-pD-C will have comparable off-rates. On the other hand, a receptor bound to one binding site of immobilised ST4-pD-C that unbinds and then rebinds the same ST4-pD-C via another binding site will have a longer apparent off-rate.

In addition to this, if one receptor is bound to immobilised ST4-pD-C with the other binding sites free, the cell and plate surface are held in close contact at this point. That could increase the likelihood of an available receptor within the cell membrane engaging with one of the free binding sites on the immobilised ST4-pD-C (illustrated in figure **5.16bi**). In comparison, even if a number of receptors are bound to immobilised ST1-pD-C, the cell membrane is less likely to be held in close proximity to a free ST1-pD-C and so it is relatively less likely that a freely diffusing receptor will engage the available ST1-pD-C (figure **5.16bii**). This would result in increased receptor activation in response to immobilised ST4-pD-C than in response to immobilised ST1-pD-C.

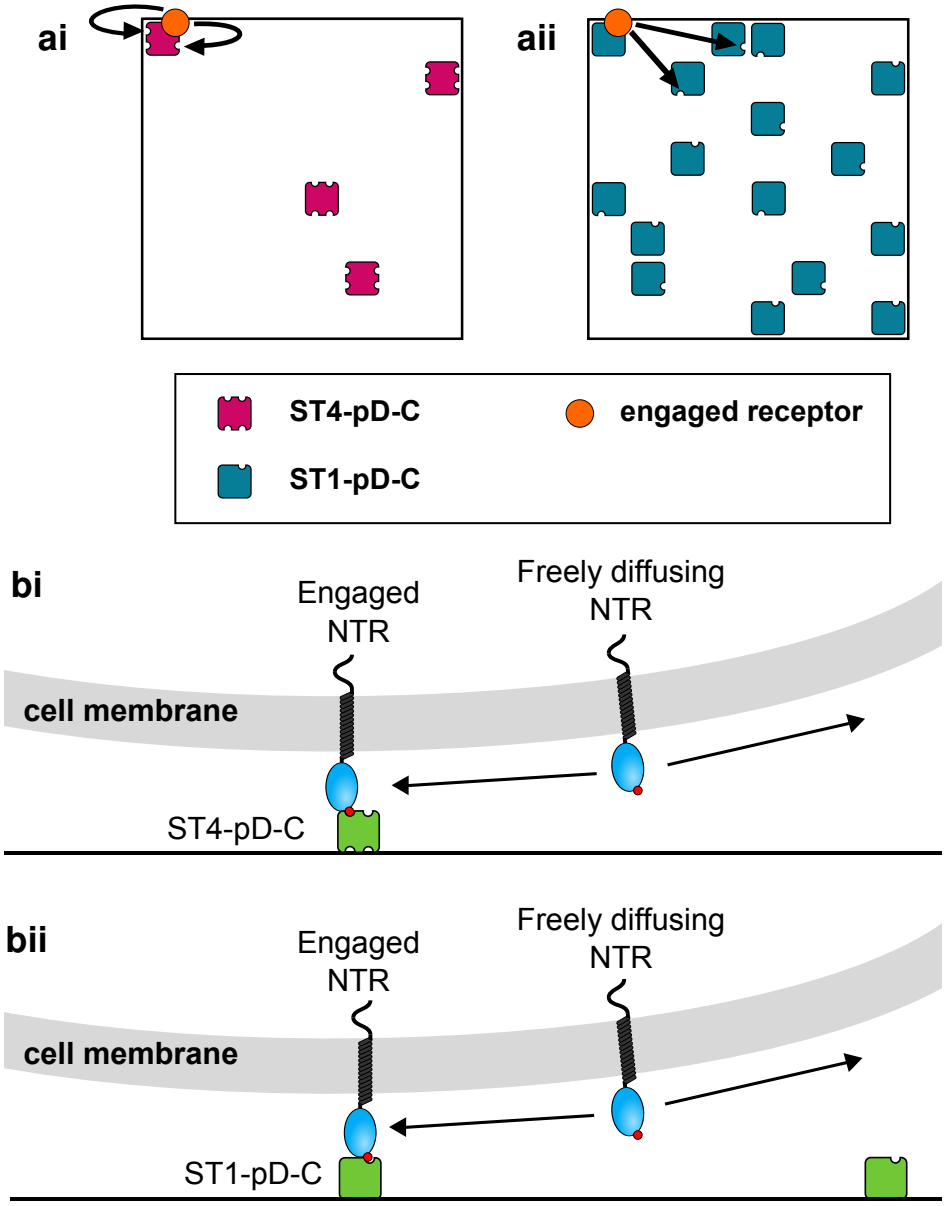


Fig. 5.16: **The close proximity of ST4-pD-C binding sites may increase the likelihood of further receptor - ST-pD-C interactions.** A section of a ST4-pD-C- (**ai**) or ST1-pD-C- (**aii**) coated well with the same number of total binding sites is qualitatively illustrated. A single receptor bound to either ST1-pD-C or ST4-pD-C is shown in orange. The two closest binding sites to the engaged receptors are indicated by black arrows in both ai and aii. A section of an NTR-expressing cell with a single NTR bound to immobilised ST4-pD-C (**bi**) is illustrated. Within the close cell-plate surface interface that results from this interaction, a free binding site on the ST4-pD-C is available for engagement of an NTR freely diffusing within the cell membrane. (**bii**) A NTR-expressing cell is also held in close contact to the surface of a ST1-pD-C-coated plate at the point of a receptor - ST-pD-C bond. However, as the cell membrane is less likely to be in close proximity to a free ST1-pD-C, it is also less likely that an unbound receptor freely diffusing in the cell membrane will interact with the available ST1-pD-C.

Accessibility of the binding sites

Another possible reason for the difference in potency between plate-immobilised ST1-pD-C and ST4-pD-C involves the method we use to measure the the number of accessible binding sites. Perhaps the number of sites measured using biotin:atto 680 does not accurately reflect the number of possible receptor-ligand interactions. Biotin:atto 680 is a small reagent and therefore may be able to bind to a site on immobilised StrepTactin-SpyCatcher that is inaccessible to Strep-Tag II-tagged SIRPβ1 expressed on cells. If the number of possible interactions between SIRPβ1 and ST1-pD-C or ST4-pD-C is overestimated, the log(EC_{50}) values of the response will also be overestimated.

To consider the accessibility of immobilised ST1-pD-C and ST4-pD-C binding sites, we show the two proteins in cartoon form in figure **5.17ai-ii** in 6 different orientations in which they can be immobilised onto the plate. ST1-pD-C and ST4-pD-C are both shown as 3D cubes without the SpyCatcher for simplicity. We assume the orientation in which ST-pD-C binds to the plate is random and therefore these orientations are equally likely. Binding sites of the StrepTactin-SpyCatcher proteins are also shown.

Binding sites in close proximity to the plate surface are the most likely to be inaccessible for receptor engagement. In figure **5.17bi**, we arbitrarily assigned binding sites of ST1-pD-C located close to the plate surface as inaccessible. The corresponding binding sites of ST4-pD-C (i.e. sites that are similarly in close proximity to the plate surface) are also defined as inaccessible (figure **5.17bii**). If the 6 orientations of protein binding shown in figure **5.17bi-ii** are equally likely, then the proportion of binding sites unavailable for receptor engagement are identical between immobilised ST1-pD-C and ST4-pD-C: 2/6 versus 8/24. The same will be true if more or fewer binding site positions are accessible to soluble biotin:atto 680 but inaccessible for receptor engagement.

Correcting for such an overestimation in the number of possible receptor-ligand interactions would alter the absolute log(EC_{50}) values of both the ST1-pD-C and ST4-pD-C data, but the values would be lowered by the same proportion. The potency of ST1-pD-C- and ST4-pD-C-mediated SIRPβ1 activation would therefore still be different.

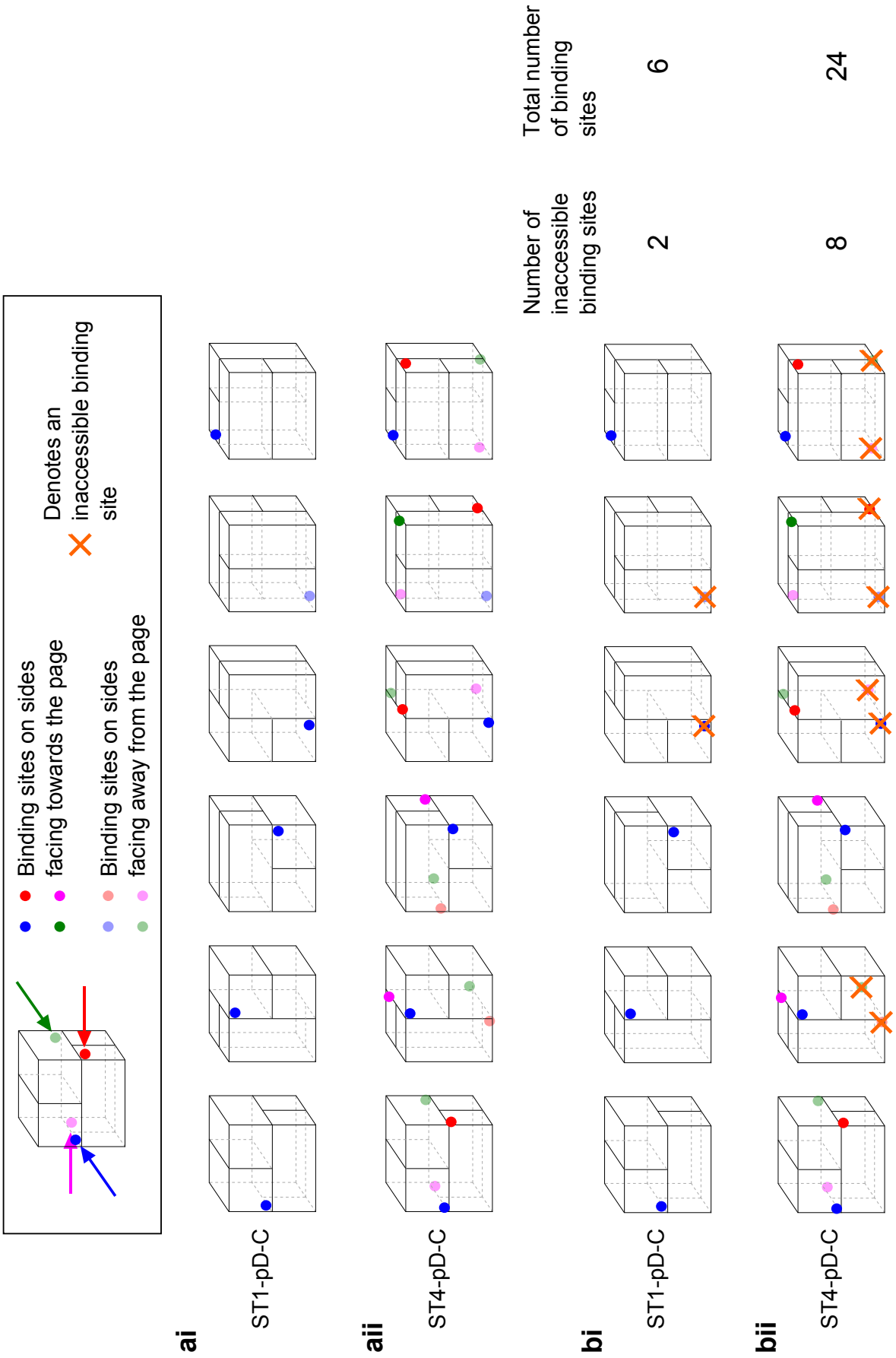


Fig. 5.17: **Provided there is no bias in binding orientation, the proportion of inaccessible binding sites between plate-immobilised ST1-pD-C and ST4-pD-C are the same.** *Continued on the next page.*

Fig. 5.17: **Provided there is no bias in binding orientation, the proportion of inaccessible binding sites between plate-immobilised ST1-pD-C and ST4-pD-C are the same.** *Continued.* The possible orientations in which ST1-pD-C (**ai**) or ST4-pD-C (**aii**) can be immobilised on a plate surface are illustrated. ST1-pD-C and ST4-pD-C are shown without the SpyCatcher and polyaspartate loop, and as 3D cubes made up of the 4 individual subunits of tetrameric StrepTactin. Biotin/Strep-Tag II-binding sites on the proteins are presented as coloured circles. Opaque colours represent binding sites that are facing the plane of the page and paler colours represent the corresponding binding sites situated at a position that is facing away from the page i.e. would not be visible in this figure if the StrepTactin proteins were shown as opaque structures. We assume that the orientation in which both proteins are immobilised is random and therefore assume each orientation is equally likely. ST1-pD-C (**bi**) and ST4-pD-C (**bii**) are again shown immobilised to a plate surface in various possible orientations. ST1-pD-C binding sites in close proximity to the plate surface are arbitrarily defined as inaccessible to Strep-Tag II-tagged receptor binding to illustrate the concept. These sites are shown with orange crosses through them. Likewise, any binding site of immobilised ST4-pD-C that corresponds to an inaccessible ST1-pD-C binding site is defined as inaccessible (also shown with an orange cross). Out of the 6 possible orientations of both ST1-pD-C and ST4-pD-C, the number of inaccessible binding sites and the total number of binding sites is displayed.

If there is a bias in the orientation in which ST1-pD-C and ST4-pD-C are immobilised onto a plate surface however, the potential error in the number of ST1-pD-C and ST4-pD-C binding sites measured by biotin:atto 680 could be significantly different. This could account for, or contribute to, the observed difference in potency between ST1-pD-C- and ST4-pD-C - mediated activation.

In addition to these factors, it is possible that 4 individual receptors are unable to interact with one ST4-pD-C protein simultaneously due to steric effects. Whereas because biotin:atto 680 is small, it is likely that 4 biotin:atto 680 dyes can interact with one ST4-pD-C. If this was the case, the number of immobilised ST4-pD-C binding sites measured using biotin:atto 680, and so also the log(EC_{50}) value, will be an overestimate. Correcting this theoretical ST4-pD-C - specific error would again increase the difference in potency between ST1-pD-C - and ST4-pD-C - mediated NTR activation.

Determining if all 4 sites of immobilised ST4-pD-C can be bound simultaneously will be useful to our studies. Surface plasmon resonance will be used for this. A soluble Strep-Tag II-tagged protein as analyte will be added to immobilised ST1-pD-C or ST4-pD-C. Relative to the amount of protein immobilised, we would expect 4 times the amount of soluble Strep-Tag II-tagged protein to bind to ST4-pD-C at equilibrium than the amount bound to ST1-pD-C. While a soluble protein does not completely represent a cell surface-

presented receptor it may give an initial indication as to how many ST4-pD-C binding sites can be engaged simultaneously by Strep-Tag II-tagged proteins.

The SpyCatcher may interfere with receptor - ST-pD-C binding

The accessibility of ST1-pD-C and ST4-pD-C binding sites for receptor engagement, independent of immobilisation of the proteins, may also differ. Three of the binding sites of ST4-pD-C are positioned on StrepTactin subunits whereas the fourth site is positioned on a subunit that is also fused to the SpyCatcher protein. This fourth binding site will be in relatively close proximity to the SpyCatcher protein and therefore may be less accessible for receptor binding due to a steric effect. The lone binding site of ST1-pD-C is positioned on the subunit fused to the SpyCatcher and so may also have a reduced accessibility. If this was the case, binding of a Strep-Tag II-tagged receptor to the one binding site of ST1-pD-C would always be affected whereas binding of a receptor to only one of the four binding sites of ST4-pD-C would be affected. This difference in binding site accessibility between ST1-pD-C and ST4-pD-C would not be reflected in the biotin:atto 680 measurements and could contribute to the difference in potency observed between ST1-pD-C- and ST4-pD-C-mediated SIRPβ1 activation.

Surface plasmon resonance could be used to investigate if the binding properties between a Strep-Tag II-tagged receptor and the binding site of either StrepTactin or StrepTactin-SpyCatcher subunits vary. More specifically, if the interaction between a Strep-Tag II-tagged protein and StrepTactin-SpyCatcher subunit is sterically inhibited, we would expect the on-rate for a soluble Strep-Tag II-tagged protein binding to immobilised ST1-pD-C to be lower than that for binding to immobilised ST4-pD-C.

5.3.3 Immobilised monovalent ligand can stimulate a representative NTR

We have also provided evidence that immobilised monovalent artificial ligand activates a representative NTR. This is consistent with the hypothesis that receptor clustering is not required for activation. However, the lowest density of immobilised ST1-pD-C that elicited an activation response from THP-1 SIRPβ1 cells is relatively high ($\sim$3000-5000 μm^{-2}, figure **5.8b**). At this density, engaged receptors could be considered as being held in close proximity to each other, or clustered. Therefore, perhaps receptor clustering

does play a vital role in activation, and at the lower densities of ST1-pD-C used in our experiments, the engaged receptors are not clustered enough for the THP-1 SIRPβ1 cell to be activated. Alternatively, it is possible that at the lower densities of ST1-pD-C it is the absolute number of receptor-ligand interactions, not the density, that is insufficient for a cell response to be detected. Using ST1-pD-C - coated beads instead of plate-immobilised ST1-pD-C could be investigated as a method of increasing the total number of ST1-pD-C binding sites a THP-1 SIRPβ1 cell is exposed to without increasing the density of the ligand. This may elucidate what is limiting the receptor response and whether receptor clustering is essential for activation.

5.3.4 Comparing the activation of SIRPβ1 in response to either monovalent or tetravalent StrepTactin-SpyCatcher presented on a cell surface

To further investigate if receptor clustering enhances receptor activation we incubated THP-1 SIRPβ1 cells with CHO CD80-Spy cells presenting either ST1-pD-C or ST4-pD-C. While receptors bound to immobilised ligand are constrained within the cell membrane, receptors engaged by cell-expressed ligand are mobile and therefore are capable of clustering.

The data of two independent experiments we show did not cover the range of binding sites that would presumably give a full dose-response curve. We were therefore unable to quantitatively analyse the data. A larger concentration range of ST1-pD-C and ST4-pD-C will be incubated with CHO CD80-Spy cells in future experiments in order to detect the full range of the cell response and allow more in-depth analysis.

In addition to this, the number of binding sites present on ligand-expressing cells in the first experiment was not accurately measured. In order to use these data in our analysis we assigned the data the same number of binding sites as corresponding cells measured in a separate experiment.

Qualitatively, in both experiments, the log(EC_{50}) values of THP-1 SIRPβ1 cell activation in response to cell-presented ST1-pD-C or ST4-pD-C are different. The magnitude of this difference varies between the two experiments which may be because the number of binding sites on the ligand-expressing cells were not measured within each experiment.

CHO CD80-Spy cell numbers were only counted prior to washing and incubation with either ST1-pD-C or ST4-pD-C. Following this the cells were washed again and either added to THP-1 SIRPβ1 cells or biotin:atto 680. There may be variability in the number of cells lost during these steps which would impact the accuracy of both the number of ligand cell binding sites measured using biotin:atto 680 and also the number of ligand cells used to stimulate the THP-1 SIRPβ1 cells. To remove this potential inaccuracy from future experiments, the cell numbers will be counted immediately prior to either incubation with THP-1 SIRPβ1 cells or the addition of guanidinium hydrochloride for measuring the number of binding sites. Repeats of this experiment would also indicate whether the results we see, particularly the difference in potency between ST1-pD-C- and ST4-pD-C- mediated NTR activation, are reproducible.

Again there are a number of possible reasons for the difference in log(EC_{50}) values.

Accessibility of the binding sites

In contrast to plate-immobilised StrepTactin-SpyCatcher, which we assume binds to the plate surface with a random orientation, ST1-pD-C and ST4-pD-C bound to CHO CD80-Spy cells via the SpyTag-SpyCatcher interaction will be presented in a specific orientation (figure **5.18ai-ii**). If the position of the single binding site of ST1-pD-C in this orientation is relatively less accessible for receptor engagement than other positions, the binding sites of all CHO CD80-Spy : ST1-pD-C cells will consistently be less accessible for receptor but not biotin:atto 680 binding (figure **5.18ai**). In contrast, for ST4-pD-C presented on CHO CD80-Spy cells, while one of the four binding sites will be in the equivalent less accessible position for receptor engagement, the other binding sites on each ST4-pD-C could be more available (figure **5.18aii**). This reduced accessibility with ST1-pD-C compared to with ST4-pD-C, would result in error in the number of binding sites on the ligand-expressing cells measured using biotin:atto 680 and may explain the difference in potency we observed.

However, we have shown that THP-1 SIRPβ1 cells do secrete IL-8 in response to CHO CD80-Spy cells presenting ST1-pD-C proving that the SIRPβ1 receptor can engage with the potentially less accessible binding site of ST1-pD-C. In addition to this, from qualitative analysis of the dose-response curves, the difference in log(EC_{50}) values of IL-8

secretion in response to ST1-pD-C- and ST4-pD-C-presenting ligand cells is significantly large that we believe any small reduction in the ability of ST1-pD-C to engage SIRPβ1 due to steric effects will not be wholly responsible for this difference.

As discussed for plate-immobilised ST4-pD-C, it is also unclear whether 4 receptors will be able to simultaneously bind to the 4 binding sites of a single ST4-pD-C presented on ligand cells. This would again mean that the measured number of binding sites on CHO CD80-Spy : ST4-pD-C cells, and log(EC_{50}) value, is an overestimate of the number of true available sites for receptor engagement. Correcting for this error would act to increase the difference in potency further.

To confirm that varied accessibility of the binding sites is not responsible for the difference in potency we observe, an alternative method for clustering the receptors could be investigated. Previously, a rapamycin-based system has been used to cluster proteins in liposomes [Hui and Vale, 2014]. To use this method in our studies, a CHO cell line expressing both CD80-Spy with multiple FK506 binding protein (FKBP) domains inserted into the intracellular region and CD80-Spy with multiple intracellular FKBP rapamycin-binding domains (FRB) would be made (figure **5.18b**). Addition of the membrane-permeable rapamycin, which binds a FRB and FKBP domain simultaneously and with high affinity, would result in dimerisation, or higher order aggregation, of CD80-Spy proteins. Covalent binding of ST1-pD-C to this protein complex would result in a ligand where the valency can be controlled by addition of rapamycin. Binding of ST1-pD-C to these ligand cells in the absence of rapamycin would on the other hand give a cell line expressing monovalent ligand. Any difference in the dose-response profiles of THP-1 SIRPβ1 cells incubated with either the ligand-expressing cell line in the absence or presence of rapamycin would therefore not be due to differences in binding site accessibility but due to ligand valency.

Clustering of the receptors

As for NTR activation in response to plate-immobilised ST-pD-C, an alternative reason for the difference in potency of CHO CD80-Spy : ST1-pD-C cells and CHO CD80-Spy : ST4-pD-C cells on THP-1 SIRPβ1 activation is varying levels of engaged receptor clustering.

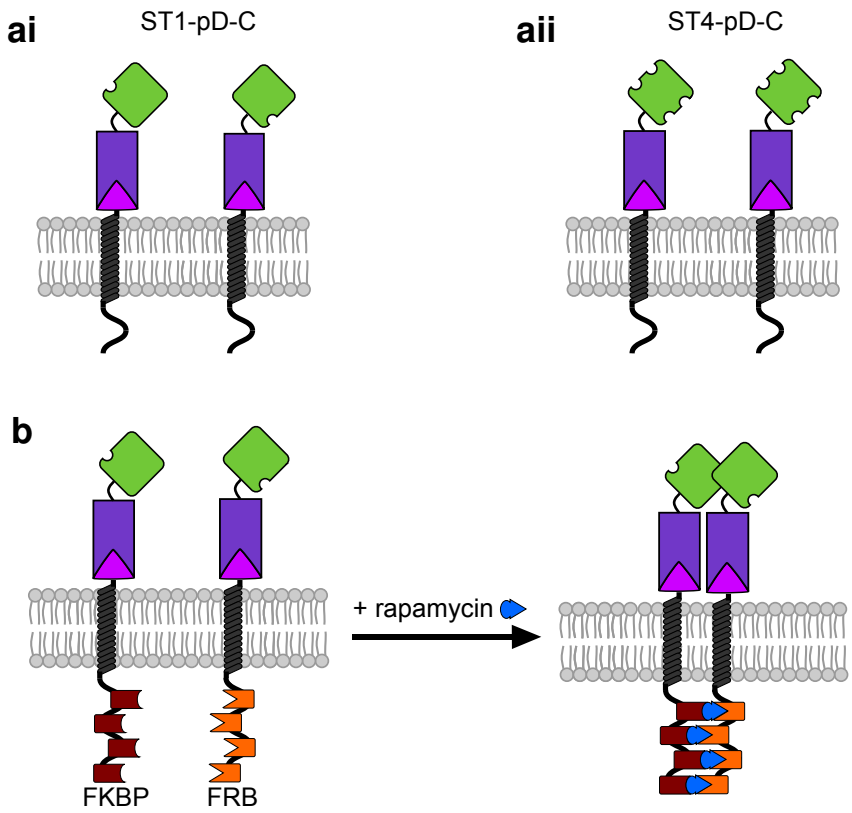


Fig. 5.18: **ST1-pD-C and ST4-pD-C bound to CHO CD80-Spy cells will be presented in a specific orientation.** Both ST1-pD-C (**ai**) and ST4-pD-C (**aii**) will covalently bind to CD80-Spy protein expressed on the surface of CHO cells using the SpyTag-SpyCatcher interaction. This will bias the orientation in which the ST-pD-C is presented. The Strep-Tag II/biotin-binding sites of ST1-pD-C and ST4-pD-C may therefore vary in their accessibility for receptor binding. (**b**) A rapamycin-based system could be used to aggregate CD80-Spy proteins bound by ST1-pD-C. A CHO cell line expressing CD80-Spy with intracellular FKBP domains and CD80-Spy with intracellular FRB domains would be made. In the absence of rapamycin, ST1-pD-C will covalently bind to the CD80-Spy proteins to form monovalent artificial ligand. In the presence of rapamycin, FKBP- and FRB- containing CD80-Spy proteins will be clustered via high affinity binding of rapamycin to both FKBP and FRB.

Compared to receptors bound to plate-immobilised ST-pD-C, receptors bound to ST-pD-C presented on ligand-expressing cells are mobile and therefore can be clustered. This includes both receptors bound to ST1-pD-C and receptors bound to ST4-pD-C. Therefore the level of clustering between these two sets of receptors may be comparable. Alternatively, despite the ability of both sets of bound receptors to cluster at the cell-cell interface, receptors bound to ST4-pD-C may still be comparatively more clustered. i.e. Four receptors each bound by one ST1-pD-C may be clustered in the cell-cell interface but the same number of receptors bound to one ST4-pD-C may be held in closer proximity to each other. Increased clustering of ST4-pD-C-bound receptors would also give increased clustering of the associated intracellular signalling motifs. This could enhance receptor signalling through favouring activating kinase activity as discussed in more detail in section 1.10.3.

Imaging and homo-FRET studies similar to those proposed in section 4.3.1 could be used to investigate if, at corresponding numbers of total binding sites, ST4-pD-C engaged receptors are indeed more clustered than ST1-pD-C engaged receptors at the cell-cell interface.

Clustering of engaged receptors will also decrease the surface area of cell membrane deformation at the cell-cell interface in comparison to when the receptors are engaged by immobile ligands, and so will also reduce the tension acting on the receptor-artificial ligand bonds. A higher level of clustering of receptors bound by cell-presented ST4-pD-C compared to receptors bound by cell-presented ST1-pD-C will similarly result in a smaller surface area of membrane deformation and therefore result in a smaller tension acting on the individual bonds. Decreased tension could yield a relatively longer off-rate and increased stability of receptor - ST4-pD-C bonds compared to receptor - ST1-pD-C bonds which in turn may act to enhance receptor signalling.

Overall, the increased potency of ST4-pD-C relative to ST1-pD-C, both when plate-immobilised and presented on cells, is consistent with receptor clustering enhancing the signalling response. Although the ligand cell experiments need to be repeated in order to extract the log(EC_{50}) values and allow more detailed analysis, the magnitude of the difference in potency of ST1-pD-C and ST4-pD-C is larger when the proteins are plate-immobilised. This is also consistent with receptor clustering enhancing signalling;

the ability of receptors bound to mobile cell-presented ST1-pD-C to cluster may partially compensate for the consistently larger average distance between ST1-pD-C-bound receptors compared to between ST4-pD-C-bound receptors and thereby reduce the difference in potency.

As discussed above and shown schematically in figure **5.19ai-aii**, the effect of receptor clustering on signalling could be mediated through the impact this has on membrane deformation and the tension placed on the receptor-artificial ligand bonds, or through bringing the receptor-associated signalling motifs into close proximity. We hypothesise that one of these mechanisms, or a combination of both, is responsible for the consistent difference in potency of ST1-pD-C and ST4-pD-C that we observe. Experimentally determining which mechanism is responsible could prove challenging however. Two possible experiments to do this are described in figure **5.19b-c**.

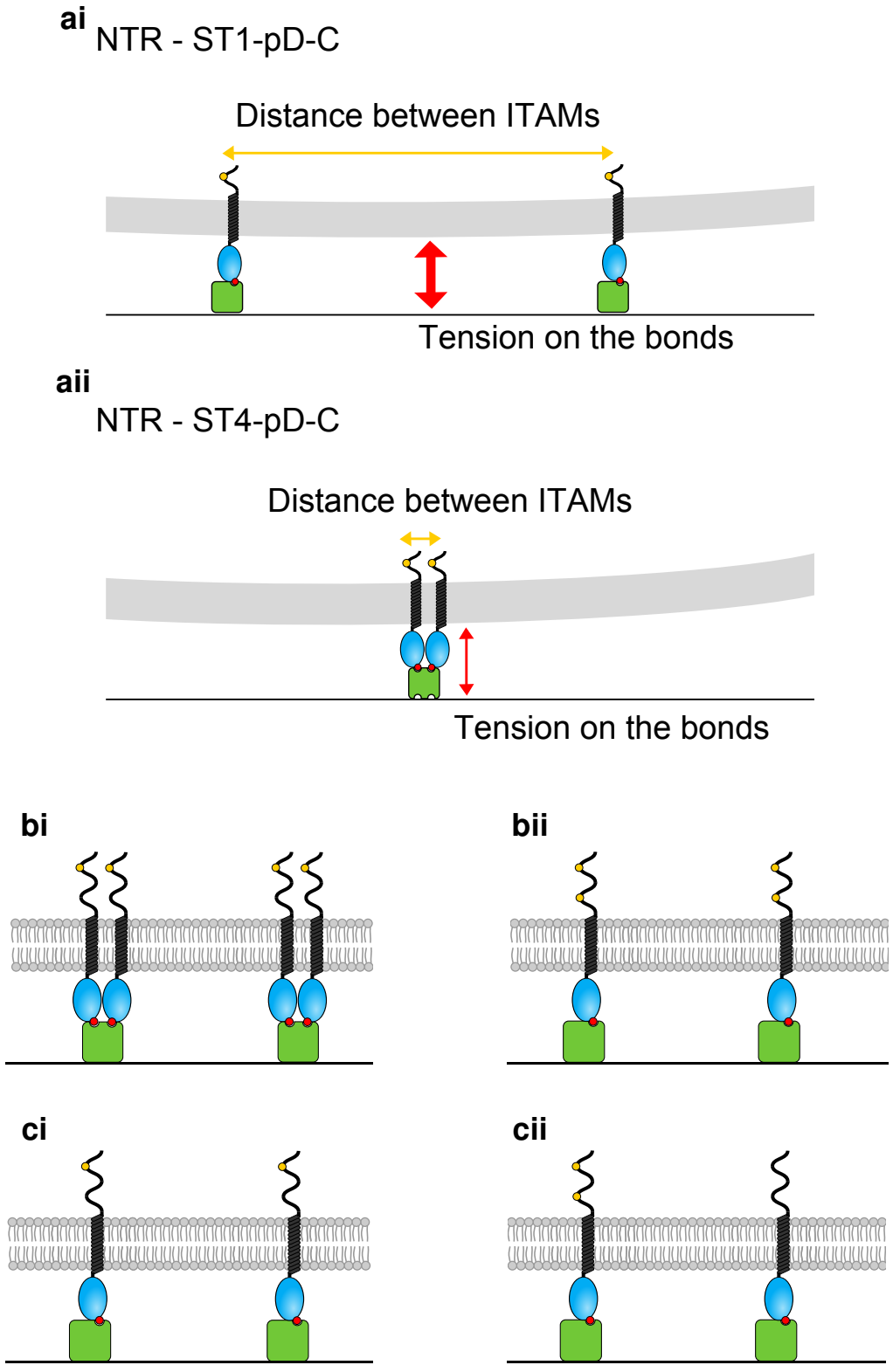


Fig. 5.19: **Clustering affects multiple properties of the receptor-artificial ligand interaction.** A Strep-Tag II-tagged NTR is shown bound to either ST1-pD-C (**ai**) or ST4-pD-C (**aii**). We show ST-pD-C presented on a surface but we hypothesise this will also occur with cell-presented ST-pD-C. Receptors bound to ST1-pD-C will not be held in as close proximity to each other as receptors bound to ST4-pD-C. This could alter the potency of the stimulus through an increased distance between receptor-associated signalling motifs (ITAMs in this case) or by a comparatively larger tension acting on the receptor - ST1-pD-C bonds, resulting in faster unbinding. *Continued on the next page.*

Fig. 5.19: **Clustering affects multiple properties of the receptor-artificial ligand interaction.** *Continued.* (**b**) To alter the receptor-ligand bond tension without altering the degree of signalling motif clustering, two receptor cell lines will be created. One expressing a Strep-Tag II-tagged NTR with the wildtype number of signalling motifs. Here we show one ITAM. These cells will be presented to plate-immobilised bivalent StrepTactin-SpyCatcher (**bi**). The other receptor cell line will express the Strep-Tag II-tagged NTR with twice as many signalling motifs (2 ITAMs per receptor in this example). By presenting these cells to plate-immobilised ST1-pD-C (**bii**), the clustering of the signalling motifs will be comparable to that in (bi) but the number of bonds per motif will be different. This will affect the bond tension only. (**c**) A different experiment could be used to alter the clustering of the signalling motifs without affecting bond tension. Cells expressing Strep-Tag II-tagged NTR with a single ITAM will be presented to plate-immobilised ST1-pD-C (**ci**). Another cell line expressing both tagged NTR with two intracellular ITAMs and a signalling-incompetent tagged NTR (no ITAMs) will also be presented to ST1-pD-C (**cii**). Between (ci) and (cii), the number of bonds does not change and so the magnitude of the tension acting on the bonds does not change but on average the ITAMs in cii are held in closer proximity.

5.3.5 Investigating the effect of elongating monovalent and tetravalent artificial ligand on NTR activation

We show the data of two independent experiments comparing the effect of elongating either monovalent or tetravalent ligand on Strep-Tag II-tagged SIRPβ1 activation. Again, the data does not form a full dose-response curve. We were therefore unable to quantitatively analyse the data.

The data consistently show that elongating the dimensions of the SIRPβ1 - ST1-pD-C interaction abolished signalling. However, we were unable to create CHO CD80-CD4-Spy : ST1-pD-C cells with the same range of binding site numbers that were measured on CHO CD80-Spy : ST1-pD-C cells. It is therefore currently unclear whether elongating the complex abolishes signalling even at high numbers of engaged receptors, or whether the potency of the response is dramatically reduced and so large numbers of engaged receptors are required for a detectable activation response. Future experiments will aim to increase the number of binding sites available on CHO CD80-CD4-Spy : ST1-pD-C cells in order to determine which is the case.

Whether elongation of the monovalent artificial ligand completely abolishes activation of engaged receptors or reduces the potency, receptor activation is significantly affected. One possible reason for this is that THP-1 SIRPβ1 cells are less able to form conjugates

with CHO CD80-CD4-Spy : ST1-pD-C cells. To test this, we can use a flow cytometry based experiment to compare conjugate formation between the receptor cell and two ligand cell lines.

In addition to this, the mobility and clustering of the receptor-ligand complex may be reduced by elongation of the ligand extracellular region (shown schematically in figure **5.20**). The difference in extracellular length between bulky glycoproteins and integrins has already been shown to play a role in integrin clustering [Paszek et al., 2014]. Similarly, the size difference between large surface molecules like CD45, and the receptor-artificial ligand complex may drive clustering of engaged NTRs in our studies. Decreasing this size difference by elongation of the receptor-ligand complex might reduce engaged receptor clustering and thereby lead to the abolished signalling that we observe. This is comparable to our hypothesis that a reduction in receptor clustering induced by engagement of lower valency ligands decreases the potency of the receptor response. To further investigate this, FRAP experiments would be used to analyse mobility of ligand-bound receptors in the cell membrane, and FRET experiments would be used to analyse the levels of clustering of Strep-Tag II-tagged SIRPβ1 receptors bound by ST1-pD-C presented either by CHO CD80-Spy cells or CHO CD80-CD4-Spy cells.

Elongating the receptor-artificial ligand complex will also impact the force acting on the protein-protein bonds. Large surface molecules in the interface between THP-1 SIRPβ1 cells and CHO CD80-CD4-Spy cells presenting ST1-pD-C will not be under as much tension as large surface molecules in the THP-1 SIRPβ1 - CHO CD80-Spy : ST1-pD-C cell interface. This is because of the reduced size difference between the receptor-ligand complex and large surface proteins. This would in turn reduce the tension placed on the receptor-elongated ligand bonds and may affect bond lifetime.

Reduced tension acting on large surface proteins present at the interface between THP-1 SIRPβ1 cells and CHO CD80-CD4-Spy : ST1-pD-C cells and also the increased intermembrane distance may alter the distribution of the large surface proteins like CD45 relative to the receptor-ligand complexes. The kinetic-segregation model predicts that at sites of NTR-ligand engagement, the small distance between the receptor cell and ligand cell will result in segregation of large proteins like the inhibitory phosphatase CD45 from the engaged receptors and consequently receptor activation. Increasing the intermem-

brane distance at sites of receptor-ligand interaction may act to decrease this segregation (figure **5.20**). Reduced segregation of CD45 from engaged receptors would have an inhibitory effect on signalling and so may play a role in the abolished SIRPβ1 signalling we observe in response to ligand cells presenting elongated monovalent ligand.

We hypothesise that either reduced clustering of receptors engaged by elongated ligand, or reduced segregation of inhibitory phosphatases from engaged receptors (or a combination of the two) is responsible for the data we observe. Immobilising the artificial ligand may aid further investigation into this. Presentation of either CD80-Spy ST1-pD-C or CD80-CD4-Spy ST1-pD-C immobilised on a surface will remove the potential clustering effects on receptor activation. Alternatively, to investigate the role of receptor-CD45 proximity in activation, CD45 could be manipulated in order to reduce the predicted segregation of this protein from receptor-'wild-type' length complexes or to increase CD45 segregation from elongated receptor-ligand complexes. These experiments have previously been used to investigate the mechanism of activation of other NTRs [He et al., 2002, Lin and Weiss, 2003, Irles et al., 2003, James and Vale, 2012, Cordoba et al., 2013].

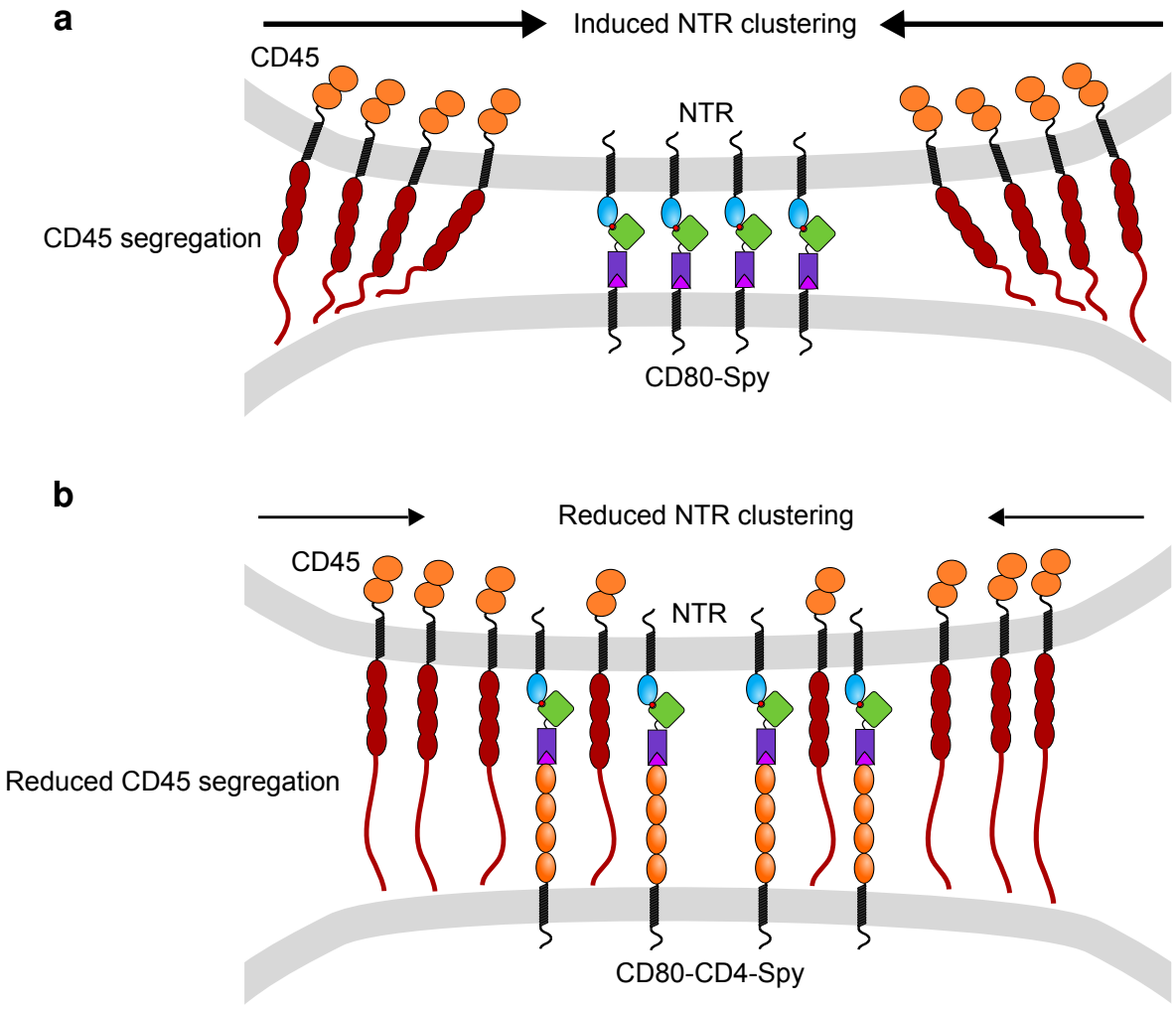


Fig. 5.20: **Elongation of the receptor - monovalent ligand complex may abolish receptor signalling by reduced engaged receptor clustering and/or reduced segregation of inhibitory phosphatases.** Schematic diagrams showing a tagged NTR-expressing cell in contact with either a CHO CD80-Spy cell presenting ST1-pD-C (**a**) or CHO CD80-CD4-Spy cell presenting ST1-pD-C (**b**). We hypothesise large surface molecules like CD45 will be segregated from NTR - monovalent CD80-Spy ligand complexes and that the engaged NTRs will cluster at the interface (a). We propose that elongating the ligand will reduce both NTR clustering and CD45 segregation from the receptor-ligand complexes and that this will dramatically reduce receptor activation (b). This is in line with what we observe.

Elongation of the tetravalent artificial ligand did not have a significant effect on SIRPβ1 activation.

As described above for elongation of monovalent ligand, we believe tagged SIRPβ1 receptors bound by CD80-CD4-Spy ST4-pD-C are less clustered than receptors bound by the shorter CD80-Spy ST4-pD-C. In addition to this, increasing the intermembrane distance at sites of receptor-ligand complexes would reduce the hypothesised segregation of large surface proteins like CD45 from the engaged receptors. We would expect this reduced segregation to significantly decrease receptor activation. This is not seen with the tetravalent ligand however.

We hypothesise that there is reduced segregation of the inhibitory phosphatase CD45 from receptors bound to CHO CD80-CD4-Spy : ST4-pD-C compared to from receptors bound to CHO CD80-Spy : ST4-pD-C. We also hypothesise that because multiple receptors bound to a single ST4-pD-C will be held in close proximity to each other, this will increase receptor activation and compensate for the reduced signalling due to decreased CD45 segregation. In contrast, receptors bound to ST1-pD-C will not be held in as close proximity and therefore cannot compensate for the reduced inhibitory phosphatase segregation. This is consistent with what we observe, that elongation of monovalent ligand abolishes signalling while elongation of tetravalent ligand has no significant effect.

Imaging studies will be used to investigate if CD45 is indeed segregated from SIRPβ1 - tetravalent CD80-Spy and from SIRPβ1 - tetravalent CD80-CD4-Spy interactions. FRET studies will also be used to compare the clustering of receptors engaged by the two different length tetravalent artificial ligands. These results will be used in combination with the existing data and results from future experiments with monovalent artificial ligand to test our hypotheses and further elucidate which mechanisms are responsible for the differences in receptor activation we have observed.

We have used the artificial ligand system to alter two properties of the NTR-ligand complex, ligand valency and ligand dimensions, and analysed the effects of this on receptor activation. Our investigations require further optimisation but have provided insight into the requirements of SIRPβ1 activation. They can now be extended to analyse SIRPβ1 signalling in more detail and also to analyse other Strep-Tag II-tagged NTRs that have

already been created to determine whether they behave similarly.

6. GENERAL DISCUSSION

In this work, we have developed an artificial generic ligand system to test our hypothesis that NTRs are activated using the KS mechanism. We also used the system to investigate other properties of receptor signalling. The artificial ligand has relatively physiological dimensions and affinity for the Strep-Tag II - tagged NTRs and so is a reasonable mimic of NTR-natural ligand interactions.

We demonstrated that both activating and inhibitory representative NTRs can be activated by the artificial ligand. This both validates the system, and indicates that NTR triggering does not require a specific ligand-induced mechanism. In support of the KS model and our hypothesis, we next showed that only ligation by surface-associated artificial ligand induced NTR activation, whilst ligation by soluble tetravalent ligand did not. We also provided evidence that the soluble ligand bound multivalently to the receptor, indicating that this level of ligand-induced receptor clustering was insufficient to trigger a representative NTR.

Using surface-immobilised artificial ligands of different valency, we showed that tetravalent StrepTactin-SpyCatcher can induce a more potent NTR activation response than monovalent StrepTactin-SpyCatcher. The difference in potency was observed both when the ligands were immobilised onto a plate and when they were presented on a cell surface. This suggests that receptor clustering can enhance activation. We postulate that the effect of increased clustering by multivalent ligand binding may enhance activation by increased proximity of signalling motifs and/or reduced tension acting on the individual bonds. Experiments to distinguish between the two mechanisms were proposed although it is possible that more than one of the mechanisms may be involved. We also suggested further mechanisms that may be responsible for the results observed and proposed experiments to investigate this further.

In further support of the KS model and our hypothesis, we showed that elongation of the artificial monovalent ligand dramatically decreased ligand-induced activation of a representative NTR. Ligand elongation may have also changed mechanical forces acting on the engaged receptor which may play a role in the results observed. Experiments were proposed to examine this in more detail. We also showed that elongation of the multivalent artificial ligand did not significantly affect the receptor response. This suggests that receptor clustering may compensate for signalling defects due to ligand elongation. Optimisation of these experiments is required to confirm the results. We proposed future experiments to investigate why elongation of multivalent ligand did not affect receptor activation.

Overall, we have provided evidence that is consistent with our hypothesis, but further work is required to exclude other potential mechanisms.

Additional future work will complete the validation of the artificial ligand system. We will compare NTR signalling in response to artificial ligand or physiological ligand to confirm the system is a good representation of physiological interactions.

We will also continue the work presented here to test other predictions the KS model makes about NTR activation, and extend the investigation to other NTRs. It would be interesting, for example, to investigate whether NTRs with relatively large ectodomains similarly show a requirement for the ligand to be presented on a surface, and whether ligand elongation affects signalling. Another NTR we would like to investigate with our artificial ligand system is the TCR. It has been shown previously that soluble dimeric pMHC can activate the TCR (discussed in Chapter 5 introduction). In the work presented here however we found that binding of soluble multivalent StrepTactin was unable to induce activation of representative receptors. It will be interesting to determine if soluble multivalent ligand binding can activate a Strep-Tag II-tagged TCR and if so, what is different between the TCR and other NTRs that gives it this property?

A potential caveat of the ligand system is the position of the Strep-Tag II on the receptor. We observed with NKG2D that the Strep-Tag II was inaccessible from solution, most likely because the receptor C terminus is close to the membrane. From the structures of other C-type lectin receptors we predicted that attaching the Strep-Tag II to the C terminus of

these receptors would similarly leave the tag inaccessible for ligand binding. We were therefore unable to study C-type lectin receptors in our system. Similar problems may arise with other NTRs or we may find that some NTRs show reduced signalling because the Strep-Tag II is less accessible for ligand binding. One way in which we could remove the potential problem of accessibility is to alter the extracellular domain of the receptors that have an inaccessible extracellular terminus. We could do this by replacing the most membrane distal extracellular domain of the receptor with that of a receptor we have shown to have an accessible Strep-Tag II.

Alternatively, instead of the Strep-Tag II - StrepTactin interaction, the well-studied interaction between NTR 2B4 and its ligand CD48 could be used. The ectodomain of each NTR could be replaced with the extracellular region of 2B4 and presented to CD48 as the artificial ligand. This system has already been used to study TCR signalling and is being used in the laboratory to investigate signalling by other NTRs [Choudhuri et al., 2005]. Elongated forms of CD48 could be created, however we would not be able to change the valency or surface density of the ligand. Such an approach, which further manipulates the NTR, would only be used for those receptors that cannot engage the artificial StrepTactin-based ligand.

The presented artificial ligand system can also be used to answer further questions about NTR signalling. For example, does changing the affinity between receptor and ligand affect signalling? The affinity can be altered by mutation of the StrepTactin protein. Additionally, by altering the membrane anchor of the ligand we can ask what effect changes in ligand mobility has on receptor signalling. This system can also be used, and is currently being used in the laboratory, to investigate the properties of activating, co-stimulatory and inhibitory NTR signal integration.

We believe this system provides a useful approach to systematically investigate the mechanism of NTR triggering and signalling. It has elucidated and will further elucidate the properties that control NTR signalling outcomes. The system can also be applied to other types of receptor-ligand interactions to similarly investigate the properties which play a fundamental role in signalling.

BIBLIOGRAPHY

[Abastado et al., 1995] Abastado, J. P., Lone, Y. C., Casrouge, a., Boulot, G., and Kourilsky, P. (1995). Dimerization of soluble major histocompatibility complex-peptide complexes is sufficient for activation of T cell hybridoma and induction of unresponsiveness. *The Journal of experimental medicine*, 182(2):439–47.

[Adams et al., 2011] Adams, J. J., Narayanan, S., Liu, B., Birnbaum, M. E., Kruse, A. C., Bowerman, N. A., Chen, W., Levin, A. M., Connolly, J. M., Zhu, C., Kranz, D. M., and Garcia, K. C. (2011). T cell receptor signaling is limited by docking geometry to peptide-major histocompatibility complex. *Immunity*, 35(5):681–93.

[Adams, 2013] Adams, K. J. (2013). Redirected T Cell Activity By High Affinity Tcr-Anti-Cd3 Bispecific Candidate Therapeutics. *A Thesis, Cardiff University*.

[Adams et al., 1998] Adams, S., van der Laan, L. J., Vernon-Wilson, E., Renardel de Lavalette, C., Döpp, E. a., Dijkstra, C. D., Simmons, D. L., and van den Berg, T. K. (1998). Signal-regulatory protein is selectively expressed by myeloid and neuronal cells. *Journal of immunology (Baltimore, Md. : 1950)*, 161(4):1853–1859.

[Aivazian and Stern, 2000] Aivazian, D. and Stern, L. J. (2000). Phosphorylation of T cell receptor zeta is regulated by a lipid dependent folding transition. *Nature structural biology*, 7(11):1023–1026.

[Akerley et al., 1991] Akerley, W. L., Guyre, P. M., and Davis, B. H. (1991). Neutrophil activation through high-affinity Fc gamma receptor using a monomeric antibody with unique properties. *Blood*, 77(3):607–15.

[Akkaya and Barclay, 2013] Akkaya, M. and Barclay, a. N. (2013). How do pathogens drive the evolution of paired receptors? *European journal of immunology*, 43(2):303–13.

[Al-Numani et al., 2003] Al-Numani, D., Segura, M., Doré, M., and Gottschalk, M. (2003). Up-regulation of ICAM-1, CD11a/CD18 and CD11c/CD18 on human THP-1 monocytes stimulated by Streptococcus suis serotype 2. *Clinical and Experimental Immunology*, 133(1):67–77.

[Alakoskela et al., 2011] Alakoskela, J.-M., Koner, A. L., Rudnicka, D., Köhler, K., Howarth, M., and Davis, D. M. (2011). Mechanisms for size-dependent protein segregation at immune synapses assessed with molecular rulers. *Biophysical journal*, 100(12):2865–74.

[Alberts et al., 2008] Alberts, B., Johnson, A., Lewis, J., Raff, M., Roberts, K., and Walter, P. (2008). *Molecular Biology of the cell*. Garland Science, New York, 5th edition.

[Alexander, 2000] Alexander, D. R. (2000). The CD45 tyrosine phosphatase: a positive and negative regulator of immune cell function. *Seminars in immunology*, 12(4):349–59.

[Ali et al., 2014] Ali, S. R., Fong, J. J., Carlin, A. F., Busch, T. D., Linden, R., Angata, T., Areschoug, T., Parast, M., Varki, N., Murray, J., Nizet, V., and Varki, A. (2014). Siglec-5 and Siglec-14 are polymorphic paired receptors that modulate neutrophil and amnion signaling responses to group B Streptococcus. *Journal of Experimental Medicine*, 211(6):1231–1242.

[Allard et al., 2012] Allard, J. F., Dushek, O., Coombs, D., and van der Merwe, P. a. (2012). Mechanical modulation of receptor-ligand interactions at cell-cell interfaces. *Biophysical journal*, 102(6):1265–73.

[Alvarez-Errico et al., 2004] Alvarez-Errico, D., Aguilar, H., Kitzig, F., Brckalo, T., Sayós, J., and López-Botet, M. (2004). IREM-1 is a novel inhibitory receptor expressed by myeloid cells. *European Journal of Immunology*, 34(12):3690–3701.

[Andersen et al., 2001] Andersen, P. S., Geisler, C., Buus, S., Mariuzza, R. A., and Karjalainen, K. (2001). Role of the T Cell Receptor Ligand Affinity in T Cell Activation by Bacterial Superantigens. *Journal of Biological Chemistry*, 276(36):33452–33457.

[Angata et al., 2006] Angata, T., Hayakawa, T., Yamanaka, M., Varki, A., and Nakamura, M. (2006). Discovery of Siglec-14, a novel sialic acid receptor undergoing concerted evolution with Siglec-5 in primates. *FASEB J*, 20(12):1964–1973.

[Angata et al., 2013] Angata, T., Ishii, T., Motegi, T., Oka, R., Taylor, R. E., Soto, P. C., Chang, Y.-C., Secundino, I., Gao, C.-X., Ohtsubo, K., Kitazume, S., Nizet, V., Varki, A., Gemma, A., Kida, K., and Taniguchi, N. (2013). Loss of Siglec-14 reduces the risk of chronic obstructive pulmonary disease exacerbation. *Cellular and molecular life sciences : CMLS*, 70(17):3199–210.

[Angata et al., 2002] Angata, T., Kerr, S. C., Greaves, D. R., Varki, N. M., Crocker, P. R., and Varki, A. (2002). Cloning and characterization of human Siglec-11: A recently evolved signaling molecule that can interact with SHP-1 and SHP-2 and is expressed by tissue macrophages, including brain microglia. *Journal of Biological Chemistry*, 277(27):24466–24474.

[Angelov et al., 2006] Angelov, G. S., Guillaume, P., Cebecauer, M., Bosshard, G., Dojcinovic, D., Baumgaertner, P., and Luescher, I. F. (2006). Soluble MHC-peptide complexes containing long rigid linkers abolish CTL-mediated cytotoxicity. *Journal of immunology (Baltimore, Md. : 1950)*, 176(6):3356–65.

[Arase and Lanier, 2004] Arase, H. and Lanier, L. L. (2004). Specific recognition of virus-infected cells by paired NK receptors. *Reviews in medical virology*, 14(2):83–93.

[Arase et al., 2002] Arase, H., Mocarski, E. S., Campbell, A. E., Hill, A. B., and Lanier, L. L. (2002). Direct recognition of cytomegalovirus by activating and inhibitory NK cell receptors. *Science (New York, N.Y.)*, 296(5571):1323–1326.

[Armstrong, 1997] Armstrong, R. N. (1997). Structure, catalytic mechanism, and evolution of the glutathione transferases. *Chemical Research in Toxicology*, 10(1):2–18.

[Arnon et al., 2005] Arnon, T. I., Achdout, H., Levi, O., Markel, G., Saleh, N., Katz, G., Gazit, R., Gonen-Gross, T., Hanna, J., Nahari, E., Porgador, A., Honigman, A., Plachter, B., Mevorach, D., Wolf, D. G., and Mandelboim, O. (2005). Inhibition of the NKp30 activating receptor by pp65 of human cytomegalovirus. *Nature immunology*, 6(5):515–523.

[Aslan et al., 2005] Aslan, F. M., Yu, Y., Mohr, S. C., and Cantor, C. R. (2005). Engineered single-chain dimeric streptavidins with an unexpected strong preference for biotin-4-fluorescein. *Proceedings of the National Academy of Sciences of the United States of America*, 102(24):8507–8512.

[Augugliaro et al., 2003] Augugliaro, R., Parolini, S., Castriconi, R., Marcenaro, E., Cantoni, C., Nanni, M., Moretta, L., Moretta, A., and Bottino, C. (2003). Selective cross-talk among natural cytotoxicity receptors in human natural killer cells. *European journal of immunology*, 33(5):1235–41.

[Avalos et al., 2014] Avalos, A. M., Bilate, A. M., Witte, M. D., Tai, A. K., He, J., Frushicheva, M. P., Thill, P. D., Meyer-Wentrup, F., Theile, C. S., Chakraborty, A. K., Zhuang, X., and Ploegh, H. L. (2014). Monovalent engagement of the BCR activates ovalbumin-specific transnuclear B cells. *The Journal of experimental medicine*, 211(2):365–79.

[Avril et al., 2004] Avril, T., Floyd, H., Lopez, F., Vivier, E., and Crocker, P. R. (2004). The Membrane-Proximal Immunoreceptor Tyrosine-Based Inhibitory Motif Is Critical for the Inhibitory Signaling Mediated by Siglecs-7 and -9, CD33-Related Siglecs Expressed on Human Monocytes and NK Cells. *The Journal of Immunology*, 173(11):6841–6849.

[Avril et al., 2005] Avril, T., Freeman, S. D., Attrill, H., Clarke, R. G., and Crocker, P. (2005). Siglec-5 (CD170) can mediate inhibitory signaling in the absence of immunoreceptor tyrosine-based inhibitory motif phosphorylation. *The Journal of biological chemistry*, 280(20):19843–19851.

[Baker et al., 2000] Baker, M., Gamble, J., Tooze, R., Higgins, D., Yang, F. T., O'Brien, P. C., Coleman, N., Pingel, S., Turner, M., and Alexander, D. R. (2000). Development of T-leukaemias in CD45 tyrosine phosphatase-deficient mutant lck mice. *The EMBO journal*, 19(17):4644–54.

[Ballek et al., 2015] Ballek, O., Valečka, J., Manning, J., and Filipp, D. (2015). The pool of preactivated Lck in the initiation of T-cell signaling: a critical re-evaluation of the Lck standby model. *Immunology and cell biology*, 93(4):384–395.

[Baqui et al., 1999] Baqui, A. A., Meiller, T. F., and Falkler, W. A. (1999). Enhanced interleukin-8 production in THP-1 human monocytic cells by lipopolysaccharide from oral microorganisms and granulocyte-macrophage colony-stimulating factor. *Oral microbiology and immunology*, 14(5):275–280.

[Barclay et al., 1997] Barclay, A. N., Brown, M. H., Law, S., McKnight, A., Tomlinson, M., and van der Merwe, P. (1997). *The Leukocyte Antigen Factsbook*. Academic Press, London, 2nd edn. edition.

[Barclay and Hatherley, 2008] Barclay, a. N. and Hatherley, D. (2008). The counterbalance theory for evolution and function of paired receptors. *Immunity*, 29(5):675–8.

[Barford, 1995] Barford, J. P. (1995). *Fundamental and Applied Aspects of Animal Cell Cultivation*. Singapore University Press, National University of Singapore.

[Barrow et al., 2011] Barrow, A. D., Raynal, N., Andersen, T. L., Slatter, D. a., Bihan, D., Pugh, N., Cella, M., Kim, T., Rho, J., Negishi-Koga, T., Delaisse, J. M., Takayanagi, H., Lorenzo, J., Colonna, M., Farndale, R. W., Choi, Y., and Trowsdale, J. (2011). OSCAR is a collagen receptor that costimulates osteoclastogenesis in DAP12-deficient humans and mice. *Journal of Clinical Investigation*, 121(9):3505–3516.

[Bartelt et al., 2009] Bartelt, R. R., Cruz-Orcutt, N., Collins, M., and Houtman, J. C. D. (2009). Comparison of T cell receptor-induced proximal signaling and downstream functions in immortalized and primary T cells. *PLoS ONE*, 4(5).

[Bashour et al., 2014] Bashour, K. T., Gondarenko, a., Chen, H., Shen, K., Liu, X., Huse, M., Hone, J. C., and Kam, L. C. (2014). CD28 and CD3 have complementary roles in T-cell traction forces. *Proceedings of the National Academy of Sciences*, 111(6):2241–2246.

[Bergman et al., 1992] Bergman, M., Mustelin, T., Oetken, C., Partanen, J., Flint, N. a., Amrein, K. E., Autero, M., Burn, P., and Alitalo, K. (1992). The human p50csk tyrosine kinase phosphorylates p56lck at Tyr-505 and down regulates its catalytic activity. *The EMBO journal*, 11(8):2919–2924.

[Billadeau and Leibson, 2002] Billadeau, D. and Leibson, P. (2002). ITAMs versus ITIMs: striking a balance during cell regulation. *Journal of Clinical Investigation*, 109(2):161–168.

[Billadeau et al., 2003] Billadeau, D. D., Upshaw, J. L., Schoon, R. a., Dick, C. J., and Leibson, P. J. (2003). NKG2D-DAP10 triggers human NK cell-mediated killing via a Syk-independent regulatory pathway. *Nature immunology*, 4(6):557–564.

[Binstadt et al., 1996] Binstadt, B. A., Brumbaugh, K. M., Dick, C. J., Scharenberg, A. M., Williams, B. L., Colonna, M., Lanier, L. L., Kinet, J. P., Abraham, R. T., and Leibson, P. J. (1996). Sequential involvement of Lck and SHP-1 with MHC-recognizing receptors on NK cells inhibits FcR-initiated tyrosine kinase activation. *Immunity*, 5(6):629–38.

[Bluemel et al., 2010] Bluemel, C., Hausmann, S., Fluhr, P., Sriskandarajah, M., Stallcup, W. B., Baeuerle, P. a., and Kufer, P. (2010). Epitope distance to the target cell membrane and antigen size determine the potency of T cell-mediated lysis by BiTE antibodies specific for a large melanoma surface antigen. *Cancer immunology, immunotherapy : CII*, 59(8):1197–209.

[Bobbitt and Justement, 2000] Bobbitt, K. R. and Justement, L. B. (2000). Regulation of MHC class II signal transduction by the B cell coreceptors CD19 and CD22. *Journal of immunology (Baltimore, Md. : 1950)*, 165(10):5588–96.

[Bodian et al., 1994] Bodian, D. L., Jones, E. Y., Harlos, K., Stuart, D. I., and Davis, S. J. (1994). Crystal structure of the extracellular region of the human cell adhesion molecule CD2 at 2.5 A resolution. *Structure (London, England : 1993)*, 2(8):755–766.

[Bonaccorsi et al., 2010] Bonaccorsi, I., Cantoni, C., Carrega, P., Oliveri, D., Lui, G., Conte, R., Navarra, M., Cavaliere, R., Traggiai, E., Gattorno, M., Martini, A., Mingari, M. C., Moretta, A., and Ferlazzo, G. (2010). The immune inhibitory receptor LAIR-1 is highly expressed by plasmacytoid dendritic cells and acts complementary with NKp44 to control IFNα production. *PloS one*, 5(11):e15080.

[Boniface et al., 1998] Boniface, J. J., Rabinowitz, J. D., Wulfing, C., Hampl, J., Reich, Z., Altman, J. D., Kantor, R. M., Beeson, C., McConnell, H. M., and Davis, M. M. (1998). Initiation of signal transduction through the T cell receptor requires the multivalent engagement of peptide/MHC ligands. *Immunity*, 9(4):459–466.

[Bouchon et al., 2000] Bouchon, A., Dietrich, J., and Colonna, M. (2000). Cutting edge: inflammatory responses can be triggered by TREM-1, a novel receptor expressed

on neutrophils and monocytes. *Journal of immunology (Baltimore, Md. : 1950)*, 164(10):4991–4995.

[Boyington et al., 2000] Boyington, J. C., Motyka, S. a., Schuck, P., Brooks, a. G., and Sun, P. D. (2000). Crystal structure of an NK cell immunoglobulin-like receptor in complex with its class I MHC ligand. *Nature*, 405(6786):537–543.

[Brandt et al., 2009] Brandt, C. S., Baratin, M., Yi, E. C., Kennedy, J., Gao, Z., Fox, B., Haldeman, B., Ostrander, C. D., Kaifu, T., Chabannon, C., Moretta, A., West, R., Xu, W., Vivier, E., and Levin, S. D. (2009). The B7 family member B7-H6 is a tumor cell ligand for the activating natural killer cell receptor NKp30 in humans. *The Journal of experimental medicine*, 206(7):1495–1503.

[Brondijk et al., 2010] Brondijk, T. H. C., Ruiter, T. D., Ballering, J., Wienk, H., Lebbink, R. J., Ingen, H. V., Boelens, R., Farndale, R. W., Meyaard, L., and Huizinga, E. G. (2010). Crystal structure and collagen-binding site of immune inhibitory receptor LAIR-1 : unexpected implications for collagen binding by platelet receptor GPVI. *Blood*, 115(7):1364–1373.

[Brown and London, 2000] Brown, D. a. and London, E. (2000). Structure and function of sphingolipid- and cholesterol-rich membrane rafts. *Journal of Biological Chemistry*, 275:17221–17224.

[Brown et al., 2007] Brown, J., O'Callaghan, C. A., Marshall, A. S. J., Gilbert, R. J. C., Siebold, C., Gordon, S., Brown, G. D., and Jones, E. Y. (2007). Structure of the fungal beta-glucan-binding immune receptor dectin-1: implications for function. *Protein science : a publication of the Protein Society*, 16(6):1042–1052.

[Brown et al., 1998] Brown, M. H., Boles, K., van der Merwe, P. a., Kumar, V., Mathew, P. a., and Barclay, a. N. (1998). 2B4, the natural killer and T cell immunoglobulin superfamily surface protein, is a ligand for CD48. *The Journal of experimental medicine*, 188(11):2083–2090.

[Bruhns, 2012] Bruhns, P. (2012). Properties of mouse and human IgG receptors and their contribution to disease models.

[Bruhns et al., 2009] Bruhns, P., Iannascoli, B., England, P., Mancardi, D. A., Fernandez, N., Jorieux, S., and Daëron, M. (2009). Specificity and affinity of human Fcgamma receptors and their polymorphic variants for human IgG subclasses. *Blood*, 113(16):3716–25.

[Brzostek et al., 2010] Brzostek, J., Chai, J.-G., Gebhardt, F., Busch, D. H., Zhao, R., van der Merwe, P. A., and Gould, K. G. (2010). Ligand dimensions are important in controlling NK-cell responses. *European journal of immunology*, 40(7):2050–9.

[Bunnell et al., 2002] Bunnell, S. C., Hong, D. I., Kardon, J. R., Yamazaki, T., McGlade, C. J., Barr, V. a., and Samelson, L. E. (2002). T cell receptor ligation induces the formation of dynamically regulated signaling assemblies. *Journal of Cell Biology*, 158(7):1263–1275.

[Burgess et al., 2003] Burgess, A. W., Cho, H. S., Eigenbrot, C., Ferguson, K. M., Garrett, T. P. J., Leahy, D. J., Lemmon, M. a., Sliwkowski, M. X., Ward, C. W., and Yokoyama, S. (2003). An open-and-shut case? Recent insights into the activation of EGF/ErbB receptors. *Molecular Cell*, 12(3):541–552.

[Burroughs et al., 2011] Burroughs, N. J., Köhler, K., Miloserdov, V., Dustin, M. L.,

van der Merwe, P. A., and Davis, D. M. (2011). Boltzmann energy-based image analysis demonstrates that extracellular domain size differences explain protein segregation at immune synapses. *PLoS Computational Biology*, 7(8):1–9.

[Burroughs et al., 2006] Burroughs, N. J., Lazic, Z., and van der Merwe, P. A. (2006). Ligand detection and discrimination by spatial relocalization: A kinase-phosphatase segregation model of TCR activation. *Biophysical journal*, 91(5):1619–29.

[Burshtyn et al., 1996] Burshtyn, D. N., Scharenberg, A. M., Wagtmann, N., Rajagopalan, S., Berrada, K., Yi, T., Kinet, J. P., and Long, E. O. (1996). Recruitment of tyrosine phosphatase HCP by the killer cell inhibitor receptor. *Immunity*, 4(1):77–85.

[Cahir McFarland et al., 1993] Cahir McFarland, E. D., Hurley, T. R., Pingel, J. T., Sefton, B. M., Shaw, A., and Thomas, M. L. (1993). Correlation between Src family member regulation by the protein-tyrosine-phosphatase CD45 and transmembrane signaling through the T-cell receptor. *Proceedings of the National Academy of Sciences of the United States of America*, 90(4):1402–6.

[Call and Wucherpfennig, 2004] Call, M. E. and Wucherpfennig, K. W. (2004). Molecular mechanisms for the assembly of the T cell receptor-CD3 complex. *Molecular Immunology*, 40(18):1295–1305.

[Call and Wucherpfennig, 2007] Call, M. E. and Wucherpfennig, K. W. (2007). Common themes in the assembly and architecture of activating immune receptors. *Nature reviews. Immunology*, 7(11):841–50.

[Campbell et al., 2004] Campbell, K. S., Yusa, S.-i., Kikuchi-Maki, A., and Catina, T. L. (2004). NKp44 triggers NK cell activation through DAP12 association that is not influenced by a putative cytoplasmic inhibitory sequence. *Journal of immunology (Baltimore, Md. : 1950)*, 172(2):899–906.

[Campi et al., 2005] Campi, G., Varma, R., and Dustin, M. L. (2005). Actin and agonist MHC-peptide complex-dependent T cell receptor microclusters as scaffolds for signaling. *The Journal of experimental medicine*, 202(8):1031–6.

[Cannons et al., 2011] Cannons, J. L., Tangye, S. G., and Schwartzberg, P. L. (2011). SLAM family receptors and SAP adaptors in immunity. *Annual review of immunology*, 29:665–705.

[Carroll-Portillo et al., 2010] Carroll-Portillo, A., Spendier, K., Pfeiffer, J., Griffiths, G., Li, H., Lidke, K. a., Oliver, J. M., Lidke, D. S., Thomas, J. L., Wilson, B. S., and Timlin, J. a. (2010). Formation of a mast cell synapse: Fc epsilon RI membrane dynamics upon binding mobile or immobilized ligands on surfaces. *Journal of immunology (Baltimore, Md. : 1950)*, 184(3):1328–1338.

[Cebecauer et al., 2005a] Cebecauer, M., Guillaume, P., Hozák, P., Mark, S., Everett, H., Schneider, P., and Luescher, I. F. (2005a). Soluble MHC-peptide complexes induce rapid death of CD8+ CTL. *Journal of immunology (Baltimore, Md. : 1950)*, 174(11):6809–6819.

[Cebecauer et al., 2005b] Cebecauer, M., Guillaume, P., Mark, S., Michielin, O., Boucheron, N., Bezard, M., Meyer, B. H., Segura, J.-M., Vogel, H., and Luescher, I. F. (2005b). CD8+ cytotoxic T lymphocyte activation by soluble major histocompatibility complex-peptide dimers. *The Journal of biological chemistry*, 280(25):23820–8.

[Chakraborty and Weiss, 2014] Chakraborty, A. K. and Weiss, A. (2014). Insights into the initiation of TCR signaling. *Nature immunology*, 15(9):798–807.

[Chang and Buehler, 2014] Chang, S. W. and Buehler, M. J. (2014). Molecular biomechanics of collagen molecules. *Materials Today*, 17(2):70–76.

[Chang et al., 2016] Chang, V. T., Fernandes, R. A., Ganzinger, K. A., Lee, S. F., Siebold, C., McColl, J., Jönsson, P., Palayret, M., Harlos, K., Coles, C. H., Jones, E. Y., Lui, Y., Huang, E., Gilbert, R. J. C., Klenerman, D., Aricescu, A. R., and Davis, S. J. (2016). Initiation of T cell signaling by CD45 segregation at 'close contacts'. *Nature Immunology*, 17(5):574–82.

[Chen et al., 2004] Chen, R., Relouzat, F., Roncagalli, R., Aoukaty, A., Tan, R., Latour, S., and Veillette, A. (2004). Molecular dissection of 2B4 signaling: implications for signal transduction by SLAM-related receptors. *Molecular and cellular biology*, 24(12):5144–5156.

[Chen and Zhu, 2013] Chen, W. and Zhu, C. (2013). Mechanical regulation of T-cell functions. *Immunological Reviews*, 256(1):160–176.

[Chen et al., 2015] Chen, X., Pan, W., Sui, Y., Li, H., Shi, X., Guo, X., Qi, H., Xu, C., and Liu, W. (2015). Acidic phospholipids govern the enhanced activation of IgG-B cell receptor. *Nature Communications*, 6:8552.

[Chen et al., 2007] Chen, X., Trivedi, P. P., Ge, B., Krzewski, K., and Strominger, J. L. (2007). Many NK cell receptors activate ERK2 and JNK1 to trigger microtubule organizing center and granule polarization and cytotoxicity. *Proceedings of the National Academy of Sciences of the United States of America*, 104(15):6329–6334.

[Cherry et al., 1998] Cherry, R. J., Wilson, K. M., Triantafilou, K., O'Toole, P., Morrison, I. E., Smith, P. R., and Fernandez, N. (1998). Detection of dimers of dimers of human leukocyte antigen (HLA)-DR on the surface of living cells by single-particle fluorescence imaging. *J Cell Biol*, 140(1):71–79.

[Chilkoti et al., 1995] Chilkoti, A., Tan, P. H., and Stayton, P. S. (1995). Site-directed mutagenesis studies of the high-affinity streptavidin-biotin complex: contributions of tryptophan residues 79, 108, and 120. *Proceedings of the National Academy of Sciences of the United States of America*, 92(5):1754–1758.

[Chlewicki et al., 2008] Chlewicki, L. K., Velikovsky, C. A., Balakrishnan, V., Mariuzza, R. a., and Kumar, V. (2008). Molecular basis of the dual functions of 2B4 (CD244). *Journal of immunology (Baltimore, Md. : 1950)*, 180(12):8159–8167.

[Choudhuri et al., 2009] Choudhuri, K., Parker, M., Milicic, A., Cole, D. K., Shaw, M. K., Sewell, A. K., Stewart-Jones, G., Dong, T., Gould, K. G., and van der Merwe, P. A. (2009). Peptide-major histocompatibility complex dimensions control proximal kinase-phosphatase balance during T cell activation. *The Journal of biological chemistry*, 284(38):26096–105.

[Choudhuri et al., 2005] Choudhuri, K., Wiseman, D., Brown, M. H., Gould, K., and van der Merwe, P. A. (2005). T-cell receptor triggering is critically dependent on the dimensions of its peptide-MHC ligand. *Nature*, 436(7050):578–82.

[Chu et al., 1998] Chu, V., Freitag, S., Le Trong, I., Stenkamp, R. E., and Stayton, P. S. (1998). Thermodynamic and structural consequences of flexible loop deletion by cir-

cular permutation in the streptavidin-biotin system. *Protein science : a publication of the Protein Society*, 7(4):848–859.

[Cochran et al., 2000] Cochran, J. R., Cameron, T. O., and Stern, L. J. (2000). The relationship of MHC-peptide binding and T cell activation probed using chemically defined MHC class II oligomers. *Immunity*, 12(3):241–250.

[Cochran et al., 2001] Cochran, J. R., Cameron, T. O., Stone, J. D., Lubetsky, J. B., and Stern, L. J. (2001). Receptor proximity, not intermolecular orientation, is critical for triggering T-cell activation. *The Journal of biological chemistry*, 276(30):28068–74.

[Connelly et al., 1990] Connelly, P. R., Varadarajan, R., Sturtevant, J. M., and Richards, F. M. (1990). Thermodynamics of protein-peptide interactions in the ribonuclease S system studied by titration calorimetry. *Biochemistry*, 29(25):6108–6114.

[Cooper et al., 1986] Cooper, J. a., Gould, K. L., Cartwright, C. a., and Hunter, T. (1986). Tyr527 is phosphorylated in pp60c-src: implications for regulation. *Science (New York, N.Y.)*, 231(4744):1431–1434.

[Cooper and Qian, 2008] Cooper, J. a. and Qian, H. (2008). A mechanism for SRC kinase-dependent signaling by noncatalytic receptors. *Biochemistry*, 47(21):5681–8.

[Cordoba et al., 2013] Cordoba, S.-P., Choudhuri, K., Zhang, H., Bridge, M., Basat, A. B., Dustin, M. L., and van der Merwe, P. A. (2013). The large ectodomains of CD45 and CD148 regulate their segregation from and inhibition of ligated T-cell receptor. *Blood*, 121(21):4295–302.

[Cosman et al., 1997] Cosman, D., Fanger, N., Borges, L., Kubin, M., Chin, W., Peterson, L., and Hsu, M. L. (1997). A novel immunoglobulin superfamily receptor for cellular and viral MHC class I molecules. *Immunity*, 7(2):273–282.

[Crites et al., 2014] Crites, T. J., Padhan, K., Muller, J., Krogsgaard, M., Gudla, P. R., Lockett, S. J., and Varma, R. (2014). TCR Microclusters pre-exist and contain molecules necessary for TCR signal transduction. *Journal of immunology (Baltimore, Md. : 1950)*, 193(1):56–67.

[Crocker et al., 2007] Crocker, P. R., Paulson, J. C., and Varki, A. (2007). Siglecs and their roles in the immune system. *Nature reviews. Immunology*, 7(4):255–266.

[Culley et al., 2009] Culley, F. J., Johnson, M., Evans, J. H., Kumar, S., Crilly, R., Casasbuenas, J., Schnyder, T., Mehrabi, M., Deonarain, M. P., Ushakov, D. S., Braud, V., Roth, G., Brock, R., Köhler, K., and Davis, D. M. (2009). Natural killer cell signal integration balances synapse symmetry and migration. *PLoS Biology*, 7(7):e1000159.

[Davis and van der Merwe, 1996] Davis, S. J. and van der Merwe, P. a. (1996). The structure and ligand interactions of CD2: implications for T-cell function. *Immunology today*, 17(4):177–87.

[Davis and van der Merwe, 2006] Davis, S. J. and van der Merwe, P. A. (2006). The kinetic-segregation model : TCR triggering and beyond. *Nature immunology*, 7(8):803–809.

[de Souza et al., 2008] de Souza, A. J., Oak, J. S., Jordanhazy, R., DeKruyff, R. H., Fruman, D. A., and Kane, L. P. (2008). T cell Ig and mucin domain-1-mediated T cell activation requires recruitment and activation of phosphoinositide 3-kinase. *Journal of immunology (Baltimore, Md. : 1950)*, 180(10):6518–6526.

[DeFord-Watts et al., 2011] DeFord-Watts, L. M., Dougall, D. S., Belkaya, S., Johnson, B. A., Eitson, J. L., Roybal, K. T., Barylko, B., Albanesi, J. P., Wülfing, C., and van Oers, N. S. C. (2011). The CD3 zeta subunit contains a phosphoinositide-binding motif that is required for the stable accumulation of TCR-CD3 complex at the immunological synapse. *Journal of immunology (Baltimore, Md. : 1950)*, 186(12):6839–47.

[Deford-Watts et al., 2009] Deford-Watts, L. M., Tassin, T. C., Becker, A. M., Medeiros, J. J., Albanesi, J. P., Love, P. E., Wülfing, C., and van Oers, N. S. C. (2009). The cytoplasmic tail of the T cell receptor CD3 epsilon subunit contains a phospholipid-binding motif that regulates T cell functions. *Journal of immunology (Baltimore, Md. : 1950)*, 183(2):1055–1064.

[Delcassian et al., 2013] Delcassian, D., Depoil, D., Rudnicka, D., Liu, M., Davis, D. M., Dustin, M. L., and Dunlop, I. E. (2013). Nanoscale ligand spacing influences receptor triggering in T cells and NK cells. *Nano letters*, 13(11):5608–14.

[Delon et al., 1998] Delon, J., Gregoire, C., Malissen, B., Darche, S., Lemaitre, F., Kourilsky, P., Abastado, J. P., Trautmann, a., Grégoire, C., and Lemaître, F. (1998). CD8 expression allows T cell signaling by monomeric peptide-MHC complexes. *Immunity*, 9(4):467–473.

[DeMond et al., 2008] DeMond, A. L., Mossman, K. D., Starr, T., Dustin, M. L., and Groves, J. T. (2008). T cell receptor microcluster transport through molecular mazes reveals mechanism of translocation. *Biophysical journal*, 94(8):3286–3292.

[Dennehy et al., 2001] Dennehy, K. M., Ferris, W. F., Veenstra, H., Zuckerman, L. A., Killeen, N., and Beyers, A. D. (2001). Determination of the tyrosine phosphorylation sites in the T cell transmembrane glycoprotein CD5. *International immunology*, 13(2):149–156.

[Dennehy et al., 2011] Dennehy, K. M., Klimosch, S. N., and Steinle, A. (2011). Cutting edge: NKp80 uses an atypical hemi-ITAM to trigger NK cytotoxicity. *Journal of immunology (Baltimore, Md. : 1950)*, 186(2):657–661.

[Depoil et al., 2008] Depoil, D., Fleire, S., Treanor, B. L., Weber, M., Harwood, N. E., Marchbank, K. L., Tybulewicz, V. L. J., and Batista, F. D. (2008). CD19 is essential for B cell activation by promoting B cell receptor-antigen microcluster formation in response to membrane-bound ligand. *Nature immunology*, 9(1):63–72.

[Desai et al., 1993] Desai, D. M., Sap, J., Schlessinger, J., and Weiss, a. (1993). Ligand-mediated negative regulation of a chimeric transmembrane receptor tyrosine phosphatase. *Cell*, 73(3):541–554.

[Dietrich et al., 2000] Dietrich, J., Cella, M., Seiffert, M., Bühring, H. J., and Colonna, M. (2000). Cutting edge: signal-regulatory protein beta 1 is a DAP12-associated activating receptor expressed in myeloid cells. *Journal of immunology (Baltimore, Md. : 1950)*, 164(1):9–12.

[Doh and Irvine, 2006] Doh, J. and Irvine, D. J. (2006). Immunological synapse arrays: patterned protein surfaces that modulate immunological synapse structure formation in T cells. *Proceedings of the National Academy of Sciences of the United States of America*, 103(15):5700–5705.

[D'Oro et al., 1996] D'Oro, U., Sakaguchi, K., Appella, E., and Ashwell, J. D. (1996). Mutational analysis of Lck in CD45-negative T cells: dominant role of tyrosine 394 phosphorylation in kinase activity. *Molecular and cellular biology*, 16(9):4996–5003.

[Doucey et al., 2001] Doucey, M. A., Legler, D. F., Boucheron, N., Cerottini, J. C., Bron, C., and Luescher, I. F. (2001). CTL activation is induced by cross-linking of TCR/MHC-peptide-CD8/p56lck adducts in rafts. *Eur J Immunol*, 31(5):1561–1570.

[Duchemin et al., 1994] Duchemin, A.-m., Ernst, L. K., and Anderson, C. L. (1994). Clustering of the High Affinity Fc Receptor for Immunoglobulin G (FcyRI) Results in Phosphorylation. *The Journal Of Biological Chemistry*, 269(16):12111–12117.

[Dushek et al., 2012] Dushek, O., Goyette, J., and van der Merwe, P. A. (2012). Non-catalytic tyrosine-phosphorylated receptors. *Immunological Reviews*, 250(1):258–276.

[Dushek and van der Merwe, 2011] Dushek, O. and van der Merwe, P. A. (2011). Mechanisms for T cell receptor triggering. *Nature reviews. Immunology*, 11(1):47–55.

[Dustin et al., 2007] Dustin, M. L., Starr, T., Varma, R., and Thomas, V. K. (2007). Supported planar bilayers for study of the immunological synapse. *Current protocols in immunology / edited by John E. Coligan ... [et al.]*, Chapter 18:Unit 18.13.

[Eggeling et al., 2009] Eggeling, C., Ringemann, C., Medda, R., Schwarzmann, G., Sandhoff, K., Polyakova, S., Belov, V. N., Hein, B., von Middendorff, C., Schönle, A., and Hell, S. W. (2009). Direct observation of the nanoscale dynamics of membrane lipids in a living cell. *Nature*, 457(7233):1159–62.

[Eiseman and Bolen, 1992] Eiseman, E. and Bolen, J. B. (1992). Engagement of the high-affinity IgE receptor activates src protein-related tyrosine kinases. *Nature*, 355(6355):78–80.

[Engel et al., 1993] Engel, P., Nojima, Y., Rothstein, D., Zhou, L. J., Wilson, G. L., Kehrl, J. H., and Tedder, T. F. (1993). The same epitope on CD22 of B lymphocytes mediates the adhesion of erythrocytes, T and B lymphocytes, neutrophils, and monocytes. *Journal of immunology (Baltimore, Md. : 1950)*, 150(11):4719–4732.

[Ernst et al., 1993] Ernst, L. K., Duchemin, A. M., and Anderson, C. L. (1993). Association of the high-affinity receptor for IgG (Fc gamma RI) with the gamma subunit of the IgE receptor. *Proceedings of the National Academy of Sciences of the United States of America*, 90(13):6023–7.

[Evan et al., 1985] Evan, G. I., Lewis, G. K., Ramsay, G., and Bishop, J. M. (1985). Isolation of monoclonal antibodies specific for human c-myc proto-oncogene product. *Molecular and cellular biology*, 5(12):3610–3616.

[Evans et al., 2005] Evans, E. J., Esnouf, R. M., Manso-Sancho, R., Gilbert, R. J. C., James, J. R., Yu, C., Fennelly, J. a., Vowles, C., Hanke, T., Walse, B., Hünig, T., Sø rensen, P., Stuart, D. I., and Davis, S. J. (2005). Crystal structure of a soluble CD28-Fab complex. *Nature immunology*, 6(3):271–9.

[Ezumi et al., 2000] Ezumi, Y., Uchiyama, T., and Takayama, H. (2000). Molecular cloning, genomic structure, chromosomal localization, and alternative splice forms of the platelet collagen receptor glycoprotein VI. *Biochemical and Biophysical Research Communications*, 277(1):27–36.

[Fairhead et al., 2014a] Fairhead, M., Krndija, D., Lowe, E. D., and Howarth, M. (2014a). Plug-and-play pairing via defined divalent streptavidins. *Journal of Molecular Biology*, 426(1):199–214.

[Fairhead et al., 2014b] Fairhead, M., Veggiani, G., Lever, M., Yan, J., Mesner, D., Robinson, C. V., Dushek, O., van der Merwe, P. A., and Howarth, M. (2014b). SpyA-

vidin hubs enable precise and ultrastable orthogonal nanoassembly. *Journal of the American Chemical Society*, 136(35):12355–63.

[Falco et al., 1999] Falco, M., Biassoni, R., Bottino, C., Vitale, M., Sivori, S., Augugliaro, R., Moretta, L., and Moretta, A. (1999). Identification and molecular cloning of p75/AIRM1, a novel member of the sialoadhesin family that functions as an inhibitory receptor in human natural killer cells. *Journal of Experimental Medicine*, 190(6):793–802.

[Feng et al., 2006] Feng, J., Call, M. E., and Wucherpfennig, K. W. (2006). The assembly of diverse immune receptors is focused on a polar membrane-embedded interaction site. *PLoS Biology*, 4(5):768–779.

[Fernandes et al., 2010] Fernandes, R. a., Yu, C., Carmo, A. M., Evans, E. J., Anton van der Merwe, P., and Davis, S. J. (2010). What Controls T Cell Receptor Phosphorylation? *Cell*, 142(5):668–669.

[Fernandez-Miguel et al., 1999] Fernandez-Miguel, G., Alarcon, B., Iglesias, A., Bluethmann, H., Alvarez-Mon, M., Sanz, E., and de la Hera, A. (1999). Multivalent structure of an $\alpha\beta$T cell receptor. *Proceedings of the National Academy of Sciences*, 96(4):1547–1552.

[Field et al., 1988] Field, J., Nikawa, J., Broek, D., MacDonald, B., Rodgers, L., Wilson, I. A., Lerner, R. A., and Wigler, M. (1988). Purification of a RAS-responsive adenylyl cyclase complex from Saccharomyces cerevisiae by use of an epitope addition method. *Molecular and cellular biology*, 8(5):2159–2165.

[Filipp et al., 2012] Filipp, D., Ballek, O., and Manning, J. (2012). Lck, membrane microdomains, and TCR triggering machinery: Defining the new rules of engagement. *Frontiers in Immunology*, 3(JUN):1–14.

[Fishler et al., 2012] Fishler, R., Artzy-Schnirman, A., Peer, E., Wolchinsky, R., Brener, R., Waks, T., Eshhar, Z., Reiter, Y., and Sivan, U. (2012). Mixed alkanethiol monolayers on submicrometric gold patterns: a controlled platform for studying cell-ligand interactions. *Nano letters*, 12(9):4992–6.

[Fleit and Kobasiuk, 1991] Fleit, H. B. and Kobasiuk, C. D. (1991). The human monocyte-like cell line THP-1 expresses Fc gamma RI and Fc gamma RII. *Journal of leukocyte biology*, 49(6):556–565.

[Florian et al., 2006] Florian, S., Sonneck, K., Czerny, M., Hennersdorf, F., Hauswirth, a. W., Bühring, H.-J., and Valent, P. (2006). Detection of novel leukocyte differentiation antigens on basophils and mast cells by HLDA8 antibodies. *Allergy*, 61(9):1054–62.

[Fournier et al., 2000] Fournier, N., Chalus, L., Durand, I., Garcia, E., Pin, J. J., Churakova, T., Patel, S., Zlot, C., Gorman, D., Zurawski, S., Abrams, J., Bates, E. E., and Garrone, P. (2000). FDF03, a novel inhibitory receptor of the immunoglobulin superfamily, is expressed by human dendritic and myeloid cells. *Journal of immunology (Baltimore, Md. : 1950)*, 165(3):1197–1209.

[Fujimoto et al., 2000] Fujimoto, M., Fujimoto, Y., Poe, J. C., Jansen, P. J., Lowell, C. A., DeFranco, A. L., and Tedder, T. F. (2000). CD19 regulates Src family protein tyrosine kinase activation in B lymphocytes through processive amplification. *Immunity*, 13(1):47–57.

[Gagnon et al., 2010] Gagnon, E., Xu, C., Yang, W., Chu, H. H., Call, M. E., Chou, J. J.,

and Wucherpfennig, K. W. (2010). Response Multilayered Control of T Cell Receptor Phosphorylation. *Cell*, 142(5):669–671.

[Garrity et al., 2005] Garrity, D., Call, M. E., Feng, J., and Wucherpfennig, K. W. (2005). The activating NKG2D receptor assembles in the membrane with two signaling dimers into a hexameric structure. *Proceedings of the National Academy of Sciences of the United States of America*, 102(21):7641–7646.

[Gasparrini et al., 2015] Gasparrini, F., Feest, C., Bruckbauer, A., Mattila, P. K., Müller, J., Nitschke, L., Bray, D., and Batista, F. D. (2015). Nanoscale organization and dynamics of the siglec CD22 cooperate with the cytoskeleton in restraining BCR signalling. *The EMBO journal*, page e201593027.

[Ge et al., 2002] Ge, Q., Stone, J. D., Thompson, M. T., Cochran, J. R., Rushe, M., Eisen, H. N., Chen, J., and Stern, L. J. (2002). Soluble peptide-MHC monomers cause activation of CD8+ T cells through transfer of the peptide to T cell MHC molecules. *Proc Natl Acad Sci U S A*, 99(21):13729–13734.

[Geppert and Lipsky, 1987] Geppert, T. D. and Lipsky, P. E. (1987). Accessory cell independent proliferation of human T4 cells stimulated by immobilized monoclonal antibodies to CD3. *Journal of immunology (Baltimore, Md. : 1950)*, 138(6):1660–6.

[Ghosh et al., 2012] Ghosh, S., Saha, S., Goswami, D., Bilgrami, S., and Mayor, S. (2012). *Dynamic imaging of homo-FRET in live cells by fluorescence anisotropy microscopy*, volume 505.

[Gil et al., 2002] Gil, D., Schamel, W. W., Montoya, M., Sánchez-Madrid, F., and Alarcón, B. (2002). Recruitment of Nck by CD3Ïţ Reveals a Ligand-Induced Conformational Change Essential for T Cell Receptor Signaling and Synapse Formation. *Cell*, 109(7):901–912.

[Gil et al., 2005] Gil, D., Schrum, A., Alarcón, B., and Palmer, E. (2005). T cell receptor engagement by peptide-MHC ligands induces a conformational change in the CD3 complex of thymocytes. *Journal of Experimental Medicine*, 201(4):517–522.

[Glebov and Nichols, 2004] Glebov, O. O. and Nichols, B. J. (2004). Lipid raft proteins have a random distribution during localized activation of the T-cell receptor. *Nature cell biology*, 6(3):238–243.

[Goodridge et al., 2011] Goodridge, H. S., Reyes, C. N., Becker, C. a., Katsumoto, T. R., Ma, J., Wolf, A. J., Bose, N., Chan, A. S. H., Magee, A. S., Danielson, M. E., Weiss, A., Vasilakos, J. P., and Underhill, D. M. (2011). Activation of the innate immune receptor Dectin-1 upon formation of a 'phagocytic synapse'. *Nature*, 472(7344):471–5.

[Gotoh and Matsumoto, 2007] Gotoh, H. and Matsumoto, Y. (2007). Cell-surface streptavidin fusion protein for rapid selection of transfected mammalian cells. *Gene*, 389(2):146–153.

[Graham et al., 2012] Graham, L. M., Gupta, V., Schafer, G., Reid, D. M., Kimberg, M., Dennehy, K. M., Hornsell, W. G., Guler, R., Campanero-Rhodes, M. a., Palma, A. S., Feizi, T., Kim, S. K., Sobieszczuk, P., Willment, J. a., and Brown, G. D. (2012). The C-type lectin receptor CLECSF8 (CLEC4D) is expressed by myeloid cells and triggers cellular activation through syk kinase. *Journal of Biological Chemistry*, 287(31):25964–25974.

[Green et al., 2003] Green, D. R., Droin, N., and Pinkoski, M. (2003). Activation-induced cell death in T cells. *Immunological reviews*, 193:70–81.

[Green, 1990] Green, N. M. (1990). Avidin and streptavidin. *Methods in Enzymology*, 184:51–67.

[Grupp et al., 1995] Grupp, S. A., Mitchell, R. N., Schreiber, K. L., McKean, D. J., and Abbas, A. K. (1995). Molecular mechanisms that control expression of the B lymphocyte antigen receptor complex. *J Exp Med*, 181(1):161–168.

[Gupta and DeFranco, 2007] Gupta, N. and DeFranco, A. L. (2007). Lipid rafts and B cell signaling. *Seminars in cell & developmental biology*, 18(5):616–26.

[Hagan et al., 2010] Hagan, R. M., Björnsson, R., McMahon, S. A., Schomburg, B., Braithwaite, V., Bühl, M., Naismith, J. H., and Schwarz-Linek, U. (2010). NMR Spectroscopic and Theoretical Analysis of a Spontaneously Formed Lys-Asp Isopeptide Bond. *Angewandte Chemie*, 122(45):8599–8603.

[Han et al., 2005] Han, S., Collins, B. E., Bengtson, P., and Paulson, J. C. (2005). Homomultimeric complexes of CD22 in B cells revealed by protein-glycan cross-linking. *Nature chemical biology*, 1(2):93–97.

[Harder and Sangani, 2009] Harder, T. and Sangani, D. (2009). Plasma membrane rafts engaged in T cell signalling: new developments in an old concept. *Cell communication and signaling : CCS*, 7:21.

[Harrison, 1993] Harrison, S. C. (1993). CD4: structure and interactions of an immunoglobulin superfamily adhesion molecule. *Accounts of Chemical Research*, 26(8):449–453.

[Hashimoto-Tane et al., 2010] Hashimoto-Tane, A., Yokosuka, T., Ishihara, C., Sakuma, M., Kobayashi, W., and Saito, T. (2010). T-cell receptor microclusters critical for T-cell activation are formed independently of lipid raft clustering. *Molecular and cellular biology*, 30(14):3421–9.

[Hayashi et al., 2004] Hayashi, A., Ohnishi, H., Okazawa, H., Nakazawa, S., Ikeda, H., Motegi, S.-i., Aoki, N., Kimura, S., Mikuni, M., and Matozaki, T. (2004). Positive Regulation of Phagocytosis by SIRPβ and Its Signaling Mechanism in Macrophages. *Journal of Biological Chemistry*, 279(28):29450 –29460.

[He et al., 2002] He, X., Woodford-Thomas, T. a., Johnson, K. G., Shah, D. D., and Thomas, M. L. (2002). Targeting of CD45 protein tyrosine phosphatase activity to lipid microdomains on the T cell surface inhibits TCR signaling. *European journal of immunology*, 32(9):2578–87.

[Hecht et al., 2009] Hecht, M.-l., Rosental, B., Horlacher, T., Hershkovitz, O., Paz, J. L. D., Noti, C., Schauer, S., Porgador, A., and Seeberger, P. H. (2009). Natural Cytotoxicity Receptors NKp30 , NKp44 and NKp46 Bind to Different Heparan Sulfate / Heparin Sequences. *Journal of proteome research*, 8(2):712–720.

[Hendrickson et al., 1989] Hendrickson, W. A., Pähler, A., Smith, J. L., Satow, Y., Merritt, E. A., and Phizackerley, R. P. (1989). Crystal structure of core streptavidin determined from multiwavelength anomalous diffraction of synchrotron radiation. *Proceedings of the National Academy of Sciences of the United States of America*, 86(7):2190–2194.

[Hermiston et al., 2009] Hermiston, M. L., Zikherman, J., and Zhu, J. W. (2009). CD45,

CD148, and Lyp/Pep: critical phosphatases regulating Src family kinase signaling networks in immune cells. *Immunological reviews*, 228(1):288–311.

[Herr et al., 2003] Herr, A. B., Ballister, E. R., and Bjorkman, P. J. (2003). Insights into IgA-mediated immune responses from the crystal structures of human FcalphaRI and its complex with IgA1-Fc. *Nature*, 423(6940):614–620.

[Herrmann et al., 2014] Herrmann, J., Berberich, H., Hartmann, J., Beyer, S., Davies, K., and Koch, J. (2014). Homo-oligomerization of the activating natural killer cell receptor NKp30 ectodomain increases its binding affinity for cellular ligands. *Journal of Biological Chemistry*, 289(2):765–777.

[Hoerter et al., 2013] Hoerter, J. a. H., Brzostek, J., Artyomov, M. N., Abel, S. M., Casas, J., Rybakin, V., Ampudia, J., Lotz, C., Connolly, J. M., Chakraborty, A. K., Gould, K. G., and Gascoigne, N. R. J. (2013). Coreceptor affinity for MHC defines peptide specificity requirements for TCR interaction with coagonist peptide-MHC. *The Journal of experimental medicine*, 210(9):1807–21.

[Hoffmann et al., 2007] Hoffmann, S. C., Schellack, C., Textor, S., Konold, S., Schmitz, D., Cerwenka, A., Pflanz, S., and Watzl, C. (2007). Identification of CLEC12B, an inhibitory receptor on myeloid cells. *Journal of Biological Chemistry*, 282:22370–22375.

[Hombach et al., 2000] Hombach, A., Heuser, C., Gerken, M., Fischer, B., Lewalter, K., Diehl, V., Pohl, C., and Abken, H. (2000). T cell activation by recombinant FcepsilonRI gamma-chain immune receptors: an extracellular spacer domain impairs antigen-dependent T cell activation but not antigen recognition. *Gene therapy*, 7(12):1067–1075.

[Hombach et al., 2007] Hombach, A. a., Schildgen, V., Heuser, C., Finnern, R., Gilham, D. E., and Abken, H. (2007). T cell activation by antibody-like immunoreceptors: the position of the binding epitope within the target molecule determines the efficiency of activation of redirected T cells. *Journal of immunology (Baltimore, Md. : 1950)*, 178(7):4650–7.

[Hopp et al., 1988] Hopp, T. P., Prickett, K. S., Price, V. L., Libby, R. T., March, C. J., Pat Cerretti, D., Urdal, D. L., and Conlon, P. J. (1988). A Short Polypeptide Marker Sequence Useful for Recombinant Protein Identification and Purification.

[Horejsí, 2005] Horejsí, V. (2005). Lipid rafts and their roles in T-cell activation. *Microbes and infection / Institut Pasteur*, 7(2):310–6.

[Hornbeck et al., 2012] Hornbeck, P. V., Kornhauser, J. M., Tkachev, S., Zhang, B., Skrzypek, E., Murray, B., Latham, V., and Sullivan, M. (2012). PhosphoSitePlus: a comprehensive resource for investigating the structure and function of experimentally determined post-translational modifications in man and mouse. *Nucleic acids research*, 40(Database issue):D261–70.

[Howard et al., 1990] Howard, F. D., Rodewald, H. R., Kinet, J. P., and Reinherz, E. L. (1990). CD3 zeta subunit can substitute for the gamma subunit of Fc epsilon receptor type I in assembly and functional expression of the high-affinity IgE receptor: evidence for interreceptor complementation. *Proceedings of the National Academy of Sciences of the United States of America*, 87(18):7015–9.

[Howarth et al., 2006] Howarth, M., Chinnapen, D. J.-F., Gerrow, K., Dorrestein, P. C., Grandy, M. R., Kelleher, N. L., El-Husseini, A., and Ting, A. Y. (2006). A monovalent

streptavidin with a single femtomolar biotin binding site. *Nature methods*, 3(4):267–273.

[Howarth et al., 2008] Howarth, M., Liu, W., Puthenveetil, S., Zheng, Y., Marshall, L. F., Schmidt, M. M., Wittrup, K. D., Bawendi, M. G., and Ting, A. Y. (2008). Monovalent, reduced-size quantum dots for imaging receptors on living cells. *Nature methods*, 5(5):397–399.

[Howarth and Ting, 2008] Howarth, M. and Ting, A. Y. (2008). Imaging proteins in live mammalian cells with biotin ligase and monovalent streptavidin. *Nature protocols*, 3(3):534–545.

[Hsu et al., 2012] Hsu, C.-J., Hsieh, W.-T., Waldman, A., Clarke, F., Huseby, E. S., Burkhardt, J. K., and Baumgart, T. (2012). Ligand mobility modulates immunological synapse formation and T cell activation. *PloS one*, 7(2):e32398.

[Huang et al., 2013] Huang, J., Brameshuber, M., Zeng, X., Xie, J., Li, Q.-j., Chien, Y.-h., Valitutti, S., and Davis, M. M. (2013). A single peptide-major histocompatibility complex ligand triggers digital cytokine secretion in CD4(+) T cells. *Immunity*, 39(5):846–57.

[Hudecek et al., 2013] Hudecek, M., Lupo-Stanghellini, M. T., Kosasih, P. L., Sommermeyer, D., Jensen, M. C., Rader, C., and Riddell, S. R. (2013). Receptor affinity and extracellular domain modifications affect tumor recognition by ROR1-specific chimeric antigen receptor T cells. *Clinical Cancer Research*, 19(12):3153–3164.

[Hui and Vale, 2014] Hui, E. and Vale, R. D. (2014). In vitro membrane reconstitution of the T-cell receptor proximal signaling network. *Nature structural & molecular biology*, 21(2):133–42.

[Hünig and Dennehy, 2005] Hünig, T. and Dennehy, K. (2005). CD28 superagonists: Mode of action and therapeutic potential. *Immunology Letters*, 100:21–28.

[Huppa et al., 2010] Huppa, J. B., Axmann, M., Mörtelmaier, M. a., Lillemeier, B. F., Newell, E. W., Brameshuber, M., Klein, L. O., Schütz, G. J., and Davis, M. M. (2010). TCR-peptide-MHC interactions in situ show accelerated kinetics and increased affinity. *Nature*, 463(7283):963–967.

[Hurley et al., 1993] Hurley, T. R., Hyman, R., and Sefton, B. M. (1993). Differential effects of expression of the CD45 tyrosine protein phosphatase on the tyrosine phosphorylation of the lck, fyn, and c-src tyrosine protein kinases. *Molecular and cellular biology*, 13(3):1651–6.

[Huse et al., 2007] Huse, M., Klein, L. O., Girvin, A. T., Faraj, J. M., Li, Q. J., Kuhns, M. S., and Davis, M. M. (2007). Spatial and Temporal Dynamics of T Cell Receptor Signaling with a Photoactivatable Agonist. *Immunity*, 27(1):76–88.

[Husson et al., 2011] Husson, J., Chemin, K., Bohineust, A., Hivroz, C., and Henry, N. (2011). Force generation upon T cell receptor engagement. *PloS one*, 6(5):e19680.

[Ikehara et al., 2004] Ikehara, Y., Ikehara, S. K., and Paulson, J. C. (2004). Negative regulation of T cell receptor signaling by Siglec-7 (p70/AIRM) and Siglec-9. *The Journal of biological chemistry*, 279(41):43117–43125.

[Ikemizu et al., 2000] Ikemizu, S., Gilbert, R. J., Fennelly, J. a., Collins, a. V., Harlos, K., Jones, E. Y., Stuart, D. I., and Davis, S. J. (2000). Structure and dimerization of a soluble form of B7-1. *Immunity*, 12(1):51–60.

[Imbert et al., 1994] Imbert, V., Peyron, J. F., Farahi Far, D., Mari, B., Auberger, P., and Rossi, B. (1994). Induction of tyrosine phosphorylation and T-cell activation by vanadate peroxide, an inhibitor of protein tyrosine phosphatases. *The Biochemical journal*, 297 (Pt 1:163–173.

[Indik et al., 1994] Indik, Z. K., Hunter, S., Huang, M. M., Pan, X. Q., Chien, P., Kelly, C., Levinson, A. I., Kimberly, R. P., and Schreiber, A. D. (1994). The high affinity Fc gamma receptor (CD64) induces phagocytosis in the absence of its cytoplasmic domain: the gamma subunit of Fc gamma RIIIA imparts phagocytic function to Fc gamma RI. *Experimental hematology*, 22(7):599–606.

[Irles et al., 2003] Irles, C., Symons, A., Michel, F., Bakker, T. R., van der Merwe, P. A., and Acuto, O. (2003). CD45 ectodomain controls interaction with GEMs and Lck activity for optimal TCR signaling. *Nature immunology*, 4(2):189–97.

[Irvine et al., 2002] Irvine, D. J., Purbhoo, M. a., Krogsgaard, M., and Davis, M. M. (2002). Direct observation of ligand recognition by T cells. *Nature*, 419(6909):845–849.

[Jackson et al., 1997] Jackson, D. E., Kupcho, K. R., and Newman, P. J. (1997). Characterization of phosphotyrosine binding motifs in the cytoplasmic domain of platelet/endothelial cell adhesion molecule-1 (PECAM-1) that are required for the cellular association and activation of the protein-tyrosine phosphatase, SHP-2. *The Journal of biological chemistry*, 272(40):24868–24875.

[James et al., 2011] James, J. R., McColl, J., Oliveira, M. I., Dunne, P. D., Huang, E., Jansson, A., Nilsson, P., Sleep, D. L., Gonçalves, C. M., Morgan, S. H., Felce, J. H., Mahen, R., Fernandes, R. a., Carmo, A. M., Klenerman, D., and Davis, S. J. (2011). The T cell receptor triggering apparatus is composed of monovalent or monomeric proteins. *The Journal of biological chemistry*, 286(37):31993–2001.

[James and Vale, 2012] James, J. R. and Vale, R. D. (2012). Biophysical mechanism of T-cell receptor triggering in a reconstituted system. *Nature*, 487(7405):64–9.

[James et al., 2007] James, J. R., White, S. S., Clarke, R. W., Johansen, A. M., Dunne, P. D., Sleep, D. L., Fitzgerald, W. J., Davis, S. J., and Klenerman, D. (2007). Single-molecule level analysis of the subunit composition of the T cell receptor on live T cells. *Proceedings of the National Academy of Sciences*, 104(45):17662–17667.

[James et al., 2008] James, S. E., Greenberg, P. D., Jensen, M. C., Lin, Y., Wang, J., Till, B. G., Raubitschek, A. a., Forman, S. J., and Press, O. W. (2008). Antigen sensitivity of CD22-specific chimeric TCR is modulated by target epitope distance from the cell membrane. *Journal of immunology (Baltimore, Md. : 1950)*, 180(10):7028–38.

[Janes et al., 2000] Janes, P. W., Ley, S. C., Magee, a. I., and Kabouridis, P. S. (2000). The role of lipid rafts in T cell antigen receptor (TCR) signalling. *Seminars in immunology*, 12(1):23–34.

[Ji et al., 1992] Ji, X., Zhang, P., Armstrong, R. N., and Gilliland, G. L. (1992). The three-dimensional structure of a glutathione S-transferase from the mu gene class. Structural analysis of the binary complex of isoenzyme 3-3 and glutathione at 2.2-A resolution. *Biochemistry*, 31(42):10169–10184.

[Jiang and Barclay, 2009] Jiang, L. and Barclay, N. a. (2009). New assay to detect low-affinity interactions and characterization of leukocyte receptors for collagen encluding

leukocyte-associated Ig-like receptor-1 (LAIR-1). *European Journal of Immunology*, 39:1167–1175.

[Jimenez-Perez et al., 2012] Jimenez-Perez, M. I., Jave-Suarez, L. F., Ortiz-Lazareno, P. C., Bravo-Cuellar, A., Gonzalez-Ramella, O., Aguilar-Lemarroy, A., Hernandez-Flores, G., Pereira-Suarez, A. L., Daneri-Navarro, A., and del Toro-Arreola, S. (2012). Cervical cancer cell lines expressing NKG2D-ligands are able to down-modulate the NKG2D receptor on NKL cells with functional implications. *BMC Immunology*, 13(1):7.

[Johnson et al., 2000] Johnson, K. G., Bromley, S. K., Dustin, M. L., and Thomas, M. L. (2000). A supramolecular basis for CD45 tyrosine phosphatase regulation in sustained T cell activation. *Proceedings of the National Academy of Sciences of the United States of America*, 97(18):10138–43.

[Joyce et al., 2011] Joyce, M. G., Tran, P., Zhuravleva, M. A., Jaw, J., Colonna, M., and Sun, P. D. (2011). Crystal structure of human natural cytotoxicity receptor NKp30 and identification of its ligand binding site. *Proceedings of the National Academy of Sciences of the United States of America*, 108(15):6223–6228.

[Juang et al., 2010] Juang, J., Ebert, P. J. R., Feng, D., Garcia, K. C., Krogsgaard, M., and Davis, M. M. (2010). Peptide-MHC heterodimers show that thymic positive selection requires a more restricted set of self-peptides than negative selection. *The Journal of experimental medicine*, 207(6):1223–34.

[Judokusumo et al., 2012] Judokusumo, E., Tabdanov, E., Kumari, S., Dustin, M. L., and Kam, L. C. (2012). Mechanosensing in T lymphocyte activation. *Biophysical journal*, 102(2):L5–L7.

[Kabat et al., 2002] Kabat, J., Borrego, F., Brooks, A., and Coligan, J. E. (2002). Role that each NKG2A immunoreceptor tyrosine-based inhibitory motif plays in mediating the human CD94/NKG2A inhibitory signal. *Journal of immunology (Baltimore, Md. : 1950)*, 169(4):1948–58.

[Kabouridis, 2006] Kabouridis, P. S. (2006). Lipid rafts in T cell receptor signalling . *Molecular membrane biology*, 23(February):49–57.

[Kada et al., 1999] Kada, G., Falk, H., and Gruber, H. J. (1999). Accurate measurement of avidin and streptavidin in crude biofluids with a new, optimized biotin-fluorescein conjugate. *Biochimica et Biophysica Acta - General Subjects*, 1427(1):33–43.

[Kang et al., 2015] Kang, X., Lu, Z., Cui, C., Deng, M., Fan, Y., Dong, B., Han, X., Xie, F., Tyner, J. W., Coligan, J. E., Collins, R. H., Xiao, X., You, M. J., and Zhang, C. C. (2015). The ITIM-containing receptor LAIR1 is essential for acute myeloid leukaemia development. *Nature Cell Biology*, 17(5):665–677.

[Kaye and Janeway Jr., 1984] Kaye, J. and Janeway Jr., C. A. (1984). The Fab fragment of a directly activating monoclonal antibody that precipitates a disulfide-linked heterodimer from a helper T cell clone blocks activation by either allogeneic Ia or antigen and self-Ia. *J Exp Med*, 159(5):1397–1412.

[Keefe et al., 2001] Keefe, A. D., Wilson, D. S., Seelig, B., and Szostak, J. W. (2001). One-step purification of recombinant proteins using a nanomolar-affinity streptavidin-binding peptide, the SBP-Tag. *Protein expression and purification*, 23(3):440–446.

[Ketchum et al., 2014] Ketchum, C., Miller, H., Song, W., and Upadhyaya, A. (2014). Lig-

and mobility regulates B cell receptor clustering and signaling activation. *Biophysical Journal*, 106(1):26–36.

[Kharitonenkov et al., 1997] Kharitonenkov, A., Chen, Z., Sures, I., Wang, H., Schilling, J., and Ullrich, A. (1997). A family of proteins that inhibit signalling through tyrosine kinase receptors. *Nature*, 386(6621):181–186.

[Kim et al., 2009] Kim, S. T., Takeuchi, K., Sun, Z. Y. J., Touma, M., Castro, C. E., Fahmy, A., Lang, M. J., Wagner, G., and Reinherz, E. L. (2009). The $\alpha\beta$ T cell receptor is an anisotropic mechanosensor. *Journal of Biological Chemistry*, 284(45):31028–31037.

[Kim et al., 2006] Kim, Y.-M., Pan, J. Y.-J., Korbel, G. a., Peperzak, V., Boes, M., and Ploegh, H. L. (2006). Monovalent ligation of the B cell receptor induces receptor activation but fails to promote antigen presentation. *Proceedings of the National Academy of Sciences of the United States of America*, 103:3327–3332.

[Kiyoshi et al., 2015] Kiyoshi, M., Caaveiro, J. M. M., Kawai, T., Tashiro, S., Ide, T., Asaoka, Y., Hatayama, K., and Tsumoto, K. (2015). Structural basis for binding of human IgG1 to its high-affinity human receptor FcγRI. *Nature communications*, 6:6866.

[Klages et al., 1994] Klages, S., Adam, D., Class, K., Fargnoli, J., Bolen, J. B., and Penhallow, R. C. (1994). Ctk: a protein-tyrosine kinase related to Csk that defines an enzyme family. *Proceedings of the National Academy of Sciences USA*, 91:2597–2601.

[Knabel et al., 2002] Knabel, M., Franz, T. J., Schiemann, M., Wulf, A., Villmow, B., Schmidt, B., Bernhard, H., Wagner, H., and Busch, D. H. (2002). Reversible MHC multimer staining for functional isolation of T-cell populations and effective adoptive transfer. *Nature medicine*, 8(6):631–637.

[Koegl et al., 1994] Koegl, M., Zlatkine, P., Ley, S. C., Courtneidge, S. A., and Magee, A. I. (1994). Palmitoylation of multiple Src-family kinases at a homologous N-terminal motif. *The Biochemical journal*, 303 (Pt 3:749–53.

[Köhler et al., 2010] Köhler, K., Xiong, S., Brzostek, J., Mehrabi, M., Eissmann, P., Harrison, A., Cordoba, S.-P., Oddos, S., Miloserdov, V., Gould, K., Burroughs, N. J., van der Merwe, P. A., and Davis, D. M. (2010). Matched sizes of activating and inhibitory receptor/ligand pairs are required for optimal signal integration by human natural killer cells. *PloS one*, 5(11):e15374.

[Korndörfer and Skerra, 2002] Korndörfer, I. P. and Skerra, A. (2002). Improved affinity of engineered streptavidin for the Strep-tag II peptide is due to a fixed open conformation of the lid-like loop at the binding site. *Protein science : a publication of the Protein Society*, 11(4):883–893.

[Krishna et al., 1992] Krishna, S., Benaroch, P., and Pillai, S. (1992). Tetrameric cell-surface MHC class I molecules. *Nature*, 357(6374):164–167.

[Krogsgaard et al., 2005] Krogsgaard, M., Li, Q.-J., Sumen, C., Huppa, J. B., Huse, M., and Davis, M. M. (2005). Agonist/endogenous peptide-MHC heterodimers drive T cell activation and sensitivity. *Nature*, 434(7030):238–43.

[Kuhns and Davis, 2008] Kuhns, M. S. and Davis, M. M. (2008). The Safety on the TCR Trigger. *Cell*, 135(4):594–596.

[Kuhns et al., 2010] Kuhns, M. S., Girvin, A. T., Klein, L. O., Chen, R., Jensen, K. D. C., Newell, E. W., Huppa, J. B., Lillemeier, B. F., Huse, M., Chien, Y.-h., Garcia, K. C., and Davis, M. M. (2010). Evidence for a functional sidedness to the $\alpha\beta$TCR. *Proc. Natl. Acad. Sci. USA*, 107(11):5094–5099.

[Kumar et al., 2011] Kumar, R., Ferez, M., Swamy, M., Arechaga, I., Rejas, M. T., Valpuesta, J. M., Schamel, W. W. a., Alarcon, B., and van Santen, H. M. (2011). Increased Sensitivity of Antigen-Experienced T Cells through the Enrichment of Oligomeric T Cell Receptor Complexes. *Immunity*, 35(3):375–387.

[Kuno et al., 1993] Kuno, K., Okamoto, S. I., Hirose, K., Murakami, S., and Matsushima, K. (1993). Structure and function of the intracellular portion of the mouse interleukin 1 receptor (type I): Determining the essential region for transducing signals to activate the interleukin 8 gene. *Journal of Biological Chemistry*, 268(18):13510–13518.

[Kuokkanen et al., 2015] Kuokkanen, E., Šuštar, V., and Mattila, P. K. (2015). Molecular Control of B Cell Activation and Immunological Synapse Formation. *Traffic*, 16(4):311–326.

[Kurlander and Gartrell, 1983] Kurlander, R. J. and Gartrell, J. E. (1983). The binding and processing of monoclonal human IgG1 by cells of a human macrophage-like cell line (U937). *Blood*, 62(3):652–662.

[Laitinen et al., 2001] Laitinen, O. H., Marttila, A. T., Airenne, K. J., Kulik, T., Livnah, O., Bayer, E. A., Wilchek, M., and Kulomaa, M. S. (2001). Biotin induces tetramerization of a recombinant monomeric avidin. A model for protein-protein interactions. *Journal of Biological Chemistry*, 276(11):8219–8224.

[Laitinen et al., 2003] Laitinen, O. H., Nordlund, H. R., Hytönen, V. P., Uotila, S. T. H., Marttila, A. T., Savolainen, J., Airenne, K. J., Livnah, O., Bayer, E. A., Wilchek, M., and Kulomaa, M. S. (2003). Rational design of an active avidin monomer. *Journal of Biological Chemistry*, 278(6):4010–4014.

[Lamla and Erdmann, 2004] Lamla, T. and Erdmann, V. A. (2004). The Nano-tag, a streptavidin-binding peptide for the purification and detection of recombinant proteins. *Protein Expression and Purification*, 33(1):39–47.

[Lanier, 2009] Lanier, L. L. (2009). DAP10- and DAP12-associated receptors in innate immunity. *Immunological Reviews*, 227(1):150–160.

[Lanier et al., 1998] Lanier, L. L., Corliss, B. C., Wu, J., Leong, C., and Phillips, J. H. (1998). Immunoreceptor DAP12 bearing a tyrosine-based activation motif is involved in activating NK cells. *Nature*, 391(6668):703–707.

[Latour et al., 2003] Latour, S., Roncagalli, R., Chen, R., Bakinowski, M., Shi, X., Schwartzberg, P. L., Davidson, D., and Veillette, A. (2003). Binding of SAP SH2 domain to FynT SH3 domain reveals a novel mechanism of receptor signalling in immune regulation. *Nature cell biology*, 5(2):149–154.

[Le Borgne and Shaw, 2012] Le Borgne, M. and Shaw, A. S. (2012). SAP signaling: a dual mechanism of action. *Immunity*, 36(6):899–901.

[Lebbink et al., 2006] Lebbink, R. J., de Ruiter, T., Adelmeijer, J., Brenkman, A. B., van Helvoort, J. M., Koch, M., Farndale, R. W., Lisman, T., Sonnenberg, A., Lenting, P. J., and Meyaard, L. (2006). Collagens are functional, high affinity ligands for the inhibitory immune receptor LAIR-1. *The Journal of experimental medicine*, 203(6):1419–25.

[Lee et al., 2009] Lee, H.-M., Yuk, J.-M., Shin, D.-M., and Jo, E.-K. (2009). Dectin-1 is Inducible and Plays an Essential Role for Mycobacteria-Induced Innate Immune Responses in Airway Epithelial Cells. *Journal of Clinical Immunology*, 29(6):795–805.

[Lee et al., 2011] Lee, J., Su, E. W., Zhu, C., Hainline, S., Phuah, J., Moroco, J. A., Smithgall, T. E., Kuchroo, V. K., and Kane, L. P. (2011). Phosphotyrosine-dependent coupling of Tim-3 to T-cell receptor signaling pathways. *Molecular and cellular biology*, 31(19):3963–3974.

[Lee et al., 2004] Lee, J. K., Boles, K. S., and Mathew, P. A. (2004). Molecular and functional characterization of a CS1 (CRACC) splice variant expressed in human NK cells that does not contain immunoreceptor tyrosine-based switch motifs. *European journal of immunology*, 34(10):2791–2799.

[Lee et al., 2015] Lee, M. S., Glassman, C. R., Deshpande, N. R., Badgandi, H. B., Parrish, H. L., Uttamapinant, C., Stawski, P. S., Ting, A. Y., and Kuhns, M. S. (2015). A Mechanical Switch Couples T Cell Receptor Triggering to the Cytoplasmic Juxtamembrane Regions of CD3$\zeta\zeta$. *Immunity*, 43(2):227–239.

[Lee and Tolar, 2013] Lee, W. Y. and Tolar, P. (2013). Activation of the B cell receptor leads to increased membrane proximity of the Igα cytoplasmic domain. *PLoS ONE*, 8(11):e79148.

[Leupin et al., 2000] Leupin, O., Zaru, R., Laroche, T., Müller, S., and Valitutti, S. (2000). Exclusion of CD45 from the T-cell receptor signaling area in antigen-stimulated T lymphocytes. *Current Biology*, 10(5):277–280.

[Li et al., 2014] Li, L., Fierer, J. O., Rapoport, T. A., and Howarth, M. (2014). Structural Analysis and Optimization of the Covalent Association between SpyCatcher and a Peptide Tag. *Journal of Molecular Biology*, 426(2):309–317.

[Li et al., 2001] Li, P., Morris, D. L., Willcox, B. E., Steinle, A., Spies, T., and Strong, R. K. (2001). Complex structure of the activating immunoreceptor NKG2D and its MHC class I-like ligand MICA. *Nature immunology*, 2(5):443–451.

[Li et al., 2009] Li, Y., Hofmann, M., Wang, Q., Teng, L., Chlewicki, L. K., Pircher, H., and Mariuzza, R. A. (2009). Structure of Natural Killer Cell Receptor KLRG1 Bound to E-Cadherin Reveals Basis for MHC-Independent Missing Self Recognition. *Immunity*, 31(1):35–46.

[Li et al., 2013] Li, Y., Wang, Q., Chen, S., Brown, P. H., and Mariuzza, R. a. (2013). Structure of NKp65 bound to its keratinocyte ligand reveals basis for genetically linked recognition in natural killer gene complex. *Proceedings of the National Academy of Sciences of the United States of America*, 110(28):11505–10.

[Li et al., 2011] Li, Y., Wang, Q., and Mariuzza, R. A. (2011). Structure of the human activating natural cytotoxicity receptor NKp30 bound to its tumor cell ligand B7-H6. *The Journal of experimental medicine*, 208(4):703–714.

[Li et al., 2010] Li, Y.-C., Chen, B.-M., Wu, P.-C., Cheng, T.-L., Kao, L.-S., Tao, M.-H., Lieber, A., and Roffler, S. R. (2010). Cutting Edge: mechanical forces acting on T cells immobilized via the TCR complex can trigger TCR signaling. *Journal of immunology (Baltimore, Md. : 1950)*, 184(11):5959–63.

[Liao et al., 1992] Liao, F., Shin, H. S., and Rhee, S. G. (1992). Tyrosine phosphorylation of phospholipase C-gamma 1 induced by cross-linking of the high-affinity or low-affinity

Fc receptor for IgG in U937 cells. *Proceedings of the National Academy of Sciences of the United States of America*, 89(8):3659–63.

[Lillemeier et al., 2010] Lillemeier, B. F., Mörtelmaier, M. a., Forstner, M. B., Huppa, J. B., Groves, J. T., and Davis, M. M. (2010). TCR and Lat are expressed on separate protein islands on T cell membranes and concatenate during activation. *Nature immunology*, 11(1):90–96.

[Lim et al., 2015] Lim, H.-S., Cordoba, S.-P., Dushek, O., Goyette, J., Taylor, A., Rudd, C. E., and van der Merwe, P. A. (2015). Costimulation of IL-2 Production through CD28 Is Dependent on the Size of Its Ligand. *The Journal of Immunology*, 195(11):5432–5439.

[Lim et al., 2013] Lim, K. H., Huang, H., Pralle, A., and Park, S. (2013). Stable, high-affinity streptavidin monomer for protein labeling and monovalent biotin detection. *Biotechnology and Bioengineering*, 110(1):57–67.

[Lim et al., 2011] Lim, T. S., Mortellaro, A., Lim, C. T., Hämmerling, G. J., and Ricciardi-Castagnoli, P. (2011). Mechanical interactions between dendritic cells and T cells correlate with T cell responsiveness. *Journal of immunology (Baltimore, Md. : 1950)*, 187(1):258–265.

[Lin and Weiss, 2003] Lin, J. and Weiss, A. (2003). The tyrosine phosphatase CD148 is excluded from the immunologic synapse and down-regulates prolonged T cell signaling. *The Journal of cell biology*, 162(4):673–82.

[Liu et al., 2014] Liu, B., Chen, W., Evavold, B. D., and Zhu, C. (2014). Accumulation of dynamic catch bonds between TCR and agonist peptide-MHC triggers T cell signaling. *Cell*, 157(2):357–368.

[Liu et al., 2013] Liu, S., Zhang, H., Li, M., Hu, D., Li, C., Ge, B., Jin, B., and Fan, Z. (2013). Recruitment of Grb2 and SHIP1 by the ITT-like motif of TIGIT suppresses granule polarization and cytotoxicity of NK cells. *Cell death and differentiation*, 20(3):456–464.

[Liu et al., 2010] Liu, W., Won Sohn, H., Tolar, P., Meckel, T., and Pierce, S. K. (2010). Antigen-induced oligomerization of the B cell receptor is an early target of Fc gamma RIIB inhibition. *Journal of immunology (Baltimore, Md. : 1950)*, 184(4):1977–89.

[Liu et al., 1997] Liu, Y., Hultén, L. M., and Wiklund, O. (1997). Macrophages isolated from human atherosclerotic plaques produce IL-8, and oxysterols may have a regulatory function for IL-8 production. *Arteriosclerosis, thrombosis, and vascular biology*, 17(2):317–323.

[Liu et al., 2005] Liu, Y., Soto, I., Tong, Q., Chin, A., Bühring, H. J., Wu, T., Zen, K., and Parkos, C. a. (2005). SIRPβ1 is expressed as a disulfide-linked homodimer in leukocytes and positively regulates neutrophil transepithelial migration. *Journal of Biological Chemistry*, 280(43):36132–36140.

[Locksley et al., 1993] Locksley, R. M., Reiner, S. L., Hatam, F., Littman, D. R., and Killeen, N. (1993). Helper T cells without CD4: control of leishmaniasis in CD4-deficient mice. *Science (New York, N.Y.)*, 261(5127):1448–51.

[Lu et al., 2015] Lu, J., Chu, J., Zou, Z., Hamacher, N. B., Rixon, M. W., and Sun, P. D. (2015). Structure of FcγRI in complex with Fc reveals the importance of glycan recog-

nition for high-affinity IgG binding. *Proceedings of the National Academy of Sciences of the United States of America*, 112(3):833–8.

[Lu et al., 2011] Lu, J., Ellsworth, J. L., Hamacher, N., Oak, S. W., and Sun, P. D. (2011). Crystal structure of Fcgamma receptor I and its implication in high affinity gamma-immunoglobulin binding. *J Biol Chem*, 286(47):40608–40613.

[Lu et al., 2006] Lu, X., Gross, A. W., and Lodish, H. F. (2006). Active conformation of the erythropoietin receptor: random and cysteine-scanning mutagenesis of the extracellular juxtamembrane and transmembrane domains. *The Journal of biological chemistry*, 281(11):7002–11.

[Lu et al., 1994] Lu, Y., Phillips, C. a., Bjorndahl, J. M., and Trevillyan, J. M. (1994). CD28 signal transduction: tyrosine phosphorylation and receptor association of phosphoinositide-3 kinase correlate with Ca(2+)-independent costimulatory activity. *European journal of immunology*, 24(11):2732–9.

[Lühder et al., 2003] Lühder, F., Huang, Y., Dennehy, K. M., Guntermann, C., Müller, I., Winkler, E., Kerkau, T., Ikemizu, S., Davis, S. J., Hanke, T., and Hünig, T. (2003). Topological requirements and signaling properties of T cell-activating, anti-CD28 antibody superagonists. *The Journal of experimental medicine*, 197(8):955–966.

[Ma et al., 2012] Ma, Z., Discher, D. E., and Finkel, T. H. (2012). Mechanical Force in T Cell Receptor Signal Initiation. *Frontiers in Immunology*, 3(217):1–3.

[Ma et al., 2008a] Ma, Z., Janmey, P. a., and Finkel, T. H. (2008a). The receptor deformation model of TCR triggering. *The FASEB journal : official publication of the Federation of American Societies for Experimental Biology*, 22(4):1002–1008.

[Ma et al., 2014] Ma, Z., LeBard, D. N., Loverde, S. M., Sharp, K. a., Klein, M. L., Discher, D. E., and Finkel, T. H. (2014). TCR Triggering by pMHC Ligands Tethered on Surfaces via Poly(Ethylene Glycol) Depends on Polymer Length. *PloS one*, 9(11):e112292.

[Ma et al., 2008b] Ma, Z., Sharp, K. a., Janmey, P. a., and Finkel, T. H. (2008b). Surface-anchored monomeric agonist pMHCs alone trigger TCR with high sensitivity. *PLoS biology*, 6(2):e43.

[Maasho et al., 2005] Maasho, K., Masilamani, M., Valas, R., Basu, S., Coligan, J. E., and Borrego, F. (2005). The inhibitory leukocyte-associated Ig-like receptor-1 (LAIR-1) is expressed at high levels by human naive T cells and inhibits TCR mediated activation. *Molecular Immunology*, 42:1521–1530.

[Macauley et al., 2014] Macauley, M. S., Crocker, P. R., and Paulson, J. C. (2014). Siglec-mediated regulation of immune cell function in disease. *Nature reviews. Immunology*, 14(10):653–66.

[Magalhães et al., 2011] Magalhães, M. L. B., Czekster, C. M., Guan, R., Malashkevich, V. N., Almo, S. C., and Levy, M. (2011). Evolved streptavidin mutants reveal key role of loop residue in high-affinity binding. *Protein Science*, 20(7):1145–1154.

[Majeti et al., 1998] Majeti, R., Bilwes, a. M., Noel, J. P., Hunter, T., and Weiss, a. (1998). Dimerization-induced inhibition of receptor protein tyrosine phosphatase function through an inhibitory wedge. *Science (New York, N.Y.)*, 279(5347):88–91.

[Marti et al., 1998] Marti, F., Xu, C. W., Selvakumar, a., Brent, R., Dupont, B., and King, P. D. (1998). LCK-phosphorylated human killer cell-inhibitory receptors recruit and ac-

tivate phosphatidylinositol 3-kinase. *Proceedings of the National Academy of Sciences of the United States of America*, 95(20):11810–5.

[Mason et al., 1997] Mason, L. H., Gosselin, P., Anderson, S. K., Fogler, W. E., Ortaldo, J. R., and McVicar, D. W. (1997). Differential tyrosine phosphorylation of inhibitory versus activating Ly-49 receptor proteins and their recruitment of SHP-1 phosphatase. *Journal of immunology (Baltimore, Md. : 1950)*, 159(9):4187–96.

[McCall et al., 1992] McCall, M. N., Shotton, D. M., and Barclay, A. N. (1992). Expression of soluble isoforms of rat CD45. Analysis by electron microscopy and use in epitope mapping of anti-CD45R monoclonal antibodies. *Immunology*, 76(2):310–7.

[McCann et al., 2003] McCann, F. E., Vanherberghen, B., Eleme, K., Carlin, L. M., Newsam, R. J., Goulding, D., and Davis, D. M. (2003). The size of the synaptic cleft and distinct distributions of filamentous actin, ezrin, CD43, and CD45 at activating and inhibitory human NK cell immune synapses. *Journal of immunology (Baltimore, Md. : 1950)*, 170(6):2862–70.

[McNeill et al., 2007] McNeill, L., Salmond, R. J., Cooper, J. C., Carret, C. K., Cassady-Cain, R. L., Roche-Molina, M., Tandon, P., Holmes, N., and Alexander, D. R. (2007). The differential regulation of Lck kinase phosphorylation sites by CD45 is critical for T cell receptor signaling responses. *Immunity*, 27(3):425–437.

[Melendez et al., 1998] Melendez, A. J., Gillooly, D. J., Harnett, M. M., and Allen, J. M. (1998). Aggregation of the human high affinity immunoglobulin G receptor (Fc gamma RI) activates both tyrosine kinase and G protein-coupled phosphoinositide 3-kinase isoforms. *Proceedings of the National Academy of Sciences of the United States of America*, 95(5):2169–2174.

[Merlo et al., 2005] Merlo, A., Tenca, C., Fais, F., Battini, L., Ciccone, E., Grossi, C. E., and Saverino, D. (2005). Inhibitory receptors CD85j, LAIR-1, and CD152 down-regulate immunoglobulin and cytokine production by human B lymphocytes. *Clinical and diagnostic laboratory immunology*, 12(6):705–712.

[Mestas and Hughes, 2004] Mestas, J. and Hughes, C. C. W. (2004). Of mice and not men: differences between mouse and human immunology. *Journal of immunology (Baltimore, Md. : 1950)*, 172(5):2731–2738.

[Meyaard et al., 1997] Meyaard, L., Adema, G. J., Chang, C., Woollatt, E., Sutherland, G. R., Lanier, L. L., and Phillips, J. H. (1997). LAIR-1, a novel inhibitory receptor expressed on human mononuclear leukocytes. *Immunity*, 7(2):283–90.

[Meyaard et al., 1999] Meyaard, L., Hurenkamp, J., Clevers, H., Lanier, L. L., and Phillips, J. H. (1999). Leukocyte-associated Ig-like receptor-1 functions as an inhibitory receptor on cytotoxic T cells. *Journal of immunology (Baltimore, Md. : 1950)*, 162:5800–5804.

[Meyer et al., 2001] Meyer, D. L., Schultz, J., Lin, Y., Henry, A., Sanderson, J., Jackson, J. M., Goshorn, S., Rees, A. R., and Graves, S. S. (2001). Reduced antibody response to streptavidin through site-directed mutagenesis. *Protein science : a publication of the Protein Society*, 10(3):491–503.

[Miah and Campbell, 2010] Miah, S. M. S. and Campbell, K. S. (2010). Expression of cDNAs in human Natural Killer cell lines by retroviral transduction. *Methods in molecular biology (Clifton, N.J.)*, 612:199–208.

[Mingueneau et al., 2008] Mingueneau, M., Sansoni, A., Grégoire, C., Roncagalli, R., Aguado, E., Weiss, A., Malissen, M., and Malissen, B. (2008). The proline-rich sequence of CD3epsilon controls T cell antigen receptor expression on and signaling potency in preselection CD4+CD8+ thymocytes. *Nature immunology*, 9(5):522–32.

[Minguet et al., 2010] Minguet, S., Dopfer, E. P., and Schamel, W. W. a. (2010). Low-valency, but not monovalent, antigens trigger the B-cell antigen receptor (BCR). *International Immunology*, 22(3):205–212.

[Minguet and Schamel, 2008] Minguet, S. and Schamel, W. W. a. (2008). A permissive geometry model for TCR-CD3 activation. *Trends in biochemical sciences*, 33(2):51–7.

[Minguet et al., 2007] Minguet, S., Swamy, M., Alarcón, B., Luescher, I. F., and Schamel, W. W. a. (2007). Full Activation of the T Cell Receptor Requires Both Clustering and Conformational Changes at CD3. *Immunity*, 26(1):43–54.

[Mócsai et al., 2010] Mócsai, A., Ruland, J., and Tybulewicz, V. L. J. (2010). The SYK tyrosine kinase: a crucial player in diverse biological functions. *Nature reviews. Immunology*, 10(6):387–402.

[Moore et al., 1967] Moore, G. E., Gerner, R. E., and Franklin, H. A. (1967). Culture of normal human leukocytes. *JAMA : the journal of the American Medical Association*, 199(8):519–524.

[Mossman et al., 2005] Mossman, K. D., Campi, G., Groves, J. T., and Dustin, M. L. (2005). Altered TCR signaling from geometrically repatterned immunological synapses. *Science (New York, N.Y.)*, 310(5751):1191–1193.

[Mousseau et al., 2000] Mousseau, D. D., Banville, D., L'Abbé, D., Bouchard, P., and Shen, S. H. (2000). PILRalpha, a novel immunoreceptor tyrosine-based inhibitory motif-bearing protein, recruits SHP-1 upon tyrosine phosphorylation and is paired with the truncated counterpart PILRbeta. *The Journal of biological chemistry*, 275(6):4467–74.

[Munro, 2003] Munro, S. (2003). Lipid Rafts: Elusive or Illusive? *Cell*, 115(4):377–388.

[Murphy, 2011] Murphy, K. (2011). *Janeway's Immunobiology*. Garland Science, New York, 8th edition.

[Nada et al., 1991] Nada, S., Okada, M., MacAuley, A., Cooper, J. A., and Nakagawa, H. (1991). Cloning of a complementary DNA for a protein-tyrosine kinase that specifically phosphorylates a negative regulatory site of p60c-src. *Nature*, 351(6321):69–72.

[Nam et al., 2005] Nam, H.-J., Poy, F., Saito, H., and Frederick, C. a. (2005). Structural basis for the function and regulation of the receptor protein tyrosine phosphatase CD45. *The Journal of experimental medicine*, 201(3):441–52.

[Nguyen et al., 2014] Nguyen, P. Q., Botyanszki, Z., Tay, P. K. R., and Joshi, N. S. (2014). Programmable biofilm-based materials from engineered curli nanofibres. *Nature Communications*, 5:4945.

[Nika et al., 2010] Nika, K., Soldani, C., Salek, M., Paster, W., Gray, A., Etzensperger, R., Fugger, L., Polzella, P., Cerundolo, V., Dushek, O., Höfer, T., Viola, A., and Acuto, O. (2010). Constitutively active lck kinase in T cells drives antigen receptor signal transduction. *Immunity*, 32(6):766–777.

[Nimmerjahn and Ravetch, 2008] Nimmerjahn, F. and Ravetch, J. V. (2008). Fcgamma receptors as regulators of immune responses. *Nature reviews. Immunology*, 8(1):34–47.

[O'Connor et al., 2012] O'Connor, R. S., Hao, X., Shen, K., Bashour, K., Akimova, T., Hancock, W. W., Kam, L. C., and Milone, M. C. (2012). Substrate rigidity regulates human T cell activation and proliferation. *Journal of immunology (Baltimore, Md. : 1950)*, 189(3):1330–9.

[Okada et al., 1991] Okada, M., Nada, S., Yamanashi, Y., Yamamoto, T., and Nakagawa, H. (1991). CSK: a protein-tyrosine kinase involved in regulation of src family kinases. *J Biol Chem*, 266(36):24249–24252.

[Okazawa et al., 2005] Okazawa, H., Motegi, S.-i., Ohyama, N., Ohnishi, H., Tomizawa, T., Kaneko, Y., Oldenborg, P.-A., Ishikawa, O., Matozaki, T., and Alerts, E. (2005). Negative regulation of phagocytosis in macrophages by the CD47-SHPS-1 system. *Journal of immunology (Baltimore, Md. : 1950)*, 174(4):2004–11.

[Oke et al., 2010] Oke, M., Carter, L. G., Johnson, K. A., Liu, H., McMahon, S. A., Yan, X., Kerou, M., Weikart, N. D., Kadi, N., Sheikh, M. A., Schmelz, S., Dorward, M., Zawadzki, M., Cozens, C., Falconer, H., Powers, H., Overton, I. M., Van Niekerk, C. A. J., Peng, X., Patel, P., Garrett, R. A., Prangishvili, D., Botting, C. H., Coote, P. J., Dryden, D. T. F., Barton, G. J., Schwarz-Linek, U., Challis, G. L., Taylor, G. L., White, M. F., and Naismith, J. H. (2010). The scottish structural proteomics facility: Targets, methods and outputs. *Journal of Structural and Functional Genomics*, 11(2):167–180.

[Omiya et al., 2009] Omiya, R., Tsushima, F., Narazaki, H., Sakoda, Y., Kuramasu, A., Kim, Y., Xu, H., Tamura, H., Zhu, G., Chen, L., and Tamada, K. (2009). Leucocyte-associated immunoglobulin-like receptor-1 is an inhibitory regulator of contact hypersensitivity. *Immunology*, 128:543–555.

[Orloff et al., 1990] Orloff, D. G., Ra, C., Frank, S. J., Klausner, R. D., and Kinet, J.-P. (1990). Family of disulphide-linked dimers containing the ζ and η chains of the T-cell receptor and the γ chain of Fc receptors. *Nature*, 347(6289):189–191.

[O'Shea et al., 1992] O'Shea, J. J., McVicar, D. W., Bailey, T. L., Burns, C., and Smyth, M. J. (1992). Activation of human peripheral blood T lymphocytes by pharmacological induction of protein-tyrosine phosphorylation. *Proceedings of the National Academy of Sciences of the United States of America*, 89(21):10306–10310.

[Ostergaard et al., 1989] Ostergaard, H. L., Shackelford, D. a., Hurley, T. R., Johnson, P., Hyman, R., Sefton, B. M., and Trowbridge, I. S. (1989). Expression of CD45 alters phosphorylation of the lck-encoded tyrosine protein kinase in murine lymphoma T-cell lines. *Proceedings of the National Academy of Sciences of the United States of America*, 86(22):8959–63.

[Owen et al., 2012] Owen, D. M., Magenau, A., Williamson, D., and Gaus, K. (2012). The lipid raft hypothesis revisited - New insights on raft composition and function from super-resolution fluorescence microscopy. *BioEssays*, 34(9):739–747.

[Panwar et al., 2012] Panwar, P., Deniaud, A., and Pebay-Peyroula, E. (2012). Contamination from an affinity column: an encounter with a new villain in the world of membrane-protein crystallization. *Acta Crystallographica Section D Biological Crystallography*, 68(10):1272–1277.

[Parolini et al., 2000] Parolini, S., Bottino, C., Falco, M., Augugliaro, R., Giliani, S., Franceschini, R., Ochs, H. D., Wolf, H., Bonnefoy, J. Y., Biassoni, R., Moretta, L., Notarangelo, L. D., and Moretta, A. (2000). X-linked lymphoproliferative disease. 2B4 molecules displaying inhibitory rather than activating function are responsible for the inability of natural killer cells to kill Epstein-Barr virus-infected cells. *The Journal of experimental medicine*, 192(3):337–346.

[Parrott and Barry, 2001] Parrott, M. B. and Barry, M. A. (2001). Metabolic biotinylation of secreted and cell surface proteins from mammalian cells. *Biochem Biophys Res Commun*, 281(4):993–1000.

[Paszek et al., 2014] Paszek, M. J., DuFort, C. C., Rossier, O., Bainer, R., Mouw, J. K., Godula, K., Hudak, J. E., Lakins, J. N., Wijekoon, A. C., Cassereau, L., Rubashkin, M. G., Magbanua, M. J., Thorn, K. S., Davidson, M. W., Rugo, H. S., Park, J. W., Hammer, D. a., Giannone, G., Bertozzi, C. R., and Weaver, V. M. (2014). The cancer glycocalyx mechanically primes integrin-mediated growth and survival. *Nature*, 511(7509):319–25.

[Peaker and Neuberger, 1993] Peaker, C. J. and Neuberger, M. S. (1993). Association of CD22 with the B cell antigen receptor. *Eur J Immunol*, 23(6):1358–1363.

[Pegram et al., 2011] Pegram, H. J., Andrews, D. M., Smyth, M. J., Darcy, P. K., and Kershaw, M. H. (2011). Activating and inhibitory receptors of natural killer cells. *Immunology and cell biology*, 89(2):216–224.

[Pende et al., 1999] Pende, D., Parolini, S., Pessino, A., Sivori, S., Augugliaro, R., Morelli, L., Marcenaro, E., Accame, L., Malaspina, A., Biassoni, R., Bottino, C., Moretta, L., and Moretta, A. (1999). Identification and molecular characterization of NKp30, a novel triggering receptor involved in natural cytotoxicity mediated by human natural killer cells. *The Journal of experimental medicine*, 190(10):1505–1516.

[Perez-Montfort et al., 1983] Perez-Montfort, R., Kinet, J. P., and Metzger, H. (1983). A previously unrecognized subunit of the receptor for immunoglobulin E. *Biochemistry*, 22(25):5722–5728.

[Perica et al., 2014] Perica, K., Tu, A., Richter, A., Bieler, J. G., Edidin, M., and Schneck, J. P. (2014). Magnetic field-induced t cell receptor clustering by nanoparticles enhances t cell activation and stimulates antitumor activity. *ACS Nano*, 8(3):2252–2260.

[Pessino et al., 1998] Pessino, A., Sivori, S., Bottino, C., Malaspina, A., Morelli, L., Moretta, L., Biassoni, R., and Moretta, A. (1998). Molecular cloning of NKp46: a novel member of the immunoglobulin superfamily involved in triggering of natural cytotoxicity. *The Journal of experimental medicine*, 188(5):953–960.

[Piatier-Tonneau et al., 1991] Piatier-Tonneau, D., Gastinel, L. N., Moussy, G., Bénichou, B., Amblard, F., Vaigot, P., and Auffray, C. (1991). Mutations in the D strand of the human CD4 V1 domain affect CD4 interactions with the human immunodeficiency virus envelope glycoprotein gp120 and HLA class II antigens similarly. *Proceedings of the National Academy of Sciences of the United States of America*, 88(15):6858–62.

[Piccio et al., 2005] Piccio, L., Vermi, W., Boles, K. S., Fuchs, A., Strader, C. A., Facchetti, F., Cella, M., and Colonna, M. (2005). Adhesion of human T cells to antigen-presenting cells through SIRPbeta2-CD47 interaction costimulates T-cell proliferation. *Blood*, 105(6):2421–2427.

[Pignata et al., 1993] Pignata, C., Prasad, K. V., Robertson, M. J., Levine, H., Rudd, C. E., and Ritz, J. (1993). Fc gamma RIIIA-mediated signaling involves src-family lck in human natural killer cells. *Journal of immunology (Baltimore, Md. : 1950)*, 151(12):6794–6800.

[Pillai et al., 2012] Pillai, S., Netravali, I. A., Cariappa, A., and Mattoo, H. (2012). Siglecs and Immune Regulation. *Annual Review of Immunology*, 30(1):357–392.

[Pizzo et al., 2002] Pizzo, P., Giurisato, E., Tassi, M., Benedetti, A., Pozzan, T., and Viola, A. (2002). Lipid rafts and T cell receptor signaling: a critical re-evaluation. *European journal of immunology*, 32(11):3082–91.

[Pogge von Strandmann et al., 2007] Pogge von Strandmann, E., Simhadri, V. R., von Tresckow, B., Sasse, S., Reiners, K., Hansen, H. P., Rothe, A., Böll, B., Simhadri, V. L., Borchmann, P., McKinnon, P. J., Hallek, M., and Engert, A. (2007). Human Leukocyte Antigen-B-Associated Transcript 3 Is Released from Tumor Cells and Engages the NKp30 Receptor on Natural Killer Cells. *Immunity*, 27(6):965–974.

[Powell et al., 1993] Powell, L. D., Sgroi, D., Sjoberg, E. R., Stamenkovic, I., and Varki, A. (1993). Natural ligands of the B cell adhesion molecule CD22 beta carry N-linked oligosaccharides with alpha-2,6-linked sialic acids that are required for recognition. *The Journal of biological chemistry*, 268(10):7019–7027.

[Pryshchep et al., 2014] Pryshchep, S., Zarnitsyna, V. I., Hong, J., Evavold, B. D., and Zhu, C. (2014). Accumulation of Serial Forces on TCR and CD8 Frequently Applied by Agonist Antigenic Peptides Embedded in MHC Molecules Triggers Calcium in T Cells. *The Journal of Immunology*, 193:68–76.

[Puech et al., 2011] Puech, P. H., Nevoltris, D., Robert, P., Limozin, L., Boyer, C., and Bongrand, P. (2011). Force measurements of TCR/pMHC recognition at T cell surface. *PLoS ONE*, 6(7):e22344.

[Puffer et al., 2007] Puffer, E. B., Pontrello, J. K., Hollenbeck, J. J., Kink, J. a., and Kiessling, L. L. (2007). Activating B cells signalling with defined multivalent ligands. *ACS Chemical Biology*, 2(4):252–262.

[Purbhoo et al., 2004] Purbhoo, M. a., Irvine, D. J., Huppa, J. B., and Davis, M. M. (2004). T cell killing does not require the formation of a stable mature immunological synapse. *Nature immunology*, 5(5):524–530.

[Qureshi et al., 2001] Qureshi, M. H., Yeung, J. C., Wu, S. C., and Wong, S. L. (2001). Development and Characterization of a Series of Soluble Tetrameric and Monomeric Streptavidin Muteins with Differential Biotin Binding Affinities. *Journal of Biological Chemistry*, 276(49):46422–46428.

[Raab et al., 1995] Raab, M., Cai, Y. C., Bunnell, S. C., Heyeck, S. D., Berg, L. J., and Rudd, C. E. (1995). p56Lck and p59Fyn regulate CD28 binding to phosphatidylinositol 3-kinase, growth factor receptor-bound protein GRB-2, and T cell-specific protein-tyrosine kinase ITK: implications for T-cell costimulation. *Proceedings of the National Academy of Sciences of the United States of America*, 92(19):8891–5.

[Raab et al., 1994] Raab, M., Yamamoto, M., and Rudd, C. E. (1994). The T-cell antigen CD5 acts as a receptor and substrate for the protein-tyrosine kinase p56lck. *Molecular and cellular biology*, 14(5):2862–2870.

[Rankin et al., 1993] Rankin, B. M., Yocum, S. A., Mittler, R. S., and Kiener, P. A. (1993).

Stimulation of tyrosine phosphorylation and calcium mobilization by Fc gamma receptor cross-linking. Regulation by the phosphotyrosine phosphatase CD45. *J Immunol*, 150(2):605–616.

[Razi and Varki, 1998] Razi, N. and Varki, A. (1998). Masking and unmasking of the sialic acid-binding lectin activity of CD22 (Siglec-2) on B lymphocytes. *Proceedings of the National Academy of Sciences of the United States of America*, 95(13):7469–7474.

[Reich et al., 1997] Reich, Z., Boniface, J. J., Lyons, D. S., Borochov, N., Wachtel, E. J., and Davis, M. M. (1997). Ligand-specific oligomerization of T-cell receptor molecules. *Nature*, 387(6633):617–620.

[Resh, 1999] Resh, M. (1999). Fatty acylation of proteins: new insights into membrane targeting of myristoylated and palmitoylated proteins. *Biochimica et Biophysica Acta (BBA) - Molecular Cell Research*, 1451(1):1–16.

[Reznik et al., 1998] Reznik, G. O., Vajda, S., Sano, T., and Cantor, C. R. (1998). A streptavidin mutant with altered ligand-binding specificity. *Proceedings of the National Academy of Sciences of the United States of America*, 95(23):13525–13530.

[Rickert, 2013] Rickert, R. C. (2013). New insights into pre-BCR and BCR signalling with relevance to B cell malignancies. *Nature reviews. Immunology*, 13(8):578–91.

[Romero et al., 2004] Romero, X., Benítez, D., March, S., Vilella, R., Miralpeix, M., and Engel, P. (2004). Differential expression of SAP and EAT-2-binding leukocyte cell-surface molecules CD84, CD150 (SLAM), CD229 (Ly9) and CD244 (2B4). *Tissue Antigens*, 64(2):132–144.

[Rosental et al., 2011] Rosental, B., Brusilovsky, M., Hadad, U., Oz, D., Appel, M. Y., Afergan, F., Yossef, R., Rosenberg, L. A., Aharoni, A., Cerwenka, A., Campbell, K. S., Braiman, A., and Porgador, A. (2011). Proliferating cell nuclear antigen is a novel inhibitory ligand for the natural cytotoxicity receptor NKp44. *Journal of immunology (Baltimore, Md. : 1950)*, 187(11):5693–702.

[Roskoski, 2005] Roskoski, R. (2005). Src kinase regulation by phosphorylation and dephosphorylation. *Biochemical and Biophysical Research Communications*, 331:1–14.

[Rossy et al., 2013] Rossy, J., Owen, D. M., Williamson, D. J., Yang, Z., and Gaus, K. (2013). Conformational states of the kinase Lck regulate clustering in early T cell signaling. *Nature immunology*, 14(1):82–9.

[Rutledge et al., 1992] Rutledge, T., Cosson, P., Manolios, N., Bonifacino, J. S., and Klausner, R. D. (1992). Transmembrane helical interactions: zeta chain dimerization and functional association with the T cell antigen receptor. *The EMBO journal*, 11(9):3245–3254.

[Sandusky et al., 2006] Sandusky, M. M., Messmer, B., and Watzl, C. (2006). Regulation of 2B4 (CD244)-mediated NK cell activation by ligand-induced receptor modulation. *European Journal of Immunology*, 36(12):3268–3276.

[Sano and Cantor, 1995] Sano, T. and Cantor, C. R. (1995). Intersubunit contacts made by tryptophan 120 with biotin are essential for both strong biotin binding and biotin-induced tighter subunit association of streptavidin. *Proceedings of the National Academy of Sciences of the United States of America*, 92(8):3180–3184.

[Saverino et al., 2002] Saverino, D., Fabbi, M., Merlo, A., Ravera, G., Grossi, C. E., and Ciccone, E. (2002). Surface density expression of the leukocyte-associated Ig-like receptor-1 is directly related to inhibition of human T-cell functions. *Human immunology*, 63(7):534–46.

[Sayos et al., 1998] Sayos, J., Wu, C., Morra, M., Wang, N., Zhang, X., Allen, D., van Schaik, S., Notarangelo, L., Geha, R., Roncarolo, M. G., Oettgen, H., De Vries, J. E., Aversa, G., and Terhorst, C. (1998). The X-linked lymphoproliferative-disease gene product SAP regulates signals induced through the co-receptor SLAM. *Nature*, 395(6701):462–469.

[Schamel and Reth, 2000] Schamel, W. W. and Reth, M. (2000). Monomeric and oligomeric complexes of the B cell antigen receptor. *Immunity*, 13(1):5–14.

[Schamel and Alarcón, 2013] Schamel, W. W. a. and Alarcón, B. (2013). Organization of the resting TCR in nanoscale oligomers. *Immunological reviews*, 251(1):13–20.

[Schamel et al., 2005] Schamel, W. W. A., Arechaga, I., Risueño, R. M., van Santen, H. M., Cabezas, P., Risco, C., Valpuesta, J. M., and Alarcón, B. (2005). Coexistence of multivalent and monovalent TCRs explains high sensitivity and wide range of response. *The Journal of Experimental Medicine*, 202(4):493–503.

[Schiff et al., 1997] Schiff, D. E., Rae, J., Martin, T. R., Davis, B. H., and Curnutte, J. T. (1997). Increased phagocyte Fc gammaRI expression and improved Fc gamma-receptor-mediated phagocytosis after in vivo recombinant human interferon-gamma treatment of normal human subjects. *Blood*, 90(8):3187–94.

[Schilham et al., 1993] Schilham, M. W., Fung-Leung, W. P., Rahemtulla, A., Kuendig, T., Zhang, L., Potter, J., Miller, R. G., Hengartner, H., and Mak, T. W. (1993). Alloreactive cytotoxic T cells can develop and function in mice lacking both CD4 and CD8. *European journal of immunology*, 23(6):1299–304.

[Schmidt et al., 1996] Schmidt, T. G., Koepke, J., Frank, R., and Skerra, A. (1996). Molecular interaction between the Strep-tag affinity peptide and its cognate target, streptavidin. *Journal of molecular biology*, 255(5):753–766.

[Schmidt et al., 2013] Schmidt, T. G. M., Batz, L., Bonet, L., Carl, U., Holzapfel, G., Kiem, K., Matulewicz, K., Niermeier, D., Schuchardt, I., and Stanar, K. (2013). Development of the Twin-Strep-tagÂő and its application for purification of recombinant proteins from cell culture supernatants.

[Scholl and Geha, 1993] Scholl, P. R. and Geha, R. S. (1993). Physical association between the high-affinity IgG receptor (Fc gamma RI) and the gamma subunit of the high-affinity IgE receptor (Fc epsilon RI gamma). *Proceedings of the National Academy of Sciences of the United States of America*, 90(19):8847–8850.

[Schott et al., 2002] Schott, E., Bertho, N., Ge, Q., Maurice, M. M., and Ploegh, H. L. (2002). Class I negative CD8 T cells reveal the confounding role of peptide-transfer onto CD8 T cells stimulated with soluble H2-Kb molecules. *Proceedings of the National Academy of Sciences of the United States of America*, 99(21):13735–13740.

[Schwartz et al., 2001] Schwartz, J. C., Zhang, X., Fedorov, a. a., Nathenson, S. G., and Almo, S. C. (2001). Structural basis for co-stimulation by the human CTLA-4/B7-2 complex. *Nature*, 410(6828):604–608.

[Secrist et al., 1993] Secrist, J. P., Burns, L. a., Karnitz, L., Koretzky, G. a., and Abraham, R. T. (1993). Stimulatory effects of the protein tyrosine phosphatase inhibitor, pervanadate, on T-cell activation events. *The Journal of biological chemistry*, 268(8):5886–93.

[Sgroi et al., 1993] Sgroi, D., Varki, A., Braesch-Andersen, S., and Stamenkovic, I. (1993). CD22, a B cell-specific immunoglobulin superfamily member, is a sialic acid-binding lectin. *The Journal of biological chemistry*, 268(10):7011–8.

[Shaw and Dustin, 1997] Shaw, A. S. and Dustin, M. L. (1997). Making the T Cell Receptor Go the Distance: A Topological View of T Cell Activation. *Immunity*, 6(4):361–369.

[Shen et al., 2009] Shen, K., Tsai, J., Shi, P., and Kam, L. C. (2009). Self-aligned supported lipid bilayers for patterning the cell-substrate interface. *Journal of the American Chemical Society*, 131(37):13204–13205.

[Shi et al., 2013] Shi, X., Bi, Y., Yang, W., Guo, X., Jiang, Y., Wan, C., Li, L., Bai, Y., Guo, J., Wang, Y., Chen, X., Wu, B., Sun, H., Liu, W., Wang, J., and Xu, C. (2013). Ca2+ regulates T-cell receptor activation by modulating the charge property of lipids. *Nature*, 493(7430):111–5.

[Sicheri et al., 1997] Sicheri, F., Moarefi, I., and Kuriyan, J. (1997). Crystal structure of the Src family tyrosine kinase Hck.

[Siegers et al., 2006] Siegers, G. M., Yang, J., Duerr, C. U., Nielsen, P. J., Reth, M., and Schamel, W. W. a. (2006). Identification of disulfide bonds in the Ig-alpha/Ig-beta component of the B cell antigen receptor using the Drosophila S2 cell reconstitution system. *International Immunology*, 18(9):1385–1396.

[Sigalov et al., 2006] Sigalov, A. B., Aivazian, D. a., Uversky, V. N., and Stern, L. J. (2006). Lipid-binding activity of intrinsically unstructured cytoplasmic domains of multichain immune recognition receptor signaling subunits. *Biochemistry*, 45(51):15731–15739.

[Sil et al., 2007] Sil, D., Lee, J. B., Luo, D., Holowka, D., and Baird, B. (2007). Trivalent ligands with rigid DNA spacers reveal structural requirements for IgE receptor signaling in RBL mast cells. *ACS chemical biology*, 2(10):674–84.

[Simons and Ikonen, 1997] Simons, K. and Ikonen, E. (1997). Functional rafts in cell membranes. *Nature*, 387(6633):569–72.

[Simons and Toomre, 2000] Simons, K. and Toomre, D. (2000). Lipid rafts and signal transduction. *Nature reviews. Molecular cell biology*, 1(1):31–9.

[Sivori et al., 2000] Sivori, S., Parolini, S., Falco, M., Marcenaro, E., Biassoni, R., Bottino, C., Moretta, L., and Moretta, A. (2000). 2B4 functions as a co-receptor in human NK cell activation. *European journal of immunology*, 30(3):787–93.

[Sivori et al., 1999] Sivori, S., Pende, D., Bottino, C., Marcenaro, E., Pessino, A., Biassoni, R., Moretta, L., and Moretta, A. (1999). NKp46 is the major triggering receptor involved in the natural cytotoxicity of fresh or cultured human NK cells. Correlation between surface density of NKp46 and natural cytotoxicity against autologous, allogeneic or xenogeneic target cells. *European Journal of Immunology*, 29(5):1656–1666.

[Smart et al., 1981] Smart, J. E., Oppermann, H., Czernilofsky, a. P., Purchio, a. F., Erikson, R. L., and Bishop, J. M. (1981). Characterization of sites for tyrosine phosphorylation in the transforming protein of Rous sarcoma virus (pp60v-src) and its normal

cellular homologue (pp60c-src). *Proceedings of the National Academy of Sciences of the United States of America*, 78(10):6013–6017.

[Smith and Morrissey, 2004] Smith, S. a. and Morrissey, J. H. (2004). Rapid and efficient incorporation of tissue factor into liposomes. *Journal of Thrombosis and Haemostasis*, 2(7):1155–1162.

[Son and Diamond, 2014] Son, M. and Diamond, B. (2014). C1q-mediated repression of human monocytes is regulated by leukocyte-associated Ig-like receptor 1 (LAIR-1). *Molecular medicine (Cambridge, Mass.)*, 20:559–68.

[Sondermann et al., 2000] Sondermann, P., Huber, R., Oosthuizen, V., and Jacob, U. (2000). The 3.2-A crystal structure of the human IgG1 Fc fragment-Fc gammaRIII complex. *Nature*, 406(6793):267–273.

[Spaggiari et al., 2001] Spaggiari, G. M., Carosio, R., Pende, D., Marcenaro, S., Rivera, P., Zocchi, M. R., Moretta, L., and Poggi, A. (2001). NK cell-mediated lysis of autologous antigen-presenting cells is triggered by the engagement of the phosphatidylinositol 3-kinase upon ligation of the natural cytotoxicity receptors NKp30 and NKp46. *European Journal of Immunology*, 31:1656–1665.

[Spörri and Reis e Sousa, 2002] Spörri, R. and Reis e Sousa, C. (2002). Self peptide/MHC class I complexes have a negligible effect on the response of some CD8+ T cells to foreign antigen. *European Journal of Immunology*, 32(11):3161–3170.

[Springer, 1990] Springer, T. a. (1990). Adhesion receptors of the immune system. *Nature*, 346(6283):425–434.

[Stamenkovic et al., 1991] Stamenkovic, I., Sgroi, D., Aruffo, A., Sy, M. S., and Anderson, T. (1991). The B lymphocyte adhesion molecule CD22 interacts with leukocyte common antigen CD45RO on T cells and alpha 2-6 sialyltransferase, CD75, on B cells. *Cell*, 66(6):1133–1144.

[Stefanová et al., 2002] Stefanová, I., Dorfman, J. R., and Germain, R. N. (2002). Self-recognition promotes the foreign antigen sensitivity of naive T lymphocytes. *Nature*, 420(6914):429–434.

[Stepanek et al., 2011] Stepanek, O., Kalina, T., Draber, P., Skopcova, T., Svojgr, K., Angelisova, P., Horejsi, V., Weiss, A., and Brdicka, T. (2011). Regulation of Src family kinases involved in T cell receptor signaling by protein-tyrosine phosphatase CD148. *The Journal of biological chemistry*, 286(25):22101–12.

[Stone and Stern, 2006] Stone, J. D. and Stern, L. J. (2006). CD8 T Cells, Like CD4 T Cells, Are Triggered by Multivalent Engagement of TCRs by MHC-Peptide Ligands but Not by Monovalent Engagement. *The Journal of Immunology*, 176(3):1498–1505.

[Straus and Weiss, 1992] Straus, D. B. and Weiss, A. (1992). Genetic evidence for the involvement of the lck tyrosine kinase in signal transduction through the T cell antigen receptor. *Cell*, 70(4):585–593.

[Sun et al., 2014] Sun, F., Zhang, W.-B., Mahdavi, A., Arnold, F. H., and Tirrell, D. a. (2014). Synthesis of bioactive protein hydrogels by genetically encoded SpyTag-SpyCatcher chemistry. *Proceedings of the National Academy of Sciences of the United States of America*, 2014:1–6.

[Sun et al., 2001] Sun, Z. Y. J., Kim, K. S., Wagner, G., and Reinherz, E. L. (2001). Mechanisms contributing to T cell receptor signaling and assembly revealed by

the solution structure of an ectodomain fragment of the CD3$\epsilon\gamma$ heterodimer. *Cell*, 105(7):913–923.

[Suzuki et al., 2000] Suzuki, T., Kono, H., Hirose, N., Okada, M., Yamamoto, T., Yamamoto, K., and Honda, Z. (2000). Differential involvement of Src family kinases in Fc gamma receptor-mediated phagocytosis. *Journal of immunology (Baltimore, Md. : 1950)*, 165(1):473–482.

[Swisher and Feldman, 2015] Swisher, J. F. A. and Feldman, G. M. (2015). The many faces of FcγRI: implications for therapeutic antibody function. *Immunological Reviews*, 268(1):160–174.

[Sykulev et al., 1994] Sykulev, Y., Brunmark, a., Jackson, M., Cohen, R. J., Peterson, P. a., and Eisen, H. N. (1994). Kinetics and affinity of reactions between an antigen-specific T cell receptor and peptide-MHC complexes. *Immunity*, 1(1):15–22.

[Sykulev et al., 1996] Sykulev, Y., Joo, M., Vturina, I., Tsomides, T. J., and Eisen, H. N. (1996). Evidence that a Single Peptide MHC Complex on a Target Cell Can Elicit a Cytolytic T Cell Response. *Immunity*, 4:565–571.

[Takata et al., 1994] Takata, M., Sabe, H., Hata, A., Inazu, T., Homma, Y., Nukada, T., Yamamura, H., and Kurosaki, T. (1994). Tyrosine kinases Lyn and Syk regulate B cell receptor-coupled Ca2+ mobilization through distinct pathways. *The EMBO journal*, 13(6):1341–1349.

[Tang et al., 2009] Tang, X., Narayanan, S., Peruzzi, G., Apara, A., Natarajan, K., Margulies, D. H., Coligan, J. E., and Borrego, F. (2009). A single residue, arginine 65, is critical for the functional interaction of leukocyte-associated inhibitory receptor-1 with collagens. *Journal of immunology (Baltimore, Md. : 1950)*, 182(9):5446–52.

[Tangye et al., 2000a] Tangye, S. G., Cherwinski, H., Lanier, L. L., and Phillips, J. H. (2000a). 2B4-mediated activation of human natural killer cells. *Molecular Immunology*, 37(9):493–501.

[Tangye et al., 1999] Tangye, S. G., Lazetic, S., Woollatt, E., Sutherland, G. R., Lanier, L. L., and Phillips, J. H. (1999). Cutting edge: human 2B4, an activating NK cell receptor, recruits the protein tyrosine phosphatase SHP-2 and the adaptor signaling protein SAP. *Journal of immunology (Baltimore, Md. : 1950)*, 162(12):6981–6985.

[Tangye et al., 2000b] Tangye, S. G., Phillips, J. H., Lanier, L. L., and Nichols, K. E. (2000b). Functional requirement for SAP in 2B4-mediated activation of human natural killer cells as revealed by the X-linked lymphoproliferative syndrome. *Journal of immunology (Baltimore, Md. : 1950)*, 165(6):2932–2936.

[Tassi and Colonna, 2005] Tassi, I. and Colonna, M. (2005). The cytotoxicity receptor CRACC (CS-1) recruits EAT-2 and activates the PI3K and phospholipase Cgamma signaling pathways in human NK cells. *Journal of immunology (Baltimore, Md. : 1950)*, 175(12):7996–8002.

[Thornton and McDaniel, 2005] Thornton, J. and McDaniel, L. S. (2005). THP-1 monocytes up-regulate intercellular adhesion molecule 1 in response to pneumolysin from Streptococcus pneumoniae. *Infection and Immunity*, 73(10):6493–6498.

[Tolar et al., 2009] Tolar, P., Hanna, J., Krueger, P. D., and Pierce, S. K. (2009). The Constant Region of the Membrane Immunoglobulin Mediates B Cell-Receptor Clustering and Signaling in Response to Membrane Antigens. *Immunity*, 30(1):44–55.

[Tolar and Pierce, 2010] Tolar, P. and Pierce, S. K. (2010). A conformation-induced oligomerization model for B cell receptor microclustering and signaling. *Current topics in microbiology and immunology*, 340:155–69.

[Tolar et al., 2005] Tolar, P., Sohn, H. W., and Pierce, S. K. (2005). The initiation of antigen-induced B cell antigen receptor signaling viewed in living cells by fluorescence resonance energy transfer. *Nature immunology*, 6(11):1168–1176.

[Tolar et al., 2008] Tolar, P., Won Sohn, H., and Pierce, S. K. (2008). Viewing the antigen-induced initiation of B-cell activation in living cells. *Immunological Reviews*, 221(1):64–76.

[Toledano et al., 2013] Toledano, N., Gur-Wahnon, D., Ben-Yehuda, A., and Rachmilewitz, J. (2013). Novel CD47: SIRPα dependent mechanism for the activation of STAT3 in antigen-presenting cell. *PloS one*, 8(9):e75595.

[Tomasello et al., 2000] Tomasello, E., Cant, C., and Bühring, H. (2000). Association of signalâĂŘregulatory proteins β with KARAP/DAPâĂŘ12. *European journal of immunology*, pages 2147–2156.

[Tsai and Discher, 2008] Tsai, R. K. and Discher, D. E. (2008). Inhibition of "self" engulfment through deactivation of myosin-II at the phagocytic synapse between human cells. *Journal of Cell Biology*, 180(5):989–1003.

[Tsai et al., 2010] Tsai, R. K., Rodriguez, P. L., and Discher, D. E. (2010). Self inhibition of phagocytosis: The affinity of 'marker of self' CD47 for SIRPalpha dictates potency of inhibition but only at low expression levels. *Blood Cells, Molecules, and Diseases*, 45(1):67–74.

[Valitutti et al., 1995a] Valitutti, S., Dessing, M., Aktories, K., Gallati, H., and Lanzavecchia, A. (1995a). Sustained signaling leading to T cell activation results from prolonged T cell receptor occupancy. Role of T cell actin cytoskeleton. *The Journal of experimental medicine*, 181(2):577–84.

[Valitutti et al., 1995b] Valitutti, S., Müller, S., Cella, M., Padovan, E., and Lanzavecchia, A. (1995b). Serial triggering of many T-cell receptors by a few peptide-MHC complexes. *Nature*, 375(6527):148–151.

[van der Merwe et al., 2000] van der Merwe, P. A., Davis, S. J., Shaw, a. S., and Dustin, M. L. (2000). Cytoskeletal polarization and redistribution of cell-surface molecules during T cell antigen recognition. *Seminars in immunology*, 12(1):5–21.

[van der Merwe et al., 1995] van der Merwe, P. a., McNamee, P. N., Davies, E. a., Barclay, a. N., and Davis, S. J. (1995). Topology of the CD2-CD48 cell-adhesion molecule complex: implications for antigen recognition by T cells. *Current biology : CB*, 5(1):74–84.

[Van Valen, 1974] Van Valen, L. (1974). Molecular evolution as predicted by natural selection. *Journal of molecular evolution*, 3:89–101.

[Van Vugt et al., 1998] Van Vugt, Van Den Herik-Oudijk, and Van DE Winkel (1998). FcgammaRIa-gamma-chain complexes trigger antibody-dependent cell-mediated cytotoxicity (ADCC) in CD5+ B cell/macrophage IIA1.6 cells. *Clinical and Experimental Immunology*, 113(3):415–422.

[Varma et al., 2006] Varma, R., Campi, G., Yokosuka, T., Saito, T., and Dustin, M. L.

(2006). T cell receptor-proximal signals are sustained in peripheral microclusters and terminated in the central supramolecular activation cluster. *Immunity*, 25(1):117–27.

[Veillette and Fournel, 1991] Veillette, A. and Fournel, M. (1991). The cd4 associated tyrosine protein kinase p56lck is positively regulated through its site of autophosphorylation. *Oncogene*, 5 (10):1455–1462.

[Veillette et al., 1998] Veillette, A., Thibaudeau, E., and Latour, S. (1998). High expression of inhibitory receptor SHPS-1 and its association with protein-tyrosine phosphatase SHP-1 in macrophages. *The Journal of biological chemistry*, 273(35):22719–22728.

[Velikovsky et al., 2007] Velikovsky, C. A., Deng, L., Chlewicki, L. K., Fernández, M. M., Kumar, V., and Mariuzza, R. a. (2007). Structure of Natural Killer Receptor 2B4 Bound to CD48 Reveals Basis for Heterophilic Recognition in Signaling Lymphocyte Activation Molecule Family. *Immunity*, 27(4):572–584.

[Vitale et al., 1998] Vitale, M., Bottino, C., Sivori, S., Sanseverino, L., Castriconi, R., Marcenaro, E., Augugliaro, R., Moretta, L., and Moretta, a. (1998). NKp44, a novel triggering surface molecule specifically expressed by activated natural killer cells, is involved in non-major histocompatibility complex-restricted tumor cell lysis. *The Journal of experimental medicine*, 187(12):2065–2072.

[Vivian et al., 2011] Vivian, J. P., Duncan, R. C., Berry, R., O'Connor, G. M., Reid, H. H., Beddoe, T., Gras, S., Saunders, P. M., Olshina, M. a., Widjaja, J. M. L., Harpur, C. M., Lin, J., Maloveste, S. M., Price, D. a., Lafont, B. a. P., McVicar, D. W., Clements, C. S., Brooks, A. G., and Rossjohn, J. (2011). Killer cell immunoglobulin-like receptor 3DL1-mediated recognition of human leukocyte antigen B. *Nature*, 479(7373):401–5.

[Voss and Skerra, 1997a] Voss, S. and Skerra, a. (1997a). Mutagenesis of a flexible loop in streptavidin leads to higher affinity for the Strep-tag II peptide and improved performance in recombinant protein purification. *Protein engineering*, 10(8):975–82.

[Voss and Skerra, 1997b] Voss, S. and Skerra, A. (1997b). Mutagenesis of a flexible loop in streptavidin leads to higher affinity for the Strep-tag II peptide and improved performance in recombinant protein purification. *Protein engineering*, 10(8):975–82.

[Wan et al., 2013] Wan, Z., Zhang, S., Fan, Y., Liu, K., Du, F., Davey, A. M., Zhang, H., Han, W., Xiong, C., and Liu, W. (2013). B cell activation is regulated by the stiffness properties of the substrate presenting the antigens. *Journal of immunology (Baltimore, Md. : 1950)*, 190(9):4661–75.

[Wang et al., 2010a] Wang, H., Holst, J., Woo, S.-R., Guy, C., Bettini, M., Wang, Y., Shafer, A., Naramura, M., Mingueneau, M., Dragone, L. L., Hayes, S. M., Malissen, B., Band, H., and Vignali, D. a. a. (2010a). Tonic ubiquitylation controls T-cell receptor:CD3 complex expression during T-cell development. *The EMBO journal*, 29(7):1285–1298.

[Wang et al., 2010b] Wang, H., Kadlecek, T. A., Au-Yeung, B. B., Goodfellow, H. E. S., Hsu, L.-Y., Freedman, T. S., and Weiss, A. (2010b). ZAP-70: an essential kinase in T-cell signaling. *Cold Spring Harbor perspectives in biology*, 2(5):a002279.

[Wang et al., 2001] Wang, J. H., Meijers, R., Xiong, Y., Liu, J. H., Sakihama, T., Zhang, R., Joachimiak, A., and Reinherz, E. L. (2001). Crystal structure of the human CD4 N-terminal two-domain fragment complexed to a class II MHC molecule. *Proceedings*

of the National Academy of Sciences of the United States of America, 98(19):10799–10804.

[Wang et al., 2012] Wang, R., Jaw, J. J., Stutzman, N. C., Zou, Z., and Sun, P. D. (2012). Natural killer cell-produced IFN-gamma and TNF-alpha induce target cell cytolysis through up-regulation of ICAM-1.

[Watson et al., 2007] Watson, A. A., Brown, J., Harlos, K., Eble, J. A., Walter, T. S., and O'Callaghan, C. A. (2007). The crystal structure and mutational binding analysis of the extracellular domain of the platelet-activating receptor CLEC-2. *Journal of Biological Chemistry*, 282(5):3165–3172.

[Watson et al., 2009] Watson, A. a., Christou, C. M., James, J. R., Fenton-May, A. E., Moncayo, G. E., Mistry, A. R., Davis, S. J., Gilbert, R. J. C., Chakera, A., and O'Callaghan, C. a. (2009). The platelet receptor CLEC-2 is active as a dimer. *Biochemistry*, 48(46):10988–96.

[Weber et al., 1989] Weber, P. C., Ohlendorf, D. H., Wendoloski, J. J., and Salemme, F. R. (1989). Structural origins of high-affinity biotin binding to streptavidin. *Science (New York, N.Y.)*, 243(4887):85–88.

[Willcox et al., 2003] Willcox, B. E., Thomas, L. M., and Bjorkman, P. J. (2003). Crystal structure of HLA-A2 bound to LIR-1, a host and viral major histocompatibility complex receptor. *Nature immunology*, 4(9):913–9.

[Wilson et al., 2001] Wilson, D. S., Keefe, A. D., and Szostak, J. W. (2001). The use of mRNA display to select high-affinity protein-binding peptides. *Proceedings of the National Academy of Sciences of the United States of America*, 98(7):3750–3755.

[Wilson et al., 1991] Wilson, G. L., Fox, C. H., Fauci, A. S., and Kehrl, J. H. (1991). cDNA cloning of the B cell membrane protein CD22: a mediator of B-B cell interactions. *The Journal of experimental medicine*, 173(1):137–146.

[Won et al., 2006] Won, W.-j., Foote, J. B., Odom, M. R., Pan, J., Kearney, J. F., and Davis, R. S. (2006). Fc receptor homolog 3 is a novel immunoregulatory marker of marginal zone and B1 B cells. *Journal of immunology (Baltimore, Md. : 1950)*, 177(10):6815–23.

[Woodruff et al., 1967] Woodruff, M. F. A., Reid, B., and James, K. (1967). Effect of Antilymphocytic Antibody and Antibody Fragments on Human Lymphocytes in vitro. *Nature*, 215(5101):591–594.

[Wright et al., 2000] Wright, G. J., Puklavec, M. J., Willis, a. C., Hoek, R. M., Sedgwick, J. D., Brown, M. H., and Barclay, a. N. (2000). Lymphoid/neuronal cell surface OX2 glycoprotein recognizes a novel receptor on macrophages implicated in the control of their function. *Immunity*, 13(2):233–242.

[Wu et al., 1997] Wu, H., Kwong, P. D., and Hendrickson, W. A. (1997). Dimeric association and segmental variability in the structure of human CD4. *Nature*, 387(6632):527–530.

[Wu et al., 2000] Wu, J., Cherwinski, H., Spies, T., Phillips, J. H., and Lanier, L. L. (2000). DAP10 and DAP12 form distinct, but functionally cooperative, receptor complexes in natural killer cells. *The Journal of experimental medicine*, 192(7):1059–68.

[Wu et al., 1999] Wu, J., Song, Y., Bakker, A. B., Bauer, S., Spies, T., Lanier, L. L., and

Phillips, J. H. (1999). An activating immunoreceptor complex formed by NKG2D and DAP10. *Science (New York, N.Y.)*, 285(5428):730–732.

[Wu et al., 2011] Wu, L., Zhang, C., and Zhang, J. (2011). HMBOX1 negatively regulates NK cell functions by suppressing the NKG2D/DAP10 signaling pathway. *Cellular and Molecular Immunology*, 8(5):433–440.

[Wülfing et al., 2002] Wülfing, C., Sumen, C., Sjaastad, M. D., Wu, L. C., Dustin, M. L., and Davis, M. M. (2002). Costimulation and endogenous MHC ligands contribute to T cell recognition. *Nature immunology*, 3(1):42–47.

[Xie and Gu, 2008] Xie, H. and Gu, X.-X. (2008). Moraxella catarrhalis lipooligosaccharide selectively upregulates ICAM-1 expression on human monocytes and stimulates adjacent naïve monocytes to produce TNF-α through cellular cross-talk. *Cellular Microbiology*, 10(7):1453–1467.

[Xie et al., 2012] Xie, J., Huppa, J. B., Newell, E. W., Huang, J., Ebert, P. J. R., Li, Q.-J., and Davis, M. M. (2012). Photocrosslinkable pMHC monomers stain T cells specifically and cause ligand-bound TCRs to be 'preferentially' transported to the cSMAC. *Nature immunology*, 13(7):674–80.

[Xu et al., 2008] Xu, C., Gagnon, E., Call, M. E., Schnell, J. R., Schwieters, C. D., Carman, C. V., Chou, J. J., and Wucherpfennig, K. W. (2008). Regulation of T Cell Receptor Activation by Dynamic Membrane Binding of the CD3epsilon Cytoplasmic Tyrosine-Based Motif. *Cell*, 135(4):702–713.

[Xu et al., 2002] Xu, M.-j., Zhao, R., Cao, H., and Zhao, Z. J. (2002). SPAP2, an Ig family receptor containing both ITIMs and ITAMs. *Biochemical and biophysical research communications*, 293(3):1037–46.

[Xu et al., 2000] Xu, M. J., Zhao, R., and Zhao, Z. J. (2000). Identification and characterization of leukocyte-associated Ig-like receptor-1 as a major anchor protein of tyrosine phosphatase SHP-1 in hematopoietic cells. *Journal of Biological Chemistry*, 275(23):17440–17446.

[Xu et al., 2001] Xu, M. J., Zhao, R., and Zhao, Z. J. (2001). Molecular cloning and characterization of SPAP1, an inhibitory receptor. *Biochemical and biophysical research communications*, 280(3):768–75.

[Xu et al., 1999] Xu, W., Doshi, A., Lei, M., Eck, M. J., and Harrison, S. C. (1999). Crystal structures of c-Src reveal features of its autoinhibitory mechanism. *Molecular Cell*, 3(5):629–638.

[Xu et al., 1997] Xu, W., Harrison, S. C., and Eck, M. J. (1997). Three-dimensional structure of the tyrosine kinase c-Src.

[Xu and Weiss, 2002] Xu, Z. and Weiss, A. (2002). Negative regulation of CD45 by differential homodimerization of the alternatively spliced isoforms. *Nature Immunology*, 3(8):764–71.

[Yachi et al., 2005] Yachi, P. P., Ampudia, J., Gascoigne, N. R. J., and Zal, T. (2005). Nonstimulatory peptides contribute to antigen-induced CD8-T cell receptor interaction at the immunological synapse. *Nature immunology*, 6(8):785–92.

[Yamada and McVicar, 2008] Yamada, E. and McVicar, D. W. (2008). Paired receptor systems of the innate immune system. *Current protocols in immunology / edited by John E. Coligan ... [et al.]*, Chapter 1(April):Appendix 1X.

[Yamaguchi and Hendrickson, 1996] Yamaguchi, H. and Hendrickson, W. a. (1996). Structural basis for activation of human lymphocyte kinase Lck upon tyrosine phosphorylation.

[Yamanaka et al., 2009] Yamanaka, M., Kato, Y., Angata, T., and Narimatsu, H. (2009). Deletion polymorphism of SIGLEC14 and its functional implications. *Glycobiology*, 19(8):841–846.

[Yamao et al., 2002] Yamao, T., Noguchi, T., Takeuchi, O., Nishiyama, U., Morita, H., Hagiwara, T., Akahori, H., Kato, T., Inagaki, K., Okazawa, H., Hayashi, Y., Matozaki, T., Takeda, K., Akira, S., and Kasuga, M. (2002). Negative regulation of platelet clearance and of the macrophage phagocytic response by the transmembrane glycoprotein SHPS-1. *The Journal of biological chemistry*, 277(42):39833–9.

[Yang and Reth, 2010] Yang, J. and Reth, M. (2010). The dissociation activation model of B cell antigen receptor triggering. *FEBS Letters*, 584(24):4872–4877.

[Yin et al., 2012] Yin, Y., Wang, X. X., and Mariuzza, R. A. (2012). Crystal structure of a complete ternary complex of T-cell receptor, peptide-MHC, and CD4. *Proceedings of the National Academy of Sciences of the United States of America*, 109(14):5405–10.

[Yokosuka et al., 2008] Yokosuka, T., Kobayashi, W., Sakata-Sogawa, K., Takamatsu, M., Hashimoto-Tane, A., Dustin, M. L., Tokunaga, M., and Saito, T. (2008). Spatiotemporal Regulation of T Cell Costimulation by TCR-CD28 Microclusters and Protein Kinase C theta Translocation. *Immunity*, 29(4):589–601.

[Yokosuka et al., 2010] Yokosuka, T., Kobayashi, W., Takamatsu, M., Sakata-Sogawa, K., Zeng, H., Hashimoto-Tane, A., Yagita, H., Tokunaga, M., and Saito, T. (2010). Spatiotemporal Basis of CTLA-4 Costimulatory Molecule-Mediated Negative Regulation of T Cell Activation. *Immunity*, 33(3):326–339.

[Yokosuka et al., 2005] Yokosuka, T., Sakata-Sogawa, K., Kobayashi, W., Hiroshima, M., Hashimoto-Tane, A., Tokunaga, M., Dustin, M. L., and Saito, T. (2005). Newly generated T cell receptor microclusters initiate and sustain T cell activation by recruitment of Zap70 and SLP-76. *Nature immunology*, 6(12):1253–1262.

[Yokosuka et al., 2012] Yokosuka, T., Takamatsu, M., Kobayashi-Imanishi, W., Hashimoto-Tane, A., Azuma, M., and Saito, T. (2012). Programmed cell death 1 forms negative costimulatory microclusters that directly inhibit T cell receptor signaling by recruiting phosphatase SHP2.

[Yokoyama et al., 1991] Yokoyama, S., Staunton, D., Fisher, R., Amiot, M., Fortin, J. J., and Thorley-Lawson, D. A. (1991). Expression of the Blast-1 activation/adhesion molecule and its identification as CD48. *The Journal of Immunology*, 146(7):2192–2200.

[Yu et al., 2008] Yu, M.-C., Su, L.-L., Zou, L., Liu, Y., Wu, N., Kong, L., Zhuang, Z.-H., Sun, L., Liu, H.-P., Hu, J.-H., Li, D., Strominger, J. L., Zang, J.-W., Pei, G., and Ge, B.-X. (2008). An essential function for beta-arrestin 2 in the inhibitory signaling of natural killer cells. *Nature immunology*, 9(8):898–907.

[Yu et al., 2001] Yu, Z., Lai, C. M., Maoui, M., Banville, D., and Shen, S. H. (2001). Identification and characterization of S2V, a novel putative siglec that contains two V set Ig-like domains and recruits protein-tyrosine phosphatases SHPs. *The Journal of biological chemistry*, 276(26):23816–24.

[Yusa et al., 2002] Yusa, S.-i., Catina, T. L., and Campbell, K. S. (2002). SHP-1- and phosphotyrosine-independent inhibitory signaling by a killer cell Ig-like receptor cytoplasmic domain in human NK cells. *Journal of immunology (Baltimore, Md. : 1950)*, 168(10):5047–57.

[Zakeri et al., 2012] Zakeri, B., Fierer, J. O., Celik, E., Chittock, E. C., Schwarz-Linek, U., Moy, V. T., and Howarth, M. (2012). PNAS Plus: Peptide tag forming a rapid covalent bond to a protein, through engineering a bacterial adhesin. *Proceedings of the National Academy of Sciences*, 109(12):E690–E697.

[Zeng et al., 2015] Zeng, Y., Yi, J., Wan, Z., Liu, K., Song, P., Chau, A., Wang, F., Chang, Z., Han, W., Zheng, W., Chen, Y.-H., Xiong, C., and Liu, W. (2015). Substrate stiffness regulates B-cell activation, proliferation, class switch, and T-cell-independent antibody responses in vivo. *European journal of immunology*, 45(6):1621–34.

[Zhang et al., 2011] Zhang, H., Cordoba, S.-P., Dushek, O., and van der Merwe, P. A. (2011). Basic residues in the T-cell receptor ζ cytoplasmic domain mediate membrane association and modulate signaling. *Proceedings of the National Academy of Sciences of the United States of America*, 108(48):19323–8.

[Zhang et al., 2004] Zhang, J., Xu, X., and Liu, Y. (2004). Activation-induced cell death in T cells and autoimmunity. *Cellular & molecular immunology*, 1(3):186–192.

[Zhang et al., 2012] Zhang, J.-G., Czabotar, P. E., Policheni, A. N., Caminschi, I., San Wan, S., Kitsoulis, S., Tullett, K. M., Robin, A. Y., Brammananth, R., van Delft, M. F., Lu, J., O'Reilly, L. A., Josefsson, E. C., Kile, B. T., Chin, W. J., Mintern, J. D., Olshina, M. A., Wong, W., Baum, J., Wright, M. D., Huang, D. C. S., Mohandas, N., Coppel, R. L., Colman, P. M., Nicola, N. A., Shortman, K., and Lahoud, M. H. (2012). The Dendritic Cell Receptor Clec9A Binds Damaged Cells via Exposed Actin Filaments. *Immunity*, 36(4):646–57.

[Zhang et al., 2015a] Zhang, L., Liu, S.-H., Wright, T. T., Shen, Z.-Y., Li, H.-Y., Zhu, W., Potempa, L. A., Ji, S.-R., Szalai, A. J., and Wu, Y. (2015a). C-Reactive Protein Directly Suppresses Th1 Cell Differentiation and Alleviates Experimental Autoimmune Encephalomyelitis. *The Journal of Immunology*, 194(11):5243–5252.

[Zhang and Phillips, 2006] Zhang, S. and Phillips, J. H. (2006). Identification of tyrosine residues crucial for CD200R-mediated inhibition of mast cell activation. *Journal of leukocyte biology*, 79(2):363–368.

[Zhang et al., 2013] Zhang, W. B., Sun, F., Tirrell, D. A., and Arnold, F. H. (2013). Controlling macromolecular topology with genetically encoded SpyTag-SpyCatcher chemistry. *Journal of the American Chemical Society*, 135(37):13988–13997.

[Zhang et al., 2003] Zhang, X., Schwartz, J.-C. D., Almo, S. C., and Nathenson, S. G. (2003). Crystal structure of the receptor-binding domain of human B7-2: insights into organization and signaling. *Proceedings of the National Academy of Sciences of the United States of America*, 100(5):2586–2591.

[Zhang et al., 2015b] Zhang, Z., Wu, N., Lu, Y., Davidson, D., Colonna, M., and Veillette, A. (2015b). DNAM-1 controls NK cell activation via an ITT-like motif. *The Journal of experimental medicine*, 212(12):2165–2182.

[Zhu et al., 2013] Zhu, Y., Yao, S., Iliopoulou, B. P., Han, X., Augustine, M. M., Xu, H., Phennicie, R. T., Flies, S. J., Broadwater, M., Ruff, W., Taube, J. M., Zheng, L., Luo,

L., Zhu, G., Chen, J., and Chen, L. (2013). B7-H5 costimulates human T cells via CD28H. *Nature communications*, 4:2043.